Environmental Chemistry for a Sustainable World 42

Zhien Zhang
Wenxiang Zhang
Eric Lichtfouse *Editors*

Membranes for Environmental Applications

Springer

Environmental Chemistry for a Sustainable World

Volume 42

Other Publications by the Editors

Books
Environmental Chemistry
http://www.springer.com/978-3-540-22860-8

Organic Contaminants in Riverine and Groundwater Systems
http://www.springer.com/978-3-540-31169-0

Sustainable Agriculture
Volume 1: http://www.springer.com/978-90-481-2665-1
Volume 2: http://www.springer.com/978-94-007-0393-3

Book series
Environmental Chemistry for a Sustainable World
http://www.springer.com/series/11480

Sustainable Agriculture Reviews
http://www.springer.com/series/8380

Journals
Environmental Chemistry Letters
http://www.springer.com/10311

Agronomy for Sustainable Development
http://www.springer.com/13593

More information about this series at http://www.springer.com/series/11480

Zhien Zhang • Wenxiang Zhang • Eric Lichtfouse
Editors

Membranes for Environmental Applications

Springer

Editors
Zhien Zhang
William G. Lowrie Department of
Chemical and Biomolecular Engineering
The Ohio State University
Columbus, OH, USA

Wenxiang Zhang
Department of Civil and Environmental
Engineering, Faculty of Science
University of Macau
Macau, China

Eric Lichtfouse
Aix-Marseille University, CNRS, IRD,
INRA, Coll France, CEREGE
Aix-en-Provence, France

ISSN 2213-7114 ISSN 2213-7122 (electronic)
Environmental Chemistry for a Sustainable World
ISBN 978-3-030-33977-7 ISBN 978-3-030-33978-4 (eBook)
https://doi.org/10.1007/978-3-030-33978-4

This Springer imprint is published by the registered company Springer Nature Switzerland AG.
The registered company address is: Gewerbestrasse 11, 6330 Cham, Switzerland

Preface

With the development of industrialization and urbanization, a large number of wastewater and waste gases are discharged into natural environment. Various pollutants from these wastes cause serious environmental issues. In order to protect the environment, it is necessary to purify and treat wastewater and waste gases with a highly efficient environmental technology. Membrane technology is a high-efficiency and precision separation method. Membrane filtration has the advantages

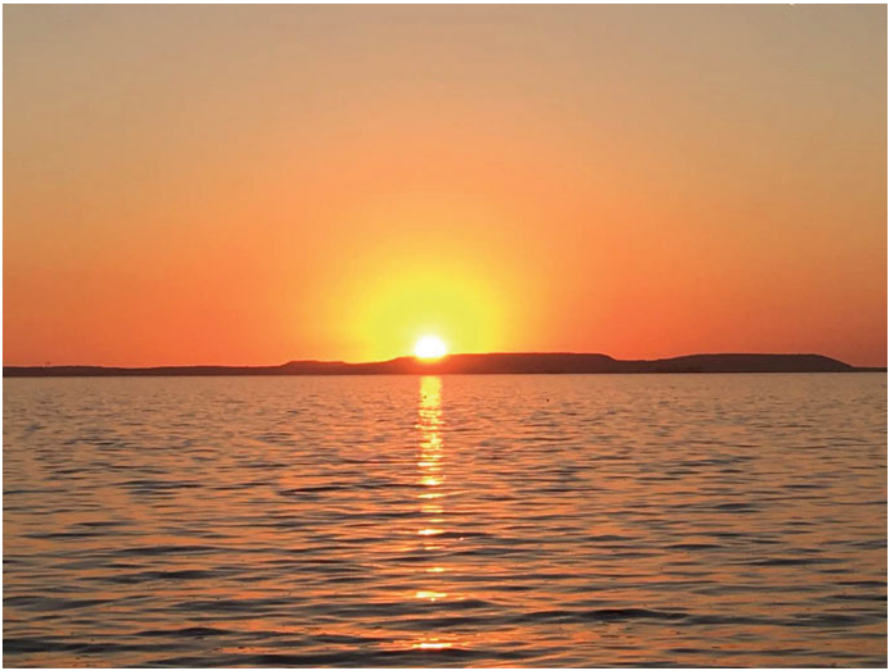

of high-efficiency separation, simple equipment, energy-saving, normal temperature operation, and without secondary pollution. Membrane filtration has been widely used for wastewater and waste gases treatment. This book provides a comprehensive overview of membrane technologies applied for wastewater and waste gas treatments and of energy issues of the processes. Novel knowledge on membrane fabrication and usage in energy, chemical, and environmental engineering is presented. Mechanisms and applications in a variety of processes to solve the environmental issues are explained.

The *Etang de Berre*, near Marseille, France, is a nice-looking lake though polluted by increasing urbanization and decades of industrial development. Picture taken at the Marettes Beach, Vitrolles. Copyright: Eric Lichtfouse 2018

In Chap. 1, Boucif et al. introduce the state-of-the-art and recent developments of the carbonic anhydrase-driven processes for CO_2 capture. They also discuss the current and prospective research and engineering achievements on enhanced enzymatic carbon capture. In Chap. 2, Sarfraz reviews the latest advances in the field of carbon capture from flue gas using polymer-based mixed-matrix membranes, containing various microporous metal organic frameworks and other nanomaterials, to signify their prospective applications on an industrial scale. CO_2 capture and separation by mixed-matrix membranes as compared to other existing approaches has been found to be better in terms of sustainability, economics, environment, and operation. Baena-Moreno et al. present the status of biogas upgrading by using membrane technologies in Chap. 3. In addition, gas permeation phenomena, membrane materials, membrane modules, different types of process configuration, and commercial biogas plants based on membrane technologies are deeply discussed. These three chapters demonstrate the feasibility of membranes applied for gas removal and separation.

In Chap. 4, Li et al. review the progress in the fabrication and synthesis mechanisms of the carbon-based membrane materials, characterization methods, and practical applications in water treatment. In Chap. 5 by Wei et al., the mechanisms, efficiency, and influencing factors of pharmaceuticals and personal care products removal in water treatments by ultrafiltration membranes, reverse osmosis membranes, and nanofiltration membranes are introduced. In Chap. 6, Xie and co-workers present an overview of the different dynamic filtration modules used for wastewater treatment. It indicates dynamic shear-enhanced membrane system shows more desirable filtration efficiency than conventional membrane process. Furthermore, Zhong et al. present the membrane fabrication methods for unconventional desalination by membrane distillation and pervaporation in Chap. 7. Moreover, in Chap. 8, Agboola et al. discuss the role and characterizations of nano-based membranes for environmental applications, including gas separation, air and solid pollution control, and desalination.

In terms of membrane applications in energy areas, Chang et al. introduce the membrane applied in the processes of liquid and gaseous biofuels production, and microbial fuel cells, and also present the membrane biofouling issues and the antibiofouling approaches in Chap. 9. In Chap. 10, Hafeez et al. discuss the membrane reactors applications in the renewable fuel production and the main advantages of different methods for hydrogen production. Additionally, in Chap. 11, Saidi et al. also review the hydrogen production from wastes by using membrane reactor. In the last chapter (Chap. 12), the recent developments of hydrogen production from residual biomass and wastes using the Pd membranes are reviewed by Maroño and Alique.

We first highly acknowledge the Springer Nature team from the acceptance of the proposal to the production of the book. We extend our sincere thanks to all the authors and reviewers who have put considerable efforts into their contributions and consistent cooperation during the manuscript writing and revision process. We hope this book will be an excellent resource to all researchers, students, professors, and scientists working on membrane and related fields.

Columbus, OH, USA Zhien Zhang
Macau, China Wenxiang Zhang
Marseille, France Eric Lichtfouse

Contents

About the Editors

Zhien Zhang is currently Research Fellow in William G. Lowrie Department of Chemical and Biomolecular Engineering at the Ohio State University. His research interests include advanced processes and materials, i.e., membranes, for CO_2 capture; carbon capture, utilization, and storage (CCUS) processes; gas separation; and gas hydrates. He has published more than 80 journal articles and 13 editorials in high-impact journals, e.g., *Renewable and Sustainable Energy Reviews*. He has authored three “hot papers” (top 0.1%) and ten “highly cited papers” (top 1%). He is Editor and Guest Editor of several international journals, e.g., *Environmental Chemistry Letters*, *Applied Energy*, *Fuel*, and *Journal of Natural Gas Science and Engineering* and is also a Visiting Professor at the University of Cincinnati.

Wenxiang Zhang is a Research Fellow at the University of Macau, working on the theory and technology of membrane water treatment, specifically including dynamic filtration for resource recovery of pollutants from food processing wastewater, filtration characteristics of granular sludge for fouling control, and the development of multifunctional membrane for advanced water treatment. He has published more than 40 journal papers in the high-impact journals, e.g., *Water Research* and *Journal of Membrane Science*.

Eric Lichtfouse is Biogeochemist at the University of Aix-Marseille, France, and Visiting Professor at Xi'an Jiaotong University. He has invented carbon-13 dating, a method allowing to measure the relative age of organic molecules occurring in different temporal pools of complex media. He is teaching scientific writing and communication and has published the book *Scientific Writing for Impact Factor Journals*, which includes a new tool – the micro-article – to identify the novelty of research results. He is Founder and Chief Editor of scientific journals and series in environmental chemistry and agriculture. He has founded the European Association of Chemistry and the Environment. He got the Analytical Chemistry Prize by the French Chemical Society, the Grand Prize of the Universities of Nancy and Metz, and a Journal Citation Award by the Essential Indicators.

Contributors

Oluranti Agboola Department of Chemical Engineering, Covenant University, Ota, Ogun State, Nigeria
Department of Chemical, Metallurgical and Materials Engineering, Tshwane University of Technology, Pretoria, South Africa

Peter Adeniyi Alaba Department of Chemical, Metallurgical and Materials Engineering, Tshwane University of Technology, Pretoria, South Africa

D. Alique Department of Chemical, Energy and Mechanical Technology, Rey Juan Carlos University, Móstoles, Spain

S. M. Al-Salem Environment & Life Sciences Research Centre, Kuwait Institute for Scientific Research, Safat, Kuwait

Francisco M. Baena-Moreno Chemical and Environmental Engineering Department, Technical School of Engineering, University of Seville, Sevilla, Spain
Department of Chemical and Process Engineering, University of Surrey, Guildford, UK

Noureddine Boucif Laboratoire des Réactions et du Génie des procédés (LRGP, UMR n° 7274), Université de Lorraine, BP, Nancy Cedex, France

Haixing Chang School of Chemistry and Chemical Engineering, Chongqing University of Technology, Chongqing, China

Jinyuan Chen College of Environment, Zhejiang University of Technology, Hangzhou, China
Key Laboratory of Microbial Technology for Industrial Pollution Control of Zhejiang Province, Hangzhou, China

Shunquan Chen Guangzhou Institute of Advanced Technology, Chinese Academy of Sciences, Guangzhou, China
Shenzhen Institutes of Advanced Technology, Chinese Academy of Sciences, Shenzhen, China

Achilleas Constantinou Division of Chemical & Petroleum Engineering, School of Engineering, London South Bank University, London, UK
Department of Chemical Engineering, University College London, London, UK

Luhui Ding Sorbonne University, Université de Technologire de Compiègne, ESCOM, EA 4297 TIMR, Centre de Recherch Royallieu, CS 60319, Compiègne Cedex, France

Xinfei Fan College of Environmental Science and Engineering, Dalian Maritime University, Dalian, China

Victoria Oluwaseun Fasiku Department of Pharmaceutical Sciences, University of KwaZulu-Natal, Durban, South Africa

Eric Favre Laboratoire des Réactions et du Génie des procédés (LRGP, UMR n° 7274), Université de Lorraine, BP, Nancy Cedex, France

Luc Fillaudeau TBI, Université de Toulouse, CNRS UMR5504, INRA UMR792, INSA, 31055, 135, avenue de Rangueil, Toulouse, France
FERMAT, Université de Toulouse, CNRS, INPT, INSA, UPS, Toulouse, France

Mohammad Hossein Gohari School of Chemistry, College of Science, University of Tehran, Tehran, Iran

Sanaa Hafeez Division of Chemical & Petroleum Engineering, School of Engineering, London South Bank University, London, UK

Rui Hu School of Chemistry and Chemical Engineering, Chongqing University of Technology, Chongqing, China

Estelle le Saché Department of Chemical and Process Engineering, University of Surrey, Guildford, UK

Chen Li College of Environmental Science and Engineering, Dalian Maritime University, Dalian, China

Cuixia Li College of Environment, Zhejiang University of Technology, Hangzhou, China
Key Laboratory of Microbial Technology for Industrial Pollution Control of Zhejiang Province, Hangzhou, China

Qiyuan Li UNESCO Centre for Membrane Science and Technology, School of Chemical Engineering, The University of New South Wales (UNSW), Kensington, NSW, Australia
School of Mechanical and Manufacturing Engineering, The University of New South Wales (UNSW), Kensington, NSW, Australia

Shibo Li College of Environmental Science and Engineering, Dalian Maritime University, Dalian, China

Bosheng Lv College of Environment, Zhejiang University of Technology, Hangzhou, China
Key Laboratory of Microbial Technology for Industrial Pollution Control of Zhejiang Province, Hangzhou, China

M. Maroño CIEMAT, Combustion and Gasification Division, Madrid, Spain

Mukuna Patrick Mubiayi Department of Mechanical Engineering Science, University of Johannesburg, Johannesburg, South Africa

Daniel Temitayo Oyekunle Department of Chemical Engineering, Covenant University, Ota, Ogun State, Nigeria

Laura Pastor-Pérez Department of Chemical and Process Engineering, University of Surrey, Guildford, UK

Patricia Popoola Department of Pharmaceutical Sciences, University of KwaZulu-Natal, Durban, South Africa

Xueqiang Qi School of Chemistry and Chemical Engineering, Chongqing University of Technology, Chongqing, China

Xuejun Quan School of Chemistry and Chemical Engineering, Chongqing University of Technology, Chongqing, China

Ali Talesh Ramezani School of Chemistry, College of Science, University of Tehran, Tehran, Iran

T. R. Reina Department of Chemical and Process Engineering, University of Surrey, Guildford, UK

Denis Roizard Laboratoire des Réactions et du Génie des procédés (LRGP, UMR n° 7274), Université de Lorraine, BP, Nancy Cedex, France

Rotimi Sadiku Department of Chemical, Metallurgical and Materials Engineering, Tshwane University of Technology, Pretoria, South Africa

Majid Saidi School of Chemistry, College of Science, University of Tehran, Tehran, Iran

Samuel Eshorame Sanni Department of Chemical Engineering, Covenant University, Ota, Ogun State, Nigeria

Muhammad Sarfraz Department of Polymer and Process Engineering, University of Engineering and Technology, Lahore, Pakistan

Philippe Schmitz TBI, Université de Toulouse, CNRS UMR5504, INRA UMR792, INSA, 31055, 135, avenue de Rangueil, Toulouse, France
FERMAT, Université de Toulouse, CNRS, INPT, INSA, UPS, Toulouse, France

Chengwen Song College of Environmental Science and Engineering, Dalian Maritime University, Dalian, China

Yahui Sun School of Energy and Mechanical Engineering, Nanjing Normal University, Nanjing, China

Chengyang Wang School of Chemistry and Chemical Engineering, Chongqing University of Technology, Chongqing, China

Jianli Wang College of Chemical Engineering, Zhejiang University of Technology, Hangzhou, China

Xiuzhen Wei College of Environment, Zhejiang University of Technology, Hangzhou, China
Key Laboratory of Microbial Technology for Industrial Pollution Control of Zhejiang Province, Hangzhou, China

Jiawei Wu College of Environment, Zhejiang University of Technology, Hangzhou, China
Key Laboratory of Microbial Technology for Industrial Pollution Control of Zhejiang Province, Hangzhou, China

Xin Xiao College of Environmental Science and Engineering, Dalian Maritime University, Dalian, China

Xiaomin Xie Institute of Environmental & Ecological Engineering, School of Environmental Science of Engineering, Guangdong University of Technology, Guangzhou, China

Xufeng Xu College of Environment, Zhejiang University of Technology, Hangzhou, China
Key Laboratory of Microbial Technology for Industrial Pollution Control of Zhejiang Province, Hangzhou, China

Jie Yang College of Environmental Science and Engineering, Dalian Maritime University, Dalian, China

Yin Yuan College of Environmental Science and Engineering, Dalian Maritime University, Dalian, China

Luying Zhang College of Environmental Science and Engineering, Dalian Maritime University, Dalian, China

Ting Zhang School of Intellectual Property, Chongqing University of Technology, Chongqing, China

Wenxiang Zhang Institute of Environmental & Ecological Engineering, School of Environmental Science of Engineering, Guangdong University of Technology, Guangzhou, China
Department of Civil and Environmental Engineering, Faculty of Science and Technology, University of Macau, Macau, China

Xiaodong Zhao Guangzhou Institute of Advanced Technology, Chinese Academy of Sciences, Guangzhou, China

Nianbing Zhong Chongqing Key Laboratory of Fiber Optic Sensor and Photodetector, Chongqing Key Laboratory of Modern Photoelectric Detection Technology and Instrument, Chongqing University of Technology, Chongqing, China

Wenwei Zhong Guangzhou Institute of Advanced Technology, Chinese Academy of Sciences, Guangzhou, China
UNESCO Centre for Membrane Science and Technology, School of Chemical Engineering, The University of New South Wales (UNSW), Kensington, NSW, Australia

Chapter 1
The Carbonic Anhydrase Promoted Carbon Dioxide Capture

Noureddine Boucif, Denis Roizard, and Eric Favre

Contents

N. Boucif (✉) · D. Roizard · E. Favre
Laboratoire des Réactions et du Génie des procédés (LRGP, UMR n° 7274), Université de Lorraine, BP, Nancy Cedex, France

Z. Zhang et al. (eds.), *Membranes for Environmental Applications*, Environmental Chemistry for a Sustainable World 42, https://doi.org/10.1007/978-3-030-33978-4_1

Abstract To match simultaneously the climate change mitigation with the increasing global demand for energy is a tremendous paradox for this century. To satisfy both criteria, carbon capture seems to be a mandatory technology for the development of sustainable energy infrastructures. Post-combustion capture is a mature and proven technology, but not economically attractive unless novel solvents and optimized processes are implemented. The use of carbonic anhydrase, inspired by the CO_2 metabolic process in cells, a natural fast biocatalyst, is a promising technique which can dramatically improve the implementation and economics of carbon capture under stringent environment demands. In this tutorial review, the authors address the state of the art of the carbonic anhydrase-driven processes for carbon capture, recent developments, current and prospective research and engineering achievements.

Keywords Carbon capture · Enzyme · Carbonic anhydrase · Enzyme immobilization

1.1 Introduction

Global warming, resulting from the continuously increasing Earth's temperature, has become a major focus of the environmental agenda worldwide. The tremendous rise in greenhouse gases is thought to be one of the most contributing factors to global warming. Six gases have been identified and reported as major contributors to the global warming, i.e., carbon dioxide (CO_2), methane (CH_4), nitrous oxide (N_2O), hydrofluorocarbons (HFC), perfluorocarbons (PFC), and sulfur hexafluoride (SF_6), among which, CO_2 plays a key role in global warming. Carbon dioxide can be emitted from various sources including the burning of coal and fossil fuels (Figueroa et al. 2008).

According to the IPCC (2017), there are four main anthropogenic greenhouse gases, namely, methane (CH_4), fluorinated gases, nitrous oxides (NO_x), and carbon dioxide (CO_2). In 2004, 1.1% of the total anthropogenic greenhouse gas emissions were attributable to fluorinated gases, 7.9% to nitrous oxides, 14.3% to methane, and 76.7% to CO_2 (IPCC 2017). It is well noted that CO_2 is by far the greenhouse gas of anthropogenic origin whose emissions are the most abundant. Coal, oil, and natural gas-fired power plants which release over nine billion metric tons every year worldwide of carbon dioxide are the overwhelming anthropogenic sources of CO_2 emission. The forecasted consumption of coal and fossil fuels is estimated by the US Department of Energy (DOE) to increase by 27% over the next 20 years, and the overall CO_2 emissions from India and China in 2030 from coal use will be around three times that of the Unites States (1371 million tons of CO_2 for India, 3226 million tons for the United States, and 8286 million tons for China) (DOE 2016).

Henceforth, it is mandatory at present to address the effect of global environmental changes due to increasing emission of CO_2. Many approaches have been suggested such as switching from fossil fuel to alternate renewable energy sources such as nuclear, solar, or wind energy (Sims et al. 2003).

Most of the political and apolitical organizations worldwide are urging the use of alternate energy sources with less or no greenhouse gas emissions. However, considering the increasing energy demand, the complete substitution of fossil fuels by clean energies is extremely difficult. Furthermore, steadying the atmospheric concentration of CO_2 is equally important and requires developing new technologies or improving existing ones to alleviate this issue through various mechanisms and protocols.

The CO_2 capture and sequestration has several features. A potential solution to stabilize and ultimately reduce the release of CO_2 into the atmosphere is the implementation of carbon capture and sequestration (CCS) technology which is a combinatorial implementation of CO_2 separation from industrial and energy-related sources, transport to a storage location, and long-term isolation from the atmosphere. This technology, which is one of the upcoming fields of interests, requires a thoughtful strategy development to mitigate the impact of CO_2 as greenhouse gas on environment (Wang et al. 2011). There are three methods for capturing CO_2 from industrial emissions (natural gas combustion fumes, coal, and fuel oil), pre-combustion, oxy-fuel capture, and post-combustion (Abu-Khader 2006), as detailed in Fig. 1.1.

- In the pre-combustion processes, the primary fossil fuel is gasified in a first reactor by injection of steam and air to produce a mixture of carbon monoxide and hydrogen. Subsequently, the mixture is introduced into a second reactor where steam is added. A mixture of mainly CO_2 and hydrogen is obtained from

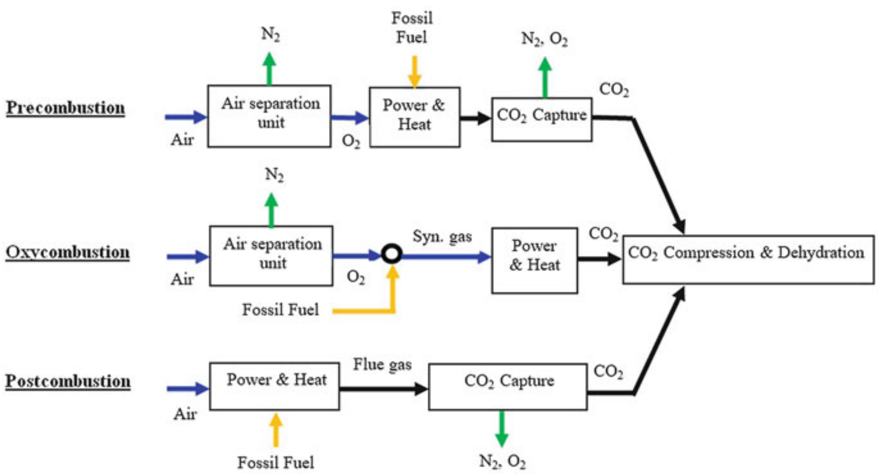

Fig. 1.1 Carbon dioxide capture systems

the reaction between steam and carbon monoxide. This mixture can be separated into a stream of CO_2 and a stream of hydrogen. The hydrogen flux separated from the mixture can be used as a "green" carbon-free fuel, and the CO_2 can be stored or used for many industrial purposes (Blomen et al. 2009).

- The oxycombustion process is characterized by the use of pure oxygen instead of air as oxidizer in the combustion of the primary fossil fuel, producing a gas mixture solely composed of water vapor and CO_2. Following oxycombustion, the gas flow is cooled down and compressed to separate the water and making it possible to recover a gas flow with a very high CO_2 content (more than 80 vol. %) (Blomen et al. 2009).
- Whereas, the post-combustion processes involve separation of dilute CO_2 from flue gas after fuel combustion where air is used, which results in a CO_2 low concentration flue gas. The post-combustion is the most promising technology among the three strategies of CO_2 capture, since it can be integrated to new power plants and applied to existing power plants. Besides, it has a relatively lower cost and provides flexibility to the power plant (Leung et al. 2014).

Various techniques have been developed to achieve CO_2 capture, the majority of which are, however, too expensive and of limited efficiency. At present, one of the most viable technology options uses amine solvents to remove CO_2 from flue gases. Therefore, some biological methodologies, also called "bio-mimetic" CO_2 capture systems, are being implemented as more economic and more sustainable technologies. These methods are based on the use of enzymes involved in the CO_2 biological processes, occurring naturally in living organisms such as the respiratory system in mammalian cells or photosynthetic systems in plant cells. The carbonic anhydrases (specifically the EC 4.2.1.1) catalyze the reversible hydration of the CO_2 molecule and could be efficiently used in these processes (Di Fiore et al. 2015). On the basis of CO_2-catalyzing enzymes, the "bio-mimic" CO_2 capture systems can show high performance and efficiency in CO_2 capture and release comparable to biomechanisms (Di Fiore et al. 2015). The last decade has seen the emergence of one of the most innovative technologies in the field of CO_2 capture, namely, the use of carbonic anhydrase, an enzyme that catalyzes the CO_2 hydration reaction very efficiently ($k_h \approx 10^{-6}\ s^{-1}$) (Whitford 2005).

Although the number of new research articles published has recently increased significantly, only few papers, to our knowledge, have specifically reviewed the use of enzymes in this field such as Pierre (2012), Yadav and coworkers (Yadav et al. 2014), Shekh and coworkers (Shekh et al. 2012), and Long and their respective coworkers (Long et al. 2017).

This paper aims to provide a state-of-the-art evaluation of the research programs carried out so far in the carbonic anhydrase accelerated carbon dioxide capture. This paper will introduce the beginners to this technology with a summary of literatures. For experienced scientists, this paper will review the available achievements and predict the progress of future research directions. In addition to previous publications on carbon dioxide capture (Figueroa et al. 2008) and enzyme accelerated CO_2 capture (Pierre 2012; Shi et al. 2015), this paper will:

(a) Elaborate historical and recent discoveries of carbonic anhydrase and its usage for carbon capture
(b) Draw the reader's attention on enzyme kinetic mechanisms for carbon dioxide capture
(c) Discuss thoroughly the carbonic anhydrase uses in free and immobilized forms
(d) Provide an update of major research activities worldwide and important pilot plant studies

In Sect. 1.2, the major carbon capture techniques are thoroughly reviewed. Then, Sect. 1.3 overviews the enzymatic carbon capture with an emphasis on the enzyme immobilization. Section 1.4 is a detailed survey of the kinetics and catalytic mechanisms of carbon dioxide capture promoted by carbonic anhydrase. In Sect. 1.5, most recent achievements on enhanced enzymatic carbon capture are overviewed. Then, major research programs worldwide and experimental studies based on pilot plants are reviewed in Sect. 1.6. Conclusions are drawn at the end of the article.

1.2 Carbon Dioxide Capture Processes

Various methods are available for carbon capture from product gas streams. Some of the more commonly used methods include absorption (physical and chemical), membrane contacting, adsorption, and cryogenic separation. Conventional processes with some emerging technologies involving a combination of products and/or processes are briefly reviewed in this section.

1.2.1 Physical Absorption

The physical absorption of CO_2 into a solvent involves Henry's law where atoms or molecules transfer from a gas phase into a liquid phase. The solubility of the solute is sensitive to the partial pressure of the gas to be removed. The solvent regeneration is achieved mainly by desorption, i.e., by pressure reduction (flashing), some additional heating and sometimes both. However, physical solvents can usually be stripped of impurities by reducing the pressure without any heat addition. The main energy requirements originate from the flue gas pressurization because the physical absorption takes place at high CO_2 partial pressures (IEA 2004). In addition, physical solvents can usually be stripped of impurities by reducing the pressure without any heat addition. Furthermore, heat requirements are usually much less for physical solvents than for chemical ones such as amines since the heat of desorption of the acid gas for the physical solvent is only a fraction of that for the chemical ones (Dindore et al. 2004a).

In physical absorption, CO_2 is transferred from gas to liquid phase without chemical reaction with the absorbent. This process is suitable for bulk removal of CO_2 from gas streams having a high CO_2 partial pressure. Furthermore, this technique is easy to design, not very toxic with a low solvent loss but has limited CO_2 selectivity. It is not, therefore, suitable for the treatment of power plant flue gases with low CO_2 partial pressure (Olajire 2010).

The physical absorption is therefore not economical for flue gas streams with CO_2 partial pressures lower than 15 vol. % (Chakravati et al. 2001). Henceforth, physical solvents tend to be favored over chemical solvents when the concentration of acid gases or other impurities is very high. Typical physical absorption solvents used in industry are propylene carbonate (*Fluor*), n-methyl-2-pyrrolidone (*Purisol*), methanol (*Rectisol* and *Ifpexol*), and dimethyl ethers of polyethylene glycol (*Selexol*), some of which are becoming increasingly efficient (Green et al. 2004).

1.2.2 Chemical Absorption

Chemical absorption is dictated by the chemical reaction of CO_2 with a solvent to form a weakly bonded intermediate compound which may be regenerated with heat addition producing the original solvent and a CO_2 stream. The form of this separation displays a relatively high selectivity and can produce a relatively pure CO_2 stream. These features make chemical absorption well suited for CO_2 capture for industrial flue gas treatment (Dindore et al. 2004a). The acidic nature of dissolved CO_2 in water dictates the types of physical and chemical solvents that would potentially be successful for efficient CO_2 absorption. Applicable chemical solvents include amine solvents and solutions, which result in CO_2 absorption by zwitterion formation and easy deprotonation by a weak base (Boucif et al. 2012). There are many possible solvents and solvent mixtures under investigation for CO_2 absorption, including amines, sterically hindered amines, carbonate solvents, as well as ionic liquids (Vaidya and Kenig 2007).

However, the disadvantage of this technology is the high energy penalty associated with solvent regeneration in the stripping column. Around 80–90% (depending on the process conditions and the solvent) of the total process energy is needed for the solvent regeneration in the desorber, making this the most important chapter in the operational costs (Svendsen et al. 2011; Notz et al. 2011).

Energy is needed to heat up the solution in the desorber to generate stripping steam and reverse the CO_2 reactions (Notz et al. 2011). To optimize the process costs, an obvious approach would be to select a solvent with higher reaction kinetics and lower heat of desorption. Unfortunately, the heat of desorption and the kinetics are interrelated (Svendsen et al. 2011). Solvents with substantially less energy needs (tertiary amine or carbonate salt solutions) require absorber tower heights of several hundred meters for the same separation task. On the other hand, solvents with high reaction rates (primary or secondary amines) need more energy in the desorber reversing the reactions (Penders-van Elk et al. 2013).

1.2.3 Membrane Gas Permeation

In the membrane-based CO_2 capture, gases dissolve and diffuse into polymeric thin film materials (membranes) which provide a selectivity to separate mixtures with respect to relative rates at which constituent species permeate (Powell and Qiao 2006) (Fig. 1.2). The permeation rates would differ based on the relative sizes of the molecules or diffusion coefficients in the membrane material. The driving force for the permeation is the difference in partial pressure of the components at either side of the membrane, and the acid gas is recovered at low pressure (Baker 2004; Boucif et al. 1986). The terms permeability and selectivity are used to describe the performance of a gas separation membrane.

The gas permeation rate is controlled by the solubility coefficient and diffusion coefficient of the gas membrane system. Polysulfone, polyimide, or polydimethylsiloxane are the most common membrane materials used in carbon capture in various geometries such as plane, spiral-wound, or hollow fibers (Henis and Tripodi 1980). In the mid-1980, Monsanto (*Prism*), Cynara (*Natco*), Separex (*UOP*), and Grace Membrane Systems started selling membranes made from cellulose acetate to remove CO_2 from CH_4 in natural gas (Ho and Sirkar 1992). For post-combustion carbon capture, block copolymers (such as polyetherblockamides, PEBA) have shown excellent trade-off performances for the CO_2/N_2 gas pair, with a CO_2/N_2 selectivity around 50 and permeability up to 2000 GPU.

Membrane separations are particularly appealing for carbon capture due to their lower energy consumption, good selectivity, easily engineered modules, and consequently lower costs. The main disadvantage of membrane separation is that multiple steps are required to reach high purity. A maximum of three stages is usually reported for industrial applications, due to the increasing cost of compressors for multistage systems. For instance, multistage separation is employed to capture a

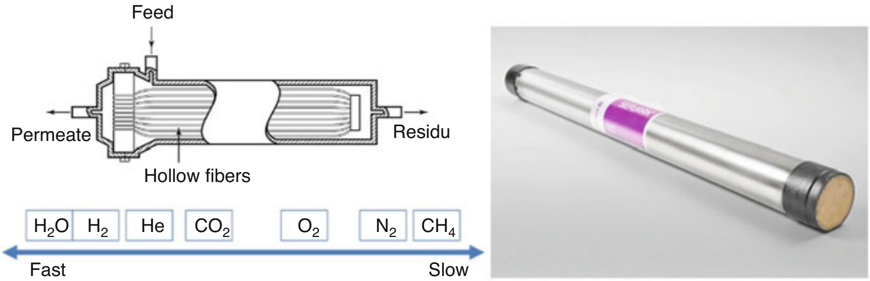

Fig. 1.2 CO_2 capture by membrane gas permeation

higher proportion of CO_2 incurring extra capital and operating cost (Chakravati et al. 2001). However, if the gas is available at a high pressure, physical solvents might be a better choice than chemical solvents. Membrane gas separation technique is generally considered as suitable for high CO_2 concentration applications (well above 20 vol. %) such as flue gas streams from oxy-fuel (Favre 2007).

Furthermore, membranes have been extensively used in many industrial separation processes in recent years. The polymeric membranes usually dominate in most industrial applications. The inorganic membranes are progressing faster in the development of new application fields such as membrane reactors and fuel cells. These membrane separation processes are overwhelming the classical processes (Xu et al. 2001).

Based on their structure, the inorganic membranes can be classified into two categories: porous and dense. In the first category, a porous thin top layer is casted on a porous ceramic or metallic support which provides mechanical strength but reduces mass transfer resistance. Alumina, carbon, glass, zeolite, and zirconia membranes are mainly used as porous inorganic membranes supported on different substrates, such as α-alumina, γ-alumina, zirconia, zeolite, or porous stainless steel. This modification changes the mean pore size and promotes an eventual specific interaction between the membrane surface and the permeating molecules enhancing the separation and improving the performance. Gas separation by means of porous inorganic membranes is achieved by four main transport mechanisms, i.e., Knudsen diffusion, surface diffusion, capillary condensation, and molecular sieving (Luebke et al. 2006).

The second category consists of a metallic thin layer such as palladium and its alloys or solid electrolytes such as zirconia. These dense membranes are highly selective for hydrogen or oxygen permeation in which gas transport occurs though a solution–diffusion mechanism. However, the low permeability across the dense inorganic membranes limits their wide applications as compared to porous inorganic membranes (Powell and Qiao 2006).

1.2.4 Membrane Gas–Liquid Absorption

The membrane gas–liquid CO_2 absorption technology act as contacting devices between the gas stream and the liquid solvent where the membrane, as a barrier, may or may not provide additional selectivity. In the gas–liquid membrane contactor concept, flue gas is passed through the lumen of a bundle of membrane fibers, while an absorbent solution is flowed through the shell side of the contactor (Fig. 1.3). CO_2 diffuses through the membrane and is absorbed in the absorbent solution, while the impurities are blocked from contact to amine, thus decreasing the loss of amine as a result of stable salt formation. It is also possible to achieve a higher loading

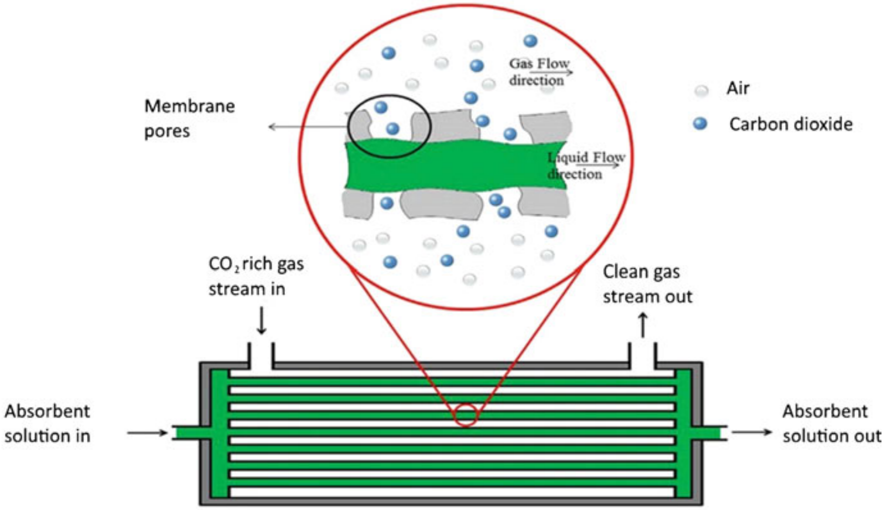

Fig. 1.3 Membrane gas–liquid CO_2 absorption contactor

differential between rich amine and lean amine. After leaving the membrane bundle, the amine is regenerated before being recycled (Darde et al. 2010).

Several absorbents such as pure water, aqueous alkaline solutions, amines, and amino acids have been theoretically and experimentally studied for CO_2 absorption in gas–liquid contacting processes. An ideal absorbent for CO_2 absorption should have the following properties (Dindore et al. 2004b):

- Higher surface tension to prevent membrane wetting leading to a high breakthrough pressure, thereby reducing the membrane susceptibility to membrane wetting
- Chemical compatibility with the membrane (to not damage the membrane)
- Low viscosity to avoid high mass transfer resistance and pressure drop

Unfortunately, the absorbent satisfying all those criteria has not been found yet.

This chemical scrubbing process uses as liquid solvent various aqueous solutions of different alkylamines to remove CO_2. The most popular alkanolamines used in industry are monoethanolamine (MEA), diethanolamine (DEA), and methyldiethanolamine (MDEA) and some sterrically hindered amines such as 2-amino-2-méthylpropanol (AMP) or a blend of some of them. In addition, ammonia has been identified as a possible alternative to the MEA solvent as it is relatively cheap and commercially available (Davison 2007; Darde et al. 2010).

This process offers some advantages over the conventional contacting devices such as packed towers for their high compactness and their low susceptibility to flooding, entrainment, channeling, or foaming. This process requires, however, that the pressures on the liquid and gas chambers are equal to allow and promote CO_2 transport across the membrane, and consequently, their separation efficiency depends on the CO_2 partial pressure. However, although the amines react with CO_2 rapidly, selectively, and reversibly, and are relatively nonvolatile and inexpensive, they are corrosive and require more expensive construction materials.

1.2.5 Adsorption

The adsorption carbon capture technology involves the contacting of a CO_2-containing phase with a solid adsorbent to which CO_2 (and potentially other components of the gas phase) is adhered, either via physical adsorption (physisorption) or chemical adsorption (chemisorption). The physisorption technique involves sorption through weak molecular interactions, namely, van der Waals forces. On the other hand, the chemisorption technique involves chemical bond formation between the adsorbate (molecule being adsorbed) and adsorbent (solid to which the molecules adsorb), causing it to be energetically favorable to bond to the surface of the adsorbate (Seader and Henley 2006).

The adsorption processes involve the use of "swings" in which the system cycles between states of high amount adsorbed (adsorption) and low amount adsorbed (desorption) to selectively separate components in a fluid stream (typically gas), where certain components of the stream preferentially adsorb over others. The adsorption processes can be categorized as pressure swing adsorption (PSA), vacuum swing adsorption (VSA), temperature swing adsorption (TSA), and electrical swing (ESA) (Seader and Henley 2006).

The adsorbing materials generally used are different types of activated carbon, alumina, molecular sieves, metallic oxides, or zeolites, depending on the gas molecular characteristics and affinity of the adsorbing material (Zhao et al. 2007). These adsorbing materials can preferably adsorb CO_2 from flue gas. The higher the pressure, the more gas is adsorbed and the gas is freed and desorbed while reducing the pressure.

When the adsorbed bed is close to saturation, the regeneration reaction takes place by reducing pressure, thereby freeing the adsorbed gases. It is then ready to cycle again. The advantages of PSA are the direct gas delivery at high pressure (no need of compression), and their disadvantages are high investment and operation costs with extensive process control. The process of VSA is a special case of PSA where the pressure is reduced to near-vacuum condition.

In the case of TSA, adsorbent regeneration is achieved by an increase in temperature as increasing temperature at constant partial pressure decreases the amount adsorbed in the gas phase (or concentration in the liquid phase) (Mason et al. 2011). A very important characteristic of TSA is that it is used exclusively for treating low adsorbate concentration feeds. TSA disadvantages are low energy efficiency and thermal ageing of the adsorbent. In ESA swing, a voltage is applied to heat the adsorbent and release the adsorbed gas. This technique is not very common in industrial practice (Emamipour et al. 2007).

1.2.6 *Cryogenic Carbon Capture*

The cryogenic CO_2 capture (referred to as CCC) is a physical process that operates at sufficiently low temperatures and moderately high pressures to separate CO_2 and other components according to their different boiling temperatures. This technique produces direct liquefied CO_2 or CO_2 vapor at high pressure saving the additional cost of compression for storage. This method is suitable only for concentrated CO_2 stream. For dilute stream, this technique is not economically sound and energetically viable (Maqsood et al. 2014a, b).

The technique of this process is based on the principle that different gases liquefy under different temperature and pressure conditions. It is a distillation process operated under very low temperatures (close to $-170\ ^{\circ}C$) and high pressure (around 80 bars). The process consists of cooling and compressing the flue gas in order to liquefy CO_2, which is then easily separated from the flue gas. It allows direct production of liquid CO_2 at a low pressure, so that the liquid CO_2 can be stored or sequestered via liquid pumping instead of compression of gaseous CO_2 to a very high pressure, thereby saving on compression energy (Pierce et al. 1995).

This physical process is suitable for treating flue gas streams with high CO_2 concentrations considering the costs of refrigeration. This is typically used for CO_2 capture for oxy-fuel process where CO_2 can potentially be recovered at 99% purity. However, this type of process requires the use of a large amount of equipments and instruments such as turbines, compressors, distillation columns, and heat exchangers (Fig. 1.4).

For this, the investment capital and operating costs are extremely high (Wellinger and Lindberg 2000). Cryogenic fractionation has the advantage that the CO_2 can be obtained at relatively high pressure as opposed to the other methods of recovering

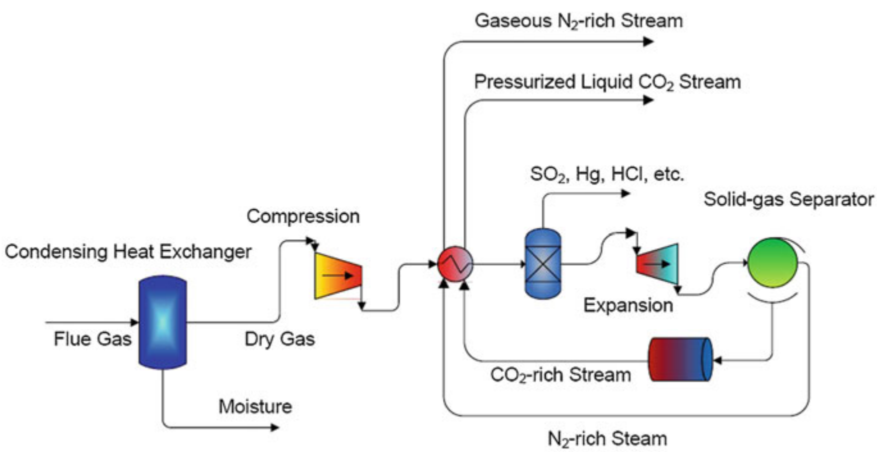

Fig. 1.4 Simple schematic diagram of the cryogenic carbon capture (CCC) process

CO_2. This advantage may, however, be offset by the large refrigeration requirement (Hart and Gnanendran 2009).

1.2.7 Metal–Organic Frameworks

The metal–organic frameworks (MOF) are hybrid organic/inorganic structures containing metal ions geometrically coordinated and bridged with organic ligands which hold great potential as adsorbents or membrane materials in gas separation. This arrangement increases surface area for adsorption, enabling them to be used as sorbents or as nanoporous membranes (Furukawa et al. 2015).

The metal–organic framework materials are nanoporous crystals that combine metal–organic complexes with organic linkers to create highly porous frameworks to offer various important advantages for membrane separations such as high surface area, better porosity, low density, and both thermal and mechanical stabilities (Furukawa et al. 2013).

A major breakthrough in the chemistry of CO_2 capture came with the development of reticular chemistry (Fig. 1.5) (Li et al. 2011). The motivation on developing MOFs for CO_2 capture has focused on reversible adsorption, a process that significantly lowers the need for energy input during regeneration and overcomes a key

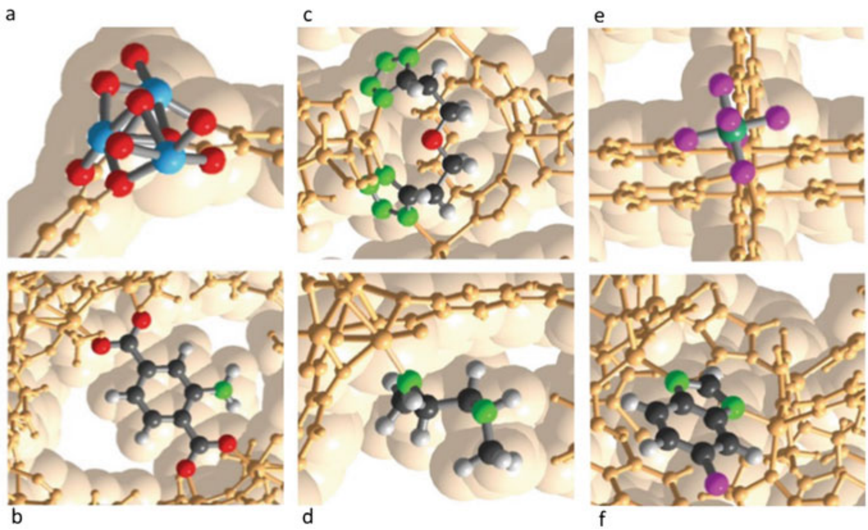

Fig. 1.5 Some structural design features of effective metal–organic framework (MOF) adsorbents for selective CO_2 capture. (**a**) Coordinatively unsaturated metal sites; (**b**) covalently linked polar functionalities; (**c**) heteroatomic amines; (**d**) alkylamines, either primary, secondary, or tertiary; (**e**) specific nonmetallic interactions within the backbone (or pores) of a MOF structure; (**f**) hydrophobicity and/or pore metrics for selectively capturing CO_2 in the presence of water (Trickett et al. 2017)

challenge of using traditional sorbents such as alkanolamine solutions. Consequently, the MOFs structures have since been systematically developed, fine-tuned, and studied in detail. The MOF features are (1) the presence of accessible unsaturated metal sites in the pores; (2) the integration of heteroatoms within, as well as covalently linked functionality to, the backbone; (3) the specific interactions of MOF building units; (4) the hydrophobicity of the pores; and (5) a hybrid of these structural features (Trickett et al. 2017).

The MOFs possess enormous potential due to the numerous possible structures that can be developed using various combinations of metal ions and organic ligands which can be tailor-made to suit a particular application such as CO_2 capture. MOFs containing zinc and magnesium ions provide higher CO_2 adsorption and are hence being thoroughly investigated (Trickett et al. 2017). The other advantage is the lower energy regeneration required compared to conventional sorbents and solvents. The study of metal–organic frameworks is still in its infancy, with investigations being made primarily on a laboratory scale.

1.3 Enzymatic Carbon Capture Overview

This chapter gives a definition of an enzyme and provides a general overview of the principles of enzyme reactions and describes in detail the mechanism for carbonic anhydrase. It also gives an up-to-date literature review on comparable mass transfer experiments for enzyme-enhanced CO_2 capture in lab and in pilot scale.

1.3.1 Historical Background

The existence of enzymes has been known for well over two centuries. In early nineteenth century, Persoz with Payen isolated in a malt extract a substance that catalyzes the transformation of starch into glucose (Payen and Persoz 1833). The scientists called this substance *diastase*, from the Greek *to separate*, due to its ability to separate the constitutive blocks of starch into individual units of glucose. This enzyme is also called g-amylase. This is the first time an enzyme is isolated, a compound that has the properties of an organic catalyst. The suffix *ase* of diastase has been since then used to name enzymes. However, the first enzyme in pure form was obtained in 1926 by James Sumner who isolated and crystallized the enzyme *urease* from the jack bean. Thereafter, Northrop and Stanley discovered a complex procedure to isolate pepsin by a precipitation technique and crystallized several enzymes (Roberts et al. 1997).

These enzymes are bulky proteins made of amino acid polymers linked by peptide bonds. They catalyze biochemical reactions occurring in living organisms. Like any other catalyst, they do not modify the thermodynamic equilibria, but allow them to be reached more rapidly. The catalytic properties of enzymes are related to the existence in their structure of an active site, which can be schematically described as having the shape of a cavity adapted specifically to the substrates to be transformed, to which they are fixed by weak chemical bonds, but able to eliminate the random aspect of the contacts prevailing during collisions in homogeneous medium. This active site is in fact subdivided into two parts:

- The binding site (fixation or recognition) consisting of amino acids, characterized by a complementarity of shape of the cavity with a specific substrate to be transformed
- The catalytic site which realizes the transformation of the substrate into a product

1.3.2 Enzymes Classification

The International Enzyme Commission, created at the Third International Biochemistry Congress held in 1955 in Brussels, in agreement with the International Union of Pure and Applied Chemistry (IUPAC), decided to divide the enzymes into six classes according to the chemical reaction they catalyzed, a classification kept up to date by the Nomenclatures Committee of the International Union of Biochemistry and Molecular Biology (Webb 1992). Hence, there are six classes called "EC n," for "Enzyme Commission number," where n stands for a number from 1 to 6 designating:

- EC 1: Oxidoreductases that catalyze oxidation–reduction reactions in which oxygen or hydrogen is gained or lost.
- EC 2: Transferases that transfer a functional group of the amino, acetyl, or phosphate type from one molecule to another.
- EC 3: Hydrolases which catalyze the hydrolysis (decomposition by water) of various bonds.
- EC 4: Lyases that catalyze the formation of a C–C, C–O, C–S, or P–O bond by processes other than hydrolysis or oxidation.
- EC 5: Isomerases that catalyze isomerization in a single molecule or allow intramolecular rearrangements.
- EC 6: Ligases that catalyze C–C, C–S, C–O, and C–N bonds in condensation reactions coupled with the use of adenosine triphosphate (= ATP).

Enzymes can be denatured and precipitated with salts, solvents, and other reagents. They have molecular weights ranging from 10,000 to 2,000,000.

1.3.3 Enzyme Catalytic Properties

Many catalysts such as arsenite, formaldehyde, hypochlorite, and sulfide have been used to catalyze the CO_2 absorption into various aqueous solutions (Sharma and

Danckwerts 1963; Pohorecki 1968; Augugliaro and Rizzuti 1987). These catalysts can accelerate the CO_2–H_2O hydration reaction by 2–4 orders of magnitude. However, the most effective CO_2 hydration catalyst known to date is the CA family of enzymes. It has been reported that the turnover number of the CA enzyme could reach more than one million per second (Davy 2009).

Enzymes are biological catalysts that reduce the activation energy of chemical and biochemical reactions. Their function is dependent on the amino acid sequence and their three-dimensional structure forming an active site with a catalytic activity into which a certain reactant (substrate S) can bind (Grunwald 2011).

There are interactions between the enzyme (E) and its substrate (S), and usually, van der Waals forces and hydrogen bonding take place to form an enzyme–substrate (ES) complex. The enzyme being a much larger molecule, the substrate fits into an active site of the enzyme molecule. Figure 1.6 shows the simplest lock-and-key interaction model where the enzyme represents the lock and the substrate the key (Whitford 2005).

In enzyme catalytic process, the enzyme and its substrate build reversible enzyme–substrate (ES) complex first, and then a chemical reaction occurs with a rate constant *k*cat called turnover number. The *k*cat expresses the maximum number of substrate molecules converted into product molecules per active site of enzyme per unit time (Whitford 2005). The reaction rate is expressed by the Michaelis–Menten expression as:

$$\mathcal{R} = \frac{k_{\text{cat}}[\text{E}][\text{S}]}{K_{\text{M}} + [\text{S}]} \tag{1.1}$$

A typical enzymatic reaction curve is shown in Fig. 1.7. The reaction curve can be represented by a Michaelis–Menten equation, Eq. (2.10).

The effect of higher product concentration on the enzyme reaction rate is often regarded as product inhibition, but it is basically a reversible reaction between

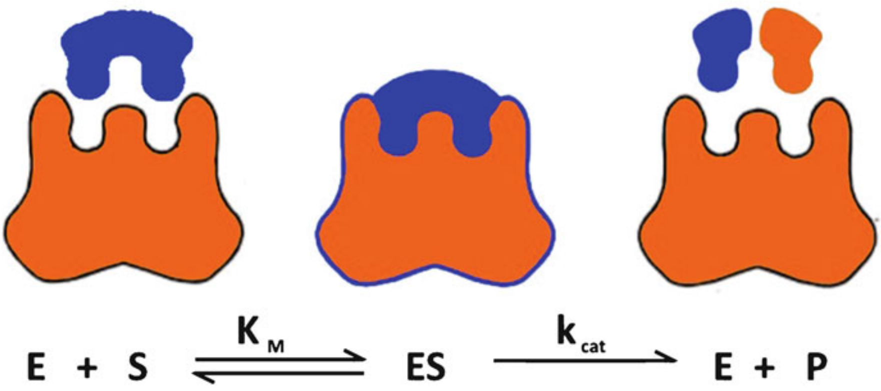

Fig. 1.6 Schematic reversible enzyme reaction key–lock mechanism

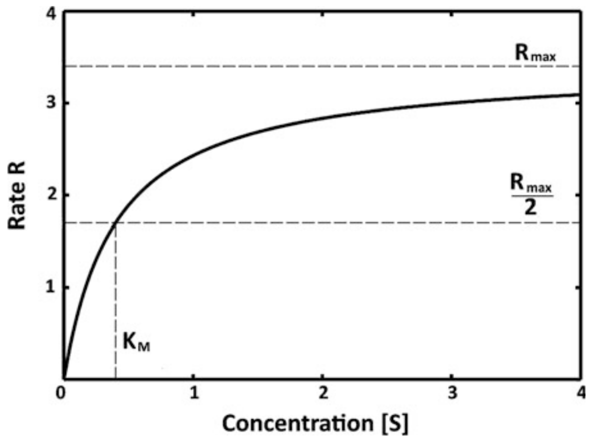

Fig. 1.7 Michaelis–Menten enzymatic reaction curve

substrate S and product P where both steps are considered reversible and following the Michaelis–Menten kinetics. The decrease in reaction rate with higher product concentration can be explained as the substrate and product are competing for binding onto the enzymes active site and the enzyme becomes more occupied by the product when its concentration increases and therefore less substrate can bind.

1.3.4 Enzyme Immobilization

The enzymes provide high potentialities in a wide range of applications due to their high selectivity, specificity, and activity under mild conditions. These industrial biocatalysts offer tremendous advantages with regard to their short processing time, low energy need, cost-effectiveness, and nontoxicity. Singh and coworkers (Singh et al. 2016) reviewed in detail the current industrial enzyme application, in food, organic synthesis, pharmaceutical and diagnostics, textile, as well as waste treatments.

Nevertheless, the use of enzymes in the industrial applications could be limited by their high cost, their isolation and purification, the instability of their structures once they are isolated from their natural environment, and their sensitivity both to process conditions, resulting in a short processing lifetime. The retention of enzymes by immobilization may be a valid method to overcome these shortcomings (Krajewska 2004; Rodrigues et al. 2013; Dos Santos et al. 2015).

Various immobilization techniques (Fig. 1.8) are available providing a wide flexibility for the solid biocatalyst preparation with regard to the enzyme applications and reactor configurations. These techniques are divided, in general, in three main categories based on the nature of the interaction between the enzyme and other reagents/phases involved in the process (Moehlenbrock and Minteers 2011; Sirisha et al. 2016).

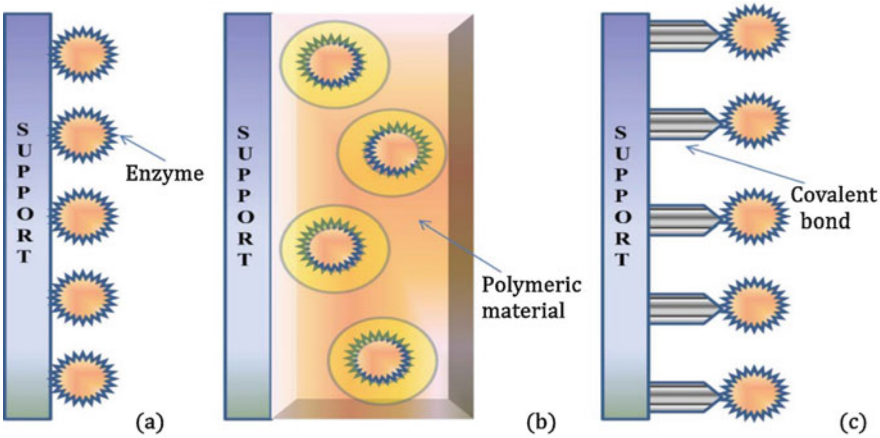

Fig. 1.8 The most common enzyme immobilization techniques: (**a**) physical adsorption, (**b**) entrapment, and (**c**) covalent attachment and cross-linking. (Spahn and Minteer 2008)

1.3.5 Physical Adsorption

This technique is characterized by the physical interactions between proteins and the surface of solid carriers by means of van der Waals forces, hydrogen bridge bonds, and electrostatic interactions (Moehlenbrock and Minteers 2011). The physical adsorption enzyme immobilization is quite simple and may have a higher commercial potential, a lower cost, and a higher retaining enzyme activity as well as a relatively chemical-free enzyme binding (Huang and Cheng 2008).

However, in general, the physical bonding is too weak to keep the enzyme fixed to the carrier and subject to enzyme leaching (Kumakura and Kaetsu 2003), resulting in a considerable contamination of the substrate.

1.3.6 Enzyme Entrapment

The enzyme entrapment is an irreversible enzyme immobilization technique where enzymes are entrapped in a support or inside fibers, either in polymer membranes or in the lattice structures of a material that filtrate the substrate and products from the enzyme (Chiang et al. 2004). The entrapment consists of a physical restriction of the enzyme within a confined network space. Mechanical stability, enzyme leaching, and chemical interaction with polymer are typically improved by the enzyme entrapment immobilization technique (Won et al. 2005). This method modifies the encapsulating material providing therefore an optimal microenvironment for the enzyme, i.e., matching the enzyme physicochemical environment with the immobilizing material. The ideal microenvironment could be optimal pH, polarity, or amphilicity which may be achieved with a variety of materials including polymers, sol–gels, polymer/sol–gel composites, and other inorganic materials (Mohamad et al. 2015).

1.3.7 Covalent Bonding and Cross-Linking

The covalent bonding enzyme immobilization technique is one of the most prominent methods. The formation of covalent bonding is required, for more stable attachment, and these are generally formed through reaction with functional groups present in the protein surface (Guisan 2006). The functional groups' contribution to the enzyme binding involves side chains of lysine (e-amino group), cysteine (thiol group), and aspartic and glutamic acids (carboxylic group) (Guisan 2006). The activity of the covalent bonded enzyme depends on the coupling method, the carrier material composition, as well as its size and shape and specific conditions during coupling (Mohamad et al. 2015).

The cross-linking enzyme immobilization technique, also called carrier-free immobilization, is another irreversible method which does not require a support to prevent enzyme loss into the substrate solution (Mohamad et al. 2015). In this method, the enzyme acts as its own carrier, and virtually pure enzyme is obtained eliminating, therefore, the drawbacks associated with carriers (Sheldon 2011). The use of carrier leads ineluctably to an activity depletion due to the introduction of a large portion of non-catalytic aggregates, the percentage of which may reach and even exceed 90%, resulting in low space–time efficiencies with a considerable cost (Sheldon 2011). The production of cross-linked enzyme aggregates (CLEA) consists of the formation of enzyme aggregates made of insoluble supramolecular structures and the cross-linking with a bifunctional agent to stabilize the aggregates in the aqueous medium (Barbosa et al. 2014).

1.3.8 Enzyme Immobilization Overview

The quality of the solid biocatalyst depends on the selection of the immobilization technique. In many cases, immobilizing enzymes may cause alter their activity. It provides, however, a great stability improvement under the various process conditions (Rodrigues et al. 2013). Criteria for selecting solid supports include the mechanical properties. The ideal supports for biocatalyst utilization in (a) internal mechanical stirring reactors are flexible polymers such as agarose, cellulose, etc., and (b) fixed bed reactors are rigid structures such as inorganic supports like porous glass, silicates, etc. Besides, the immobilized enzyme entrapment in polymeric matrices may offer a good mechanical resistance (Bentagor et al. 2005).

Several techniques and materials have been used for the CA immobilization, and only the relevant ones are summarized in this review with their relative success in terms of activity, stability, and reusability.

Oviya and Yadav and coworkers obtained good results using chitosan-based nanoparticles or hydrogels (Yadav et al. 2011; Oviya et al. 2012). Both chitosan and alginate are biocompatible and were used in many enzymatic applications (Machida-Sano et al. 2012; Zhai et al. 2013). Sharma and collaborators have purified and immobilized live *P. fragi* cells to chitosan and were able to observe $CaCO_3$ precipitation, a measure of catalyzed conversion of CO_2 to bicarbonate (Sharma et al. 2011).

Vinoba and coworkers (Vinoba et al. 2013) immobilized bovine carbonic anhydrase (BCA) covalently onto functionalized Fe_3O_4/SiO_2 nanoparticles by using glutaraldehyde as a spacer. They observed that, after 30 cycles, the Fe–CA displayed strong activity, and the CO_2 capture efficiency was 26-fold higher than that of the free enzyme. They have shown that the magnetic nanobiocatalyst is an excellent reusable catalyst for the sequestration of CO_2. Vinoba and his group synthesized a biocatalyst by immobilizing human carbonic anhydrase onto gold nanoparticles assembled over amine/thiol-functionalized mesoporous SBA-15. They demonstrate that these nanobiocatalysts are highly efficient potential for industrial-scale CO_2 sequestration (Vinoba et al. 2011).

A group of researchers studied other methods to attach the enzyme, including covalent attachment, enzyme adsorption, and cross-linked enzyme aggregation. In general, the enzyme activity was similar to that of the free enzyme, but displayed additional desirable features such as stability, reusability, and storage endurance (Vinoba et al. 2012). Wanjari et al. used mesoporous aluminosilicate as a support for CA immobilization due to its large surface area and pore size. Interestingly, the K_M for the immobilized enzyme was higher compared to the free form, indicating decreased affinity of the enzyme for the substrate due to suboptimal substrate/product exchange (Wanjari et al. 2012).

The enzymes trapping in porous materials are also possible. The original irreversible enzyme entrapment protocol in polyurethane foam was introduced in the 1980s by Wood and his group (Wood et al. 1982). Bovine carbonic anhydrase was immobilized by covalent attachment within a polyurethane (PU) foam matrix (Ozdemir 2009). This process is relatively fast, and a high percentage of active enzymes are covalently obtained in the final PU. In contrast to other materials, after seven cycles, there was no detectable enzyme leaching or a reduction in CA activity. And, after 45 days of storage of the CA-PU foam at room temperatures, it was still 100% active, while the free enzyme was completely inactive after the same period at 4 °C (Ozdemir 2009).

Many groups have attempted to immobilize CA between thin liquid membranes for CO_2 extraction from flue gas. The process comprises a thin liquid containing CA layer sandwiched between two membranes made of some polypropylene derivative strengthened to prevent curving of the pliable membrane. Kimmel and his group studied the covalent immobilization of carbonic anhydrase on the surface of polypropylene hollow fiber membranes using glutaraldehyde-activated chitosan tethering to amplify the density of reactive amine functional groups (Kimmel et al. 2013). Hou and his group developed a novel "Janus" (hydrophilic–superhydrophobic) biocatalytic gas–liquid membrane contactor for CO_2 capture. The carbonic anhydrase (CA) was immobilized on the hydrophilic carbon nanotube (CNT) side, while the superhydrophobic porous side was located in the gas phase, resulting in a permanent hydration of the immobilized CA and a reduction of the CO_2 diffusion in the solvent. The authors confirmed that catalytic efficiency with immobilized CA has significantly improved compared with the equal amount of free CA, and effective enzyme coating regeneration lasted over five cycles.

1.4 Kinetics and Catalytic Mechanisms of Enzymatic Carbon Dioxide Capture

In 1933, the carbonic anhydrase was independently discovered by Meldrum and Roughton (Meldrum and Roughton 1933). CA was first characterized while searching a catalytic factor necessary for fast transportation of HCO_3^- from the erythrocyte to pulmonary capillary. Meldrum and Roughton purified the erythrocyte carbonic anhydrase, and Keilin and Martin (Keilin and Mann 1939) presented the role for Zn in catalysis by finding the fact that activity was directly proportional to the Zn content; hence, carbonic anhydrase was the first Zn metalloenzyme identified. CA regulates important biological processes within humans and other living organisms such as the acid–base balance within the blood, the photosynthesis mechanism in plants, and the carbon concentration mechanism in microorganisms (Bhattacharya et al. 2004).

1.4.1 Classes of Carbonic Anhydrase Enzymes

The carbonic anhydrase, an ancient enzyme widespread among the entire prokaryotic and eukaryotic domain, has been known to catalyze the reversible hydration of carbon dioxide as follows:

$$\left[CO_2 + H_2O \rightleftharpoons HCO_3^- + H^+\right] \tag{1.2}$$

The CA can be produced via fermentation, and it may be disposed of with minimum detrimental impact on the environment. CAs are typically classified into five different classes defined by the Enzyme Commission as EC 4.2.1.1, namely, αCAs (predominant within animals), βCAs (predominant within plants), γCAs (predominant within Archaea) (Aggarwal et al. 2013; Rowlett 2010), as well as δCA and ζCA found in diatoms and in other marine phytoplankton (Boone et al. 2013). CA's are expressed in numerous plant tissues and in different cellular

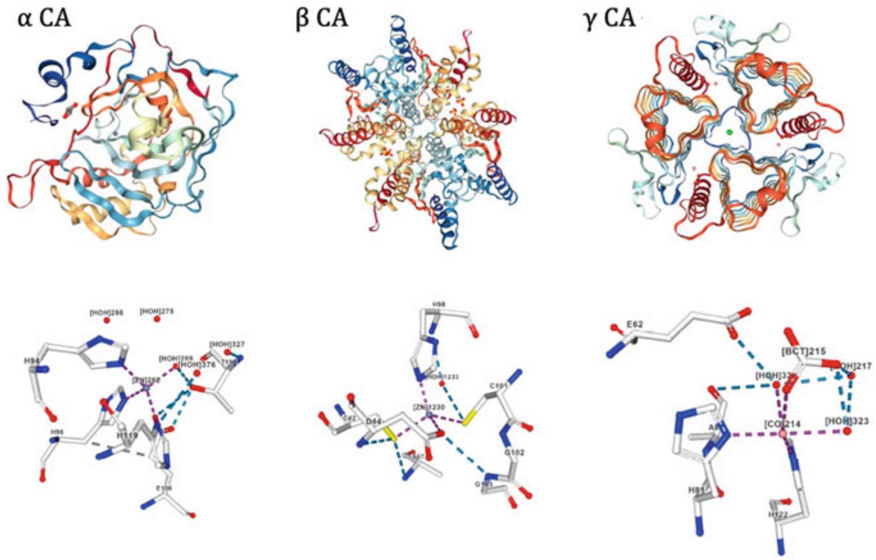

Fig. 1.9 Representative structures of α, β, and γ carbonic anhydrase (CA) enzymes with their respective metal active sites. (Aspatwar et al. 2018)

locations, the most prevalent of which are those in the chloroplast, cytosol, and mitochondria. This diversity in location is paralleled in the many physiological and biochemical roles that CAs play in plants (DiMario et al. 2017).

The most commonly investigated class of CA is the *α* form which is generally found in mammals. Figure 1.9 illustrates the structure of *α*, *β*, and *γ*CA. In *α*CA, the enzymatic activity is derived from a Zn_2^+ ion that is coordinated to three histidine residues near the center of the molecule in a cone-shaped cavity.

The catalytically active alpha carbonic anhydrases are similar in structure with their conserved motifs of the active site cavity. To date, the crystallographic structure of human CA-I, CA-II, CA-III, CA-IV, CA-VI, CA-VII, CA-VIII, CA-IX, CA-XII, CA-XIII, and CA-XIV has been determined and is available in the protein data bank (www.PDB.org). All the *α*CA have similar tertiary structure and centrally bind a divalent metal ion, most often a zinc (Zn_2^+), held as a prosthetic group (Aspatwar et al. 2018).

1.4.2 Carbonic Anhydrase Mechanism

The metal ion Zn atom in all *α*CAs is essential to catalysis. The structure-based mechanism of human carbonic anhydrase *h*CAII has been exemplified and detailed (Berg et al. 2010).

The catalytic mechanism of hCA II consists of five distinct steps as reported by many authors (Supuran 2016; Gladis et al. 2017) and detailed in Fig. 1.10.

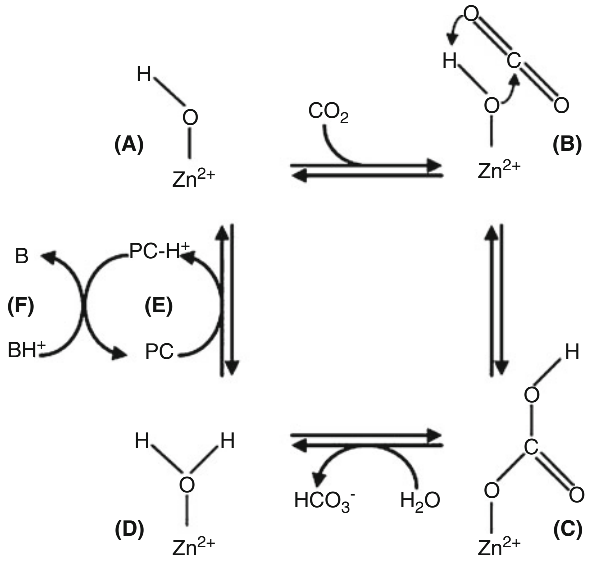

Fig. 1.10 The overall catalytic mechanism of carbonic anhydrases (Gladis et al. 2017). PC stands for proton channel

The first step in this mechanism is the binding of a CO_2 molecule to the enzyme. The water molecule linked to the amino acid is replaced by a CO_2 molecule which is linked to the enzyme by a hydrogen bond. The formation of a bicarbonate molecule forms in the second step occurring by a nucleophilic attack of the hydroxyl ion bound to the zinc ion on the CO_2 molecule. The bicarbonate molecule is linked through three bonds, two hydrogen bonds and one ionic bond. In the third step, the bicarbonate molecule is released with the partial regeneration of the active site leaving space for a water molecule. In the fourth step, depicted as isomerization or intramolecular proton transfer step, where the proton is first transferred to an amino acid side chain called a proton channel (PC), the enzyme is activated with binding a hydroxyl ion to the zinc ion.

But after the product is released, a water molecule is bound to the zinc ion with a proton expulsion as a result. The fifth and final stage of the mechanism is the intermolecular transfer where a molecule of unprotonated cationic buffer recovers the proton bound to the residue. The cycle is then completed, a bicarbonate molecule is produced, a buffer molecule is protonated, and the enzyme regenerated to its active state. It has been demonstrated that the enzyme recycling is the rate-reaction controlling step in this cycle.

The simplest process may be schematically represented by the following reactions:

Table 1.1 CA isozymes kinetic constants with CO_2

Carbonic anhydrase	Substrate	Kinetic constants		References
		K_M [mM]	k_{cat}/K_M $\left[(Ms)^{-1}\right]$	
Carbonic anhydrase	CO_2	12.0	8.3 10^7	Whitford (2005)
Human CA I	CO_2	4.0	5.0 10^7	Supuran (2008)
Human CA II	CO_2	9.3	1.5 10^8	
Human CA III	CO_2	52	2.5 10^5	
Human CA III	CO_2	–	3.0 10^5	Duda et al. (2005)
Bovine CA	CO_2	0.65	36.31	Mirjafari et al. (2007)

$$\mathrm{CA} + \mathrm{CO_2} + \mathrm{H_2O} \underset{k_{-1}}{\overset{k_1}{\rightleftharpoons}} \mathrm{CA}\cdot\mathrm{CO_2} \underset{k_{-2}}{\overset{k_{\mathrm{cat}}}{\rightleftharpoons}} \mathrm{CA} + \mathrm{HCO_3^-} + \mathrm{H^+} \tag{1.3}$$

As a potential model, the linear approximation of the Michaelis-Menten kinetics equation (Eq. 1.4) is a satisfactory tool:

$$\mathcal{R}_{\mathrm{CA}} = \frac{k_{\mathrm{cat}}}{K_{\mathrm{M}}}[\mathrm{CA}]\left\{[\mathrm{CO_2}] - [\mathrm{CO_2}]_{\mathrm{eq}}\right\} \tag{1.4}$$

where K_{M} refers to the Michaelis constant of the reaction and k_{cat} is defined as the turnover number and ranges between 10^4 and 10^6 molecules of CO_2 per molecule of CA per second depending on the strain of CA that is being used (Tripp et al. 2001; Shekh et al. 2012). The $[CO_2]$ term represents the quantity of CO_2 that is being converted into HCO_3^-, and the $[CO_2]_{eq}$ term represents the concentration of HCO_3^- that is being converted back into CO_2.

Table 1.1 summarizes typical kinetic parameters of the many carbonic anhydrase isozymes with various substrates.

1.4.3 Catalytic Models of the CO_2 Conversion Activity

Nevertheless, further studies demonstrated that the CO_2 hydration kinetics may be substantially modified by the nature of a buffer mixed in the enzymatic solution, whereas the Michaelis-Menten rate equation model implies that this proton exchange is not rate limiting. Therefore, several models were developed to specifically correct this omission.

Steiner and coworkers (Steiner et al. 1975) proposed a model in a classical Michaelis-Menten reversible kinetics with two reagents, i.e., the substrate $[CO_2]$ and the product $\left[HCO_3^-\right]$. As for the enzyme, it comes in two forms: the active form [E] and the form of a transient complex [ES]. Several steps of the reaction mechanism are omitted in this model; only two steps are represented, including the bonding of CO_2 and the release of bicarbonate $\left[HCO_3^-\right]$.

Jonsson and collaborators (Jonsson et al. 1976) improved the model by adding an isomerization step (intramolecular proton transfer) to improve the Michaelis–Menten kinetics proposed. The model still includes only two reagents, but the enzyme comes in three different forms: the active form [E], a transient complex form, [ES] and a form in which a water molecule is bound to the zinc ion [E_w].

Rowlett and Silverman suggested a model (Rowlett and Silverman 1982) where the enzyme is found in three forms: the active form [E], the form of a transient complex, [ES] and the form where the residue is protonated [$_H$E]. This model is divided into three stages, namely, CO_2 binding, bicarbonate release, and intermolecular proton transfer. It is identified by the Ter Bi Ping Pong kinetics where the term Ter means that the model includes three substrates, namely, CO_2, water, and buffer in basic form. The term Bi means that the model includes two products, bicarbonate and buffer, in the form of conjugated acid.

Larachi (2010) presented four models to correct the discrepancies observed in the previous models. The model has three substrates, CO_2, water, and buffer, in basic form, as well as two products, including bicarbonate and buffer, in the form of conjugated acid. In this model, the enzyme is present in three forms: the active form [E], the form where a water molecule is bound to the zinc ion [E_w], and the form where the residue is protonated [$_H$E]. This model does not include a transient complex [#ES]. The steps included in this model are CO_2 binding and product release, intramolecular proton transfer (isomerization), and intermolecular proton transfer. The novelty of this model comes from the fact that it includes inter- and intramolecular transfer. Model (a) is represented by ordered Ter Bi Iso Ping Pong kinetics. Model (b) is represented as a random Quad Quad Iso Ping Pong kinetic. Model (c) is an ordered Ter Bi Iso Ping Pong kinetics. This model is similar to model (a) except that it includes a transient complex. Model (d) is represented by random Quad Quad Iso Ping Pong kinetics. This model is very similar to model (b) except that it includes a transient complex:

$$[\mathrm{E}] + [\mathrm{S}] \underset{k_{-1}}{\overset{k_1}{\rightleftharpoons}} [\mathrm{ES}] \tag{1.5}$$

$$[\mathrm{ES}] + [\mathrm{W}] \underset{k_{-2}}{\overset{k_2}{\rightleftharpoons}} [\mathrm{E_w}] + [\mathrm{P}] \tag{1.6}$$

$$[E_w] \underset{k_{-2}}{\overset{k_2}{\rightleftharpoons}} [{}_HE] \tag{1.7}$$

$$[B] + [{}_HE] \underset{k_{-4}}{\overset{k_4}{\rightleftharpoons}} [BH^+] + [E] \quad \text{and} \quad [P] + [{}_HE] \underset{k_{-5}}{\overset{k_5}{\rightleftharpoons}} [W] + [S] + [W] \tag{1.8}$$

The reaction rate defined by the production of bicarbonate [P] is expressed according to the following differential equation:

$$\frac{d[P]}{dt} = k_1[W]\,[ES] - k_{-2}[P]\,[E_w] + k_{-5}[W]\,[S]\,[E] - k_5[P]\,[{}_HE] \tag{1.9}$$

Using the method of King and Altman (1956), the reaction rate is written in the following form:

$$\frac{d[P]}{[E_0]dt} = \frac{\left([S][B] - \frac{K_{a2}}{K_{a1}}[P][BH^+]\right)\left(\frac{K_{a1}k_3}{K_E k_1}k_4\left(\frac{K_E}{K_{a1}}k_1 + k_5\left(1 + \frac{k_{-1}}{k_2[W]}\right)\right) + k_4k_5[P]\right)}{\begin{array}{l}\frac{k_3}{k_1}\left(\frac{K_E}{K_{a1}}k_1 + k_5\left(1 + \frac{k_{-1}}{k_2[W]}\right)\right)\left(2\frac{K_{a1}}{K_E}[S] + [P]\right) + \frac{k_3}{k_1}k_4\left(1 + \frac{k_{-1}}{k_2[W]}\right)\left([B] + 2\frac{K_{a2}}{K_E}[BH^+]\right) \\ +k_4\left(1 + \frac{k_3}{k_2[W]}\right)[S][B] + \left(2k_5 + \frac{k_3k_1}{k_1k_{-1}}\left(\frac{K_E}{K_{a1}}k_1 + k_5\left(1 + \frac{k_{-1}}{k_2[W]}\right)\right)\right)[S][P] \\ +k_4\left(\frac{K_E}{K_{a1}}[B] + \frac{K_{a2}}{K_{a1}}\left(\frac{k_3}{k_{-1}} + 1\right)[BH^+]\right)[P] + \frac{K_E}{K_{a1}}k_5[P]^2 + \frac{K_E k_1}{K_{a1}k_{-1}}k_5[S][P]^2 + \frac{K_E k_1}{K_{a1}k_{-1}}k_4[S][B][P]\end{array}}$$

These models being very complex and lengthy to develop herein, the interested readers are advised to refer to Larachi's paper (Larachi 2010). Figure 1.11 represents the five sets of data compared to model (d). This model represents fairly well the transition between regimes where the intramolecular transfer is the stage controlling the rate of reaction and a regime where the intermolecular transfer controls the reaction rate (Larachi 2010).

1.4.4 The Carbonic Anhydrase Biomimetic CO_2 Capture

The process design of the biomimetic CO_2 capture depends closely on the selection of the enzyme forms able to handle the severe operational conditions, such as high temperature, high salt concentration, and elevated alkalinity which may affect the enzyme performance. In general, the absorption processes are run at temperatures ranging between 40 and 60 °C, while the desorption temperature is around 100 °C, although it can be lowered when running the unit under vacuum (about 0.3 bar) (Russo et al. 2013). Furthermore, the enzyme performance could be seriously

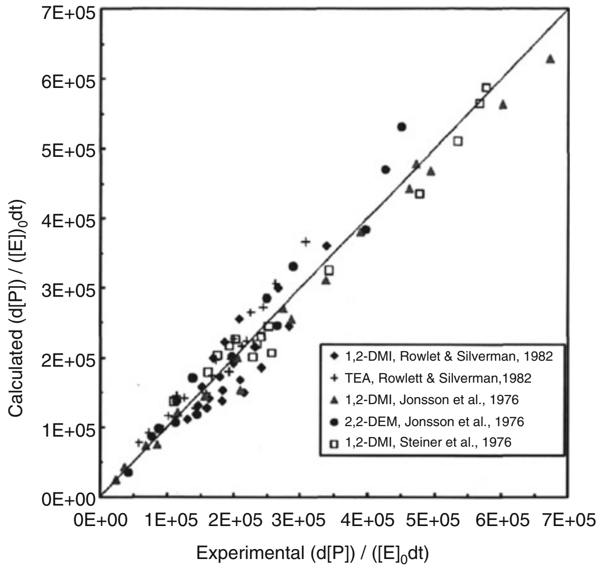

Fig. 1.11 Measured CO_2 hydration rate versus calculated using the Larachi model (d). (Larachi 2010)

damaged by some pollutant present in the flue gases, such as Cl, Hg, NO_x, SO_2, and fly ashes. The enzyme characterizations under typical process conditions are expressed in terms of kinetic assessment and long-term stability. The CO_2 loading capacity is increased by adding solvents, usually inorganic carbonate salts or amines.

Bicarbonate

Bicarbonates are regarded as solvents with the highest potential for use with CA: they do not degrade, are less corrosive, and require low regeneration energy. Besides, CA has high stability in bicarbonate with stable activity for long period of time (Ye and Lu 2014).

Lu and coworkers studied the CO_2 absorption in a stirred cell reactor using a characterized CA form of microbial origin. Tests were run using pure CO_2 as gas phase and 20% wt K_2CO_3 aqueous solutions as liquid phase, at 25, 40, and 50 °C and at CA concentration of 300 mg/l . Results showed that the CA enhanced the CO_2 absorption rate of about 10, 5, and 4 times with respect to tests run without promoter at 25, 40, and 50 °C, respectively.

Zhang and Lu characterized an engineered CA form provided by *Novozymes*. They run CO_2 batch absorption tests into K_2CO_3 20% in lean solvent conditions (20% CTB conversion) and rich conditions (55% CTB conversion) at 50 °C. They evaluated k_{cat}/K_M as 9.0 10^8 $M^{-1}s^{-1}$, without any CTB conversion influence. They further developed a theoretical model to simulate the CA performance in a packed-bed column at the scheduled conditions including the measured kinetic parameters.

Hu and coworkers (Hu et al. 2017) characterized a CA form of microbial origin using of a wetted wall column absorption via the stop flow technique. They used K_2CO_3 30% aqueous solutions as liquid phase at 50 °C and different carbonate to bicarbonate (CTB) conversions (0–20%). The CA Michaelis–Menten catalysis parameter k_{cat}/K_M was determined to be around 5.3 10^8 $M^{-1}s^{-1}$ and showed a slight decrease with the CTB conversion. The decrease may be due to the CA catalysis of the backward reaction of CO_2 hydration that occurs at high bicarbonate concentration and that influences the apparent reaction rate. The CA retained more than 70% of its initial activity after incubation into K_2CO_3 30% at 50 °C for 8 h.

Gladis and coworkers (Gladis et al. 2017) characterized a recombinant CA form provided by *Novozymes* through absorption tests run in a wetted wall column. They compared the activity of four different solvents: the primary amine (MEA), the sterically hindered primary amine (AMP), the tertiary amine (MDEA), and the carbonate salt solution K_2CO_3 with and without enzyme in concentrations ranging from 5 to 50 wt% and temperatures from 298 to 328 K. The results revealed that the addition of carbonic anhydrase (CA) dramatically increases the liquid side mass transfer coefficient for MDEA and K_2CO_3, AMP has a moderate increase, whereas MEA was unchanged. The results confirmed that only the bicarbonate forming systems benefit from CA, showing that the enzyme activity was particularly influenced by the temperature, reaching in all the cases a k_{cat}/K_M of about $5 \cdot 10^3$ m^3/kg. s at low solvent concentrations (5–15 wt%). On the other hand, at 20% wt K_2CO_3, a considerable increase of the rate constant was noticed, passing from 1.2 10^4 m^3/kg. s at 25 °C to 2.1 10^4 m^3/kg. s at 55 °C.

Iliuta and Iliuta (2017) developed an enzyme–CO_2 dynamic 3D model removal performance of countercurrent packed-bed column reactors based on continuity, momentum, and species balance equations in the liquid and gas phases with simultaneous diffusion and chemical reaction at the enzyme washcoat/liquid film scale level. They observed that the packed-bed column reactor performance with immobilized human enzyme hCA II on random packings can be enhanced by reducing the washcoat thickness, increasing the inlet buffer concentration and pKa constant, and increasing the liquid velocity maintaining a low pressure drop level. Also, operating with extra hCA II loadings allows obtaining higher CO_2 conversion and avoids the degradation of the CO_2 hydration rate in long-term operation attributable to the decrease of hCA II enzyme activity.

Solvents

Many other solvents (ammonia, amino acids, primary, secondary, tertiary, and hindered amines) have all been used with CA. For amine solvents, the noncatalyzed rate increases linearly with increasing pKa (Penders-Van Elk et al. 2016a, b).

Penders-van Elk and coworkers studied extensively the carbonic anhydrase kinetics for CO_2 absorption with various solvents using different process conditions (Penders-Van Elk et al. 2012, 2013, 2016a, b). They investigated in their first study (Penders-Van Elk et al. 2012) the kinetics of two types of carbonic anhydrase with MDEA at 298 K in a stirred cell reactor and reported that the CO_2 physical solubility is not affected by enzyme addition. They observed a neat overall reaction rate increase of the solvent with the enzyme concentration increase at a fixed solvent concentration, with a linear relationship at lower enzyme concentration and a flattening out at higher enzyme concentrations. They also examined several new alkanolamines (Penders-van Elk et al. 2015): N,N-diethylethanolamine (DEMEA), N,N-dimethylethanolamine (DMEA), monoethanolamine (MEA), triethanolamine (TEA), and triisopropanolamine (TIPA) at 298 K. In both TEA and DMEA, they observed a decrease in enzymatic activity. A very low MEA concentration was chosen (0.1 mol/l) for measuring the enzymatic reaction. In a most recent study (Penders-Van Elk et al. 2016a, b), they looked at the enzyme kinetics with the temperature dependency in MDEA solutions and derived a simplified kinetic model based on their experimental results in a temperature range from 278 to 313 K. The model, however, underpredicted the results obtained at 298 K and overpredicted the ones at 343 K.

Vinoba and coworkers (Vinoba et al. 2013) used a vapor–liquid equilibrium device to investigate the CO_2 absorption using MEA, DEA, MDEA, and AMP solutions enhanced by bovine carbonic anhydrase. The results showed that the overall CO_2 absorption flux and reaction rate constant followed the order MEA > DEA > AMP > MDEA in the absence or presence of CA. The hydration of CO_2 by MDEA in the presence of CA directly produced bicarbonate, whereas AMP produced unstable carbamate intermediate and then underwent hydrolytic reaction and converted to bicarbonate. The MDEA > AMP > DEA > MEA reverse ordering of the enhanced CO_2 flux and reaction rate constant in the presence of CA was due to bicarbonate formation by the tertiary and sterically hindered amines. They reported that CA increased the CO_2 absorption rate by MDEA by a factor of 3 relatively to the absorption rate by MDEA alone. Furthermore, the thermal effects suggested that CA yielded a higher activity at 40 °C.

Zhang and Lu carried out the same simulation considering 5 M MEA as liquid phase, in condition of lean (40% MEA conversion) and rich (90% MEA conversion) solvent. Their results pointed out that the overall rate of CO_2 absorption into 5 M MEA solution and into K_2CO_3 20% promoted by 3g/l CA was about the same.

Recently, Gladis and collaborators (Gladis et al. 2017) studied the effect of carbonic anhydrase addition on the absorption of CO_2 in a wetted wall column apparatus where they compared four solvents, the MEA, AMP, and MDEA with K_2CO_3, in concentrations ranging from 5 to 50 wt% in a temperature interval from 298 to 328 K with and without an enzyme. The results showed that the addition of carbonic anhydrase increased dramatically the liquid side mass transfer coefficient for MDEA and K_2CO_3, AMP had moderately increased, whereas MEA was unchanged. The results confirmed that only bicarbonate forming systems benefit from the enzyme catalyst.

Sivanesan and his group (Sivanesan et al. 2015) used model complexes based on the carbonic anhydrase in aqueous tertiary amine medium to improve CO_2 sequestration. They used a stopped-flow spectrophotometer to follow pH changes coupled to pH indicator in a continuous stirred-tank reactor (CSTR) to determine the effect of substituents on the CA model complexes on CO_2 absorption and desorption. The CO_2 hydration rate constants were determined under basic conditions, and a compound which contained a hydrophilic group showed the highest absorption or hydration levels of CO_2 (2.860 10^3L/(mol. s)). Furthermore, the CSTR experimental results for simple model CA complexes may be suitable for post-combustion processing.

1.4.5 Temperature Effect on Carbonic Anhydrase Activity and Structure

At high temperature, enzymes lose their biological activity and become irreversibly denaturated. This inactivation by heat denaturation has a profound effect on the enzyme productivity (Sheldon 2007). The temperature limitation of enzymes is an important parameter for industrial applications affecting the cost of the process if the enzyme could not be reused. Lavecchia and Zugaro studied the thermal behavior of bovine carbonic anhydrase (Lavecchia and Zugaro 1991) who reported that carbonic anhydrase was active under 60 °C, but it lost its activity between 60 and 65 °C.

Many authors reported recently a decrease in enzyme activity when exposed to higher temperatures for a longer time (Russo et al. 2013; Gundersen et al. 2014; Ye and Lu 2014). The positive results from the large-scale experiments encourage the application of CA in carbon capture and show that it is possible to develop thermostable enzymes through protein engineering.

1.5 Enhanced Enzymatic Carbon Capture Overview

A wide spectrum of reactor configurations is reported in literature. However, the absorption unit designs are still an open and challenging issue. The reactor configurations, in general, are strongly associated with the enzyme form used, i.e., dissolved (homogeneous catalysis) or immobilized (heterogeneous catalysis). Nevertheless, the use of heterogeneous catalysts provides numerous advantages, in particular:

1. The use of immobilized carbonic anhydrase allows its easy recovery and reuse.
2. The use of the dedicated enzyme immobilization technique improves substantially its stability under the industrial processing conditions (Garcia-Galan et al. 2011).
3. Because the CO_2 absorption requires high salts and enzyme concentrations, the free CA may aggregate and then reduce the homogeneous enzyme efficiency (Ye and Lu 2014).
4. The suitable immobilization technique allows the use of high enzyme loadings, concentrations larger than 300 mg/l (Ye and Lu 2014).

The morphology of the solid biocatalyst and the reactor configuration should be carefully designed to maximize the CO_2 absorption rate. Several authors (Iliuta and Larachi 2012; Russo et al. 2013) reported that the enzyme catalysis on the CO_2 absorption rate is enhanced by the immobilized enzyme availability at the gas–liquid interface, by virtue of which various technical designs are available in the literature.

Iliuta and Larachi (2012) proposed a novel conceptual model of a multiscale monolith slurry reactor where hCA II was covalently immobilized on a monolith wall. The monolith is a bundle of parallel channels (honeycomb like) with a 3 mm cross-sectional diameter. The solvent was permanently regenerated by ion-exchange beads (Amberlite IRN-150) which remove ions, preventing CA product inhibition and enhancing CO_2 hydration rate. The reactor was run continuously with respect to both liquid and gas phases in a cocurrent flow pattern. They simulated the effects of enzyme loading, channel washcoat thickness, resin concentration, buffer acid–base constant and concentration, fluid fluxes, gas composition, and channel length on CO_2 scrubbing for monolith three-phase slurry enzymatic reactor enabled assessment.

Zhang and his group used hollow fiber membrane reactor filled with immobilized carbonic anhydrase by nanocomposite hydrogel to study the CO_2 facilitated transport. They reported that simulated results of CO_2 and CA concentrations, and flow rate of feed gas on CO_2 removal performance were in agreement with the experimental data with a maximum deviation of up to 18.7%. Besides, they also investigated the effect of CO_2 concentration on the required membrane areas for the same CO_2 removal target (1 kg/day).

Hou and colleagues developed a novel biocatalytic gas–liquid membrane contactor for CO_2 capture with virgin and superhydrophobic PP hollow fibers. To promote CO_2 hydration, biocatalytic TiO_2 nanoparticles with covalently immobilized CA were suspended in the solvent absorbent. The CA immobilization on titania nanoparticles was proved beneficial for higher immobilization yields and easier biocatalyst recovery with respect to CA adsorbed to the inner wall of the membrane. They also showed that the enzymatic promotion is more efficient at low liquid Reynolds number, which correspond to operating conditions of most conventional gas–liquid membrane contactors.

Leimbrink and his group (Leimbrink et al. 2017a) compared the use of some intensified contacting devices (ICD), especially membrane contactor (MC) and rotating packed beds (RPB) to classical packed columns (PC) to achieve enzyme accelerated carbon capture. They investigated a 30 wt. % aqueous MDEA solution with and without dissolved CA in a packed column and in the two ICDs to evaluate the potential improvement of a joint application of the ICD intensified contacting devices and the application of CA absorption. While all three equipments show similar absorption performance without adding CA, the authors claimed that the RPB can handle exceptionally high gas loads, while the MC can be operated over a much wider range of liquid loads. When CA is added to the solvent, the PC and the RPB show superior performance compared to the MC.

Kim and colleagues (Kim et al. 2017) studied the use of carbonic anhydrase for the acceleration of CO_2 reaction in MEA and MDEA solutions in a lab-scale membrane contactor module. They used specific microporous membranes which have both hydrophilic (surface) and hydrophobic (bulk) properties in order to avoid wetting of solution and reduce fouling by the enzymes simultaneously. They reported that enzyme addition improved substantially the CO_2 absorption rate in MDEA solution but had a negative effect in MEA solution. They coated, in the meantime, the porous hydrophobic membranes with a highly selective polyionic liquid layer to increase the affinity of CO_2 towards the interfacial area and consequently the driving force. They obtained promising results with the activated membrane material to accelerate CO_2 transport in MDEA solution. They concluded that polyionic liquid membrane coating combined with enzyme enhances considerably the CO_2 absorption in MDEA solution.

Gaspar and collaborators (Gaspar et al. 2017) developed a rate-based model for CO_2 absorption using carbonic anhydrase-enhanced MDEA solution and validated it against pilot-scale absorption experiments. The authors reported that the developed model is suitable for CO_2 capture simulation and optimization using MDEA and MDEA enhanced with CA. Besides, they studied the accuracy of the enhancement factor model for CO_2 absorption/desorption using wetted wall column for various CO_2 loadings and temperatures.

Leimbrink and his team (Leimbrink et al. 2017b) studied the combination of the effects of an aqueous MDEA solution with carbonic anhydrase in a packed column pilot plant to offset the loss of separation efficiency caused by the lower driving force in CO_2 capture from power plant flue gases.

They explored two different CA application strategies as a biocatalyst in reactive absorption processes to understand their influence on absorption efficiency: (i) dissolution of the enzyme in the solvent to allow the enzyme to react in the liquid boundary layer. However, due to the enzyme temperature sensitivity, the enzyme recovery requires an additional operation before desorption at high temperatures. (ii) Immobilization of the enzyme inside the absorption column is an alternative to this drawback but may create additional mass transfer resistance at the solid particles. Although this strategy allows locating the enzyme at convenient process conditions and avoiding high temperature in the desorber, the enzyme immobilization and the suitable packing selection increase the difficulty of this strategy.

Absorption performance with enzyme dissolution was three times higher than of the enzyme immobilization under equivalent operating conditions, but the immobilized enzyme concentration used was 50 times lower. On the other hand, the authors (Leimbrink et al. 2017b) reported that, with a liquid inlet temperature of 20 °C, a 30 wt. % MDEA concentration, and a liquid flow rate of 24 $m^3/(m^2 . h)$, the best absorption performance with the enzyme dissolution and the measured absorption rate was 7.57 times higher than without enzyme added.

1.6 Major Research Programs and Pilot Plants Worldwide

Several companies are developing novel carbonic anhydrase-based CO_2 capture technologies. These attempts are focusing to improve the enzyme forms and functions to develop new methods for the enzyme use in engineered systems and to develop specialized mass transfer unit operations to implement the enzyme function.

1.6.1 *Enzyme-Enhanced Amines by* CO_2 Solution Inc.

CO_2 *Solutions Inc. (CSI)* of Québec, Canada, has been developing CO_2 capture systems based on the biocatalyst carbonic anhydrase use in packed-bed absorption tower-type absorber–stripper systems [CO_2 Solutions, 2009]. This concept allows solutions with low regeneration temperatures having low absorption rates technically viable candidates for post-combustion capture.

Recently (2015), CO_2 *Solutions Inc.* has successfully demonstrated a 10 tpd CO_2 enzyme accelerated solvent carbon capture project from a natural gas fired boiler in Salaberry-de-Valleyfield near Montreal, Canada (Fig. 1.12). The plant was successfully run for 2500 h with biocatalyst stable performance, negligible solvent deterioration, no toxic waste generation, and production of 99.95% pure CO_2 suitable for many reuse applications. The plant reached 95% CO_2 capture which illustrates a wide range achievement of performance objectives. The inventors found that the enzyme remaining in the solvent kept excellent activity throughout the test period and demonstrated an easy enzyme addition during plant running. CO_2 *Solution Inc.* (CSI), which has proved the ability to erect up to 300 tpd plant, is presently erecting a 30 tpd plant in Canada and start-up is estimated in late 2018.

Lalande and Tremblay of CO_2 *Solutions Inc.* (Lalande and Tremblay 2005) invented a process and built a CO_2 recovery and recycling unit for gas emissions from a cement clinker production plant. In that process, a gas/liquid CO_2 packed column absorption catalyzed by carbonic anhydrase is used and subsequent with the production of limestone ($CaCO_3$). The sequence is accomplished when the $CaCO_3$ is used as first class raw material for the fabrication of Portland cement.

In addition, *Codexis Inc.*, in a joint venture with CO_2 *Solution Inc.*, has built a pilot-scale CO_2 capture process at the National Carbon Capture Center in Wilsonville, Alabama, USA, in which the observed CO_2 absorption rate was enhanced 25-fold compared to the noncatalyzed absorption process (Alvizo et al. 2014).

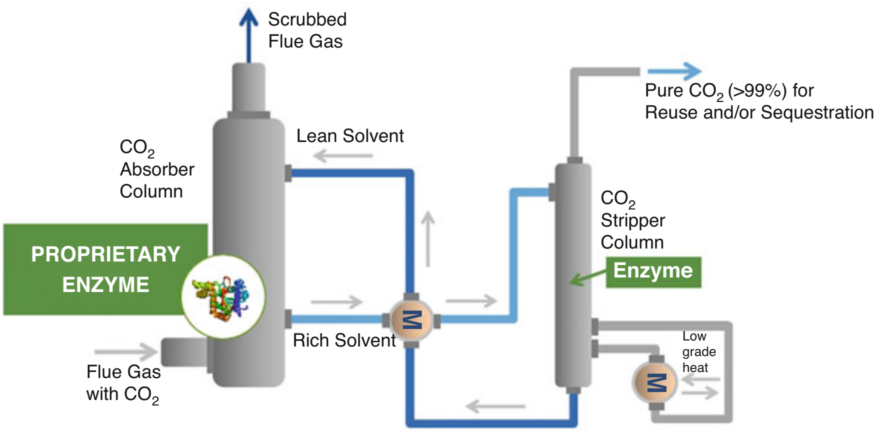

Fig. 1.12 Carbonic anhydrase-catalyzed amine absorber plant for carbon capture from fuel-fired power plant flue gas. (www.CO2solutions.com)

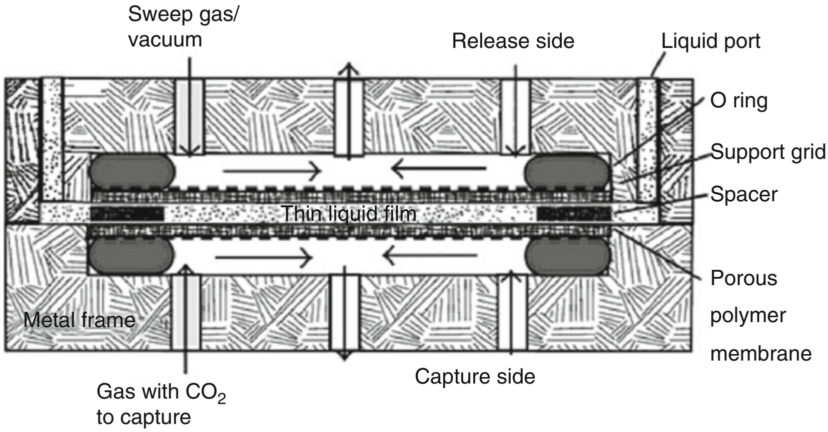

Fig. 1.13 Thin liquid membrane for CO_2 capture developed by NASA. (Ge et al. 2002)

1.6.2 NASA Thin Liquid Membrane System

The *National Aeronautics and Space Administration* (NASA) has initially developed another process to clean the ambient air in the confined inhabited crew cabins where CO_2 is captured in thin aqueous films with some immobilized CA (Ge et al. 2002; Cowan et al. 2003).

The CO_2 concentration of such ambient air is relatively low ($\leq 0.1\%$). Figure 1.13 illustrates the membrane rector constructed by sandwiching a thin (330 μm thick) enzymatic solution layer CA containing phosphate-buffered solution between two polypropylene membranes, themselves retained by thin metallic screens to insure the liquid membrane thickness and rigidity. The incoming CO_2 from the ambient atmosphere dissolves immediately in the liquid membrane on one face and then diffuses across the liquid membrane and evaporates out on the liquid membrane opposite face, either in vacuum or in a carrier gas. Capture and release gases analysis showed a selective CO_2 diffusion in a ratio of 1400 to 1 compared to N_2 and 866 to 1 compared to O_2. The collected data elected this enzyme-based contained liquid membrane as a viable and suitable technique for NASA applications to control CO_2 in the crew cabins.

1.6.3 Hollow Fiber Membrane Program by **Carbozyme Inc.**

Carbozyme, Inc. has developed a biomimetic CO_2 capture apparatus able to accept a wide spectrum of gas streams and generate a stream acceptable to a pipeline operator. The *Carbozyme* permeator design consists of two fibrous microporous membranes portioned by a thin liquid membrane (CLM). To optimize the conversion

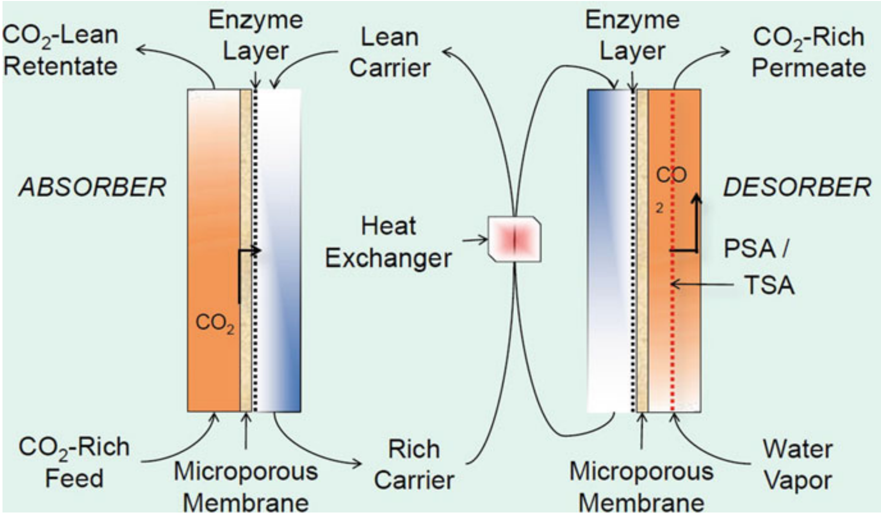

Fig. 1.14 *Carbozyme* permeator operation diagram. (Trachtenberg et al. 2009)

efficiency, the enzymatic biocatalyst is immobilized in the hollow fiber wall to insure an intimate contact between CO_2 and the carbonic anhydrase at the gas–liquid interface (Fig. 1.14).

Contained liquid membranes (CLM) are a gas-to-gas application and operated in the same way as simple selective membranes. Absorption and desorption are carried out in the same unit where CO_2 dissolves into the liquid in the membrane and is desorbed on the other side producing an ultrapure CO_2 stream. They may be used as flat membranes or hollow fiber membranes to increase contact area but increasing operating difficulty. Sweep gas (argon or nitrogen) is usually used for desorption in experimental setups, whereas it would be done with vacuum in industrial scale. The advantage of this aims reducing energy which is beneficial for the enzyme stability (Figueroa et al. 2008). However, the process requires energy to pressurize the incoming gas and to create vacuum on the exit side. In addition, solvent loss through evaporation in the membrane pores may also be a serious problem, and higher capture ratios often require exponentially higher energy needs (Russo et al. 2013). The application of such technology may be suitable for cases where the inlet CO_2 concentration is fairly high and sufficiently low carbon capture rates are needed. This technology has led to satisfactory experimental results on laboratory scale. Bao and Trachtenberg have shown that CA in bicarbonate gave higher carbon capture rates than both uncatalyzed bicarbonate and the secondary amine diethanolamine (DEA) (Bao and Trachtenberg 2006).

The *Carbozyme* system achieved 85% CO_2 removal from a 15.4% CO_2 feed stream in a 0.5 m^2 permeator as predicted by the model calculations (Trachtenberg et al. 2009).

Most recently, *Carbozyme* has reported on the use of a proprietary absorber–stripper arrangement based on the same concept of using carbonic anhydrase immobilized at the gas–liquid interface (Smith et al. 2010).

However, in this process, some technical difficulties may appear due to the drying of aqueous film during continuous longtime process running. To overcome this drawback, Trachtenberg and his group suggested humidifiers such as polysulfone to humidify the capture and release gases (Cowan et al. 2003). Nevertheless, for a better solution to this problem, the investigators adapted the technique to hollow microporous fiber networks where the flue gas and the release gases could flow (Bao and Trachtenberg 2006; Trachtenberg et al. 2009). Following this progress, *Carbozyme* developed a new technology based on hollow microporous propylene microfibers, separated by control separators made of thin oxide powders, the whole system bathing in an excess aqueous enzyme solution. The enzyme was directly immobilized on the external faces of the microfibers, and water vapor under moderate vacuum (15 kPa) was used as sweep gas at low flow rates in the release microfibers. The CO_2 content in the sweep gas almost reached 95%, for a flue gas containing 15% of CO_2. No significant loss of enzyme activity was observed during a 5-day continuous run, and a conservative run time of 2500 h was selected before needing to change the enzyme (Trachtenberg et al. 2009).

Yong and his team (Yong et al. 2016) developed a similar strategy to promote the reaction rate by the electrostatic adsorption of carbonic anhydrase onto the surface of both porous polypropylene (PP) and nonporous polydimethoxysilane (PDMS) hollow fiber membranes via layer-by-layer (LbL) assembly. They reported that CO_2 absorption rate into K_2CO_3 is increased approximately threefold when CA is adsorbed onto the PP membrane surface, while the absorption rate of the modified PDMS membrane was slightly lower, within 70–90% of the PP values. The CO_2 hydration is enhanced in all cases, and the wetting of the porous PP membranes is significantly reduced by the pore blockage induced by the LbL adsorption of the polyelectrolytes. The company *Carbozyme* is developing a similar hollow fiber membrane system.

Furthermore, *Novozymes* has deposited some patents, the latter of which proposed the combination of various CO_2 capture and release units, such as those developed by the CO_2 *Solutions* or *Carbozyme* companies interconnected by fluid circulation pipes (Saunders et al. 2010).

1.6.4 Other Miscellaneous Programs

Akermin, Inc.

Akermin, Inc. has developed a carbonic anhydrase immobilization–stabilization technique for CO_2 capture from flue gas. The conceptual idea is to encapsulate the enzyme in custom polymer structures, thus protecting the enzyme and allowing a long life. Besides, the enzyme is spread out in the capture solution to be present at all the gas–liquid interface, where it can provide higher benefit.

The immobilized biocatalyst was shown to enhance kinetic rates compared to coated packing, and modeling showed a 30% lower energy needs (Reardon et al. 2014).

Akermin has been working on the technology for approximately 5 years and was recently awarded a 2-year project to optimize its enzyme-containing solvent formulation and demonstrate process efficacy by treating up to 2 standard cubic meters of simulated flue gas per hour (*US Department of Energy National Energy Technology Laboratory*, *NETL*, 2016h).

Akermin, Inc. has carried out field tests with their surface-immobilized packing absorption device at the National Carbon Capture Center (NCCC) in Wilsonville, Alabama. They achieved 80% capture in an absorption column with around 0.21 m diameter and a total packing height of around 8 m with 20 wt% K_2CO_3 with a liquid to gas ratio of 7.88 (kg/kg) over a timeframe of 5 months and 1 month, respectively. A six to sevenfold higher mass transfer rates was observed with the use of the surface-immobilized enzyme (Reardon et al. 2014).

Sulzer BX **Gauze Packing**

Kunze and coworkers (Kunze et al. 2015) carried out laboratory-scale experiments and showed chemical capability and evaluated various solvents. They measured CO_2 absorption rates of 30 wt.% MEA, 30 wt.% MDEA, 30 wt.% DEEA, and 10 wt.% K_2CO_3 with the addition of 0.2 wt.% carbonic anhydrase. They identified aqueous solutions of 30 wt.% MDEA as well as 30 wt.% K_2CO_3 as promising solvents whose CO_2 absorption rate was accelerated by the enzyme, as the addition of 0.2 wt.% carbonic anhydrase led to an increase of the absorbed mole flow by a factor larger than 4. Next, they tested the technical feasibility of the enzyme–solvent concept packed columns to check for scaling of laboratory size performance to pilot size (56 mm diameter, 2.3 m high, Sulzer BX gauze packing). Absorption runs at 317 K and 15 vol. % CO_2 in the gas phase resulted in comparable intensification of absorption compared to the results from the spray reactor, and CE_{CA} values of 4.0–5.9 for K_2CO_3 and 3.3–4.2 for MDEA were reported. They reported a good agreement in the increase of the absorbed mole flow in pilot scale in the presence of biocatalyst with the laboratory-scale experiments and did not observed any undesired effects such as foaming or aggregation.

Sandia National Laboratories **Ultrathin Liquid Membrane**

The Sandia National Laboratories group in collaboration with the University of New Mexico (Fu et al. 2018) has very recently developed a CA-catalyzed, ultrathin liquid membrane nano-immobilized via capillary forces for CO_2 separation (Fig. 1.15). Using atomic layer deposition and oxygen plasma processing, the silica mesopores are engineered to be hydrophobic except for an 18-nm-deep region at the pore surface which is hydrophilic. Carbonic anhydrase enzymes and water fill

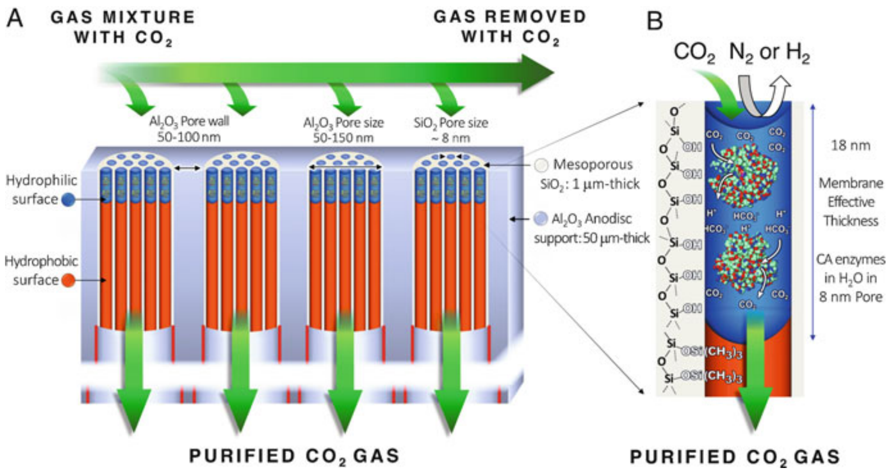

Fig. 1.15 The ultrathin liquid membrane by courtesy of Sandia National Laboratories. (Fu et al. 2018)

spontaneously the hydrophilic mesopores through capillary condensation to form an array of immobilized enzymes with an effective concentration ten times greater than that achievable in solution.

The metalloenzyme rapidly catalyzes CO_2 and H_2O conversion into HCO_3^-. Fu and his team (Fu et al. 2018) found that the enzymatic liquid membrane separates CO_2 at room temperature and atmospheric pressure at a rate of 2600 GPU with CO_2/N_2 and CO_2/H_2 selectivities as high as 788 and 1500, respectively, the highest combined flux and selectivity yet assessed for ambient condition operation by minimizing diffusional constraints, stabilizing and concentrating CA within the nanopore array to a concentration ten times greater than achievable in solution.

The authors have created in this device a mechanically stable liquid membrane just 18 nm thick, whereas in the *Carbozyme* configurations (Trachtenberg 2011), the characteristic membrane thicknesses were limited to 10–100 μm invalidating, therefore, the potential advantage of the liquid membrane compared to a polymer membrane. Furthermore, the advantage of this membrane compared to Carbozyme's is that the confinement within the close-packed array of hydrophilic nanopores allows for higher enzyme concentration. In addition, the higher hydrophilic nanopore density in this new membrane, when filled with CA, would provide a considerably higher local CA concentration.

1.7 Conclusion

Although the use of carbonic anhydrase for biomimetic CO_2 capture is still in its infancy, it is an effective and rapidly advancing technology. However, the industrial applications of enzymes in carbon capture processes are restricted by their high cost, low catalytic activity, poor stability in time, high sensitivity to temperature, low resistance to pollutants such as sulfur compounds, and reusability. To overcome these adversities, further developments are still needed so that improved economic feasibility and significant progress on several features may also be expected.

Although the well-understood physicochemical laws governing the carbon capture in aqueous and solvent mediums are allowing development of various efficient reactor types, much effort should be made not only to improve the state-of-the-art technology but also to develop several innovative chemical reactor concepts for enzymatic gas–liquid contactors.

Besides, carbon dioxide may be turned into chemicals and fuel using chemical, photochemical, electrochemical, and enzymatic methods such as conversion to carbon monoxide, to methanol, to formic acid, to glucose, or to methane. Although facing harsh barriers, the enzymatic conversion of carbon dioxide into useful chemicals is making great strides and could be used to recycle considerable amounts of carbon. The implementation of these technologies with enzymatic conversion would very likely enhance selectivity and productivity and ought to be given further attention in the future.

In addition, only few conceptual processes have been tested on a lab scale, but just a very few of them have demonstrated potential interest on an industrial scale. Emerging processes that have successfully completed smaller pilot-scale tests and are in the process of scaling up to larger demonstrations are likely to be available commercially in the next 5–10 years. Nonetheless, several interesting routes have not yet been sufficiently explored.

In conclusion, all these studies confirm the remarkable potential of some CA forms as biocatalysts, providing a realistic demonstration of the feasibility of the biomimetic CO_2 capture processes.

References

Abu-Khader MM (2006) Recent progress in CO_2 capture/sequestration: a review. Energy Sources 28:1261–1279

Aggarwal M, Boone CD, Kondeti B, McKenna R (2013) Structural annotation of human carbonic anhydrases. J Enzyme Inhib Med Chem 28:267–277

Alvizo O, Nguyen LJ, Savile CK, Bresson JA, Lakhapatri SL, Solis EOP, Fox RJ, Broering JM, Benoit MR, Zimmerman SA, Novicka SJ, Lianga J, Lalonde JJ (2014) Directed evolution of an ultrastable carbonic anhydrase for highly efficient carbon capture from flue gas. Proc Natl Acad Sci 111(46):16436–16441

Aspatwar A, Haapanen S, Parkkila S (2018) An update on the metabolic roles of carbonic anhydrases in the model alga, *Chlamydomonas reinhardtii*. Meta 8:22

Augugliaro V, Rizzuti L (1987) Kinetics of carbon dioxide absorption into catalyzed potassium carbonate solutions. Chem Eng Sci 42(10):2339–2343

Baker RW (2004) Membrane technology and applications, 2nd edn. Wiley, Chichester

Bao L, Trachtenberg MC (2006) Facilitated transport of CO_2 across a liquid membrane: comparing enzyme, amine, and alkaline. J Membr Sci 280:330–334

Barbosa O, Ortiz C, Berenguer-Murcia A, Torres R, Rodrigues RC, Fernandez-Lafuente R (2014) Glutaraldehyde in bio-catalysts design: a useful crosslinker and a versatile tool in enzyme immobilization. RSC Adv 4:1583–1600

Bentagor L, Lopez-Gallego F, Hindalgo A, Fuentes M, Podrasky O, Kuncova G, Guisan JM, Fernandez-Lafuente R (2005) Advantages of the pre-immobilization of enzymes on porous supports for their entrapment in sol−gels. Biomacromolecules 6:1027–1030

Berg JM, Tymoczko JL, Stryer L (2010) Biochemistry, 7th edn. Freeman and Company, New York

Bhattacharya S, Nayak A, Schiavone M, Bhattacharya SK (2004) Solubilization and concentration of carbon dioxide: novel spray reactors with immobilized carbonic anhydrase. Biotechnol Bioeng 86:37–46

Blomen E, Hendriks C, Neele F (2009) Capture technologies: improvements and promising developments. Energy Procedia 1(1):1505–1512

Boone CD, Habibzadegan A, Gill S, McKenna R (2013) Carbonic anhydrases and their biotechnological applications. Biomol Ther 3:553–562

Boucif N, Sengupta A, Sirkar KK (1986) Hollow fiber gas permeator with countercurrent or cocurrent flow: series solutions. Ind Eng Chem Fundam 25(2):217–228

Boucif N, Corriou JP, Roizard D, Favre E (2012) Carbon dioxide absorption by monoethanolamine in hollow fiber membrane contactors: A parametric investigation. AICHE J 58(9):2843–2855

Chakravati S, Gupta A, Hunek B (2001) Advanced technology for the capture of carbon dioxide from flue gases. In: 1st National Conference on carbon sequestration. Washington, DC

Chiang C-J, Hsiau L-T, Lee W-C (2004) Immobilization of cell-associated enzymes by entrapment in polymethacrylamide beads. Biotechnol Tech 11(2):121–125

Cowan RM, Ge JJ, Qin YJ, McGregor ML, Trachtenberg MC (2003) CO_2 capture by means of an enzyme-based reactor. Ann N Y Acad Sci 984:453–469

Darde V, Thomsen K, van Well WJM, Stenby EH (2010) Chilled ammonia process for CO_2 capture. Int J Greenhouse Gas Control 4:131–136

Davison J (2007) Performance and costs of power plants with capture and storage of CO_2. Energy 32:1163–1176

Davy R (2009) Development of catalysts for fast, energy efficient post combustion capture of CO_2 into water; an alternative to monoethanolamine (MEA) solvents. Energy Procedia 1:885–892

Department of Energy, Energy Information Administration (EIA) (2016) Annual Energy, Outlook. http://www.eia.doe.gov/oiaf/aeo/

Di Fiore A, Alterio V, Monti SM, De Simone G, D'Ambrosio K (2015) Thermostable carbonic anhydrases in biotechnological applications. Int J Mol Sci 16:15456–15480

DiMario RJ, Clayton H, Mukherjee A, Ludwig M, Moroney JV (2017) Plant carbonic anhydrases: structures, locations, evolution, and physiological roles. Mol Plant 10:30–46

Dindore VY, Brilman DWF, Geuzebroek FH, Versteeg GF (2004a) Membrane solvent selection for CO_2 removal using membrane gas–liquid contactors. Sep Purif Technol 40:133–145

Dindore V, Brilman D, Feron P, Versteeg G (2004b) CO_2 absorption at elevated pressures using a hollow fiber membrane contactor. J Membr Sci 235(1):99–109

Dos Santos JC, Barbosa O, Ortiz C, Berenguer-Murcia A, Rodrigues RC, Fernandez-Lafuente R (2015) Importance of the support properties for immobilization or purification of enzymes. ChemCatChem 7:2413–2432

Duda DM, Tu C, Fisher SZ, An H, Yoshioka C, Govindasamy L, Laipis JL, McKenna MA, Silverman DN, McKenna R (2005) Human carbonic anhydrase III: structural and kinetic study of catalysis and proton transfer. Biochemistry 44:10046–10053

Emamipour H, Hashisho Z, Cevallos D, Rood MJ, Thurston DL, Hay KJ (2007) Steady-state and dynamic desorption of organic vapor from activated carbon with electrothermal swing adsorption. Environ Sci Technol 41:5063–5069

Favre E (2007) Carbon dioxide recovery from post-combustion processes: can gas permeation membranes compete with absorption? J Membr Sci 294:50–59

Figueroa JD, Fout T, Plasynski S, McIlvried H, Rameshwar DS (2008) Advances in CO_2 capture technology-The U.S. Department of Energy's carbon sequestration program. Int J Greenhouse Gas Control 2:19–20

Fu Y, Jiang Y-B, Dunphy D, Xiong H, Coker E, Chou SS, Zhang H, Vanegas JM, Croissant JG, Cecchi JL, Rempe SB, Brinker CJ (2018) Ultra-thin enzymatic liquid membrane for CO_2 separation and capture. Nat Commun 9:990

Furukawa H, Cordova KE, O'Keeffe M, Yaghi OM (2013) The chemistry and applications of metal-organic frameworks. Science 341:1230444

Furukawa H, Muller U, Yaghi OM (2015) Heterogeneity within order, in metal-organic frameworks. Angew Chem Int Ed 54:3417–3430

Garcia-Galan C, Berenguer-Murcia A, Fernandez-Lafuente R, Rodrigues RC (2011) Potential of different enzyme immobilization strategies to improve enzyme performance. Adv Synth Catal 313:2885–2904

Gaspar J, Gladis A, Woodley JM, Thomsen K, von Solms N, Fosbøl PL (2017) Rate-base modelling and validation of a pilot absorber using MDEA enhanced with carbonic anhydrase (CA). Energy Procedia 114:707–718

Ge J, Cowan RM, Tu C, McGregor ML, Trachtenberg MC (2002) Enzyme-based CO_2 capture for advanced life support. Life Support Biosph Sci 8(3–4):181–189

Gladis A, Gundersen MT, Fosbøl PL, Woodley JM, von Solms N (2017) Influence of temperature and solvent concentration on the kinetics of the enzyme carbonic anhydrase in carbon capture technology. *Chem Eng J* 309:772–786

Green DA, Turk BS, Portzer JW et al (2004) Carbon dioxide capture from flue gas using dry regenerable sorbents. U.S. DOE, National Energy Technology Laboratory, NETL, Washington, DC

Grunwald P (2011) Biocatalysis, 1st edn. Imperial College Press, London

Guisan JM (2006) Immobilization of enzymes as the 21st century begins. In: Guisan JM (ed) Immobilization of enzymes and cells, 2nd edn. Humana Press Inc, Totowa

Hart A, Gnanendran N (2009) Cryogenic CO_2 capture in natural gas. Energy Procedia 1:697–706

Henis JMS, Tripodi MK (1980) A novel approach to gas separation using composite hollow fiber membranes. Sep Sci Technol 15:1059–1068

Ho WSW, Sirkar KK (eds) (1992) Membrane handbook. Van Nostrand Reinhold, New York

Hu G, Smith KH, Nicholas NJ, Yong J, Kentish SE, Stevens GW (2017) Enzymatic carbon dioxide capture using a thermally stable carbonic anhydrase as a promoter in potassium carbonate solvents. Chem Eng J 307:49–55

Huang L, Cheng ZM (2008) Immobilization of lipase on chemically modified bimodal ceramic foams for olive oil hydrolysis. Chem Eng J 144:103–109

IEA (2004) Prospects for CO_2 capture and storage. OECD/IEA, Paris

Iliuta I, Iliuta MC (2017) Enzymatic CO_2 capture in countercurrent packed-bed column reactors with high performance random packings. Int J Greenhouse Gas Control 63:462–474

Iliuta I, Larachi F (2012) New scrubber concept for catalytic CO_2 hydration by immobilized carbonic anhydrase II and in-situ inhibitor removal in three-phase monolith slurry reactor. Sep Purif Technol 86:199–214

IPCC (2017) Intergovernmental panel on climate change (IPCC) special report on carbon dioxide capture and storage. Cambridge University Press, Cambridge, UK

Jonsson BH, Steiner H, Lindskog S (1976) Participation of buffer in the catalytic mechanism of carbonic anhydrase. FEBS Lett 64:310–314

Keilin D, Mann T (1939) Carbonic anhydrase. Nature 144:442–443

Kim T-J, Lang A, Chikukwa A, Sheridan E, Inge DP, Leimbrink M, Skiborowski M, Roubroeks J (2017) Enzyme carbonic anhydrase accelerated CO_2 absorption in membrane contactor. Energy Procedia 114:17–24

Kimmel JD, Arazawa DT, Ye S-H, Shankarraman V, Wagner WR, Federspiel WJ (2013) Carbonic anhydrase immobilized on hollow fiber membranes using glutaraldehyde activated chitosan for artificial lung applications. J Mater Sci Mater Med 24(11):2611–2621

King EL, Altman C (1956) A schematic method of deriving the rate laws for enzyme-catalyzed reactions. J Phys Chem 60(10):1375–1378

Krajewska B (2004) Application of chitin- and chitosan-based materials for enzyme immobilizations: a review. Enzym Microb Technol 35:126–139

Kumakura M, Kaetsu I (2003) Immobilization of cellulase using porous polymer matrix. J Appl Polym Sci 29(9):2713–2718

Kunze A, Dojchinov G, Haritos VS, Lutze P (2015) Reactive absorption of CO_2 into enzyme accelerated solvents: from laboratory to pilot scale. Appl Energy 156:676–685

Lalande JM, Tremblay A (2005) Process and a plant for the production of Portland cement clinker. *Patent US6908507*, USA

Larachi F (2010) Kinetic model for the reversible hydration of carbon dioxide catalyzed by human carbonic anhydrase II. Ind Eng Chem Res 49:9095–9104

Lavecchia R, Zugaro M (1991) Thermal denaturation of erythrocyte carbonic anhydrase. *Fed Eur Biochem Soc 292*:162–164

Leimbrink M, Neumann K, Kupitz K, Górak A, Skiborowski M (2017a) Enzyme accelerated carbon capture in different contacting equipment – a comparative study. Energy Procedia 114:795–812

Leimbrink M, Limberg T, Kunze A-K, Skiborowski M (2017b) Different strategies for accelerated CO_2 absorption in packed columns by application of the biocatalyst carbonic anhydrase. Energy Procedia 114:781–794

Leung DY, Caramanna G, Maroto-Valer MM (2014) An overview of current status of carbon dioxide capture and storage technologies. Renew Sust Energ Rev 39:426–443

Li JR, Ma Y, McCarthy MC, Sculley J, Yu J, Jeong H-K, Balbuena PB, Zhou H-C (2011) Carbon dioxide capture-related gas adsorption and separation in metal-organic frameworks. Coord Chem Rev 255:1791–1823

Long NVD, Lee J, Koo K-K, Luis P, Lee M (2017) Recent progress and novel applications in enzymatic conversion of carbon dioxide. Energies 10:473–492

Luebke D, Myers C, Pennline H (2006) Hybrid membranes for selective carbon dioxide separation from fuel gas. Energy Fuel 20(5):1906–1913

Machida-Sano I, Ogawa S, Ueda H, Kimura Y, Satoh N, Namiki H (2012) Effects of composition of iron-cross-linked alginate hydrogels for cultivation of human dermal fibroblasts. Int J Biomater 2012:1–8., 820513

Maqsood K, Mullick A, Ali A, Kargupta K, Ganguly S (2014a) Cryogenic carbon dioxide separation from natural gas: a review based on conventional and novel emerging technologies. Rev Chem Eng 30(5):453–477

Maqsood K, Pal J, Turunawarasu D, Pal A, Ganguly S (2014b) Performance enhancement and energy reduction using hybrid cryogenic distillation networks for purification of natural gas with high CO_2 content. Korean J Chem Eng 31:1120–1135

Mason JA, Sumida K, Herm ZR, Krishna R, Long JR (2011) Evaluating metal-organic frameworks *for* post-combustion carbon dioxide capture via temperature swing adsorption. Energy Environ Sci 4(8):3030–3040

Meldrum NU, Roughton FJW (1933) Carbonic anhydrase. Its preparation and properties. J Physiol 80(2):113–142

Mirjafari P, Asghari K, Mahinpey N (2007) Investigating the application of enzyme carbonic anhydrase for CO_2 sequestration purposes. Ind Eng Chem Res 46:921–926

Moehlenbrock MJ, Minteers DM (2011) Introduction to the field of enzyme immobilization and stabilization. Methods Mol Biol 679:1–7

Mohamad NR, Marzuki NHC, Buang NA, Huyop F, Abdul Wahab R (2015) An overview of technologies for immobilization of enzymes and surface analysis techniques for immobilized enzymes. Biotechnol Biotechnol Equip 29(2):205–220

Notz R, Tönnies I, Mangalapally HP, Hoch S, Hasse H (2011) A short-cut method for assessing absorbents for post-combustion carbon dioxide capture. Int J Greenhouse Gas Control 5 (3):413–421

Olajire AA (2010) CO_2 capture and separation technologies for end-of-pipe applications – a review. Energy 35(6):2610–2628

Oviya M, Giri SS, Sukumaran V, Natarajan P (2012) Immobilization of carbonic anhydrase enzyme purified from *Bacillus Subtilis* Vsg-4 and its application as CO_2 sequesterer. Prep Biochem Biotechnol 42:462–475

Ozdemir E (2009) Biomimetic CO_2 sequestration: 1. immobilization of carbonic anhydrase within polyurethane foam. Energy Fuel 23:5725–5730

Payen A, Persoz J-F (1833) Memoire sur la Diastase, les Principaux Produits de ses Réactions et leurs Applications aux Arts Industriels. Ann Chim Phys 2(53):73–92

Penders-Van Elk NJMC, Derks PWJ, Fradette S, Versteeg GF (2012) Kinetics of absorption of carbon dioxide in aqueous MDEA solutions with carbonic anhydrase at 298 K. Int J Greenhouse Gas Control 9:385–392

Penders-van Elk N, Hamborg ES, Carley JA, Fradette S, Versteeg GF (2013) Kinetics of absorption of carbon dioxide in aqueous amine and carbonate solutions with carbonic anhydrase. Int J Greenhouse Gas Control 12:259–268

Penders-van Elk NJMC, Fradette S, Versteeg GF (2015) Effect of pKa on the kinetics of carbon dioxide absorption in aqueous alkanolamine solutions containing carbonic anhydrase at 298 K. Chem Eng J 259:682–691

Penders-Van Elk NJMC, Van Aken C, Versteeg GF (2016a) Influence of temperature on the kinetics of enzyme catalysed absorption of carbon dioxide in aqueous MDEA solutions. Int J Greenhouse Gas Control 49:64–72

Penders-Van Elk NJMC, Oversteegen SM, Versteeg GF (2016b) Combined effect of temperature and pKa on the kinetics of absorption of carbon dioxide in aqueous alkanolamine and carbonate solutions with carbonic anhydrase. Ind Eng Chem Res 55(38):10044–10054

Pierce WF, Riemer P, William GO (1995) International perspectives, the results of carbon dioxide capture disposal and utilization studies. Energy Convers Manag 36:813–818

Pierre AC (2012) Enzymatic carbon dioxide capture. ISRN Chem Eng 2012. Article ID 753687:1–22

Pohorecki R (1968) The absorption of CO_2 in carbonate-bicarbonate buffer solutions containing hypochlorite catalyst on a sieve plate. Chem Eng Sci 23:1447–1451

Powell CE, Qiao GG (2006) Polymeric CO_2/N_2 gas separation membranes for the capture of carbon dioxide from power plant flue gases. J Membr Sci 279:1–49

Reardon J, Bucholz T, Hulvey M, Tuttle J, Shaffer A, Pulvirenti D, Weber L, Killian K, Zaks A (2014) Low energy CO_2 capture enabled by biocatalyst delivery system. Energy Procedia 63:301–321

Roberts SB, Lane T, Morel FMM (1997) Carbonic anhydrase in the marine diatom Thalassiosira Weissflogii (Bacillariophyta). J Phycol 33:845–850

Rodrigues RC, Ortiz C, Berenguer-Murcia A, Torres R, Fernandez-Lafuente R (2013) Modifying enzyme activity and selectivity by immobilization. Chem Soc Rev 42:6290–6307

Rowlett RS (2010) Structure and catalytic mechanism of the beta-carbonic anhydrases. Biochim Biophys Acta 1804:362–373

Rowlett RS, Silverman DN (1982) Kinetics of the protonation of buffer and hydration catalyzed by human carbonic anhydrase II. J Am Chem Soc 104:6737–6741

Russo ME, Olivieri G, Marzocchella A, Salatino P, Caramuscio P, Cavaleiro C (2013) Post-combustion carbon capture mediated by carbonic anhydrase. Sep Purif Technol 107:331–339

Saunders P, Salmon S, Borchert M, Lessard LP (2010) Modular membrane reactor and process for carbon dioxide extraction. Novozymes. *International Patent WO 2010/014774 A2*

Seader JD, Henley EJ (2006) Separation process principles, 2nd edn. John Wiley & Sons, Hoboken

Sharma MM, Danckwerts PV (1963) Fast reactions of CO_2 in alkaline solutions-(A) carbonate buffers with arsenite, formaldehyde and hypochlorite as catalysts, (B) aqueous monoisopropanolamine (1-Amino-2-Propanol) solutions. Chem Eng Sci 18:729–735

Sharma A, Bhattacharya A, Shrivastava A (2011) Biomimetic CO_2 sequestration using purified carbonic anhydrase from indigenous bacterial strains immobilized on biopolymeric materials. Enzym Microb Technol 48:416–426

Shekh AY, Krishnamurthi K, Mudliar S, Yadav RR, Fulke AB, Devi SS, Chakrabarti T (2012) Recent advancements in carbonic anhydrase driven processes for CO_2 sequestration: minireview. Crit Rev Environ Sci Technol 42(14):1419–1440

Sheldon RA (2007) Enzyme immobilization: the quest for optimum performance. Adv Synth Catal 349:1289–1307

Sheldon RA (2011) Characteristic features and biotechnological applications of cross-linked enzyme aggregates (CLEAs). Appl Microbiol Biotechnol 92:467–477

Shi J, Jiang Y, Jiang Z, Wang X, Wang X, Zhang S, Han P, Yang C (2015) Enzymatic conversion of carbon dioxide. Chem Soc Rev 44:5981–6000

Sims REH, Rogner HH, Gregory K (2003) Carbon emission and mitigation cost comparisons between fossil fuel, nuclear and renewable energy resources for electricity generation. Energy Policy 31:1315–1326

Singh R, Kumar M, Mittal A, Kumar Mehta P (2016) Microbial enzymes: industrial progress in 21st century. Biotechnology 174:1–15

Sirisha VL, Jain A, Jain A (2016) Chapter nine – enzyme immobilization: an overview on methods, support material, and applications of immobilized enzymes. Adv Food Nutr Res 79:179–211

Sivanesan D, Choi Y, Lee J, Youn MH, Park KT, Grace AN, Kim H-J, Kwan JS (2015) Carbon dioxide sequestration by using a model carbonic anhydrase complex in tertiary amine medium. ChemSusChem 8:3977–3982

Smith D, Ghazi I, Wood DW, Trachtenberg MC (2010) Enzyme-catalyzed capture of CO_2. Presented at the 9th Annual Conference on Carbon Capture & Sequestration. David L. Lawrence Convention Center, Pittsburgh, Pennsylvania, May 10, 2010

Spahn C, Minteer SD (2008) Enzyme immobilization in biotechnology. Recent Pat Eng 2:195–200

Steiner H, Jonsson BH, Lindskog S (1975) The catalytic mechanism of carbonic anhydrase: hydrogen-isotope effects on the kinetic parameters of the human C isoenzyme. Eur J Biochem 59:253–259

Supuran CT (2008) Carbonic anhydrases – an overview. Curr Pharm Des 14:603–614

Supuran CT (2016) Structure and function of carbonic anhydrases. Biochem J 473(14):2023–2032

Svendsen HF, Hessen ET, Mejdell T (2011) Carbon dioxide capture by absorption, challenges and possibilities. Chem Eng J 171(3):718–724

Trachtenberg MC (2011) Enzyme facilitated carbon dioxide capture. In Carbon capture and storage: technology innovation and market viability. *Agrion*

Trachtenberg MC, Cowan RM, Smith DA, Horazak DA, Jensen MD, Laumb JD, Vucelic AP, Chen H, Wang L, Wu X (2009) Membrane-based, enzyme-facilitated, efficient carbon dioxide capture. Energy Procedia 1:353–360

Trickett CA, Helal A, Al-Maythalony BA, Yamani ZH, Cordova KE, Yaghi OM (2017) The chemistry of metal-organic frameworks for CO_2 capture, regeneration and conversion. Nat Rev Mater 2, Article ID 17045

Tripp BC, Smith K, Ferry JG (2001) Carbonic anhydrase: new insights for an ancient enzyme. J Biol Chem 276:48615–48618

Vaidya PD, Kenig EY (2007) CO_2-alkanolamine reaction kinetics: a review of recent studies. Chem Eng Technol 30(11):1467–1474

Vinoba M, Lim KS, Lee SH, Jeong SK, Alagar M (2011) Immobilization of human carbonic anhydrase on gold nanoparticles assembled onto amine/thiol-functionalized mesoporous SBA-15 for biomimetic sequestration of CO_2. Langmuir 27:6227–6234

Vinoba M, Bhagiyalakshmi M, Jeong SK, Yoon YI, Nam SC (2012) Immobilization of carbonic anhydrase on spherical SBA-15 for hydration and sequestration of CO_2. Colloids Surf B: Biointerfaces 90:91–96

Vinoba M, Bhagiyalakshmi M, Grace AN, Kim DH, Yoon Y, Nam SC, Baek IH, Jeong SK (2013) Carbonic anhydrase promotes the absorption rate of CO_2 in post-combustion processes. J Phys Chem B 117(18):5683–5690

Wang M, Lawal A, Stephenson P, Sidders J, Ramshaw C (2011) Post-combustion CO_2 capture with chemical absorption: a state-of-the-art review. Chem Eng Res Des 89:1609–1624

Wanjari S, Prabhu C, Satyanarayana T, Vinu A, Rayalu S (2012) Immobilization of carbonic anhydrase on mesoporous aluminosilicate for carbonation reaction. Microporous Mesoporous Mater 160:151–158

Webb EC (1992) Enzyme nomenclature. Academic Press, San Diego

Wellinger A, Lindberg A (2000) Biogas upgrading and utilization. In: IEA bioenergy, task 24: energy from biological conversion of organic waste. *IEA Bioenergy*

Whitford D (2005) Proteins: structure and function. Wiley, New-York

Won K, Kim S, Kim KJ, Park HW, Moon SJ (2005) Optimization of lipase entrapment in Ca-alginate gel beads. Process Biochem 40:2149–2154

Wood LL, Hartdegen FJ, Hahn PA (1982) Enzymes bound to polyurethane. *US Patent 4*, 342, 834

Xu Z, Wang J, Chen W, Xu Y (2001) Separation and fixation of carbon dioxide using polymeric membrane. In: Proceedings of *1st National Conference on carbon sequestration*. NETL, National Energy Technology Laboratory, Washington DC

Yadav R, Satyanarayanan T, Kotwal S, Rayalu S (2011) Enhanced carbonation reaction using chitosan-based carbonic anhydrase nanoparticles. Curr Sci 100:520–524

Yadav RR, Krishnamurthi K, Mudliar SN, Devi SS, Naoghare PK, Bafana A, Chakrabarti T (2014) Carbonic anhydrase mediated carbon dioxide sequestration: promises, challenges and future prospects. J Basic Microbiol 54(6):472–481

Ye X, Lu Y (2014) CO_2 absorption into catalyzed potassium carbonate–bicarbonate solutions: kinetics and stability of the enzyme carbonic anhydrase as a biocatalyst. Chem Eng Sci 116:567–575

Yong JKJ, Stevens GW, Caruso F, Kentish SE (2016) In situ layer-by-layer assembled carbonic anhydrase-coated hollow fiber membrane contactor for rapid CO_2 absorption. J Membr Sci 514:556–565

Zhai P, Chen XB, Schreyer DJ (2013) Preparation and characterization of alginate microspheres for sustained protein delivery within tissue scaffolds. Biofabrication 5:015009

Zhao Z, Cui X, Ma J, Li R (2007) Adsorption of carbon dioxide on alkali-modified zeolite 13x adsorbents. Int J Greenhouse Gas Control 1:355–359

Chapter 2
Carbon Capture via Mixed-Matrix Membranes Containing Nanomaterials and Metal–Organic Frameworks

Muhammad Sarfraz

Contents

Abstract Global warming issues arise due to the emission of carbon dioxide gas into the atmosphere. Carbon dioxide concentration in the environment has appreciably increased due to burning of carbon-based fossil fuels which releases large quantities of greenhouse gas into the atmosphere. Global warming can be controlled

M. Sarfraz (✉)
Department of Polymer and Process Engineering, University of Engineering and Technology, Lahore, Pakistan
e-mail: msarfraz@uet.edu.pk

Z. Zhang et al. (eds.), *Membranes for Environmental Applications*, Environmental Chemistry for a Sustainable World 42, https://doi.org/10.1007/978-3-030-33978-4_2

by minimizing greenhouse gas emissions into the atmosphere by capturing carbon dioxide from current effluent sources by applying carbon capture and sequestration technology. Carbon dioxide can be readily captured from post-combustion flue gas using mixed-matrix membranes filled with various nanofillers. This chapter comprehensively discusses recent developments made in the field of carbon capture from post-combustion flue gas using polymer-based mixed-matrix membranes containing different microporous metal–organic frameworks and other nanomaterials to signify their prospective application on an industrial scale. A comparison of membrane separation technology with conventional processes in terms of carbon capture performance is made here. Carbon capture performance of various mixed-matrix membranes prepared from different polymer matrices and selected microporous nanofillers is reviewed in terms of CO_2 permeability and CO_2/N_2 selectivity. Notable polymer matrices used to prepare mixed-matrix membranes include polysulfone, polyimide, polydimethylsiloxane, Matrimid®, Ultrason®, Pebax, SPEEK, and Ultem®. Currently investigated prominent nanomaterials comprise carbon nanotubes, graphene oxide nanosheets, and silica, while noteworthy microporous metal–organic frameworks encompass HKUST-1, ZIF-7, ZIF-8, ZIF-300, ZIF-301, ZIF-302, MIL-53, and MIL-101. Nanomaterial-filled membranes offer superior carbon dioxide separation performance as compared to their respective pure polymer counterparts and higher selectivities than the associated pure metal–organic framework membranes. Main advantages of these membranes include easy processability, casting and handling, improved mechanical and chemical properties, and superior gas separation performances.

Keywords Global warming · CO_2 capture · Post-combustion · Mixed-matrix membranes · Polymer · Metal–organic frameworks · Zeolitic imidazolate frameworks · Permeability · Selectivity · Porous materials

2.1 Introduction

One of the major issues currently being faced by the Earth's sphere is global warming due to continuous release of carbon dioxide (CO_2) gas into the atmosphere. In contrast to its natural fluctuation, carbon concentration in atmosphere has significantly been increased in a quick succession of time due to anthropogenic activities (Fig. 2.1). With the beginning of industrial revolution in the late eighteenth century, the CO_2 level in the atmosphere has enormously increased, thus disturbing the energy balance by raising the average surface temperature of the Earth (ESRL 2019). Burning of fossil fuels, required to fulfill ever-expanding energy demands of the world, discharges large volumes of carbon dioxide into the atmosphere (Quadrelli and Peterson 2007). These carbon-based fuels are still needed in the upcoming decades, especially in power plants and other industries. Growing world

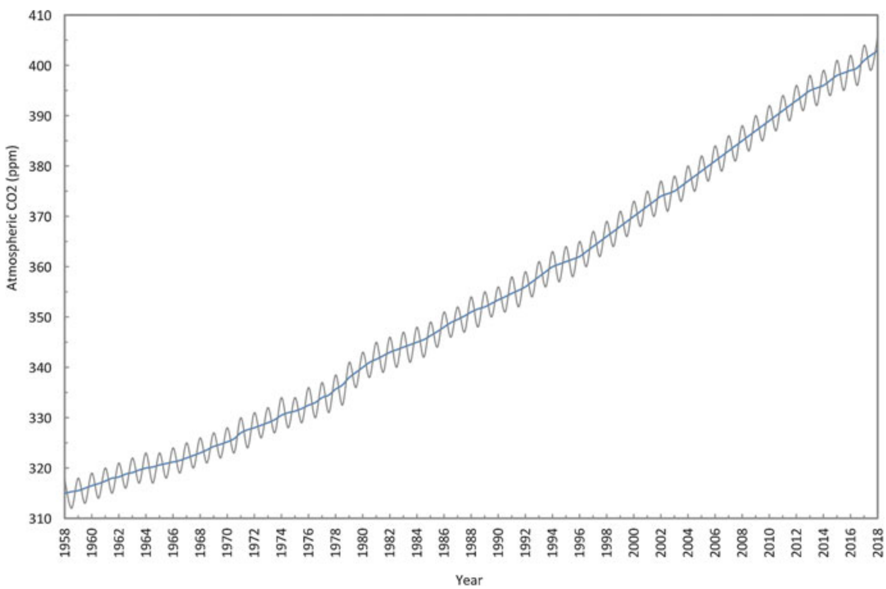

Fig. 2.1 Atmospheric CO_2 concentration during 1958–2019 measured at the Mauna Loa Observatory, Hawaii, displaying successive elevation of CO_2 in atmosphere. Note the CO_2 concentration in the atmosphere steadily and consistently increased in the last few decades. Modified after (ESRL 2019)

industry and expanding economy would result in further accumulation of atmospheric CO_2 in the future and disturb the poised carbon balance of the Earth planet (Pachauri and Reisinger 2007). Being the main promoter in raising the climate temperature, it is urgently needed to launch international measures to mitigate greenhouse gas emissions in order to control global warming and protect world environment.

Ideally the switch of the current energy-providing setup from carbon-based sources to clean-energy alternatives like solar energy or hydrogen fuel is considered to be the best option in this regard. Shifting to such cleaner alternative sources demands extensive alterations to the existing energy infrastructure; majority of the suggested technologies are still under refining process so as to implement them on large industrial scale. Consequently, existing carbon capture and sequestration (CCS) technologies effectively capturing carbon dioxide from current effluent sources are believed to play a vibrant role until substantial alterations to the energy framework can be recognized. The Intergovernmental Panel on Climate Change (IPCC) estimates 80–90% reduction in CO_2 emissions for a recent power plant furnished with an appropriate CO_2 capture and sequestration technology (Metz et al. 2005). The application of CCS technology is supposed to go in parallel with other important techniques like shifting to clean energy sources.

As compared to mobile sources, it is easy to implement CO_2 capture technologies at stationary point sources, such as natural gas- and coal-fired energy plants. The insertion of effectual CO_2 capture systems to modern power plant designs is likely to provide huge reduction in CO_2 discharges. Carbon capture and sequestration approach is accomplished in three stages, namely, CO_2 capture and its transportation and permanent storage (Haszeldine 2009). The process of CO_2 capture involves its separation from a mixture of gases originated in a certain operation. After transporting it to a storing location, the captured CO_2 is subjected to perpetual sequestration by inserting it into subterranean geographical structures, such as saline water aquifers or exhausted petroleum reservoirs.

In contrast to its capture technologies, transportation of CO_2 to a storing location and its perpetual storage are comparatively established technologies. This chapter is proposed to familiarize the reader with a comprehensive overview of the advancement made in the field of carbon dioxide capture from post-combustion flue gas using polymer-based mixed-matrix membranes (MMMs) filled with micro- and meso-porous metal–organic frameworks (MOFs) and nanomaterials, a short comparison of their capture performance with the current technologies, a summary of chemistry of mixed-matrix membranes, and an emphasis on the highly demanding properties requiring improvements. After giving a brief introduction to CO_2 capture technology and recent advancements made in this field, this chapter will discuss various membrane preparation and characterization techniques used to correlate chemical and structural characteristics of mixed-matrix membranes with their separation performances and associated study directly related to CO_2 separation in mixed-matrix membranes. Although a few review articles on CO_2 capture and sequestration using mixed-matrix membranes filled with various nanomaterials and metal–organic frameworks are available (Jeazet et al. 2012; Daturi and Chang 2011; Hedin et al. 2010; Keskin et al. 2010; Choi et al. 2010), a comprehensive review is required to make some directed outlook available for prospective research owing to a large number of research articles published in this field.

2.2 Controlling Global Warming via Carbon Capture

2.2.1 Carbon Capture and Sequestration

One of the current issues the Earth is facing today is global warming due to continuous increase in emissions of atmospheric carbon dioxide mainly owing to anthropogenic activities. In contrast to its natural fluctuation, the increased carbon release due to anthropogenic activities has noticeably affected the Earth's climate in a quick succession of time (ESRL 2019). With the beginning of industrial revolution in the late eighteenth century, the CO_2 level in the atmosphere has enormously increased (Fig. 2.1), thus disturbing the energy balance and raising the average surface temperature of the Earth. Being the main culprit in raising the climate temperature, it is urgently needed to minimize CO_2 emissions into the atmosphere.

Burning of fossil fuels, required to fulfill ever-expanding energy demands of the world, discharges large volumes of carbon dioxide (ca. 80% of CO_2 emissions over the globe) (Quadrelli and Peterson 2007; Girault et al. 2018). These carbon-based fuels are still needed in the upcoming decades, especially in power plants and other carbon-burning industries. Growing world industry and expanding economy would result in further accumulation of atmospheric CO_2 in the future and disturb the poised carbon balance of the Earth planet.

Ideally the switch of the current energy-providing setup from carbon-based sources to clean-energy alternatives, e.g., solar energy or hydrogen fuel, is considered to be the best option in this regard. Shifting to such cleaner alternative sources demands extensive modifications to the existing energy infrastructure; majority of the suggested technologies are still under refining process so as to implement them on large industrial scale. Consequently, existing carbon capture and sequestration (CCS) technologies effectively capturing carbon dioxide from current effluent sources are believed to play a vibrant role until substantial alterations to the energy framework can be recognized. The fundamental theory of CCS includes capturing CO_2 emissions without discharging them into the atmosphere followed by their storage or sequestration under high pressures. The Intergovernmental Panel on Climate Change (IPCC) estimates 80–90% reduction in CO_2 emissions for a recent power plant furnished with appropriate CO_2 capture and sequestration technologies. The application of CCS is supposed to go in parallel with other important techniques like shifting to clean energy sources.

As compared to mobile sources, it is easy to implement CO_2 capture technologies at stationary point sources, such as natural gas- and coal-fired energy plants. The insertion of effectual CO_2 capture systems to modern power plant designs is likely to provide huge reduction in CO_2 discharges. CCS is accomplished in three stages, namely, CO_2 capture and its transportation and permanent storage. The process of CO_2 capture involves its separation from a mixture of gases originated in a certain operation. After transporting it to a storing location, the captured CO_2 is subjected to perpetual sequestration by inserting it into subterranean geographical structures, such as saline water aquifers or exhausted petroleum reservoirs.

In contrast to its capture technologies, transporting CO_2 to a storing location and its perpetual storage are comparatively established technologies. Well-established techniques for CO_2 sequestration are already in practice (such as enhanced oil recovery (EOR) processes) along with the construction of numerous probationary CO_2 sequestration locations. Alternative utilization pathways for the captured CO_2 include its reuse as a reactant in chemical transformations, though it does not seem to be a feasible enduring scheme owing to huge volumes of CO_2 releases worldwide (about 30 Gt per annum). Another promising method to consume substantial quantity of captured CO_2 is its chemical transformation into useful petroleum products if proficient techniques for accomplishing the conversion through a renewable energy source can be established (Kumar et al. 2010).

2.2.2 Technologies/Methods in Carbon Capture

Quest for scalable commercial methods and technologies for carbon dioxide capture from gas- or coal-fired electricity generating plants and other industrial processes where carbon dioxide is generated due to burning of carbon-based fuels is considered as the main valuable approach in managing anthropogenic CO_2 emissions. Depending on its production quantities, various suggested CO_2 capture techniques have been executed. In general, based on chemical processes engaged in the combustion of fossil fuels, three basic CO_2 capture options under which new materials could serve to reduce the energy requirements include (1) post-combustion capture, (2) pre-combustion capture, and (3) oxy-fuel combustion (Sumida et al. 2012). As an illustration three options for CO_2 capture from power generation plants are schematically illustrated in Fig. 2.2.

In post-combustion capture, CO_2 obtained as a result of combustion of fossil fuel in air is separated from flue gas before releasing it into the atmosphere. Owing to large amount of N_2 in air employed in fuel combustion, this is mainly the separation of CO_2 from CO_2/N_2 gas mixture. Post-combustion capture is considered to be the most feasible technique since it can easily be retrofitted to currently operating power plants and befoul-producing bioreactors. A supplementary benefit of post-combustion capture is to generate power even if CO_2 capture facility is not functioning due to emergency, which is not probable with other complex capture technologies.

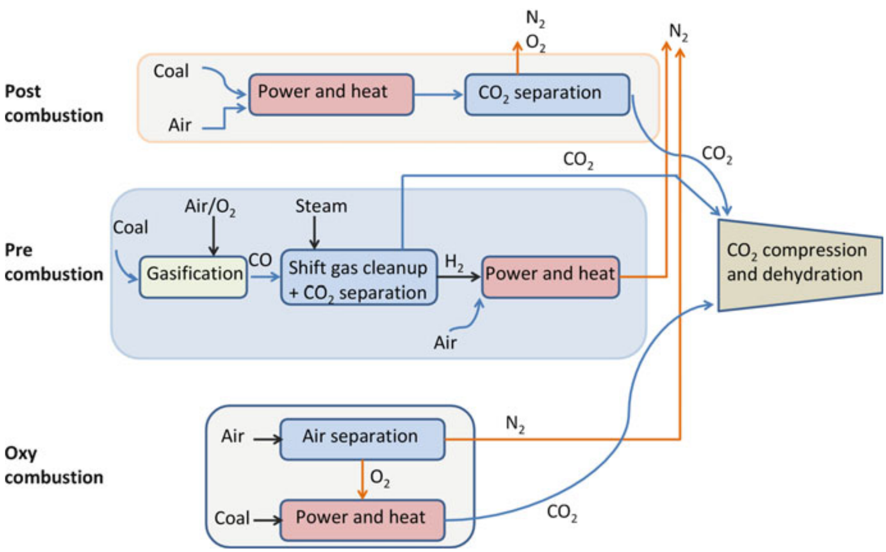

Fig. 2.2 Basic schemes showing the types of CO_2 capture technologies from power generation plants

Table 2.1 Physical properties of gases associated with carbon dioxide capture processes (Sumida et al. 2012)

Gas molecule	Kinetic diameter (Å)	Polarizability (10^{-25} cm^{-3})	Dipole moment (10^{-19} esu^{-1} cm^{-1})	Quadrupole moment (10^{-27} esu^{-1} cm^{-1})
CO_2	3.30	29.1	0	43.0
CO	3.76	19.5	1.10	25.0
N_2	3.64	17.4	0	15.2
H_2O	2.65	14.5	18.5	–
NO_2	–	30.2	0	–
NO	3.49	17.0	1.59	–
O_2	3.46	15.8	0	3.9
H_2	2.89	8.04	0	6.62
H_2S	3.60	37.8	9.78	–

In pre-combustion capture, gasification of a primary fuel such as coal in presence of oxygen or air produces a high-pressure flue gas containing H_2 and CO_2 or in some cases CO, which can subsequently be converted to CO_2 followed by separation of H_2 and CO_2. The separated H_2 is subsequently used for power generation, thus giving only H_2O as the end product. As compared to post-combustion CO_2 capture, pre-combustion process carries the advantage of easier CO_2/H_2 separation and lower energy requirements. The challenges with pre-combustion capture include high capital cost, elevated operating temperature, low process efficiency, and community clash for new construction.

To reduce CO_2 emissions via oxy-fuel combustion, coal or natural gas is combusted using pure O_2 by performing O_2/N_2 separation from air. O_2 separated from air is diluted with CO_2 before combustion, resulting in a flue gas consisting of a mixture of H_2O and CO_2. The gaseous mixture obtained here can be directly stored as almost pure CO_2. However, air separation to render pure O_2, normally obtained via conventional cryogenic process, leads to high capital cost.

All these CO_2 capture techniques involve separation of different gases with varying physical properties. Owing to their singular physical characteristics, gases subjected to separation demand a totally different group of materials' properties for each separation as tabulated in Table 2.1. It helps to realize the significance of materials optimization, necessary to develop the next-generation CO_2 capture materials.

2.2.3 Current Carbon Capture Materials

The main existing CO_2 capture technologies and methods normally applied for CO_2 separation are schematically illustrated in Fig. 2.2. Different types of materials are used as the carriers in each case; cryogenic separation is an exception.

Solvent scrubbing or absorption is a mature CO_2 separation method currently applied in various petroleum and chemical industries. Solvent scrubbing can be accomplished via either physical or chemical absorption. The former scheme efficiently absorbs CO_2 well at low temperature subjected to high pressure, while the latter one effectively works on the basis of acid–base neutralization reaction using caustic solvents. The preferred scrubbing solvents include aqueous alkanolamine solutions (e.g., monoethanolamine, *N*-methyldiethanolamine, 2-amino-2-methyl-1-propanol, piperazine) (David et al. 2011), imidazolium-based ionic liquids (Wappel et al. 2010), Rectisol, Selexol, ammonia solutions, and fluorinated solvents (Mirzaei et al. 2015). Significant drawbacks of aqueous alkanolamine solutions as adsorbents for extensive CO_2 capture include relative instability towards heating, high heat capacity, material decomposition, and equipment corrosion.

Cryogenic distillation, separating CO_2 on the basis of cooling and condensation, seems to be more effective when the gas stream contains high CO_2 concentration (typically >90%) subjected to high pressures and is less suitable for dilute streams. The advantage of this condensation-based CO_2 separating technique is its capability to directly produce liquid CO_2 required for transportation purposes. Main drawbacks of CO_2 separation via cryogenic processes include large energy penalties for refrigeration and removal of some hygroscopic components before cooling the gas stream to avoid blockages.

Adsorption-based gas separation has been well developed; the important consideration for a particular separation involves the selection of a proper adsorbent material. Despite the establishment of appropriate adsorptive materials for gas separation and the availability of a wide variety of handy CO_2-separating adsorbent materials, still the performance optimization of the existing sorbent materials and investigation of novel sorbents is needed. Typical solid adsorbents comprise silica gel, activated carbons, activated alumina, zeolites, ion-exchange resins, metal oxides, mesoporous silicates, and other surface-modified porous media (Sumida et al. 2012). Recently developed CO_2-separating sorbents include metal–organic frameworks (MOFs), carbon fibers, and their composites. A recently designed simple strategy is to convert metal–organic frameworks into controlled porous carbon (Ferey et al. 2011; Li et al. 2016). In order to attain cost-effective CO_2 separation, various adsorption methods can be implemented depending on sorbent restoration methods. Commonly used regeneration methods include temperature swing adsorption, pressure swing adsorption, vacuum swing adsorption, electric swing adsorption, simulated moving bed, and purge displacement.

Gas separation via membranes is accomplished via principles of kinetics (physical size exclusion) and/or thermodynamics (chemical affinity/interaction between gases and the membrane material) so as to allow some components to pass preferentially through the membrane. Membranes find wide prospective applications in post-combustion CO_2/N_2 separation and pre-combustion CO_2/H_2 capture. A wide range of various membrane materials and processes have already been applied on large industrial scale, and other new materials have potential to implement for CO_2 separation. When applied to CO_2 capture on large scale, the cost and separation efficiency of membrane-based technologies mainly depend on the cost of membrane materials themselves. Organic polymeric membranes and inorganic ceramic membranes have already been applied in post-combustion CO_2 separation from flue gas streams. Although feasible in terms of cost, attaining an improved CO_2 separation efficiency using single-stage polymeric or ceramic membrane is not an easy task to accomplish. Novel membrane materials still need to be developed to obtain the required CO_2 separation performance by membranes.

In addition to the aforementioned physical and chemical processes, some biological methods have also been anticipated to capture CO_2 (Benemann 1993). For instance, bio-fixation of CO_2 via algal in photo-bioreactors and via chemo-autotrophic microorganisms using inorganic chemicals has also been investigated to capture CO_2 (Kwak et al. 2006).

The implementation of these techniques on industrial scale greatly depends on the development of capturing materials. Maximizing the separation efficiency at minimum cost coupled with transferring CO_2-capture technology from laboratory to harsh industrial conditions is the main challenge arising in the advancement of these techniques and materials.

2.2.4 Performance Criteria for Carbon Capture Materials

The CO_2-capture materials required for gas- and coal-fired power plants have led to induce the rapid exploration of different types of materials to date. Depending on the definite structure of power plant along with the specific type of CO_2 capture technique, several finely tunable performance parameters need to be considered while developing such materials. Appropriate optimization of these parameters helps to reduce the cost and energy penalty of CO_2 capture processes, thus facilitating extensive application subjected to different scenarios.

High selectivity for CO_2 over other gases is the most critical performance parameter for any CO_2 capture material to ensure complete removal of CO_2 contents from the flue gas. Ratio of CO_2 uptake to the detention of any other gas (typically nitrogen for post-combustion capture and hydrogen for pre-combustion) is characterized as CO_2 selectivity over that gas. Size-based kinetic separation and adsorption-based thermodynamic separation are two dominant mechanisms which give rise to selectivity. Selectivity based on kinetic separation owes to small pores present within membrane structure which allow only smaller molecules to diffuse into the pores, thus separating the molecules based on size difference. In case of post-combustion CO_2/N_2 separation, the controlled gas diffusion through membranes' structure demands tiny pores owing to comparable kinetic diameters of CO_2 and N_2 molecules as displayed in Table 2.1. Selectivity based on thermodynamic adsorption occurs due to the preferential affinity of membrane surface for CO_2 molecules over other constituents of the gas mixture. The specific gas–membrane interaction owes to unique physical properties like polarizability/quadrupole moment of adsorbing gas molecules, which in turn elevates the adsorption enthalpy of certain molecules as compared to others. Incorporating charged groups, for instance, exposed metal cations or polar organic substituents can further improve the selectivity due to polarizability difference of various molecules (Li et al. 2009).

Also the chemical affinity of the capturing material for CO_2 molecules needs to be optimized to lower the energy requirements for its capture. The stronger the material–CO_2 interaction, the higher the energy penalty for desorption of captured CO_2, while the weaker the interactions between material and CO_2 molecules, the lesser the regeneration cost but at the expense of low selectivity for CO_2 over other flue gas components. In addition, the capturing material should be highly stable under the operating conditions of capture and regeneration so as to increase the lifetime of the separation plant. Furthermore, since huge volumes of CO_2 need to be captured from the flue gas, CO_2 take-up of the material should be high so as to minimize the volume of membrane material.

As discussed previously, since none of the aforementioned materials satisfy all of the separation performance criteria, there is an urgent need to develop novel materials which can fulfill all the requirements for efficient CO_2 capture. Mixed-matrix membranes filled with microporous metal–organic frameworks and/or nanomaterials offer an opportunity to develop next-generation optimized materials for real-world applications to capture CO_2. Nonetheless, other kinds of adsorbent materials are also advantageous provided they are optimized to fulfill many of the performance criteria stated above.

2.3 Carbon Capture via Mixed-Matrix Membranes

2.3.1 Metal–Organic Frameworks

During the past decade or so, the synthesis, development, characterization, and applications of a novel class of crystalline porous materials called metal–organic frameworks (MOFs) or three-dimensional porous coordination polymers (PCPs) have been extensively studied to efficiently capture CO_2 from flue gases on account of their high porosity, high gas adsorption capacity, large surface area, tunable pore sizes, and chemical and structural tunability (Kitagawa and Matsuda 2007; Maji and Kitagawa 2007; Stock and Biswas 2012). Metal–organic framework structures are constructed via reticular synthesis by bridging metal-containing nodes (single ions or clusters) with organic ligands through strong coordination bonds to build a one-, two-, or three-dimensional porous crystalline network (Zhou et al. 2012; Furukawa et al. 2013). Topographically and geometrically well-established strong framework structures of metal–organic frameworks let the encompassed guest species to eject, resulting in perpetual porosity. Structurally, metal–organic frameworks can be flexible or rigid: owing to their dynamic frameworks, the former type responds to outside stimulus like temperature, pressure, and guest molecules, whereas later type generally possesses tough established permanent porous structures like activated carbons and zeolites. Absolutely identical and fixed pore size throughout the entire framework structure is a unique feature of metal–organic frameworks as compared to other porous materials.

The liberty to systematically link different combinations of organic linkers and metal nodes has resulted in the development of thousands of metal–organic framework materials in the recent years (Sumida et al. 2012). In addition to their abstract design and actual synthesis to form porous crystalline structures by sensibly linking different building blocks (Zhao et al. 2009; Yuan et al. 2010), the microporous properties and structural features of metal–organic frameworks can be systematically tuned by post-synthetic functionalizing methods (Wang and Cohen 2009) to optimize the essential properties required for particular applications such as selective capture of CO_2. Highly porous metal–organic frameworks can be synthesized by reacting organic linkers and metal salts using cold, hot, microwave, and solid-state synthesis (Klinowski et al. 2011).

Standard synthesis methods are used to prepare MOFs by bridging metal-based nodes through organic ligands to render a crystalline structure having permanent porosity. A number of synthetic techniques under varying conditions of reagent concentrations, reagent ratios, solvent formulations, temperatures, and reaction times have been widely used in the recent years to get the required material (Dey et al. 2014). Slight change in all of these operating conditions plays a vital role to optimize the production of MOF materials. Novel synthesis techniques such as electrosynthetic deposition (Li and Dinca 2011), sonication-assisted synthesis (Thompson et al. 2012), microwave heating (Wu et al. 2014; Burgaz et al. 2019), dry-gel synthesis (Das et al. 2016), sonochemical methods (Hassanpoor et al. 2018), and mechanochemical methods (Klimakow et al. 2010) have also been used to prepare these porous structures. To access all the available surface area and pore volume of MOFs, the void spaces within the pores occupied by solvent molecules are removed by heating under vacuum.

Metal–organic frameworks find numerous applications in molecular gas separation and sequestration, heterogeneous catalysis, drug delivery, super capacitors, fuel cells, and catalytic conversions (Yaghi et al. 2003; Allen et al. 2013). Owing to their large surface areas, adjustable pore surface properties, controllable pore sizes, and prospective scalability to industrial scale, metal–organic frameworks are considered to be the best adsorbents or membrane materials for CO_2 capture and sequestration.

2.3.2 Polymer Membranes

Polymer membranes find carbon-capture applications in numerous industrial gas separation processes for the last few decades (Koros and Mahajan 2000; Ohlrogge and Stürken 2001; Baker 2002). They are used to (i) treat natural gas (CO_2/CH_4 separation), (ii) recover and isolate hydrogen (CO_2/H_2 separation), (iii) enrich oxygen from air (CO_2/O_2 separation), and (iv) enrich nitrogen from air (CO_2/N_2). Vapor recovery (gas recovery from buried waste), monomer recovery (C_2H_4/N_2, C_3H_6/N_2 or olefin/paraffin separation), polar molecules removal from equilibrium

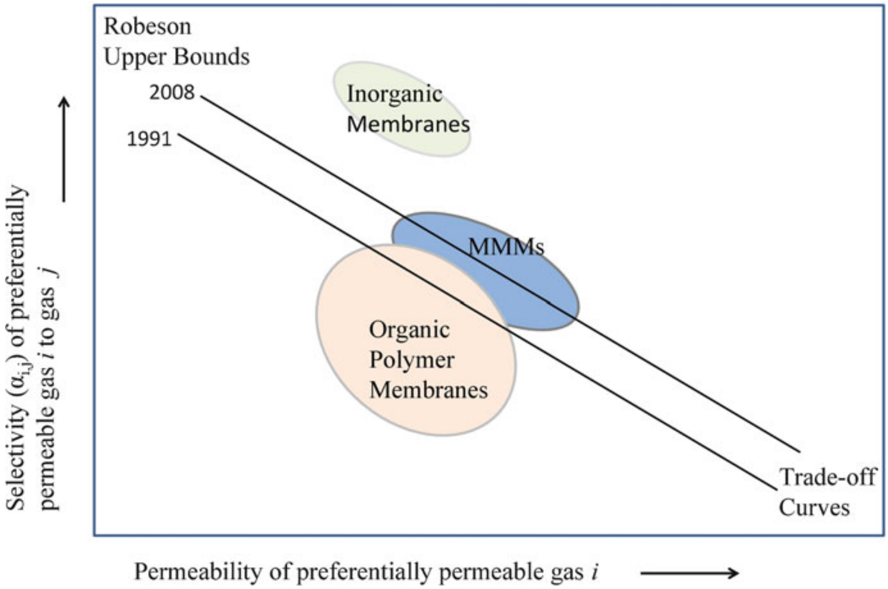

Fig. 2.3 Schematic representation of 1991 and 2008 Robeson trade-off curves between permeability of preferentially permeating CO_2 gas and its selectivity over less permeating gas like N_2 in nonporous membranes (Robeson 2008)

reactions, and organic solvents dehydration (solvent/H_2O separation) are other processes where polymer membranes are being extensively applied.

Owing to its unique and unparallel characteristic features, membrane-based separation technology finds great potential in CCS in contrast to conventional carbon capture processes. Main advantages of membrane-based separation process over other techniques are (i) low capital and operating costs, (ii) compactness and light weight, (iii) low energy requirement, (iv) simple design, (v) relatively easy fabrication of commercial modules, (vi) ease of scalability, (vii) stability at high pressures, (viii) high mechanical and chemical resistances, (ix) ability to integrate multi-processes in single unit, and (x) ease of transportation to remote areas (Basu et al. 2010a).

Membranes rendering gas separation performance close to or above the Robeson 2008 upper bound are considered to be more interesting with respect to economy and technology (Robeson 2008). Pure organic polymer membranes exhibit relatively low gas permeability and selectivity as compared to porous inorganic membranes as shown in Fig. 2.3. Bare polymer membranes can approach but rarely exceed the Robeson upper bound limit. Gas separation performance of polymer membranes needs to be optimized in terms of permeability and selectivity of concerned gas. Gas separation performance of membranes can significantly be improved by developing novel materials as well as introducing advanced fabrication processes to fulfill future demands and challenges related to global warming issues.

2.3.3 Inorganic Membranes

Owing to their high permeability and selectivity, inorganic membranes are developed from porous inorganic materials like ceramics (Smart et al. 2010), carbon (Ismail and David 2001), zeolites or perovskites (Caro and Noack 2008), metal oxides (Basu et al. 2010b), metal–organic frameworks (Gascon et al. 2012), metals and their alloys (Ockwig and Nenoff 2007), and glass (Strathmann 2012). Depending on their pore structure and size, inorganic membranes can be broadly classified into porous and nonporous (dense) membranes. Morphology of microporous inorganic membranes can be crystalline or amorphous.

As compared to polymer membranes, inorganic membranes (like zeolite membranes) have the advantages of high gas permeability and selectivity, excellent thermal and chemical stabilities, good erosion resistance, and high porosity. Complex fabricating steps (e.g., substrate treatment, selective layer deposition, controlled pyrolysis, maintaining inert atmosphere, etc.), reduced reproducibility, less stability, low mechanical resistance, difficult scaling up, and high fabrication cost of inorganic membranes make their fabrication difficult as compared to polymer membranes (Saracco et al. 1999; Strathmann 2012).

2.3.4 Mixed-Matrix Membranes

Inadequacies of both inorganic and polymeric membranes can be compensated and their valuable properties exploited by developing nanomaterial-doped polymer-based mixed-matrix membranes (MMMs) since the properties of both phases directly affect their gas separation performance. Mixed-matrix membranes are fabricated by incorporating nanoparticles of inorganic filler(s) (discrete phase) into a thermoplastic glassy or rubbery polymeric matrix (continuous phase) (Fig. 2.4).

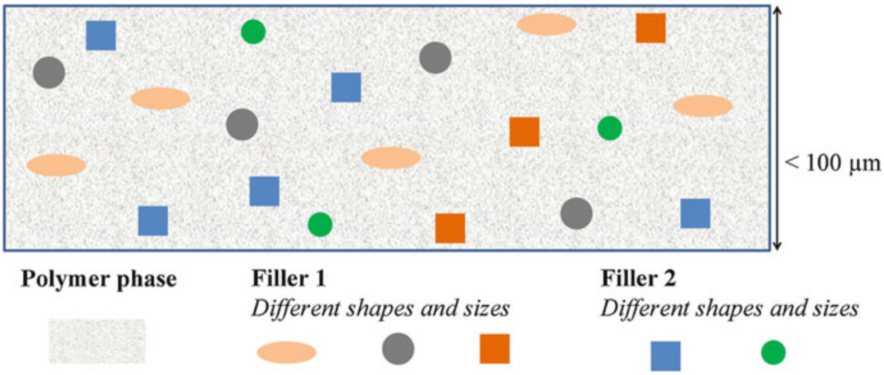

Fig. 2.4 Schematic illustration of a mixed-matrix membrane composed of organic polymer matrix (continuous phase) filled with two different types of inorganic nanofillers (dispersed phase) existing in various possible shapes and sizes

Salient features of fabricating mixed-matrix membranes by doping conventional fillers and/or microporous nanofillers into thermoplastic polymer matrix are the ability to combine the easy and low-cost fabrication, better mechanical strength and chemical resistance of polymers with the improved gas separation efficiency, tunable surface functionalities, and high surface areas of mesoporous nanomaterials (Jeazet et al. 2012). As compared to inorganic membranes, nanomaterials-filled polymer-based mixed-matrix membranes can be economically fabricated and/or easily functionalized to render high surface area membranes possessing improved mechanical, chemical, physical, and thermal properties to withstand harsh environmental conditions. Owing to synergistic effect of combining polymers and nanofillers, mixed-matrix membranes afford an opportunity to achieve gas separation performance closer to Robeson upper bound limit for polymer membranes (Robeson 2008). Good compatibility and effective interfacial adhesion between polymer and filler phases are the prerequisite to make faultless void-free membranes. Other challenges associated with mixed-matrix membranes which need to be addressed include large-scale fabrication, relatively high cost, and occasional fragility as compared to their pure polymer counterparts.

Since their inception in the 1980s, remarkable advancement has been made to improve gas separation performance of mixed-matrix membranes in the last few decades (Chung et al. 2007). A variety of glassy polymers have been filled with inorganic fillers (e.g., mesoporous silicas, carbon nanotubes, layered silicates, activated carbons, metal oxides, zeolites, nonporous solids, etc.) to develop various mixed-matrix membranes (Bae et al. 2010; Zimmerman et al. 1997; Zornoza et al. 2009, 2011a, 2013). The trend of selecting filler material has recently switched to more sophisticated novel microporous nanostructured materials called metal–organic frameworks (MOFs) as prospective nanofillers to be incorporated into polymers to fabricate efficient carbon capture mixed-matrix membranes (Galve et al. 2011). Metal–organic frameworks not only possess high internal porous structure, pore volume, and surface area, but also their chemical nature can precisely be tailored by choosing suitable organic linkers and/or via post-synthetic functionalization techniques. All these characteristic features of metal–organic frameworks make them the foremost carbon-capture materials for a sustainable world.

Right selection of metal–organic framework organic linkers as well as polymer matrix plays a key role to improve the compatibility and adhesion at framework–polymer interface by eliminating boundary imperfections between two phases. Low interfacial compatibility between filler and polymer phases can lead to the formation of nonselective voids at their interface, thus affecting the gas separation performance of fabricated mixed-matrix membranes. Separation efficiency of membranes can further be enhanced by optimizing the fabrication conditions, rheological properties of dope solution, concentration, phase morphology, wettability, and shape and size of the incorporated filler particles. Some proposed guidelines and criteria regarding material selection and fabrication procedures can help to successfully prepare high-performance membranes (Zimmerman et al. 1997; Mahajan and Koros 2000).

Separation performance of membranes can be evaluated in terms of Robeson upper bound plot (Fig. 2.3) which is a trade-off between permeability of key gas (e.g., CO_2) and selectivity of that gas with respect to another gas (e.g., N_2) subjected to standardized experimental conditions. CO_2 separation performance acquired from metal–organic framework-filled polymer-based mixed-matrix membranes is capable to exceed Robeson upper bound limit for most of the CO_2-enriched industrial effluent gas streams.

2.4 Metal–Organic Framework- and Nanomaterials-Based Mixed-Matrix Membranes for Carbon Capture

Metal–organic frameworks (MOFs), a special class of porous materials, find potential applications in carbon capture processes. Gas separation performance of continuous membranes made from pure metal–organic framework materials has not been found appealing except for few metal–organic frameworks (Yoo et al. 2009; Guo et al. 2009; Ranjan and Tsapatsis 2009; Venna and Carreon 2010; McCarthy et al. 2010; Zou et al. 2011). Their low separation efficiency can be ascribed to various factors such as the presence of open channels and morphological defects in membrane structure as well as undesirable orientation and deformation of metal–organic framework crystals. Essential carbon capture potentialities of metal–organic frameworks can be exploited by incorporating them into polymer matrices to fabricate mixed-matrix membranes.

2.4.1 General Considerations in Preparation of Mixed-Matrix Membranes

Owing to their significant advantages over other conventional porous materials, a large number of metal–organic frameworks have been incorporated into various glassy and rubbery polymers to prepare efficient carbon capture mixed-matrix membranes (Noble 2011). For instance, the presence of organic linkers and functionalities on metal–organic frameworks structure render high affinity towards polymer chains as compared to other inorganic fillers. Good affinity between polymer chains and metal–organic framework particles helps to suppress the formation of void spaces at framework-polymer interfaces, thus improving gas selectivity. In addition, metal–organic framework cavities can be finely tuned by adjusting their pore size, shape, and chemical functional groups either by choosing suitable ligands during synthesis (Gascon et al. 2009) or by post-synthesis functionalization (Wang and Cohen 2009). Furthermore, metal–organic frameworks have higher internal pore volume and lower bulk density in contrast to other conventional fillers, thus resulting in overall reduced weight of prepared membranes.

Mixed-matrix membranes can be fabricated by the same techniques as those employed for preparation of bare polymer membranes. Different lab-scale methods to prepare mixed matrix membranes are schematically illustrated in Fig. 2.5.

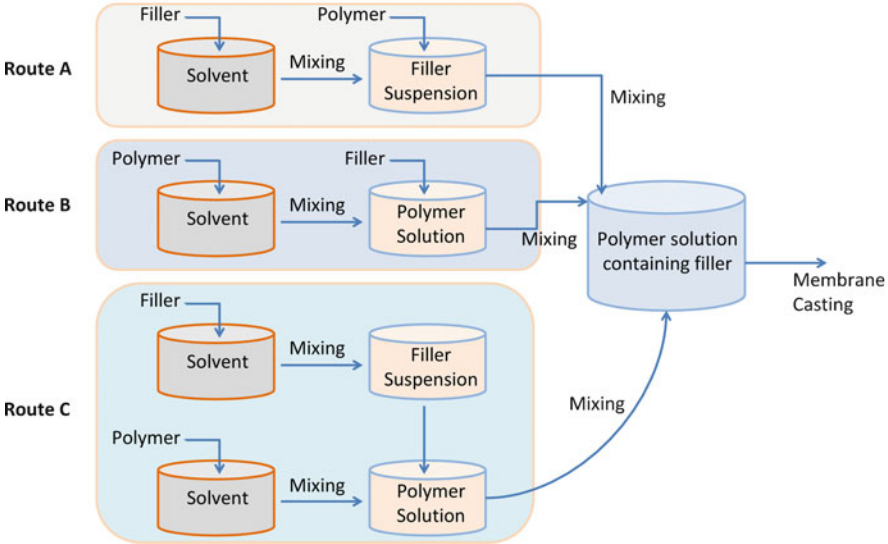

Fig. 2.5 Schematic illustration of lab-scale fabrication methods to prepare mixed-matrix membranes composed of organic polymer matrix and inorganic nanofiller

Polymer-based mixed-matrix membranes containing nanofillers can be fabricated by following either of the three main routes: (i) homogeneous dispersion of nanofiller particles into a suitable solvent followed by addition of polymer (Ismail et al. 2008; Guo et al. 2015; Shen et al. 2016); (ii) dissolution of polymer into a solvent followed by addition of nanofiller particles into the polymer solution (Kim et al. 2007; Ahn et al. 2008); and (iii) separate dissolution of polymer and nanofiller particles in the solvent followed by mixing the two suspensions (Sarfraz and Ba-Shammakh 2018c). Polymer solution containing nanofillers acquired from either of the aforementioned routes can be used to fabricate mixed-matrix membranes via solution casting or spin coating method. Solvent from the prepared membranes can be removed by evaporation and vacuum drying at different temperatures.

Gas separation performance of metal–organic framework-filled mixed-matrix membranes, with reference to the corresponding pure polymer membranes, is assessed in terms of CO_2 permeability and CO_2/N_2 selectivity. Majority of glassy and rubbery polymers have been filled with various metal-organic frameworks and nanomaterials in order to design efficient composite membranes rendering improved gas permeation properties as compared to their pure polymer membranes. Main polymer matrices in combination with different metal-organic frameworks and other nanomaterials used to prepare mixed-matrix membranes are described in this section and summarized in Table 2.2.

Table 2.2 CO_2 permeability (Barrer) and CO_2/N_2 selectivity of common mixed-matrix membranes as measured from permeation experiments performed on single- or mixed-gas feed streams

Polymer matrix	Nanomaterial(s)	CO_2 Permeability (Barrer)	CO_2/N_2 Selectivity	Gas permeation experiment performed on	References
6FDA-DAM	ZIF-94	2310	22	Mixed gas	Benavides et al. (2018)
6FDA-Durene	HKUST-1	1101.6	27.1	Mixed gas	Lin et al. (2016)
	ZIF-8	1192	2.3	Mixed gas	Wijenayake et al. (2013)
6FDA-Durene diamine	ZIF-8	2185	17	Single gas	Nafisi and Hägg (2014)
Matrimid®	Cu-HFS-BIPY	7.2	42	Single gas	Zornoza et al. (2011b)
	HKUST-1	18 GPU	24	Mixed gas	Basu et al. (2011)
	NH_2-MIL-53(Al)	8.2	42	Mixed gas	Sabetghadam et al. (2016)
	JUC-62	30.9	56	Single gas	Prasetya et al. (2018)
	PCN-250	30.7	60	Single gas	
Matrimid®/Polysulfone	HKUST-1	12 GPU	30	Mixed gas	Basu et al. (2010b)
Polydimethylsiloxane/polysulfone	Before swelling	12.7	–	Single gas	Suleman et al. (2016)
	After swelling	4.3	–	Single gas	
PMDA-ODA	HKUST-1	64.9	5.6	Single gas	Hu et al. (2010)
Poly(1-trimethylsilyl-1-propyne)	ZIF-7	28,205	5.5	Mixed gas	Dai et al. (2018)
	TiO_2	16,550	6.6		
	ZIF-8	14,760	6.1		
	ZIF-L	1255	14.9		
Poly(ether block amide)	Unfilled	20% CO_2 recovery	2.2	Mixed gas	Liu et al. (2005)
Poly(vinyl alcohol)/poly(ethylene glycol)	Silica	730	305	Mixed gas	Barooah and Mandal (2018)
Polydimethylsiloxane	Unfilled	2950	10.6	Mixed gas	Russo et al. (2017)
	Silica	8.17 $kg/m^2 \cdot h$	36	Single gas	Ataeivarjovi et al. (2018)
	CNTs	1970	6.9	Single gas	Silva et al. (2017)
Polyetherimide	Unfilled	1943 GPU	10.8	Single gas	Ahmad et al. (2017)

(continued)

Table 2.2 (continued)

Polymer matrix	Nanomaterial(s)	CO_2 Permeability (Barrer)	CO_2/N_2 Selectivity	Gas permeation experiment performed on	References
Polyethyleneimine/PVAm	ZIF-8	1990 GPU	79.9	Mixed gas	Gao et al. (2018)
Polyimide	Graphene oxide	12.3	38.6	Single gas	Ge et al. (2018)
Polyimide/ polydimethylsiloxane	Cross-linked by piperazinium	800	16	Mixed gas	You et al. (2018)
Polysulfone	HKUST-1	Optimum	Optimum	Single gas	Venna and Carreon (2010)
	ZIF-8	950 GPU	112	Mixed gas	Gong et al. (2017)
	ZIF-301	21.4	22.7	Single gas	Sarfraz and Ba-Shammakh (2016a)
	S1C	9.4	23	Mixed gas	Zornoza et al. (2011a)
	HKUST-1	9.5	24	Mixed gas	Zornoza et al. (2011a)
	ZIF-8	12.2	19	Mixed gas	Zornoza et al. (2011a)
	ZIF-301 + CNTs	19	48	Single gas	Sarfraz and Ba-Shammakh (2018c)
	ZIF-302 + CNTs	18	35	Single gas	Sarfraz and Ba-Shammakh (2018c)
	HKUST-1 + S1C	8.4	38	Mixed gas	Zornoza et al. (2011a)
	S1C + ZIF-8	7.6	14.4	Mixed gas	Zornoza et al. (2011a)
	ZIF-301 + GO	25	63	Single gas	Sarfraz and Ba-Shammakh (2016c)
	ZIF-302 + GO	13	25	Single gas	Sarfraz and Ba-Shammakh (2016d)
Polyurethane	SAPO-34	0.5	59	Single gas	Sodeifian et al. (2018)
Polyvinylacetate	Cu(BDC)	3.3	35	Single gas	Adams et al. (2010)
PVC/Pebax	Unfilled	76	56	Single gas	Khalilinejad et al. (2017)
	Silica gel	107	61	Single gas	

SPEEK	MIL-101	2490	80	Mixed gas	Xin et al. (2015)
Ultem®	NH_2-MIL-53	30.9 GPU	34.7	Single gas	Zhu et al. (2017)
Ultrason®	ZIF-300	27.8	26.1	Single gas	Sarfraz and Ba-Shammakh (2018a)
	ZIF-302	13.2	32.1	Single gas	Sarfraz and Ba-Shammakh (2018b)
	ZIF-300 + GO	20	63	Single gas	Sarfraz and Ba-Shammakh (2018d)

2.4.2 Polysulfone-Based Mixed-Matrix Membranes

Microporous metal–organic framework Cu-BTC or HKUST-1 having chemical formula Cu_3(benzene-1,3,5-tricarboxylate)$_2$(H_2O)$_3$ has been intensively studied in the preparation of mixed-matrix membranes due to its thermal stability up to 240 °C (Venna and Carreon 2010; McCarthy et al. 2010). Physisorption of gas molecules to copper metal-sites leads to high CO_2 adsorption under a pressure of few bars. Mixed-matrix membranes prepared by incorporating varying amounts of HKUST-1 into glassy polymer polysulfone (PSF) imparted gradual improvement in CO_2 permeability with raising HKUST-1 loading up to 10 wt %. Composite membrane filled with 5 wt % HKUST-1 depicted an optimized ideal CO_2/N_2 selectivity compared to pure polysulfone membrane. Further increase in HKUST-1 loadings resulted in reduced CO_2/N_2 selectivity.

Zeolitic imidazolate framework (ZIF)-based mixed-matrix membranes have been prepared by incorporating mesoporous ZIF-8 particles into polysulfone matrix to assess their CO_2 permeation properties by gas permeation experiments (Gong et al. 2017). Addition of ZIF-8 into polysulfone resulted in significant improvement in CO_2 permeability due to increase in gas diffusion and solubility within the membrane structure.

Addition of water stable ZIF-301 into polysulfone matrix significantly improved CO_2 permeation properties of resulting composite membranes (Sarfraz and Ba-Shammakh 2016a). As compared to CO_2 permeability of 6.3 Barrer and CO_2/N_2 ideal selectivity of 26.3 for bare polysulfone membrane, the CO_2 permeability of ZIF-301/PSF mixed-matrix membrane was increased to 21.4 Barrer at the expense of reduced CO_2/N_2 ideal selectivity dropping to 22.7 for 40% filler loading. The improved gas separation performance can mainly be attributed to chabazite-type structural topology of ZIF-301 nanocrystals showing great chemical affinity for quadrupolar CO_2 molecules as compared to nonpolar N_2 molecules.

Addition of water stable ZIFs such as ZIF-300 and ZIF-302 into commercial grade of polysulfone, namely, Ultrason® (US), greatly enhanced CO_2 permeation properties of resulting membranes (Sarfraz and Ba-Shammakh 2018a; Sarfraz and Ba-Shammakh 2018b). In contrast to CO_2 permeability of 6.2 Barrer and CO_2/N_2 ideal selectivity of 26.1 for neat Ultrason® membrane, the CO_2 permeability of ZIF-300/Ultrason® and ZIF-302/Ultrason® mixed-matrix membranes was found to 27.8 and 13.2 Barrer, respectively, with corresponding CO_2/N_2 expected selectivities of 26.1 and 32.1 for 40% filler loading in each case. Enhanced gas separation performance can largely be ascribed to chabazite-type structural topology of ZIF particles showing high chemical affinity for CO_2 molecules as compared to N_2 molecules.

Different combinations of metal–organic frameworks, e.g., HKUST-1 and ZIF-8, and zeolites, e.g., silicate-1 (S1C), were synergistically added to polysulfone matrix to prepare a variety of mixed-matrix membranes to investigate separation performance of CO_2/N_2 gas mixture (Zornoza et al. 2011a). In contrast to CO_2 permeability of 5.9 Barrer for pure polysulfone membrane, the CO_2 permeability of composite membranes doped with only one filler such as S1C/PSF, HKUST-1/PSF, and ZIF-8/

PSF mixed-matrix membranes were raised to 9.4, 9.5, and 12.2 Barrer, respectively, with corresponding CO_2/N_2 selectivities of 23, 24, and 19. On the contrary, mixed-matrix membranes filled with two fillers having total loading of 16 wt % demonstrated significant improvement in CO_2 permeability due to synergetic effect of adding both fillers. Both the CO_2 permeability and CO_2/N_2 selectivity of HKUST-1/S1C/PSF mixed-matrix membrane were increased to 8.4 Barrer and 38, respectively. CO_2 permeability of composite membrane containing S1C and ZIF-8 fillers was increased to 7.6, but the CO_2/N_2 selectivity was dropped to 14.4. Addition of fillers into polysulfone matrix widens the polymer inter-chain spacing and increases its free volume, thus resulting in an improvement of permeation properties of composite membranes. In addition, different surface chemistry of the fillers leads to their proper distribution and good adhesion with the polymer matrix.

Collegial impact of adding nanoparticles of water-stable ZIFs such as ZIF-301 and ZIF-302 along with carbon nanotubes (CNTs) into polysulfone matrix leads to improve CO_2 separation performance of fabricated membranes (Sarfraz and Ba-Shammakh 2016b; Sarfraz and Ba-Shammakh 2018c). As compared to CO_2 permeability of 6.4 Barrer determined for bare polysulfone membrane, the CO_2 permeability of ZIF-301/CNTs/PSF composite membrane was promoted to 19 Barrer with corresponding ideal CO_2/N_2 selectivity of 48 when filled with an optimal loading of 6 wt % carbon nanotubes and 18 wt % ZIF-301 nanoparticles. CO_2 permeability and ideal CO_2/N_2 selectivity of ZIF-302/CNTs/PSF hybrid membrane containing 8 wt % carbon nanotubes and 12 wt % ZIF-302 were improved to 18 Barrer and 35, respectively. Smooth internal pores of carbon nanotubes resulted in an improvement of CO_2 permeability, whereas the high affinity of amine-containing ZIF-302 nanocrystals for quadrupolar CO_2 molecules as compared to nonpolar N_2 molecules resulted in high CO_2/N_2 selectivity. Gas permeation experiments performed under wet conditions did not influence CO_2 permeability and CO_2/N_2 ideal selectivity.

CO_2 separation performance of water-stable composite membranes was substantially improved due to harmonious interaction of hydro-stable ZIF-300 nanoparticles and graphene oxide (GO) nanosheets synergistically added to Ultrason® (US) matrix (Sarfraz and Ba-Shammakh 2018d). In contrast to pure Ultrason® membrane, values of both the CO_2 permeability and CO_2/N_2 ideal selectivity were improved by almost three times when filled with an optimum loading of 30 wt % ZIF-300 nanoparticles and 1 wt % graphene oxide nanosheets in ZIF-300/GO/US composite membranes. Again the gas permeation properties were not affected by performing experiments under moist conditions.

High-performance membranes offering excellent enhancement both in CO_2 permeability and CO_2/N_2 selectivity were prepared by synergistically incorporating highly selective nanosheets of graphene oxide (GO) in combination with hydro-stable ZIF-301 or ZIF-302 in polysulfone matrix (Sarfraz and Ba-Shammakh 2016c, d). CO_2 permeability and CO_2/N_2 ideal selectivity of ZIF-301/GO/PSF mixed-matrix membrane containing 30 wt % ZIF-301 nanoparticles and 1 wt % graphene oxide nanoplates were respectively increased by almost 4 and 3 times as compared to bare polysulfone membrane. As compared to bare polysulfone membrane, both the

CO_2 permeability and CO_2/N_2 ideal selectivity were doubled for ZIF-302/GO/PSF mixed-matrix membrane filled with an optimum loading of 1 wt % graphene oxide nanoplates and 30 wt % ZIF-302 nanoparticles under dry and wet experimental conditions. High chemical affinity of ZIF-302 nanocrystals for CO_2 as compared to N_2 resulted in an increase in CO_2 permeability. The layered structure of graphene oxide nanosheets generated sieving effect allowing smaller CO_2 molecules to pass through the membrane while rejecting relatively larger N_2 molecules, consequently improving ideal CO_2/N_2 selectivity.

2.4.3 Polyimide-Based Mixed-Matrix Membranes

Carbon capture performance of composite membranes prepared by incorporating microporous crystalline metal–organic framework Cu-HFS-BIPY (4,4′-bipyridine-hexafluorosilicate copper(II)) into glassy polyimide Matrimid® matrix was assessed in terms of CO_2 permeability and CO_2/N_2 ideal selectivity by performing permeation experiments on single gases (Zornoza et al. 2011b). As compared to pure Matrimid® membrane, the CO_2 permeability through fabricated mixed-matrix membranes was considerably enhanced while ideal CO_2/N_2 selectivity was dropped due to the addition of Cu-HFS-BIPY crystals into Matrimid®.

Various hybrid membranes based on HKUST-1 ($Cu_3(BTC)_2$) were fabricated by adding microporous crystals of HKUST-1 either to pure Matrimid® or to a Matrimid®/polysulfone blend in 3:1 ratio by weight (Basu et al. 2010b, 2011). Mixed-gas permeation experiments performed over CO_2-N_2 binary gas mixtures containing 10–75 vol % CO_2 showed noticeable improvement in CO_2 permeance and CO_2/N_2 selectivity with filler loading as compared to unfilled membranes made from pure Matrimid® or Matrimid®/polysulfone blend. On adding 30 wt % HKUST-1 crystals in each case, CO_2 permeance of bare Matrimid® membrane increased from 10 GPU to 18 GPU, while that of the blend membrane raised from 7 GPU to 12 GPU as measured at 35 °C under 10 bar for a 35/65 vol % CO_2-N_2 binary gas mixture. Improved gas permeation taking place via diffusion mechanism can be assigned to higher chain mobility as well as pore volume expansion due to addition of porous HKUST-1 crystals.

CO_2 separation performance of polyetherimide (PEI) Ultem® 1000 matrix can significantly be improved by adding metal–organic framework MIL-53 and its amino-functionalized derivative NH_2-MIL-53 (Zhu et al. 2017). As compared to non-functionalized MIL-53, loading levels of functionalized NH_2-MIL-53 crystals as high as 15 wt % can be added to Ultem® 1000 matrix most probably due to the formation of hydrogen bonding between imide groups available on Ultem® 1000 matrix and amine groups present on MIL crystals. Functionalized MIL-53 rendered outstanding gas permeance properties: as compared to CO_2 permeance of 12.2 GPU and CO_2/N_2 ideal selectivity of 25.4 for bare Ultem® membrane, CO_2 permeance and CO_2/N_2 ideal selectivity were respectively raised to 30.9 GPU and 34.7. Solution-diffusion mechanism of gas transport through prepared composite membranes helped to increase CO_2 permeance and decrease CO_2/N_2 selectivity with increasing temperature.

High-performance membranes, rendering outstanding improvement in CO_2 permeability and CO_2/N_2 ideal selectivity as compared to pristine sulfonated poly(ether ether ketone) (SPEEK) membrane, can be prepared by incorporating water-stable MIL-101 crystals immobilized in PEI matrix (Xin et al. 2015). These hydro-stable mixed-matrix membranes, in contrast to bare SPEEK, showed a remarkable increase in CO_2 permeability and CO_2/N_2 selectivity for 40% loading of MIL-101 crystals. High loading levels of MIL-101 crystals in SPEEK matrix are achievable due to good adhesion and compatibility between MIL-101 particles and polymer chains in the resulting mixed-matrix membranes. SPEEK/PEI@MIL-101(Cr) mixed-matrix membranes showed outstanding long-term stability and very high CO_2 permeabilities as compared to other metal–organic framework-based mixed-matrix membranes (Robeson 2008).

Mixed-matrix membranes fabricated by addition of MIL-53(Al) crystals with different morphologies to Matrimid® matrix displayed improved CO_2 permeance in contrast to pure Matrimid® membrane (Sabetghadam et al. 2016). Gas permeation properties of composite membranes comprising 5–20 wt % of MIL-53(Al) crystals were tested by performing gas permeation experiments. CO_2 permeance through prepared membranes considerably improved with increasing loadings of all three types of MIL-53(Al).

Composite membranes prepared by exclusive incorporation of light-responsive JUC-62 and PCN-250 metal–organic frameworks into Matrimid® matrix were investigated to determine their post-combustion carbon capture performance by conducting gas permeation experiments on a custom-designed membrane testing cell (Prasetya et al. 2018). As compared to most of the available metal–organic framework-Matrimid® mixed-matrix membranes, CO_2 permeability and CO_2/N_2 ideal selectivity of Matrimid®-based mixed-matrix membranes containing 15 wt % of light-responsive metal–organic frameworks were significantly improved. Assessment of their long-term separation performance indicated that mixed-matrix membranes fabricated by adding both types of metal–organic frameworks were able to sustain their permeation properties for a month except Matrimid®-based composite membrane containing 10 wt % PCN-250 filler for which CO_2 permeability was observed to decrease slightly.

Glassy polyimide PMDA-ODA, made by combining PMDA (pyromellitic dianhydride) and ODA (4,4′-oxydianiline) together, was filled with microporous crystals of HKUST-1 to fabricate CO_2-separating hybrid membranes (Hu et al. 2010). Owing to homogeneous filler dispersion and good interfacial adhesion between polymer and filler phases, the prepared membranes were able to be spun into hollow fibers via dry/wet spinning method. Single-gas permeation experiments performed over prepared membranes at 25 °C and 1 MPa indicated significant improvement in CO_2 permeance as well as CO_2/N_2 ideal selectivity of PMDA-ODA/HKUST-1 hollow-fiber membranes with increasing HKUST-1 loading as compared to pristine PMDA-ODA membrane.

High-performance membranes obtained by evenly distributing nanocrystals of ZIF-94 within a highly permeable polyimide 6FDA-DAM

(4,4′-hexafluoroisopropylidene diphthalic anhydride- diaminomesitylene) matrix displayed high potential for post-combustion CO_2 capture applications (Benavides et al. 2018). In contrast to pure 6FDA-DAM membrane, the prepared composite membranes filled with ZIF-94 nanocrystals exhibited significant improvement in CO_2 permeability without affecting CO_2/N_2 permselectivity as established by mixed-gas (CO_2:N_2:: 15:85) permeation experiments performed at 298 K subjected to a transmembrane pressure difference of 1–4 bar. Addition of ZIF-94 nanoparticles into 6FDA-DAM polymer substantially increased CO_2 permeability while upholding a fixed CO_2/N_2 permselectivity of about 22. CO_2 permeability of fabricated mixed-matrix membrane was almost doubled when the polymer was loaded with 40 wt% ZIF-94 nanocrystals.

Mixed-matrix membranes consisting of 6FDA-Durene (4,4-′-hexafluoroisopropylidene diphthalic anhydride-2,3,5,6-tetramethyl-1,3-phenyldiamine) matrix were fabricated by incorporating microparticles of HKUST-1 immobilized with thin layer of ionic liquid (Lin et al. 2016). Thin-layered coating of ionic liquid on HKUST-1 particles helped to improve metal–organic framework–polymer affinity in membrane structure by eliminating nonselective voids at polymer–filler interface. The role of ionic liquid as a binder promoted metal–organic framework–liquid and liquid–polymer interactions, which improved the overall metal–organic framework/polymer interfacial adhesion and restricted the creation of nonselective voids at metal–organic framework/polymer interface. Both CO_2 permeability and CO_2/N_2 selectivity of (6FDA-Durene)-based mixed-matrix membranes filled with liquid-coated HKUST-1 particles were significantly improved in comparison to (6FDA-Durene)-based mixed-matrix membranes filled with uncoated HKUST-1 particles.

Mixed-matrix membranes fabricated by incorporating varying loadings of microporous ZIF-8 crystals into cross-linked 6FDA-Durene significantly improved CO_2 permeability as measured by single gas permeation experiments performed at 35 °C and 3.5 bar (Wijenayake et al. 2013). As compared to unfilled 6FDA-Durene membrane, CO_2 permeability of 6FDA-Durene-based composite membrane comprising 33.3 wt % ZIF-8 crystals was almost doubled with slight increase in CO_2/N_2 selectivity.

Hybrid membranes based on polyimide 6FDA-Durene diamine were prepared by filling it with varying loadings of inorganic crystals of ZIF-8 (Nafisi and Hägg 2014). Permeation properties of CO_2 and N_2 gases through fabricated composite membranes were determined by performing experiments on single as well as mixed gas feed streams. Single gas (CO_2 or N_2) permeation tests were carried out at two different upstream pressures of 2 and 6 bar, while CO_2/N_2 gas mixture was tested at an upstream pressure of 2.6 bar. Uniform distribution of ZIF-8 crystals in polymer matrix, as corroborated by SEM micrographs, leads to considerable improvement in CO_2 permeability from 1468 Barrer for unfilled polymer membrane to 2185 Barrer for composite membrane containing 30 wt% ZIF-8 particles for a feed pressure of 2 bar. CO_2/N_2 selectivity of mixed-matrix membranes filled with ZIF-8 crystals was slightly dropped due to broadening of void spaces of membrane structure.

The effect of functionalization of graphene oxide (GO) on gas permeation properties of polyimide-based membranes was assessed by testing hybrid membranes prepared by doping polyimide (PI) matrix with pristine and aminated graphene oxide nanosheets (Ge et al. 2018). Pristine GO/PI mixed-matrix membranes were fabricated by conventional solution casting method, while amine-functionalized GO/PI mixed-matrix membranes were prepared via novel in situ polymerization method. Aminated GO/PI mixed-matrix membranes were prepared by dispersing ethylenediamine-functionalized graphene oxide nanoplates into polyimide precursor (poly(amic acid) solution) followed by chemical imidization. Use of in situ polymerization technique improved graphene oxide–polyimide interfacial interaction as well as homogeneous distribution of graphene oxide nanoplates dispersion in polyimide matrix as indicated by SEM micrographs. As compared to pristine GO/PI mixed-matrix membranes, both CO_2 permeability and CO_2/N_2 selectivity of aminated GO/PI mixed-matrix membranes were drastically improved due to the presence of amino groups on functionalized graphene oxide nanosheets. Owing to their intrinsically basic nature, amino groups have high affinity for quadrupolar acidic CO_2 molecules over nonpolar N_2 molecules, which results in considerable improvement in solubility and permeability of CO_2 gas molecules. Maximum CO_2 permeability of 12.3 Barrer and CO_2/N_2 selectivity of 38.6 were obtained for composite membrane containing 3 wt% aminated graphene oxide nanosheets.

2.4.4 Polydimethylsiloxane-Based Mixed-Matrix Membranes

A flexible polymer membrane for carbon capture applications fabricated from pure polydimethylsiloxane (PDMS) rubber rendered much improved CO_2 separation performance as compared to other polymer-based membranes (Sadrzadeh et al. 2010). Permeation, sorption, and diffusion properties of CO_2 and N_2 gases through prepared membrane were analyzed at 35 °C under different feed-side pressures. The fabricated membrane was found to be more permeable to CO_2 as compared to N_2. Gas sorption and diffusion data obtained from permeation experiments were used to estimate Flory–Huggins (FH) interaction parameters as well as coefficients of diffusion and solubility.

Mixed-matrix membranes fabricated by adding different loadings of HKUST-1 into rubbery polymer polydimethylsiloxane showed considerable improvement in CO_2 permeability with slight increase in ideal CO_2/N_2 selectivity. CO_2 separation performance was decreased with further loading of the filler (Chui et al. 2007).

Clinoptilolite zeolites, in its different cationic forms such as H, Na, K, and Mg, were incorporated in polydimethylsiloxane matrix to fabricate zeolite-based mixed-matrix membranes for carbon capture applications (Oral 2018). Gas permeation experiments indicated that incorporation of clinoptilolite into polydimethylsiloxane significantly improved both CO_2 permeability and CO_2/N_2 ideal selectivity as compared to pure polydimethylsiloxane membrane. Furthermore the permeation tests helped to determine the optimum loading of zeolite filler rendering maximum

CO_2 permeability through prepared membranes. CO_2 permeability and CO_2/N_2 selectivity of the zeolite-filled mixed-matrix membranes were affected by the presence of different types of cationic forms of clinoptilolite filler.

Varying concentrations of multi-walled carbon nanotubes were incorporated into polydimethylsiloxane rubber to fabricate high permeation composite membranes for efficient CO_2 separation (Silva et al. 2017). Gas permeation experiments performed over CO_2 and N_2 gases indicated slight improvement in CO_2/N_2 ideal selectivity, as compared to pure polydimethylsiloxane, but at the cost of reduced CO_2 permeability when filled with 1% carbon nanotubes. CO_2 permeability kept on improving, while CO_2/N_2 ideal selectivity continuously declined with increasing carbon nanotubes contents up to 6.7 wt % due to enhanced gas transport through membrane structure occurring via diffusion mechanism.

Copolymers comprising low permeable rigid glassy polyimide (major component) and highly permeable rubbery polydimethylsiloxane (minor component) were synthesized and cross-linked by CO_2-philic ionic piperazinium groups (You et al. 2018). Membranes fabricated from cross-linked copolymers (xPIPDMSs) rendered excellent CO_2 permeability of about 800 Barrer and CO_2/N_2 permselectivity of about 16. Incorporation of cross-linking piperazinium groups highly enhanced thermochemical stability of copolymer membranes on account of their improved resistance to CO_2 plasticization.

Microporous inorganic silica (SiO_2) nanoparticles were incorporated into rubbery polydimethylsiloxane (PDMS) matrix to prepare PDMS-SiO_2 composite membranes (Ataeivarjovi et al. 2018). Experiments performed on prepared membranes showed that an increase in silica contents from 1.5 to 3 wt % largely improved CO_2 flux from 1.7 to 5.38 kg/m^2·h while dropping CO_2/N_2 selectivity from 94 to 47. Best CO_2 separation performance of PDMS-SiO_2 mixed-matrix membranes was achieved when filled with 10 wt % silica nanoparticles. CO_2 permeability was further increased, at the expense of reduced CO_2/N_2 selectivity, by elevating the operating temperature. The maximum permeability value of 8.17 kg/m^2·h was attained at 40 °C for 10% contents of silica particles; correspondingly the CO_2/N_2 selectivity was dropped to about 36. Inclusion of silica nanoparticles into polydimethylsiloxane matrix to prepare PDMS-SiO_2 mixed-matrix membranes improved both the CO_2 separation performance and process economy in contrast to conventional gas stripping process.

Separation efficiency of rubbery polydimethylsiloxane membranes to separate CO_2 from CO_2–N_2 mixtures was studied by performing gas permeation experiments on a bench-scale membrane module which is capable to separate CO_2–N_2 binary gas mixtures having 5–20% CO_2 by volume (Russo et al. 2017). Permeation properties of pure CO_2 and N_2 gases as well as their binary mixtures through polydimethylsiloxane membrane investigated at different feed pressures, varying compositions of feed gas, and using N_2 as sweep gas indicated an average CO_2 permeability of about 2950 Barrer. By varying the feed pressure in the range 1–2.4 bar, CO_2 permeability was marginally changed. A maximum CO_2/N_2 permselectivity of 10.55 was obtained for a CO_2–N_2 binary mixture having 10% CO_2 by volume for a feed pressure of 1.8 bar. A real post-combustion flue gas produced by burning of natural gas was analyzed on a pilot-scale polydimethylsiloxane membrane module to assess the potentiality of prepared polydimethylsiloxane membrane system in carbon-capture applications.

2.4.5 Miscellaneous Polymer-Based Mixed-Matrix Membranes

Mixed-matrix membranes consisting of low-T_g glassy polyvinylacetate (PVAc) were prepared to attain a faultless void-free ideal morphology by resolving the problem of non-ideal morphological behavior at microporous filler-polymer matrix interface (Adams et al. 2010). In contrast to membrane fabricated from unfilled PVAc matrix, mixed-matrix membranes prepared by incorporating microporous crystals of metal–organic framework Cu(BDC) having chemical formula (Cu_3(benzene-1,4-dicarboxylate)$_2$) into PVAc significantly improved their carbon capture efficiency as established by gas permeation experiments performed at 4.5 bar and 35 °C. 34% increase in CO_2 permeability and 10% increase in CO_2/N_2 ideal selectivity were obtained for PVAc-based composite membrane filled with 15 wt % Cu(BDC) crystals. Improved metal–organic framework-polymer interfacial adhesion and controlled pore size of metal–organic framework structure lead to improve gas separation performance of fabricated membranes.

High-performance carbon-capture poly(vinyl chloride) (PVC)-based ultrafiltration composite membranes were developed by coating thin films of Pebax 1657 (poly(ether-block-amide)) and nanoparticles of hydrophobic/hydrophilic silica gel (Khalilinejad et al. 2017). SEM micrographs confirmed successful deposition of 4-μm-thick nonporous faultless dense layer as well as homogeneous distribution (up to 8 wt% loading) of silica nanoparticles in Pebax matrix. Increasing contents of silica nanoparticles in polymer matrix resulted in an increased CO_2 permeability and ideal CO_2/N_2 selectivity as measured by gas permeation tests performed at 25 °C and 1 bar. Improved gas separation performance of prepared membranes can be associated with enhanced CO_2 solubility governed by the chemical nature (hydrophilic and hydrophobic) of silica nanoparticles dispersed in Pebax matrix. As compared to bare Pebax membrane having CO_2 permeability of 76 Barrer and ideal CO_2/N_2 selectivity of 56, corresponding values of Pebax/PVC membrane containing 8 wt% contents of hydrophilic silica nanoparticles were found to be 124 Barrer and 76, respectively. CO_2 permeability and ideal CO_2/N_2 selectivity of Pebax/PVC membrane filled with 8 wt% loading of hydrophobic silica nanoparticles were measured to be 107 Barrer and 61, respectively. In addition, the gas separation performance of prepared composite membranes was improved with increasing feed-side pressure (1–10 bar) due to plasticization of membrane structure. Furthermore, increasing temperature (25–50 °C) results in an increase in CO_2 permeability and a drop in ideal CO_2/N_2 selectivity on account of increased polymer chain mobility.

Polyurethane (PU)-based mixed-matrix membranes were prepared by incorporating different loadings of zeolite silicoaluminophosphate (SAPO-34) particles into polyurethane matrix to explore permeation properties of CO_2 and N_2 gases (Sodeifian et al. 2018). Increasing contents of SAPO-34 nanoparticles resulted in improved ideal CO_2/N_2 selectivity with slight drop in CO_2 permeability as indicated by gas permeation tests carried out on PU/SAPO-34 mixed-matrix membranes filled with 5, 10, and 20 wt% loadings of SAPO-34 filler. As compared to bare polyurethane membrane, 4.5% reduction in CO_2 permeability, and 37.5% increase in CO_2/N_2 selectivity was achieved by PU/SAPO-34 hybrid membrane containing optimum loading (20 wt%) of SAPO-34 particles at a feed-side pressure of 12 bar.

Incompatibility issues arising at metal–organic framework–polymer interface in mixed-matrix membranes structure can be resolved by grafting hyperbranched chains of polyethyleneimine (PEI) and microporous nanocrystals of ZIF-8 at room temperature to synthesize PEI-g-ZIF-8 nanoparticles via in situ synthesis technique (Gao et al. 2018). PEI-g-ZIF-8 nanoparticles were deposited on poly(vinylamine) (PVAm) substrate to develop high performance mixed-matrix membrane indicating improved compatibility at PVAm/PEI-*g*-ZIF-8 interface. Owing to its aminated nature and high pore volume, PVAm/PEI-*g*-ZIF-8 composite membrane rendered a CO_2 permeance of 1990 GPU and CO_2/N_2 permselectivity of 79.9 under a mixed-gas (15% CO_2/85% N_2 by volume) feed pressure of 0.30 MPa.

High-performance CO_2-selective composite membranes were prepared via solution casting method by incorporating different loadings of hydrophilic silica (SiO_2) nanoparticles into a mixed-polymer matrix that comprised poly(vinyl alcohol) (PVA) and poly(ethylene glycol) (PEG) (Barooah and Mandal 2018). SiO_2 nanoparticles synthesized through in situ sol–gel method were homogeneously dispersed into PVA/PEG matrix due to good interfacial compatibility between SiO_2 nanoparticles and polymer matrix. Owing to better filler-polymer interaction, incorporation of SiO_2 nanoparticles into PVA/PEG matrix led to reasonable improvement in CO_2 separation performance. In contrast to bare PVA/PEG membrane, CO_2 permeability and CO_2/N_2 selectivity of PVA/PEG/SiO_2 mixed-matrix membranes containing 3.34 wt % SiO_2 contents were improved by 78 and 45%, respectively, at 100 °C subjected to set experimental conditions.

Exceptionally highly permeable pristine poly(1-trimethylsilyl-1-propyne) (PTMSP) membrane finds limited application in carbon capture processes due to low CO_2/N_2 selectivity and aging issues caused by its high internal free volume and large void spaces. CO_2 separation performance of bare PTMSP membrane can be improved by preparing mixed-matrix membranes consisting of inorganic nanoparticles incorporated in PTMSP matrix (Dai et al. 2018). CO_2 separation performance of composite membranes fabricated by doping PTMSP matrix with different nanofillers (such as TiO_2, ZIF-7, ZIF-8, and ZIF-L) was assessed by performing mixed-gas permeation experiments in presence of water vapor in order to imitate real flue gas situation. Permeation tests indicated that CO_2 separation performance of prepared membranes strongly depends on the type of filler added to PTMSP matrix: the incorporation of ZIF-7, ZIF-8, and TiO_2 nanofillers led to improve CO_2 permeability at the expense of reduced CO_2/N_2 permselectivity, while the addition of 2-dimensional microporous ZIF-L filler enhanced CO_2/N_2 permselectivity with reduced CO_2 permeability.

2.4.6 Polymer-Based Asymmetric Composite Membranes

An asymmetric polydimethylsiloxane/polysulfone composite membrane was developed by dip coating of polydimethylsiloxane over polysulfone membrane via phase inversion method (Suleman et al. 2016). Scanning electron microscopic (SEM) images of developed membranes established asymmetric micro-structural morphology of polysulfone membrane having dense polydimethylsiloxane coating layer over it. Swelling resistivity of polydimethylsiloxane/polysulfone composite membrane against water was improved in contrast to bare polysulfone membrane. CO_2 separation performance of asymmetric membrane was declined due to swelling effect as assessed by permeation tests performed before and after swelling in the pressure range of 2–10 bar.

Flat-sheet asymmetric polyetherimide (PEI) membranes prepared via phase inversion method were used to efficiently separate CO_2 from N_2 (Ahmad et al. 2017). The membranes were synthesized by dissolving varying loadings (20, 25, and 30 wt %) of PEI matrix in *N*-methyl-2-pyrrolidone (NMP) solvent using water–isopropanol as coagulant. Structural morphology of fabricated membranes was examined via scanning electron microscopy (SEM). Single-gas permeation tests conducted at 1 bar and 25 °C indicated that increasing PEI contents leads to significant increase in CO_2/N_2 selectivity but at the expense of sharp drop in CO_2 permeance. Maximum CO_2 permeance of 1943 GPU was achieved for 20 wt % loading of PEI, while maximum CO_2/N_2 selectivity of 10.8 was obtained at 30 wt % PEI contents. Considerably high CO_2/N_2 selectivity of asymmetric membrane made from commercial PEI resin makes it a valuable material for carbon capture applications.

Asymmetric poly(ether block amide) (PEBA)-based composite membranes were prepared to efficiently capture CO_2 from flue gas (Liu et al. 2005). PEBA/PEI composite membranes were developed by coating thin layer of highly selective PEBA matrix on PEI-based microporous substrate available in the form of hollow fibers. Gas permeation properties of fabricated membranes were assessed by introducing CO_2/N_2 mixed gas feed (15.3% CO_2 and 84.7% N_2 by volume) to pilot-plant hollow fiber membrane modules designed to operate in different flow configurations. The best CO_2 separation performance in terms of product recovery and product purity was achieved with counter current flow configuration with feed entering from shell. Single-staged countercurrent flow membrane module operating at 23 °C under a feed-side pressure of 790 kPa rendered a permeate stream comprising 62 mol % CO_2 with 20% CO_2 recovery and a retentate stream containing 99.4 mol % N_2 with 36% N_2 recovery. As compared to permeance values obtained from permeation experiments performed over CO_2/N_2 mixed-gas feed stream, permeance values of CO_2 and N_2 assessed using pure gas feed streams were slightly reduced when operating at the same pressure. Counter current flow configuration with feed entering from tube side was not found to be appropriate on account of possible issues related to concentration polarization in microporous substrate as well as deformation of membrane structure under high operating pressure.

High-performance facilitated transport membranes were fabricated by depositing thin layer of polyethylenimine (PEI) on reverse osmosis (RO) membrane substrate via aqueous self-assembly method (Sun et al. 2017). For an optimized PEI concentration of 50 mg/L, the fabricated composite membranes exhibited maximum CO_2 permeance and CO_2/N_2 selectivity. Systemic investigation performed over prepared membranes in terms of pH of electrostatic-assembly, concentration of PEI matrix and other working conditions suggested facilitated-transport and solution-diffusion mechanisms for CO_2 and N_2, respectively, owing to presence of amine groups on PEI molecules.

Efficient carbon-capture asymmetric composite membranes were developed by depositing thin layers of polyhedral oligomeric silsesquioxane (POSS®)-doped polyvinyl alcohol (PVA) matrix on polysulfone porous substrate (Guerrero et al. 2018). The deposited selective layer of nanocomposite membranes was prepared by doping PVA matrix with POSS® nanoparticles functionalized with either amidine (amidino POSS®) or lactamide (lactamide POSS®) groups. Functionalization of POSS® nanoparticles reasonably improved polymer-particle compatibility as indicated by Fourier-transform infrared spectroscopy. Increasing contents of POSS® nanoparticles in PVA layer significantly improved crystalline regions as well as inter-crystallites slippage as corroborated by differential scanning calorimetry and dynamic mechanical analysis. Gas permeation tests indicated reduced CO_2 permeability and increased CO_2/N_2 selectivity with increasing feed-side pressure as well as nanofiller loading. Permeation results suggest that the fabricated nonporous dense membranes transport gas via solution-diffusion mechanism. As compared to amidino POSS®-filled composite membrane, lactamide POSS®-filled composite membrane results into reduced permeability on account of its strong interaction with PVA matrix and enhanced degree of crystallinity.

2.5 Gas Transport Through Membranes

2.5.1 Membrane Separation Mechanisms

Disparity in chemical and/or physical properties of different gas molecules as well as their dissimilar interaction with membrane material causes different gases to permeate through the membrane structure at different rates. Difference in permeabilities of different gases permeating through the membrane helps to separate a gas mixture into its individual component gases. Depending on their chemical and physical nature, molecular size and shape, and interaction with membrane material, gases can be separated in membranes via different mechanisms. Size sieving, surface diffusion, and Knudsen diffusion are the gas separating mechanisms operating in

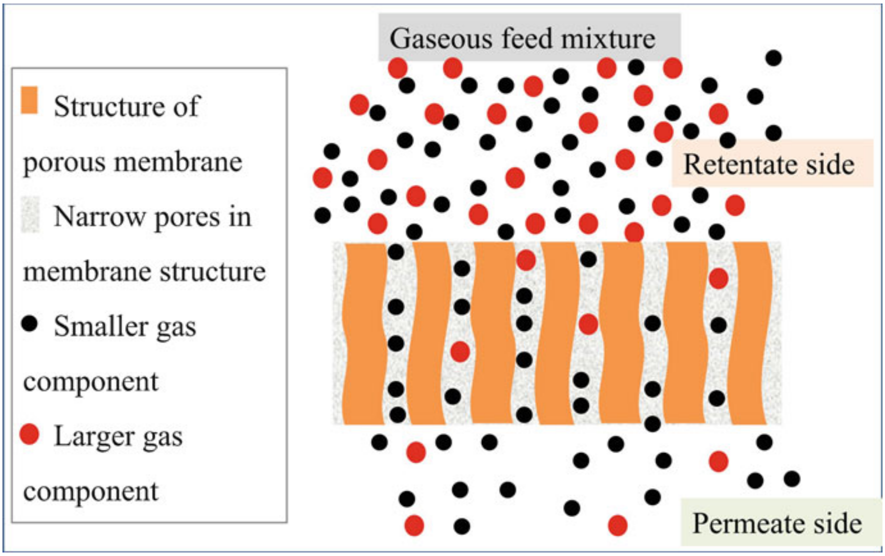

Fig. 2.6 Schematic representation of gas separation via size sieving mechanism occurring through narrow pores of micro-porous membranes

micro- or meso-porous membranes, while dense (nonporous) membranes separate gases via solution–diffusion and/or facilitated transport separation mechanisms.

Size sieving mechanism functions well when membrane pore size is between the molecular sizes of bigger and smaller gas molecules as illustrated in Fig. 2.6. Controlled pore size permits smaller gas molecule to transport freely through it while restricting larger ones to penetrate the membrane pore. Owing to its smaller size, CO_2 can effectively be separated from post-combustion flue gas via size sieving effect. This is the most dominant gas separation mechanism operating in narrow-pored microporous membranes used to separate gas molecules having dissimilar molecular sizes, e.g., CO_2/H_2, CO_2/N_2, CO_2/hydrocarbons mixtures, etc.

Surface diffusion is the dominant transport mechanism when a specific gas component, owing to its high affinity for membrane material, preferentially adsorbs on membrane surface as compared to other one. This results in higher concentration of highly adsorbable gas component within membrane structure as compared to less adsorbable gas component. Adsorbed gas molecules diffuse through the membrane pores to be extracted on permeate side of membrane, thus resulting in higher permeability of highly adsorbed gas component as compared to other one. Difference in permeabilities of high and low adsorbable gas components leads to the separation of a gas mixture (see Fig. 2.7). This transport mechanism occurs in micro- and meso-porous membranes to separate gas mixtures comprised of adsorbing and non-adsorbing gas components such as CO_2/He, CO_2/H_2, etc.

Gas separation via molecular weight-dependent Knudsen diffusion occurs when the mean free path of gas molecules is larger than membrane pore size and/or low

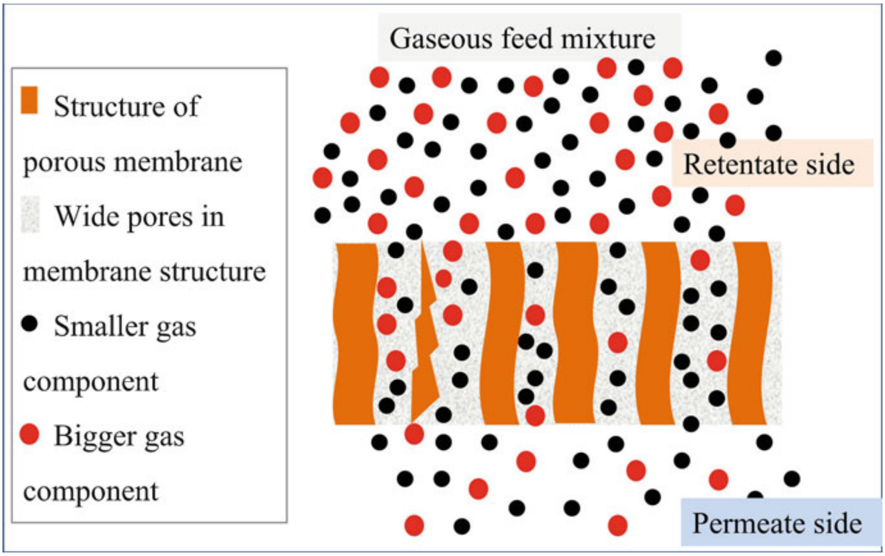

Fig. 2.7 Schematic representation of gas separation via surface diffusion mechanism occurring through micro- and meso-porous structure of porous membranes

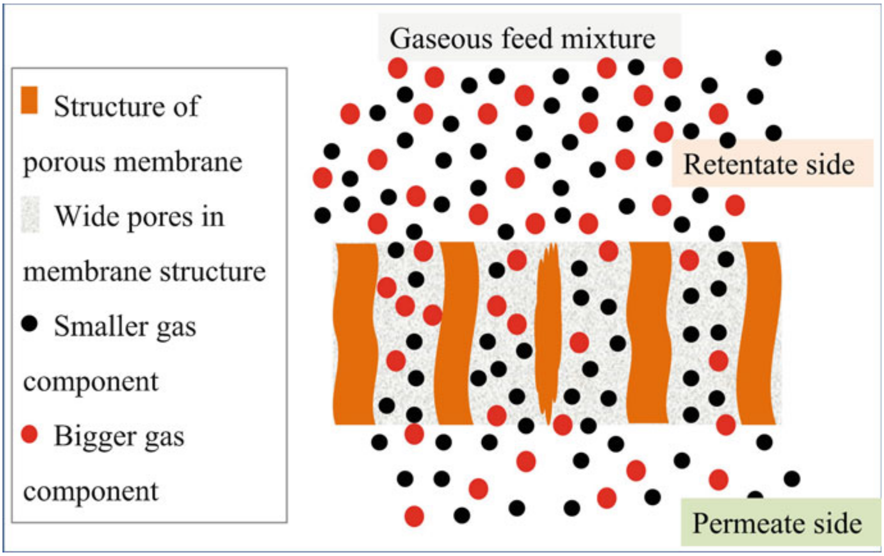

Fig. 2.8 Schematic representation of gas separation via Knudsen diffusion mechanism occurring through wide-pored structure of porous membranes

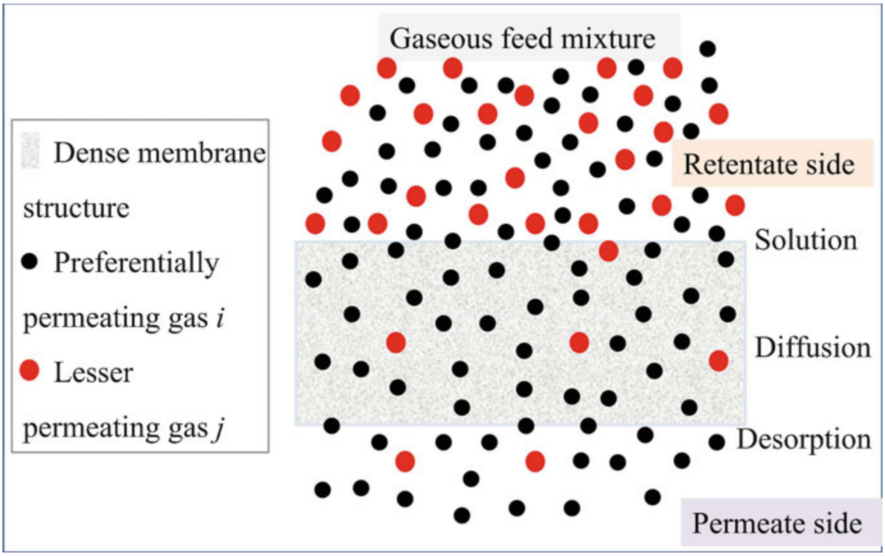

Fig. 2.9 Simplified diagram of gas separation by solution-diffusion mechanism in non-facilitated dense membranes

pressure (usually vacuum) is applied across the membrane. Knudsen diffusion arises due to collision of gas molecules having different molecular masses (and different interaction energies) with the porous membrane surface, thus resulting into different transport rates through the membrane (Fig. 2.8). In Knudsen diffusion the permeability of heavier gas component is low as compared to lighter one. Due to its high molecular weight, CO_2 permeates through the membrane at a relatively slower rate as compared to N_2 in an attempt to separate post-combustion flue gas into its component gases.

In contrast to transport via Knudsen diffusion, transport mechanisms of molecular sieving and surface diffusion dictate high permeability of CO_2 through the porous membranes as compared to N_2.

Separation in non-facilitated dense membranes takes place via solution diffusion mechanism since they do not have porous channels to transport gas molecules. The separation mechanism depends on two factors: solubility of a particular gas component in membrane material and its diffusivity through the bulk membrane as shown in Fig. 2.9. Solubility at the feed–membrane interface is determined by preferential dissolution or interaction of one of the gas components with membrane material while leaving the less soluble gas component behind in the feed gas. Diffusion of dissolved gas component through the membrane structure is driven by concentration gradient. Rate of diffusion is generally determined by molecular size of highly

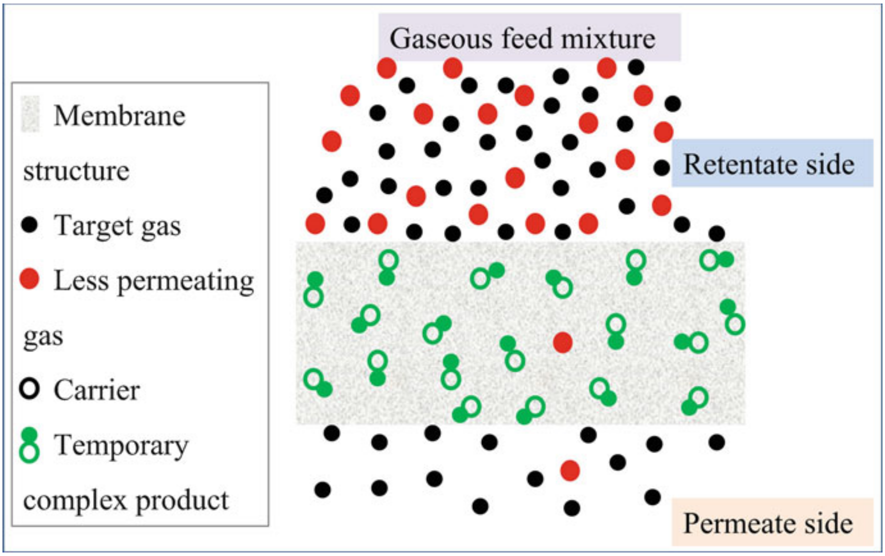

Fig. 2.10 Schematic diagram of gas separation via facilitated transport mechanism in facilitated liquid membranes

permeating gas component coupled with polymer chain mobility and interchain spacing. Highly soluble and diffusing component desorbs at permeate–membrane interface, thus completing the process of gas separation via solution–diffusion mechanism.

Low solubility and/or low diffusivity of key gas component through membrane material may result in low permeability via solution–diffusion mechanism. Both the permeability and selectivity of the key component through membrane can be enhanced by making use of facilitated transport mechanism. This mechanism transports gases not only by usual solution–diffusion mechanism but also by an active transport mechanism by involving a fixed or mobile carrier present in the membrane. The gas component to be separated reversibly reacts with carrier to form a temporary complex product which traverses through the membrane due to concentration gradient of intermediate complex rather than that of target component. Reverse reaction occurring at the permeate–membrane interface regenerates the target component as well as the carrier. Regenerated target component is desorbed on the permeate side, while carrier diffuses in reverse direction to feed–membrane interface so as to react with more key component molecules and carry the formed temporary product across the membrane. This type of transport mechanism usually works well in liquid membranes. To illustrate the mechanism of facilitated transport, the schematic diagram of a facilitated membrane, having amine as fixed carrier, to separate CO_2 form CO_2/N_2 mixture is demonstrated in Fig. 2.10. After its adsorption in membrane at feed side, the target gas component CO_2 reacts with amine carrier to form temporary bicarbonate. Bicarbonate diffuses through the membrane and dissociates back into CO_2 and amine at permeate–membrane interface releasing CO_2 at permeate side. Contrary to their non-facilitated counterparts, unique feature of facilitated membranes is the drop in CO_2 permeability as well as CO_2/N_2 selectivity with increasing partial pressure of CO_2 on feed side.

2.5.2 General Membrane-Specific Terminologies

Effective separation a gas mixture into its components using a membrane demands high production rate and high purity of the key component being separated. Some important terminologies needed to assess gas separation performance of a membrane are discussed here.

Molar flux across the membrane: The permeation of a certain species i diffusing through a thin membrane can be described in terms of its molar flux N_i which is equivalent to product of permeance $\overline{P}_{\mathrm{M},i}$ of key component i and driving force (partial pressure or concentration of component i) operating across the membrane, i.e.,

$$N_i \equiv \frac{V_i/t}{A_\mathrm{M}} = \left(\overline{P}_{\mathrm{M},i}\right)(\text{driving force}) = \left(\frac{P_{\mathrm{M},i}}{l_\mathrm{M}}\right)(\text{driving force}) \tag{2.1}$$

where V_i is the volume of gas component i permeated through the membrane having active cross-sectional area A_M in time interval dt. The gas permeance $\overline{P}_{\mathrm{M},i}$ can be defined as the ratio of permeability $P_{\mathrm{M},i}$ of key gas component i to membrane thickness l_M.

Permeability: Gas permeability P, defined as the transmembrane permeate flux through unit cross-sectional area subjected to unit pressure gradient, can be deduced from Eq. (2.1) and expressed as:

$$\text{Permeability} = \frac{\left(\frac{\text{volumetric gas flow rate}}{\text{membrane cross sectional area}}\right)}{\left(\frac{\text{transmembrane pressure difference}}{\text{membrane thickness}}\right)}$$

or

$$P = \frac{\left(\frac{V}{A_\mathrm{M} dt}\right)}{\left(\frac{\Delta P}{l_\mathrm{M}}\right)} \tag{2.2}$$

Gas permeability of a single gas permeating through a membrane can be assessed for isochoric permeation experiments via the following equation:

$$P = \frac{22414}{RT} \times \frac{V}{A_{\mathrm{M}}} \times \frac{l_{\mathrm{M}}}{\Delta P} \times \frac{dP}{dt} \tag{2.3}$$

where P, R, T, V, A_{M}, l_{M}, ΔP, and dP/dt denote gas permeability (*Barrer*), universal gas constant (6236.56 cm^3cmHg/mol/K), absolute temperature (K), downstream collection chamber volume (cm^3), membrane effective cross-sectional area (cm^2), membrane thickness (cm), upstream pressure (psi), and rate of pressure rise on permeate side (psi/s), respectively. Gas permeability can be measured either in terms of *Barrer* or *gas permeation unit (GPU)*.

Barrer: Gas permeability through a membrane, measured in cgs-system, corresponds to 1 Barrer if a gas flow rate of 10^{-10} cm^3/s (volume measured at standard temperature and pressure conditions of 0 °C and 1 atm, respectively) occurs through a membrane of cross-sectional area 1 cm^2 and thickness 1 cm by maintaining a pressure difference of 1 cm Hg across the membrane, i.e.,

$$P(1\ \text{Barrer}) = 10^{-10}\,\frac{\text{cm}^3(\text{STP}).\text{cm}}{\text{cm}^2.\text{s}.\text{cm Hg}}$$

Gas permeability of 1 Barrer in SI units can be expressed as:

$$P(1\ \text{Barrer}) = 7.50062 \times 10^{-18}\,\frac{\text{m}^3(\text{STP}).\text{m}}{\text{m}^2.\text{s}.\text{Pa}}$$

Gas permeation unit (GPU): Permeability of a single gas permeating through a membrane is equivalent to 1 gas permeation unit (GPU) if it flows at a rate of 10^{-6} cm^3/s (at 0 °C and 1 atm) through a membrane of cross-sectional area 1 cm^2 and thickness 1 cm under a transmembrane pressure difference of 1 cm Hg, i.e.,

$$P(1\ \text{GPU}) = 10^{-6}\,\frac{\text{cm}^3(\text{STP}).\text{cm}}{\text{cm}^2.\text{s}.\text{cm Hg}}$$

For a gas mixture flowing through a membrane, the permeability P_i of a certain component i expressed in GPU can be determined via below equation:

$$P_i(1\ \text{GPU}) = \frac{6 \times 10^4}{T} \times \frac{V}{A_{\mathrm{M}}} \times \frac{l_{\mathrm{M}}}{\Delta \mathrm{P}} \times \frac{dP}{dt} \times \frac{Y_i}{X_i} \tag{2.4}$$

where T, V, A_{M}, l_{M}, ΔP, dP/dt, X_i, and Y_i represent absolute temperature (K), volume of downstream collection chamber (cm^3), membrane effective cross-sectional area (cm^2), membrane thickness (cm), upstream pressure (mbar), rate of pressure rise on permeate side (mbar min^{-1}), mole fraction of component i on feed side, and mole fraction of component i on permeate side, respectively (Basu et al. 2010b).

Ideal selectivity: Ideal selectivity $\alpha_{i,j}$ of gas A over gas B, defined as the ratio of permeability of A to that of B, is generally determined via isochoric single-gas permeation experiments by assuming that the permeation behavior of a gas remains the same whether it permeates through the membrane exclusively or as a component of a certain gas mixture. Ideal selectivity of gas i over j can be calculated from Eq. (2.5):

$$\alpha_{i,j} = \frac{P_i}{P_j} \tag{2.5}$$

where P_i and P_j are the permeabilities of gases i and j, respectively, as measured by single gas permeation experiments.

Solution–diffusion mechanism of gas transport through a membrane can be accounted for in terms of Fick's first law stating that the gas permeability P_i of penetrant i equals the product of its diffusivity D_i and solubility S_i through the membrane, i.e.,

$$P_i = D_i \times S_i \tag{2.6}$$

Ideal selectivity of gas i over j can be expressed in terms of diffusion-based selectivity (D_i/D_j) and solubility-based selectivity (S_i/S_j) of the two penetrating gas components as follows:

$$\alpha_{i,j} \equiv \frac{P_i}{P_j} = \left(\frac{D_i}{D_j}\right)\left(\frac{S_i}{S_j}\right) \tag{2.7}$$

Ideal selectivity based on single-gas permeation experiment may differ from actual selectivity based on separation experiment performed over real gas mixture owing to mutual interaction of permeating gases of the mix. For a permeating mixture of gases through a membrane, the real selectivity of the key component i over gas component j can be calculated by the following equation:

$$\alpha_{i,j} = \frac{Y_i/Y_j}{X_i/X_j} \tag{2.8}$$

where X_i and X_j denote feed-side mole fractions of components i and j, respectively, while Y_i and Y_j represent corresponding permeate-side mole fractions of components i and j (Basu et al. 2010b).

2.5.3 Models to Predict Gas Permeability Through Mixed-Matrix Membranes

Designing of gas separation process using mixed-matrix membranes requires permeation data of gas species transporting through polymer matrix (continuous phase) and filler particles (dispersed phase) (Keskin and Sholl 2010). Essential permeability data for majority of metal–organic framework-filled membranes is usually acquired through experimentation. Complex mathematical models based on atomistic simulation of adsorption, diffusion, solubility, and separation of gas molecules can be used to theoretically predict gas permeation data for various mixed-matrix membranes (Keskin et al. 2009; Song et al. 2012).

Analogous to electrical and/or thermal conductivity models, various theoretical models are available to predict gas permeation through mixed-matrix membranes (Pal 2008; Cheetham et al. 2012). Depending on phase morphology of mixed-matrix membranes, theoretical models predicting gas permeability through mixed-matrix membranes can be classified into two-phase (particle-polymer) and three-phase (particle-interface-polymer) permeation models. A two-phase model depicting perfect morphology of mixed-matrix membranes is characterized by good polymer-filler adhesion corroborating a defect-free, faultless, and non-deformable interface between continuous (polymer matrix) and dispersed (nanofiller) phases. Noteworthy two-phase permeation models include Maxwell, Bruggeman, Singh, Lewis–Nielsen, Pal, Chiew–Galandt, Bottcher, and Higuchi models. A three-phase model, in addition to polymer and filler phases, also considers polymer-filler interface as the third phase of the system. It is characterized by a poor polymer-filler adhesion as well as a non-ideal morphology suggesting some defects, faults, and imperfections at the polymer-filler interface. A three-phase system can assume non-ideal morphology due to interfacial defects such as the creation of a rigidified polymer layer around filler particle, the pore blockage in porous particles, and/or the formation of void spaces between polymer and filler phases. Modified Maxwell, modified Felske, and modified Pal permeation models are considered to be some of the important three-phase permeation models.

Relative permeability (P_r) of a gas permeating through a mixed-matrix membrane with respect to its pure polymer counterpart can be anticipated by Maxwell permeation model as follows:

$$P_{\mathrm{r}} = \frac{1 + 2\Phi\left(\frac{\lambda_{\mathrm{dm}}-1}{\lambda_{\mathrm{dm}}+2}\right)}{1 - \Phi\left(\frac{\lambda_{\mathrm{dm}}-1}{\lambda_{\mathrm{dm}}+2}\right)} \tag{2.9}$$

where

$$P_r = \frac{P_{eff}}{P_m} = \frac{\text{Effective permeability of MMM}}{\text{Permeability of polymer matrix}}$$

$$\lambda_{dm} = \frac{P_d}{P_m} = \frac{\text{Permeability of dispersed phase}}{\text{Permeability of polymer matrix}}$$

$$\Psi = 1 + \left(\frac{1 - \Phi_m}{\Phi_m^2}\right)\Phi \tag{2.10}$$

Φ_m = *volume fraction of fillers at maximum packing* = *0.64.*
and Φ = *volume fraction of filler(s)*

This model is valid for low concentration ($\Phi < 0.2$) of filler particles and cannot accurately predict gas permeability through mixed-matrix membranes for higher volume fractions of the filler. Maxwell model has nothing to do with filler morphological parameters such as particle shape, particle size distribution, and aggregation state of particles.

Bruggeman model, an advanced version of Maxwell model, correlates relative gas permeability with filler volume fraction by the following numerically solvable implicit relationship.

$$P_r^{\frac{1}{3}}\left(\frac{\lambda_{dm} - 1}{\lambda_{dm} - P_r}\right) = (1 - \Phi)^{-1} \tag{2.11}$$

Both the Maxwell and Bruggeman models are applied for well-dispersed isotropic filler particles in polymeric matrix due to their dependence on volume fraction of filler particles and has nothing to do with morphology or size of the filler particle.

Lewis–Nielsen model accounts for morphological effects like size, shape, size distribution, and aggregation state of filler particles on gas permeability through mixed-matrix membranes. It can calculate gas permeation at maximum packing of filler volume fraction:

$$P_r = \frac{1 + 2\left(\frac{\lambda_{dm}-1}{\lambda_{dm}+2}\right)\Phi_m}{1 - \Psi\left(\frac{\lambda_{dm}-1}{\lambda_{dm}+2}\right)\Phi_m} \tag{2.12}$$

Pal model, just like Lewis–Nielsen model, can be applied to determine gas permeability at maximum packing volume fraction of fillers since it considers the influence of particle shape, particle size distribution, and particle aggregation state:

$$P_r^{1/3}\left(\frac{\lambda_{dm} - 1}{\lambda_{dm} - P_r}\right) = \left(1 - \frac{\Phi}{\Phi_m}\right)^{-\Phi_m} \tag{2.13}$$

Three-phase Felske permeation model used to estimate relative permeability (P_r) of a gas through a mixed-matrix membrane can be expressed as follows:

$$P_{\mathrm{r}} = \frac{1 + \frac{2\Phi(\beta-\gamma)}{(\beta+2\gamma)}}{1 - \frac{\Phi\Psi(\beta-\gamma)}{(\beta+2\gamma)}} \tag{2.14}$$

where

$$\beta = \left(2+\delta^3\right)\lambda_{dm} - 2\left(1-\delta^3\right)\lambda_{im}$$

$$\gamma = 1 + 2\delta^3 - \left(1-\delta^3\right)\lambda_{di}$$

$$\lambda_{\mathrm{di}} = \frac{P_{\mathrm{d}}}{P_{\mathrm{i}}} = \frac{\text{Permeability of dispersed phase}}{\text{Permeability of interphase}}$$

$$\lambda_{\mathrm{im}} = \frac{P_{\mathrm{i}}}{P_{\mathrm{m}}} = \frac{\text{Permeability of interphase}}{\text{Permeability of matrixphase}}$$

$$\lambda_{\mathrm{dm}} = \lambda_{\mathrm{di}}\lambda_{\mathrm{im}} = \frac{\beta}{\gamma}$$

and $\delta =$ *ratio of interphase to particle radii*

Felske model turns to original Maxwell model in the absence of an interfacial layer, i.e., when $\delta = 1$. Although the computing of Felske model to determine gas permeability is relatively easy as compared to Maxwell model, its limitations are the same as those of modified Maxwell model. It can accurately predict gas permeability through mixed-matrix membranes for volume fractions of filler particles less than 0.2.

All the abovementioned permeation models are used to predict permeability of a single gas permeating exclusively through mixed-matrix membranes with the assumption that their flow behavior would be unaffected even if they permeate with other gases of the mixture. If the permeability of a certain gas species is affected by the presence of other gas components while permeating in a gas mixture, the prediction of gas permeability through mixed-matrix membrane requires more complicated mathematical equations. An exclusive approach based on partial pressures of permeating gases along with other parameters obtained from single gas permeation experiments is partial immobilization model (Vu et al. 2003). This model can be used to estimate gas permeability P_i of component i of a gas mixture permeating through mixed-matrix membranes as follows:

$$P_i = (K_i D_i)\left(1 + \frac{F_i K_i}{1 + \sum_{i=1}^{n} b_i p_i}\right) \tag{2.15}$$

Here p_i is the partial pressure of gas component i on feed side of membrane while maintaining vacuum on permeate side of the membrane. K_i and D_i are Henry adsorption coefficient and ordinary diffusivity of species i, respectively; b_i and F_i are corresponding Langmuir affinity constant and ratio of diffusivities of permeating gas components.

2.6 Conclusion

Global warming can be efficiently controlled by capturing carbon dioxide via mixed-matrix membranes prepared by incorporating high surface area porous metal–organic frameworks and nanomaterials in polymer matrix. Carbon capture and separation performance of mixed-matrix membranes as compared to other existing technologies has been found to be better in terms of sustainability, economics, environment, and operation. Chemistry of metal–organic frameworks to be incorporated in mixed-matrix membranes can be tailored to improve essential properties of membranes by modifying their fundamental crystal structure, chemical nature, and/or functionalization. A variety of hybrid membranes have been prepared by incorporating different mesoporous materials like MOF-5, HKUST-1, ZIF-8, ZIF-94, ZIF-300, ZIF-301, ZIF-302, carbon nanotubes, silica, graphene oxide, etc. in various thermoplastic and rubbery polymers such as polysulfone, polyimides, polydimethylsiloxane, polyvinylacetate, poly(vinyl chloride), polyethyleneimine, poly(ether block amide), etc. Remarkable improvement in CO_2 permeability and CO_2/N_2 selectivity has been revealed to be possessed by these composite membrane materials. This in turn results in lowered operational energy demands for CO_2 capture process in contrast to existing technologies. Solution–diffusion mechanism dominates the gas transport phenomena through these dense nonporous membranes. CO_2 permeability and CO_2/N_2 selectivity can be theoretically predicted via different gas permeation models and measured by performing gas permeation experiments over single- or mixed-gas feed streams at varying feed pressures. Improvement in CO_2 separation performance of composite membranes can be owned to porous structure of metal–organic frameworks. As compared to bare polymers, the precisely adjustable porosity of nanomaterials added to mixed-matrix membranes offers the opportunity to considerably improve CO_2/N_2 selectivity in contrast to pure polymeric matrix. Finding intensive utility in carbon capture applications, mixed-matrix membranes filled with metal–organic frameworks and other nanomaterials would be considered important materials of choice to control global warming in the future.

Nomenclature

Abbreviations

6FDA	4,4′-hexafluoroisopropylidene diphthalic anhydride
CCS	carbon capture and sequestration
CNT	carbon nanotube
Cu(BDC)	Cu_3(benzene-1,4-dicarboxylate)$_2$
Cu-BTC	Cu_3(benzene-1,3,5-tricarboxylate)$_2(H_2O)_3$
Cu-HFS-BIPY	4,4′-bipyridine-hexafluorosilicate copper(II)
DAM	diaminomesitylene
Durene	2,3,5,6-tetramethyl-1,3-phenyldiamine
EOR	enhanced oil recovery
GPU	gas permeation unit

GO	graphene oxide
IPCC	Intergovernmental Panel on Climate Change
HKUST-1	Cu_3(benzene-1,3,5-tricarboxylate)$_2$(H_2O)$_3$
MOF	metal–organic framework
MMM	mixed-matrix membrane
NMP	*N*-methyl-2-pyrrolidone
PDMS	polydimethylsiloxane
PEBA	poly(ether block amide)
PEG	poly(ethylene glycol)
PEI	polyetherimide
PI	polyimide
PMDA	pyromellitic dianhydride
POSS®	silsesquioxanes
PTMSP	poly(1-trimethylsilyl-1-propyne)
PSF	polysulfone
PU	polyurethane
PVAc	polyvinylacetate
PVAm	poly(vinylamine)
PVC	poly(vinyl chloride)
ODA	4,4′-oxydianiline
S1C	silicate-1
SAPO-34	silicoaluminophosphate
SPEEK	sulfonated poly(ether ether ketone)
US	Ultrason®
ZIF	zeolitic imidazolate framework

Symbols

A	effective membrane area (cm^2)
b	Langmuir affinity constant
D	diffusivity *or* diffusion coefficient (cm^2/s)
F	ratio of diffusivities of permeating gas components
K	Henry adsorption parameter determined from Langmuir adsorption isotherm
l	membrane thickness (cm)
m	mass or weight of the specimen
N	molar flux
n	number of gas components
P	gas permeability (Barrer; 1 Barrer = 10^{-10} cm^3 (STP) cm/(cm s cmHg))
$\overline{P}$	permeance (Barrer/cm)
p	partial pressure of gaseous component on feed side
R	universal gas constant (6236.56 cm^3cmHg/mol/K)
S	solubility coefficient (cm^3 (STP)/cm^3cmHg)
T	absolute temperature (K)
t	time (s)

V gas volume *or* cell downstream volume (cm^3)
X mole fraction of gaseous component on feed side
Y mole fraction of gaseous component on permeate side
y parameter to be determined from Langmuir adsorption isotherm
Δp pressure difference across the membrane (psi)
$\Delta P/dt$ gas permeation rate (psi/s) in terms of time rate of pressure

Greek Letters

α membrane gas selectivity
β matrix rigidification or chain immobilization factor
γ ratio of interphase thickness to particle radius
δ ratio of outer radius of rigidified interfacial matrix chain layer to radius of core particle
λ permeability ratio
ψ function of packing volume fraction of filler particles
Φ fractional volume of filler(s) (%)

Subscripts

C continuous phase
D dispersed phase
eff effective
i interphase
i gas '*i*'
j gas '*j*'
M membrane
m polymer matrix
r relative

References

Adams R, Carson C, Ward J, Tannenbaum R, Koros W (2010) Metal organic framework mixed matrix membranes for gas separations. Microporous Mesoporous Mater 131:13–20. https://doi.org/10.1016/j.micromeso.2009.11.035

Ahmad AL, Salaudeen YO, Jawad ZA (2017) Synthesis of asymmetric polyetherimide membrane for CO_2/N_2 separation. IOP Conf Ser: Mater Sci Eng 206:012068. https://doi.org/10.1088/1757-899X/206/1/012068

Ahn J, Chung W-J, Pinnau I, Guiver MD (2008) Polysulfone/silica nanoparticle mixed-matrix membranes for gas separation. J Membr Sci 314:123–133. https://doi.org/10.1016/j.memsci.2008.01.031

Allen CA, Boissonnault JA, Cirera J, Gulland R, Paesani F, Cohen SM (2013) Chemically crosslinked isoreticular metal-organic frameworks. Chem Commun 49:3200–3202. https://doi.org/10.1039/C3CC40635K

Ataeivarjovi E, Tang Z, Chen J (2018) Study on CO_2 desorption behavior of a PDMS-SiO_2 hybrid membrane applied in a novel CO_2 capture process. ACS Appl Mater Interfaces 10:28992–29002. https://doi.org/10.1021/acsami.8b08630

Bae TH, Lee JS, Qiu W, Koros WJ, Jones CW, Nair S (2010) A high-performance gas-separation membrane containing submicrometer-sized metal-organic framework crystals. Angew Chem Int Ed Engl 49:9863–9866. https://doi.org/10.1002/anie.201006141

Baker RW (2002) Future directions of membrane gas separation technology. Ind Eng Chem Res 41:1393–1411. https://doi.org/10.1021/ie0108088

Barooah M, Mandal B (2018) Enhanced CO_2 separation performance by PVA/PEG/silica mixed matrix membrane. J Appl Polym Sci 135:46481–46483. https://doi.org/10.1002/app.46481

Basu S, Khan AL, Odena AC, Liu C, Vankelecom IFJ (2010a) Membrane-based technologies for biogas separations. Chem Soc Rev 39:750–768. https://doi.org/10.1039/b817050a

Basu S, Odena AC, Vankelecom IFJ (2010b) Asymmetric Matrimid®/[$Cu_3(BTC)_2$] mixed-matrix membranes for gas separations. J Membr Sci 362:478–487. https://doi.org/10.1016/j.memsci.2010.07.005

Basu S, Odena AC, Vankelecom IFJ (2011) MOF-containing mixed-matrix membranes for CO_2/CH_4 and CO_2/N_2 binary gas mixture separations. Sep Purif Technol 81:31–40. https://doi.org/10.1016/j.seppur.2011.06.037

Benavides ME, David O, Johnson T, Łozińska MM, Orsic A, Wright PA, Mastel S, Hillenbrand R, Kapteijn F, Gascon J (2018) High performance mixed matrix membranes (MMMs) composed of ZIF-94 filler and 6FDA-DAM polymer. J Membr Sci 550:198–207. https://doi.org/10.1016/j.memsci.2017.12.033

Benemann JR (1993) Utilization of carbon dioxide from fossil fuel-burning power plants with biological systems. Energy Convers Manag 34:999–1004. https://doi.org/10.1016/0196-8904(93)90047-E

Burgaz E, Erciyes A, Andac M, Andac O (2019) Synthesis and characterization of nano-sized metal organic framework-5 (MOF-5) by using consecutive combination of ultrasound and microwave irradiation methods. Inorg Chim Acta 485:118–124. https://doi.org/10.1016/j.ica.2018.10.014

Caro J, Noack M (2008) Zeolite membranes – recent developments and progress. Microporous Mesoporous Mater 115:215–233. https://doi.org/10.1016/j.micromeso.2008.03.008

Choi S, Drese JH, Jones CW (2010) Adsorbent materials for carbon dioxide capture from large anthropogenic point sources. ChemSusChem 2:796–854. https://doi.org/10.1002/cssc.200900036

Cheetham AK, Al-Muhtaseb SA, Sivaniah E (2012) Zeolitic imidazolate framework (ZIF-8) based polymer nanocomposite membranes for gas separation. Energy Environ Sci 5:8359–8369. https://doi.org/10.1039/C2EE21996D

Chui SS, Lo SM, Charmant JPH, Orpen AG, Williams ID (2007) A chemically functionalizable nanoporous material $[Cu_3(TMA)_2(H_2O)_3]_n$. Science 283:1148–1150. https://doi.org/10.1126/science.283.5405.1148

Chung TS, Jiang LY, Li Y, Kulprathipanja S (2007) Mixed matrix membranes (MMMs) comprising organic polymers with dispersed inorganic fillers for gas separation. Prog Polym Sci 32:483–507. https://doi.org/10.1016/j.progpolymsci.2007.01.008

Dai Z, Løining V, Deng J, Ansaloni L, Deng L (2018) Poly(1-trimethylsilyl-1-propyne)-based hybrid membranes: effects of various nanofillers and feed gas humidity on CO_2 permeation. Membranes 8:76. https://doi.org/10.3390/membranes8030076

Das AK, Vemuri RS, Kutnyakov I, McGrail BP, Motkuria RK (2016) An efficient synthesis strategy for metal-organic frameworks: dry-gel synthesis of MOF-74 framework with high yield and improved performance. Sci Rep 6:28050–28057. https://doi.org/10.1038/srep28050

Daturi M, Chang JS (2011) Why hybrid porous solids capture greenhouse gases? Chem Soc Rev 40(2):550-562. https://doi.org/10.1039/c0cs00040j

David H, Wagener V, Rochelle GT (2011) Stripper configurations for CO_2 capture by aqueous monoethanolamine and piperazine. Energy Procedia 4:1323–1330. https://doi.org/10.1016/j.egypro.2011.01.190

Dey C, Kundu T, Biswal BP, Mallick A, Banerjee R (2014) Crystalline metal-organic frameworks (MOFs): synthesis, structure and function. Acta Cryst 70:3–10. https://doi.org/10.1107/S2052520613029557

ESRL (2019) Trends in atmospheric carbon dioxide. Earth System Research Laboratory, Global Monitoring Division, 2019

Ferey G, Serre C, Devic T, Maurin G, Jobic H, Llewellyn PL, De Weireld G, Vimont A, Daturi M, Chang JS (2011) Why hybrid porous solids capture greenhouse gases? Chem Soc Rev 40 (2):550–562. https://doi.org/10.1039/c0cs00040j

Furukawa H, Cordova KE, O'Keeffe M, Yaghi OM (2013) The chemistry and applications of metal-organic frameworks. Science 341:1230444–1230456. https://doi.org/10.1126/science.1230444

Galve A, Sieffert D, Vispe E, Tellez C, Coronas J, Staudt C (2011) Copolyimide mixed matrix membranes with oriented microporous titanosilicate JDF-L1 sheet particles. J Membr Sci 370:131–140. https://doi.org/10.1016/j.memsci.2011.01.011

Gao Y, Qiao Z, Zhao S, Wang Z, Wang J (2018) In situ synthesis of polymer grafted ZIFs and application in mixed matrix membrane for CO_2 separation. J Mater Chem A 6:3151–3161. https://doi.org/10.1039/C7TA10322K

Gascon J, Aktay U, Alonso MDH, van Klink GPM, Kapteijn F (2009) Amino-based metal-organic frameworks as stable, highly active basic catalysts. J Catal 261:75–87. https://doi.org/10.1016/j.jcat.2008.11.010

Gascon J, Kapteijn F, Zornoza B, Sebastian V, Casado C, Coronas J (2012) Practical approach to zeolitic membranes and coatings: state of the art, opportunities, barriers, and future perspectives. Chem Mater 24:2829–2844. https://doi.org/10.1021/cm301435j

Ge BS, Wang T, Sun HX, Gao W, Zhao HR (2018) Preparation of mixed matrix membranes based on polyimide and aminated graphene oxide for CO_2 separation. Polym Adv Technol 29:1334–1343. https://doi.org/10.1002/pat.4245

Girault F, Adhikari LB, Lanord CF, Agrinier P, Koirala BP, Bhattarai M, Mahat SS, Groppo C, Rolfo F, Bollinger L, Perrier F (2018) Persistent CO_2 emissions and hydrothermal unrest following the 2015 earthquake in Nepal. Nat Commun 9:2956–2965. https://doi.org/10.1038/s41467-018-05138-z

Gong X, Wnag Y, Kuang T (2017) ZIF-8-based membranes for carbon dioxide capture and separation. ACS Sustain Chem Eng 5:11204–11214. https://doi.org/10.1021/acssuschemeng.7b03613

Guerrero G, Hägg MB, Simon C, Peters T, Rival N, Denonville C (2018) CO_2 separation in nanocomposite membranes by the addition of amidine and lactamide functionalized POSS® nanoparticles into a PVA layer. Membranes 8:28. https://doi.org/10.3390/membranes8020028

Guo HL, Zhu GS, Hewitt IJ, Qiu SL (2009) "Twin copper source" growth of metal-organic framework membrane: $Cu_3(BTC)_2$ with high permeability and selectivity for recycling H_2. J Am Chem Soc 131:1646–1647. https://doi.org/10.1021/ja8074874

Guo X, Huang H, Ban Y, Yang Q, Xiao Y, Li Y, Yang W, Zhong C (2015) Mixed matrix membranes incorporated with amine-functionalized titanium-based metal-organic framework for CO_2/CH_4 separation. J Membr Sci 478:130–139. https://doi.org/10.1016/j.memsci.2015.01.007

Hassanpoor A, Mirzaei M, Eshtiagh-Hosseini H (2018) Syntheses and characterization of two new coordination compounds containing an azide ligand in the presence of o-donor co-ligands with nickel and copper(II) metal ions and an investigation into the effects of sonochemical methods on morphology and particle size. J Iran Chem Soc 15:1287–1292. https://doi.org/10.1007/s13738-018-1327-x

Haszeldine RS (2009) Carbon capture and storage: how green can black be? Science 325:1647–1652. https://doi.org/10.1126/science.1172246

Hedin N, Chen L, Laaksonen A (2010) Sorbents for CO_2 capture from flue gas- aspects from materials and theoretical chemistry. Nanoscale 2:1819–1841. https://doi.org/10.1039/C0NR00042F
Hu J, Cai H, Ren H, Wei YM, Xu Z, Liu H, Hu Y (2010) Mixed-matrix membrane hollow fibers of $Cu_3(BTC)_2$ MOF and polyimide for gas separation and adsorption. Ind Eng Chem Res 49:12605–12612. https://doi.org/10.1021/ie1014958
Ismail AF, David L (2001) A review on the latest development of carbon membranes for gas separation. J Membr Sci 193:1–18. https://doi.org/10.1016/S0376-7388(01)00510-5
Ismail AF, Kusworo TD, Mustafa A (2008) Enhanced gas permeation performance of polyethersulfone mixed matrix hollow fiber membranes using novel Dynasylan Ameo silane agent. J Membr Sci 319:306–312. https://doi.org/10.1016/j.memsci.2008.03.067
Jeazet HT, Staudt C, Janiak C (2012) Metal-organic frameworks in mixed-matrix membranes for gas separation. Dalton Trans 41:14003–14027. https://doi.org/10.1039/C2DT31550E
Keskin S, Sholl DS (2010) Selecting metal organic frameworks as enabling materials in mixed matrix membranes for high efficiency natural gas purification. Energy Environ Sci 3:343–351. https://doi.org/10.1039/B923980B
Keskin S, Liu J, Johnson JK, Sholl DS (2009) Atomically detailed models of gas mixture diffusion through CuBTC membranes. Microporous Mesoporous Mater 125:101–106. https://doi.org/10.1016/j.micromeso.2009.01.016
Keskin S, van Heest TM, Sholl DS (2010) Can metal-organic framework materials play a useful role in large-scale carbon dioxide separations? ChemSusChem 3(8):879–891. https://doi.org/10.1002/cssc.201000114
Khalilinejad I, Kargari A, Sanaeepur H (2017) Preparation and characterization of (Pebax 1657 + silica nanoparticle)/PVC mixed matrix composite membrane for CO_2/N_2 separation. Chem Pap 71:803–818. https://doi.org/10.1007/s11696-016-0084-5
Kim S, Chen L, Johnson JK, Marand E (2007) Polysulfone and functionalized carbon nanotube mixed matrix membranes for gas separation: theory and experiment. J Membr Sci 294:147–158. https://doi.org/10.1016/j.memsci.2007.02.028
Kitagawa S, Matsuda R (2007) Chemistry of coordination space of porous coordination polymers. Coord Chem Rev 251:2490–2509. https://doi.org/10.1016/j.ccr.2007.07.009
Klimakow M, Klobes P, Thünemann AF, Rademann K, Emmerling F (2010) Mechanochemical synthesis of metal−organic frameworks: a fast and facile approach toward quantitative yields and high specific surface areas. Chem Mater 22:5216–5221. https://doi.org/10.1021/cm1012119
Klinowski J, Paz FAA, Silva P, Rocha J (2011) Microwave-assisted synthesis of metal-organic frameworks. Dalton Trans 40:321–330. https://doi.org/10.1039/C0DT00708K
Koros WJ, Mahajan R (2000) Pushing the limits on possibilities for large scale gas separation: which strategies? J Membr Sci 175:181–196. https://doi.org/10.1016/S0376-7388(00)00418-X
Kumar B, Smieja JM, Kubiak CP (2010) Photoreduction of CO_2 on p-type silicon using Re(bipy-Bu^t)$(CO)_3Cl$: Photovoltages exceeding 600 mV for the selective reduction of CO_2 to CO. J Phys Chem C 114:14220–14223. https://doi.org/10.1021/jp105171b
Kwak KO, Jung SJ, Chung SY, Kang CM, Huh YI, Bae SO (2006) Optimization of culture conditions for CO_2 fixation by a chemoautotrophic microorganism, strain YN-1 using factorial design. Biochem Eng J 31:1–7. https://doi.org/10.1016/j.bej.2006.05.001
Li M, Dinca M (2011) Reductive electrosynthesis of crystalline metal-organic frameworks. J Am Chem Soc 133:12926–12929. https://doi.org/10.1021/ja2041546
Li JR, Kuppler RJ, Zhou HC (2009) Selective gas adsorption and separation in metal-organic frameworks. Chem Soc Rev 38:1477–1504. https://doi.org/10.1039/b802426j
Li X, Sun Q, Liu J, Xiao B, Li R, Sun X (2016) Tunable porous structure of metal organic framework derived carbon and the application in lithium-sulfur batteries. J Power Sources 302:174–179. https://doi.org/10.1016/j.jpowsour.2015.10.049
Lin R, Ge L, Diao H, Rudolph V, Zhu Z (2016) Ionic liquids as the MOFs/polymer interfacial binder for efficient membrane separation. ACS Appl Mater Interfaces 8:32041–32049. https://doi.org/10.1021/acsami.6b11074

Liu L, Chakma A, Feng X (2005) CO_2/N_2 separation by poly(ether block amide) thin film hollow fiber composite membranes. Ind Eng Chem Res 44:6874–6882. https://doi.org/10.1021/ie050306k
Mahajan R, Koros WJ (2000) Factors controlling successful formation of mixed-matrix gas separation materials. Ind Eng Chem Res 39:2692–2696. https://doi.org/10.1021/ie990799r
Maji TK, Kitagawa S (2007) Chemistry of porous coordination polymers. Pure Appl Chem 79:2155–2177. https://doi.org/10.1351/pac200779122155
McCarthy MC, Guerrero VV, Barnett GV, Jeong HK (2010) Synthesis of zeolitic imidazolate framework films and membranes with controlled microstructures. Langmuir 26:14636–14641. https://doi.org/10.1021/la102409e
Metz B, Davidson O, de Coninck H, Loos M, Meyer L (2005) IPCC special report on carbon dioxide capture and storage. Cambridge University Press, Cambridge, pp 1–431
Mirzaei S, Shamiri A, Aroua MK (2015) A review of different solvents, mass transfer, and hydrodynamics for postcombustion CO_2 capture. Int J Eng Res 3:742–744. https://doi.org/10.1515/revce-2014-0045
Nafisi V, Hägg MB (2014) Gas separation properties of ZIF-8/6FDA-durene diamine mixed matrix membrane. Sep & Purif Technol 128:31–38. https://doi.org/10.1016/j.seppur.2014.03.006
Noble RD (2011) Perspectives on mixed matrix membranes. J Membr Sci 378:393–397. https://doi.org/10.1016/j.memsci.2011.05.031
Ockwig NW, Nenoff TM (2007) Membranes for hydrogen separation. Chem Rev 107:4078–4110. https://doi.org/10.1021/cr0501792
Ohlrogge K, Stürken K (2001) The separation of organic vapors from gas streams by means of membranes. In: Membrane technology: in the chemical industry. Wiley, Weinheim. https://doi.org/10.1002/3527600388.ch7. Ch II-1
Oral CA (2018) Gas permeability of polydimethylsiloxane membranes filled with clinoptilolite in different cationic forms. Turk J Chem 42:112–120. https://doi.org/10.3906/kim-1707-8
Pachauri RK, Reisinger A (2007) Contribution of working groups I, II and III to the fourth assessment report of the intergovernmental panel on climate change. In: IPCC climate change 2007: synthesis report, pp 1–104
Pal R (2008) Permeation models for mixed matrix membranes. J Colloid Interface Sci 317:191–198. https://doi.org/10.1016/j.jcis.2007.09.032
Prasetya N, Teck AA, Ladewig BP (2018) Matrimid-JUC-62 and Matrimid-PCN-250 mixed matrix membranes displaying light-responsive gas separation and beneficial ageing characteristics for CO_2/N_2 separation. Sci Rep 8:2944. https://doi.org/10.1038/s41598-018-21263-7
Quadrelli R, Peterson S (2007) The energy-climate challenge: recent trends in CO_2 emissions from fuel combustion. Energy Policy 35:5938–5952. https://doi.org/10.1016/j.enpol.2007.07.001
Ranjan R, Tsapatsis M (2009) Microporous metal organic framework membrane on porous support using the seeded growth method. Chem Mater 21:4920–4924. https://doi.org/10.1021/cm902032y
Robeson LM (2008) The upper bound revisited. J Membr Sci 320:390–400. https://doi.org/10.1016/j.memsci.2008.04.030
Russo G, Prpich G, Anthony EJ, Montagnaro F, Jurado N, Lorenzo GD, Darabkhani HG (2017) Selective-exhaust gas recirculation for CO_2 capture using membrane technology. J Membr Sci 549:649–659. https://doi.org/10.1016/j.memsci.2017.10.052
Sabetghadam A, Seoane B, Keskin D, Duim N, Rodenas T, Shahid S, Sorribas S (2016) Metal organic framework crystals in mixed-matrix membranes: impact of the filler morphology on the gas separation performance. Adv Funct Mater 26:3154–3163. https://doi.org/10.1002/adfm.201505352
Sadrzadeh M, Shahidi K, Mohammadi T (2010) Synthesis and gas permeation properties of a single layer PDMS membrane. J Appl Polym Sci 117:33–48. https://doi.org/10.1002/app.31180
Saracco G, Neomagus HWJP, Versteeg GF, van Swaaij WPM (1999) High-temperature membrane reactors: potential and problems. Chem Eng Sci 54:1997–2017. https://doi.org/10.1016/S0009-2509(99)00009-3

Sarfraz M, Ba-Shammakh M (2016a) A novel zeolitic imidazolate framework based mixed-matrix membrane for efficient CO_2 separation under wet conditions. J Taiwan Inst Chem Eng 65:427–436. https://doi.org/10.1016/j.jtice.2016.04.033
Sarfraz M, Ba-Shammakh M (2016b) Combined effect of CNTs with ZIF-302 into polysulfone to fabricate MMMs for enhanced CO_2 separation from flue gases. Arab J Sci Eng 41:2573–2582. https://doi.org/10.1007/s13369-016-2096-4
Sarfraz M, Ba-Shammakh M (2016c) Synergistic effect of adding graphene oxide and ZIF-301 to polysulfone to develop high performance mixed matrix membranes for selective carbon dioxide separation from post combustion flue gas. J Membr Sci 514:35–43. https://doi.org/10.1016/j.memsci.2016.04.029
Sarfraz M, Ba-Shammakh M (2016d) Synergistic effect of incorporating ZIF-302 and graphene oxide to polysulfone to develop highly selective mixed-matrix membranes for carbon dioxide separation from wet post-combustion flue gases. J Ind Eng Chem 36:154–162. https://doi.org/10.1016/j.jiec.2016.01.032
Sarfraz M, Ba-Shammakh M (2018a) Water-stable ZIF-300/Ultrason® mixed-matrix membranes for selective CO_2 capture from humid post combustion flue gas. Chin J Chem Eng 26:1012–1021. https://doi.org/10.1016/j.cjche.2017.11.007
Sarfraz M, Ba-Shammakh M (2018b) ZIF-based water-stable mixed-matrix membranes for effective CO_2 separation from humid flue gas. Can J Chem Eng 96:2475–2483. https://doi.org/10.1002/cjce.23170
Sarfraz M, Ba-Shammakh M (2018c) Harmonious interaction of incorporating CNTs and zeolitic imidazole frameworks into polysulfone to prepare high performance MMMs for CO_2 separation from humidified post combustion gases. Braz J Chem Eng 35:217–228. https://doi.org/10.1590/0104-6632.20180351s20150595
Sarfraz M, Ba-Shammakh M (2018d) Pursuit of efficient CO_2-capture membranes: graphene oxide- and MOF-integrated Ultrason® membranes. Polym Bull 75:5039–5059. https://doi.org/10.1007/s00289-018-2301-6
Shen J, Liu G, Huang K, Li Q, Guan K, Li Y, Jin W (2016) UiO-66-polyether block amide mixed matrix membranes for CO_2 separation. J Membr Sci 513:155–165. https://doi.org/10.1016/j.memsci.2016.04.045
Silva EA, Windmoller D, Silva GG, Figueiredo KCS (2017) Polydimethylsiloxane membranes containing multi-walled carbon nanotubes for gas separation. Mater Res 20:1454–1460. https://doi.org/10.1590/1980-5373-MR-2016-0825
Smart S, Lin CXC, Ding L, Thambimuthu K, da Costa JCD (2010) Ceramic membranes for gas processing in coal gasification. Energy Environ Sci 3:268–278. https://doi.org/10.1039/B924327E
Sodeifian G, Raji M, Asghari M, Rezakazemi M, Dashti A (2018) Polyurethane-SAPO-34 mixed matrix membrane for CO_2/CH_4 and CO_2/N_2 separation. Chin J Chem Eng. https://doi.org/10.1016/j.cjche.2018.03.012
Song Q, Nataraj SK, Roussenova MV, Tan JC, Hughes DJ, Li W, Bourgoin P, Alam MA, Cheetham AK, Al-Muhtaseb SA, Sivaniah E (2012) Zeolitic imidazolate framework (ZIF-8) based polymer nanocomposite membranes for gas separation. Energy Environ Sci 5:8359–8369. https://doi.org/10.1039/C2EE21996D
Stock N, Biswas S (2012) Synthesis of metal-organic frameworks (MOFs): routes to various MOF topologies, morphologies, and composites. Chem Rev 112:933–969. https://doi.org/10.1021/cr200304e
Strathmann H (2012) Introduction to membrane science and technology. Wiley-VCH. Ch 3, p 114. https://doi.org/10.1002/anie.201205786
Suleman MS, Lau KK, Yeong YF (2016) Development and performance evaluation of polydimethyl siloxane/polysulfone (PDMS/PSF) composite membrane for CO_2/CH_4 separation. IOP Conf Ser: Earth Environ Sci 36:012014. https://doi.org/10.1088/1755-1315/36/1/012014

Sumida K, Rogow DL, Mason JA, McDonald TM, Bloch ED, Herm ZR, Bae TH, Long JR (2012) Carbon dioxide capture in metal-organic frameworks. Chem Rev 112:724–781. https://doi.org/10.1021/cr2003272

Sun J, Yi Z, Zhao X, Zhou Y, Gao C (2017) CO_2 separation membranes with high permeability and CO_2/N_2 selectivity prepared by electrostatic self-assembly of polyethylenimine on reverse osmosis membranes. RSC Adv 7:14678–14687. https://doi.org/10.1039/c7ra00094d

Thompson JA, Chapman KW, Koros WJ, Jones CW, Nair S (2012) Sonication-induced Ostwald ripening of ZIF-8 nanoparticles and formation of ZIF-8/polymer composite membranes. Microporous Mesoporous Mater 158:292–299. https://doi.org/10.1016/j.micromeso.2012.03.052

Venna SR, Carreon MA (2010) Highly permeable zeolite imidazolate framework-8 membranes for CO_2/CH_4 separation. J Am Chem Soc 132:76–78. https://doi.org/10.1021/ja909263x

Vu DQ, Koros WJ, Miller SJ (2003) Mixed matrix membranes using carbon molecular sieves. J Membr Sci 211:335–348. https://doi.org/10.1016/S0376-7388(02)00429-5

Wang ZQ, Cohen SM (2009) Postsynthetic modification of metal-organic frameworks. Chem Soc Rev 38:1315–1329. https://doi.org/10.1039/b802258p

Wappel D, Gronald G, Kalb R, Draxler J (2010) Ionic liquids for post-combustion CO_2 absorption. Int J Greenhouse Gas Control 4:486–494. https://doi.org/10.1016/j.ijggc.2009.11.012

Wijenayake SN, Panapitiya NP, Versteeg SH, Nguyen CN, Goel S, Balkus KJ Jr, Musselman IH, Ferraris JP (2013) Surface cross-linking of ZIF-8/polyimide mixed matrix membranes (MMMs) for gas separation. Ind Eng Chem Res 52:6991–7001. https://doi.org/10.1021/ie400149e

Wu X, Yuan B, Bao Z, Deng S (2014) Adsorption of carbon dioxide, methane and nitrogen on an ultramicroporous copper metal-organic framework. J Colloid Interface Sci 430:78–84. https://doi.org/10.1016/j.jcis.2014.05.021

Xin Q, Ouyang J, Liu T, Li Z, Li Z, Liu Y, Wang S, Wu H, Jiang Z, Cao X (2015) Enhanced interfacial interaction and CO_2 separation performance of mixed matrix membrane by incorporating polyethylenimine-decorated metal-organic frameworks. ACS Appl Mater Interfaces 7:1065–1077. https://doi.org/10.1021/am504742q

Yaghi OM, O'Keeffe M, Ockwig NW, Chae HK, Eddaoudi M, Kim J (2003) Reticular synthesis and the design of new material. Nature 423:705–714. https://doi.org/10.1038/nature01650

Yoo Y, Lai Z, Jeong HK (2009) Fabrication of MOF-5 membranes using microwave-induced rapid seeding and solvothermal secondary growth. Microporous Mesoporous Mater 123:100–106. https://doi.org/10.1016/j.micromeso.2009.03.036

You H, Hossain I, Kim TH (2018) Piperazinium-mediated crosslinked polyimide-polydimethylsiloxane (PI-PDMS) copolymer membranes: the effect of PDMS content on CO_2 separation. RSC Adv 8:1328–1336. https://doi.org/10.1039/c7ra10949k

Yuan D, Zhao D, Sun D, Zhou HC (2010) An isoreticular series of metal-organic frameworks with dendritic hexacarboxylate ligands and exceptionally high gas-uptake capacity. Angew Chem Int Ed 49:5357–5361. https://doi.org/10.1002/anie.201001009

Zhao D, Yuan DQ, Sun DF, Zhou HC (2009) Stabilization of metal-organic frameworks with high surface areas by the incorporation of mesocavities with microwindows. J Am Chem Soc 131:9186–9188. https://doi.org/10.1021/ja901109t

Zhou HC, Long JR, Yaghi OM (2012) Introduction to metal-organic frameworks. Chem Rev 112:673–674. https://doi.org/10.1021/cr300014x

Zhu H, Jie X, Cao Y (2017) Fabrication of functionalized MOFs incorporated mixed matrix hollow fiber membrane for gas separation. J Chem 2017:1–9. https://doi.org/10.1155/2017/2548957

Zimmerman CM, Singh A, Koros WJ (1997) Tailoring mixed matrix composite membranes for gas separations. J Membr Sci 137:145–154. https://doi.org/10.1016/S0376-7388(97)00194-4

Zornoza B, Irusta S, Tellez C, Coronas J (2009) Mesoporous silica sphere-polysulfone mixed matrix membranes for gas separation. Langmuir 25:5903–5909. https://doi.org/10.1021/la900656z

Zornoza B, Seoane B, Zamaro JM, Téllez C, Coronas J (2011a) Combination of MOFs and zeolites for mixed-matrix membranes. ChemPhysChem 12:2781–2785. https://doi.org/10.1002/cphc.201100583

Zornoza B, Esekhile O, Koros WJ, Tellez C, Coronas J (2011b) Hollow silicalite-1 sphere-polymer mixed matrix membranes for gas separation. Sep Purif Technol 77:137–145. https://doi.org/10.1016/j.seppur.2010.11.033

Zornoza B, Tellez C, Coronas J, Gascon J, Kapteijn F (2013) Metal organic framework based mixed matrix membranes: an increasingly important field of research with a large application potential. Microporous Mesoporous Mater 166:67–78. https://doi.org/10.1016/j.micromeso.2012.03.012

Zou X, Zhang F, Thomas S, Zhu G, Valtchev V, Mintova S (2011) $Co_3(HCOO)_6$ microporous metal-organic framework membrane for separation of CO_2/CH_4 mixtures. Chem-Eur J 17:12076–12083. https://doi.org/10.1002/chem.201101733

Chapter 3
Biogas as a Renewable Energy Source: Focusing on Principles and Recent Advances of Membrane-Based Technologies for Biogas Upgrading

Francisco M. Baena-Moreno, Estelle le Saché, Laura Pastor-Pérez, and T. R. Reina

Contents

Abstract In this work, a comprehensive discussion of biogas upgrading using membrane technologies is presented. Bio-methane obtained from biogas upon carbon dioxide removal is an attractive source of clean energy, and several techniques have been developed for this purpose. These technologies are chemical absorption, water scrubbing, physical absorption, adsorption, cryogenic separation, and membrane separation. Among these techniques, membrane separation outstands

---

F. M. Baena-Moreno (✉)
Chemical and Environmental Engineering Department, Technical School of Engineering, University of Seville, Sevilla, Spain

Department of Chemical and Process Engineering, University of Surrey, Guildford, UK
e-mail: fbaena2@us.es

E. le Saché · L. Pastor-Pérez · T. R. Reina
Department of Chemical and Process Engineering, University of Surrey, Guildford, UK

Z. Zhang et al. (eds.), *Membranes for Environmental Applications*, Environmental Chemistry for a Sustainable World 42, https://doi.org/10.1007/978-3-030-33978-4_3

due to its promising economic viability. In this work, general characteristics of biogas and its upgrading processes are explained. Then membrane technology for biogas upgrading through gas permeation is analyzed in detail. Gas permeation phenomena, membrane materials, membrane modules, different types of process configuration, and commercial biogas plants based on membrane technologies are deeply investigated. Polymeric membrane materials are under continuous development, and this will facilitate the implementation of membrane-based biogas upgrading processes in many industrial areas. Single-stage configurations are not able to produce both high methane purity and a high recovery percentage. Thus, multistage configurations play an important role in biogas upgrading when membranes are selected to facilitate the CH_4/CO_2 separation. In this scenario, it is expected that membrane-based biogas upgrading methods will significantly contribute to open new approaches in the urgent matter of sustainable energy technologies.

Keywords Biogas upgrading · Bio-methane · Renewable energies · Energy sources · Membranes for biogas upgrading · Gas permeation · Carbon capture · Polymeric materials · Multistage configurations · Biogas-based plants

3.1 Introduction

Sustainable and renewable energies are the key to combating the scarcity of energy from fossil fuels, as well as addressing the climate change that has increased in recent years. The serious environmental crisis, mainly due to the incessant increase of greenhouse gases derived from anthropogenic emissions, is an important factor which forces governments to undertake new energy policies and regulations. The increase of these greenhouse gas concentrations in the atmosphere has the potential to initiate unprecedented changes in climate systems, leading to serious ecological and economic disturbances. Among the most influent greenhouse gases, carbon dioxide (CO_2) stands out due to its increasing presence in the atmosphere, as can be seen in Fig. 3.1 (Verotti et al. 2016; Ibrahim et al. 2018; Lam et al. 2017; Clift 2006).

For this reason, the development of carbon capture and storage (CCS) as well as carbon capture and utilization (CCU) technologies has been promoted by national and international organizations (Baena-Moreno et al. 2018a, b). The implementation of CCS technologies could be an essential contribution to the effort of global reduction of greenhouse gases derived from industrial and power generation plants alimented by fossil fuels. However, these techniques are not developed enough to be an economical option for greenhouse gases mitigation (Baena-Moreno et al. 2018b; Leonzio 2016).

In addition, the economic growth of developing countries in the past decades and the world population rise is catapulting the development of new technologies that

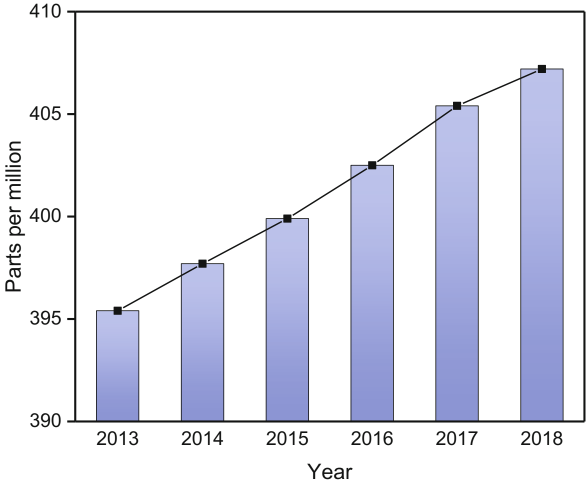

Fig. 3.1 CO_2 concentration in the atmosphere. Annual record. (Modified after Scripps Institution of Oceanography 2018)

allow the use of renewable resources. In the short term, governments are to prioritize the increase of energy efficiency, although economic and thermodynamic limitations will be encountered. Thus, in the longer term, only the further development of renewable energies combined with traditional energy sources will solve the great challenges of the future (Aresta 2010; Pfau et al. 2017).

The most important types of renewable energies are bioenergy from biomass, geothermal, hydroelectric, solar, and wind. Among these renewable sources of energy, biogas has aroused great interest in recent years, as it is one of the easiest to implement technologies especially in rural areas. Biogas comes from renewable biomass sources. Its potential development, not only considering the production of biogas, but also its potential to convert into other valuable products such as bio-fertilizer, makes attractive its utilization in sectors with abundant organic waste matter (Ullah Khan et al. 2017; Weiland 2009; Abatzoglou and Boivin 2009).

One of the main problems of biogas relies on its composition. As biogas comes from the anaerobic digestion of residues, the percentage of CO_2 in its composition is about 30–50%, which should be removed before use, in order to suppress its greenhouse potential (Ullah Khan et al. 2017; Niesner et al. 2013; Sun et al. 2015). For this purpose, biogas upgrading technologies have been studied by several groups and are an extensive area of research. pressure swing adsorption (PSA), water scrubbing, chemical scrubbing, organic physical scrubbing, membrane separation, and cryogenic separation are the most popular technologies for biogas upgrading (Wheeler et al. 1999; Persson et al. 2007).

Among the technologies exposed above, membrane separation is one of the most promising, due to the overall costs involved in its installation and operation as well as the high removal efficiency towards most of biogas contaminants (Baker and Lokhandwala 2008; Zhang et al. 2014). In this chapter, first, a preliminary presentation of the main characteristics of biogas is given, as well as a brief overview of different available technologies for biogas upgrading. Afterwards, membrane technologies for biogas upgrading will be deeply discussed, from fundamental aspects such as construction materials to commercial plants for biogas upgrading based on membrane technologies.

3.2 Biogas: General Characteristics and Upgrading Processes

As it has been addressed before, biogas is a product obtained from the anaerobic digestion of residues such as sewage wastes, landfills residues, or agricultural wastes. This section tries to detail the main characteristics and uses, as well as the main biogas transformation techniques in bio-methane.

3.2.1 Production and Applications

The biological production of biogas from organic residues is represented in Fig. 3.2. Briefly, this anaerobic process is constituted by three main steps. The first one implies the transformation of insoluble organic material to soluble organic materials by the enzymes' action and is called the hydrolysis step. The second step consists of the breakdown of the products from the previous step to obtain carbon dioxide, hydrogen, acetic acid, and other simple volatile organic acids. Finally, the last step

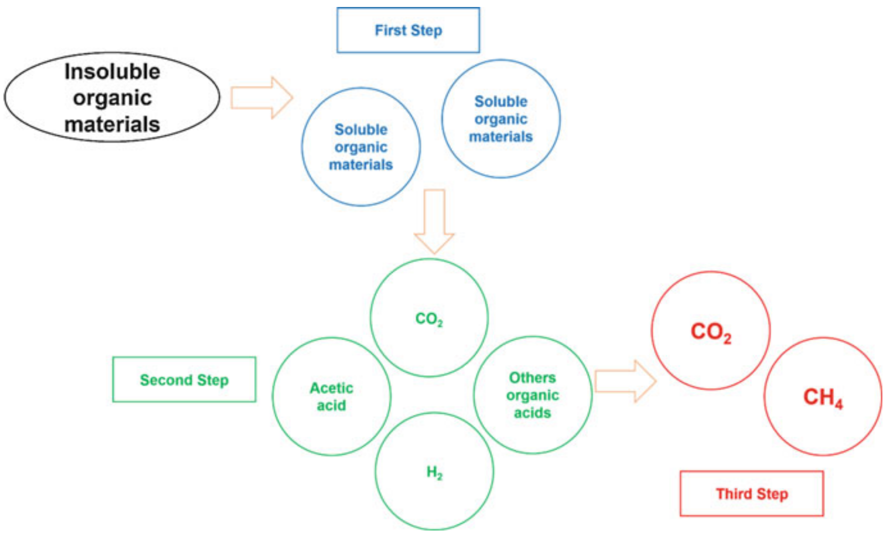

Fig. 3.2 Steps of biogas fermentation

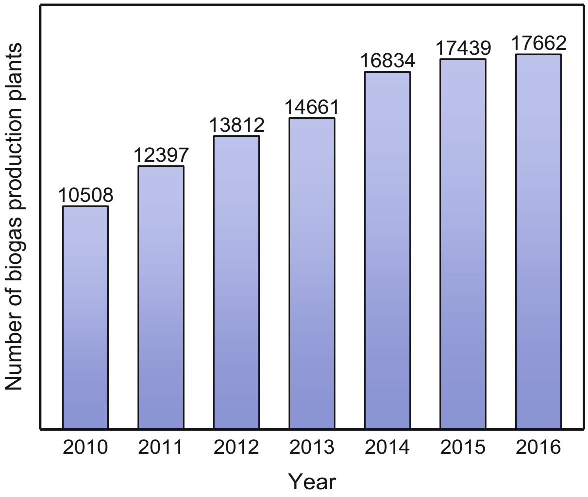

Fig. 3.3 Number of biogas production plants (2010–2016)

Table 3.1 Requirements for bio-methane to be used in different applications (Kadam and Panwar 2017; Rasi et al. 2011; Bauer et al. 2013)

End use	H_2S	CO_2	H_2O and other siloxanes
Boiler	<1000 ppm	Not allowed	Not allowed
Cooker	Allowed	Not allowed	Not allowed
Stationary engine	<250 ppm	Not allowed	Not allowed
Vehicle fuel	Allowed	Recommended	Not allowed
Natural gas grid	Not allowed	Eventually	Eventually

entails the conversion of acetic acid, hydrogen, and carbon dioxide to a mix of methane and carbon dioxide (Fig. 3.1) (Yadvika et al. 2004).

Biogas is called to have an important role within the renewable energy portfolio. It is planned that the use of biogas in the world will reach approximately the value of 30 GW in 2022. In the European Union, almost 25 million tons of oil equivalents are estimated to be produced in 2020, producing a high impact of reduction in greenhouse emissions. By 2020, renewable energies are expected to account for 20% of the total European energy demand, being biogas expected to produce the 25% of the total bioenergy (Ullah Khan et al. 2017).

This issue is being reflected in the increase of biogas production plants in recent years. As depicted in Fig. 3.3, the number of biogas plants has increased from 10,508 in 2010 to 17,662 in 2016, which represents an increase of 68% (AEBIOM 2017).

There are several applications in which biogas have been employed successfully, for example, electricity production, direct combustion to heat or steam generation, injection into the gas grid as a substitute of natural gas, and fuel for vehicles (Abatzoglou and Boivin 2009; Ullah Khan et al. 2017). The different requirements of bio-methane for some applications are indicated in Table 3.1.

Nowadays, direct combustion of biogas to produce heat or steam is the most common industrial application, due to its simplicity as only water should be separated before burning. However, direct combustion causes loss of calorific value and requires remarkable capital investment since big installations are needed to cope with relatively high gas flows (Ahmadi Moghaddam et al. 2015).

The injection into the natural gas grid has the main advantage of a minimum infrastructure cost, since these are existing facilities in the majority of countries. This reason could facilitate a greater overall performance of the upgrading biogas process and its use. However, the high operational cost of this option and the very restrictive laws imposed by governments make it one of the less preferred options (Bond and Templeton 2011; Hosseini and Wahid 2013).

Regarding the utilization of bio-methane as fuel, light vehicles are suitable to work with conventional gasoline and compressed natural gas. Bio-methane is a clean vehicle fuel and can help to balance the fast growth of the transport sector with lower vehicular emissions, since biogas comes from renewable sources. These reductions could be around 60–85% for NO_x, 10–70% for CO, and 60–80% for emitted particles, when substituting conventional fuels with bio-methane (Bauer et al. 2013; Yang et al. 2014).

3.2.2 Composition

In addition to methane and carbon dioxide, biogas is composed of water, ammonia, hydrogen, oxygen, nitrogen, and hydrogen sulfide, as stated in Table 3.2. Its composition varies depending on its origin source. In comparison with natural gas, where CH_4 content is about 90%, biogas presents a wide range of 35–70% methane.

Table 3.2 Biogas composition from different sources

Compound	Biogas from sewage	Biogas from landfill	Biogas from waste water	Natural gas
CH_4 (%)	60–70	35–65	55–58	90–95
CO_2 (%)	34–38	30–45	32–50	0.2–2
H_2O (%)	1–7	1–5	1–5	–
NH_3 (ppm)	50–100	0–5	0–100	–
H_2 (%)	Traces	0–5	Traces	–
O_2 (%)	Traces	0–1	Traces	–
N_2 (%)	0–2	5–15	Traces	0–0.5
H_2S (ppm)	0–4000	0–100	0–4000	0–10
Siloxanes (%)	0–0.2	0–0.2	0–0.5	–

Table 3.3 Biogas contaminants and its effects

Contaminant	Effect – consequence
H_2S	Corrosion, toxic and formation of SO_2–SO_3 in combustion stage
Siloxanes	Depositions on different elements provoking its wearing and microcrystalline quartz formation in combustion stage
H_2O	Corrosion in compressors and acid formation when reacting with other biogas components
NH_3	Corrosion when reacting with water
CO_2	Diminishing of calorific value

CO_2 represents about 30–50% of the biogas composition, followed by traces of water and nitrogen and parts per million (ppm) of ammonia and hydrogen sulfide. Although the latter ones are in a very low composition, they are the most problematic ones from an operational point of view, since they spark corrosion (Hertel et al. 2015; Alonso-Vicario et al. 2010; Rahman et al. 2017; Harasimowicz et al. 2007; Bekkering et al. 2010; Chen et al. 2015; Persson et al. 2007; Bauer et al. 2013; Patrizio et al. 2015; Ryckebosch et al. 2011; Niesner et al. 2013).

3.2.3 Upgrading Necessity

As exposed in the previous section, multiple biogas compositions can be obtained depending on the raw materials and the operational conditions specified during the anaerobic digestion process (Yadvika et al. 2004). Some of those components included in the biogas mixture could be detrimental for the process equipment and eventually may damage the materials of construction. Hence it is important to eliminate such components. Some of the effects and consequences of the different impurities are represented in Table 3.3.

The benefits of eliminating these components are multifold: (i) expansion of the life span of the process equipment, (ii) higher calorific value of the biogas, (iii) reduction of environmentally unfriendly emissions, and (iv) an overall boosting of the economic viability of the process. Biogas calorific value is between 20.7 and 27.8 MJ/m^3, while bio-methane calorific value is about 37.7–39.8 MJ/m^3 (Pipatmanomai et al. 2009; Bright et al. 2011). This difference has an obvious impact on the price, ranging from 0.89 to 2.97 p/kWh for biogas and from 1.49 to 3.30 p/kWh for bio-methane (Hoo et al. 2018; Ullah Khan et al. 2017).

Due to the reasons explained in this section, biogas upgrading is a necessity for applying as renewable energy industrially. Furthermore, the economic balance has been demonstrated to be more favorable for bio-methane than for raw biogas. For this purpose, many biogas upgrading technologies were studied by several authors, and their main characteristics are summarized in the next section.

3.2.4 Biogas Upgrading Technologies

A large number of biogas upgrading technologies have been developed from the beginning of the century, some of them well-established at commercial scale. Nowadays, the cutting edge of the research focuses on improving the overall efficiency of the processes and consequently the operation and investment costs.

During the first years of bio-methane construction plants, water scrubbing was the technology of choice due to its technical simplicity and cost. Nevertheless, in the last decades, the number of chemical scrubbing, membranes, and PSA plants has risen greatly as a consequence of the progress on the development of these alternatives (Angelidaki et al. 2018). A distribution of different commercial plants in Europe categorized by chosen technology for biogas treatment can be seen in Fig. 3.4.

Regarding the investment capital and operational costs, Table 3.4 presents updated data for the different biogas upgrading technologies. Membrane technology investment costs seem to be economically interesting especially in installations with relatively low gas flow. However, there are not substantial differences between membrane technology and PSA systems in terms of operational costs for small productions. This gap is considerably bigger for plants producing up to 300 m^3 h^{-1}, so in terms of operational costs, membrane technology fits in this range of production.

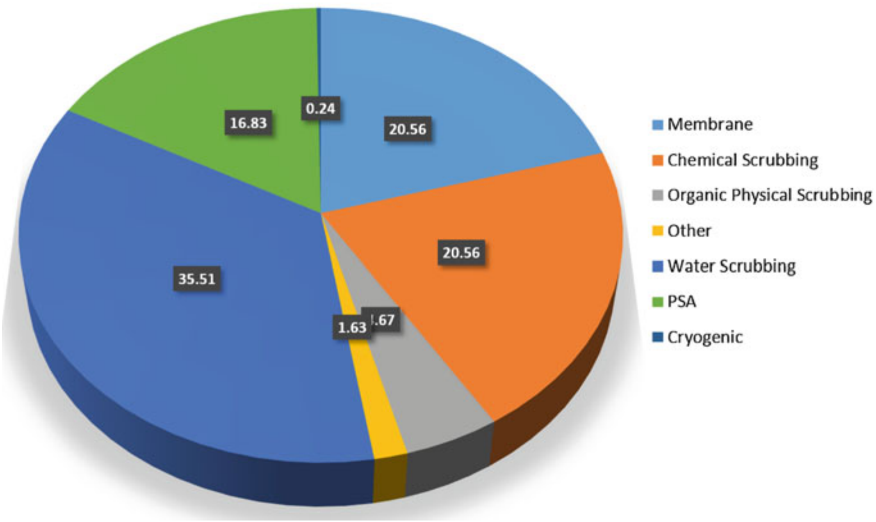

Fig. 3.4 Commercial bio-methane plant distribution. (Modified after Angelidaki et al. 2018)

Table 3.4 Biogas composition from different sources

		Water scrubbing	Organic physical scrubbing	Amine scrubbing	PSA systems	Membrane technology
Approximate investment costs (€/m^3 h^{-1} of bio-methane)	Up to 100 m^3 h^{-1}	10,100	9500	9500	10,500	7500
	Up to 200 m^3 h^{-1}	5500	5000	5000	5500	4800
	Up to 300 m^3 h^{-1}	3500	3500	3500	3800	3500
Approximate operational costs (€/m^3 h^{-1} of bio-methane)	Up to 100 m^3 h^{-1}	14.0	13.8	14.4	12.8	12.5
	Up to 200 m^3 h^{-1}	10.3	10.2	12.0	10.1	8.6
	Up to 300 m^3 h^{-1}	9.1	9.0	11.2	9.2	7.5

Modified after Chen et al. (2015)

PSA Systems

PSA processes are quite simple from an operational point of view. The raw biogas is first compressed and then dried to prevent water from reaching the sorbent filter, where activated carbon molecular sieves retain CO_2, H_2S, and NH_3 mainly. The advantageous characteristics of PSA systems are the low energy consumption and fast regeneration of the sorbent. Some industrial technologies such as the Carbotech patented system benefit from improved operational costs as well as high removal efficiency, thus leading to the implementation of a large number of plants for biogas upgrading (Kim et al. 2015; Alonso-Vicario et al. 2010; Persson 2003).

Water Scrubbing

In a water scrubber, carbon dioxide and other compounds are physically absorbed in water at high operation pressures of about 6–10 bars. This operation is normally carried out in a packed tower filled with a random packing to increase the contact surface of both phases, in a countercurrent flow disposition. As a consequence of the absorption, a small fraction of methane is lost, but overall, the efficiency of the process is reasonably high due to the high solubility of CO_2 in water (Rotunno et al. 2017; Jiang et al. 2010). After the CO_2 absorption stage, the aqueous solution obtained is regenerated by a desorption column by applying air in a countercurrent flow at atmospheric pressure (Zhou et al. 2017).

Chemical Scrubbing

Nowadays one of the most employed biogas upgrading techniques relies on a chemical scrubber in which the gas flow comes into contact with a solvent that is usually MEA, piperazine, NaOH, or KOH. This method ensures a high CO_2 absorption and no methane loss. After the absorption stage, it is necessary to regenerate the solvent to make the process economically affordable. When employing MEA or piperazine, the regeneration stage is carried out above 100 °C to release CO_2 in a pure gas flow. However, when using a caustic solvent, chemical reaction methods using high calcium or magnesium sources are employed to regenerate the solvent, forming a precipitated carbonate as a valuable by-product (Baena-moreno et al. 2018a, b; Sanna et al. 2014; Arti et al. 2017; Vega et al. 2017; Leonzio 2016).

Organic Physical Scrubbing

Dimethyl ether and polyethylene glycol are the most employed solvents for physical scrubbing. Since carbon dioxide is much more soluble in these two substances than in water, the same amount of flow gas could be absorbed using less solvent. This is an advantage over the water scrubbing process. On the other hand, these organic solvents are more expensive than water, but this can be economically balanced by a higher efficiency regeneration stage (Djas and Henczka 2018; Andriani et al. 2014; Weiland 2009).

Membrane Separation

Membranes employed in biogas upgrading retain methane and let carbon dioxide permeate through the porous membrane. This technique is based on the molecule size difference, in that way the membrane acts as a filter. Other contaminants may be separated by the membrane, but preferably they should be removed in a previous stage in order to extend the lifetime of the membrane. The selection of membrane materials is crucial for the process as it may affect the performance and selectivity due to the particular interaction between materials and the gas mixture. The development of different commercial membrane upgrading technologies led to the spread of that technology among bio-methane producers (Zhou et al. 2017; Basu et al. 2010; Yin et al. 2016).

Cryogenic Separation

This technique is based on a gradual decrease of biogas temperature, until pure CO_2 and CH_4 gas flows are achieved. Methane in this state is known as liquefied natural gas (LNG). Typically, the raw biogas is first dried and compressed to up to 80 bars and later cooled down to around −110 °C. This technique achieves really promising results regarding the overall separation efficiencies, but the high investment cost associated with the compression and cooling operations makes it presently not economically affordable (Tuinier and Van Sint Annaland 2012; Johansson 2008; Chiesa et al. 2011).

Chemical Hydrogenation Process

This process consists of the biological or chemical reduction of carbon dioxide by means of hydrogen, based on Sabatier reaction, under the action of a catalyst, typically based on nickel and ruthenium. The process is carried out at about 300 °C and 20 MPa and achieves high conversions of CO_2. However, the overall efficiency of the process is affected by the presence of H_2S or siloxanes in the raw biogas. Sulfur compounds poison the catalyst, leading to its deactivation. Hence a sulfur removal unit is required prior to the hydrogenation process (Lam et al. 2017; Angelidaki et al. 2018).

3.3 Membrane Technology for Biogas Upgrading

Membrane-based technologies for biogas upgrading are a promising alternative to conventional technologies such as water scrubbing or PSA. Previously used for natural gas treatment, gas permeation membranes have potential in biogas treatment towards bio-methane. In recent years, the application of membrane modules was developed to pilot plant scale, but the technology is not as mature as gas permeation membranes. This section explains in details the different aspects of gas permeation membranes applied for biogas upgrading. Since carbon dioxide is the major contaminant of biogas, the techniques discussed mainly focus on removing this greenhouse gas.

3.3.1 Biogas Permeation Phenomena

Mass transport phenomena in membrane reactors can be generally classified into two steps into permeation process: first the diffusion of the gas along the entire dense area of the membrane is carried out, governed by Fick's law; after that, the gas goes through another stage of diffusion along the porous zone of the membrane (Scholz et al. 2013b).

The principle in which permeation membrane technology is based is the partial pressure difference of the difference gas components from the feed side to the permeate side (see Fig. 3.5). To generate this driving force, three methods are

Fig. 3.5 Membrane configuration scheme

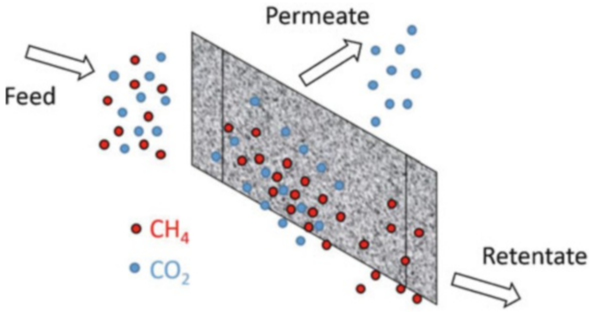

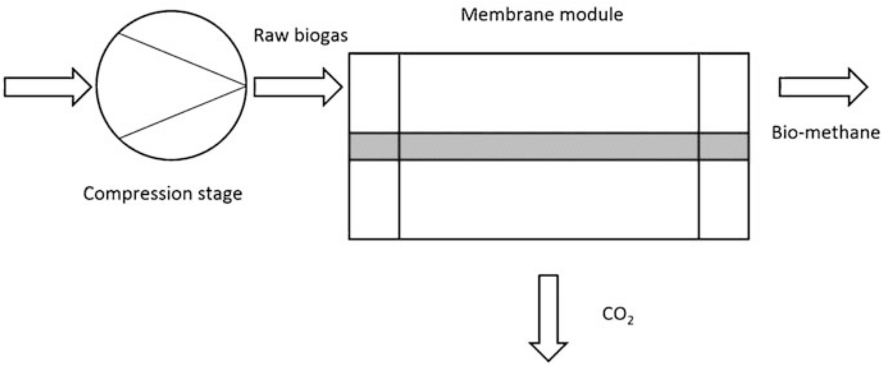

Fig. 3.6 Feed compression to generate driving force. (Modified after Scholz et al. 2013a, b)

typically applied: feed compression, vacuum in the permeate side, and a sweep gas spark application in the permeate side (Scholz et al. 2013b).

When the driving force is generated by compression (configuration in Fig. 3.6), the feed gas should remain pressurized all over the membrane surface (Basu et al. 2010). On the contrary, the permeate side operates at ambient pressure. A filter is generally fitted before the compressor in order to eliminate some particles present in the biogas that could damage it. This configuration may be more efficient than others since if the product is the retentate, then it is already pressurized for downstream processes or implementation in the natural gas grid network (Scholz et al. 2013b).

Figure 3.7 represents a vacuum in the permeate side configuration to provide the driving force in the overall of the system. This scheme is really useful when only a small amount of biogas needs to be upgraded. Nevertheless, the resulted bio-methane is not compressed, so this makes a compression stage necessary to meet natural gas grid requirements (Makaruk et al. 2010).

A sweep gas stream on the permeate side in counterflow direction can be employed to create the driving force for the permeation phenomena (Chen et al. 2016). This entails a dilution of the permeate flow and a possible additional step if the permeate component needs to be recovered for other potential application. Moreover, an extra cost is expected since the sweep gas is usually an inert gas.

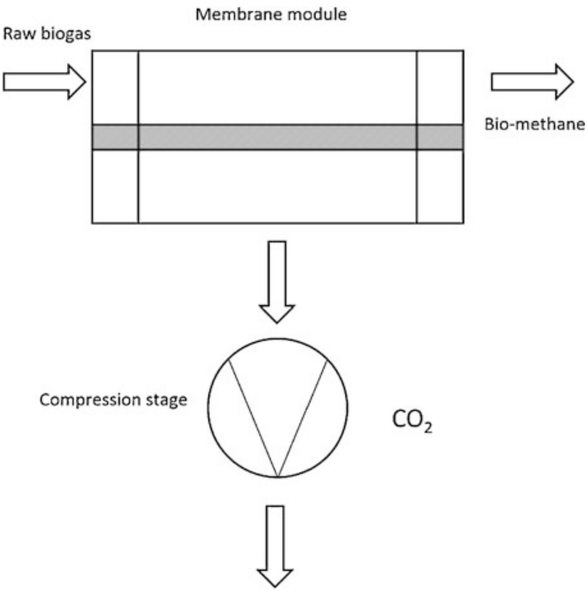

Fig. 3.7 Driving force by vacuum in the permeate side. (Modified after Scholz et al. 2013a, b)

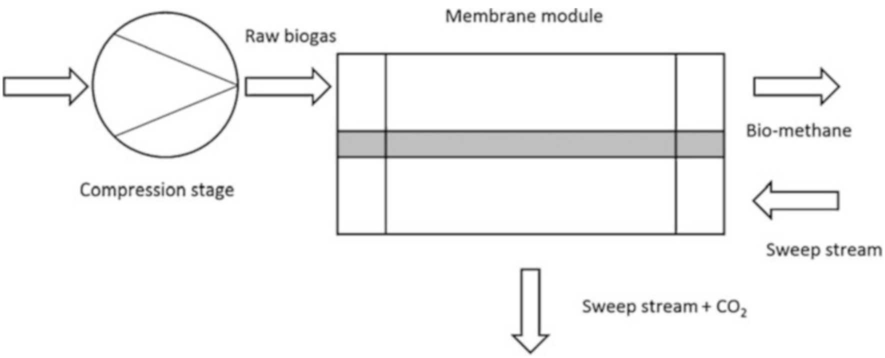

Fig. 3.8 Sweep stream configuration. (Modified after Scholz et al. 2013a, b)

Sometimes it is possible to employ the raw gas flow as sweep gas, but this usually lowers the efficiency of the membrane module (Fig. 3.8).

3.3.2 Membrane Materials

Due to the hard process conditions at which membranes must operate, the composition materials need to be resistant to chemicals such as H_2S, NH_3, or H_2O. In addition, these membrane materials should withstand pressures between 20 and 25 bars and temperatures of about 50 °C. For this purpose, the most used materials

Table 3.5 Most extended membrane materials for gas separations

Polymeric materials	Non-polymeric materials
Polysulfone	Carbon molecular sieves
Cellulose acetate	Zeolites
Polyetherimide	Silica
Polyimide	Palladium
Polymethylpentene	Perovskites

Modified after Basu et al. (2010)

Table 3.6 Commercial polymeric membranes per manufacturer

Company	Polymeric material
Membrane Technology Research	Cellulose acetate
Air Products	Polysulfone
Air Liquide	Polyimide
MTR	Polydimethylsiloxane
Cynara	Cellulose acetate

Modified after Basu et al. (2010)

are inorganic and polymeric, although composite membranes have also been studied in the last years. Materials usually employed for gas separations are collected in Table 3.5. Among these, the use of polymer membranes is widely used at industrial scale for biogas upgrading. The main reason is competitive prices when compared to others.

Non-polymeric membranes (alumina and zeolites among others) are known to have the best separation properties together with higher chemical and thermal stability. Nevertheless, their employment is limited due to their high manufacturing costs and insufficient mechanical properties to face the operational conditions.

Ceramic membranes are proved to be quite chemically stable and resist elevated temperatures in addition to having good selectivity and permeability. The composition of this kind of membranes is based on a metal, which is usually aluminum, titanium, or silicium, combined with an oxide, a nitride, or a carbide like aluminum oxide and titanium oxide or carbon nanotubes. However, intracrystalline phenomenon defects affect the behavior of the membrane in terms of selective transport.

Carbon molecular sieve membranes show high selectivity and permeability; however, they are brittle which makes their preparation at industrial scale difficult. Nevertheless, this type of membranes is still under research to improve the affordability of the production process.

Polymeric membranes have been the most employed type of membranes due to several reasons. They benefit from lower costs, facile module fabrication, and high pressure stability. Polysulfone, cellulose acetate, and polyimide have been employed widely in various industrial-scale applications, and their manufacture is presently done by Membrane Technology Research, Air Products, or Air Liquide among others (Table 3.6). Further information regarding polymeric membrane properties are given in Table 3.7. In particular, the permeability and selectivity of some polymeric membranes towards H_2, CH_4, and CO_2 are given.

Table 3.7 Properties of selected polymeric membrane materials

	Compound	Polysulfone	Cellulose acetate	Polyimide
Permeability at 30 °C/barrer	H_2	14	2.63	28.1
	CH_4	0.25	0.21	0.25
	CO_2	5.6	6.3	10.7
Selectivity	H_2-CO_2	2.5	0.41	2.63
	CO_2-CH_4	22.4	30.0	42.8

Modified after Basu et al. (2010)

Table 3.8 Main characteristics of the different membrane modules (Li et al. 2004; Peeva et al. 2010)

Parameter	Hollow fiber	Spiral wound	Envelope
Costs for module (€/m^2)	1.5–9	9–45	45–175
Packing density (m^2/m^3)	1000–10,000	100–1500	30–500
Area per module (m^2)	100–600	10–50	2–30

3.3.3 Membrane Modules: Characteristics and Operation

There are three commercially available modules for biogas permeation: hollow fiber modules, spiral-wound modules, and envelope modules (Brunetti et al. 2010; Scholz et al. 2013b). The main characteristics of these modules are collected in Table 3.8. The hollow fiber module benefits from high packing density and is the most economically viable. For this reason, it is the most used industrially.

The majority of international suppliers, Air Liquide, Air Products, Evonik, and Parker, provide hollow fiber modules. Nevertheless, other well-recognized suppliers like MTF or UOP former Grace have launched better quality spiral-wound membrane module type.

A commercial hollow fiber module needs to have the mechanical strength to withstand the high operation pressure, high-quality fibers, fits in the range of flow gases the flow patterns, and an economic balance between material costs and working life (Li et al. 2004).

Regarding the operation of membrane modules, some problems could derive from physical effects and have an impact on the module performance. These effects are pressure losses, concentration polarization, and Joule–Thomson effect which may considerably affect the driving force.

Pressure loss in biogas permeation membrane modules is the most common and inevitable effect. It is caused by the flowing medium in the fiber that decreases the transmembrane pressure. Moreover, some local fluxes are not uniform, and as a result, some inefficiencies are presented along the fiber, decreasing the overall performance. Several authors studied this influence and modeled it mathematically (Paulen and Fikar 2016; Pellegrin et al. 2015; Yoon et al. 2008; Shao and Huang 2006; Liang 2016).

Concentration polarization is caused by the accumulation of biogas molecules at the membrane surface and may result in the reduction of the mass transfer along the membrane surface. This phenomenon is directly correlated with the flux – the higher it is, the bigger is the effect – and it mainly occurs in the pores of the material (Lüdtke et al. 1998; de Nooijer et al. 2018).

The Joule–Thomson effect has been widely studied (Mushtaq et al. 2013; Rowe et al. 2010; Coker et al. 1999; Scholz et al. 2013b). This effect is due to the change in temperature under constant enthalpy that occurs when a gas tends to expand from higher pressure zones to lower ones. In biogas permeation, this effect is considerable since the pressure difference between the feed and the permeate is quite elevated (20–25 bar vs. 1 bar). For biogas feed with a high carbon dioxide concentration at normal operating pressures, the temperature drop is quite significant and thus potentially causes some condensation along the membrane surface. To remove this possible effect, Faizan Ahmad et al. (2012) proposed the installation of a heater before the membrane module (Ahmad et al. 2012).

3.3.4 *Biogas Upgrading Permeation Processes: Single- and Multistage Configurations*

There are different configurations for biogas upgrading through permeation processes, and the selection of one of them depends on the purity requirements for the final bio-methane. Generally, these different configurations can be split in two categories: single-stage gas permeation and multistage processes.

Regarding the single-stage process, two possible schemes can be found (Figs. 3.9 and 3.10). Figure 3.9 shows the simplest process for biogas upgrading but also the most inefficient one since the methane loss is very high. This configuration is hardly

Fig. 3.9 Hollow fiber membrane module

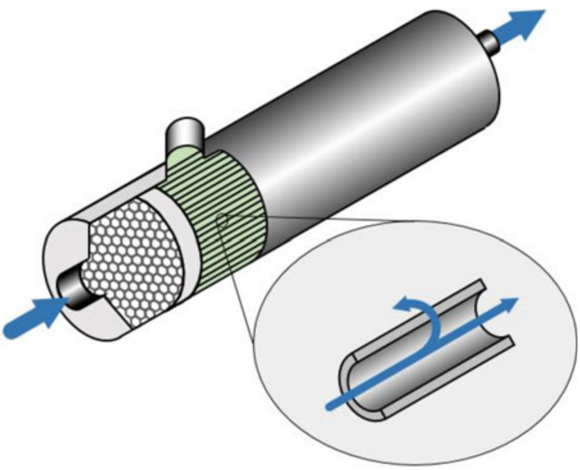

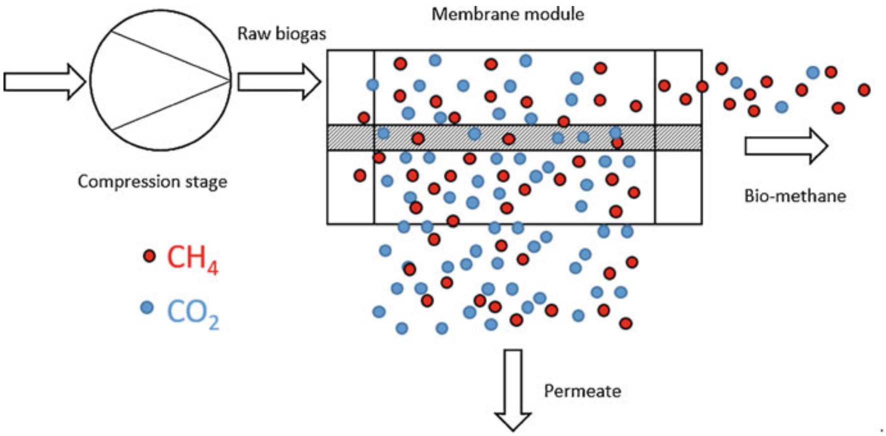

Fig. 3.10 Single-stage configuration without recirculation

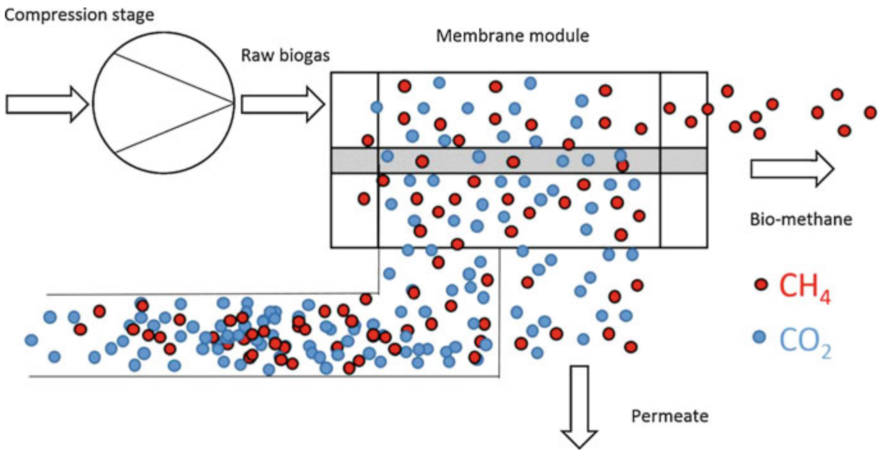

Fig. 3.11 Single-stage configuration with partial recirculation

controllable since it is solely directed by the selectivity of the membrane, and traces of CO_2 can appear in the bio-methane flow. On the other hand, the methane loss can be decreased by a partial recycling of the permeate, as shown in Fig. 3.10. This allowed the recovery of up to 95% of methane (Li et al. 2007; Niesner et al. 2013; Chen et al. 2015). Nevertheless, the energy input involved in the compression stage is higher since the gas flow increased considerably.

When higher bio-methane purity and less bio-methane losses are required, multistage processes have been applied successfully (Haider et al. 2016). The most common way to build a multistage process is to interconnect two membrane modules in series. Figures 3.11, 3.12, 3.13, and 3.14 show different multistage configurations for biogas upgrading. From these four configurations, many hybrid processes have

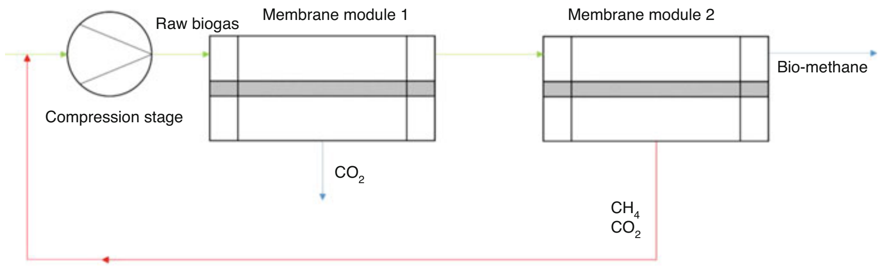

Fig. 3.12 Multistage configuration with a second membrane module and permeate recirculation. (Modified after Zeman and Zydney 2017)

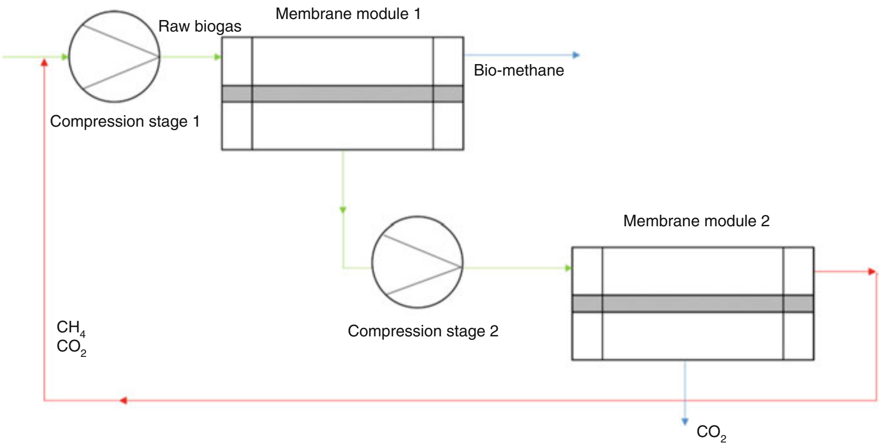

Fig. 3.13 Multistage configuration with a second membrane module, a retentate recirculation, and two compressors. (Modified after Zhao et al. 2010)

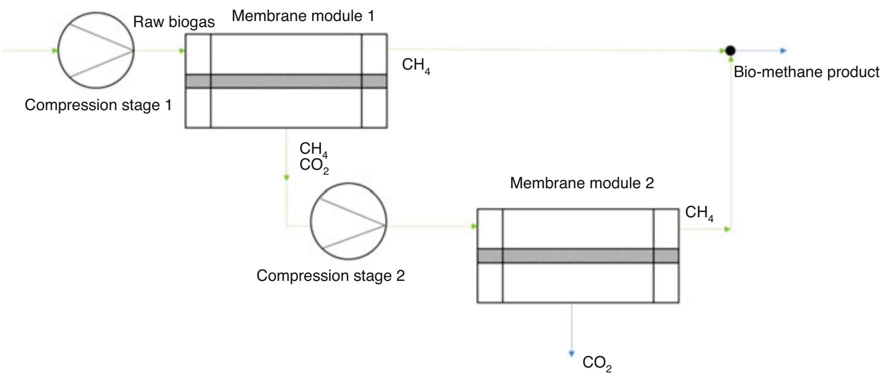

Fig. 3.14 Multistage configuration without recirculation of the second membrane module retentate. (Modified after Bailón Allegue and Bailón and Hinge 2014)

been proposed (Bauer et al. 2013; Zhou et al. 2017; Zhang et al. 2014; Deng and Hägg 2010; Baker and Lokhandwala 2008; Makaruk et al. 2010; Bhide et al. 1998; Scholz et al. 2013a, b).

Figure 3.11 describes a process in which the first module removes carbon dioxide from raw biogas, while the second one allows to obtain an adjustable bio-methane purity, according to the specifications. In order to diminish the CH_4 losses, the permeate of the second module is recirculated before the compression stage.

An alternative to increase the purity and recover the CH_4 that may have gone to the permeate flow is the further treatment of the permeate (Deng and Hägg 2010). Unfortunately, this configuration requires a second compressor prior the second stage since the permeate is an ambient pressure. This increases the process energy consumption and as a consequence lowers the overall performance.

Another variation of the previous configuration without recirculating the retentate is shown in Fig. 3.13. Here the methane-rich flow resulting from the second membrane filtration is mixed with the bio-methane stream from the first membrane module, so removing the recirculation provokes lower capital cost since the flows are smaller.

The last multistage configuration known is quite similar to the one presented in Fig. 3.11 but with the inclusion of a sweep gas in the second membrane module as shown in Fig. 3.14. This allows to increase the efficiency of the second module. However, once again, the capital cost of the installation as well as the operating compression costs increases due to larger streams circulated in the system.

3.3.5 Commercial Biogas Plants Based on Membrane Technologies

The number of biogas plant based on membrane technologies has increased recently until becoming the second most built installation for bio-methane production. In general, these bio-methane production installations are divided into high-capacity (commercial purpose) and low-capacity (usually research purpose) plants. Figure 3.15 shows a typical scheme of a commercial membrane bio-methane production (Fig. 3.16).

In a commercial membrane-based installation for biogas upgrading, first, the raw biogas is produced in a biodigester by an anaerobic digestion process. This raw biogas is then pulsed into a gas washer stage for a minimum water scrubbing operation to light up the total flow gas. After that, H_2S and NH_3 are partially removed with a carbon filter step to avoid operation problems in the compression stage. Finally, once the biogas is compressed in the membrane module unit, the bio-methane is recovered from the flow in the retentate. The carbon dioxide in the permeate could be compressed and sold if its purity is adequate.

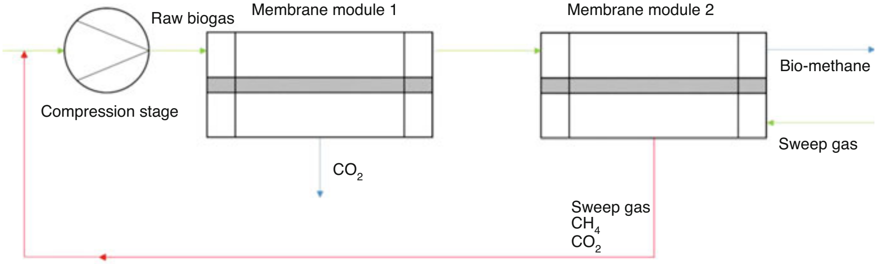

Fig. 3.15 Multistage configuration with sweep gas use and a second membrane module with permeate recirculation. (Modified after Hasan et al. 2012)

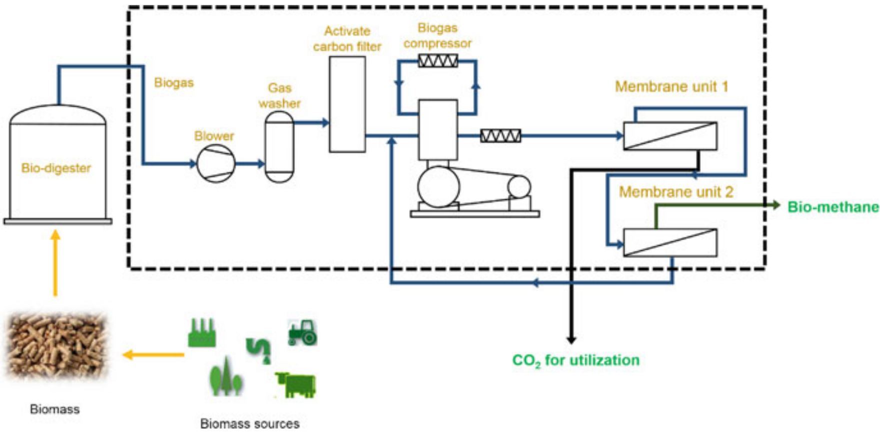

Fig. 3.16 Layout of a typical commercial membrane-based bio-methane installation. (Modified after X. Y. Chen et al. 2015)

Some of the most relevant installations in each category as well as their location are collected in Table 3.9. Curiously, the largest commercial plants are located in the United States, while the most important research plants are based in Europe.

The first commercial bio-methane production plant in Europe was set in 1990 in the Netherland, in Collendoorn with a capacity of 25 m^3/h. Nowadays its capacity multiplied by 15. Though it was the first commercial plant based in Europe, the purity of bio-methane obtained is not more than 90% (Scholz et al. 2013b).

It is expected by the biogas research world that the number of bio-methane production membrane-based plants will increase greatly in the near future, since low operational and investment costs as well as high bio-methane purities can be obtained by means of this technology. Additionally, bio-methane production processes could be easily connected to combined heat and power (CHP) engines. Makaruk et al. conducted a promising study in which they integrated a membrane-based bio-methane plants with the heating and power requirements, achieving an energy consumption of around 0.3 kWh per m^3 of bio-methane (Makaruk et al. 2010).

Table 3.9 Location of installed membrane-based bio-methane production plants per production capacity

Category	Location	Capacity (m^3/h)
High-capacity	Seattle (United States)	18,886
	Kersey (United States)	14,164
	New Orleans (United States)	10,623
	Atlanta (United States)	8263
	Winder (United States)	7082
	Imperial (United States)	7082
Low-capacity	Collendoorn (Netherland)	375
	Kisslegg-Rahmhaus (Germany)	300
	Witteveen (Netherland)	200
	Wiener Neustadt (Austria)	120
	Bruck an der Leitha (Austria)	100
	Beverwijk (Netherland)	80

Modified after X. Y. Chen et al. (2015) and Scholz et al. (2013b)

3.4 Conclusions

This study confirms that a range of biogas upgrading technologies are available to be applied on an industrial scale. Pressure swing adsorption, water scrubbing, chemical scrubbing, organic physical scrubbing, membrane separation, and cryogenic separation have been proven to be technically developed enough, while further efforts should be focused on reducing economic factors. Among these technologies, membrane-based processes for biogas upgrading present investment and operational costs which seem to be economically interesting for an immediate industrial application. This technique carried out by means of gas permeation phenomena has shown results worthy of replacing conventional biogas separation techniques such as water scrubbing. Polymeric membrane materials are under continuous development which will facilitate the implementation of membrane-based biogas upgrading processes in many industrial areas. Besides, their low cost and flexibility make polymeric membranes easy to be fabricated into hollow fiber modules. However, there are some issues that need to be improved such as methane losses in some process configurations. Single-stage membrane processes are not technologically mature since the overall efficiency of the process is affected by methane losses. Multistage configurations play an important role in biogas upgrading membrane-based processes, thanks to the outstanding results presented regarding overall costs and adjustable bio-methane purity. Moreover, this technology is even more interesting for the adaptability of the different configurations and the multiple opportunities to form hybrid processes in combination with other techniques.

Several industrial areas with biogas production potential will implement membrane-based biogas upgrading technologies in the near future. The ripeness showed by the already existing membrane-based plants is the main reason to encourage novel biogas producers to apply this technology. Future research should focus on finding a way to remove minor components, for example, H_2S, NH_3, and siloxanes, in order to improve the overall economic performance. Also the development of new construction materials cheaper than those employed nowadays will be a call for research in the near future.

References

Abatzoglou N, Boivin S (2009) A review of biogas purification processes. Biofuels Bioprod Biorefin. https://doi.org/10.1002/bbb.117

AEBIOM (2017) Key findings. European Bioenergy. AEBIOM statistical report outlook. European Biomass Association (AEBIOM)

Ahmad F, Lau KK, Shariff AM, Murshid G, Keong LK, Shariff AM, Murshid G, Petronas UT, Iskandar BS (2012) The study of Joule Thompson effect for the removal of CO2 from natural gas by membrane process. Int J Chem Environ Eng 3(2):15–18.

Alonso-Vicario A, Ochoa-Gómez JR, Gil-Río S, Gómez-Jiménez-Aberasturi O, Ramírez-López CA, Torrecilla-Soria J, Domínguez A (2010) Purification and upgrading of biogas by pressure swing adsorption on synthetic and natural zeolites. Microporous Mesoporous Mater. https://doi.org/10.1016/j.micromeso.2010.05.014

Andriani D, Wresta A, Atmaja TD, Saepudin A (2014) A review on optimization production and upgrading biogas through CO_2 removal using various techniques. Appl Biochem Biotechnol 172(4):1909–1928. https://doi.org/10.1007/s12010-013-0652-x

Angelidaki I, Treu L, Tsapekos P, Luo G, Campanaro S, Wenzel H, Kougias PG (2018) Biogas upgrading and utilization: current status and perspectives. Biotechnol Adv. https://doi.org/10.1016/j.biotechadv.2018.01.011

Aresta M (2010) Carbon dioxide as chemical feedstock. Wiley-VCH, Weinheim/Chichester. https://doi.org/10.1002/9783527629916

Arti M, Youn MH, Park KT, Kim HJ, Kim YE, Jeong SK (2017) Single process for CO_2 capture and mineralization in various alkanolamines using calcium chloride. Energy Fuel 31(1):763–769. https://doi.org/10.1021/acs.energyfuels.6b02448

Baena-moreno FM, Rodríguez-Galán M, Vega F, Bernabé Alonso-fariñas LF, Arenas V, Navarrete B (2018a) Carbon capture and utilization technologies: a literature review and recent advances. Energy Sources Part A 41(12):1403–1433. https://doi.org/10.1080/15567036.2018.1548518

Baena-Moreno FM, Rodríguez-Galán M, Vega F, Reina TR, Vilches LF, Navarrete B (2018b) Regeneration of sodium hydroxide from a biogas upgrading unit through the synthesis of precipitated calcium carbonate: an experimental influence study of reaction parameters. Processes 6:205. https://doi.org/10.3390/pr6110205

Bailón Allegue L, Hinge J (2014) Biogas upgrading evaluation of methods for H_2S removal. Danish Technological Institute. https://doi.org/10.1074/mcp.M110.002766

Baker RW, Lokhandwala K (2008) Natural gas processing with membranes: an overview. Ind Eng Chem Res 47(7):2109–2121. https://doi.org/10.1021/ie071083w

Basu S, Khan AL, Cano-Odena A, Liu C, Vankelecom IFJ (2010) Membrane-based technologies for biogas separations. Chem Soc Rev 39(2):750–768. https://doi.org/10.1039/b817050a

Bauer F, Hulteberg C, Persson T, Tamm D (2013) Biogas upgrading – review of commercial technologies. SGC Rapport 2013:270

Bekkering J, Broekhuis AA, van Gemert WJT (2010) Optimisation of a green gas supply chain – a review. Bioresour Technol 101(2):450–456. https://doi.org/10.1016/j.biortech.2009.08.106

Bhide BD, Voskericyan A, Stern SA (1998) Hybrid processes for the removal of acid gases from natural gas. J Membr Sci 140(1):27–49. https://doi.org/10.1016/S0376-7388(97)00257-3

Bond T, Templeton MR (2011) History and future of domestic biogas plants in the developing world. Energy Sustain Dev 15(4):347–354. https://doi.org/10.1016/j.esd.2011.09.003

Bright A, Bulson H, Henderson A, Sharpe N, Dorstewitz H, Pickering J (2011) An introduction to the production of biomethane gas and injection to the national grid

Brunetti A, Bernardo P, Drioli E, Barbieri G (2010) Membrane engineering: progress and potentialities in gas separations. In: Membrane gas separation. Wiley, Chichester. https://doi.org/10.1002/9780470665626.ch14

Chen XY, Vinh-Thang H, Ramirez AA, Rodrigue D, Kaliaguine S (2015) Membrane gas separation technologies for biogas upgrading. RSC Adv 5(31):24399–24448. https://doi.org/10.1039/C5RA00666J

Chen WH, Lin CH, Lin YL, Tsai CW, Chein RY, Ching Tsung Y (2016) Interfacial permeation phenomena of hydrogen purification and carbon dioxide separation in a non-isothermal palladium membrane tube. Chem Eng J 305:156–168. https://doi.org/10.1016/j.cej.2016.01.036

Chiesa P, Campanari S, Manzolini G (2011) CO_2 cryogenic separation from combined cycles integrated with molten carbonate fuel cells. Int J Hydrog Energy 36(16):10355–10365. https://doi.org/10.1016/j.ijhydene.2010.09.068

Clift R (2006) Sustainable development and its implications for chemical engineering. Chem Eng Sci 61(13):4179–4187. https://doi.org/10.1016/j.ces.2005.10.017

Coker DT, Allen T, Freeman BD, Fleming GK (1999) Nonisothermal model for gas separation hollow-fiber membranes. AICHE J 45(7):1451–1468. https://doi.org/10.1002/aic.690450709

de Nooijer N, Gallucci F, Pellizzari E, Melendez J, Tanaka DAP, Manzolini G, van Sint Annaland M (2018) On concentration polarisation in a fluidized bed membrane reactor for biogas steam reforming: modelling and experimental validation. Chem Eng J 348:232–243. https://doi.org/10.1016/j.cej.2018.04.205

Deng L, Hägg MB (2010) Techno-economic evaluation of biogas upgrading process using CO_2 facilitated transport membrane. Int J Greenh Gas Control 4(4):638–646. https://doi.org/10.1016/j.ijggc.2009.12.013

Djas M, Henczka M (2018) Reactive extraction of carboxylic acids using organic solvents and supercritical fluids: a review. Sep Purif Technol 201:106–119. https://doi.org/10.1016/j.seppur.2018.02.010

Haider S, Lindbråthen A, Hägg M-B (2016) Techno-economical evaluation of membrane based biogas upgrading system: a comparison between polymeric membrane and carbon membrane technology. Green Energy Environ 1(3):222–234. https://doi.org/10.1016/j.gee.2016.10.003

Harasimowicz M, Orluk P, Zakrzewska-Trznadel G, Chmielewski AG (2007) Application of polyimide membranes for biogas purification and enrichment. J Hazard Mater 144(3):698–702. https://doi.org/10.1016/j.jhazmat.2007.01.098

Hasan MMF, Baliban RC, Elia JA, Floudas CA (2012) Modeling, simulation, and optimization of postcombustion CO_2 capture for variable feed concentration and flow rate. 1. Chemical absorption and membrane processes. Ind Eng Chem Res 51(48):15642–15664. https://doi.org/10.1021/ie301571d

Hertel S, Navarro P, Deegener S, Körner I (2015) Biogas and nutrients from blackwater, lawn cuttings and grease trap residues: experiments for Hamburg's Jenfelder Au District. Energy Sustain Soc 5(1). https://doi.org/10.1186/s13705-015-0057-5

Hoo PY, Hashim H, Ho WS (2018) Opportunities and challenges: landfill gas to biomethane injection into natural gas distribution grid through pipeline. J Clean Prod 175:409–419. https://doi.org/10.1016/j.jclepro.2017.11.193

Hosseini SE, Wahid MA (2013) Feasibility study of biogas production and utilization as a source of renewable energy in Malaysia. Renew Sust Energ Rev 19:454–462. https://doi.org/10.1016/j.rser.2012.11.008

Ibrahim M, El-Zaart A, Adams C (2018) Smart sustainable cities roadmap: readiness for transformation towards urban sustainability. Sustain Cities Soc 37:530–540. https://doi.org/10.1016/j.scs.2017.10.008

Jiang Z, Xiao T, Kuznetsov VL, Edwards PP (2010) Turning carbon dioxide into fuel. Philos Trans R Soc A Math Phys Eng Sci 368(1923):3343–3364. https://doi.org/10.1098/rsta.2010.0119

Johansson N (2008) Production of liquid biogas, LBG, with cryogenic and conventional upgrading technology – description of systems and evaluations of energy balances. http://lup.lub.lu.se/student-papers/record/4468178/file/4469242.pdf

Kadam R, Panwar NL (2017) Recent advancement in biogas enrichment and its applications. Renew Sust Energ Rev 73:892–903. https://doi.org/10.1016/j.rser.2017.01.167

Kim YJ, Nam YS, Kang YT (2015) Study on a numerical model and PSA (pressure swing adsorption) process experiment for CH_4/CO_2 separation from biogas. Energy 91:732–741. https://doi.org/10.1016/j.energy.2015.08.086

Lam CH, Das S, Erickson NC, Hyzer CD, Garedew M, Anderson JE, Wallington TJ, Tamor MA, Jackson JE, Saffron CM (2017) Towards sustainable hydrocarbon fuels with biomass fast pyrolysis oil and electrocatalytic upgrading. Sustain Energy Fuels 1(2):258–266. https://doi.org/10.1039/C6SE00080K

Leonzio G (2016) Upgrading of biogas to bio-methane with chemical absorption process: simulation and environmental impact. J Clean Prod 131:364–375. https://doi.org/10.1016/j.jclepro.2016.05.020

Li D, Wang R, Chung TS (2004) Fabrication of lab-scale hollow fiber membrane modules with high packing density. Sep Purif Technol 40(1):15. https://doi.org/10.1016/j.seppur.2003.12.019

Li S, Falconer JL, Noble RD, Krishna R (2007) Modeling permeation of CO_2/CH_4, CO_2/N_2, and N_2/CH_4 mixtures across SAPO-34 membrane with the Max Well-Stefan equations. Ind Eng Chem Res 46(12):3904–3911. https://doi.org/10.1021/ie0610703

Liang S (2016) Performance modeling and analysis of a hollow fiber membrane system. J Membr Sci Technol 6:1. https://doi.org/10.4172/2155-9589.1000144

Lüdtke O, Behling RD, Ohlrogge K (1998) Concentration polarization in gas permeation. J Membr Sci 146(2):145–157. https://doi.org/10.1016/S0376-7388(98)00104-5

Makaruk A, Miltner M, Harasek M (2010) Membrane biogas upgrading processes for the production of natural gas substitute. Sep Purif Technol 74(1):83–92. https://doi.org/10.1016/j.seppur.2010.05.010

Moghaddam A, Elham SA, Hulteberg C, Nordberg Å (2015) Energy balance and global warming potential of biogas-based fuels from a life cycle perspective. Fuel Process Technol. https://doi.org/10.1016/j.fuproc.2014.12.014

Mushtaq A, Mukhtar HB, Shariff AM, Mannan HA (2013) A review: development of polymeric blend membrane for removal of CO_2 from natural gas. Int J Eng Technol. https://doi.org/10.1080/0300443730020210

Niesner J, Jecha D, Stehlík P (2013) Biogas upgrading technologies: state of art review in European region. Chem Eng Trans 35:517–522. https://doi.org/10.3303/CET1335086

Patrizio P, Leduc S, Chinese D, Dotzauer E, Kraxner F (2015) Biomethane as transport fuel – a comparison with other biogas utilization pathways in Northern Italy. Appl Energy 157:25–34. https://doi.org/10.1016/j.apenergy.2015.07.074

Paulen R, Fikar M (2016) Membrane processes. In: Advances in industrial control. https://doi.org/10.1007/978-3-319-20475-8_1

Peeva LG, Sairam M, Livingston AG (2010) Comprehensive membrane science and engineering. In: Comprehensive membrane science and engineering. Elsevier Science, Oxford. https://doi.org/10.1016/B978-0-08-093250-7.00020-7

Pellegrin M-L, Sadler ME, Greiner AD, Aguinaldo J, Min K, Zhang K, Arabi S, Burbano MS, Kent F, Shoaf R (2015) Membrane processes. Water Environ Res 89(10):1066–1135. https://doi.org/10.2175/106143015X14338845155345

Persson M (2003) Evaluation of upgrading techniques for biogas. Report SGC142

Persson M, Jonsson O, Wellinger A (2007) Biogas upgrading to vehicle fuel standards and grid. IEA Bioenergy:1–32

Pfau SF, Hagens JE, Dankbaar B (2017) Biogas between renewable energy and bio-economy policies—opportunities and constraints resulting from a dual role. Energy Sustain Soc 7 (1):1–15. https://doi.org/10.1186/s13705-017-0120-5

Pipatmanomai S, Kaewluan S, Vitidsant T (2009) Economic assessment of biogas-to-electricity generation system with H_2S removal by activated carbon in small pig farm. Appl Energy 86 (5):669–674. https://doi.org/10.1016/j.apenergy.2008.07.007

Rahman MA, Møller HB, Saha CK, Alam MM, Wahid R, Feng L (2017) Optimal ratio for anaerobic co-digestion of poultry droppings and lignocellulosic-rich substrates for enhanced biogas production. Energy Sustain Dev 39:59–66. https://doi.org/10.1016/j.esd.2017.04.004

Rasi S, Läntelä J, Rintala J (2011) Trace compounds affecting biogas energy utilisation – a review. Energy Convers Manag 52(12):3369–3375. https://doi.org/10.1016/j.enconman.2011.07.005

Rotunno P, Lanzini A, Leone P (2017) Energy and economic analysis of a water scrubbing based biogas upgrading process for biomethane injection into the gas grid or use as transportation fuel. Renew Energy 102:417–432. https://doi.org/10.1016/j.renene.2016.10.062

Rowe BW, Robeson LM, Freeman BD, Paul DR (2010) Influence of temperature on the upper bound: theoretical considerations and comparison with experimental results. J Membr Sci 360:58–69. https://doi.org/10.1016/j.memsci.2010.04.047

Ryckebosch E, Drouillon M, Vervaeren H (2011) Techniques for transformation of biogas to biomethane. Biomass Bioenergy 35(5):1633–1645. https://doi.org/10.1016/j.biombioe.2011.02.033

Sanna A, Vega F, Navarrete B, Mercedes Maroto-Valer M (2014) Accelerated MEA degradation study in hybrid CO_2 capture systems. Energy Proc 63:745–749. https://doi.org/10.1016/j.egypro.2014.11.082

Scholz M, Frank B, Stockmeier F, Falß S, Wessling M (2013a) Techno-economic analysis of hybrid processes for biogas upgrading. Ind Eng Chem Res 52(47):16929–16938. https://doi.org/10.1021/ie402660s

Scholz M, Melin T, Wessling M (2013b) Transforming biogas into biomethane using membrane technology. Renew Sust Energ Rev 17:199–212. https://doi.org/10.1016/j.rser.2012.08.009

Scripps Institution of Oceanography (2018) The keeling curve. UC San Diego. https://scripps.ucsd.edu/programs/keelingcurve/

Shao P, Huang RYM (2006) An analytical approach to the gas pressure drop in hollow fiber membranes. J Membr Sci 271(1–2):69–76. https://doi.org/10.1016/j.memsci.2005.06.058

Sun Q, Li H, Yan J, Liu L, Yu Z, Yu X (2015) Selection of appropriate biogas upgrading technology-a review of biogas cleaning, upgrading and utilisation. Renew Sust Energ Rev 51:521–532. https://doi.org/10.1016/j.rser.2015.06.029

Tuinier MJ, Van Sint Annaland M (2012) Biogas purification using cryogenic packed-bed technology. Ind Eng Chem Res 51(15):5552–5558. https://doi.org/10.1021/ie202606g

Ullah Khan I, Hafiz Dzarfan Othman M, Hashim H, Matsuura T, Ismail AF, Rezaei-DashtArzhandi-M, Wan Azelee I (2017) Biogas as a renewable energy fuel – a review of biogas upgrading, utilisation and storage. Energy Convers Manag 150:277–294. https://doi.org/10.1016/j.enconman.2017.08.035

Vega F, Cano M, Gallego M, Camino S, Camino JA, Navarrete B (2017) Evaluation of MEA 5 M performance at different CO_2 concentrations of flue gas tested at a CO_2 capture lab-scale plant. Energy Procedia 114(114):6222–6228. https://doi.org/10.1016/j.egypro.2017.03.1760

Verotti M, Servadio P, Bergonzoli S (2016) Biogas upgrading and utilization from ICEs towards stationary molten carbonate fuel cell systems. Int J Green Energy 13(7):655–664. https://doi.org/10.1080/15435075.2015.1018992

Weiland P (2009) Biogas production: current state and perspectives. Appl Microbiol Biotechnol 85 (4):849–860. https://doi.org/10.1007/s00253-009-2246-7

Wheeler P, Holm-Nielsen JB, Jaatinen T, Wellinger A, Lindberg A, Pettigrew A (1999) Biogas upgrading and utilisation. IEA Bioenergy:3–20. http://www.energietech.info/pdfs/Biogas_upgrading.pdf

Yadvika S, Sreekrishnan TR, Kohli S, Rana V (2004) Enhancement of biogas production from solid substrates using different techniques – a review. Bioresour Technol 95(1):1–10. https://doi.org/10.1016/j.biortech.2004.02.010

Yang L, Ge X, Wan C, Yu F, Li Y (2014) Progress and perspectives in converting biogas to transportation fuels. Renew Sust Energ Rev 40:1133–1152. https://doi.org/10.1016/j.rser.2014.08.008

Yin F, Li Z, Zhou X, Bai X, Lian J (2016) Effects of temperature and relative humidity on the methane permeability rate of biogas storage membranes. Int J Green Energy 13(9):951–956. https://doi.org/10.1080/15435075.2015.1088446

Yoon SH, Lee S, Yeom IT (2008) Experimental verification of pressure drop models in hollow fiber membrane. J Membr Sci 310(1–2):7–12. https://doi.org/10.1016/j.memsci.2007.11.048

Zeman LJ, Zydney AL (2017) Microfiltration and ultrafiltration: principles and applications. Taylor and Francis, London. https://doi.org/10.1201/9780203747223

Zhang Z, Yan Y, Zhang L, Chen Y, Ju S (2014) CFD investigation of CO_2 capture by methyldiethanolamine and 2-(1-piperazinyl)-ethylamine in membranes: Part B. Effect of membrane properties. J Nat Gas Sci Eng 19:311–316. https://doi.org/10.1016/j.jngse.2014.05.023

Zhao L, Riensche E, Blum L, Stolten D (2010) Multi-stage gas separation membrane processes used in post-combustion capture: energetic and economic analyses. J Membr Sci 359:160–172. https://doi.org/10.1016/j.memsci.2010.02.003

Zhou K, Chaemchuen S, Verpoort F (2017) Alternative materials in technologies for biogas upgrading via CO_2 capture. Renew Sust Energ Rev 79:1414–1441. https://doi.org/10.1016/J.RSER.2017.05.198

Chapter 4
Developments of Carbon-Based Membrane Materials for Water Treatment

Chen Li, Jie Yang, Luying Zhang, Shibo Li, Yin Yuan, Xin Xiao, Xinfei Fan, and Chengwen Song

Contents

Abstract Serious water contamination and freshwater shortage result in the urgent requirements of advanced technologies for water treatment. Membrane separation is an alternative technology to address the global water crisis. Hence the research for membrane materials with excellent properties is being undertaken vigorously. Recently, successful attempts have been made towards applying carbon-based membrane materials, such as carbon membranes, carbon nanotube membranes,

C. Li · J. Yang · L. Zhang · S. Li · Y. Yuan · X. Xiao · X. Fan · C. Song (✉)
College of Environmental Science and Engineering, Dalian Maritime University, Dalian, China
e-mail: chengwensong@dlmu.edu.cn

Z. Zhang et al. (eds.), *Membranes for Environmental Applications*, Environmental Chemistry for a Sustainable World 42, https://doi.org/10.1007/978-3-030-33978-4_4

carbon fiber membranes, activated carbon membranes, graphene-based membranes, etc. for achieving a high separation performance. The intrinsic properties of the carbon materials can potentially lead to enhancements in fouling mitigation, hydrophilicity, and permeate quality. This chapter provides a brief and comprehensive overview of the fabrication and synthesis mechanisms of the carbon-based membrane materials, characterization methods, and practical applications in water treatment. The major points are:

1. Carbon membranes, derived from phenolic resin and coal as precursors, have been widely used in water treatment, specifically utilizing the electrical conductivity of coal-based carbon membrane as the electrode and membrane filter simultaneously demonstrate great potential on water treatment.
2. Four types of carbon nanotube membranes are presented and indicate high separation performance due to the remarkable physicochemical properties of carbon nanotubes.
3. Carbon fiber membranes possess abundant functional groups on the surface, favoring high permeability in water treatment.
4. Activated carbon membranes are promising for organic matter removal owing to high surface area, micro–meso and macroscopic structure, and various chemical functional groups.
5. Graphene-based membranes as the novel carbon-based membrane materials with unique laminar pores are attracting more and more attentions.

Keywords Membrane · Carbon materials · Wastewater treatment · Water purification · Separation

4.1 Introduction

The industrial development and population growth have led to serious and sustainable challenge towards the water resources in the twenty-first century (Menachem and William 2011; Ma et al. 2017; Salgot and Folch 2018). The prediction from the United Nations indicates that half of the countries worldwide will be confronted with water shortage in the coming decades (Goh and Ismail 2018). The World Health Organization (WHO) also estimates that more than 1.2 billion people worldwide have gotten sick or died through drinking contaminated water, and the number is expected to significantly grow in the coming years (Montgomery and Elimelech 2007; Wilson et al. 2018). Hence, in order to reduce the hazards from water pollution to humankind, various technologies and industrial processes for water treatment or purification have been developed and applied rapidly in recent years (Zheng et al. 2015; Pintor et al. 2016; Hayat et al. 2017; Jiao et al. 2017).

Among them, membrane separation has been accepted as a promising and pervasive technology arising from its numerous advantages of no chemical additives requirement, low energy demand, easy operation, high separation selectivity, and good stability (Gin and Noble 2011; Li et al. 2016b; Thakur and Voicu 2016; Chowdhury et al. 2018; Lau et al. 2018). To date, membrane separation has been widely applied in industrial wastewater treatment and drinking water purification and desalinization (Pendergast and Hoek 2011; Singh and Hankins 2016; Parimal 2017; Zhang et al. 2018). As one of the dominated factors to determine membrane performance, membrane materials should be primarily concerned for exploring high-performance membranes.

Recently, carbon-based materials have been used to develop membranes with optimal structure and performance due to their excellent physicochemical properties (Goh et al. 2016; Thines et al. 2017; Anand et al. 2018; Wei et al. 2018). The carbon-based materials not only can improve the wetting ability and surface charges of the membranes but also introduce additional functions such as antimicrobial ability and photocatalytic and electrochemical reactions (Liu et al. 2011; Ong et al. 2018). According to previous works, several kinds of carbon-based membrane materials including carbon membranes, carbon nanotube membranes, carbon fiber membranes, activated carbon membranes, graphene-based membranes, etc. (Inagaki et al. 2014; Jiang et al. 2016; Lawler 2016; Vatanpour and Safarpour 2018) are described. This chapter aims to provide an overview on recent developments of carbon-based membrane materials for water treatment. A brief discussion of the existing challenges and their prospects are also considered.

4.2 Carbon Membranes

Carbon membranes, as novel porous inorganic membranes, are usually prepared by pyrolysis of carbonaceous materials, such as polyimide and its derivatives, polyacrylonitrile, poly(furfuryl alcohol), phenol–formaldehyde, coal, etc. In the past several decades, carbon membranes have demonstrated excellent gas separation performance (Hamm et al. 2017), however, only a few carbon membranes are applied on water treatment due to their high cost and complex preparation process. In the following parts, several kinds of carbon membranes used in water treatment will be introduced.

4.2.1 Phenolic Resin-Based Carbon Membranes

Phenolic resins have presented suitable features to be applied as the precursors of carbon membranes due to their low cost, thermosetting property, and high carbon yield (Muylaert et al. 2012). Several scholars have successfully prepared carbon membranes with phenolic resins for water treatment. Song et al. (2017) developed carbon alumina mixed-matrix membranes by impregnating phenolic resin in porous alumina matrix via a vacuum-assisted method. Their results showed that carbon alumina mixed-matrix membranes with high water fluxes and salt rejections could be easily tailored. However, the carbon membrane, formed by dip coating a phenolic resin solution on an alumina substrate, could not exclude small molecules of glucose and sucrose. It only demonstrated high removal rates (80% and 100%, respectively) for 36 kda and 400 kda of polyvinylpyrrolidone polymers (Abd et al. 2017). Wu et al. (2016) prepared phenolic resin-based carbon membrane to treat oily wastewater. The oil concentration dramatically reduced from initial 200 mg/L in feed to below 10 mg/L in permeate, with the oil rejection rate of 95.3%. Zhao et al. (2018) prepared the original precursor membrane by compressing the mushy mixture composed of phenolic resin, hexamethylenetetramine, carboxymethylcellulose sodium, and distilled water. The results showed that these carbon membranes could effectively remove phenol and phosphoric acid from water. The maximum removal rates were 81.9% for phenol and 55.3% for phosphoric acid. In addition, the carbon membrane derived from phenolic resin was also effective to treat dye wastewater. Asymmetric tubular carbon membranes on an ultrafiltration substrate were prepared by thermosetting phenolic resin and carbon black (Tahri et al. 2016), and such carbon membranes could be applied efficiently to the treatment of industrial dyeing effluent. According to the above research, carbon membranes made from phenolic resin as raw material or part of raw material have been applied in many aspects of water treatment and showed their unique performance.

4.2.2 Coal-Based Carbon Membranes

Coal, as a kind of natural mixture composed of macromolecular cross-linked polymers and inorganic minerals, is a good candidate for preparing carbon membranes because of its low price and abundant deposit. In the past two decades, our group explored the preparation technology of carbon membranes derived from coal, which was shown in Fig. 4.1. The coal was ground into fine particles first, and then mixed with binder into a dough, which was extruded into a tube of 10 mm external diameter by a hydraulic extruder at 2.5–3.0 MPa. After drying at ambient atmosphere, the tubular membrane was carbonized in Ar up to 900 °C at the rate of 3 °C/min and held for 1 h. The final product was cooled to room temperature naturally. A series of systematic investigations on the controlled preparation of coal-based carbon membranes were carried out, and the pore structure, mechanical strength, and electrical conductivity of CBCMs were further optimized. As expected, the coal-based carbon membranes showed excellent water treatment performance (Song et al. 2006).

During treatment, the retention and accumulation of pollutants on the membrane surface and inside the membrane pores would give rise to serious membrane fouling. In order to improve the antifouling ability of coal-based carbon membranes, an electric field was exerted on the treatment system; our group utilized the electrical conductivity of coal-based carbon membranes and designed a coupling system

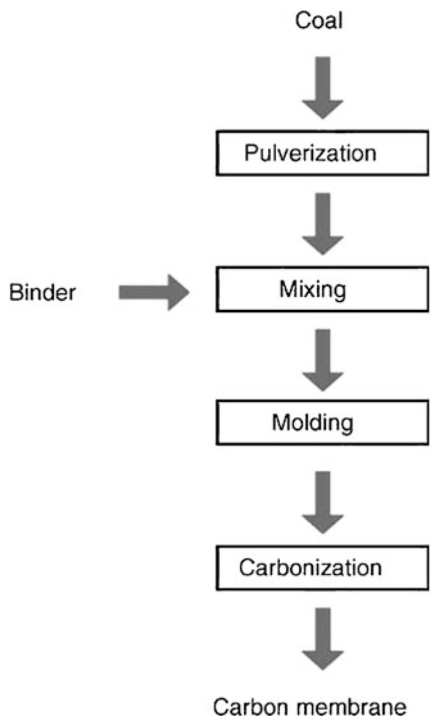

Fig. 4.1 Preparation process of coal-based carbon membranes. (Reprinted with permission of (Song et al. 2006))

which employs coal-based carbon membranes as the anode and Ti plate surrounding the membrane as the cathode. This system achieved significant improvement on removal efficiency and antifouling ability under an external electric field due to the electrochemical oxidation (Fig. 4.2). This system not only displayed excellent removal efficiency for organic pollutants (such as oil droplets) larger than the membrane pores (Li et al. 2016a) but also demonstrated great potential on those pollutants with a smaller molecule size than the membrane pore size including dyes, phenol, etc. (Yin et al. 2016); Tao et al. 2017b; Sun et al. 2018). Moreover, microorganisms such as microalgae and *Vibrio cholerae* were also effectively removed (Tao et al. 2017a). Compared with other membrane processes such as ultrafiltration, nanofiltration, and reverse osmosis, this technology possessed obvious advantages on processing capacity and energy consumption.

Although the coupling system has been proved to be effective for organic wastewater treatment, further potential for improvement in the removal efficiency and life span of the coupling system is often limited by the relatively low electrochemical activity of membrane electrode materials. Therefore, improving electrochemical activity of the membrane electrode material is a key to make a significant breakthrough in this field. Yang et al. (2011) presented the design of a novel electrocatalytic membrane reactor by loading electrocatalyst on carbon membrane (Fig. 4.3). In the research, TiO_2 as the electrocatalyst and hydrophilic agent was coated on the membrane surface by a sol–gel approach to enhance electron transfer

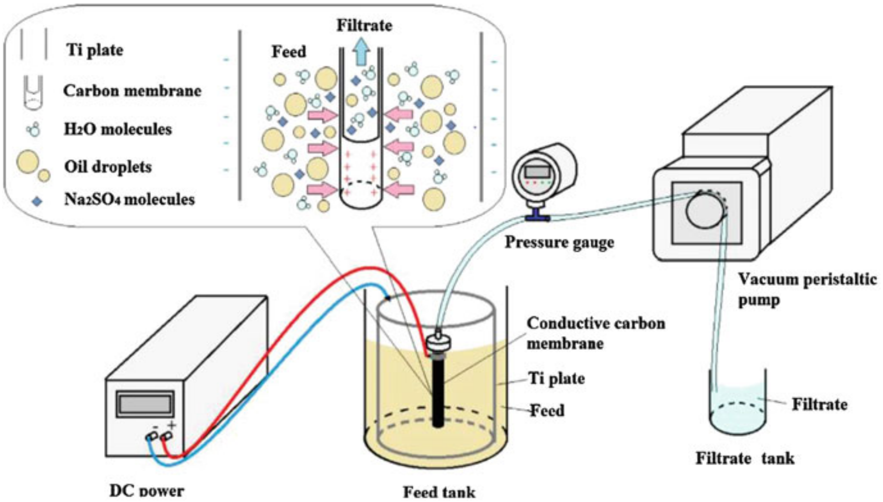

Fig. 4.2 Flow schematic diagram of carbonized membrane coupling with an electric field. (Reprinted with permission of (Li et al. 2016a))

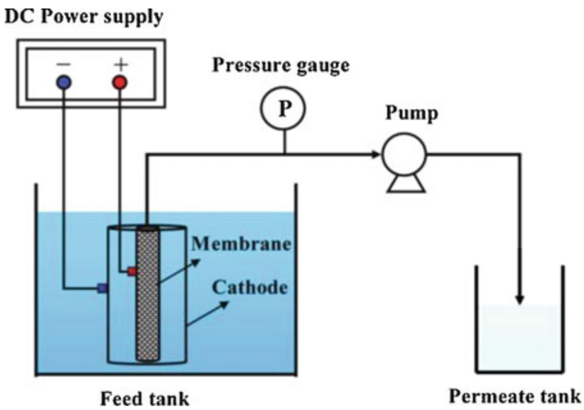

Fig. 4.3 Scheme of electrocatalytic membrane reactor. The figure shows an electrocatalytic membrane reactor with self-cleaning function for industrial water treatment. (Reprinted with permission of (Yang et al. 2011))

and improve membrane permeability. In this operation process, once the membrane anode was electrified, excitation of electrons in the conduction band took place at the TiO_2 surface. The obtained electrons and holes not only electrochemically decomposed H_2O into O_2 and H_2, inducing gas and liquid microflows to reduce concentration polarization and avoid membrane fouling, but also reacted with the adsorbed H_2O and O_2 at the TiO_2 surface to generate reactive intermediates, which could indirectly decompose the organic foulants into CO_2 and H_2O or biodegradable products, so as to realize the self-cleaning function of the electrocatalytic membrane. Similarly, Wang et al. (2014) also used an electrocatalytic membrane reactor constituted by TiO_2 loading carbon membrane to treat phenol wastewater. Besides, the Bi–SnO_2/C electrocatalytic membrane was fabricated via a simple electrochemical reduction and hydrothermal method by Wang et al. (2018b). The Bi–SnO_2/C membrane could continuously remove and inactivate *E. coli* in water through flow-through mode. As a result, the sterilization efficiency reached more than 99.99% under the conditions of cell voltage of 4 V, flow rate of 1.4 mL/min, and *E. coli* initial concentration of 1.0×10^4 CFU/mL, owing to the synergistic effect of the membrane separation and electrocatalytic oxidation.

4.3 Carbon Nanotube Membranes

Carbon nanotubes (CNTs), as an important kind of carbon materials, have many remarkable electrical, thermal, mechanical, and optical properties, which make them be widely used in sensor, supercapacitor, lithium–ion battery, etc. (Ren et al. 2011; Gupta et al. 2013; Yu et al. 2014; Apul and Karanfil 2015; Patino et al. 2015). Generally, carbon nanotubes can be divided into single-walled carbon nanotubes and multi-walled carbon nanotubes (Fig. 4.4) (Ahn et al. 2012; Ihsanullah 2019). As we have known, carbon nanotubes were firstly discovered by Sumio Iijima (1991). Soon after, researchers observed ultrahigh water flow rates in carbon nanotubes, and this discovery produced great expectation that carbon nanotubes could be used as an ideal material for water treatment (Whitby and Quirk 2007; Lee et al. 2011; Ahn et al. 2012).

The concept of carbon nanotube membrane was introduced by Li and Richard (2000) when they studied the mass transfer phenomenon in single-walled carbon nanotubes. Recently, carbon nanotube membranes for water purification are getting more and more attention. According to the arrangement patterns of carbon nanotubes, carbon nanotube membranes are usually classified into vertically aligned carbon nanotubes (VA-CNT) membranes, horizontally aligned carbon nanotubes (HA-CNT) membranes, mixed-matrix carbon nanotube membranes, and electrochemical carbon nanotube membranes (as shown in Fig. 4.5).

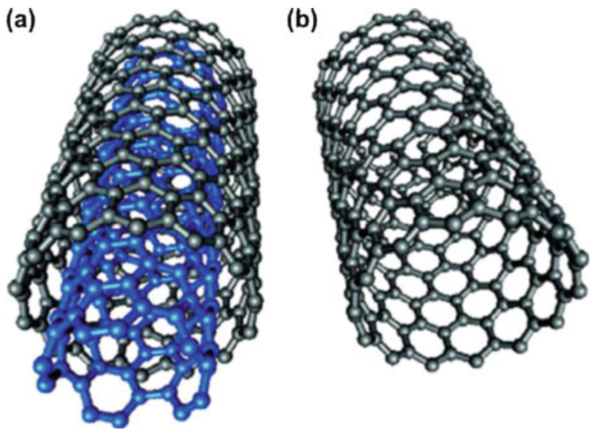

Fig. 4.4 The structure of multi-walled carbon nanotubes and single-walled carbon nanotubes. (Reprinted with permission of (Ihsanullah 2019))

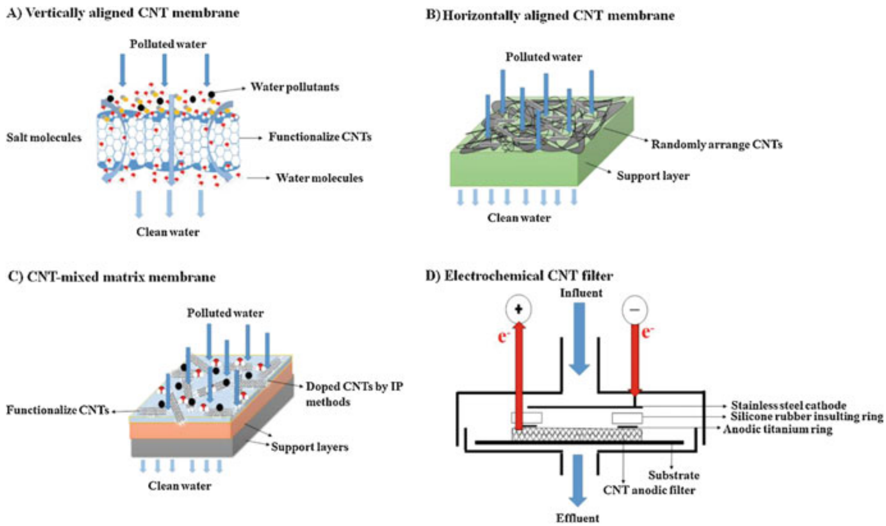

Fig. 4.5 Mechanism of water passing through the four types of carbon nanotube membranes: (**a**) vertically aligned carbon nanotube membrane, (**b**) horizontally aligned carbon nanotube membrane which is randomly arranged horizontally on a porous support layer, (**c**) mixed-matrix carbon nanotube membrane which is directly doped into the polymer membranes by interfacial polymerization or phase inversion, (**d**) electrochemical carbon nanotube membrane. (Reprinted with permission of (Ali et al. 2019))

4.3.1 Vertically Aligned Carbon Nanotube Membranes

Bruce et al. (2004) firstly constructed a multi-walled vertically aligned carbon nanotube membrane, and its typical preparation process was shown in Fig. 4.6 (Das et al. 2014), and the separation performance of vertically aligned carbon nanotube membranes was listed in Table 4.1. The work from Baek et al. (2014) showed the superiority of vertically aligned carbon nanotube membrane with the water permeation almost three times higher than a typical ultrafiltration membrane. Besides, the membrane prepared by Holt (2004) with silicon nitride (Si_3N_4)-filled carbon nanotube array obtained much higher water flux which was three times larger than that calculated by the Hagen–Poiseuille equation. This was mainly owing to the effect of the compact nanotube forest and short nanochannel length. In addition, some researchers prepared novel vertically aligned carbon nanotube membranes that possessed certain antimicrobial and antifouling capacities (Lee et al. 2015). A key challenge on preparing these kinds of membranes was to align the carbon nanotubes over a sufficiently large area for comprehensive water treatment (Ali et al. 2019). Instead of conventional preparation methods, Wu et al. (2014) utilized an electric field to obtain vertically aligned carbon nanotube membranes. Electro-casting allowed multi-walled carbon nanotubes to grow vertically and disperse more evenly. However, complex manufacturing techniques were still major obstacle to make these membranes suitable for large-scale applications (Ihsanullah 2019).

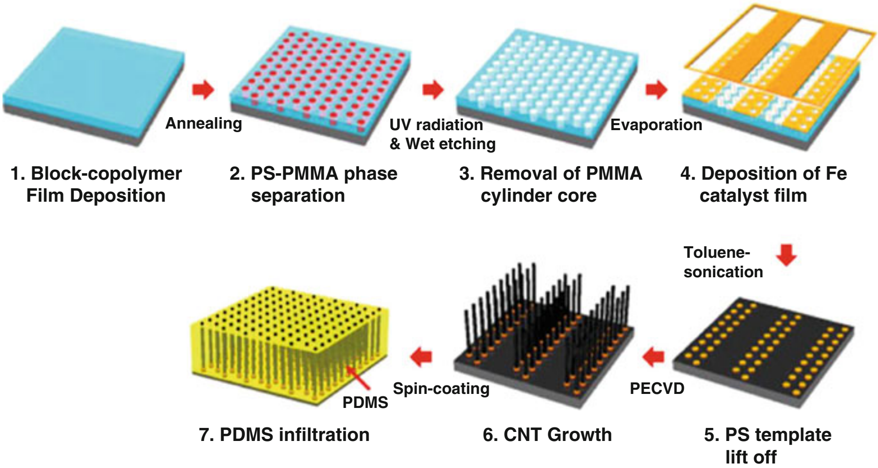

Fig. 4.6 Process flow for the fabrication of a vertically aligned carbon nanotube membrane using a block copolymer lithography method. (Reprinted with permission of (Ahn et al. 2012))

4.3.2 Horizontally Aligned Carbon Nanotube Membranes

In addition to vertically aligned pattern, carbon nanotubes can aggregate with each other by the van der Waals interactions to form horizontally aligned carbon nanotube membranes (Fig. 4.5B) (Ihsanullah 2019). This type of carbon nanotube membranes possesses several advantages such as a high specific surface area, large porous 3D network, etc. The most common methods for synthesizing horizontally aligned carbon nanotube membranes are electrospinning, vacuum filtration, and layer-by-layer deposition (Sears et al. 2010).

The preparation processes of horizontally aligned carbon nanotube membranes usually involve two steps: the functionalization of carbon nanotubes and vacuum filtration (Fig. 4.7). Firstly, the functionalized carbon nanotubes (horizontally aligned carbon nanotubes) are ultrasonically treated for uniformly dispersing in water or other solvents. Then, the dispersion is placed on the substrate membrane by vacuum filtration, after drying in an oven to remove the solvent (Lee et al. 2016a).

The related works on horizontally aligned carbon nanotube membranes are listed in Table 4.2. Due to the disordered arrangement of functionalized carbon nanotubes, the horizontally aligned carbon nanotube membranes can provide rich porous structure and large specific surface area (Sears et al. 2010), which makes the horizontally aligned carbon nanotube membranes possess high adsorption capacity to natural organic matter (Yang et al. 2013) and strong antimicrobial actions (Kang et al. 2007). Li et al. (2015) found that a “slanted carbon nanotube membrane” exhibited a higher water flux than a typical vertically aligned carbon nanotube membrane, because this kind of art structure could obviously lower the energy barrier for filling water into the carbon nanotubes. Brady Estevez et al. (2008) reported that the horizontally aligned single-walled carbon nanotube membrane

Table 4.1 Membrane performance of some vertically aligned carbon nanotube membranes

Membrane material	Membrane performance	Reference
CNT/polystyrene	The membrane flux of ruthenium bipyridine and methyl viologen was 9.57 (±0.91) and 21.05 (±2.32) nmol/h, respectively	Mainak et al. (2005)
CNT/stainless steel	The flux of diesel and water was 4692 kg/(m^2·h) (400 Pa) and 85.6 kg/(m^2·h) (1820 Pa) when the membrane was used to separate diesel–water mixture	Lee and Baik (2010)
CNT/polyethersulfone	The water flux was ~100 L/(m^2·h) at 60 Psi	Li et al. (2014)
CNT/PS/epoxy resin	The water flux was 1100 ± 130 L/m^2·h·bar (3 times higher than a commercial membrane). The VA-CNT membrane showed better biofouling resistance	Baek et al. (2014)
CNT/ polytetrafluoroethylene/ Si	The water flux was 30,000 L/m^2·h·bar (almost 12.5 times higher than the reported CNT membranes). The carbon nanotube walls of the membrane were proved to hinder the formation of biofilms and prevent bacterial adhesion	Lee et al. (2015)
CNT/Fe/Al_2O_3/Si	The BSA rejection increased from 71% to 90% with the modification of methacrylic acid. The pure water flux was 1000 ± 100 L/(m^2·h·bar)	Park et al. (2014)
CNT/Si wafer	The rejection rate of NaCl was 41.4%. The water flux was $1.31 \times 10^{-3} - 6.57 \times 10^{-2}$ L/(cm^2·day·MPa)	Matsumoto et al. (2017)
CNTs–TiO_2/Al_2O_3	The rejection rate of polyethylene glycol was 70% and the flux was 980 L/(m^2·h)	Zhao et al. (2013a)
Fe_3O_4/CNT	Membranes with a 10 and 1% iron oxide exhibited the best removal of 90 and 88% of SA after 3 h	Ihsanullah et al. (2016)
CNT–carbon fabrics	The hydrophobicity of the membrane increased; the wetted surface fraction and adhesion were lower. The separation efficiency of oil–water mixture was much higher	Hsieh et al. (2016)
PdO–CNT	The removal efficiency of atrazine was almost 100%	Vijwani et al. (2018)

displayed high removal rate for the virus MS_2 bacteriophage. Ihsanullah et al. (2015) synthesized a silver-doped carbon nanotube membrane and demonstrated good antibiofouling and antibacterial properties. Subsequently, they found that an iron oxide composite carbon nanotube membrane could present excellent antifouling property (Ihsanullah et al. 2016). Dumée et al. (2010) applied horizontally aligned carbon nanotube membranes to direct contact membrane distillation. Their work proved that horizontally aligned carbon nanotube membranes possessed high water flux and good desalination ability. After that, they modified high-purity carbon nanotubes by two chemical ways, and the resultant horizontally aligned carbon nanotube membrane had a larger contact angle (140° compared with 125°), which further improved the performance of the horizontally aligned carbon nanotube membrane (Dumée et al. 2011).

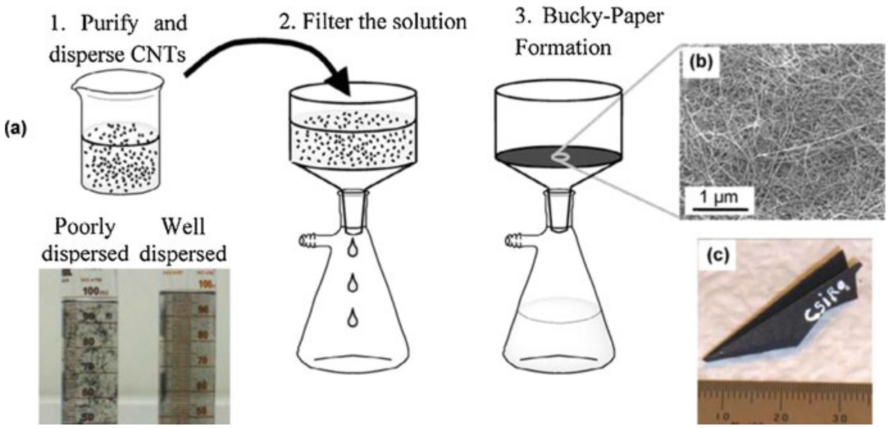

Fig. 4.7 Process flow for the fabrication of horizontally aligned carbon nanotube membrane. (**a**) Flow of manufacturing horizontally aligned carbon nanotube membrane. (**b**) SEM image of the membrane surface. (**c**) Fold it into a paper airplane to show its flexibility and mechanical robustness. (Reprinted with permission of (Sears et al. 2010))

Table 4.2 Application and membrane performance of some horizontally aligned carbon nanotube membranes

Membrane material	Membrane performance	Reference
CNT	The salt rejection was more than 95%. The water vapor flux was $4.5 \pm 0.1 \times 1012$ kg/(m·s·Pa)	Dumée et al. (2011)
CNT	The salt rejection was more than 99%. Flux rate was ~12 kg/(m^2 h) at a water vapor partial pressure difference of 22.7 kPa	Dumée et al. (2010)
CNT/PP/PES/PS/PVDF	The salt rejection was 95%. The water vapor flux was $3.3\times10{-}^{12}$ kg/(m·s·Pa)	Dumée et al. (2012)
f-CNT	The rejection rate of humic acid was more than 93%	Yang et al. (2013)
CNT/PVDF	The rejection rate of *E. coli* was 94% (exhibited good anti-microbial capacity). The water flux was 13,800 L/m^2·h·bar and 6500 L/(m^2·h·bar) at SWNT loading of 0.3 mg/cm^2 and 0.8 mg/cm^2	Brady Estevez et al. (2008)
Cu–CNT/PVDF	The rejection rate of As(III) was above 90%. The pure water flux was 4639–4854 L/m^2·h·bar).	Luan et al. (2019)

However, carbon nanotubes usually tended to aggregate when they were dispersed in a polymer matrix or solvent. Therefore, it was difficult to prepare a uniform dispersion. For this reason, several surfactants such as Triton X-100, sodium lauryl sulfate, etc. were adopted to improve the dispersion of carbon nanotubes in aqueous solution (Wu et al. 2010c). Besides, another efficient method was chemical functionalization (Yang et al. 2013), which had been proved to increase the hydrophilicity and stability of carbon nanotube suspensions (Ansón-Casaos et al. 2010). For example, some researchers covalently grafted functional groups including amines, fluorine, and sulfhydryl groups onto carbon nanotubes to help them disperse in horizontally aligned carbon nanotube membranes (Ansón-Casaos et al. 2010; Darryl et al. 2010).

4.3.3 Mixed-Matrix Carbon Nanotube Membranes

The main role of carbon nanotubes in mixed-matrix carbon nanotube membranes is to improve the performance of conventional polymer membrane (Ihsanullah 2019). Compared with the above two types of membranes, mixed-matrix membranes are easier to be commercialized for their simple preparation procedures. For preparing mixed-matrix carbon nanotube membranes, functional carbon nanotubes are generally added into polymeric membranes by several synthesis techniques (Ali et al. 2019; Ihsanullah 2019). The most common methods are phase inversion (Choi et al. 2006; Brunet et al. 2008; Majeed et al. 2012), interfacial polymerization (Shen et al. 2013; Kim et al. 2014), solution mixing (Ahmed et al. 2013), spray-assisted layer-by-layer (Liu et al. 2013), polymer grafting (Shawky et al. 2011), in situ polymerization (Zhao et al. 2014; Zarrabi et al. 2016), and in situ colloidal precipitation (Ho et al. 2017). The prepared membranes often exhibit excellent properties for reverse osmosis, ultrafiltration, and forward osmosis applications (Lee et al. 2016a). Some researches about the membrane performance of mixed-matrix nanotube membranes are listed in Table 4.3.

Mixed-matrix carbon nanotube membranes typically exhibited high removal efficiency and water flux. Zheng et al. (2017) prepared a novel sulfonated multi-walled carbon nanotube membrane by using the interfacial polymerization method. By adding 0.01% multi-walled carbon nanotubes, the membrane showed high salt rejection (96.8%) and water permeation (13.2 $L/(m^2 \cdot h \cdot bar)$). Moreover, a polysulfone membrane (Choi et al. 2006) and a polyether sulfone membrane (Celik et al. 2011b) doped with carbon nanotubes were more hydrophilic and demonstrated an enhanced antifouling ability because of the hydrophilic carboxylic groups of functionalized carbon nanotubes.

4.3.4 Electrochemical Carbon Nanotube Membranes

Electrochemical carbon nanotube membrane for wastewater treatment is a novel technique which combines electrochemical degradation with conventional membrane filtration to remove target contaminants (de Lannoy et al. 2012; Lalia et al. 2015; Ahmed et al. 2016; Elimelech and Boo 2017; Ho et al. 2018; Yi et al. 2018). In this process, the electrochemical carbon nanotube membranes are used both as a filter for contaminant sorption and an electrode for electrochemical degradation of aqueous pollutants (Ali et al. 2019).

Table 4.3 Application, membrane performance, and other conditions of mixed-matrix carbon nanotube membranes

Material	Synthesis technique	CNT amount (wt %)	Application	Membrane performance	Reference
MWNCTs/polysulfone (PSf)	Phase inversion	1.5	UF	The rejection rate of PEO was more than 99%. The flux was ~21 $m^3/m^2 \cdot$day at 4 bar	Choi et al. (2006)
MWCNTs/PSf	Phase inversion	4	UF	The flux increased from 24.6 ± 12.6 to 28 ± 10.7 $L/(m^2 \cdot h)$ by the addition of 4 wt% CNTs	Brunet et al. (2008)
MWCNTs/PAN	Phase inversion	2	UF	The flux increased from ~41 to 53 $L/(m^2 \cdot h)$ at 2 bar by the addition of 2 wt% CNTs	Majeed et al. (2012)
MWCNT/PSf (C/P)	Phase inversion	2	UF	The water flux was ~90 $L/(m^2 \cdot h)$ at 60 Psi with the addition of 2% MWCNTs	Celik et al. (2011b)
MWCNT/PSf	Phase inversion	0–1	UF	The removal efficiency of Cr(VI)/Cr(II)was from 10.2% and 9.9% to 94.2% and 78.2%	Shah and Murthy (2013)
MWCNTs/PSf hollow fiber membrane	Phase inversion	0.1	UF	The flux increased from 36.1 ± 4.0 to 70.7 ± 1.8 $L/(m^2 \cdot h)$ with the addition of 0.1% MWCNTs	Yin et al. (2013)
f-CNTs/PA	Interfacial polymerization	0–20	–	The flux increased by more than a factor of 4 with the addition of CNTs from 0 to 20%	Chan et al. (2013)
MWCNTs/PPSU	Phase inversion	0.5	UF	The pure water flux increased from 7.91 to 56.91 $L/(m^2 \cdot h)$ at 345 kPa with addition of 0.5 wt % F-MWCNTs. The rejection rate of pepsin and trypsin decreased from 97 and 90% to ~90 and 84% with addition of 0.5 wt% f-MWCNTs.	Lawrence et al. (2012)
CNT/PA	Interfacial polymerization	0.2 g	RO	The rejection rate of NaCl was more than 95% (at 2000 ppm). The pure water flux increased from ~37 to 44 $L/(m^2 \cdot h)$ at 15.5 bar of feed pressure with addition of 2 wt% MWCNTs. The water flux of PA-CNT membrane decreased by only 18.40%, compared with the PA membrane decreased by 32.80% after 48 h	Kim et al. (2014)

(continued)

Table 4.3 (continued)

Material	Synthesis technique	CNT amount (wt %)	Application	Membrane performance	Reference
MWCNTs/BPPO/ Triethanolamine (TEOA)	Phase inversion	5	UF	The rejection rate of egg albumin was 94%. The water flux increased from 197 to 487 L/(m^2·h) at 0.2 MPa	Wu et al. (2010a)
MWCNTs/polyester TFN	Interfacial polymerization	0.05	NF	The water flux through TFN membrane with 0.05% (w/v) MWNTs was 4.7 L/(m^2·h) . The salt separation capability of the membrane was improved	Wu et al. (2010b)
MWCNTs/MPDA	Interfacial polymerization	0.1	RO	The salt rejection rate of the membrane was 93.4%. The water flux increased from 11.1 to 13.6 L/(m^2·h)	Park et al. (2012)
MWCNT/polypropylene (PP) or PES	Interfacial polymerization	0.01–0.06	NF	The degradation rate of Brilliant Blue was more than 96%	Roy et al. (2011)
MWCNT/PSU	Phase inversion	1–20	MF	Pure water flux of MWCNT/PSU membranes was 1200 L/(m^2·h·bar)	Medina-Gonzalez and Remigy (2011)
MWNT/PA	Interfacial polymerization	0.005–0.2	RO	The water flux increased from 26 L/(m^2·h) to 71 L/(m^2·h)	Zhang et al. (2011)
MWNTs/PMMA	Interfacial polymerization	0.67	NF	The rejection rate of Na_2SO_4 was 99%. The water flux of the resultant membrane was $\sim 1.94 \times 10^{-3}$ cm^3/(cm^2·s)	Shen et al. (2013)
MWCNTs/polyester TFN	Interfacial polymerization	0–2.0 mg/ mL	NF	The water flux increased from 10.8 L/(m^2·h) to 21.2 L/(m^2·h) .	Wu et al. (2013)
f-MWCNT/PA/PSf	Interfacial polymerization	0.1	FO	The water flux was 95.7 L/(m^2·h) (nearly 160% higher)	Amini et al. (2013)
f-MWNTs/PA	Interfacial polymerization	0.1	RO	The water flux increased from 14.86 to 28.05 L/ (m^2·h) with the addition of 0.1% MWCNTs	Zhao et al. (2014)

DDA-MWNTs/PSf	Phase inversion	0.25	UF	The water flux of the resulting membrane was ~12 L/(m^2·h) at 1 bar.	Khalid et al. (2015)
NH2-functionalized MWCNT/PA	Interfacial polymerization	0–0.01	NF	The rejection rate of Na_2SO_4 and NaCl was 36.71% and 95.72% The flux increased from 48.6 (Na_2SO_4) and 48.1 L/(m^2·h) (NaCl) to 61.7 and 60.8 L/(m^2·h)	Zarrabi et al. (2016)
Sulfonated MWCNTs/ poly(piperazine amide)	Interfacial polymerization	0–0.02	NF/UF	The rejection rate of Na_2SO_4 was 96.8%. The water flux of the resulting membrane was 13.2 L/ (m^2·h·bar) (1.6 times higher)	Zheng et al. (2017)
PMMA-modified MWNTs/PA	Interfacial polymerization	0.67–2.0 g/L	NF	The rejection rate of Na_2SO_4 was above 98% with the addition of 0.67 g/L PMMA-MWNTs, and the water flux was almost 1.5 times higher than the TFC membrane	Yu et al. (2013)
f-MWCNTs/PES	Layer-by-layer	1	UF	The irreversible fouling ratio of BSA was reduced from 49.3 ± 0.5 to 12.3 ± 2.9 after bilayer deposition of polyelectrolyte/MWCNTs	Liu et al. (2013)
Polycaprolactone (PCL)-MWCNTs/PES	Solution casting	3	–	The removal efficiency of Cd(II) increased from 8.7% to 27%. The water flux increased from 28 L/ (m^2·h) to 61 L/(m^2·h)	Mansourpanah et al. (2011)
PVK/SWCNTs	Solution mixing	3	–	The membrane was tested by removing MS_2 bacteriophage virus (~2.5 logs)	Ahmed et al. (2013)
MWCNTs/aromatic PA	Polymer grafting	2.5–15 mg/g PA polymer	RO	The rejection rate of NaCl and HA increases to 3.17% and 1.67%. The permeability was decreased by 6.5%.	Shawky et al. (2011)
f-MWCNTs/GO/PVDF	In situ colloidal precipitation	0.001–0.1 g/ L	UF	The removal efficiency of TDS, phosphorus, hardness, COD, chlorine, turbidity, color, and TSS was 1.51%, 6.55%, 21.79%, 75.5%, 76%, 81.94%, 86.3%, and 100%, respectively. The water flux were 43.99 , 52.62 , and 43.38 L/ (m^2·h·bar) with the concentration of 0.1, 0.001, and 0.01 g/L	Ho et al. (2017)

(continued)

Table 4.3 (continued)

Material	Synthesis technique	CNT amount (wt %)	Application	Membrane performance	Reference
SBS/f-MWCNTs	Solution blending	0.01–0.1	NF	The PVDF/SBS-MWCNTs-SCN-Ag membrane had a tensile strength in the range of 12.6–20.1 MPa and a maximum decomposition temperature of 567–599 °C	Mehwish et al. (2015)
TiO_2-MWCNTs/PES	Phase inversion	0.1–1	NF	The pure water flux increased from ~3.71 to 5.66 kg/(m^2·h) at 5 bar with the addition of 1 wt% TiO_2-coated MWCNTs. The antifouling property of the PES membrane was decreased from 46.9% to 21.6% with addition of 1 wt% TiO_2 coated MWCNTs	Vatanpour et al. (2012)
f-MWCNTs/PES	Phase inversion precipitation	0.1	–	The water flux of the PCA-CNT membrane increased from ~10 to ~30 kg/(m^2·h) after 1 h with the addition of 0.1 wt% f-MWCNTs. The flux recovery ratio (FR) after passing whey solution increased from 44% to 95%. The membrane had a smooth and hydrophilic membrane surface	Daraei et al. (2013b)
f-MWCNTs/PES	Phase inversion	0.04–0.4	NF	The rejection rate of Na_2SO_4 had increased with the addition of 0.04 wt% MWCNTs. The pure water flux increased from ~5.5 to 9 kg/m^2·h at 4 bar with addition of 0.2 wt% MWCNTs	Vatanpour et al. (2011)
MWCNT/PVDF	Phase inversion	0–2	UF	The PVDF exhibited the highest protein adsorption (~70 mg/cm^2) with the addition of 2% MWNTHPAE content in casting solution. The pure water flux was to reach maximum when the MWNTHPAE/PVDF ratio was 1.5%. The flux	Zhao et al. (2012)

				recovery increased from 82% to 95.7% with the addition of MWCNTs	
f-MWCNTs/PES	Phase inversion	0–2	UF	The rejection rate of BSA increased from 81 to 88% with addition of 2% f-MWCNTs. The water flux was 184 L/(m^2·h) at 3 bar with the addition of 1 wt% f-MWCNTs	Rahimpour et al. (2012)
NH_2-MWCNTs/PES	Phase inversion	0–0.06	NF	The rejection rate of Na_2SO_4/$MgSO_4$/NaCl was 65%/45%/20% after 180 min of filtration. The water flux increased from 13.6 to 23.7 L/(m^2·h)	Vatanpour et al. (2014)
PVDF/GO/MWCNTs	Phase inversion	1	UF	The pure water flux was 251.73% higher than that of the original membrane when GO/OMWCNTs ratio was 5:5	Zhang et al. (2013)
MWCNTs/PANI/PES	In situ polymerization and phase inversion	0–2	UF	The water flux was1400 L/(m^2·h) (LMH)/bar (30 times higher). The NOM rejection rate (80%) was 4 times higher than that of the PES membrane	Lee et al. (2016b)
MWCNTs/TiO_2/PSf	Phase inversion	0–1	UF	The rejection rate of HA increased from 6% to 56% with the addition of 0.5% TiO_2–0.5% MWCNTs. The water flux increased from 10 L/(m^2·h) to 210 L/(m^2·h) with the addition of 1% MWCNTs	Esfahani et al. (2015)
MWCNTs/PVA	Pressure filtering deposition	0–20	UF	The rejection rate of the PEO was more than 90% with the addition of 5 wt% MWCNTs. The water flux increased from 1440 L/(m^2·h) by 20 w/% CNT concentration	de Lannoy et al. (2012)
MWCNTs/PVDF/ polydimethylsiloxane	Deposition and coating	0.05	MF	The rejection rate of Na_2SO_4 was ~80%. The water flux of the composite membrane was ~38 kg/(m^2·h) at 4 bar	Madaeni et al. (2013)

(continued)

Table 4.3 (continued)

Material	Synthesis technique	CNT amount (wt %)	Application	Membrane performance	Reference
MWCNT/PSf	–	0–10.55	UF	The water flux of the membrane increased from 2.5 to ~5.5 L/(m^2·h) with the addition of 6.94 wt % f-CNT	de Lannoy et al. (2013)
f-CNT/PSf	Phase inversion	0–0.5	UF	The pure water flux of the membrane increased from ~46 to 175 L/(m^2·h) at 100 kPa with the addition of 0.19% f-MWNTs. The adsorption of proteins was inhibited after the CNTs were added to the membrane	Qiu et al. (2009)
CNT/PES (C/P)	Phase inversion	0–4	UF	The highest pure water flux was 93 L/(m^2·h) with the addition of 0.5% CNT. The adsorption amount of BSA decreased from ~210 to ~75 μg/cm^2 at pH = 3 with the addition of 4% CNT	Celik et al. (2011a)
MWCNT/PVDF	Phase inversion	0–2	UF	The contact angle of the membrane decreased from 75.8° to 54.7° with the addition of 1 wt% f-MWCNTs. The pure water flux was 225 L/(m^2·h) (11 times higher) with the addition of 1 wt % f-MWCNTs. The rejection rate of BSA increased significantly (86.0%) with the addition of 0.5 wt% f-MWCNTs	Ma et al. (2013)
PVA/MWNTs/PAN	Electrospinning	10	UF	The membrane had a high water flux of about 270.1 L/(m^2·h) even at very low feeding pressure (0.1 MPa) with the addition of 10 wt% MWNTs. The same membrane also had a high separation rate (99.5%) of oil–water emulsion	You et al. (2013)

PVDF/MWCNTs	Phase inversion	1	UF	The PVDF/MWCNTs membrane had the highest water flux of about 620 L/(m^2·h) (114% higher). The rejection rate of BSA increased to about 31.8%.	Zhao et al. (2013b)
f-MWCNTs/ polyetherimide (PEI)/PA	Electrospinning	0.3	FO	The substrate porosity and the substrate tensile modulus of the membrane increased by 18% and 53%, and the structural parameter (S value) decreased by 30% with the addition of f-CNTs	Tian et al. (2015)
f-MWCNTs/chitosan/poly (vinyl) alcohol	Casting and evaporation	0–2	–	The amount of Cu(II) adsorbed doubled with the addition of 2 wt% MWCNTs (20.1 mg/g compared with 11.1 mg/g at 40 °C)	Salehi et al. (2012)
f-MWNTs/nano-silver/ PSf	Phase inversion and interfacial polymerization	0–5	UF	The addition of 5.0 wt% f-MWNTs in the support layer enhanced the pure water permeability of the n-TFN membrane by 23%	Kim et al. (2012)
f-MWCNTs/PES	Phase inversion	0–2	UF	COD and total phenol removal capacity of the prepared membrane was 72.6% and 89.5%, respectively. The pure water flux was 21.2 (kg/(m^2·h))	Zirehpour et al. (2014)
MWCNTs/PA and MWCNTs/PSf	Phase inversion and interfacial polymerization	5 and 10	MF/UF	PSU membrane with MWCNTs had a higher water flux (from 16.4 L/(m^2·h) at 2.3 bar to 18.4 L/(m^2·h) at 2.1 bar)	Kim et al. (2013)
PAA-modified MWCNTs (PAA-g-MWCNT)/PES	Phase inversion	0–0.1	NF	The resultant membrane had a high water flux of 40 kg/(m^2·h) at 0.4 MPa, excellent antifouling properties, and higher salt rejection	Daraei et al. (2013a)
f-MWCNTs/PES	Phase inversion	0–0.5	UF	The pure water flux increased from 24.28 L/ (m^2·h) to 53.91 L/(m^2·h) with the addition of 0.5 wt% of f-MWCNTs. The hydrophilic property of PES/f-MWCNTs was improved by 18.7%. The rejection rate of the membrane was 27–30%, much higher than that of a PES membrane	Saranya et al. (2014)

(continued)

Table 4.3 (continued)

Material	Synthesis technique	CNT amount (wt %)	Application	Membrane performance	Reference
f-CNTs/PES	Phase inversion	0–0.5	–	The water flux increased from 260 to 375 and 450 L/(m^2·h) with the addition of 0.02 and 0.04 wt % f-CNTs	Phao et al. (2013)
f-MWCNTs/ polyvinylpyrrolidone (PVP)/PES	Phase inversion	0–0.5	UF	The removal efficiency of bovine serum albumin, pepsin, and trypsin was 93.4%, 74.7%, and 59.4%, respectively	Masoomaa et al. (2015)
PES/f-MWCNTs	Phase inversion	0.01	UF and hemodialysis	The water flux increased from 22.57 to 149.67 L/(m^2·h·bar) with the addition of 0.1 wt% of f-MWCNTs	Abidin et al. (2017)
PES membrane/ZnO–MWCNTs	Non-solvent-induced phase inversion	0–1	NF	The rejection rate of Direct Red 16 was more than 90%. The water flux was 16.7 kg/(m^2·h) with the addition of 0.5 wt% ZnO–MWCNTs	Zinadini et al. (2017)
Mixed isotactic polypropylene membrane/f-MWCNTs	Melt mixing and melt pressing	4	–	The water permeability of the membrane increases by a factor of ~35 with the addition of 4 wt% MWCNT-g-PP	Bounos et al. (2017)
PVDF/Fe_2O_3/MWCNTs	In situ polymerization	0.2	–	For degradation of cyclohexanoic acid (CHA) by membrane in the presence of H_2O_2, the removal rate reached 48% in 24 h. For HAs, removal in the presence of H_2O_2 was much higher than that without H_2O_2	Alpatova et al. (2015)
PA/MWCNTs RO membrane	Interfacial polymerization	0–0.01	RO	The saline solution fluxes of the membrane increased from 20.3 ~25.9 to 28.9 L/(m^2·h) by adding f-MWCNTs. The salt (NaCl) rejection rate was >96% by adding MWCNTs. The membranes with f-MWCNTs had better antifouling properties than the original membrane	Farahbakhsh et al. (2017)

MWCNTs/PES	Phase inversion	0–3	UF	The adsorption amount of BSA decreased from 58.96 μg/cm^2 to 41.63 μg/cm^2. The water flux increased from 5.18 L/(m^2·h) to 71.26 L/(m^2·h) with the addition of 1.5 wt% f-MWCNTs	Wang et al. (2015b)
PA/MWCNTs NF membranes	Non-solvent-induced phase inversion	0.001–0.01	NF	The membrane with 0.005 wt% f-MWCNT added had the largest water flux. The membrane was improved in the rejection rate of Na_2SO_4 by the addition of f-MWCNTs	Mahdavi et al. (2017)
MWCNTs/PSf TFN membrane	Solution mixing	0.01–0.05	RO	The membrane with 0.03% f-MWCNTs added to the PA layer reached the highest water permeability after 48 hours of treatment with 1.5 M H_2SO_4. The NaCl rejection rate was higher than 96%	Wan Azelee et al. (2018)
f-MWCNTs-PAN/PP	Electrostatic spraying	1	–	The removal rate of Indigo was 98.73%. The water flux was 3891.85 L/m^2·h at a low pressure of 0.1 MPa	Xu et al. (2017b)
PHB–CaAlg/CMWCNT	Electrospinning	–	–	The adsorption rate of Brilliant Blue was 98.20%. The water flux of the resultant membrane was 32.95 L/m^2·h	Guo et al. (2016)
PSF/PVP/gCNT	Phase inversion	0.2	UF	The separation efficiency of oil–water was nearly 100% and the flux reached 121 LMH	Santosh et al. (2018)
f-MWCNT/PES	Phase inversion	0.4	NF	The rejection rate of Rhodamine B, crystal violet, indigo carmine, and orange G was 99.23%, 98.43%, 87.12%, and 82.13%, respectively	Mohammad et al. (2018)
PVDF/CNT	Layer-by-layer and simultaneous	0.02%	–	CNT blend membrane showed better wettability, higher permeability, and better MB removal efficiency and had a more open structure	Mavukkandy et al. (2018)
PSf/pebax/f-MWCNTs	Solution casting and solvent evaporation	0–2	NF	The separation efficiency of oil–water was 99.79% with the addition of 2 wt% f-MWCNTs	Saadati and Pakizeh (2017)

(continued)

Table 4.3 (continued)

Material	Synthesis technique	CNT amount (wt %)	Application	Membrane performance	Reference
PVDF-CNT/PU/PVDF-CNT	Sequential electrospinning	0–1	UF	The separation efficiency of oil–water was more than 94%	Gu et al. (2018)
CNT-PA	Interfacial polymerization	0–0.01	RO	The rejection rate of BSA was more than 96%. The water flux increased from 20.3 to 28.9 L/(m^2·h) with the addition of CNTs	Farahbakhsh et al. (2017)
PES/CNT	Phase inversion	0.01–1	NF	The rejection rate of Na_2SO_4 was 87.25%. The water flux was 38.91 L/m^2 h by the addition of 0.1 wt% CNT	Wang et al. (2015a)
PES/CNT	Phase inversion	0–0.1	NF	Membrane blended with 0.1 wt% f-MWCNTs had a highest permeation flux as well as dye (acid orange 7) removal efficiency (99%)	Ghaemi et al. (2015)
PES-SWCNT	Phase inversion	0–0.5	–	The rejection rate of bisphenol A and nonylphenol was 56% and 76% (improve more than 60%)	Kaminska et al. (2015)

Table 4.4 Application of electrochemical carbon nanotube membranes

CNT membrane	Voltage (V)	Target contaminant	Removal efficiency	Reference
COOH-MWNT	2.0	Ibuprofen	~100%	Bakr and Rahaman (2016)
CNT-PTFE	8.0	Pb^{2+}	98.8%	Gao et al. (2017b)
CNT-PVA	7.0	Cr (VI)	>99%	Duan et al. (2017)
N-CNT	–	TOC/NH^{4+}	95.2%/97.7%	Zuo et al. (2016)
Fe-CNT	1.0	Metoprolol	97%	Yanez et al. (2017)

The electrochemical carbon nanotube membranes exhibited great potential on wastewater treatment due to high degradation efficiency, low energy consumption, and simple operation process (Motoc et al. 2013; Bakr and Rahaman 2016, 2017; Liu et al. 2017). Besides, by transferring electrons directly through the surface of the electrochemical carbon nanotube membrane electrode, the solute transfer restriction of the conventional batch electrochemical process was overcome. Therefore, this method was more advantageous than conventional batch electrolysis. Table 4.4 provides some works on electrochemical carbon nanotube membranes. For example, Wei et al. (2017b) prepared a novel carbon nanotube-based hollow fiber membrane with a sandwich-like structure. Low concentration of microcystin-LR (0.5 mg/L) was removed economically and efficiently (>99.8%) by simple switching with adsorption and desorption as well as electrochemical oxidation by these carbon nanotube ultrafiltration membranes.

4.4 Graphene-Based Membranes

Graphene, consisting of a compact accumulation of sp2 hybrid carbon atoms, was reported for the first time by Geim and Novoselov (2004). Since then, graphene and graphene-based materials have been extensively studied and used to synthesize various multifunctional materials. As we know, graphene can be obtained by chemical vapor deposition or chemical reduction of graphene oxide. Generally, it is easy to fabricate single-layered or several-layered graphene on some catalytic substrates via chemical vapor deposition. Compared with the tedious and expensive chemical vapor deposition, reducing graphene oxide is more favorable for scale production. Graphene oxide is usually prepared by oxidizing graphite through the famous Hummer's method, which has abundant oxygen-containing functional groups on its surface and edges. After chemical reduction by hydrogen iodide acid, hydrazine, or thermal treatment, the oxygen-containing groups are reduced to obtain reduced graphene oxide which possesses similar properties to graphene. To date, both graphene and graphene oxide have also been applied to construct novel membranes with laminar pores. Besides, these materials are also used as blender to improve the hydrophilicity, surface charges, and antifouling ability of the polymeric membranes.

4.4.1 Support-Free Graphene Membranes

The ideal separation membrane should possess uniform pore size, ultrathin thickness, high mechanical strength, and excellent physicochemical properties to provide good permeability and selectivity. Graphene membrane may be a suitable candidate to meet such requirements. According to the theoretical calculation, the single-layered graphene membrane can completely desalinate brine water and seawater, showing great potential for water treatment (Cohen-Tanugi and Grossman 2012).

Previous research suggested that salt rejection was negatively correlated to improve pore size and applied pressure (Anand et al. 2018). Meanwhile, ionization of functional groups surrounding nanopores could influence desalination efficiency of single-layered graphene membrane (Chao et al. 2017). Therefore, single-layered graphene membranes could achieve highly permeable desalination by controlling the pore size and functional groups of nanopores (Cohen-Tanugi and Grossman 2012). To date, the nanopores in single-layered graphene membranes were usually produced by ion beam and electron beam exposure, ion bombardment, UV-induced oxidation etching, hydroxyl radical etching, oxygen plasma etching, etc. (Anand et al. 2018). O'Hern et al. (2014) reported their works on the controllable high-density subnanometer pores in single-layered graphene membranes which allowed the transport of salt but rejected larger organic molecules.

Compared with single-layered graphene membranes, Celebi et al. (2014) reported highly efficient mass transfer across physically perforated double-layered graphene membrane. Wei et al. (2017a) reported a four-layered graphene membrane with about 2 nm thickness, indicating outstanding permeability and selectivity. Cohen-Tanugi et al. (2016) also reported a reverse osmosis membrane stacked by multilayer nanoporous graphene for desalination by using classical molecular dynamic simulation. They found that double-layered nanoporous graphene membranes with the 3.0 Å of nanopore radius exhibited full salt rejection. Compared to the single-layered graphene membranes, the bilayer nanoporous graphene membranes showed excellent salt rejection. Recently, the effects of pressure and wall interaction on the water transport through multilayer nanoporous graphene membranes were carried out by molecular dynamic simulation (Shahbabaei et al. 2017). They found the water flux was mostly doubled in the multilayered hydrophilic pore membrane owing to strong hydrogen bonds. And then Chang et al. (2017) reported the nanofiltration properties of reduced graphene-based membrane with adjustable porous structure. Similarly, Yi (2013) prepared ultrathin (≈22–53 nm thick) graphene nanofiltration membranes on microporous substrates. The performance of such ultrathin graphene nanofiltration membranes was tested on a dead-end filtration device, and the pure water flux of ultrathin graphene nanofiltration membranes was high (21.8 L/

m^2·h·bar). Furthermore, Kabiri et al. (2016) synthesized a thiol-functionalized graphene composite with a unique three-dimensional porous structure to remove mercury ions (Hg^{2+}) from water. The results indicated that the removal efficiency of the membrane reached almost 100% for low (4 mg/L) and high (120 mg/L) concentration of Hg^{2+}. Due to excellent permeability and selectivity, support-free graphene membranes exhibited great potential in selective ion transportation and separation.

4.4.2 Graphene Oxide Membranes

Recently, graphene oxide has attracted increasing attention on membrane preparation and modification due to its excellent hydrophilic properties (Choi et al. 2013). Graphene oxide is usually obtained by oxidizing graphite with a strong acid or oxidant. Graphene oxide is a reforming form of graphene in which oxygen and hydrogen atoms are bonded with carbon atoms (Hu and Mi 2013). Due to the presence of oxygen- and hydrogen-based functional groups, graphene oxide can be well dispersed in water and other organic solvents, which favors the preparation of graphene oxide-based membranes (Stankovich et al. 2007).

Sun et al. (2014a) used graphene oxide membranes to recover acids from iron-based electrolyte wastewater. The mechanism was that Fe^{3+} was blocked by graphene oxide membranes, while H^+ could migrate fast. Sun et al. (2014b) also studied ion mobility and interactions with graphene oxide membranes. They found that ion permeability exhibited the order of $Mg^{2+} > Na^+ > Cd^{2+} > Ba^{2+} = > Ca^{2+} > K^+ > Cu^{3+} > Fe^{3+}$. Various interactions between ions and graphene oxide sheets, such as chelation, static electricity, van der Waals forces, etc., were attributed to the selectivity of graphene oxide membranes. Figure 4.8 showed the schematic diagram of

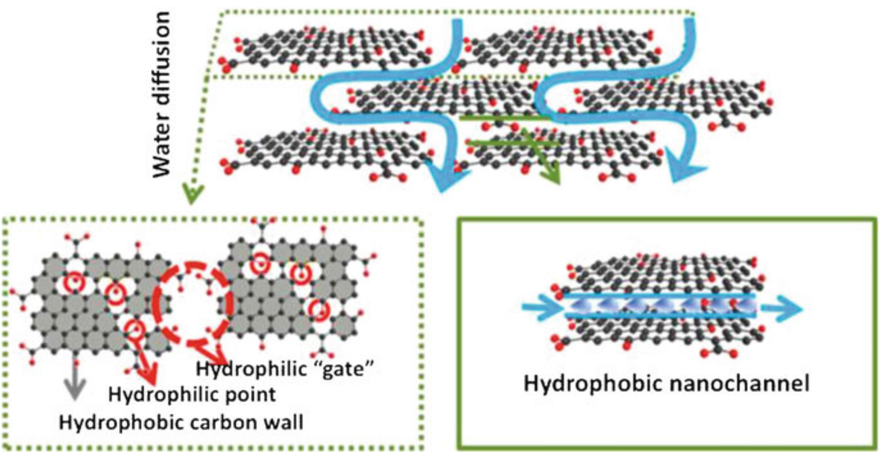

Fig. 4.8 Nanochannels in a graphene oxide membrane and hydrophilic pores for water flow in desalination. (Reprinted with permission of (Wang et al. 2016a))

graphene oxide membranes for water transport (Wang et al. 2016a). Water molecules firstly arrived in the hydrophilic sites in graphene oxide and then slipped through the hydrophobic nanochannel with low or no friction.

A dopamine-coated polysulfone membrane has been prepared to investigate the dependence of water flux and charge effect on separation. They revealed that the water flux was independent of the number of graphene oxide layers and salt exclusion but depended on interlayer spacing (Hu and Mi 2013). However, the volume of graphene oxide membrane would swell in the aqueous environment. Nair et al. (2012) studied the water mobility in nanochannels between graphene oxide tablets under different condition. They showed that the interlayer spacing between the original graphene oxide membrane region and the stacked graphene oxide membrane was about 0.6 nm in the dry conditions. Because of the diffusion of water molecules to graphene oxide layer, the increased interlayer spacing between graphene oxide membranes resulted in high mobility for water molecules. However, when the graphene oxide membrane was immerged in an ionic solution, the increased gap by the hydration cannot repel K^+ and Na^+ ions, making the membrane inappropriate for desalination applications (Joshi et al. 2014). Addressing to this issue, graphene oxide was functionalized with glycine and carboxylation for preparing membrane by pressure-assisted self-assembly to achieve high salt rejection efficiency (Yuan et al. 2017). Xu et al. (2017a) reported that the water flux and separation ability of graphene oxide membrane was related to the inner nanostructure of graphene oxide membrane. In addition to the interlayer spacing, it was found that the morphological characteristics of graphene oxide membranes, such as corrugation, could improve the separation performance (Qiu et al. 2011). Wang et al. (2012) presented that a graphene oxide/polyelectrolyte composite membrane had obvious nanofiltration performance in removing dyes, separating monovalent and divalent ions, and dehydrating solvent–water mixture. O'Hern et al. (2014) also verified the water purification and ion permeation (rather selective) properties of the graphene oxide membrane.

Similar to the study of graphene oxide membrane in ion transport, Chang et al. (2017) reported that carboxylation could increase the hydrophilicity of graphene oxide membrane, improving the efficiency of dye removal. Such improvement was potentially attributed to surface charge density. On the contrary, it was found that reduced preoxidized graphene membrane could increase the rejection efficiency of methyl orange dye to >90%. In addition, a graphene oxide hydrogel membrane was synthesized by Qin et al. (2012) via suspending the graphene oxide (graphene oxide) in water. This graphene oxide hydrogel exhibited pH responsiveness and good mechanical properties. Meanwhile, graphene oxide hydrogel had a good adsorption capacity for organic dye Rhodamine B and anionic chromate.

Graphene oxide membrane also possessed superior metal ion adsorption characteristics. The graphene oxide membranes, which were modified with hyperbranched polyethylenimine, were applied to obtain high permeability and rejection (>90%) of heavy metal ions (Zhang et al. 2015). The divalent metal ions, such as Co^{2+}, Ni^{2+}, Cu^{2+}, Zn^{2+}, Cd^{2+}, Pb^{2+}, etc., could be chemically adsorbed by graphene oxide membranes, and the membranes could be reused for up to ten cycles (Sitko et al. 2016).

Nowadays, graphene oxide membranes were also applied to oil–water separation. With vacuum-assisted filtration, Zhao et al. (2016) intercalated palygorskite nanorods into adjacent graphene oxide nanosheets and assembled graphene oxide nanosheets into laminate structures to prepare the freestanding graphene oxide membranes. Under various conditions (different concentration, pH, or oil species), the graphene oxide membranes showed excellent anti-oil performance in the separation process of water-containing oil emulsion.

4.4.3 Graphene Oxide Hybrid Membranes

Although graphene oxide membranes with a good desalination capability can be prepared by simple methods, these membranes could be trapped by the use of pressure-driven systems. Liu et al. (2015) found that the composite membrane prepared by adding graphene oxide to polysulfone displayed superior pressure-resisted ability, mechanical strength, and water permeability.

In order to increase water flux further, Dai et al. (2015) introduced a large quantity of nitrogen-containing and oxygen-containing groups into the surface of graphene oxide membrane and filled the interlayer space with polypropylene. The novel polypropylene-based composite membrane apparently improved the hydrophilicity and adsorption capacity. With the development of materials science, membranes consisted of polymeric materials, including nylon, aromatic polyamides, polyvinylidene fluoride, polysulfone, and polyethersulfone, as well as non-polymer materials, such as ceramics, metals, and composites, which have been readily fabricated and applied on the filtration of diverse solutions. Compared to pure polymer membranes, the polyamide membranes doped with graphene oxide showed higher water flux and desalination rate (Bano et al. 2015). The resultant increase in the permeate water flux was from 1.8 L/($m^{2\cdot}$ h^1) to 22 L /($m^{2\cdot}$ h^1), while salt rejection maintained at essentially above 80%. Similarly, research conducted by Lai et al. (2016) demonstrated that water flux and salt removal were improved by integrating graphene oxide in polyamide membrane. Moreover, Ali et al. (2016) prepared thin composite membranes embedded with graphene oxide to evaluate their desalination performance. They found that adding a small amount of graphene oxide (100 ppm) significantly improved water flux and mechanical stability and reduced membrane fouling. For salt solution with 2000 ppm NaCl, the launching flux at 1.5 MPa was 29.6 L/m^2, and the salt removal rate was 97%. Besides, Kochameshki et al. (2017) synthesized a polysulfone nanocomposite membrane modified with graphene grafted with diallyldimethylammonium chloride. The results showed that the water flux increased to about 450 L/m^2·h, the antifouling performance was improved, and the heavy metal ion rejection rate increased to 86.68% (Cu^{2+}) and 88.68% (Cd^{2+}).

In addition, polyethylenimine membrane integrated with tannic acid-functionalized graphene oxide showed excellent ion separation performance against NaCl and $MgSO_4$ (Lim et al. 2017). A thin nanofiltration membrane was prepared by aggregating piperazine and trimesoyl chloride with reduced graphene oxide/TiO_2 composite, which demonstrated good separation performance and antifouling property in cross-flow filtration system due to the hydrophilicity of reduced graphene oxide (Safarpour et al. 2015b). Zhang et al. (2017c) synthesized a novel layered structure membrane which was prepared by coating graphene oxide sheets on the surface of electrospun aminated polyacrylonitrile (APAN) fibers, exhibiting ultrahigh flux (10,000 L/(m^2·h)), promising rejection (98%) and excellent antifouling performance for the separation of oil–water emulsions. Besides, Choi et al. (2013) also fabricated a dual-action barrier coating layer of graphene oxide on the surface of polyamide reverse osmosis membrane. The antifouling tests indicated that the graphene oxide coating layer can increase the surface hydrophilicity and decrease the surface roughness, which promoted the significantly improved antifouling performance against a protein foulant. Similarly, graphene oxide nanosheets were successfully doped across 200-nm-thick polyamide membranes by He et al. (2015). They observed the significant increase of water flux (80%) in the reverse osmosis membranes modified with graphene oxide nanosheets. Moreover, polyamide nanofiltration membranes modified with reduced graphene oxide–NH_2 were prepared by Li et al. (2017b) to enhance water flux and antifouling capability. There were some researchers reporting the improvement in the chlorine resistance of the polyamide membranes incorporated with graphene oxide (Safarpour et al. 2015a). In their opinion, the chemically stable graphene oxide plate embedded in the polyamide layer acted as a barrier layer, protecting the polyamide from chlorine erosion, as shown in Fig. 4.9 (Choi et al. 2013).

The researchers also identified that adding graphene to polymer membranes had positive influences on dye absorption. Polypyrrole-hydrolyzed polyacrylonitrile composite NF membrane doped with graphene oxide was prepared by Shao et al. (2014). It is found that the effectiveness of Rose Bengal dye rejection was approximately 99.0%, and the solvent permeability was enhanced. And the NF performance of graphene oxide mixed polyether sulfone membrane used for dyestuff (Direct red 16) removal was higher than that of polyethersulfone membrane (99% vs. 90%) (Zinadini et al. 2014). The NF membrane fabricated by multilayered deposition of graphene oxide on a polysulfone support exhibited high water permeability and superior rejection (93–95%) of Rhodamine B dye (Qiu et al. 2011). In addition, a polyamide membrane assembled with carboxyl-functionalized graphene oxide showed 98.1% dye rejection rate of the New Coccine (Zhang et al. 2017b).

Due to superior separation characteristic, graphene oxide-doped polymer membranes were also applied on oil–water separation. Hu et al. (2015) successfully fabricated a novel graphene oxide hybrid membrane on commercial 19-channel ceramic by adopting a vacuum method. During the treatment, the water permeation fluxes of modified membranes were about 667 L/(m^2·h·bar) after 150-min operation,

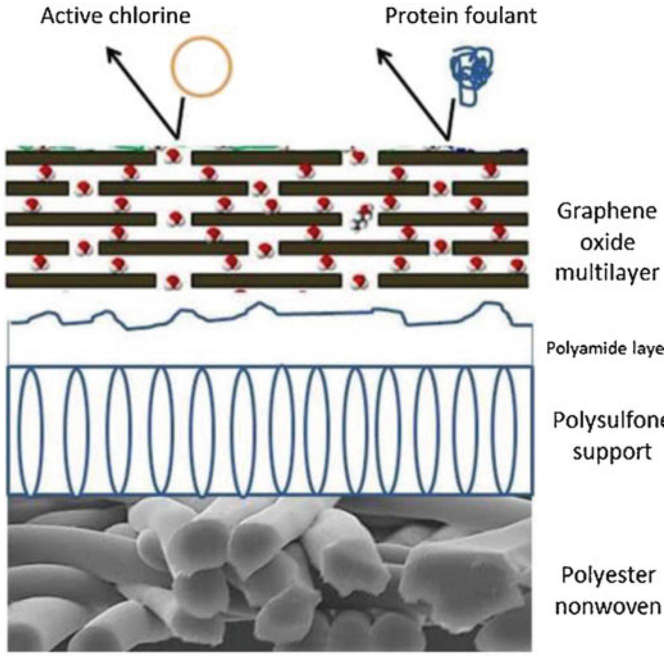

Fig. 4.9 Graphene oxide protective layer against foulants and active chlorine in the polyamide membrane. (Reprinted with permission of (Choi et al. 2013))

which was higher about 27.8% than that of the unmodified membrane (522 L/(m^2·h·bar)). These results showed that graphene oxide modification played a crucial role on improving oil–water separation performance. Similarly, in addition to the application of membrane in above wastewater treatment, the novel membranes were more widely applied to more intricate wastewater (Huang et al. 2015). Zinadini et al. (2015) synthesized three different hybrid membranes which were fabricated in three concentrations of 13, 15, and 17 wt% of polyethersulfone polymer. Polyethersulfone/graphene oxide membrane with 15 wt% of polyether sulfone and graphene oxide content of 0.5 wt% showed the most superior performances and was selected as optimal membrane for treatment of milk processing wastewater. Similarly, Sun et al. (2015) developed an antibiofouling membrane by in situ fabrication of graphene oxide–AgNPs onto cellulose acetate membranes. The presence of graphene oxide–AgNPs composite on the membrane caused an inactivation of 86% *Escherichia coli* after contacting with the membrane for 2 h. Compared to modifying graphene oxide with active substances, graphene oxide hybrid membranes by adding graphene oxide into polymer membranes achieve more significant advantages on improved water flux, mechanical stability, and fouling resistance. There is no doubt that graphene oxide hybrid membranes will provide us the new insight on the optimization of graphene-based membranes (Table 4.5).

Table 4.5 Application, membrane performance, and other conditions of mixed-matrix graphene oxide membranes

Membrane material	Synthesis technique	Application	Membrane performance	Reference
PES/GO/PAA	Solution casting	Remove synthetic melanoidin solution	54% color removal	Kiran et al. (2015)
Polycation/GO multilayer membrane	Self-assembly-assisted layer-by-layer deposition	Remove dye from water	The flux and retention rate could reach 6.42 kg/(m^2·h·bar) and 99.2%	Wang et al. (2016b)
MgSi@RGO/PAN composite membrane	Vacuum filtration and deposition	Desalination, wastewater treatment, separation, and purification	The membranes can effectively reject small molecules	Liang et al. (2016a)
PES-GO-4	Interfacial polymerization	Water or wastewater treatment applications	The PES-GO-4 membrane exhibited 2.6 times greater flux recovery than an unmodified PES-UF membrane	Efosa et al. (2016)
GO/APAN membrane	Electrospinning-assisted layer-by-layer assembly technique	Separation of oil–water emulsion	This membrane exhibited ultrahigh flux (~10,000 LMH), preferable rejection rate (≥98%), and remarkable antifouling performance	Zhang et al. (2017c)
Polysulfone–Fe_3O_4/GO mixed-matrix membrane	Immersion phase inversion	Water treatment during the backwashing procedure	The novel polysulfone–Fe_3O_4/GO mixed-matrix membrane was having 3 times higher permeate flux than the neat PSf membrane	Chai et al. (2016)
GO-ZnO membranes	Double-casting phase inversion (DCPI)	Wastewater reclamation	The novel membranes exhibited higher fluxes, with less fouling and high rejection rate of TOCs.	Mahlangua et al. (2016)
TA/GOQDs TFN membrane	Interfacial polymerization	Wastewater treatment, separation, and purification	The TA/GOQDs TFN membrane showed a pure water flux up to 23.33 L/(m^2·h) (0.2 MPa), and high dye rejection to Congo red (99.8%) and methylene blue (97.6%) was kept	Zhang et al. (2017a)

(continued)

Table 4.5 (continued)

Membrane material	Synthesis technique	Application	Membrane performance	Reference
3D PPy@GO membrane	One-step electrochemical co-deposition	Wastewater treatment	The 3D PPy@GO composite-coated electrodes showed excellent permselectivity of Pb^{2+} with a flux of 4.7 g/(m^2·h), a current efficiency of 51.9%, and excellent cycling stability	Gao et al. (2017a)
PVA/PAA/GO-COOH@PDA	Electrospinning technique	Wastewater treatment and dye removal	The PVA/PAA/GO-COOH@PDA composite materials showed efficient adsorption capacity towards the three model dyes. The composite membranes can be easily separated and regenerated from wastewater dye solution and demonstrated excellent reusability	Xing et al. (2017)
GPC ultrafiltration membrane	Drop-coating combined with vacuum filtration	Complex industrial wastewater streams	The membrane exhibited an excellent rejection coefficient of 99.2% for methylene blue and the permeation flux was 12 L/(m^2·h) at 0.1 bar	Wang et al. (2018a)
CG RO membranes	Embedding and melting method	Desalination	The RO membrane performance showed that the permeate flux of membrane increased from 1.67 L/(m^2·h) to 4.74 L/(m^2·h)	Chen et al. (2017)
PVA–GA composite membranes	Cross-linking and polymerization methods	Removing an industrial textile dye from wastewater	The nanofiltration membrane showed lowest fouling rate during removal of the industrial direct dye (flux recovery ratio, 96.60%; reversible fouling ratio, 23.82%; and irreversible fouling ratio, 3.39%)	Liu et al. (2018)

4.5 Carbon Fiber Membranes

Since Shimpei (1986) accidentally found that carbon fibers facilitated microbial attachment, and possessed excellent adsorption capacity for pollutants, the research works focused on carbon fibers for water treatment were widely carried out. It was believed that these advantages opened the "surprise door" for the application of carbon fibers (Xu and Luo 2012; Manawi et al. 2018). Especially, carbon fiber membranes, as one of the novel membrane materials, have been explored and applied in recent years (Xiao et al. 2016).

4.5.1 Support-Free Carbon Fiber Membranes

The support-free carbon fiber membranes are generally obtained by forming carbon fiber precursors into membrane shape and then stabilized and carbonized via thermal treatment. Beck et al. (2017) prepared carbon nanofiber membranes by electrospinning followed by carbonization (Fig. 4.10). The adsorption capacity, permeability, and adsorption kinetics of the carbon nanofiber membranes were about 10, 6, and 2 times larger than that of the traditional activated carbon

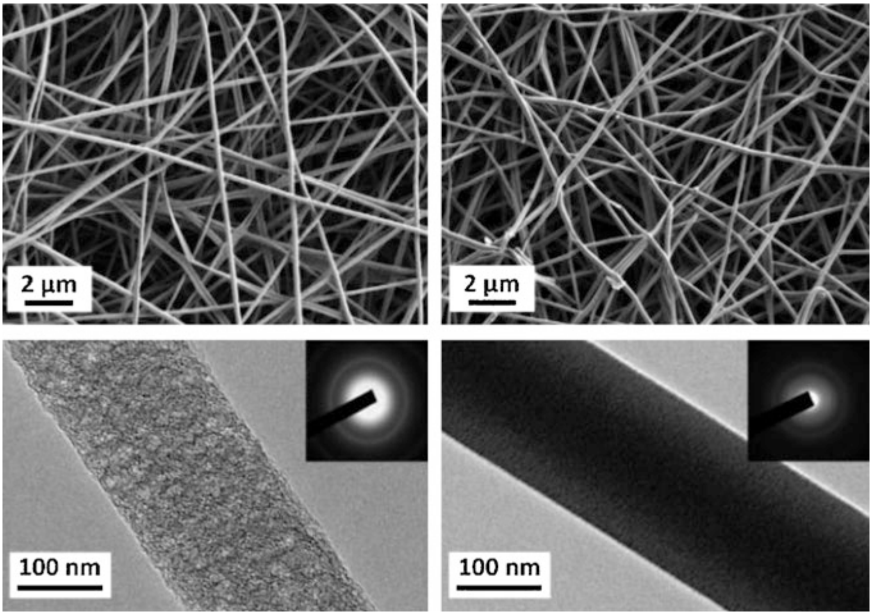

Fig. 4.10 SEM (top) and TEM (bottom) images of electrospun carbon nanofiber membranes prepared from the precursors of lignin/PVA (left) and PAN (right). The insets in the TEM images show the electron diffraction patterns. (Reprinted with permission of (Beck et al. 2017))

membrane, respectively. However, such carbon fiber membranes usually suffered from serious membrane fouling, limiting their application.

4.5.2 Carbon Fiber Hybrid Membranes

In order to expand the application of carbon fiber membrane in water treatment and improve the removal efficiency of pollutants, researchers have developed a variety of carbon fiber hybrid membranes, which combined the advantages of carbon fiber and membrane technology, improving its treatment efficiency.

Yang and Tsai (2008, 2009) prepared carbon fibers/carbon/alumina tubular composite membrane and applied it in a cross-flow electrocoagulation/electrofiltration module for Cu chemical mechanical polishing wastewater treatment. Under the optimal experimental conditions, the turbidity of the permeate was less than 1 NTU, and the removal rates of total solid content, copper, total organic carbon, and silicon were 72%, 92%, 81%, and 87%, respectively. Li et al. (2013a, b) reported their works on domestic sewage treatment using biological carbon fiber membrane. The biological carbon fiber membrane could effectively intercept sludge and most organic matter. Moreover, the bio-carbon fiber inside the membrane had a strong adsorption performance, which could further adsorb the organic matter across the membrane surface, thus ensuring a higher and more stable removal rate of organic matter.

Besides, Tai et al. (2014) developed a novel freestanding and flexible electrospun carbon–silica composite nanofibrous membrane. This composite membrane was more tough than the original carbon nanofibers when the SiO_2 concentration was 2.7 wt%. They found that after coating with silicone oil, the composite membrane became ultrahydrophobic and superoleophilic, which enabled the membrane to serve as an effective substrate for separating free oil from water. Yue et al. (2018) fabricated layered porous dynamic separation membranes containing primary and secondary nanostructures by in situ growth of ZnO nanowires on carbon fibers (Fig. 4.11). The

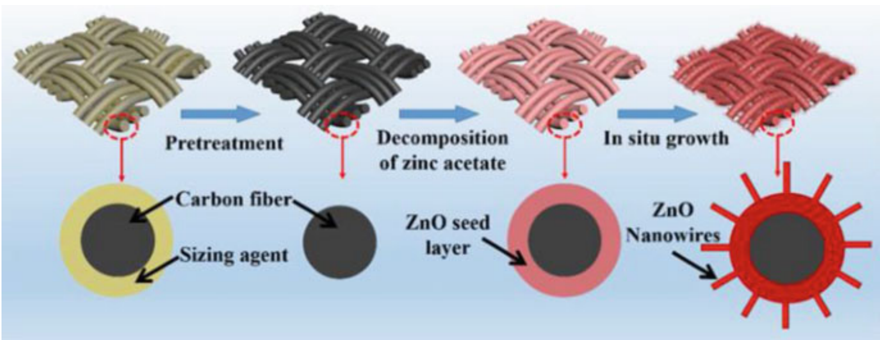

Fig. 4.11 Fabrication process of ZnO–carbon fiber dynamic membrane. (Reprinted with permission of (Yue et al. 2018))

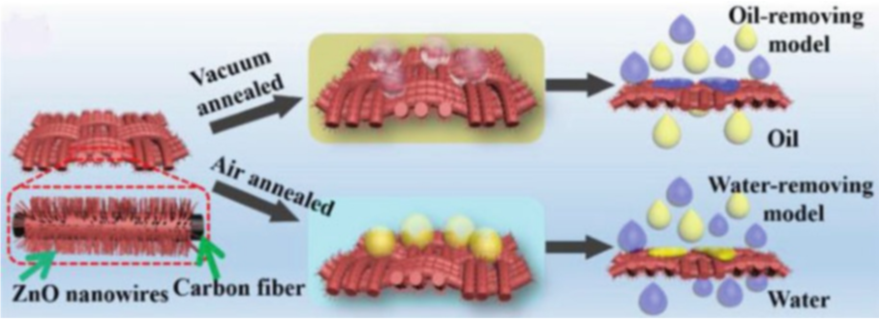

Fig. 4.12 The switchable wettability of ZnO–carbon fiber dynamic membrane when annealed in different atmosphere and the corresponding separation capacities of oil–water mixtures. (Reprinted with permission of (Yue et al. 2018))

membrane could switch wettability between high hydrophobicity and superhydrophilicity by simply annealing alternatively in vacuum and air environment (Fig. 4.12) and indicated more than 98% separation efficiency in deoiling and dewater modes. Han et al. (2017) prepared 3D structural Fe_2O_3–TiO_2@activated carbon fiber membranes by a modified electrospinning process followed by a thermal treatment. The membrane possessed high adsorption and visible light excitable photocatalytic properties and could be used to remove dyes and heavy metal ions.

4.5.3 The Composite Membranes Using Carbon Fiber Cloth as the Substrate

These composite membranes usually are obtained by loading various functional materials on carbon fiber cloth, which is adopted as the substrate. They can combine the advantages of functional materials and membrane technology. Meanwhile, the carbon fiber substrate has good mechanical properties and can reduce the loss of functional material in the process of water treatment.

Li et al. (2016c) successfully prepared a catalytic cathode membrane on the basis of low-cost carbon fiber cloth with Pd-reduced graphene oxide–$CoFe_2O_4$ catalyst (Fig. 4.13). The cathode membrane was used in microbial fuel cell/membrane bioreactor coupling system, exhibiting great potential on simulated wastewater treatment. Xiao et al. (2017) obtained carbon fiber/C_3N_4 cloth by a dip-coating and thermal condensation method with carbon fiber cloth as substrate (Fig. 4.14). The carbon fiber/C_3N_4 cloth possessed excellent flexibility and strong visible light absorption, which displayed good treatment performance for the degradation of flowing wastewater. To further improve the treatment efficiency, Shen et al. (2018) inserted TiO_2 between C_3N_4 and carbon fiber (Fig. 4.15). The carbon fiber/TiO_2/C_3N_4 cloth showed enhanced photocatalytic activity for degrading various organic pollutants in comparison with carbon fiber/C_3N_4 cloth.

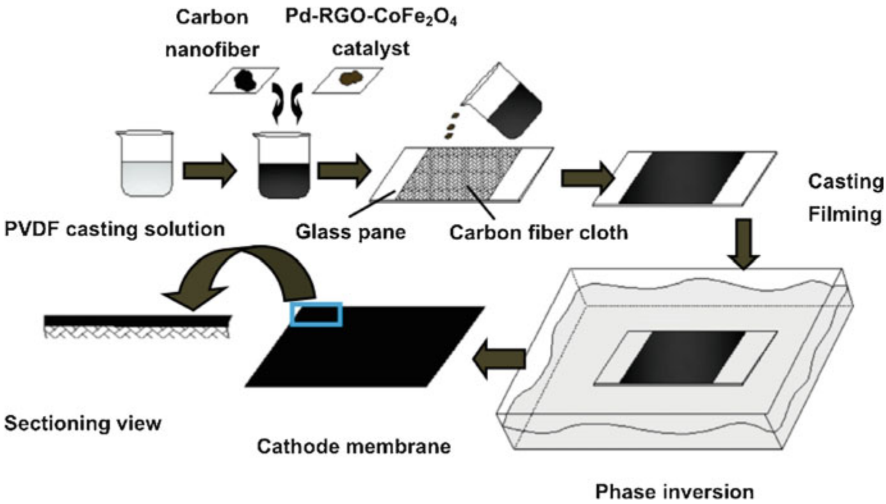

Fig. 4.13 The preparation process of cathode membrane. (Reprinted with permission of (Li et al. 2016c))

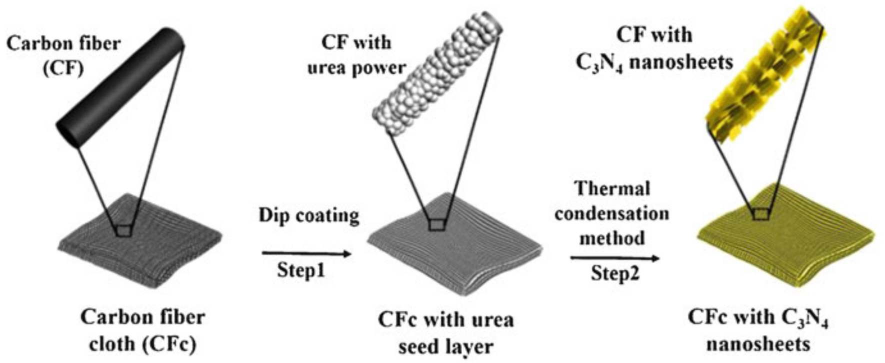

Fig. 4.14 Schematic illustration of the preparation process of carbon fiber/C_3N_4 cloth. (Reprinted with permission of (Xiao et al. 2017))

4.6 Activated Carbon Membranes

Activated carbon, as a unique multifunctional material with high surface area, micro–meso and macroscopic structure, and various chemical functional groups, is recognized worldwide as one of the most popular adsorbents in water treatment (Amit et al. 2013; Danish and Ahmad 2018). Up to now, activated carbon has been widely used in various industrial processes including food processing (Alvarez et al. 2011), chemical manufacturing (Jaria et al. 2018), pharmaceutical (Karelid et al. 2017), paper making (Ou Yang et al. 2013), etc. to remove water-soluble chemical

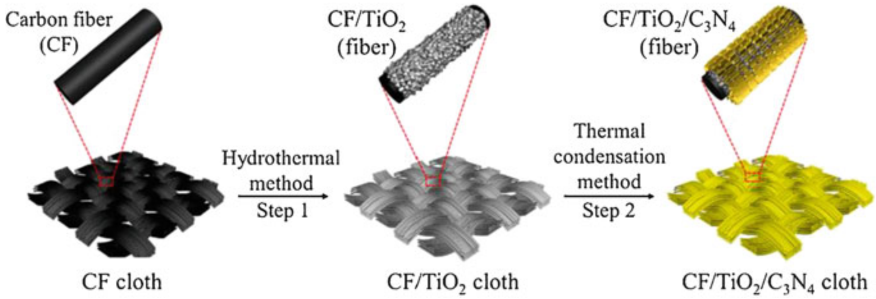

Fig. 4.15 Schematic illustration of the preparation of TiO_2/C_3N_4 heterojunctions on carbon fiber cloth. (Reprinted with permission of (Shen et al. 2018))

pollutants from inorganic and organic wastewater (Abdel-Nasser and El-Hendawy 2001; Mohammed 2011). Jacangelo (1995) found that activated carbon could adsorb organics to prevent the formation of membrane fouling in membrane separation processes. Several studies also demonstrated that membrane bioreactor achieved high removal efficiency for trace organic pollutants in synthetic and real wastewater by the use of granular activated carbon (Amaral et al. 2014; Jia et al. 2014). In this section, the membrane materials integrated with activated carbon, including activated carbon-coated membranes, support-free activated carbon membranes, and activated carbon mixed-matrix membranes for wastewater treatment, were described as follows.

4.6.1 Activated Carbon-Coated Membranes

Activated carbon could be coated on membranes to enhance membrane separation performance while removing contaminants from wastewater. Thiruvenkatachari et al. (2006) prepared activated carbon pre-coated microfiltration hollow fiber membrane using wood-based, coal-based, and coconut shell-based activated carbon for wastewater treatment (Fig. 4.16). After 8 h of operation, 63% of organic pollutants were removed by wood-based activated carbon-coated membrane, 57% by coal-based activated carbon-coated membrane, and 56% by coconut shell-based activated carbon-coated membrane, which were higher than that of non-pre-coated membrane. Simultaneously, the decrease of membrane flux was prevented effectively (less than 20% of initial flux). This work strongly confirmed that the membranes coated by activated carbon could significantly relieved membrane fouling, enhance membrane treatment performance, and improve membrane life. Amaral et al. (2016) developed microfiltration membranes coated by superfine powdered activated carbon for drinking water treatment. The coated membranes achieved excellent removal efficiency because superfine powdered activated carbon was more favorable for the adsorption of pollutants due to its smaller particle size compared with conventional activated carbon. Bae et al. (2007) designed activated carbon membrane with carbon whiskers for

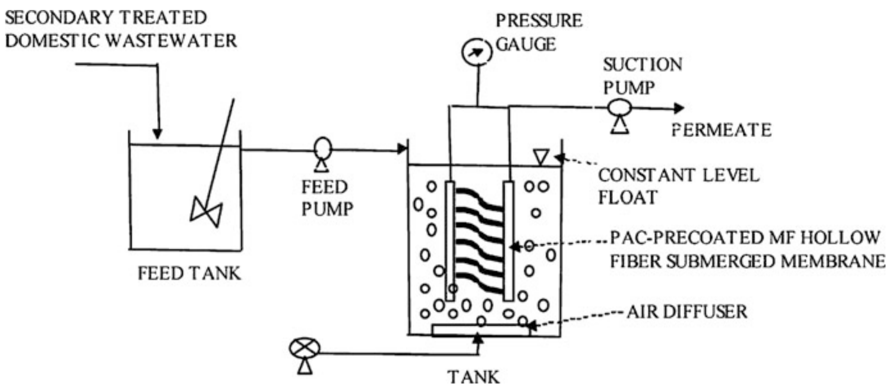

Fig. 4.16 Schematic of membrane hybrid system with pre-coated membrane. (Reprinted with permission of (Thiruvenkatachari et al. 2006))

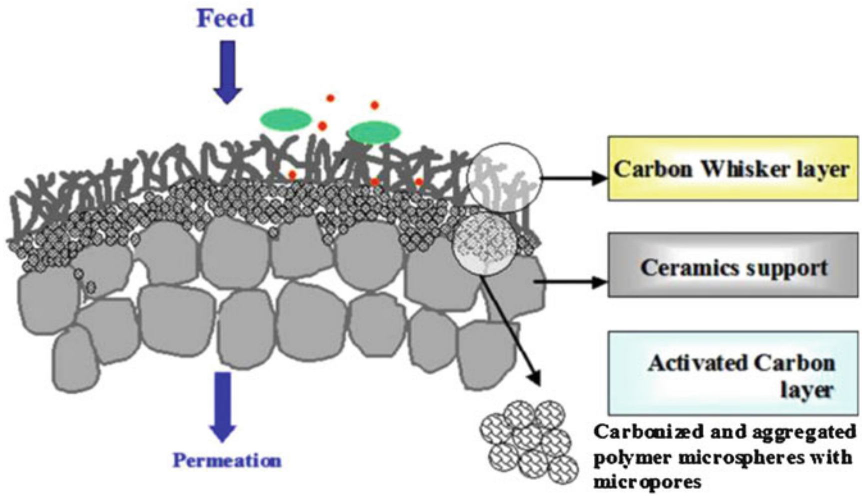

Fig. 4.17 Structure of an activated carbon membrane with carbon whiskers. (Reprinted with permission of (Bae et al. 2007))

wastewater and drinking water treatments. The carbon whiskers on the activated carbon membrane could significantly prevent the deposition and accumulation of particles, extending membrane lifetime (Fig. 4.17).

4.6.2 Support-Free Activated Carbon Membranes

Activated carbon membrane is a novel carbon-based membrane, which not only has excellent thermal stability and chemical stability of inorganic membrane materials but also has excellent electrical conductivity and rich pore structure of carbon materials. Li et al. (2017a) designed and prepared a support-free activated carbon membrane by mixing activated carbon, binder, pore former, and conductive agent followed by compression modeling and carbonization. The activated carbon membrane realized the integration of the triple function of adsorption/electrocatalysis/membrane separation for deep water purification.

4.6.3 Activated Carbon Hybrid Membranes

In order to further improve membrane performance, activated carbon was also adopted as function material to be mixed in membrane matrix. Aghili et al. (2017) prepared a novel powdered activated carbon mixed-matrix membrane for cheese whey wastewater treatment. This membrane integrated a powdered activated carbon adsorption mechanism with the separation property of the polysulfone membrane, indicating high treatment efficiency for organic matter removal. Ahmad et al. (2018) fabricated high-performance hybrid ceramic/activated carbon symmetric membrane to purify oily wastewater (Fig. 4.18). The hybrid Al_2O_3/activated carbon membrane

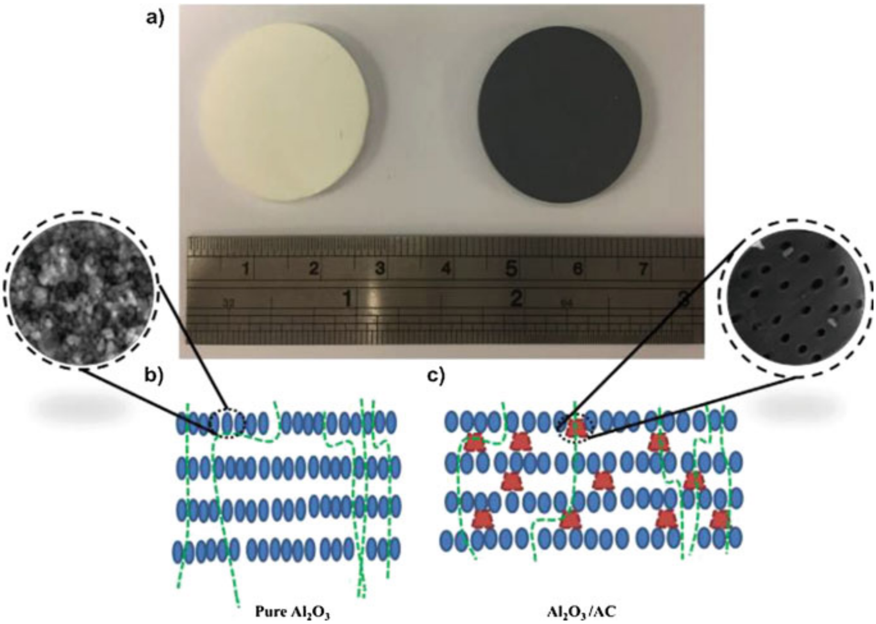

Fig. 4.18 Optical images of (**a**) Al_2O_3 membrane and Al_2O_3/activated carbon hybrid membrane. Schematic illustration of (**b**) Al_2O_3 and (**c**) Al_2O_3/activated carbon hybrid membranes. (The SEM image in (**b**) shows the particle size of the Al_2O_3 after sintering, while the SEM image in (**c**) shows the morphological structure of the activated carbon with highly porous structure and distribution of cylindrical-shaped pores.) (Reprinted with permission of (Ahmad et al. 2018))

possessed complex microchannel–nanochannel networks, which achieved two times higher porosity in comparison with Al_2O_3 membrane. As expected, the oil removal efficiency of the hybrid Al_2O_3/activated carbon membrane could reach 99.02%. On the whole, the development of a cost-effective membrane by doping a cheap material, such as activated carbon, could create a complementary structure, producing strong competitiveness in wastewater treatment.

4.7 Other Carbon Materials Incorporated Membrane

In addition to these carbon materials mentioned above, several other carbon materials such as asphalt were also be adopted to prepare membranes for water treatment. Liang et al. (2016b) used a tubular electrochemically reactive graphite membrane acting as cathode and evidenced the advantages of coupled advanced oxidation process (electro-Fenton reaction) for dynamic filtration. Liu et al. (2017) designed a novel b-cyclodextrin (β-CD)-functionalized g–C_3N_4 composite membrane with the integration of dual function of microfiltration and visible light-driven photocatalytic degradation. The membrane could remove the organic dye by adsorption, microfiltration, and photodegradation. Yvonne (2014) prepared a sulfonated asphalt sodium alginate hybrid membrane.

4.8 Conclusion and Future Prospects

Numerous studies have been performed in membrane technologies with diverse materials for highly efficient water treatment. Among them, carbon materials with outstanding properties have been proven with potential benefits to prepare carbon-based membranes and exhibit superiority over other membrane processes. To further enhance membrane separation performance and antifouling properties, several kinds of carbon-based membrane materials including carbon membranes, carbon nanotube membranes, carbon fiber membranes, activated carbon membranes, graphene-based membranes, etc. are explored for highly efficient water treatment. Various methods including surface modification, operation parameter optimization, and technologies combination are adopted to optimize membrane performance. All these attempts have been proved with fruitful results and make great progress in this field.

Although these carbon-based membrane materials have exhibited promising potential in the field of water treatment, further studies are still required to achieve the commercial application level. The concerned challenges are listed below:

1. More advanced membrane preparation technology should be developed to fabricate high-performance carbon-based membrane materials.
2. The electric assistance might speed up the corrosion of carbon-based membrane materials, shorten the lifetime, and cause secondary pollution. Therefore,

developing the modification technology of existing carbon materials and exploring novel carbon materials with great potential are important to pursue higher separation efficiency and better antifouling performance.

3. Besides electrochemical action, other innovative coupling processes should be further extended.
4. The vast majority of carbon-based membrane materials are carried out in laboratory scale, while much efforts should be paid before the pilot- and industrial-scale applications. In this process, the stability of carbon-based membrane materials needs to be further investigated during long-term operation.

Thus, these issues deserve more attention for membrane researchers. Although it would take a long time and quite great effort to resolve the remaining challenges, it is worth affirming that carbon-based membrane materials have promising potential in dealing with a large variety of industrial wastewater application in the future.

Acknowledgments This work was supported by the National Natural Science Foundation of China (21476034) and Key R&D Program Projects in Liaoning Province (2017308005).

References

Abd JSN, Wang DK, Yacou C, Motuzas J, Smart S, Diniz da Costa CJ (2017) Vacuum-assisted tailoring of pore structures of phenolic resin derived carbon membranes. J Membr Sci 525:240–248. https://doi.org/10.1016/j.memsci.2016.11.002

Abdel-Nasser A, El-Hendawy Samra SE (2001) Adsorption characteristics of activated carbons obtained from corncobs. Colloid Surf A 180:209–221

Abidin MNZ, Goh PS, Ismail AF, Othman MHD, Hasbullah H, Said N, Kadir S, Kamal F, Abdullah MS, Ng BC (2017) Development of biocompatible and safe polyethersulfone hemodialysis membrane incorporated with functionalized multi-walled carbon nanotubes. Mater Sci Eng C 77:572–582. https://doi.org/10.1016/j.msec.2017.03.273

Aghili F, Ghoreyshi AA, Rahimpour A, Rahimnejad M (2017) Coating of mixed-matrix membranes with powdered activated carbon for fouling control and treatment of dairy effluent. Process Saf Environ 107:528–539. https://doi.org/10.1016/j.psep.2017.03.013

Ahmad K, Anita B, Marijke J, Gordon M, Muataz AA (2018) Novel hybrid ceramic/carbon membrane for oil removal. J Membr Sci 559:42–53. https://doi.org/10.1016/j.memsci.2018.05.003

Ahmed F, Santos CM, Mangadlao J, Advincula R, Rodrigues DF (2013) Antimicrobial PVK: SWNT nanocomposite coated membrane for water purification: performance and toxicity testing. Water Res 47:3966–3975. https://doi.org/10.1016/j.watres.2012.10.055

Ahmed F, Lalia BS, Kochkodan V, Hilal N, Hashaikeh R (2016) Electrically conductive polymeric membranes for fouling prevention and detection: a review. Desalination 391:1–15. https://doi.org/10.1016/j.desal.2016.01.030

Ahn C, Baek Y, Lee C, Kim S, Kim S, Lee S, Kim SH, Bae SS, Park J, Yoon J (2012) Carbon nanotube-based membranes: fabrication and application to desalination. J Ind Eng Chem 18:1551–1559. https://doi.org/10.1016/j.jiec.2012.04.005

Ali MEA, Wang L, Wang X, Feng X (2016) Thin film composite membranes embedded with graphene oxide for water desalination. Desalination 386:67–76. https://doi.org/10.1016/j.desal.2016.02.034

Ali S, Rehman SAU, Luan HY, Farid MU, Huang H (2019) Challenges and opportunities in functional carbon nanotubes for membrane-based water treatment and desalination. Sci Total Environ 646:1126–1139. https://doi.org/10.1016/j.scitotenv.2018.07.348

Alpatova A, Meshref M, McPhedran KN, Gamal El-Din M (2015) Composite polyvinylidene fluoride (PVDF) membrane impregnated with Fe_2O_3 nanoparticles and multiwalled carbon nanotubes for catalytic degradation of organic contaminants. J Membr Sci 490:227–235. https://doi.org/10.1016/j.memsci.2015.05.001

Alvarez PM, Pocostales JP, Beltran FJ (2011) Granular activated carbon promoted ozonation of a food-processing secondary effluent. J Hazard Mater 185:776–783. https://doi.org/10.1016/j.jhazmat.2010.09.088

Amaral MCS, Lange LC, Borges CP (2014) Evaluation of the use of powdered activated carbon in membrane bioreactor for the treatment of bleach pulp mill effluent. Water Environ Res 86:788–799. https://doi.org/10.2175/106143014x13975035526383

Amaral P, Partlan E, Li M, Lapolli F, Mefford OT, Karanfil T, Ladner DA (2016) Superfine powdered activated carbon (S-PAC) coatings on microfiltration membranes: effects of milling time on contaminant removal and flux. Water Res 100:429–438. https://doi.org/10.1016/j.watres.2016.05.034

Amini M, Jahanshahi M, Rahimpour A (2013) Synthesis of novel thin film nanocomposite (TFN) forward osmosis membranes using functionalized multi-walled carbon nanotubes. J Membr Sci 435:233–241. https://doi.org/10.1016/j.memsci.2013.01.041

Amit B, William H, Marcia M, Mika S (2013) An overview of the modification methods of activated carbon for its water treatment applications. Chem Eng J 219:499–511. https://doi.org/10.1016/j.cej.2012.12.038

Anand A, Unnikrishnan B, Mao J, Lin H, Huang C (2018) Graphene-based nanofiltration membranes for improving salt rejection, water flux and antifouling–a review. Desalination 429:119–133. https://doi.org/10.1016/j.desal.2017.12.012

Ansón-Casaos A, González-Domínguez JM, Terrado E, Martínez MT (2010) Surfactant-free assembling of functionalized single-walled carbon nanotube buckypapers. Carbon 48:1480–1488. https://doi.org/10.1016/j.carbon.2009.12.043

Apul OG, Karanfil T (2015) Adsorption of synthetic organic contaminants by carbon nanotubes: a critical review. Water Res 68:34–55. https://doi.org/10.1016/j.watres.2014.09.032

Bae SD, Lee CW, Kang LS, Sakoda A (2007) Preparation, characterization, and application of activated carbon membrane with carbon whiskers. Desalination 202:247–252. https://doi.org/10.1016/j.desal.2005.12.061

Baek Y, Kim C, Seo D, Kim T, Lee J, Kim Y, Ahn K, Bae S, Lee S, Lim J, Lee K, Yoon J (2014) High performance and antifouling vertically aligned carbon nanotube membrane for water purification. J Membr Sci 460:171–177. https://doi.org/10.1016/j.memsci.2014.02.042

Beck RH, Zhao Y, Fong H, Menkhaus TJ (2017) Electrospun lignin carbon nanofiber membranes with large pores for highly efficient adsorptive water treatment applications. J Water Process Eng 16: 240-248. https://doi.org/10.1016/j.jwpe.2017.02.002

Bakr AR, Rahaman MS (2016) Electrochemical efficacy of a carboxylated multiwalled carbon nanotube filter for the removal of ibuprofen from aqueous solutions under acidic conditions. Chemosphere 153:508–520. https://doi.org/10.1016/j.chemosphere.2016.03.078

Bakr AR, Rahaman MS (2017) Removal of bisphenol A by electrochemical carbon-nanotube filter: influential factors and degradation pathway. Chemosphere 185:879–887. https://doi.org/10.1016/j.chemosphere.2017.07.082

Bano S, Mahmood A, Kim S, Lee K (2015) Graphene oxide modified polyamide nanofiltration membrane with improved flux and antifouling properties. J Mater Chem A 3:2065–2071. https://doi.org/10.1039/c4ta03607g

Bounos G, Andrikopoulos KS, Moschopoulou H, Lainioti GC, Roilo D, Checchetto R, Ioannides T, Kallitsis JK, Voyiatzis GA (2017) Enhancing water vapor permeability in mixed matrix polypropylene membranes through carbon nanotubes dispersion. J Membr Sci 524:576–584. https://doi.org/10.1016/j.memsci.2016.11.076

Brady Estevez AS, Kang S, Elimelech M (2008) A single-walled-carbon-nanotube filter for removal of viral and bacterial pathogens. Small 4:481–484. https://doi.org/10.1002/smll.200700863

Bruce J, Hinds N, Chopra T, Rantell R, Andrews VG, Leonidas GB (2004) Aligned multiwalled carbon nanotube membranes. Science 303:62–65

Brunet L, Lyon DY, Zodrow K, Rouch JC, Caussat B, Serp P, Remigy JC, Wiesner MR, Alvarez PJJ (2008) Properties of membranes containing semi-dispersed carbon nanotubes. Environ Eng Sci 25:565–576. https://doi.org/10.1089/ees.2007.0076

Celebi K, Buchheim J, Wyss RM, Droudian A, Gasser P, Shorubalko I, Kye JI, Lee C, Park HG (2014) Ultimate permeation across atomically thin porous graphene. Science 344:289–292. https://doi.org/10.1126/science.1249097

Celik E, Liu L, Choi H (2011a) Protein fouling behavior of carbon nanotube/polyethersulfone composite membranes during water filtration. Water Res 45:5287–5294. https://doi.org/10.1016/j.watres.2011.07.036

Celik E, Park H, Choi H, Choi H (2011b) Carbon nanotube blended polyethersulfone membranes for fouling control in water treatment. Water Res 45:274–282. https://doi.org/10.1016/j.watres.2010.07.060

Chai PV, Mahmoudi E, Teow YH, Mohammad AW (2016) Preparation of novel polysulfone-Fe_3O_4/GO mixed-matrix membrane for humic acid rejection. Water Process Eng 15:83–88. https://doi.org/10.1016/j.jwpe.2016.06.001

Chan W, Chen H, Surapathi A, Taylor MG, Shao X, Marand E, Johnson JK (2013) Zwitterion functionalized carbon nanotube/polyamide nanocomposite membranes for water desalination. ACS Nano 7:5308–5319

Chang Y, Shen Y, Kong D, Ning J, Xiao Z, Liang J, Zhi L (2017) Fabrication of the reduced preoxidized graphene-based nanofiltration membranes with tunable porosity and good performance. RSC Adv 7:2544–2549. https://doi.org/10.1039/c6ra24746f

Chao F, Zhou Y, Rui Q (2017) Impact of surface ionization on water transport and salt leakage through graphene oxide membranes. J Phys Chem C 121:13412–13420. https://doi.org/10.1021/acs.jpcc.7b04283

Chen K, Xiao C, Huang Q, Liu H, Tang Y (2017) Fabrication and properties of graphene oxide-embedded cellulose triacetate RO composite membrane via melting method. Desalination 425:175–184. https://doi.org/10.1016/j.desal.2017.10.004

Choi J, Jegal J, Kim W (2006) Fabrication and characterization of multi-walled carbon nanotubes/polymer blend membranes. J Membr Sci 284:406–415. https://doi.org/10.1016/j.memsci.2006.08.013

Choi W, Choi J, Bang J, Lee JH (2013) Layer-by-layer assembly of graphene oxide nanosheets on polyamide membranes for durable reverse-osmosis applications. ACS Appl Mater Inter 5:12510–12519. https://doi.org/10.1021/am403790s

Chowdhury ZZ, Sagadevan S, Johan RB, Shah ST, Adebesi A, Md SI, Rafique RF (2018) A review on electrochemically modified carbon nanotubes (CNTs) membrane for desalination and purification of water. Mater Res Express 5:102001. https://doi.org/10.1088/2053-1591/aada65

Cohen-Tanugi D, Grossman JC (2012) Water desalination across nanoporous graphene. Nano Lett 12:3602–3608. https://doi.org/10.1021/nl3012853

Cohen-Tanugi D, Lin LC, Grossman JC (2016) Multilayer nanoporous graphene membranes for water desalination. Nano Lett 16:1027–1033. https://doi.org/10.1021/acs.nanolett.5b04089

Dai J, Liu X, Xiao Y, Yang J, Qi P, Wang J, Wang Y, Zhou Z (2015) High hydrophilicity and excellent adsorption ability of a stretched polypropylene/graphene oxide composite membrane achieved by plasma assisted surface modification. RSC Adv 5:71240–71252. https://doi.org/10.1039/c5ra10310j

Danish M, Ahmad T (2018) A review on utilization of wood biomass as a sustainable precursor for activated carbon production and application. Renew Sust Energ Rev 87:1–21. https://doi.org/10.1016/j.rser.2018.02.003

Daraei P, Madaeni SS, Ghaemi N, Ahmadi Monfared H, Khadivi MA (2013a) Fabrication of PES nanofiltration membrane by simultaneous use of multi-walled carbon nanotube and surface graft polymerization method: comparison of MWCNT and PAA modified MWCNT. Sep Purif Technol 104:32–44. https://doi.org/10.1016/j.seppur.2012.11.004

Daraei P, Madaeni SS, Ghaemi N, Khadivi MA, Astinchap B, Moradian R (2013b) Enhancing antifouling capability of PES membrane via mixing with various types of polymer modified multi-walled carbon nanotube. J Membrane Sci 444:184–191. https://doi.org/10.1016/j.memsci.2013.05.020

Darryl NV, Rebecca AS, Kan-Sheng C, Haifa HH, Kimberly AR, Thomas JF, Chol SY, Geoffrey FS, Harold WK, Steve FAA (2010) Assembly of cross-linked multi-walled carbon nanotube mats. Carbon 48:987–994. https://doi.org/10.1016/j.carbon.2009.11.016

Das R, Ali ME, Hamid SBA, Ramakrishna S, Chowdhury ZZ (2014) Carbon nanotube membranes for water purification: a bright future in water desalination. Desalination 336:97–109. https://doi.org/10.1016/j.desal.2013.12.026

de Lannoy CF, Jassby D, Davis DD, Wiesner MR (2012) A highly electrically conductive polymer–multiwalled carbon nanotube nanocomposite membrane. J Membr Sci 415–416:718–724. https://doi.org/10.1016/j.memsci.2012.05.061

de Lannoy CF, Soyer E, Wiesner MR (2013) Optimizing carbon nanotube-reinforced polysulfone ultrafiltration membranes through carboxylic acid functionalization. J Membr Sci 447:395–402. https://doi.org/10.1016/j.memsci.2013.07.023

Duan W, Chen G, Chen C, Sanghvi R, Iddya A, Walker S, Liu H, Ronen A, Jassby D (2017) Electrochemical removal of hexavalent chromium using electrically conducting carbon nanotube/polymer composite ultrafiltration membranes. J Membr Sci 531:160–171. https://doi.org/10.1016/j.memsci.2017.02.050

Dumée LF, Sears K, Schütz J, Finn N, Huynh C, Hawkins S, Duke M, Gray S (2010) Characterization and evaluation of carbon nanotube Bucky-Paper membranes for direct contact membrane distillation. J Membr Sci 351:36–43. https://doi.org/10.1016/j.memsci.2010.01.025

Dumée L, Germain V, Sears K, Schütz J, Finn N, Duke M, Cerneaux S, Cornu D, Gray S (2011) Enhanced durability and hydrophobicity of carbon nanotube bucky paper membranes in membrane distillation. J Membr Sci 376:241–246. https://doi.org/10.1016/j.memsci.2011.04.024

Dumée L, Sears K, Schütz J, Finn N, Duke M, Gray S (2012) Carbon nanotube based composite membranes for water desalination by membrane distillation. Desalin Water Treat 17:72–79. https://doi.org/10.5004/dwt.2010.1701

Efosa I, Yaolin F, Ramamoorthy M, Kimberly LJ, Vernon M (2016) Graphene oxide functionalized polyethersulfone membrane to reduce organic fouling. J Membr Sci 514:518–526. https://doi.org/10.1016/j.memsci.2016.05.024

Elimelech M, Boo C (2017) Thermal desalination membranes: carbon nanotubes keep up the heat. Nat Nanotechnol. https://doi.org/10.1038/nnano.2017.114

Esfahani MR, Jameson TL, Holly SA, Martha WJM (2015) Effects of a dual nanofiller, nano-TiO_2 and MWCNT, for polysulfone-based nanocomposite membranes for water purification. Desalination 372:47–56. https://doi.org/10.1016/j.desal.2015.06.014

Farahbakhsh J, Delnavaz M, Vatanpour V (2017) Investigation of raw and oxidized multiwalled carbon nanotubes in fabrication of reverse osmosis polyamide membranes for improvement in desalination and antifouling properties. Desalination 410:1–9. https://doi.org/10.1016/j.desal.2017.01.031

Gao F, Du X, Hao X, Li S, Zheng J, Yang Y, Han N, Guan G (2017a) A potential-controlled ion pump based on a three-dimensional PPy@GO membrane for separating dilute lead ions from wastewater. Electrochim Acta 236:434–442. https://doi.org/10.1016/j.electacta.2017.03.187

Gao F, Du X, Hao X, Li S, Zheng J, Yang Y, Han N, Guan G (2017b) Electrical double layer ion transport with cell voltage-pulse potential coupling circuit for separating dilute lead ions from wastewater. J Membr Sci 535:20–27. https://doi.org/10.1016/j.memsci.2017.04.009

Ghaemi N, Madaeni SS, Daraei P, Rajabi H, Shojaeimehr T, Rahimpour F, Shirvani B (2015) PES mixed matrix nanofiltration membrane embedded with polymer wrapped MWCNT: fabrication

and performance optimization in dye removal by RSM. J Hazard Mater 298:111–121. https://doi.org/10.1016/j.jhazmat.2015.05.018
Gin DL, Noble RD (2011) Designing the next generation of chemical separation membranes. Science 332:674–676
Goh PS, Ismail AF (2018) A review on inorganic membranes for desalination and wastewater treatment. Desalination 434:60–80. https://doi.org/10.1016/j.desal.2017.07.023
Goh K, Karahan HE, Wei L, Bae TH, Fane AG, Wang R, Chen Y (2016) Carbon nanomaterials for advancing separation membranes: a strategic perspective. Carbon 109:694–710. https://doi.org/10.1016/j.carbon.2016.08.077
Gu J, Gu H, Zhang Q, Zhao Y, Li N, Xiong J (2018) Sandwich-structured composite fibrous membranes with tunable porous structure for waterproof, breathable, and oil-water separation applications. J Colloid Interf Sci 514:386–395. https://doi.org/10.1016/j.jcis.2017.12.032
Guo J, Zhang Q, Cai Z, Zhao K (2016) Preparation and dye filtration property of electrospun polyhydroxybutyrate–calcium alginate/carbon nanotubes composite nanofibrous filtration membrane. Sep Purif Technol 161:69–79. https://doi.org/10.1016/j.seppur.2016.01.036
Gupta VK, Kumar R, Nayak A, Saleh TA, Barakat MA (2013) Adsorptive removal of dyes from aqueous solution onto carbon nanotubes: a review. Adv Colloid Interface Sci 193–194:24–34. https://doi.org/10.1016/j.cis.2013.03.003
Hamm JBS, Griebeler JG, Marcilio NR, Tessaro IC, Pollo LD (2017) Recent advances in the development of supported carbon membranes for gas separation. Int J Hydrogen Energ 42:24830–24845. https://doi.org/10.1016/j.ijhydene.2017.08.071
Han C, Mao X, Xiang Q, Guan J (2017) Preparation and characterization of 3D nano Fe_2O_3–TiO_2@activated carbon fiber membrane for waste water treatment. J Nanosci Nanotechnol 17:5327–5334. https://doi.org/10.1166/jnn.2017.13811
Hayat K, Menhas S, Bundschuh J, Chaudhary HJ (2017) Microbial biotechnology as an emerging industrial wastewater treatment process for arsenic mitigation: a critical review. J Clean Prod 151:427–438. https://doi.org/10.1016/j.jclepro.2017.03.084
He L, Dumée LF, Feng C, Velleman L, Reis R, She F, Gao W, Kong L (2015) Promoted water transport across graphene oxide–poly(amide) thin film composite membranes and their antibacterial activity. Desalination 365:126–135. https://doi.org/10.1016/j.desal.2015.02.032
Ho KC, Teow YH, Ang WL, Mohammad AW (2017) Novel GO/OMWCNTs mixed-matrix membrane with enhanced antifouling property for palm oil mill effluent treatment. Sep Purif Technol 177:337–349. https://doi.org/10.1016/j.seppur.2017.01.014
Ho KC, Teow YH, Mohammad AW, Ang WL, Lee PH (2018) Development of graphene oxide (GO)/multi-walled carbon nanotubes (MWCNTs) nanocomposite conductive membranes for electrically enhanced fouling mitigation. J Membr Sci 552:189–201. https://doi.org/10.1016/j.memsci.2018.02.001
Holt JK, Noy A, Huser T, Eaglesham D, Bakajin O (2004) Fabrication of a carbon nanotube-embedded silicon nitride membrane for studies of nanometer-scale mass transport. J Am Chem Soc 4:2245–2250
Hsieh C, Hsu J, Hsu H, Lin W, Juang R (2016) Hierarchical oil–water separation membrane using carbon fabrics decorated with carbon nanotubes. Surf Coat Technol 286:148–154. https://doi.org/10.1016/j.surfcoat.2015.12.035
Hu M, Mi B (2013) Enabling graphene oxide nanosheets as water separation membranes. Environ Sci Technol 47:3715–3723. https://doi.org/10.1021/es400571g
Hu X, Yu Y, Zhou J, Wang Y, Liang J, Zhang X, Chang Q, Song L (2015) The improved oil/water separation performance of graphene oxide modified Al_2O_3 microfiltration membrane. J Membrane Sci 476:200–204. https://doi.org/10.1016/j.memsci.2014.11.043
Huang Y, Li H, Wang L, Qiao Y, Tang C, Jung C, Yoon Y, Li S, Yu M (2015) Ultrafiltration membranes with structure-optimized graphene-oxide coatings for antifouling oil/water separation. Adv Mater Interfaces 2:1400433. https://doi.org/10.1002/admi.201400433

Ihsanullah (2019) Carbon nanotube membranes for water purification: Developments, challenges, and prospects for the future. Sep Purif Technol 209:307–337. https://doi.org/10.1016/j.seppur.2018.07.043

Ihsanullah LT, Al-Amer AM, Khalil AB, Abbas A, Khraisheh M, Atieh MA (2015) Novel anti-microbial membrane for desalination pretreatment: a silver nanoparticle-doped carbon nanotube membrane. Desalination 376:82–93. https://doi.org/10.1016/j.desal.2015.08.017

Ihsanullah, Al Amer AM, Laoui T, Abbas A, Al-Aqeeli N, Patel F, Khraisheh M, Atieh MA, Hilal N (2016) Fabrication and antifouling behaviour of a carbon nanotube membrane. Mater Des 89:549–558. https://doi.org/10.1016/j.matdes.2015.10.018

Inagaki M, Kang F, Toyoda M, Konno H (2014) Nanoporous carbon membranes and webs. In: Advanced materials science and engineering of carbon, pp 215–236. https://doi.org/10.1016/B978-0-12-407789-8.00010-7

Jacangelo JG, Laîné JM, Cummings EW, Adham SS (1995) UF with pretreatment for removing DBP precursors. J Am Water Works Assoc 87:100–112

Jaria G, Calisto V, Silva CP, Gil MV, Otero M, Esteves VI (2018) Obtaining granular activated carbon from paper mill sludge – a challenge for application in the removal of pharmaceuticals from wastewater. Sci Total Environ 653:393–400. https://doi.org/10.1016/j.scitotenv.2018.10.346

Jia S, Han H, Hou H, Zhuang H, Fang F, Zhao Q (2014) Treatment of coal gasification wastewater by membrane bioreactor hybrid powdered activated carbon (MBR-PAC) system. Chemosphere 117:753–759. https://doi.org/10.1016/j.chemosphere.2014.09.085

Jiang Y, Biswas P, Fortner JD (2016) A review of recent developments in graphene-enabled membranes for water treatment. Environ Sci-Water Res 2:915–922. https://doi.org/10.1039/c6ew00187d

Jiao W, Luo S, He Z, Liu Y (2017) Applications of high gravity technologies for wastewater treatment: a review. Chem Eng J 313:912–927. https://doi.org/10.1016/j.cej.2016.10.125

Joshi RK, Carbone P, Wang FC, Kravets VG, Su Y, Grigorieva WHA IV, Geim AK, Nair RR (2014) Precise and ultrafast molecular sieving through graphene oxide membranes. Science 343:752–754. https://doi.org/10.1126/science.1245711

Kabiri S, Tran DNH, Cole MA, Losic D (2016) Functionalized three-dimensional (3D) graphene composite for high efficiency removal of mercury. Environ Sci-Water Res 2:390–402. https://doi.org/10.1039/c5ew00254k

Kaminska G, Bohdziewicz J, Calvo JI, Prádanos P, Palacio L, Hernández A (2015) Fabrication and characterization of polyethersulfone nanocomposite membranes for the removal of endocrine disrupting micropollutants from wastewater. Mechanisms and performance. J Membr Sci 493:66–79. https://doi.org/10.1016/j.memsci.2015.05.047

Kang S, Pinault M, Pfefferle LD, Elimelech M (2007) Single-walled carbon nanotubes exhibit strong antimicrobial activity. Langmuir 23:8670–8673

Karelid V, Larsson G, Bjorlenius B (2017) Pilot-scale removal of pharmaceuticals in municipal wastewater: comparison of granular and powdered activated carbon treatment at three wastewater treatment plants. J Environ Manag 193:491–502. https://doi.org/10.1016/j.jenvman.2017.02.042

Khalid A, Al-Juhani AA, Al-Hamouz OC, Laoui T, Khan Z, Atieh MA (2015) Preparation and properties of nanocomposite polysulfone/multi-walled carbon nanotubes membranes for desalination. Desalination 367:134–144. https://doi.org/10.1016/j.desal.2015.04.001

Kim E, Hwang G, Gamal El-Din M, Liu Y (2012) Development of nanosilver and multi-walled carbon nanotubes thin-film nanocomposite membrane for enhanced water treatment. J Membr Sci 394–395:37–48. https://doi.org/10.1016/j.memsci.2011.11.041

Kim E, Liu Y, Gamal El-Din M (2013) An in-situ integrated system of carbon nanotubes nanocomposite membrane for oil sands process-affected water treatment. J Membr Sci 429:418–427. https://doi.org/10.1016/j.memsci.2012.11.077

Kim HJ, Choi K, Baek Y, Kim DG, Shim J, Yoon J, Lee JC (2014) High-performance reverse osmosis CNT/polyamide nanocomposite membrane by controlled interfacial interactions. ACS Appl Mater Interfaces 6:2819–2829. https://doi.org/10.1021/am405398f

Kiran SA, Thuyavan YL, Arthanareeswaran G, Matsuura TAF, Ismail AF (2015) Impact of graphene oxide embedded polyethersulfone membranes for the effective treatment of distillery effluent. Chem Eng J 286:528–537. https://doi.org/10.1016/j.cej.2015.10.091

Kochameshki MG, Marjani A, Mahmoudian M, Farhadi K (2017) Grafting of diallyldimethylammonium chloride on graphene oxide by RAFT polymerization for modification of nanocomposite polysulfone membranes using in water treatment. Chem Eng J 309:206–221. https://doi.org/10.1016/j.cej.2016.10.008

Lai GS, Lau WJ, Goh PS, Ismail AF, Yusof N, Tan YH (2016) Graphene oxide incorporated thin film nanocomposite nanofiltration membrane for enhanced salt removal performance. Desalination 387:14–24. https://doi.org/10.1016/j.desal.2016.03.007

Lalia BS, Ahmed FE, Shah T, Hilal N, Hashaikeh R (2015) Electrically conductive membranes based on carbon nanostructures for self-cleaning of biofouling. Desalination 360:8–12. https://doi.org/10.1016/j.desal.2015.01.006

Lau WJ, Emadzadeh D, Shahrin S, Goh PS, Ismail AF (2018) Ultrafiltration membranes incorporated with carbon-based nanomaterials for antifouling improvement and heavy metal removal. In: Carbon-based polymer nanocomposites for environmental and energy applications, pp 217–232. https://doi.org/10.1016/B978-0-12-813574-7.00009-5

Lawler J (2016) Incorporation of graphene-related carbon nanosheets in membrane fabrication for water treatment: a review. Membranes (Basel) 6. https://doi.org/10.3390/membranes6040057

Lawrence AD, Alam J, Alhoshan M (2012) Carbon nanotubes-blended poly(phenylene sulfone) membranes for ultrafiltration applications. Appl Water Sci 3:93–103. https://doi.org/10.1007/s13201-012-0063-0

Lee C, Baik S (2010) Vertically-aligned carbon nano-tube membrane filters with superhydrophobicity and superoleophilicity. Carbon 48:2192–2197. https://doi.org/10.1016/j.carbon.2010.02.020

Lee KP, Arnot TC, Mattia D (2011) A review of reverse osmosis membrane materials for desalination—development to date and future potential. J Membr Sci 370:1–22. https://doi.org/10.1016/j.memsci.2010.12.036

Lee B, Baek Y, Lee M, Jeong DH, Lee HH, Yoon J, Kim YH (2015) A carbon nanotube wall membrane for water treatment. Nat Commun 6:7109. https://doi.org/10.1038/ncomms8109

Lee J, Jeong S, Liu Z (2016a) Progress and challenges of carbon nanotube membrane in water treatment. Crit Rev Environ Sci Technol 46:999–1046. https://doi.org/10.1080/10643389.2016.1191894

Lee J, Ye Y, Ward AJ, Zhou C, Chen V, Minett AI, Lee S, Liu Z, Chae S, Shi J (2016b) High flux and high selectivity carbon nanotube composite membranes for natural organic matter removal. Sep Purif Technol 163:109–119. https://doi.org/10.1016/j.seppur.2016.02.032

Li S, Richard MC (2000) Single carbon nanotube membranes: a well-defined model for studying mass transport through nanoporous materials. J Am Chem Soc 122:12340–12345. https://doi.org/10.1021/ja002429w

Li M, Hai R, Yang L, Wang X, Li Y (2013a) Comparative study on biological carbon fiber membrane and common membrane treating sewage. Environ Sci Technol 36:126–130. (in Chinese)

Li M, Hai R, Yang L, Wang X, Li Y (2013b) Performance parameter optimization of biological carbon fiber membrane treating domestic wastewater. Environ Sci Technol 36:54–60. (in Chinese)

Li S, Liao G, Liu Z, Pan Y, Wu Q, Weng Y, Zhang X, Yang Z, Tsui OKC (2014) Enhanced water flux in vertically aligned carbon nanotube arrays and polyethersulfone composite membranes. J Mater Chem A 2:12171–12176. https://doi.org/10.1039/c4ta02119c

Li J, Kong X, Lu D, Liu Z (2015) Italicized carbon nanotube facilitating water transport: a molecular dynamics simulation. Sci Bull 60:1580–1586. https://doi.org/10.1007/s11434-015-0888-7

Li C, Song C, Tao P, Sun M, Pan Z, Wang T, Shao M (2016a) Enhanced separation performance of coal-based carbon membranes coupled with an electric field for oily wastewater treatment. Sep Purif Technol 168:47–56. https://doi.org/10.1016/j.seppur.2016.05.020

Li L, Chen M, Dong Y, Dong X, Cerneaux S, Hampshire S, Cao J, Zhu L, Zhu Z, Liu J (2016b) A low-cost alumina-mullite composite hollow fiber ceramic membrane fabricated via phase-inversion and sintering method. J Eur Ceram Soc 36:2057–2066. https://doi.org/10.1016/j.jeurceramsoc.2016.02.020

Li Y, Liu L, Yang F (2016c) High flux carbon fiber cloth membrane with thin catalyst coating integrates bio-electricity generation in wastewater treatment. J Membr Sci 505:1300–1137. https://doi.org/10.1016/j.memsci.2016.01.038

Li L, Pan Z, Yang J, Tao P, Song C, Wang C, Wang T (2017a) Carbon membranes with triple functions of adsorption/electrocatalysis/membrane separation and their preparation methods. China patent No. CN 107051218A

Li X, Zhao C, Yang M, Yang B, Hou D, Wang T (2017b) Reduced graphene oxide-NH_2 modified low pressure nanofiltration composite hollow fiber membranes with improved water flux and antifouling capabilities. Appl Surf Sci 419:418–428. https://doi.org/10.1016/j.apsusc.2017.04.080

Liang B, Zhang P, Wang J, Qu J, Wang L, Wang X, Guan C, Pan K (2016a) Membranes with selective laminar nanochannels of modified reduced graphene oxide for water purification. Carbon 103:94–100. https://doi.org/10.1016/j.carbon.2016.03.001

Liang P, Rivallin M, Cerneaux S, Lacour S, Petit E, Cretin M (2016b) Coupling cathodic Electro-Fenton reaction to membrane filtration for AO7 dye degradation: a successful feasibility study. J Membr Sci 510:182–190. https://doi.org/10.1016/j.memsci.2016.02.071

Lim MY, Choi YS, Kim J, Kim K, Shin H, Kim JJ, Shin DM, Lee JC (2017) Cross-linked graphene oxide membrane having high ion selectivity and antibacterial activity prepared using tannic acid-functionalized graphene oxide and polyethyleneimine. J Membr Sci 521:1–9. https://doi.org/10.1016/j.memsci.2016.08.067

Liu S, Zeng T, Hofmann M, Burcombe E, Wei J, Jiang R, Kong J, Chen Y (2011) Antibacterial activity of graphite, graphite oxide, graphene oxide, and reduced graphene oxide: membrane and oxidative stress. ACS Nano 5:6971–6980

Liu L, Son M, Chakraborty S, Bhattacharjee C, Choi H (2013) Fabrication of ultra-thin polyelectrolyte/carbon nanotube membrane by spray-assisted layer-by-layer technique: characterization and its anti-protein fouling properties for water treatment. Desalin Water Treat 51:6194–6200. https://doi.org/10.1080/19443994.2013.780767

Liu X, Duan J, Yang J, Huang T, Zhang N, Wang Y, Zhou Z (2015) Hydrophilicity, morphology and excellent adsorption ability of poly(vinylidene fluoride) membranes induced by graphene oxide and polyvinylpyrrolidone. Colloid Surf A 486:172–184. https://doi.org/10.1016/j.colsurfa.2015.09.036

Liu Z, Zhu M, Zhao L, Deng C, Ma J, Wang Z, Liu H, Wang H (2017) Aqueous tetracycline degradation by coal-based carbon electrocatalytic filtration membrane: Effect of nano antimony-doped tin dioxide coating. Chem Eng J 314:59–68. https://doi.org/10.1016/j.cej.2016.12.093

Liu Y, Hou C, Jiao T, Song J, Zhang X, Xing R, Zhou J, Zhang L, Peng Q (2018) Self-assembled AgNP-containing nanocomposites constructed by electrospinning as efficient dye photocatalyst materials for wastewater treatment. Nanonaterials-Basel 8:35. https://doi.org/10.1002/pat.4186

Luan H, Teychene B, Huang H (2019) Efficient removal of As(III) by Cu nanoparticles intercalated in carbon nanotube membranes for drinking water treatment. Chem Eng J 355:341–350. https://doi.org/10.1016/j.cej.2018.08.104

Ma J, Zhao Y, Xu Z, Min C, Zhou B, Li Y, Li B, Niu J (2013) Role of oxygen-containing groups on MWCNTs in enhanced separation and permeability performance for PVDF hybrid ultrafiltration membranes. Desalination 320:1–9. https://doi.org/10.1016/j.desal.2013.04.012

Ma L, Dong X, Chen M, Zhu L, Wang C, Yang F, Dong Y (2017) Fabrication and water treatment application of carbon nanotubes (CNTs)-based composite membranes: a review. Membranes (Basel) 7:16. https://doi.org/10.3390/membranes7010016

Madaeni SS, Zinadini S, Vatanpour V (2013) Preparation of superhydrophobic nanofiltration membrane by embedding multiwalled carbon nanotube and polydimethylsiloxane in pores of microfiltration membrane. Sep Purif Technol 111:98–107. https://doi.org/10.1016/j.seppur.2013.03.033

Mahdavi MR, Delnavaz M, Vatanpour V (2017) Fabrication and water desalination performance of piperazine–polyamide nanocomposite nanofiltration membranes embedded with raw and oxidized MWCNTs. J TAIWAN Inst Chem E 75:189–198. https://doi.org/10.1016/j.jtice.2017.03.039

Mahlangua OT, Nackaertsb R, Thwalac JM, Mambaa BB, Verliefdeb ARD (2016) Hydrophilic fouling-resistant GO-ZnO/PES membranes for wastewater reclamation. J Membr Sci 524:43–55. https://doi.org/10.1016/j.memsci.2016.11.018

Mainak M, Nitin C, Bruce JH (2005) Effect of tip functionalization on transport through vertically oriented carbon nanotube membranes. J Am Chem Soc 127:9062–9070

Majeed S, Fierro D, Buhr K, Wind J, Du B, Boschetti-de-Fierro A, Abetz V (2012) Multi-walled carbon nanotubes (MWCNTs) mixed polyacrylonitrile (PAN) ultrafiltration membranes. J Membr Sci 403–404:101–109. https://doi.org/10.1016/j.memsci.2012.02.029

Manawi YM, Ihsanullah SA, Al-Ansari T, Atieh MA (2018) A review of carbon nanomaterials' synthesis via the chemical vapor deposition (CVD) method. Materials (Basel) 11:882. https://doi.org/10.3390/ma11050822

Mansourpanah Y, Madaeni SS, Rahimpour A, Adeli M, Hashemi MY, Moradian MR (2011) Fabrication new PES-based mixed matrix nanocomposite membranes using polycaprolactone modified carbon nanotubes as the additive: property changes and morphological studies. Desalination 277:171–177. https://doi.org/10.1016/j.desal.2011.04.022

Masoomaa HB, Irfanc M, Woei-Jye L (2015) Acid functionalized MWCNT/PVP nanocomposite as new additive for fabrication of ultrafiltration membrane with improved anti-fouling resistance. RSC Adv 5:1–17

Matsumoto H, Tsuruoka S, Hayashi Y, Abe K, Hata K, Zhang S, Saito Y, Aiba M, Tokunaga T, Iijima T, Hayashi T, Inoue H, Amaratunga GAJ (2017) Water transport phenomena through membranes consisting of vertically-aligned double-walled carbon nanotube array. Carbon 120:358–365. https://doi.org/10.1016/j.carbon.2017.05.034

Mavukkandy MO, Zaib Q, Arafat HA (2018) CNT/PVP blend PVDF membranes for the removal of organic pollutants from simulated treated wastewater effluent. J Environ Chem Eng. https://doi.org/10.1016/j.jece.2018.10.029

Medina-Gonzalez Y, Remigy JC (2011) Sonication-assisted preparation of pristine MWCNT–polysulfone conductive microporous membranes. Mater Lett 65:229–232. https://doi.org/10.1016/j.matlet.2010.10.016

Mehwish N, Kausar A, Siddiq M (2015) High-performance polyvinylidene fluoride/poly(styrene–butadiene–styrene)/functionalized MWCNTs-SCN-Ag nanocomposite membranes. Iran Polym J 24:549–559. https://doi.org/10.1007/s13726-015-0346-z

Menachem E, William AP (2011) The future of seawater desalination: energy, technology, and the environment. Science 333:712–717

Mohammed D (2011) Activated carbons: preparations and characterizations. In: Taylor JC (ed) Adv Chem Res, pp 1–38

Mohammad P, Toraj M, Omid B (2018) Effective treatment of dye wastewater via positively charged TETA-MWCNT/PES hybrid nanofiltration membranes. Sep Purif Technol 194:488–502. https://doi.org/10.1016/j.seppur.2017.11.070

Montgomery MA, Elimelech M (2007) Water and sanitation in developing countries: including health in the equation. Environ Sci Technol 41:17–24. https://doi.org/10.1021/es072435t

Motoc S, Remes A, Pop A, Manea F, Schoonman J (2013) Electrochemical detection and degradation of ibuprofen from water on multi-walled carbon nanotubes-epoxy composite electrode. J Environ Sci 25:838–847. https://doi.org/10.1016/s1001-0742(12)60068-0

Muylaert I, Verberckmoes A, De Decker J, Van Der Voort P (2012) Ordered mesoporous phenolic resins: highly versatile and ultra stable support materials. Adv Colloid Interface 175:39–51. https://doi.org/10.1016/j.cis.2012.03.007

Nair RR, Wu HA, Jayaram PN, Grigorieva IV, Geim AK (2012) Unimpeded permeation of water through helium-leak-tight graphene-based membranes. Science 335:442–444. https://doi.org/10.1126/science.1211694

Novoselov KS, Geim AK, Morozov SV, Jiang D, Zhang Y, Dubonos SV, Grigorieva IV, Firsov AA (2004) Electric field effect in atomically thin carbon films. Science 306:666–669

O'Hern SC, Boutilier MS, Idrobo JC, Song Y, Kong J, Laoui T, Atieh M, Karnik R (2014) Selective ionic transport through tunable subnanometer pores in single-layer graphene membranes. Nano Lett 14:1234–1241. https://doi.org/10.1021/nl404118f

Ong C, Al-Anzi BS, Lau WJ (2018) Recent developments of carbon nanomaterials-incorporated membranes, carbon nanofibers and carbon membranes for oily wastewater treatment. In: Carbon-based polymer nanocomposites for environmental and energy applications, pp 261–280. https://doi.org/10.1016/C2016-0-01539-5

Ou Yang Z, Xu H, Xiong C, Huang W, Xie D, Luo B, Lv B (2013) Preparation of TiO-supported activated carbon and its application in papermaking wastewater. Adv Mater Res 791–793:7–11. https://doi.org/10.4028/www.scientific.net/AMR.791-793.7

Parimal P (2017) Water treatment by membrane-separation technology. In: Industrial water treatment process technology. Butterworth-Heinemann, Oxford, pp 173–242

Park J, Choi W, Kim SH, Chun BH, Bang J, Lee KB (2012) Enhancement of chlorine resistance in carbon nanotube based nanocomposite reverse osmosis membranes. Desalin Water Treat 15:198–204. https://doi.org/10.5004/dwt.2010.1686

Park S, Jung J, Lee S, Baek Y, Yoon J, Seo D, Kim Y (2014) Fouling and rejection behavior of carbon nanotube membranes. Desalination 343:180–186. https://doi.org/10.1016/j.desal.2013.10.005

Patino Y, Diaz E, Ordonez S, Gallegos-Suarez E, Guerrero-Ruiz A, Rodriguez-Ramos I (2015) Adsorption of emerging pollutants on functionalized multiwall carbon nanotubes. Chemosphere 136:174–180. https://doi.org/10.1016/j.chemosphere.2015.04.089

Pendergast MTM, Hoek EMV (2011) A review of water treatment membrane nanotechnologies. Energ Environ Sci 4:1946. https://doi.org/10.1039/c0ee00541j

Phao N, Nxumalo EN, Mamba BB, Mhlanga SD (2013) A nitrogen-doped carbon nanotube enhanced polyethersulfone membrane system for water treatment. Phys Chem Earth 66:148–156. https://doi.org/10.1016/j.pce.2013.09.009

Pintor AMA, Vilar VJP, Botelho CMS, Boaventura RAR (2016) Oil and grease removal from wastewaters: sorption treatment as an alternative to state-of-the-art technologies. A critical review. Chem Eng J 297:229–255. https://doi.org/10.1016/j.cej.2016.03.121

Qin S, Liu X, Zhuo R, Zhang X (2012) Microstructure-controllable graphene oxide hydrogel film based on a pH-responsive graphene oxide hydrogel. Macromol Chem Phys 213:2044–2051. https://doi.org/10.1002/macp.201200281

Qiu S, Wu L, Pan X, Zhang L, Chen H, Gao C (2009) Preparation and properties of functionalized carbon nanotube/PSF blend ultrafiltration membranes. J Membr Sci 342:165–172. https://doi.org/10.1016/j.memsci.2009.06.041

Qiu L, Zhang X, Yang W, Wang Y, Simon GP, Li D (2011) Controllable corrugation of chemically converted graphene sheets in water and potential application for nanofiltration. Chem Commun (Camb) 47:5810–5812. https://doi.org/10.1039/c1cc10720h

Rahimpour A, Jahanshahi M, Khalili S, Mollahosseini A, Zirepour A, Rajaeian B (2012) Novel functionalized carbon nanotubes for improving the surface properties and performance of polyethersulfone (PES) membrane. Desalination 286:99–107. https://doi.org/10.1016/j.desal.2011.10.039

Ren X, Chen C, Nagatsu M, Wang X (2011) Carbon nanotubes as adsorbents in environmental pollution management: a review. Chem Eng J 170:395–410. https://doi.org/10.1016/j.cej.2010.08.045
Roy S, Ntim SA, Mitra S, Sirkar KK (2011) Facile fabrication of superior nanofiltration membranes from interfacially polymerized CNT-polymer composites. J Membr Sci 375:81–87. https://doi.org/10.1016/j.memsci.2011.03.012
Saadati J, Pakizeh M (2017) Separation of oil/water emulsion using a new PSf/pebax/F-MWCNT nanocomposite membrane. J TAIWAN Inst Chem E 71:265–276. https://doi.org/10.1016/j.jtice.2016.12.024
Safarpour M, Khataee A, Vatanpour V (2015a) Thin film nanocomposite reverse osmosis membrane modified by reduced graphene oxide/TiO_2 with improved desalination performance. J Membr Sci 489:43–54. https://doi.org/10.1016/j.memsci.2015.04.010
Safarpour M, Vatanpour V, Khataee A, Esmaeili M (2015b) Development of a novel high flux and fouling-resistant thin film composite nanofiltration membrane by embedding reduced graphene oxide/TiO_2. Sep Purif Technol 154:96–107. https://doi.org/10.1016/j.seppur.2015.09.039
Salehi E, Madaeni SS, Rajabi L, Vatanpour V, Derakhshan AA, Zinadini S, Ghorabi S, Ahmadi Monfared H (2012) Novel chitosan/poly(vinyl) alcohol thin adsorptive membranes modified with amino functionalized multi-walled carbon nanotubes for Cu(II) removal from water: preparation, characterization, adsorption kinetics and thermodynamics. Sep Purif Technol 89:309–319. https://doi.org/10.1016/j.seppur.2012.02.002
Salgot M, Folch M (2018) Wastewater treatment and water reuse. Curr Opin Environ Sci Health 2:64–74. https://doi.org/10.1016/j.coesh.2018.03.005
Santosh V, Gopinath J, Babu PV, Sainath AVS, Reddy AVR (2018) Acetyl-d-glucopyranoside functionalized carbon nanotubes for the development of high performance ultrafiltration membranes. Sep Purif Technol 191:134–143. https://doi.org/10.1016/j.seppur.2017.09.018
Saranya R, Arthanareeswaran G, Dionysiou DD (2014) Treatment of paper mill effluent using Polyethersulfone/functionalised multiwalled carbon nanotubes based nanocomposite membranes. Chem Eng J 236:369–377. https://doi.org/10.1016/j.cej.2013.09.096
Sears K, Dumée L, Schütz J, She M, Huynh C, Hawkins S, Duke M, Gray S (2010) Recent developments in carbon nanotube membranes for water purification and gas separation. Materials 3:127–149. https://doi.org/10.3390/ma3010127
Shah P, Murthy CN (2013) Studies on the porosity control of MWCNT/polysulfone composite membrane and its effect on metal removal. J Membr Sci 437:90–98. https://doi.org/10.1016/j.memsci.2013.02.042
Shahbabaei M, Tang D, Kim D (2017) Simulation insight into water transport mechanisms through multilayer graphene-based membrane. Comput Mater Sci 128:87–97. https://doi.org/10.1016/j.commatsci.2016.10.044
Shao L, Cheng X, Wang Z, Ma J, Guo Z (2014) Tuning the performance of polypyrrole-based solvent-resistant composite nanofiltration membranes by optimizing polymerization conditions and incorporating graphene oxide. J Membr Sci 452:82–89. https://doi.org/10.1016/j.memsci.2013.10.021
Shawky HA, Chae S, Lin S, Wiesner MR (2011) Synthesis and characterization of a carbon nanotube/polymer nanocomposite membrane for water treatment. Desalination 272:46–50. https://doi.org/10.1016/j.desal.2010.12.051
Shen J, Yu C, Ruan H, Gao C, Van der Bruggen B (2013) Preparation and characterization of thin-film nanocomposite membranes embedded with poly(methyl methacrylate) hydrophobic modified multiwalled carbon nanotubes by interfacial polymerization. J Membr Sci 442:18–26. https://doi.org/10.1016/j.memsci.2013.04.018
Shen X, Song L, Luo L, Zhang Y, Zhu B, Liu J, Chen Z, Zhang L (2018) Preparation of TiO_2/C_3N_4 heterojunctions on carbon-fiber cloth as efficient filter-membrane-shaped photocatalyst for removing various pollutants from the flowing wastewater. J Colloid Interfac Sci 532:798–807. https://doi.org/10.1016/j.jcis.2018.08.028

Shimpei G, Tomio A, Fumio M, Kunio M, Sugio O (1986) Process for the preparation of carbon fibers. Carbon 24:II patent No. 4554148 https://doi.org/10.1016/0008-6223(86)90196-X

Singh R, Hankins NP (2016) Introduction to membrane processes for water treatment. In: Emerging membrane technology for sustainable water treatment. LLC, Colorado Springs, pp 15–52

Sitko R, Musielak M, Zawisza B, Talik E, Gagor A (2016) Graphene oxide/cellulose membranes in adsorption of divalent metal ions. RSC Adv 6:96595–96605. https://doi.org/10.1039/c6ra21432k

Song C, Wang T, Pan Y, Qiu J (2006) Preparation of coal-based microfiltration carbon membrane and application in oily wastewater treatment. Sep Purif Technol 51:80–84. https://doi.org/10.1016/j.seppur.2005.12.026

Song Y, Wang DK, Birkett G, Smart S, Diniz da Costa JC (2017) Vacuum film etching effect of carbon alumina mixed matrix membranes. J Membr Sci 541:53–61. https://doi.org/10.1016/j.memsci.2017.06.082

Stankovich S, Dikin DA, Piner RD, Kohlhaas KA, Kleinhammes A, Jia Y, Wu Y, Nguyen ST, Ruoff RS (2007) Synthesis of graphene-based nanosheets via chemical reduction of exfoliated graphite oxide. Carbon 45:1558–1565. https://doi.org/10.1016/j.carbon.2007.02.034

Sumio Iijima (1991) Helical microtubules of graphitic carbon. Nature 354:56–58. https://doi.org/10.1038/354056a0

Sun P, Wang K, Wei J, Zhong M, Wu D, Zhu H (2014a) Effective recovery of acids from iron-based electrolytes using graphene oxide membrane filters. J Mater Chem A 2:7734–7737. https://doi.org/10.1039/c4ta00668b

Sun P, Zheng F, Zhu M, Wang K, Zhong M, Wu D, Zhu H (2014b) Realizing synchronous energy harvesting and ion separation with graphene oxide membranes. Sci Rep-UK 4:5528. https://doi.org/10.1038/srep05528

Sun X, Qin J, Xia P, Guo B, Yang C, Song C, Wang S (2015) Graphene oxide–silver nanoparticle membrane for biofouling control and water purification. Chem Eng J 281:53–59. https://doi.org/10.1016/j.cej.2015.06.059

Sun M, Feng G, Zhang M, Song C, Tao P, Wang T, Shao M (2018) Enhanced removal ability of phenol from aqueous solution using coal-based carbon membrane coupled with electrochemical oxidation process. Colloid Surf A 540:186–193. https://doi.org/10.1016/j.colsurfa.2018.01.006

Tahri N, Jedidi I, Ayadi S, Cerneaux S, Cretin M, Ben Amar R (2016) Preparation of an asymmetric microporous carbon membrane for ultrafiltration separation: application to the treatment of industrial dyeing effluent. Desalin Water Treat 57:23473–23488. https://doi.org/10.1080/19443994.2015.1135826

Tai MH, Gao P, Tan BY, Sun DD, Leckie JO (2014) Highly efficient and flexible electrospun carbon-silica nanofibrous membrane for ultrafast gravity-driven oil-water separation. ACS Appl Mater Inter 6:9393–9401. https://doi.org/10.1021/am501758c

Tao P, Xu Y, Zhou Y, Song C, Shao M, Wang T (2017a) Coal-based carbon membrane coupled with electrochemical oxidation process for the enhanced microalgae removal from simulated ballast water. Water Air Soil Pollut 228. https://doi.org/10.1007/s11270-017-3608-x

Tao P, Xu Y, Song C, Yin Y, Yang Z, Wen S, Wang S, Liu H, Li S, Li C, Wang T, Shao M (2017b) A novel strategy for the removal of rhodamine B (RhB) dye from wastewater by coal-based carbon membranes coupled with the electric field. Sep Purif Technol 179:175–183. https://doi.org/10.1016/j.seppur.2017.02.014

Thakur VK, Voicu SI (2016) Recent advances in cellulose and chitosan based membranes for water purification: a concise review. Carbohyd Polym 146:148–165. https://doi.org/10.1016/j.carbpol.2016.03.030

Thines RK, Mubarak NM, Nizamuddin S, Sahu JN, Abdullah EC, Ganesan P (2017) Application potential of carbon nanomaterials in water and wastewater treatment: a review. J TAIWAN Inst Chem E 72:116–133. https://doi.org/10.1016/j.jtice.2017.01.018

Thiruvenkatachari R, Shim W, Lee J, Aim R, Moon H (2006) A novel method of powdered activated carbon (PAC) pre-coated microfiltration (MF) hollow fiber hybrid membrane for

domestic wastewater treatment. Colloid Surf A 274:24–33. https://doi.org/10.1016/j.colsurfa.2005.08.026
Tian M, Wang Y, Wang R (2015) Synthesis and characterization of novel high-performance thin film nanocomposite (TFN) FO membranes with nanofibrous substrate reinforced by functionalized carbon nanotubes. Desalination 370:79–86. https://doi.org/10.1016/j.desal.2015.05.016
Vatanpour V, Safarpour M (2018) Carbon-based polymer nanocomposite membranes for desalination. In: Carbon-based polymer nanocomposites for environmental and energy applications, pp 281–304. https://doi.org/10.1016/C2016-0-01539-5
Vatanpour V, Madaeni SS, Moradian R, Zinadini S, Astinchap B (2011) Fabrication and characterization of novel antifouling nanofiltration membrane prepared from oxidized multiwalled carbon nanotube/polyethersulfone nanocomposite. J Membr Sci 375:284–294. https://doi.org/10.1016/j.memsci.2011.03.055
Vatanpour V, Madaeni SS, Moradian R, Zinadini S, Astinchap B (2012) Novel antibifouling nanofiltration polyethersulfone membrane fabricated from embedding TiO_2 coated multiwalled carbon nanotubes. Sep Purif Technol 90:69–82. https://doi.org/10.1016/j.seppur.2012.02.014
Vatanpour V, Esmaeili M, Farahani MHDA (2014) Fouling reduction and retention increment of polyethersulfone nanofiltration membranes embedded by amine-functionalized multi-walled carbon nanotubes. J Membr Sci 466:70–81. https://doi.org/10.1016/j.memsci.2014.04.031
Vijwani H, Nadagouda MN, Mukhopadhyay SM (2018) Robust nanocatalyst membranes for degradation of atrazine in water. J Water Process Eng 25:15–21. https://doi.org/10.1016/j.jwpe.2018.05.016
Wan Azelee I, Goh PS, Lau WJ, Ismail AF (2018) Facile acid treatment of multiwalled carbon nanotube-titania nanotube thin film nanocomposite membrane for reverse osmosis desalination. J Clean Prod 181:517–526. https://doi.org/10.1016/j.jclepro.2018.01.212
Wang N, Ji S, Zhang G, Li J, Wang L (2012) Self-assembly of graphene oxide and polyelectrolyte complex nanohybrid membranes for nanofiltration and pervaporation. Chem Eng J 213:318–329. https://doi.org/10.1016/j.cej.2012.09.080
Wang H, Guan Q, Li J, Wang T (2014) Phenolic wastewater treatment by an electrocatalytic membrane reactor. Catal Today 236:121–126. https://doi.org/10.1016/j.cattod.2014.05.003
Wang L, Song X, Wang T, Wang S, Wang Z, Gao C (2015a) Fabrication and characterization of polyethersulfone/carbon nanotubes (PES/CNTs) based mixed matrix membranes (MMMs) for nanofiltration application. Appl Surf Sci 330:118–125. https://doi.org/10.1016/j.apsusc.2014.12.183
Wang W, Shi J, Wang J, Li Y, Gao N, Liu Z, Lian W (2015b) Preparation and characterization of PEG-g-MWCNTs/PSf nano-hybrid membranes with hydrophilicity and antifouling properties. RSC Adv 5:84746–84753. https://doi.org/10.1039/c5ra16077d
Wang J, Zhang P, Liang B, Liu Y, Xu T, Wang L, Cao B, Pan K (2016a) Graphene oxide as an effective barrier on a porous nanofibrous membrane for water treatment. Acs Appl Mater Inter 8:6211–6218. https://doi.org/10.1021/acsami.5b12723
Wang L, Wang N, Li J, Li J, Bian W, Ji S (2016b) Layer-by-layer self-assembly of polycation/GO nanofiltration membrane with enhanced stability and fouling resistance. Sep Purif Technol 160:123–131. https://doi.org/10.1016/j.seppur.2016.01.024
Wang J, Huang T, Zhang L, Yu QJ, Hou L (2018a) Dopamine crosslinked graphene oxide membrane for simultaneous removal of organic pollutants and trace heavy metals from aqueous solution. Environ Technol 39:3055–3065. https://doi.org/10.1080/09593330.2017.1371797
Wang P, Deng Y, Hao L, Zhao L, Zhang X, Deng C, Liu H, Zhu M (2018b) Continuous efficient removal and inactivation mechanism of E. coli by bismuth doped SnO_2/C electrocatalytic membrane. Environ Sci Pollut Res 26(11):11399–11409
Wei G, Quan X, Chen S, Yu H (2017a) Superpermeable atomic-thin graphene membranes with high selectivity. ACS Nano 11:1920–1926. https://doi.org/10.1021/acsnano.6b08000

Wei G, Quan X, Fan X, Chen S, Zhang Y (2017b) Carbon-nanotube-based sandwich-like hollow fiber membranes for expanded microcystin-LR removal applications. Chem Eng J 319:212–218. https://doi.org/10.1016/j.cej.2017.02.125

Wei Y, Zhang Y, Gao X, Ma Z, Wang X, Gao C (2018) Multilayered graphene oxide membrane for water treatment: a review. Carbon 139:964–981. https://doi.org/10.1016/j.carbon.2018.07.040

Whitby M, Quirk N (2007) Fluid flow in carbon nanotubes and nanopipes. Nat Nanotechnol 2:87–94. https://doi.org/10.1038/nnano.2006.175

Wilson R, George G, Jose AJ (2018) Polymer membranes reinforced with carbon-based nanomaterials for water purification. In: New polymer nanocomposites for environmental remediation, pp 457–468. https://doi.org/10.1016/C2016-0-00649-6

Wu H, Tang B, Wu P (2010a) Novel ultrafiltration membranes prepared from a multi-walled carbon nanotubes/polymer composite. J Membr Sci 362:374–383. https://doi.org/10.1016/j.memsci.2010.06.064

Wu H, Tang B, Wu P (2010b) MWNTs/polyester thin film nanocomposite membrane: an approach to overcome the trade-off effect between permeability and selectivity. J Phys Chem C 114:16395–16400. https://doi.org/10.1021/jp107280m

Wu Q, Zhu W, Zhang C, Liang Z, Wang B (2010c) Study of fire retardant behavior of carbon nanotube membranes and carbon nanofiber paper in carbon fiber reinforced epoxy composites. Carbon 48:1799–1806. https://doi.org/10.1016/j.carbon.2010.01.023

Wu H, Tang B, Wu P (2013) Optimization, characterization and nanofiltration properties test of MWNTs/polyester thin film nanocomposite membrane. J Membr Sci 428:425–433. https://doi.org/10.1016/j.memsci.2012.10.042

Wu B, Li X, An D, Zhao S, Wang Y (2014) Electro-casting aligned MWCNTs/polystyrene composite membranes for enhanced gas separation performance. J Membr Sci 462:62–68. https://doi.org/10.1016/j.memsci.2014.03.015

Wu Y, Zhang X, Liu S, Zhang B, Lu Y, Wang T (2016) Preparation and applications of microfiltration carbon membranes for the purification of oily wastewater. Sep Sci Technol 51:1872–1880. https://doi.org/10.1080/01496395.2016.1187169

Xiao L, Jing N, Shi X, Yan L, Xin Z, Hai N (2016) Research process of new material carbon fiber in water treatment applications. J Environ Eng 10:1577–1587. (in Chinese)

Xiao F, Tian Y, Peng F, Li S, Jian S, Zhi G (2017) Growth of C_3N_4 nanosheets on carbon-fiber cloth as flexible and macroscale filter-membrane-shaped photocatalyst for degrading the flowing wastewater. Appl Catal B-Environ 219:425–431. https://doi.org/10.1016/j.apcatb.2017.07.059

Xing R, Wang W, Jiao T, Ma K, Zhang Q, Hong W, Qiu H, Zhou J, Zhang L, Peng Q (2017) Bioinspired polydopamine sheathed nanofibers containing carboxylate graphene oxide nanosheet for high-efficient dyes scavenger. ACS Sustain Chem Eng 5:4948–4956. https://doi.org/10.1021/acssuschemeng.7b00343

Xu D, Luo Y (2012) The application of carbon fiber in harness of water environment- new task in 21th century. Hi-Tech Fiber Appl 37:49–56. (in Chinese)

Xu W, Fang C, Zhou F, Song Z, Liu Q, Qiao R, Yu M (2017a) Self-assembly: a facile way of forming ultrathin, high-performance graphene oxide membranes for water purification. Nano Lett 17:2928–2933. https://doi.org/10.1021/acs.nanolett.7b00148

Xu Z, Li X, Teng K, Zhou B, Ma M, Shan M, Jiao K, Qian X, Fan J (2017b) High flux and rejection of hierarchical composite membranes based on carbon nanotube network and ultrathin electrospun nanofibrous layer for dye removal. J Membr Sci 535:94–102. https://doi.org/10.1016/j.memsci.2017.04.029

Yanez HJ, Wang Z, Lege S, Obst M, Roehler S, Burkhardt CJ, Zwiener C (2017) Application and characterization of electroactive membranes based on carbon nanotubes and zerovalent iron nanoparticles. Water Res 108:78–85. https://doi.org/10.1016/j.watres.2016.10.055

Yang GCC, Tsai CM (2008) Preparation of carbon fibers/carbon/alumina tubular composite membranes and their applications in treating Cu-CMP wastewater by a novel electrochemical process. J Membr Sci 321. https://doi.org/10.1016/j.memsci.2008.04.060

Yang GCC, Tsai CM (2009) Preparation of carbon fibers/carbon/alumina tubular composite membranes and their applications in treating Cu-CMP wastewater by a novel electrochemical process: Part 2. J Membr Sci 331:100–108. https://doi.org/10.1016/j.memsci.2009.01.021

Yang Y, Li J, Wang H, Song X, Wang T, He B, Liang X, Ngo HH (2011) An electrocatalytic membrane reactor with self-cleaning function for industrial wastewater treatment. Angew Chem Int Ed 50:2148–2150. https://doi.org/10.1002/anie.201005941

Yang X, Lee J, Yuan L, Chae S, Peterson VK, Minett AI, Yin Y, Harris AT (2013) Removal of natural organic matter in water using functionalised carbon nanotube buckypaper. Carbon 59:160–166. https://doi.org/10.1016/j.carbon.2013.03.005

Yi H, Zhen X, Chao G (2013) Ultrathin graphene nanofiltration membrane for water purification. Adv Funct Mater 23:3693–3700. https://doi.org/10.1002/adfm.201202601

Yi G, Chen S, Quan X, Wei G, Fan X, Yu H (2018) Enhanced separation performance of carbon nanotube–polyvinyl alcohol composite membranes for emulsified oily wastewater treatment under electrical assistance. Sep Purif Technol 197:107–115. https://doi.org/10.1016/j.seppur.2017.12.058

Yin J, Zhu G, Deng B (2013) Multi-walled carbon nanotubes (MWNTs)/polysulfone (PSU) mixed matrix hollow fiber membranes for enhanced water treatment. J Membr Sci 437:237–248. https://doi.org/10.1016/j.memsci.2013.03.021

Yin Y, Li C, Song C, Tao P, Sun M, Pan Z, Wang T, Shao M (2016) The design of coal-based carbon membrane coupled with the electric field and its application on the treatment of malachite green (MG) aqueous solution. Colloid Surf A 506:629–636. https://doi.org/10.1016/j.colsurfa.2016.07.038

You H, Li X, Yang Y, Wang B, Li Z, Wang X, Zhu M, Hsiao BS (2013) High flux low pressure thin film nanocomposite ultrafiltration membranes based on nanofibrous substrates. Sep Purif Technol 108:143–151. https://doi.org/10.1016/j.seppur.2013.02.014

Yu C, Yu H, Chu Y, Ruan H, Shen J (2013) Preparation thin film nanocomposite membrane incorporating PMMA modified MWNT for nanofiltration. Key Eng Mater 562-565:882–886. https://doi.org/10.4028/www.scientific.net/KEM.562-565.882

Yu JG, Zhao XH, Yang H, Chen XH, Yang Q, Yu LY, Jiang JH, Chen XQ (2014) Aqueous adsorption and removal of organic contaminants by carbon nanotubes. Sci Total Environ 482–483:241–251. https://doi.org/10.1016/j.scitotenv.2014.02.129

Yuan Y, Gao X, Wei Y, Wang X, Wang J, Zhang Y, Gao C (2017) Enhanced desalination performance of carboxyl functionalized graphene oxide nanofiltration membranes. Desalination 405:29–39. https://doi.org/10.1016/j.desal.2016.11.024

Yue X, Yang D, Qiu F, Zhu Y, Fang J (2018) In situ fabrication dynamic carbon fabrics membrane with tunable wettability for selective oil–water separation. J Ind Eng Chem 61:188–196. https://doi.org/10.1016/j.jiec.2017.12.016

Yvonne LFM, Catherine MS, Maria Lourdes PD, Debora FR (2014) Surface modification of membrane filters using graphene and graphene oxide-based nanomaterials for bacterial inactivation and removal. ACS Sustain Chem Eng. https://doi.org/10.1021/sc500044p

Zarrabi H, Yekavalangi ME, Vatanpour V, Shockravi A, Safarpour M (2016) Improvement in desalination performance of thin film nanocomposite nanofiltration membrane using amine-functionalized multiwalled carbon nanotube. Desalination 394:83–90. https://doi.org/10.1016/j.desal.2016.05.002

Zhang L, Shi G, Qiu S, Cheng L, Chen H (2011) Preparation of high-flux thin film nanocomposite reverse osmosis membranes by incorporating functionalized multi-walled carbon nanotubes. Desalin Water Treat 34:19–24. https://doi.org/10.5004/dwt.2011.2801

Zhang J, Xu Z, Shan M, Zhou B, Li Y, Li B, Niu J, Qian X (2013) Synergetic effects of oxidized carbon nanotubes and graphene oxide on fouling control and anti-fouling mechanism of polyvinylidene fluoride ultrafiltration membranes. J Membr Sci 448:81–92. https://doi.org/10.1016/j.memsci.2013.07.064

Zhang Y, Sui Z, Chung TS (2015) Nanometric graphene oxide framework membranes with enhanced heavy metal removal via nanofiltration. Environ Sci Technol 49:10235–10242

Zhang C, Wei K, Zhang W, Bai Y, Sun Y, Gu J (2017a) Graphene oxide quantum dots Incorporated into a thin film nanocomposite membrane with high flux and antifouling properties for

low-pressure nanofiltration. ACS Appl Mater Interfaces 9:11082–11094. https://doi.org/10.1021/acsami.6b12826
Zhang H, Bin L, Pan J, Qi Y, Shen J, Gao C, Van der Bruggen B (2017b) Carboxyl-functionalized graphene oxide polyamide nanofiltration membrane for desalination of dye solutions containing monovalent salt. J Membr Sci 539:128–137. https://doi.org/10.1016/j.memsci.2017.05.075
Zhang J, Xue Q, Pan X, Lu W, Ding D, Guo Q (2017c) Graphene oxide/polyacrylonitrile fiber hierarchical-structured membrane for ultra-fast microfiltration of oil-water emulsion. Chem Eng J 307:643–649. https://doi.org/10.1016/j.cej.2016.08.124
Zhang Y, Wei S, Hu Y, Sun S (2018) Membrane technology in wastewater treatment enhanced by functional nanomaterials. J Clean Prod 197:339–348. https://doi.org/10.1016/j.jclepro.2018.06.211
Zhao X, Ma J, Wang Z, Wen G, Jiang J, Shi F, Sheng L (2012) Hyperbranched-polymer functionalized multi-walled carbon nanotubes for poly (vinylidene fluoride) membranes: from dispersion to blended fouling-control membrane. Desalination 303:29–38. https://doi.org/10.1016/j.desal.2012.07.009
Zhao H, Yu H, Chang H, Quan X, Chen S (2013a) CNTs–TiO_2/Al_2O_3 composite membrane with a photocatalytic function: fabrication and energetic performance in water treatment. Sep Purif Technol 116:360–365. https://doi.org/10.1016/j.seppur.2013.06.007
Zhao Y, Xu Z, Shan M, Min C, Zhou B, Li Y, Li B, Liu L, Qian X (2013b) Effect of graphite oxide and multi-walled carbon nanotubes on the microstructure and performance of PVDF membranes. Sep Purif Technol 103:78–83. https://doi.org/10.1016/j.seppur.2012.10.012
Zhao H, Qiu S, Wu L, Zhang L, Chen H, Gao C (2014) Improving the performance of polyamide reverse osmosis membrane by incorporation of modified multi-walled carbon nanotubes. J Membr Sci 450:249–256. https://doi.org/10.1016/j.memsci.2013.09.014
Zhao X, Su Y, Liu Y, Li Y, Jiang Z (2016) Free-standing graphene oxide-palygorskite nanohybrid membrane for oil/water separation. ACS Appl Mater Interfaces 8:8247–8256. https://doi.org/10.1021/acsami.5b12876
Zhao W, Liang Y, Wu Y, Wang D, Zhang B (2018) Removal of phenol and phosphoric acid from wastewater by microfiltration carbon membranes. Chem Eng Commun 205:1432–1441. https://doi.org/10.1080/00986445.2018.1457027
Zheng X, Zhang Z, Yu D, Chen X, Cheng R, Min S, Wang J, Xiao Q, Wang J (2015) Overview of membrane technology applications for industrial wastewater treatment in China to increase water supply. Resour Conserv Recycl 105:1–10. https://doi.org/10.1016/j.resconrec.2015.09.012
Zheng J, Li M, Yu K, Hu J, Zhang X, Wang L (2017) Sulfonated multiwall carbon nanotubes assisted thin-film nanocomposite membrane with enhanced water flux and anti-fouling property. J Membr Sci 524:344–353. https://doi.org/10.1016/j.memsci.2016.11.032
Zinadini S, Zinatizadeh AA, Rahimi M, Vatanpour V, Zangeneh H (2014) Preparation of a novel antifouling mixed matrix PES membrane by embedding graphene oxide nanoplates. J Membr Sci 453:292–301. https://doi.org/10.1016/j.memsci.2013.10.070
Zinadini S, Vatanpour V, Zinatizadeh AA, Rahimi M, Rahimi Z, Kian M (2015) Preparation and characterization of antifouling graphene oxide/polyethersulfone ultrafiltration membrane: application in MBR for dairy wastewater treatment. J Water Process Eng 7:280–294. https://doi.org/10.1016/j.jwpe.2015.07.005
Zinadini S, Rostami S, Vatanpour V, Jalilian E (2017) Preparation of antibiofouling polyethersulfone mixed matrix NF membrane using photocatalytic activity of ZnO/MWCNTs nanocomposite. J Membr Sci 529:133–141. https://doi.org/10.1016/j.memsci.2017.01.047
Zirehpour A, Rahimpour A, Jahanshahi M, Peyravi M (2014) Mixed matrix membrane application for olive oil wastewater treatment: process optimization based on Taguchi design method. J Environ Manage 132:113–120. https://doi.org/10.1016/j.jenvman.2013.10.028
Zuo K, Liu H, Zhang Q, Liang P, Vecitis CD, Huang X (2016) Enhanced performance of nitrogen-doped carbon nanotube membrane-based filtration cathode microbial fuel cell. Electrochim Acta 211:199–206. https://doi.org/10.1016/j.electacta.2016.05.104

Chapter 5
Removal of Pharmaceuticals and Personal Care Products in Aquatic Environment by Membrane Technology

Xiuzhen Wei, Xufeng Xu, Cuixia Li, Jiawei Wu, Jinyuan Chen, Bosheng Lv, and Jianli Wang

Contents

Abstract Pharmaceuticals and personal care products (PPCPs) as emerging environmental contaminants have attracted increasing attention because of their potential adverse effects on humans and wildlife. PPCPs are frequently detected in surface and groundwater worldwide at concentrations of ng/L or ug/L. However, traditional activated sludge treatment process used in sewage treatment plants cannot effectively remove PPCPs from water. It has been confirmed that trace PPCPs can cause

X. Wei (✉) · X. Xu · C. Li · J. Wu · J. Chen · B. Lv (✉)
College of Environment, Zhejiang University of Technology, Hangzhou, China

Key Laboratory of Microbial Technology for Industrial Pollution Control of Zhejiang Province, Hangzhou, China
e-mail: xzwei@zjut.edu.cn; zjhzlbs@zjut.edu.cn

J. Wang (✉)
College of Chemical Engineering, Zhejiang University of Technology, Hangzhou, China
e-mail: wangjl@zjut.edu.cn

Z. Zhang et al. (eds.), *Membranes for Environmental Applications*, Environmental Chemistry for a Sustainable World 42, https://doi.org/10.1007/978-3-030-33978-4_5

fish growth malformations, sex disorders, and even death, which raises concerns about the potential adverse effects of PPCPs. Membrane separation technologies have been confirmed to be suitable for the removal of PPCPs from water because they are simple to operate, effective, and economical.

This work will present a review on mechanisms, efficiency, and influence factors of PPCPs removal by ultrafiltration membranes, reverse osmosis membranes, and nanofiltration membranes. For ultrafiltration membranes, the removal efficiencies of PPCPs are relatively lower. But ultrafiltration membranes can be used to treat wastewater that contains PPCPs if they are combined with other treatment processes. Reverse osmosis membranes can effectively remove PPCPs molecules. However, the reverse osmosis process is not economical compared with nanofiltration membranes. Normally, the main mechanisms for nanofiltration membranes to remove PPCPs include size exclusion, electrostatic exclusion, and hydrophobic adsorption. For nanofiltration membranes, the removal efficiencies of PPCPs are affected by many factors, including the PPCPs characteristics, water quality conditions, and nanofiltration membrane characteristics. Nanofiltration membranes show great prospects for PPCPs wastewater treatment because of their relatively higher removal efficiency and lower energy consumption.

Keywords PPCPs · Removal efficiency · Activated sludge · Surface water · Groundwater · Environmental risk · Membrane technology · Ultrafiltration membrane · Reverse osmosis membrane · Nanofiltration membrane

5.1 Introduction

Water is the source of life and is important for our daily life. Climate change, population growth, and increased urbanization pose major challenges for water supply systems and place an ever-increasing demand on finite freshwater resources (Baghbanzadeh et al. 2017; Leijon and Boström 2018; Yao et al. 2016). The World Health Organization estimates that 844 million people worldwide lack a safe drinking water source, including 159 million people who are dependent on surface water. Normally, ammonium (NH^{4+}), nitrite (NO^{2-}), nitrate (NO^{3-}), phosphorous, compounds from eutrophication effects, heavy metals, natural organic matter, and some organic molecules that have different molecular weights can be found in water. Nutrients and natural organic matter can be removed by processes such as activated sludge and sand filtration, and the microorganisms produced because of nutrient enrichment can be removed via microfiltration and ultrafiltration (Chollom et al. 2017; Liu 2019; Zhang and Fu 2018). The new emerging low-concentration pollutants that are difficult to degrade in water, such as pharmaceuticals and personal care products (PPCPs), are worrisome. As emerging contaminants, PPCPs have been detected in surface water, groundwater, and other aquatic environments around the world in concentrations ranging from ng/l to μg/l (Peng et al. 2014; Dai et al. 2015; Yu and Cao 2016; Li et al. 2018a; Ma et al. 2018). Although the concentration of PPCPs is very low, and some may be mobilized and converted into other active (or inactive) compounds during the migration process (Yang et al. 2017), PPCPs are easy to accumulate in organisms due to their poor degradability, which can have a serious impact on the health of plants, animals, and humans (Kim and Tanaka 2009; Yang et al. 2017).

The objective of this paper is to review the current situation of PPCPs in water environments, including surface water and groundwater throughout the world, and the harm of PPCPs to aquatic organisms to provide a clear and concise overview of the current application of membrane technology for the removal of PPCPs. This includes assessing cost aspects and cost-effectiveness. In particular, we provide an overview of the potential of nanofiltration membranes for PPCPs removal.

5.2 Pharmaceuticals and Personal Care Products

PPCPs are important components of human life and include a variety of pharmaceutical compounds, such as Chinese medicine, analgesics, antibiotics, hormones, analgesics/anti-inflammatories, psychiatric drugs, lipid regulators, contraceptives, and sedatives, and personal care products, such as cosmetics, aromatics, detergents, disinfectants, hair dyes, and hairstyling agents. The specific classes, corresponding purposes, and main properties of PPCPs are listed in Table 5.1. Most PPCPs are highly polar and have relatively low volatilities, making them difficult to dissipate from water environments, resulting in the water environment becoming a "savings bank" of PPCPs.

The use of pharmaceuticals for humans and livestock is becoming increasingly common (Tappin et al. 2016; Tran et al. 2015) because of their beneficial properties, resulting in their continuous accumulation in the environment, especially in water environments (Jones et al. 2005; Nikolaou et al. 2007). The production of antibiotics in China approached 2.48×10^5 t in 2013, which approximately tripled since 2009. Meanwhile, the usage of antibiotics approached 1.62×10^5 t, with antibiotic penetration in the water and soil environment at 5.0×10^4 t/year (Liu et al. 2018). In the United Kingdom, the annual usage of acetaminophen and aspirin reached 2000 and 770 tons, respectively, resulting in a considerable increase in the possibility that they are entering the environment (Dodgen et al. 2015). Moreover, personal care products, such as musk, cosmetics, and shading agents, are widely used by people to improve their quality of life. Thus, the demand for personal care products has greatly increased. For example, the amount of decamethylcyclopentasiloxane and dodecamethylcyclohexasiloxane used as carrier solvents and emollients in personal care products has increased tenfold in the last 25 years and accounts for more than 225,000 and 22,500 tons, respectively (Vita et al. 2018).

After pharmaceuticals are ingested by humans or livestock, only a few are absorbed by the body, and most are excreted via the body's metabolism process

Table 5.1 The specific classes and main properties of pharmaceuticals and personal care products

Compound group/class	Compound	Functions	CAS	Molecular weight	Molecular formula	Solubility	LogKow	Pka	Vapor pressure
Pharmaceuticals									
Hormones	Estriol	Regulation of metabolism; control of the sexual development; keep homeostasis	50-27-1	288.4	$C_{18}H_{24}O_3$	2.73E-02	2.45	10.54	9.93E-12
	Bisphenol A		80-05-7	228.3	$C_{15}H_{16}O_2$	1.20E-04	3.32	9.60	4.00E-08
	Estrone		53-16-7	270.4	$C_{18}H_{22}O_2$	3.00E-02	3.13	10.34	2.49E-10
	Estradiol		50-28-2	272.4	$C_{18}H_{24}O_2$	3.60E-03	4.01	10.46	6.38E-09
Veterinary and human antibiotics	Sulfamethazine	Vital medicines for the treatment of bacterial infections in both humans and animals	57-68-1	278.3	$C_{12}H_{14}N_4O_2S$	1.5	0.14	7.59	6.82E-09
	Sulfamethoxazole		723-46-6	253.3	$C10H_{11}N_3O_3S$	4.59E-01	0.89	1.60, 5.70	6.93E-08
	Trimethoprim		738-70-5	290.3	$C_{14}H_{18}N_4O_3$	4.00E-01	0.91	7.12	
	Amoxicillin		26787-78-0	365.4	$C_{16}H_{19}N_3O_5S$	3.43	0.87	3.20, 11.70	4.69E-17
	Erythromycin		643-22-1	733.9	$C_{37}H_{67}NO_{13}$	2	3.06	8.88	2.12E-25
	Norfloxacin		70458-96-7	319.3	$C_{16}H_{18}FN_3O_3$	2.80E-01	0.46	6.34, 8.75	
	Ofloxacin		82419-36-1	361.4	$C_{18}H_{20}FN_3O_4$	10.8	0.39	5.97, 9.28	9.84E-13
	Clarithromycin		81103-11-9	748	$C_{38}H_{69}NO_{13}$	1.69E-03	3.16	8.99	2.32E-25
	Ciprofloxacin		85721-33-1	331.3	$C_{17}H_{18}FN_3O_3$	30	0.28	6.09, 8.74	2.85E-13
	Ampicillin		69-53-4	349.4	$C_{16}H_{19}N_3O_4S$	10.1	1.45	2.50, 7.30	

	Cefalexin		15686-71-2	347.4	$C_{16}H_{17}N_3O_4S$	2.97E-01	0.65	5.20, 7.30	
	Tetracycline		64-75-5	444.4	$C_{22}H_{24}N_2O_8$	2.31E-01	−1.37	3.30	
	Chloramphenicol		56-75-7	323.1	$C_{11}H_{12}Cl_2N_2O_5$	2.5	1.14		1.73E-12
Analgesics and anti-inflammatory drugs	Ibuprofen	Reduce pain and inflammation	15687-27-1	206.3	$C_{13}H_{18}O_2$	2.10E-02	3.97	4.91	4.74E-05
	Caffeine			194.2	$C_8H_{10}N_4O_2$	2.16E+01	−0.07	10.40	1.50E+01
	Diclofenac		15307-86-5	296.1	$C_{14}H_{11}Cl_2NO_2$	2.37E-03	4.51	4.15	6.14E-08
	Acetaminophen		103-90-2	151.2	$C_8H_9NO_2$	14	0.46	9.38	6.29E-05
	Azithromycin		117772-70-0	749	$C_{38}H_{72}N_2O_{12}$	2.37E-03	4.02	8.74	2.65E-24
	Naproxen		26159-31-9	230.3	$C_{14}H_{14}O_3$	1.59E-02	3.18	4.15	1.89E-06
	Phenazone			188.2	$C_{11}H_{12}N_2O$	5.19E-01	0.38	1.50	3.06E-05
	Salicylic acid		69-72-7	138.1	$C_7H_6O_3$	2.24	2.26	2.98, 13.60	8.20E-05
	Paracetamol		58-80	151.2	$C_8H_9NO_2$	14	0.33	9.38	6.42E-13
	Ketoprofen		22071-15-4	254.3	$C_{16}H_{14}O_3$	5.10E-02	2.80	4.45	
	Mefenamic acid		61-68-7	241.3	$C_{15}H_{15}NO_2$	1.37E-02	4.20	4.20	

(continued)

Table 5.1 (continued)

Compound group/class	Compound	Functions	CAS	Molecular weight	Molecular formula	Solubility	LogKow	Pka	Vapor pressure
Psychiatric drugs	Carbamazepine	Treat mood disorders	298-46-4	236.3	$C_{15}H_{12}N_2O$	1.80E-02	2.45	13.90	1.84E-07
	Primidone		125-33-7	218.3	$C_{12}H_{14}N_2O_2$	5.00E-01	0.91		
Lipid regulators	Bezafibrate	Regulation of triglycerides and cholesterol in blood	41859-67-0	361.8	$C_{19}H_{20}ClNO_4$	1.55E-03	3.61		
	Clofibric acid		882-09-7	214.6	$C_{10}H_{11}ClO_3$	5.83E-01	2.57	3.20	1.13E-04
	Gemfibrozil		25812-30-0	250.3	$C_{15}H_{22}O_3$	1.10E-02	4.77	4.50	3.10E-05
β-Blockers	Atenolol	Inhibit the hormone adrenalin and the neurotransmitter noradrenalin	29122-68-7	266.3	$C_{14}H_{22}N_2O_3$	13.3	0.16	9.60	
	Metoprolol		51384-51-1	267.4	$C_{15}H_{25}NO_3$	16.9	1.88	9.60	
	Propranolol		525-66-6	259.3	$C_{16}H_{21}NO_2$	6.17E-02	3.48	9.42	
Personal care products									
Fragrances	Galaxolide	Create a pleasant odor	1222-05-5	258.4	$C_{18}H_{26}O$	1.75E-03	5.90		5.45E-04
	Tonalide		21145-77-7	258.4	$C_{18}H_{26}O$	1.25E-03	5.70		5.12E-04
Sunscreen agents	Benzophenone	Protect the skin from the sun's ultraviolet radiation and reduce sunburn and other skin damage	119-61-9	182.2	$C_{14}H_8O_2$	1.37E-01	3.18		1.93E-03
	Octocrylene		6197-30-4	361.5	$C_{24}H_{27}NO_2$		6.90		

Insect repellents	N,N diethyl-m-toluamide	Kill unwanted insect	134-62-3	191.3	$C_{12}H_{17}NO$	9.12E-01	2.02		2.00E-03
Antiseptics	Methylparaben	Prevent decomposition by microbial growth or by undesirable chemical changes	99-76-3	152.1	$C_8H_8O_3$	2.5	1.96	8.40	2.37E-04
	Triclocarban		101-20-2	315.6	$C_{13}H_9Cl_3N_2O$	2.37E-06	4.90		3.60E-09
	Triclosan		3380-34-5	289.5	$C1_2H_7Cl_3O_2$	1.00E-02	4.76	7.90	4.60E-06
	Sulfadiazine		68-35-9	250.3	$C_{10}H_{10}N_4O_2S$	7.70E-02	−0.09	6.36	
	Butylparaben		94-26-8	194.2	$C_{11}H_{14}O_3$	2.07E-01	3.57	8.47	2.51E-04

via feces or are washed off during use or over time (Liu and Wong 2013; Schlüsener and Bester 2006). These direct and indirect discharged pharmaceuticals from humans and livestock then end up in sewage treatment plants. Compared with pharmaceuticals, personal care products enter the sewage system more directly in larger amounts. For example, kitchen detergents and toilet cleaners, which are frequently used, are directly discharged into the sewer network at higher concentrations. However, in addition to used PPCPs, a large number of these compounds are directly abandoned in the environment because they expire or are discarded for other reasons. In addition, direct or indirect discharge from industrial, hospital, and agricultural wastewater is an important source of PPCPs. Thus, large amounts of PPCPs molecules are accumulating in sewage treatment plants.

Normally, activated sludge treatment processes are used in sewage treatment plants. However, most PPCPs are relatively stable and cannot be degraded by the activated sludge treatment process, and the removal efficiencies of PPCPs in biological wastewater treatment plants are very low (Carmona et al. 2014; Kosma et al. 2014). The un-degraded PPCPs in sewage treatment plants are discharged into open water bodies. PPCPs in open waters may be consumed by aquatic organisms, accumulated in the organism's body and transferred along the food chain. Eventually, PPCPs will be concentrated in surface water and groundwater (Nödler et al. 2012; Tang et al. 2015).

Thus, it is increasingly necessary to find a suitable method to effectively remove PPCPs. Membrane technology, as a novel separation and purification technology, plays an important role in a variety of domains. Because of their unique screening mechanisms, membrane technologies, especially nanofiltration and reverse osmosis, have been confirmed to be effective in removing PPCPs (Kimura et al. 2009; Lin and Lee 2014; Radjenović et al. 2008).

5.2.1 Removal Efficiencies of Pharmaceuticals and Personal Care Products by Sewage Treatment Plants

All domestic sewage and industrial wastewaters are treated by sewage treatment plants before they are discharged into open water. Normally, sewage treatment plants include screening, a regulation pool, an anaerobic pool, an aerobic pool, and a sedimentation tank treatment unit. However, the activated sludge treatment process has little effect on most PPCPs because most PPCPs are relatively stable and cannot be degraded by the activated sludge treatment process, which makes the problem of PPCPs in the water environment more serious. The concentrations of some PPCPs detected in the influents and effluents from sewage treatment plants and the corresponding removal efficiencies are summarized in Table 5.2. As the results in Table 5.2 indicate, the removal efficiencies of different sewage treatment plants are different even for the same PPCPs molecules, and the removal efficiencies are relatively lower. Sometimes, more than half of PPCPs detected in the influents still

Table 5.2 The influent and effluent concentration of pharmaceuticals and personal care products detected in sewage treatment plants and corresponding removal efficiency

Selected compounds	Sampling sites	Influent concentration (μg/L)	Effluent concentration (μg/L)	Removal efficiency (%)	References
Bisphenol A	China	0.837	0.004	99.6	Nie et al. (2012)
Estrone	USA	0.057	–	93.7	Blair et al. (2015)
	Korea	0.070	0.024	87.1	Behera et al. (2011)
	Czech Republic	0.041	<0.003	>94.0	Vymazal et al. (2015)
	France	0.007	0.009	−28.0	Mailler et al. (2014)
	China	0.052	0.013	75.4	Nie et al. (2012)
Estradiol	Korea	0.004	0	100	Behera et al. (2011)
	Czech Republic	0.009	<0.001	>88.0	Vymazal et al. (2015)
	China	0.008	ND	>90.0	Nie et al. (2012)
Estriol	Korea	0.802	0	100	Behera et al. (2011)
	Czech Republic	0.013	<0.010	>23.0	Vymazal et al. (2015)
	China	0.078	ND	>95.0	Nie et al. (2012)
	USA	0.060	ND	66.8	Blair et al. (2015)
Erythromycin-H_2O	China	0.460	0.455	1.0	Leung et al. (2012)
Sulfamethoxazole	Korea	0.216	0.162	51.9	Behera et al. (2011)
	EU	0.530	0.310	52.0	Martin Ruel et al. (2010)
	USA	7.400	–	−35.8	Blair et al. (2015)
Sulfamethazine	Greece	ND-0.507	ND-0.08	84.0	Papageorgiou et al. (2016)
	China	0.140	0.037	74.0	Leung et al. (2012)
	Korea	0.343	0.408	13.1	Behera et al. (2011)

(continued)

Table 5.2 (continued)

Selected compounds	Sampling sites	Influent concentration (μg/L)	Effluent concentration (μg/L)	Removal efficiency (%)	References
Trimethoprim	Korea	0.277	0.154	69.0	Behera et al. (2011)
	China	0.114	0.068	40.0	Leung et al. (2012)
	USA	0.570	–	−53.1	Blair et al. (2015)
Amoxicillin	China	0.261	0.066	74.0	Leung et al. (2012)
Ampicillin	Greece	ND-1.805	ND-0.498	72.0	Papageorgiou et al. (2016)
	USA	0.160	–	1.3	Blair et al. (2015)
Cefalexin	China	0.040	ND	>90.0	Leung et al. (2012)
Chloramphenicol	China	0.206	0.234	−14.0	Leung et al. (2012)
Ofloxacin	China	1.020	0.980	4.0	Leung et al. (2012)
	USA	2.100	–	−1.2	Blair et al. (2015)
Tetracycline	China	0.257	0.152	44.0	Leung et al. (2012)
Lincomycin	Korea	19.401	21.278	−11.2	Behera et al. (2011)
	USA	0.032	–	−50.4	Blair et al. (2015)
Acetaminophen	Korea	10.234	0.027	99.9	Behera et al. (2011)
	USA	13	–	97.1	Blair et al. (2015)
Aspirin	USA	0.17–0.93	ND-0.070	58.8–92.5	Yu et al. (2013)
Diclofenac	Greece	0.377	0.125	66.8	Stamatis and Konstantinou (2013)
	Korea	0.243	0.049	81.4	Behera et al. (2011)
	Greece	ND-4.869	ND-2.668	45.0	Papageorgiou et al. (2016)
	Spain	1.660	0.430	74.0	Fernández-López et al. (2016)
	USA	0.086–0.580	ND-0.120	−39.5-79.3	Yu et al. (2013)
Ibuprofen	Greece	0.504	0.036	92.9	Stamatis and Konstantinou (2013)
	Korea	2.853	0.075	98.2	Behera et al. (2011)
	UK	1.681–33.764	0.143–4.239	>80.0	Petrie et al. (2014)
	Greece	ND-0.793	ND-0.220	72.0	Papageorgiou et al. (2016)
	USA	4.500	–	99.7	Blair et al. (2015)
	Spain	2.800	0.720	72.0	Fernández-López et al. (2016)

Caffeine	Greece	3.203	0.070	97.8	Stamatis and Konstantinou (2013)
	Korea	3.217	0.060	99.2	Behera et al. (2011)
Ketoprofen	Korea	0.286	0.037	94.2	Behera et al. (2011)
	USA	0.150–1.300	ND-0.065	56.7–95.0	Yu et al. (2013)
Mefenamic acid	Korea	0.328	0.392	−26.3	Behera et al. (2011)
Naproxen	Greece	0.096	0.007	92.7	Stamatis and Konstantinou (2013)
	Korea	5.033	0.166	95.7	Behera et al. (2011)
	USA	3		96.2	Blair et al. (2015)
	Spain	1.180	0.190	84.0	Fernández-López et al. (2016)
Salicylic acid	Greece	1.157	0.120	89.6	Stamatis and Konstantinou (2013)
Paracetamol	Greece	1.629	0.191	88.3	Stamatis and Konstantinou (2013)
	USA	0.370-218	ND-0.210	43.2–100	Yu et al. (2013)
Fluoxetine	USA	0.050	–	23.1	Blair et al. (2015)
Carbamazepine	Greece	0.566	0.304	46.3	Stamatis and Konstantinou (2013)
	Korea	0.127	0.074	23.1	Behera et al. (2011)
	Spain	15.780	7.570	52.0	Fernández-López et al. (2016)
	USA	0.220	–	−92.4	Blair et al. (2015)
Fluoxetine	Australia	0.051	–	68.2	Roberts et al. (2016)
Bezafibrate	EU-wide, Korea	0.05–1.39	0.030–0.670	9.10–70.5	Loos et al. (2013) and Yu et al. (2013)
Clofibric acid	EU-wide	0–0.74	ND–0.330	0–93.6	Loos et al. (2013)
	Greece	0.527	0.135	74.4	Stamatis and Konstantinou (2013)
	Korea	0.065	0.006	93.6	Behera et al. (2011)
	USA	0.057-0.42	ND-0.081	−122.8	Yu et al. (2013)
Gemfibrozil	EU-wide	0.10-17.1	0.0025–5.24	0–92.3	Loos et al. (2013)
	Greece	0.862	0.229	73.4	Stamatis and Konstantinou (2013)
	Korea	0.318	0.026	92.3	Behera et al. (2011)
	USA	0.190	–	50.8	Blair et al. (2015)

(continued)

Table 5.2 (continued)

Selected compounds	Sampling sites	Influent concentration (μg/L)	Effluent concentration (μg/L)	Removal efficiency (%)	References
Atenolol	Korea	11.239	5.911	64.5	Behera et al. (2011)
	Switzerland	2.140	0.730	65.8	Alder et al. (2010)
	Australia	0.255	0.135	47.1	Roberts et al. (2016)
Metoprolol	Switzerland	0.247	0.200	19.0	Alder et al. (2010)
	Korea	0.006	0.003	23.0	Behera et al. (2011)
Propranolol	Switzerland	0.050	0.030	40.0	Alder et al. (2010)
Sotalol	Switzerland	0.340	0.260	23.5	Alder et al. (2010)
	Australia	0.711	0.760	−6.8	Roberts et al. (2016)
Galaxolide	Spain, WB	0.03–25	0.06–2.77	87.8	Pothitou and Voutsa (2008) and Terzić et al. (2008)
Tonalide	Spain, WB	0.05–1.93	0.05–0.32	84.7	
4-Methyl-benzilidine-camphor	China	0.169	0.043	12.0	Tsui et al. (2014)
2-Ethyl-hexyl-4-trimethoxycinnamate	China	0.462	0.150	93.0	Tsui et al. (2014)
Butyl methoxydibenzoylmethane	China	0.289	0.147	49.0	Tsui et al. (2014)
Ethylhexyl salicylate	China	0.093	0.008	91.0	Tsui et al. (2014)
Homosalate	China	0.151	0.031	79.0	Tsui et al. (2014)
Isoamyl p-methoxycinnamate	China	0.043	0.024	44.0	Tsui et al. (2014)
Octyl-dimethyl-p-aminobenzoic acid	China	0.138	0.056	17.0	Tsui et al. (2014)
Octocrylene	China	8.000	0	>99.0	Tsui et al. (2014)
Oxycodone	India		0.041	1.5	Subedi et al. (2015)

Benzophenone-3	Korea, Spain	0.079–0.900	0.079–0.23	63.8–98.2	Behera et al. (2011) and Pothitou and Voutsa (2008)
N,N diethyl-m-toluamide	EU-wide	2.560–3.190	0.610–15.80	65.6–79.5	Loos et al. (2013) and Terzić et al. (2008)
	China	0.066	0.040	40.0	Wang et al. (2014)
Triclosan	Greece	0.156	0.056	64.1	Stamatis and Konstantinou (2013)
	EU	0.450	–	99.0	Martin Ruel et al. (2010)
	Korea	0.785	0.149	79.6	Behera et al. (2011)
	India	892	202	77.0	Subedi et al. (2015)
	USA	0.300	–	55.3	Blair et al. (2015)
Triclocarban	USA	0.540	–	11.4	Blair et al. (2015)
	India	1.150	0.049	>80.0	Subedi et al. (2015)
Sulfadiazine	USA	0.020	–	−64.1	Blair et al. (2015)
Methylparaben	China	0.570	–	98.8	Li et al. (2015)
	Spain	0.334	0.011	96.0	Carmona et al. (2014)
Butylparaben	China	0.028	–	99.7	Li et al. (2015)

ND not detected

remain in the effluents after the treatment by sewage treatment plants, such as estriol, erythromycin-H_2O, sulfamethazine, and amoxicillin. Antibiotics are among the most commonly used PPCPs, and erythromycin-H_2O, sulfamethoxazole, trimethoprim, chloramphenicol, ofloxacin, and lincomycin exhibit high concentrations both in influents and effluents. This is inextricably linked to the mass use of antibiotics. However, they cannot be degraded easily because they are antimicrobial agents or are specifically designed to achieve a biological response (McClellan and Halden 2010; Parolini et al. 2013). An interesting phenomenon is that trimethoprim, chloramphenicol, ofloxacin, and lincomycin all have negative growth trends compared with their concentrates in influents and effluents, which is due to the degradation of precursors or the formation of conjugated states (Behera et al. 2011; Blair et al. 2015; Leung et al. 2012; Martin Ruel et al. 2010). Thus, the severity of antibiotics in the water environment is beyond doubt, and the conventional activated sludge treatment system has serious limitations.

With improvements in medical management, the mortality of cardiovascular disease patients is decreasing. β-Blockers are common pharmaceuticals that are widely used to treat cardiovascular diseases. They have been detected in the influents and effluents of several sewage treatment plants, and their removal efficiencies are only -6.8% to 65.8%. For example, atenolol in the influents and effluents from Korean sewage treatment plants was detected by Behera et al. (2011), and their concentrations were as high as 11.239 and 5.911 μg/L, respectively, which are far beyond the normal standard (for pharmaceuticals, UK PNECs are currently estimated at typically 0.01 μg/L) (Gardner et al. 2012). The concentrations of sotalol detected in the influents and effluents from Australian sewage treatment plants ranged from 0.711 μg/L to 0.760 μg/L and showed negative growth (McClellan and Halden 2010). This is due to the deconjugation of metabolites, transformation products from hydrolysis, and desorption from suspended solids/sludge during treatment processes. Similarly, sewage treatment plants cannot effectively remove these pharmaceuticals.

Conventional sewage treatment plants not only remove PPCPs ineffectively but are easily affected by environmental conditions, such as the environmental temperature and pH (Li et al. 2016). For instance, Kosma et al. found that the removal efficiency for bezafibrate was higher in summer than in winter at sewage treatment plants in Greece (Kosma et al. 2014). This may be because the environmental temperature is lower in winter than in summer, and the biodegradation kinetics are slower at a low temperature (Ma et al. 2013).

In general, conventional sewage treatment plants are not suitable for the treatment of PPCPs, which means that activated sludge treatment systems are not sufficient for the treatment of the current sewage. Many researchers even believe that sewage treatment plants are the main pathway for PPCPs release into freshwaters (Chang et al. 2010; Tarpani and Azapagic 2018; Zepon Tarpani and Azapagic 2018).

5.2.2 Pharmaceuticals and Personal Care Products in Surface Water

Surface water is one of the most important sources of drinking water for humans, including rivers, lakes, reservoirs, oceans, and so on. Currently, most oceans, rivers, and lakes are polluted, although the pollution levels differ. As we know, the annual production of PPCPs can exceed 2×10^7 tons. Most PPCPs cannot be degraded or removed by sewage treatment plants. The massive use of PPCPs has made surface water the most direct receptor. Some studies have shown that surface water is seriously polluted by PPCPs (Kasprzyk-Hordern et al. 2008; Luo et al. 2014; Nakada et al. 2007; Peng et al. 2008; Wang et al. 2015). Fortunately, because of the dilution of precipitation and runoff, the concentration of PPCPs in surface water is basically at the level of ng/L to μg/L (Balakrishna et al. 2017; Prasse et al. 2010; Zuccato et al. 2008). The PPCPs in surface water from different regions are shown in Table 5.3.

Currently, antibiotics, analgesics/anti-inflammatories, psychiatric drugs, β-blockers, insect repellents, and antiseptics have all been detected in surface waters all over the world. For example, the detection frequencies of sulfamethoxazole in the Kenya River Basin and the Yangtze River are as high as 100% and 87.5%, respectively. The former is attributed to the use of sulfamethoxazole for a broad range of bacterial infections, including opportunistic infections occurring in people with HIV in the Kenya River Basin. For the latter, the reason is that antibiotics are extensively used in animal farming and aquaculture in the central and lower Yangtze River. In addition, many compounds can be detected in other surface basins with 100% detection frequency, such as diclofenac, caffeine, mefenamic acid, and carbamazepine, indicating that PPCPs are ubiquitous in surface water (Cantwell et al. 2018; Dai et al. 2015; Hossain et al. 2018; Lin et al. 2018a; Ma et al. 2016; Sharma et al. 2019; Wu et al. 2014). The concentrations of doxycycline, ibuprofen, caffeine, acetaminophen, and ketoprofen are significantly higher than 1 μg/L, especially caffeine from Costa Rican surface water, whose concentration is as high as 1.121 mg/L (Spongberg et al. 2011). Similarly, caffeine was detected in high concentrations (0.156~2.056 μg/L) in the surface waters of China, India, and the United States. Because caffeine can be found in various products, such as painkillers, coffee, and tea, which can be regarded as necessities for life, it has been regarded as an indicator of anthropogenic contaminants (Al-Qaim et al. 2015). Thus, the high concentration of caffeine in surface water also reflects the severity of surface water contamination by PPCPs.

5.2.3 Pharmaceuticals and Personal Care Products in Groundwater

More than a quarter of the world's population relies primarily on groundwater for drinking water. However, groundwater polluted by refractory organic molecules has

Table 5.3 Concentration of pharmaceuticals and personal care products in surface water from different regions

Categories	Compound	Max concentration μg/L	Mean concentration μg/L	Area	Detection frequency (%)	References
Veterinary and human antibiotics	Sulfamethoxazole	0.007	0.001	Old Brahmaputra River, Bangladesh	70.0	K'oreje et al. (2018)
		2.400	–	Kenya River Basin	100	Hossain et al. (2018)
		0.0185	0.008	Yangtze River, China	87.5	Wu et al. (2014)
		0.100	0.015	Xiangjiang River, China	100	Lin et al. (2018a)
	Erythromycin	0.039	0.036	Surface water, Portugal	4.2	Pereira et al. (2017)
		0.808	0.296	Yangtze River, China	93.8	Wu et al. (2014)
	Clarithromycin	0.103	0.018	Yangtze River, China	93.8	Wu et al. (2014)
	Trimethoprim	0.538	–	Beiyun River of Beijing, China	100	Dai et al. (2015)
		0.017	0.003	Old Brahmaputra River, Bangladesh	95.0	K'oreje et al. (2018)
	Doxycycline	0.128	0.037	The Tejo estuary, Portugal	25.8	Reis-Santos et al. (2018)
		73.722	–	Costa Rican surface water	77.0	Spongberg et al. (2011)
	Clarithromycin	0.100	0.008	Xiangjiang River, China	100	Lin et al. 2018a)
	Amoxicillin	0.710	0.052	Xiangjiang River, China	100	Lin et al. 2018a)

Analgesics and anti-inflammatory drugs	Ibuprofen	0.099	0.011	Yangtze River, China	12.5	Wu et al. (2014)
		0.320	0.069	Xiangjiang River, China	100	Lin et al. 2018a)
		36.788	–	Costa Rican surface water	19.0	Spongberg et al. (2011)
	Diclofenac	0.231	0.040	East Dongting Lake, China	100	Ma et al. (2016)
		0.051	0.034	Surface water, Portugal	19.4	Pereira et al. (2017)
		0.150	–	Beiyun River of Beijing, China	100	Dai et al. (2015)
		0.266	–	Costa Rican surface water	8.0	Spongberg et al. (2011)
		0.0518	0.015	The Tejo estuary, Portugal	32.3	Reis-Santos et al. (2018)
	Caffeine	1121.446	–	Costa Rican surface water	29.0	Spongberg et al. (2011)
		0.743	0.196	Lower reach of Ganges River, India	100	Sharma et al. (2019)
		2.056	–	Hudson River, USA	100	Cantwell et al. (2018)
		0.786	0.142	Yangtze River, China	100	Wu et al. (2014)
		8.095	–	Beiyun River of Beijing, China	100	Dai et al. (2015)
		–	0.118	The River Thames basin, UK	75.0	Nakada et al. (2017)
		0.156	0.085	West Dongting Lake, China	100	Ma et al. (2016)
	Acetaminophen	13.216	–	Costa Rican surface water	27.0	Spongberg et al. (2011)
	Salicylic acid	0.274	–	Costa Rican surface water	41.0	Spongberg et al. (2011)

(continued)

Table 5.3 (continued)

Categories	Compound	Max concentration μg/L	Mean concentration μg/L	Area	Detection frequency (%)	References
	Paracetamol	0.011	0.002	The Tejo estuary, Portugal	80.6	Reis-Santos et al. (2018)
		0.069	0.038	Surface water, Portugal	19.4	Pereira et al. (2017)
	Ketoprofen	9.808	–	Costa Rican surface water	27.0	Spongberg et al. (2011)
	Naproxen	–	0.053	The River Thames basin, UK	75.0	Nakada et al. (2017)
	Mefenamic acid	0.008	–	Beiyun River of Beijing, China	67.0	Dai et al. (2015)
		0.011	0.005	West Dongting Lake, China	100	Ma et al. (2016)
Psychiatric drugs	Carbamazepine	0.082	–	Costa Rican surface water	10.0	Spongberg et al. (2011)
		0.006	0.002	East Dongting Lake, China	100	Ma et al. (2016)
		0.009	0.002	Old Brahmaputra River in Bangladesh	65.0	K'oreje et al. (2018)
		0.002	0.001	Yangtze River, China	50.0	Wu et al. (2014)
		0.189	–	Beiyun River of Beijing, China	100	Dai et al. (2015)
		–	0.209	The River Thames basin, UK	88.0	Nakada et al. (2017)
	Primidone	–	0.015	The River Thames basin, UK	50.0	Nakada et al. (2017)

Lipid regulators	Gemfibrozil	0.077	0.023	The Tejo estuary, Portugal	67.7	Reis-Santos et al. (2018)
		0.063	–	Beiyun River of Beijing, China	100	Dai et al. (2015)
	Bezafibrate	0.013	0.003	The Tejo estuary, Portugal	87.1	Reis-Santos et al. (2018)
		0.071	–	Beiyun River of Beijing, China	100	Dai et al. (2015)
β-Blockers	Atenolol	–	0.077	The River Thames basin, UK	88.0	Nakada et al. (2017)
	Metoprolol	0.353	–	Beiyun River of Beijing, China	100	Dai et al. (2015)
		0.002	0.001	East Dongting Lake, China	100	Ma et al. (2016)
	Propranolol	0.037	–	Beiyun River of Beijing, China	80.0	Dai et al. (2015)
Insect repellents	N,N-diethyl-m-toluamide	0.080	–	Kenya River Basin	100	Hossain et al. (2018)
		0.017	0.006	East Dongting Lake, China	100	Ma et al. (2016)
		0.229	–	Beiyun River of Beijing, China	100	Dai et al. (2015)
Antiseptics	Triclosan	0.263	–	Costa Rican surface water	34.0	Spongberg et al. (2011)

been frequently detected over the past few decades, which has attracted wide attention (Jurado et al. 2012; Lapworth et al. 2012; Meffe and de Bustamante 2014; Sacher et al. 2001; Stuart et al. 2012). PPCPs can enter groundwater in many ways, including embedding and recharging of contaminated surface water, as leachates from landfills and municipal sewage pipes, and via infiltration of chemical fertilizer. With an increasing number of research reports showing that groundwater has been polluted by PPCPs to various degrees, the investigations of PPCPs in groundwater have rapidly increased. Table 5.4 lists PPCPs that have a high detection frequency and concentration for different regions.

Yao et al. thought that lower $\log K_{ow}$ compounds could more easily accumulate in the groundwater environment (Yao et al. 2017). For example, antibiotics (sulfamethoxazole, ciprofloxacin, ofloxacin, and tetracyclines) with low $\log K_{ow}$ values are frequently detected in the groundwater in the United States (Fram and Belitz 2011; Schaider et al. 2014), Spain (Lapworth et al. 2012; López-Serna et al. 2013), China (Lapworth et al. 2012; Peng et al. 2014; Yao et al. 2017) and Europe (Sui et al. 2015). Analgesics/anti-inflammatories can be eliminated by photodegradation and biodegradation processes with an estimated half-life ranging from 8 to 32 days (Tixier et al. 2003). However, analgesics/anti-inflammatory drugs are still frequently detected in groundwater in various countries, and their concentrations are at a high level (above 0.1 μg/L) (Lapworth et al. 2012; López-Serna et al. 2013; Sharma et al. 2019; Sui et al. 2015). This can be because these kinds of PPCPs in groundwater are more durable and more difficult to eliminate because of the relatively reduced redox conditions and lack of photodegradation (Peng et al. 2014). Similar to surface water, caffeine has also been frequently detected in groundwater in the concentration range of 0.189 to 16.249 μg/L. Although the caffeine concentration in groundwater is lower than that in surface water, it is still much higher than the normal standard, especially in Singapore (Lapworth et al. 2012). Additionally, N,N diethyl-m-toluamide was also detected with 100% frequency in groundwater in Singapore with a concentration of 3.48 μg/L, which was far beyond the normal range (Lapworth et al. 2012).

In reports from all over the world, we know that PPCPs have been detected in both surface water and groundwater with a high detection frequency and concentration. The pollution of PPCPs in the water environment will have potential long-term adverse effects on humans, animals, and plants.

5.2.4 Environmental Risk

Most PPCPs molecules have strong persistence and potential bioaccumulation. After entering the water environment, PPCPs can induce changes in the biochemical functions of aquatic organisms, endangering the ecological environment and biological health. Many researchers have studied the environmental and biochemical risks of PPCPs using model organisms such as fish and cells.

Table 5.4 Detection frequency and concentration of pharmaceuticals and personal care products in groundwater from different regions

Categories	Compound	Max concentration μg/L	Mean concentration μg/L	Area	Detection frequency (%)	References
Hormones	Estrone	0.310	–	Landfills sites, Poland	9.0	Kapelewska et al. (2018)
	Bisphenol A	6.880	–	Landfills sites, Poland	100	Kapelewska et al. (2018)
Veterinary and human antibiotics	Ampicillin	3.690	0.820	Penn State, USA	11.0	Kibuye et al. (2019)
	Sulfamethoxazole	27.410	2.130	Penn State, USA	40.0	Kibuye et al. (2019)
		0.065	0.023	Mallorca Street of Barcelona, Spain	80.0	López-Serna et al. (2013)
		0.029	0.006	NE Catalonia, Spain	81.0	Peng et al. (2014)
		0.170	–	California, USA	0.4	Fram and Belitz (2011)
		0.038	–	Europe	24.2	Lapworth et al. (2012)
		0.410	–	Germany	10.0	Lapworth et al. (2012)
		0.125	0.029	Guangzhou, China	23.6	Yao et al. (2017)
		0.113	–	Massachusetts, USA	60.0	Schaider et al. (2014)
	Ciprofloxacin	0.443	0.088	Poble Sec of Barcelona, Spain	100	López-Serna et al. (2013)
	Ofloxacin	114.940	13.530	Penn State, USA	4.0	Kibuye et al. (2019)
		0.044	–	Jianghan Plain, China	10.0–68.0	Boy-Roura et al. (2018)

(continued)

Table 5.4 (continued)

Categories	Compound	Max concentration μg/L	Mean concentration μg/L	Area	Detection frequency (%)	References
		0.367	–	Barcelona, Spain	100	López-Serna et al. (2013)
	Tetracyclines	0.123	0.041	Jianghan Plain, China	11.0–67.0	Yao et al. (2017)
	Trimethoprim	6.950	0.610	Penn State, USA	7.0	Kibuye et al. (2019)
Analgesics and anti-inflammatory drugs	Acetaminophen	1.800	–	Storlien, Sweden	80.0	Gao et al. (2019)
		15.580	0.420	Penn State, USA	9.0	Kibuye et al. (2019)
	Caffeine	14.150	2.650	Penn State, USA	32.0	Kibuye et al. (2019)
		16.249	–	Singapore	80.0–83.0	Sui et al. (2015)
		4.500	–	UK	27.0	Lapworth et al. (2012)
		0.262	0.078	Ganges River Basin, India	100	Sharma et al. (2019)
		0.189	–	Europe	82.9	Lapworth et al. (2012)
	Ibuprofen	0.750	–	Storlien, Sweden	90.0	Gao et al. (2019)
		0.988	–	Barcelona, Spain	46.0–92.0	Sui et al. (2015)
		0.395	–	Europe	6.7	Peng et al. (2014)
	Diclofenac	0.094	–	Storlien, Sweden	100	Gao et al. (2019)
		2.770	–	Landfills sites, Poland	39.0	Kapelewska et al. (2018)
		0.380	–	Barcelona, Spain	40.0–100	Sui et al. (2015)
	Salicylic acid	2.015	–		98.0	Sui et al. (2015)

				Municipal landfills, China		
		0.620	–	Barcelona, Spain	100	Sui et al. (2015)
	Ketoprofen	0.215	0.081	Mallorca Street of Barcelona, Spain	100	López-Serna et al. (2013)
	Naproxen	0.200	–	Storlien, Sweden	50.0	Gao et al. (2019)
		98.390	37.700	Penn State, USA	19.0	Kibuye et al. (2019)
Psychiatric drugs	Primidone	0.097	–	Storlien, Sweden	5.0	Gao et al. (2019)
	Carbamazepine	0.019	–	Storlien, Sweden	100	Gao et al. (2019)
		0.136	–	Barcelona, Spain	92.0–100	Sui et al. (2015)
Lipid regulators	Gemfibrozil	0.751	0.209	Besòs River Delta, Spain	100	López-Serna et al. (2013)
β-Blockers	Sotalol	0.015	–	Storlien, Sweden	100	Gao et al. (2019)
	Atenolol	0.018	–	Storlien, Sweden	100	Gao et al. (2019)
	Metoprolol	0.057	–	Storlien, Sweden	100	Gao et al. (2019)
		0.355	–	Barcelona, Spain	100	Sui et al. (2015)
Fragrances	Galaxolide	0.820	–	Storlien, Sweden	100	Gao et al. (2019)
Sunscreen agents	Octocrylene	0.540	–	Storlien, Sweden	40.0	Gao et al. (2019)
	Benzophenone	1.700	–	Storlien, Sweden	65.0	Gao et al. (2019)
		3.450	–	Landfills sites, Poland	100	Kapelewska et al. (2018)

(continued)

Table 5.4 (continued)

Categories	Compound	Max concentration μg/L	Mean concentration μg/L	Area	Detection frequency (%)	References
Insect repellents	N,N diethyl-m-toluamide	0.230	–	Storlien, Sweden	100	Gao et al. (2019)
		17.280	–	Landfills sites, Poland	83.0	Kapelewska et al. (2018)
		0.0148	0.002	Ganges River Basin, India	100	Sharma et al. (2019)
		3.481	–	Singapore	100	Sui et al. (2015)
Antiseptics	Triclosan	0.210	–	Landfills sites, Poland	39.0	Kapelewska et al. (2018)
	Methylparaben	2.880	–	Landfills sites, Poland	69.0	Kapelewska et al. (2018)

Fish are the most common aquatic organisms; thus, their physiological status is usually an intuitive manifestation of water quality (Huerta et al. 2018). Recently, PPCPs have been detected in fish all over the world. In the United States, Huerta et al. detected 6 pharmaceuticals from 8 species of fish in 25 polluted river locations that are downstream of different sewage treatment plants (Huerta et al. 2018). The bioaccumulation of 11 selected psychiatric drugs (citalopram, clomipramine, haloperidol, hydroxyzine, levomepromazine, mianserin, mirtazapine, paroxetine, sertraline, tramadol, and venlafaxine) was detected in the Zivny Stream in the Czech Republic. Although only 6 of the 11 pharmaceuticals were detected in the water samples, all were detectable in the liver and kidneys of the fish exposed to the polluted stream (Grabicova et al. 2017). China is one of the countries that has the largest production and consumption of PPCPs, and PPCPs are frequently detected in fish (Gao et al. 2016; Liu and Wong 2013). Yao et al. collected 12 wild fish from 2 major river basins, the Pearl River and the Yangtze River of China, and detected 9 fungicides, 2 synthetic musks, and 2 benzotriazoles in their muscle and liver tissues (Yao et al. 2018). Concentrated fish populations are the first to be affected by a large consumption of PPCPs. However, some fish collected from sparsely populated areas, such as Antarctica, are also affected by PPCPs. 2-Hydroxy-4-methoxybenzophenone, propofol, and alkylphenol 4-tert-octylphenol were detected in fish tissues 25 kilometers away from the Cape Evans research stations with contents at 14.1, 19.2, and 5.0 ng/g, respectively (Emnet et al. 2015). This indicates that the biological hazards of PPCPs have spread all over the world, which reminds us that PPCPs should arouse great concerns.

Some studies have revealed that the prolonged exposure of zebra fish embryos to some PPCPs can cause dose-dependent hatching rates, malformations, anxious behavior, and even mortality (Wang et al. 2016; Zhang et al. 2016, 2017). For example, Yang et al. first performed an acute toxicity test for mianserin exposure using zebra fish embryos after fertilization. They found that mianserin exposure reduced the body length of zebra fish larvae. Although the environmentally relevant concentrations were much lower than the lethal doses, low concentrations of mianserin significantly affected the early development of the fish embryos (Yang et al. 2018a, b). More seriously, the accumulation of PPCPs not only occurs in fish tissues and viscera but also in fish brains, which are the most important organ. Grabicova K found citalopram, sertraline and venlafaxine in the brains of most fish upon exposure experiments (Grabicova et al. 2014). Bisesi believed that exposure to antidepressants (fluoxetine and venlafaxine) reduced the serotonin levels in the fish brain, leading to a decline in fish capture capacity (Bisesi et al. 2014). Normally, these antidepressants can affect humans through the biological chain, acting on humans via the same mechanism.

The accumulation of PPCPs in aquatic organisms and its harm to aquatic organisms highlights the risks associated with the inadvertent presence of PPCPs in the environment. However, the sewage treatment plants are not completely capable of removing PPCPs during treatment processes, indicating that the PPCPs in the environment will become worse. Therefore, an effective method to remove PPCPs is necessary.

5.3 Pharmaceuticals and Personal Care Products Treatment Using Membrane Technology

With more PPCPs molecules being detected in water environments, many reports have revealed that conventional water treatment methods are outdated regarding their removal efficiencies for PPCPs (which are relatively low). Therefore, various methods for PPCPs removal have emerged. However, the migration of degradation products after oxidation via advanced oxidation and photochemical degradation needs to be studied, and there are disadvantages such as long cycle, low efficiency, cumbersome operation, and high cost (Andrzejewski et al. 2008; Gmurek et al. 2017; Kanakaraju et al. 2018; Sharma et al. 2018). Furthermore, advanced oxidation and photochemical degradation both produce by-products (Esplugas et al. 2007; Klavarioti et al. 2009), whereas physical adsorption and membrane treatment do not produce any by-products. In contrast, physical adsorption requires periodic regeneration because of its principle of action, and the membrane treatment method is more practical, effective, and economical for PPCPs removal. The mechanism of membrane treatment is generally considered to involve the principles of screening, electrostatic repulsion, and hydrophobic adsorption. This section mainly summarizes the PPCPs removal situation and mechanism using ultrafiltration membranes, nanofiltration membranes, and reverse osmosis membranes. Additionally, the effective factors and future prospects for PPCPs removal via nanofiltration membranes are also discussed.

5.3.1 Pharmaceuticals and Personal Care Products Removal Mechanisms Using Membranes

Ultrafiltration Membranes

The removal efficiencies of PPCPs by ultrafiltration membrane are shown in Table 5.5. The pore diameters of ultrafiltration membranes usually range between 5 and 100 nm, whose molecular weight cutoff (MWCO) ranges between 10,000 and 200,000 Da. Because of the flexibility, adaptability, and sustainability of ultrafiltration membranes, they have gained increased attention and wide application in water treatment (Chew et al. 2018; Xing et al. 2018). Currently, many researchers believe that the main mechanism of ultrafiltration membrane removal of PPCPs involves hydrophobic adsorption (Comerton et al. 2007; Yoon et al. 2006). Boleda et al. (2011) combined ultrafiltration and nanofiltration membranes to treat sewage containing 40 kinds of pharmaceuticals. It was found that the removal rate of 17 pharmaceuticals in the 40 pharmaceuticals was more than 87% after ultrafiltration membrane treatment, especially for azithromycin, whose removal rate was more than 90%. Meanwhile, Garcia-Ivars et al. (2017) also found that an ultrafiltration membrane (INSIDE CéRAM™) can effectively remove erythromycin, whose

Table 5.5 Removal efficiencies of pharmaceuticals and personal care products by ultrafiltration membrane

Membrane	Company	Compounds	Membrane parameters and operating conditions	Feed liquid	Removal efficiency (%)	References
IRIS	Orelis, France	Ibuprofen	MWCO: 3000 Da, polyethersulfone, cross-flow, 1.5 bar	Model a real wastewater from sewage treatment plants	12.2	Vona et al. (2015)
		Diazepam			19.0	
		Acetaminophen			–	
		Sulfamethoxazole			10.7	
		Clonazepam			–	
		Diclofenac			24.7	
Cylinder membranes	A/G Technology	Acetaminophen	MWCO: 100 kDa	2.300 μg/L, wastewater from sewage treatment plants, USA	4.3	Sheng et al. (2016)
		Caffeine		2.500 μg/L, wastewater from sewage treatment plants, USA	0	
		Carbamazepine		0.110 μg/L, wastewater from sewage treatment plants, USA	70.9	
		Cotinine		1.000 μg/L, wastewater from sewage treatment plants, USA	44.0	
		Diclofenac		0.070 μg/L, wastewater from sewage treatment plants, USA	25.7	
		Gemfibrozil		0.270 μg/L, wastewater from sewage treatment plants, USA	51.9	
		Ibuprofen		2.500 μg/L, wastewater from sewage treatment plants, USA	0	

(continued)

Table 5.5 (continued)

Membrane	Company	Compounds	Membrane parameters and operating conditions	Feed liquid	Removal efficiency (%)	References
		Metoprolol		0.260 μg/L, wastewater from sewage treatment plants, USA	38.5	
		Naproxen		2.500 μg/L, wastewater from sewage treatment plants, USA	0	
		Sulfamethoxazole		0.490 μg/L, wastewater from sewage treatment plants, USA	18.4	
		Triclosan		2.400 μg/L, wastewater from sewage treatment plants, USA	98.8	
		Trimethoprim		0.150 μg/L, wastewater from sewage treatment plants, USA	4.0	
INSIDE CéRAM™	TAMI Industries, France	Acetaminophen	MWCO: 8 kDa, ceramic membrane, cross-flow, 2 bar, pH = 7	Sewage treatment plants secondary effluent samples, Spain	30.0	Garcia-Ivars et al. (2017)
		Caffeine			17.0	
		Diazepam			50.0	
		Diclofenac			36.0	
		Erythromycin			59.0	
		Ibuprofen			38.0	
		Naproxen			37.0	
		Sulfamethoxazole			40.0	
		Triclosan			44.0	
		Trimethoprim			25.0	

ZeeWeed® 500	GE Water and Process Technologies, Canada	Bisphenol A	A hollow fiber poly(vinylidene fluoride) membrane, outside-in, 0.345 bar	1.000 μg/L, three natural surface waters, Canada	1.5	Wray et al. (2014)
		Estriol			2.5	
		Estrone			4.0	
		Gemfibrozil			2.5	
		Carbamazepine			2.0	
PW	GE Osmonics, USA	Acetaminophen	MWCO: 20000 Da, polyethersulfone, cross-flow, 6 bar, pH = 7	500 μg/L, model wastewater	4.7	Acero et al. (2010)
		Metoprolol			8.1	
		Caffeine			2.1	
		Antipirine			2.3	
		Sulfamethoxazole			10.2	
		Flumequine			23.0	
		Ketorolac			6.1	
		Atrazine			17.9	
		Isoproturon			17.4	
		Hydroxybiphenyl			87.9	
		Diclofenac			26.5	
PLCC	Millipore, US	Estradiol	MWCO: 5000 Da, cellulose, 5 bar	0.100 μg/L, model wastewater	26.0	Neale and Schäfer (2012)
		Estrone			6.0	
		Testosterone			7.0	

MWCO molecular weight cutoff

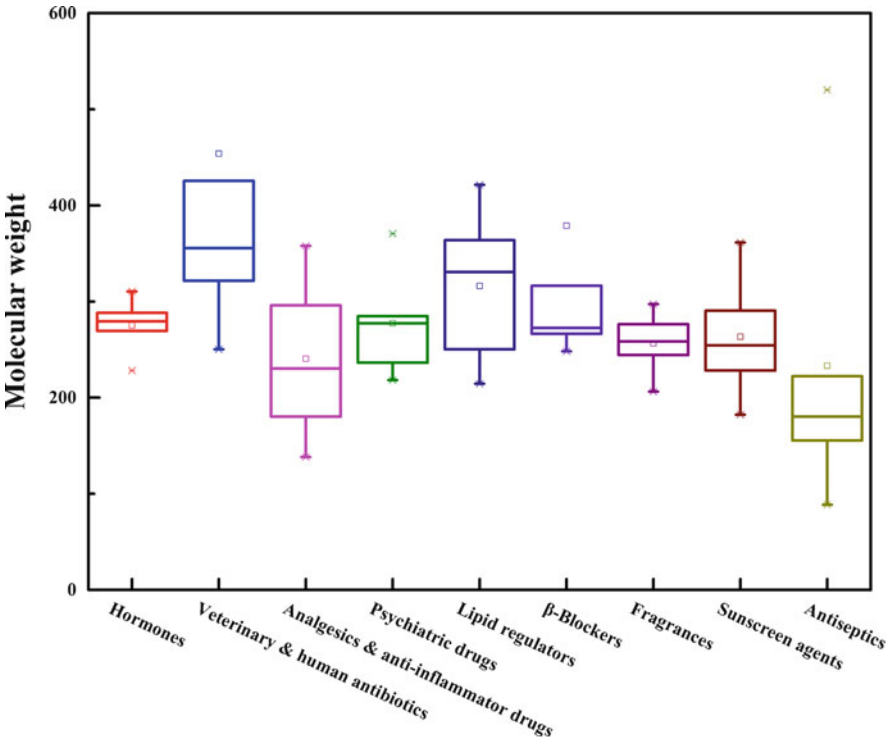

Fig. 5.1 Molecular weight range of pharmaceuticals and personal care products

removal rate was approximately 70%. However, the ultrafiltration membrane only showed good removal performance for a small part of the PPCPs (Acero et al. 2010; Sheng et al. 2016). For most PPCPs molecules, the removal rate via ultrafiltration is relatively low (Acero et al. 2010; Garcia-Ivars et al. 2017; Neale and Schäfer 2012; Sheng et al. 2016; Wray et al. 2014).

The removal rate of different PPCPs via the ultrafiltration membrane varies and is closely related to the characteristics of the PPCPs. As shown in Fig. 5.1, the molecular weights of most PPCPs range between 200 and 400 Da, which are relatively lower than the MWCO of the ultrafiltration membrane. Therefore, ultrafiltration membranes remove PPCPs mainly via hydrophobic adsorption rather than size exclusion. For example, Yoon et al. (2006) used ultrafiltration and nanofiltration membranes to treat wastewater containing PPCPs. Their results showed that the rejection rate of ultrafiltration was more than 40% for strong hydrophobic PPCPs, such as aromatic ring-containing carbon groups and chlorinated nonaromatic groups in the molecular structure; however, the rate was less than 25% for strong hydrophilic PPCPs containing the hydroxyl and amine group. Moreover, the adsorption capacity of ultrafiltration membranes is limited; thus, the removal rate of ultrafiltration membranes for PPCPs may be decreased as treatment time is prolonged

(Fonseca Couto et al. 2018). From a development perspective, the ultrafiltration membrane system is not the optimal solution for PPCPs removal.

Although a single ultrafiltration system cannot effectively remove all PPCPs, the removal efficiency of ultrafiltration combined with other processes is considerable. Sheng et al. (2016) combined ultrafiltration and powdered activated carbon, ultrafiltration, and coagulation to remove target pharmaceuticals (acetaminophen, caffeine, diazepam, diclofenac, erythromycin, ibuprofen, naproxen, sulfamethoxazole, triclosan, and trimethoprim). The results showed that the average removal efficiency of the pharmaceuticals from a single ultrafiltration system was only 29%. However, the average removal efficiency for an ultrafiltration and coagulation combined system was 33%, and a 90.3% removal efficiency was achieved for an ultrafiltration and powdered activated carbon combined in-line membrane system. Back et al. (2018) combined ultrafiltration and nonthermal plasma to degrade diclofenac, carbamazepine, and sulfamethoxazole in conventionally treated wastewater. The results also indicated that the ultrafiltration system alone could not effectively remove the three pharmaceuticals (46~67%), and the removal efficiency of the combined system was considerably improved (over 90%).

Thus, ultrafiltration membranes alone are not suitable for treating wastewater containing PPCPs molecules because the PPCPs molecules are removed only via hydrophobic adsorption of the ultrafiltration membranes and the adsorption capacity of the ultrafiltration membrane is limited. More importantly, the removal efficiency of a single ultrafiltration system to treat most PPCPs is not ideal. However, ultrafiltration membranes could be used to remove PPCPs in combination with other treatment processes, and the removal efficiency is considerable, which has been confirmed by many studies.

Reverse Osmosis Membranes

Removal efficiencies of PPCPs by reverse osmosis membrane are shown in Table 5.6. Reverse osmosis technology adds a certain pressure on the high concentration side of the solution, which can change the direction of osmosis to pressure water in the high-concentration solution to the other side of the membrane. Generally, reverse osmosis membranes are used in seawater desalination, electroplating wastewater treatment, and brackish water treatment. Reverse osmosis membranes are prepared via an interfacial polymerization process, and the selective layers of reverse osmosis membranes are relatively dense and considered nonporous. Normally, the MWCO of reverse osmosis is less than 150 Da, which is less than the molecular weight of most of the PPCPs shown in Fig. 5.1. For reverse osmosis membranes, the main rejection mechanism is size exclusion. According to this principle, reverse osmosis membranes could reject 100% of PPCPs molecules. Alonso et al. (2018) used a standard spiral-wound polyamide thin-film reverse osmosis membrane (RE2521-SHF) to remove ciprofloxacin from seawater. Eventually, ciprofloxacin removal rates were higher than 90% in all tests, and the maximum rejection value was 99.96%. Licona et al. (2018) evaluated the removal efficiencies

Table 5.6 Removal efficiencies of pharmaceuticals and personal care products by reverse osmosis membrane

Membrane	Company	Compounds	Membrane parameters and operating conditions	Feed liquid	Removal efficiency (%)	References
X-20	TriSep, USA	Estrone	Cross-flow, 10 bar, pH = 8	0.100 μg/L, surface water	> 90.0	Nghiem et al. (2004)
TFC-S					>85.0	
RE8040-FL	Woongjin Chemical, Korea	Caffeine	MWCO: 100–400 Da, polyamide, cross-flow, pH = 7	0.541 μg/L, model wastewater	72.3	Chon et al. (2013)
		Sulfamethoxazole		0.155 μg/L, model wastewater	100	
		Diclofenac		0.127 μg/L, model wastewater	100	
		Carbamazepine		0.106 μg/L, model wastewater	98.5	
		Atenolol		0.206 μg/L, model wastewater	87.3	
BW30	Dow Filmtec, USA	Carbamazepine	Cross-flow, pH = 7	Synthetic drinking water	84.3	Snyder et al. (2003)
		Acetaminophen	MWCO: ~100 Da, polyamide, cross-flow, 15 bar, pH = 5	10 mg/L, model wastewater	97.0	Licona et al. (2018)
		Ibuprofen			99.0	
		Diclofenac			98.0	
		Dipyrone			98.0	
		Caffeine			94.0	
		Acetaminophen	MWCO: ~100 Da, polyamide, cross-flow, 15.5 bar, pH = 8	130 μg/L, model water	94.3	Licona et al. (2018)
		BPA		52 μg/L, model water	98.4	
		Caffeine		610 μg/L, model water	98.4	
		Carbamazepine		43 μg/L, model water	98.2	
		Cotinine		200 μg/L, model water	97.8	
		Ethinyl estradiol-17α		15 μg/L, model water	97.9	
		Gemfibrozil		36 μg/L, model water	99.9	
		Ibuprofen		30 μg/L, model water	97.9	
		Progesterone		0.550 μg/L, model water	94.5	

		Sulfamethoxazole		160 μg/L, model water	92.5	
		Triclosan		5.7 μg/L, model water	98.5	
		Trimethoprim		140 μg/L, model water	87.1	
		Acetaminophen	MWCO <200 Da, polyamide, pH = 6	8–17 μg/l, model water	62.0	Yangali-Quintanilla et al. (2011)
		Carbamazepine			90.0	
		17β-Estradiol			87.0	
		Atrazine			87.0	
		17α-Ethynilestradiol			85.0	
		Sulfamethoxazole			85.0	
		Ketoprofen			83.0	
ESPA2	Hydranautics, USA	Phenacetine	MWCO <200 Da, polyamide, pH = 6		80.0	
		Caffeine			85.0	
		Carbamazepine			90.0	
		Bisphenol A			90.0	
		Ketoprofen			95.0	
		Ibuprofen			95.0	
		Gemfibrozil			95.0	
XLE	Dow Filmtec, USA	Carbamazepine	Polyamide, cross-flow, 6.9 bar, pH = 10	Model surface water	98.0	Lin and Lee (2014)
		Triclosan			97.0	
		Ibuprofen			99.0	
		Sulfadiazine			99.0	
		Sulfamethoxazole			99.0	
		Sulfamethazine			99.0	
RE2521-SHF	Toray Industries, Japan	Ciprofloxacin	Polyamide, cross-flow, 39.5 bar, pH = 7	Model seawater	99.96	Alonso et al. (2018)
LCF1-4040	Hydranautics, USA	Atenolol	Polyamide, cross-flow, 11 bar, pH = 7	1.044 μg/L, the secondary effluent of the sewage treatment plants, Spain	99.7	Urtiaga et al. (2013)

(continued)

Table 5.6 (continued)

Membrane	Company	Compounds	Membrane parameters and operating conditions	Feed liquid	Removal efficiency (%)	References
		Bezafibrate		0.164 μg/L, the secondary effluent of the sewage treatment plants, Spain	100	
		Caffeine		6.288 μg/L, the secondary effluent of the sewage treatment plants, Spain	99.9	
		Fenofibric acid		0.194 μg/L, the secondary effluent of the sewage treatment plants, Spain	100	
		Furosemide		0.811 μg/L, the secondary effluent of the sewage treatment plants, Spain	100	
		Gemfibrozil		1.035 μg/L, the secondary effluent of the sewage treatment plants, Spain	98.9	
		Hydrochlorothiazide		0.239 μg/L, the secondary effluent of the sewage treatment plants, Spain	96.2	
		Ibuprofen		0.574 μg/L, the secondary effluent of the sewage treatment plants, Spain	97.7	
		N-Acetyl-4-amino-antipyrine		4.472 μg/L, the secondary effluent of the sewage treatment plants, Spain	99.5	

		Naproxen		2.583 μg/L, the secondary effluent of the sewage treatment plants, Spain	99.4	
		Nicotine		0.075 μg/L, the secondary effluent of the sewage treatment plants, Spain	82.7	
		Ofloxacin		0.087 μg/L, the secondary effluent of the sewage treatment plants, Spain	95.4	
DOW 1812-50	Dow Filmtec, USA	Ibuprofen	MWCO <200 Da, polyamide, cross-flow, 8 bar	Artificial wastewater	>90.0	Yang et al. (2018b)
		Carbamazepine			>90.0	
BW30	Dow Filmtec, USA	Carbamazepine	Cross-flow, 6 bar	Membrane bioreactor effluents	100	Gur-Reznik et al. (2011)
SW30					100	
XLE					99.0	
BW30				Tap water	98.0	
SW30					98.0	
XLE					97.6	
X20	TriSep, USA	Acetaminophen	MWCO <200 Da, polyamide, cross-flow, 10 bar, pH = 8.1	Filtered (5 μm) Lake Ontario	94.5	Comerton et al. (2008)
		Bisphenol A			97.9	
		Caffeine			98.0	
		Carbamazepine			97.9	
		N,N diethyl-m-toluamide			98.6	
		Estriol			96.2	
		Estrone			98.1	
		Gemfibrozil			99.6	
LF10	Nitto Denko, Japan	Clofibric acid	MWCO: 100 Dda, cross-flow, 10 bar, pH = 7	Tertiary effluent	>90.0	Kimura et al. (2009)
		diclofenac			>95.0	
		Ketoprofen			>95.0	
		Mefenamic acid			>95.0	

(continued)

Table 5.6 (continued)

Membrane	Company	Compounds	Membrane parameters and operating conditions	Feed liquid	Removal efficiency (%)	References
		Carbamazepine			>85.0	
		Primidone			>85.0	
BW 30	Dow Filmtec, USA	Fluconazole	MWCO: 100 Da, polyamide, cross-flow, 10 bar, pH = 7	Fluconazole	100	Foureaux et al. (2019)
XLE	Dow Filmtec, USA	Sulfamethoxazole	MWCO: 100 Da, polyamide, cross-flow, 15 bar, pH = 6.96	Milli-Q water	98.9	Dolar et al. (2011)
		Trimethoprim			94.8	
		Ciprofloxacin			>99.9	
LFC-1	Hydranautics, USA	Sulfamethoxazole	MWCO: 100 Da, polyamide, cross-flow, 15 bar, pH = 6.96	Milli-Q water	97.2	
		Trimethoprim			98.3	
		Ciprofloxacin			>99.9	
BW30LE-440	Dow Filmtec, USA	Gemfibrozil	Polyamide, cross-flow	Groundwater	>50.0	Radjenović et al. (2008)
		Ketoprofen			>95.0	
		Carbamazepine			>98.0	
		Diclofenac			100	
		Mefenamic acid			>40.0	
		Acetaminophen			>85.0	
		Sulfamethoxazole			>100	
		Metoprolol			>80.0	
		Sotalol			>90.0	
DOW 1812-50	Dow Filmtec, USA	Sulfamethoxazole	MWCO <200 Da, cross-flow, 8 bar,	Real secondary effluent	>60.0	Li et al. (2018b)
		Carbamazepine			>75.0	
		Ibuprofen			>80.0	

MWCO molecular weight cutoff

of five pharmaceuticals (acetaminophen, ibuprofen, dipyrone, diclofenac, and caffeine) using nanofiltration (NF90) and reverse osmosis (BW30) membranes. The results showed that the rejection rate was higher than 98% for ibuprofen, dipyrone, and diclofenac via treatment with a reverse osmosis membrane. In addition, the reverse osmosis membrane could also remove approximately 92% of acetaminophen and caffeine from water. Similarly, Urtiaga et al. (2013) found that the removal rate of caffeine was as high as 99.5% if it was treated with reverse osmosis membranes (LCF1-4040).

Except for size exclusion, the mechanism for reverse osmosis removal of PPCPs is also related to the characteristics of the PPCPs and membrane materials. It has been recognized that reverse osmosis membranes remove PPCPs via three mechanisms, including size exclusion, electrostatic repulsion, and hydrophobicity adsorption (Lin 2017; Lin et al. 2014). For example, Yangali-Quintanilla et al. (2011) found that reverse osmosis membranes (BW30LE and ESPA2) effectively removed 18 kinds of PPCPs, and the average removal rate was 85% for neutral PPCPs and 99% for ionic PPCPs. Moreover, Lin et al. (Lin and Lee 2014) investigated the effect of pH on the removal of PPCPs by a reverse osmosis (XLE) membrane. The results showed that a change in pH changed the surface charge of the membrane and the ionic state of the PPCPs. If the reverse osmosis membranes and PPCPs have the same charge, the removal efficiencies are relatively high. In contrast, if the reverse osmosis membranes and PPCPs have opposite charges, the removal efficiencies are relatively lower. In addition, compounds (triclosan and ibuprofen) with the strongest hydrophobicity were found in the polyamide and polysulfone layers of reverse osmosis membranes after filtration of simulated PPCPs wastewater, indicating that PPCPs molecules could be rejected via the hydrophobicity adsorption effect. In addition to size exclusion, electrostatic exclusion and hydrophobicity adsorption also significantly contribute to the removal of PPCPs when using a reverse osmosis membrane.

Although a reverse osmosis membrane can remove most PPCPs from water, there are some limitations, such as low permeation, high energy consumption, poor membrane durability, membrane fouling, and high maintenance costs (Lee et al. 2012; Shrivastava et al. 2015; Wenten and Khoiruddin 2016). Because of these problems, reverse osmosis technology requires further research and optimization before it can be put into practical application to remove PPCPs from water.

Nanofiltration Membranes

Removal efficiencies of PPCPs by nanofiltration membrane are shown in Table 5.7. Nanofiltration membranes have a pore size of 0.5–2 nm and a MWCO of 200–1000 Da, and their separation properties are between those of ultrafiltration and reverse osmosis. More importantly, nanofiltration membranes show high permeation flux and rejection to multivalent salts and organic molecules simultaneously (Zhou et al. 2014). The molecular weight of most PPCPs is between the MWCO range of nanofiltration membranes, indicating that nanofiltration is suitable for

Table 5.7 Removal efficiencies of pharmaceuticals and personal care products by nanofiltration membrane

Membrane	Company	Compounds	Membrane parameters and operating conditions	Feed liquid	Removal efficiency (%)	References
HL	GE Osmonics, USA	Acetaminophen	MWCO: 150–300 Da, TF, cross-flow, 30 bar, pH = 9	500 μg/L, model wastewater	23.3	Acero et al. (2010)
		Metoprolol			100	
		Caffeine			85.8	
		Sulfamethoxazole			97.7	
		Flumequine			93.5	
		Ketorolac			95.8	
		Atrazine			91.3	
		Isoproturon			83.7	
		Hydroxybiphenyl			96.8	
		Diclofenac			96.4	
NF90	Dow Filmtec, USA	Acetaminophen	MWCO: 200–400 Da, polyamide, cross-flow, 15 bar, pH = 5	10 mg/L, model wastewater	91.0	Licona et al. (2018)
		Ibuprofen			98.0	
		Diclofenac			97.0	
		Dipyrone			87.0	
		Caffeine			93.0	
Hydranautics ESNA1-LF2-2540	Nitto Denko, Switzerland	Ibuprofen	Polyamide, cross-flow, 15 bar, pH = 6.48	Model wastewater	86.6	Vona et al. (2015)
		Diazepam			91.0	
		Acetaminophen			4.9	
		Sulfamethoxazole			70.8	
		Clonazepam			74.5	
		Diclofenac			68.7	
NF90	Dow Filmtec, USA	Carbamazepine	Polyamide, cross-flow, 6.9 bar, pH = 10	Model surface water	> 90.0	Lin and Lee (2014)
		Triclosan			> 90.0	
		Ibuprofen			> 95.0	
		Sulfadiazine			> 95.0	
		Sulfamethoxazole			> 95.0	
		Sulfamethazine			> 95.0	

NF270		Carbamazepine	Polyamide, cross-flow, 6.9 bar, pH = 10	Model surface water	15.0	
		Triclosan			45.0	
		Ibuprofen			> 90.0	
		Sulfadiazine			>90.0	
		Sulfamethoxazole			>85.0	
		Sulfamethazine			>90.0	
NTR 729HF	–	Atenolol	MWCO: 700 Da, polyvinyl alcohol/polyamides, cross-flow, 4 bar	Biologically treated sewage effluent after microfiltration and activated carbon	>95.0	Shanmuganathan et al. (2015)
		Caffeine			>95.0	
		Carbamazepine			>95.0	
		Diclofenac			>95.0	
		Gemfibrozil			>95.0	
		Naproxen			>95.0	
		Sulfamethoxazole			>95.0	
		Triclosan			>95.0	
		Trimethoprim			>95.0	
Modified cellulose acetate NF	–	Carbamazepine	Cellulose acetate, cross-flow, 6.9 bar	8.050 μg/L, the wastewater of Walkerton Clean Water Centre	23.4	Narbaitz et al. (2013)
		Sulfamethazine		5.240 μg/L, the wastewater of Walkerton Clean Water Centre	72.4	
		Ibuprofen		4.710 μg/L, the wastewater of Walkerton Clean Water Centre	80.4	
NF270	Dow Filmtec, USA	Carbamazepine	Polyamide, cross-flow, 6.9 bar	8.050 μg/L, the wastewater of Walkerton Clean Water Centre	69.0	
		Sulfamethazine		5.240 μg/L, the wastewater of Walkerton Clean Water Centre	88.4	
		Ibuprofen		4.710 μg/L, the wastewater of Walkerton Clean Water Centre	90.5	

(continued)

Table 5.7 (continued)

Membrane	Company	Compounds	Membrane parameters and operating conditions	Feed liquid	Removal efficiency (%)	References
NE40	Woongjin Chemical, Korea	Acetaminophen	MWCO: 1000 Da, polyamide, cross-flow, 3.5 bar	0.750 μg/L, primary effluents provided from Gwangju sewage treatment plants	13.0	Chon et al. (2012)
		Atenolol		0.030 μg/L, primary effluents provided from Gwangju sewage treatment plants	24.8	
		Carbamazepine		2.440 μg/L, primary effluents provided from Gwangju sewage treatment plants	41.1	
		Clopidogrel		0.010 μg/L, primary effluents provided from Gwangju sewage treatment plants	38.4	
		Diclofenac		0.140 μg/L, primary effluents provided from Gwangju sewage treatment plants	86.1	
		Dilantin		0.060 μg/L, primary effluents provided from Gwangju sewage treatment plants	40.1	
		Ibuprofen		0.110 μg/L, primary effluents provided from Gwangju sewage treatment plants	39.1	
		Iopromide		0.370 μg/L, primary effluents provided from Gwangju sewage treatment plants	38.1	
		Glimepiride		0.650 μg/L, primary effluents provided from Gwangju sewage treatment plants	52.7	

		Naproxen		0.820 μg/L, primary effluents provided from Gwangju sewage treatment plants	44.3	
		Sulfamethoxazole		0.520 μg/L, primary effluents provided from Gwangju sewage treatment plants	33.8	
NE70		Acetaminophen	MWCO: 350 Da, cross-flow, 3.5 bar	0.750 μg/L, primary effluents provided from Gwangju sewage treatment plants	16.0	
		Atenolol		0.030 μg/L, primary effluents provided from Gwangju sewage treatment plants	60.1	
		Carbamazepine		2.440 μg/L, primary effluents provided from Gwangju sewage treatment plants	72.5	
		Clopidogrel		0.010 μg/L, primary effluents provided from Gwangju sewage treatment plants	83.0	
		Diclofenac		0.140 μg/L, primary effluents provided from Gwangju sewage treatment plants	100	
		Dilantin		0.060 μg/L, primary effluents provided from Gwangju sewage treatment plants	65.4	
		Ibuprofen		0.110 μg/L, primary effluents provided from Gwangju sewage treatment plants	55.7	
		Iopromide		0.370 μg/L, primary effluents provided from Gwangju sewage treatment plants	61.9	

(continued)

Table 5.7 (continued)

Membrane	Company	Compounds	Membrane parameters and operating conditions	Feed liquid	Removal efficiency (%)	References
		Glimepiride		0.650 μg/L, primary effluents provided from Gwangju sewage treatment plants	78.5	
		Naproxen		0.820 μg/L, primary effluents provided from Gwangju sewage treatment plants	100	
		Sulfamethoxazole		0.520 μg/L, primary effluents provided from Gwangju sewage treatment plants	45.0	
NE90		Acetaminophen	MWCO: 210 Da, cross-flow, 3.5 bar	0.750 μg/L, primary effluents provided from Gwangju sewage treatment plants	31.3	
		Atenolol		0.030 μg/L, primary effluents provided from Gwangju sewage treatment plants	62.2	
		Carbamazepine		2.440 μg/L, primary effluents provided from Gwangju sewage treatment plants	82.3	
		Clopidogrel		0.010 μg/L, primary effluents provided from Gwangju sewage treatment plants	83.0	
		Diclofenac		0.140 μg/L, primary effluents provided from Gwangju sewage treatment plants	100	

		Dilantin		0.060 μg/L, primary effluents provided from Gwangju sewage treatment plants	78.0	
		Ibuprofen		0.110 μg/L, primary effluents provided from Gwangju sewage treatment plants	98.6	
		Iopromide		0.370 μg/L, primary effluents provided from Gwangju sewage treatment plants	74.0	
		Glimepiride		0.650 μg/L, primary effluents provided from Gwangju sewage treatment plants	88.1	
		Naproxen		0.820 μg/L, primary effluents provided from Gwangju sewage treatment plants	100	
		Sulfamethoxazole		0.520 μg/L, primary effluents provided from Gwangju sewage treatment plants	73.1	
NF90	Dow Filmtec, USA	Norfloxacin	MWCO: 200 Da, polyamide, cross-flow, 5–12 bar, pH = 6.5	50 mg/L, model pharmaceutical wastewater	99.5	de Souza et al. (2018)
NF270					93.6	
A tubular ceramic NF	Fraunhofer Institute, Germany	Dipyridamole	MWCO: 200 Da, ceramic, cross-flow, 0.8 bar, pH = 6.5	10 μg/L, model secondary wastewater effluents	>95.0	Fujioka et al. (2018)
		Tylosin			>70.0	
		Tetracycline			>95.0	
		Chlortetracycline			>70.0	
TS80	TriSep, USA	Acetaminophen	MWCO <200 Da, polyamide, cross-flow, 10.3 bar	Filtered (5 μm) Lake Ontario water	67.1	Comerton et al. (2008)
		Bisphenol A			93.9	
		Caffeine			100	
		Carbamazepine			97.3	

(continued)

Table 5.7 (continued)

Membrane	Company	Compounds	Membrane parameters and operating conditions	Feed liquid	Removal efficiency (%)	References
		N,N diethyl-m-toluamide			93.8	
		Estriol			96.8	
		Estrone			98.1	
		Gemfibrozil			98.4	
TS80	TriSep, USA	Salbutamol	MWCO: 200 Da, polyamide, cross-flow, pH = 7	Surface water in Weesperkarspel	>90.0	Verliefde et al. (2008)
		Pindolol			>90.0	
		Propranolol			>85.0	
		Atenolol			>90.0	
		Metoprolol			>90.0	
		Sotalol			>90.0	
		Phenazone			>90.0	
		Carbamazepine			>95.0	
		Ibuprofen			>95.0	
		Clofibric acid			>95.0	
		Fenoprofen			>95.0	
		Gemfibrozil			>95.0	
		Ketoprofen			>95.0	
		Diclofenac			>95.0	
		Bezafibrate			>95.0	
HL	GE Osmonics, USA	Salbutamol	MWCO: 150–300 Da, polyamide, cross-flow, pH = 7		>90.0	
		Pindolol			>75.0	
		Propranolol			>75.0	
		Atenolol			>85.0	

		Metoprolol			>90.0	
		Sotalol			>90.0	
		Phenazone			>85.0	
		Carbamazepine			>85.0	
		Ibuprofen			>95.0	
		Clofibric acid			>95.0	
		Gemfibrozil			>95.0	
		Ketoprofen			>95.0	
		Bezafibrate			>95.0	
PEI-NF	–	Primidone	MWCO: 500 Da, polyamide, cross-flow, 4 bar, pH = 7	Model wastewater	>85.0	Wei et al. (2018)
		Carbamazepine			>90.0	
		Sulfamethoxazole			>80.0	
		Atenolol			>95.0	
		Sulfadimidine			>90.0	
		Norfloxacin			>95.0	
PIP-NF		Primidone	MWCO: 520 Da, polyamide, cross-flow, 4 bar, pH = 7		>80.0	
		Carbamazepine			>85.0	
		Sulfamethoxazole			>90.0	
		Atenolol			>80.0	
		Sulfadimidine			>85.0	
		Norfloxacin			>90.0	
DF30	Beijing OriginWater Technology, China	Metoprolol	MWCO: 400 Da, cross-flow, 6.9 bar, pH = 6.7	Model wastewater	81.2	Xu et al. (2019)
		Trimethoprim			81.2	
		Carbamazepine			81.5	
		Chloramphenicol			85.7	
		Indomethacin			95.4	

(continued)

Table 5.7 (continued)

Membrane	Company	Compounds	Membrane parameters and operating conditions	Feed liquid	Removal efficiency (%)	References
NF270	Dow Filmtec, USA	Acetaminophen	MWCO: 230 Da, cross-flow, 8 bar, pH = 8	Sewage treatment plants effluent	>40.0	Azaïs et al. (2016)
		Carbamazepine			>90.0	
		Atenolol			>80.0	
NF90		Acetaminophen	MWCO: 150 Da, cross-flow, 8 bar, pH = 8		>90.0	
		Carbamazepine			>85.0	
		Atenolol			>85.0	
NF90	Dow Filmtec, USA	Sulfamethoxazole	Cross-flow, 8 bar, pH = 7	Model wastewater	>95.0	Nghiem and Hawkes (2007)
		Ibuprofen			>95.0	
		Carbamazepine			>95.0	
NF270		Sulfamethoxazole			>80.0	
		Ibuprofen			>90.0	
		Carbamazepine			>80.0	
$(HTCC/PDA)_3$ NF	–	Ibuprofen	MWCO: 935 Da, cross-flow, 5 bar, pH = 7	Model wastewater	89.9	Ouyang et al. (2019)
		Carbamazepine			87.3	
		Atenolol			76.2	
Cellulose acetate NF	–	Carbamazepine	Cross-flow, 10.3 bar	0.020 μg/L, aqueous solution	60.1	Rana et al. (2012)
		Ibuprofen			59.1	
		Sulfamethazine			85.2	
Macromolecule modified cellulose acetate NF	–	Carbamazepine			65.6	
		Ibuprofen			48.2	
		Sulfamethazine			84.1	

Hydrophilic SMM modified cellulose acetate NF	–	Carbamazepine			51.4	
		Ibuprofen			45.5	
		Sulfamethazine			78.6	
PIP-NF	–	Atenolol	Cross-flow, 5 bar, pH = 7.3.	50 μg/L, aqueous solution	>90.0	Liu et al. (2019)
		Trimethoprim			>95.0	
		Primidone			>95.0	
		Carbamazepine			>90.0	
		Sulfamethoxazole			>95.0	
		Indomethacin			>95.0	
M-TiO2	Inopor GmbH, Germany	Clofibric acid	MWCO: 550 Da, ceramic membrane, cross-flow, 10 bar, pH = 8.1	20 μg/L, aqueous solution	>65.0	Zhao et al. (2018)
		Sulfamethoxazole			>85.0	
		Indomethacin			>85.0	
LC2		Clofibric acid	MWCO: 440 Da, ceramic membrane, cross-flow, 10 bar, pH = 8.1.		>60.0	
		Sulfamethoxazole			>70.0	
		Indomethacin			>90.0	
NF270	Dow Filmtec, USA	Carbamazepine	Polyamide, cross-flow	Model wastewater	>30.0	Lin (2018)
		Ibuprofen			>90.0	
		Sulfadiazine			>75.0	
		Sulfamethoxazole			>80.0	
		Sulfamethazine			>70.0	
SPM modified NF270	–	Carbamazepine			>90.0	
		Ibuprofen			>85.0	
		Sulfadiazine			>90.0	
		Sulfamethoxazole			>90.0	
		Sulfamethazine			>90.0	

(continued)

Table 5.7 (continued)

Membrane	Company	Compounds	Membrane parameters and operating conditions	Feed liquid	Removal efficiency (%)	References
HEMA modified NF270	–	Carbamazepine			>90.0	
		Ibuprofen			>85.0	
		Sulfadiazine			>80.0	
		Sulfamethoxazole			>90.0	
		Sulfamethazine			>80.0	
NF90	Dow Filmtec, USA	Carbamazepine	Polyamide, cross-flow	Model wastewater	>40.0	Lin et al. (2018b)
		Ibuprofen			>95.0	
		Sulfadiazine			>95.0	
		Sulfamethoxazole			>95.0	
		Sulfamethazine			>95.0	
SPM modified NF90	–	Carbamazepine			>95.0	
		Ibuprofen			>95.0	
		Sulfadiazine			>95.0	
		Sulfamethoxazole			>95.0	
		Sulfamethazine			>95.0	
HEMA modified NF270	–	Carbamazepine			>95.0	
		Ibuprofen			>95.0	
		Sulfadiazine			>95.0	
		Sulfamethoxazole			>95.0	
		Sulfamethazine			>95.0	

MWCO molecular weight cutoff

PPCPs removal from water (Shanmuganathan et al. 2015; Zepon Tarpani and Azapagic 2018). Similar to reverse osmosis, the mechanisms of nanofiltration removal of PPCPs from water also include size exclusion, electrostatic exclusion, and hydrophobic adsorption. First, size exclusion is always regarded as one of the most important separation mechanisms for all polymer membranes to remove PPCPs (Comerton et al. 2008). Hydrophobic adsorption always exists because most materials used to prepare nanofiltration membranes are hydrophobic. Thus, it is recognized that hydrophobic adsorption can strongly contribute to the removal of PPCPs (Comerton et al. 2007; Yoon et al. 2007). Regarding electrostatic exclusion, this is determined by the charges on the surfaces of nanofiltration membranes and PPCPs molecules. Most nanofiltration membranes have negative or positive charges because of the dissociation of functional groups and the adsorption of ions from solutions, polyelectrolytes, ionic surfactants, and charged macromolecules (Schaep and Vandecasteele 2001). Regardless of hydrophobic adsorption, if PPCPs are electrically neutral, the size exclusion effect will play an important role in the rejection of PPCPs. If the surfaces of PPCPs have a charge, the synergistic effect of size exclusion and electrostatic exclusion will determine the removal rate of PPCPs. Chon et al. also found that the removal rates of negatively charged PPCPs (diclofenac, ibuprofen, glimepiride, naproxen, and sulfamethoxazole) were higher than those of nonionic PPCPs (acetaminophen, carbamazepine, clopidogrel, Dilantin, and iopromide) or positively charged PPCPs (atenolol) if these PPCPs were treated with a negatively charged nanofiltration membrane. In addition, nonionic and highly hydrophobic PPCPs (carbamazepine, clopidogrel, and Dilantin) could be considerably removed by the negatively charged nanofiltration membrane via the hydrophobic adsorption effect (Chon et al. 2012). Thus, the mechanism of nanofiltration removal of PPCPs changes with the nature of the membrane and target. Actually, the rejection rate of PPCPs is influenced by water quality, membrane characteristics, and other factors, which will be discussed below.

Compared with ultrafiltration membrane, because the MWCO range of nanofiltration includes almost all molecular weights of most PPCPs, the nanofiltration membrane process can considerably improve water quality, and the removal efficiencies of PPCPs are obviously better. Compared with reverse osmosis, nanofiltration not only has a good removal efficiency but also an improved water permeability under the same operating pressure, which means that nanofiltration is more efficient for dealing with PPCPs sewage with lower operating costs (Foureaux et al. 2019). With evolving nanofiltration technology, it is believed that the removal of PPCPs from water via this technology will be relevant in future water treatment.

5.3.2 *Affecting Factors of Pharmaceuticals and Personal Care Products Removal via Nanofiltration Membrane*

The factors that affect the efficiency of PPCPs removal via nanofiltration membrane are related to the PPCPs characteristics, the water quality conditions, and characteristics of the nanofiltration membranes. Regarding the characteristics of PPCPs, most believe that larger-molecular-weight PPCPs will experience higher removal efficiencies during the nanofiltration treatment process. In addition, many researchers believe that the nanofiltration membranes removal efficiencies of PPCPs are directly proportional to the hydrophobicity of PPCPs, indicating that more hydrophobic PPCPs exhibit a higher rejection (Comerton et al. 2008; Yoon et al. 2006). However, the type and content of PPCPs in the water environment are not controllable, and it is unrealistic to improve the removal efficiencies of PPCPs by changing their characteristics. Therefore, we can only improve the nanofiltration membranes removal efficiencies of PPCPs by controlling the water quality and the characteristics of the nanofiltration membranes. Water quality conditions currently are widely investigated, including the ionic strength, pH, temperature, and natural organic matter. The characteristics of the nanofiltration membrane that can affect their rejection rate include MWCO, charging performance, hydrophilicity/hydrophobicity, etc.

Water Quality Conditions

Ionic Strength

The presence of inorganic ions in solution will affect the surface charge of nanofiltration membrane. Inorganic ions in water can compress the thickness of the electrical double layer of nanofiltration membrane surface and neutralize and weaken the charge of the membrane surface (Luo and Wan 2011; Verliefde et al. 2008). For instance, Ca^{2+} can neutralize and weaken the negative charge of a polyamide nanofiltration membrane surface, leading to a decrease in the rejection for negatively charged PPCPs and an increase in the rejection for positively charged PPCPs. Additionally, the complexation of PPCPs with ions decreases the molecular polarity and shield-charged functional groups, leading to more PPCPs molecules being adsorbed onto the membrane surface (Wei et al. 2016). Wei et al. (2018) used a negatively charged nanofiltration membrane prepared via piperazine (PIP) and trimesoyl chloride to remove six typical pharmaceuticals (primidone, carbamazepine, sulfamethoxazole, atenolol, sulfadimidine, and norfloxacin) from water. Primidone, carbamazepine, atenolol, sulfadimidine, and norfloxacin exhibited a positive charge, and sulfamethoxazole exhibited a negative charge at $pH = 7$. The results showed that the rejection efficiency of negatively charged sulfamethoxazole ($pKa = 5.7$) decreased from 92% to 88% when the $CaCl_2$ concentration increased from 0 to 30 mmol/L in water ($pH = 7$). This was attributed to the adsorption of Ca^{2+} on the negatively charged membrane surface, which weakened the electrostatic exclusion. However, the rejection efficiency of the other pharmaceuticals all increased, especially for norfloxacin, whose rejection efficiency reached 94%. Azaïs and Xu also achieved similar results (Azaïs et al. 2016; Xu et al. 2019). Therefore, the ionic strength of the feed solution can be adjusted according to the actual situation to improve the removal efficiency when nanofiltration membranes are used to remove PPCPs.

pH

The membrane charge is usually expressed with the zeta potential. If the zeta potential is greater than zero, the membrane surface is positively charged, and conversely, the surface of the membranes is negatively charged. The number of charges is proportional to the absolute value of the zeta potential. However, the zeta potential has been confirmed to be closely related to the pH of the solution (Deshmukh and Childress 2001; Dukhin and Parlia 2012). Thus, the pH of the feed solution directly determines the charge properties and charge quantities of the membrane surface (Zhao and Jia 2012). Similarly, pH also affects the ionization state of PPCPs in solution because of the existence of the acid dissociation constant, pKa (Nghiem and Hawkes 2007; Wegst-Uhrich et al. 2014). Similar to the results reported by Vona et al. (2015), the removal efficiencies of ibuprofen (pKa = 4.91), diazepam (pKa = 3.3), and diclofenac (pKa = 4.15) treated with nanofiltration (polyamine membrane ESNA1-LF2-2540, negatively charged) increased from 80.51% to 91.38%, from 87.41% to 91.28%, and from 66.91% to 76.45%, respectively, as the wastewater pH increased from 6.11 to 8.5. This can be attributed to the amount of surface negative charge on the nanofiltration membrane, and the three PPCPs increased as the pH increased, which further enhanced the electrostatic exclusion effect between them. In addition, Licona et al. (2018) also found that the removal efficiencies of ibuprofen and diclofenac via polyamine membranes (NF90) were both over 95% when the pH in the feed solution was adjusted to 5. Thus, based on the electrostatic exclusion mechanism, adjusting the pH value in the feed solution and finding the optimum treatment condition during the nanofiltration membrane process are also a feasible way to improve the removal efficiencies of PPCPs in practical applications.

Temperature

Temperature has been regarded as one of the important factors affecting the operation of nanofiltration membranes; thus, the effect of temperature on PPCPs removal has also been studied by many researchers. First, the MWCO of nanofiltration membranes will increase as the temperatures increase (Arsuaga et al. 2008; Gonzalez et al. 2019; Tsuru et al. 2000). Second, the thermal energy generated by the temperature increase will increase the diffusivity of PPCPs and reduce the water viscosity. Both aspects make it is easy for PPCPs molecules and water to pass through the nanofiltration membrane. Wei et al. (2016) investigated the temperature influence for phthalate esters (PAEs) removed from water via nanofiltration hollow fiber membranes. With a temperature increase, the permeate flux of the nanofiltration clearly increased; however, the rejection rate of the PAEs did not obviously change.

The rejection of PAEs did not change because of the bucking effect between the permeating solute molecules and the permeating flux as the temperature increased.

In general, a high temperature will allow PPCPs to more easily pass through the nanofiltration membrane. Although some studies have shown that an increase of temperature can increase the permeation flux and improve the treatment efficiency while maintaining the rejection rate, increasing the temperature will result in a higher cost. Therefore, for temperature, it is essential to find the optimum value for actual treatment efficiency and energy consumption.

Natural Organic Matter

Natural organic matter not only can interact with PPCPs but also can affect the performance of nanofiltration membranes. First, natural organic matter can absorb PPCPs molecules, leading to an increase in the size of the PPCPs, and natural organic matter can absorb into nanofiltration membrane surface pores or even into the inner pores, resulting in narrowing of the membrane pores (Ogutverici et al. 2016; Schäfer et al. 2010). Both effects will enhance the size exclusion effect, leading to an increase in removal efficiencies of PPCPs. Second, according to the hydrophobic adsorption mechanism, natural organic matter, especially dissolved and highly hydrophobic organic matter, will preempt the adsorption sites with PPCPs on the membrane surface, resulting in a reduction in removal efficiencies of PPCPs (Lin 2017). The two conclusions contradict each other, and there is no definite explanation at present. However, natural organic matter is one of the major membrane contaminants that can reduce the service life of the membrane (Ye et al. 2018). Natural organic matter is inevitable in natural water, and the existence of natural organic matter can improve the removal efficiencies of PPCPs to some degree. However, regarding nanofiltration membrane service life, it is better to remove most natural organic matter before the water is introduced into the nanofiltration unit.

The removal efficiencies of PPCPs by nanofiltration membrane can be improved by adjusting the water quality conditions. However, nanofiltration membranes are more vulnerable, and the feed water must be pretreated before it can be treated by nanofiltration membranes to achieve the desired removal efficiencies for PPCPs and maintain a reasonable service life for nanofiltration membranes (Yuan and Kilduff 2018).

Characteristics of Nanofiltration Membrane

Molecular Weight Cutoff

Size exclusion plays an important role in the mechanism of PPCPs removal via nanofiltration membranes. PPCPs are expected to be widely retained via the physical sieving effect if their molecular weights are larger than the MWCO of the nanofiltration membranes. Interestingly, the molecular weights of most PPCPs are within 200–400 Da. Certainly, the rejection rate of PPCPs will significantly increase if the MWCO of the prepared nanofiltration membrane is approximately 200 Da or less. Yoon et al. (2007) found that a nanofiltration membrane with a MWCO of 200 Da could efficiently remove (>90%) most of the 52 PPCPs from synthetic solution and real surface water. Similarly, Radjenović et al. (2008) used a nanofiltration membrane whose MWCO was 200 Da in a full-scale drinking water treatment plant to treat groundwater. The results showed that all the PPCPs molecules in the feed solution were efficiently removed by the nanofiltration membrane and the rejection rate was higher than 85%. Normally the smaller the MWCO of the nanofiltration membrane, the higher the removal efficiencies of the PPCPs. However, the permeation flux of the nanofiltration membrane will decrease with a decrease in MWCO, indicating a lower treatment efficiency for wastewater and more energy consumption.

Charging Performance

It has been confirmed that the electrostatic exclusion considerably contributes to the removal of PPCPs by a nanofiltration membrane. Thus, it is feasible to use charged materials to prepare or modify the nanofiltration membrane to improve the rejection properties (Ji et al. 2012; Wu et al. 2016). Ouyang et al. (2019) prepared a dually charged polyelectrolyte multilayer nanofiltration membrane with an active skin layer on a polyethersulfone (PES) ultrafiltration membrane using the layer-by-layer technique using oppositely charged polyelectrolytes of polydopamine (PDA) and quaternate chitosan (HTCC) as the polyelectrolyte. The results indicated that the nanofiltration membranes removal efficiencies of PPCPs changed as the pH varied. When the pH of the feed solution was adjusted from 7 to 3, the negative charges on the nanofiltration membrane surface were transformed to positive charges, and the rejection rate of the positively charged atenolol increased from 76.22% to 81.67%. Conversely, when the pH of the feed solution was adjusted to 10, polydopamine with phenolic hydroxyl deprotonation caused more electronegativity on the surface of the membrane, enhancing the removal efficiency of the negatively charged ibuprofen from 89.85% to 94.50%. Rana et al. (2012) prepared a novel cellulose acetate (CA) nanofiltration membrane using charged surface-modifying macromolecules (CSMM) as additives. The results showed that the addition of CSMM increased the removal efficiencies of PPCPs because the negative charge density on the nanofiltration membrane surface increased. The addition of functional additives to improve the performance of nanofiltration membranes is also beneficial for improving the removal efficiencies of PPCPs. Many researchers have improved the nanofiltration membranes removal efficiencies of PPCPs by adding charged materials to increase the positive and negative charges on the nanofiltration membrane surface to enhance the electrostatic exclusion effect (Liu et al. 2019). Theory and results have indicated that improving the surface charge of the nanofiltration membrane is beneficial for the removal of PPCPs by nanofiltration membranes from water.

Hydrophilicity/Hydrophobicity

In actual nanofiltration application process, a higher permeation flux will result in a higher treatment efficiency and a lower required driving pressure (lowered energy consumption). Improving the hydrophilicity of the nanofiltration membrane surface has been extensively studied by researchers (Bagheripour et al. 2018; Yuan et al. 2018). In addition, the hydrophilicity of the membrane surface is conductive to improving the antifouling performance of the membrane surface and improving the economic practicability of the membrane.

Membrane fouling will certainly become more serious with use as time progresses, which is also a major problem for a practical application process. Many studies have found that the fouling of a nanofiltration membrane will cause a decrease in PPCPs rejection, especially for hydrophilic-ionized and hydrophobic-ionized compounds at low pH values because of the shield of the dominant electrostatic repulsion mechanism between the PPCPs and the nanofiltration membrane surface causing a cake-enhanced concentration polarization phenomenon (Lin 2017; Zhao et al. 2018). Therefore, to increase the efficiency of the nanofiltration membrane to remove PPCPs from water, antifouling performance has also been investigated by many researchers. For example, Lin (2018) used the concentration–polymerization–enhanced radical graft polarization method (3-sulfopropyl methacrylate potassium salt and 2-hydroxyethyl methacrylate) to in situ modify the nanofiltration membrane (NF270). The results showed that the silica fouling of the modified nanofiltration membrane was mitigated due to the increasing degree of grafting and hydrophilicity. In addition, the removal efficiencies of PPCPs by the modified nanofiltration membrane improved because the grafted polymer acted as an extra steric barrier layer, enhancing the electrostatic exclusion. An in situ radical graft polarization technique using monomers of 3-sulfopropyl methacrylate potassium salt (SPM) and 2-hydroxyethyl methacrylate (HEMA) was used to modify nanofiltration membrane (NF90) by Lin et al. (2018b). The results showed that the PPCPs removal by the modified nanofiltration membrane was higher than that by the virgin membrane after sodium alginate and sodium alginate + humic acid fouling, respectively. Additionally, the modified nanofiltration membrane exhibited considerably improved fouling resistance and an increased reversible fouling percentage, meaning that the practical and economic benefits of the modified membranes were obvious.

Compared with the water quality conditions and the characteristics of the nanofiltration membrane, the latter can be said to be an intrinsic factor for nanofiltration membrane removal of PPCPs. Research on membrane performance improvements has continued since the invention of the membrane, especially improvements in the MWCO, charging performance, and hydrophilicity/ hydrophobicity.

5.4 Conclusion

PPCPs are a unique group of persistently emerging environmental contaminants. Because the consumption of PPCPs is increasing and sewage treatment plants cannot effectively remove PPCPs, an increasing number of studies have confirmed the presence of various PPCPs in surface water and groundwater all over the world. However, some PPCPs are hardly removed in natural environments because of their unique physicochemical characteristics. Although there is no direct evidence regarding the impacts of PPCPs on humans, there are many studies that have investigated PPCPs, and it has been reported that even at trace concentrations, they can result in abnormal growth, gender disorders, inability to hunt, or even the death of aquatic organisms. These results highlight the risks associated with the inadvertent presence of PPCPs in the environment.

Membrane technology, as a new type of pollution-free and efficient water treatment technology, is promising for the removal of PPCPs from water. For ultrafiltration membranes, the removal efficiencies of PPCPs from water are dependent on hydrophobicity adsorption. For nanofiltration and reverse osmosis membranes, the removal efficiencies of PPCPs from water mainly depend on the size exclusion effect, while the electrostatic repulsion effect and hydrophobicity adsorption effect considerably contribute to PPCPs removal efficiencies. However, nanofiltration membranes are more suitable for the removal of PPCPs because of their MWCO range, which includes the molecular weight of most PPCPs, and relatively lower energy consumption.

According to the removal mechanism, the main factors affecting the removal efficiencies of PPCPs via nanofiltration membranes include the PPCPs characteristics, water quality conditions, and membrane characteristics. In general, the nanofiltration membrane can effectively remove PPCPs from water by optimizing the water quality and nanofiltration membrane characteristics. It is feasible to combine nanofiltration membranes with sewage treatment plants to improve the quality of the effluent and reduce the environmental risks brought on by PPCPs; however, related research needs to study this further.

Acknowledgments The authors gratefully acknowledge financial support from the Natural Science Foundation of Zhejiang Province (Grant No. LY19E030005), MOE Key Laboratory of Macromolecular Synthesis and Functionalization, Zhejiang University (2017MSF05). The authors also sincerely thank the Open Foundation from the Top Key Discipline of Environmental Science and Engineering, Zhejiang University of Technology (Grant No. 20150314).

References

Acero JL, Benitez FJ, Teva F, Leal AI (2010) Retention of emerging micropollutants from UP water and a municipal secondary effluent by ultrafiltration and nanofiltration. Chem Eng J. https://doi.org/10.1016/j.cej.2010.07.060

Alder AC, Schaffner C, Majewsky M, Klasmeier J, Fenner K (2010) Fate of β-blocker human pharmaceuticals in surface water: comparison of measured and simulated concentrations in the Glatt Valley Watershed, Switzerland. Water Res. https://doi.org/10.1016/j.watres.2009.10.002

Alonso JJS, El Kori N, Melián-Martel N, Del Río-Gamero B (2018) Removal of ciprofloxacin from seawater by reverse osmosis. J Environ Manag 217:337–345. https://doi.org/10.1016/j.jenvman.2018.03.108

Al-Qaim FF, Mussa ZH, Othman MR, Abdullah MP (2015) Removal of caffeine from aqueous solution by indirect electrochemical oxidation using a graphite-PVC composite electrode: a role of hypochlorite ion as an oxidising agent. J Hazard Mater. https://doi.org/10.1016/j.jhazmat.2015.07.007

Andrzejewski P, Kasprzyk-Hordern B, Nawrocki J (2008) N-nitrosodimethylamine (NDMA) formation during ozonation of dimethylamine-containing waters. Water Res. 42(4-5):863–870. https://doi.org/10.1016/j.watres.2007.08.032

Arsuaga JM, López-Muñoz MJ, Aguado J, Sotto A (2008) Temperature, pH and concentration effects on retention and transport of organic pollutants across thin-film composite nanofiltration membranes. Desalination. https://doi.org/10.1016/j.desal.2007.01.081

Azaïs A, Mendret J, Petit E, Brosillon S (2016) Evidence of solute-solute interactions and cake enhanced concentration polarization during removal of pharmaceuticals from urban wastewater by nanofiltration. Water Res 104:156–167. https://doi.org/10.1016/j.watres.2016.08.014

Back JO, Obholzer T, Winkler K, Jabornig S, Rupprich M (2018) Combining ultrafiltration and non-thermal plasma for low energy degradation of pharmaceuticals from conventionally treated wastewater. J Environ Chem Eng 6:7377–7385. https://doi.org/10.1016/j.jece.2018.07.047

Baghbanzadeh M, Rana D, Lan CQ, Matsuura T (2017) Zero thermal input membrane distillation, a zero-waste and sustainable solution for freshwater shortage. Appl Energy. https://doi.org/10.1016/j.apenergy.2016.10.142

Bagheripour E, Moghadassi AR, Hosseini SM, Ray MB, Parvizian F, Van der Bruggen B (2018) Highly hydrophilic and antifouling nanofiltration membrane incorporated with water-dispersible composite activated carbon/chitosan nanoparticles. Chem Eng Res Des. https://doi.org/10.1016/j.cherd.2018.02.027

Balakrishna K, Rath A, Praveenkumarreddy Y, Guruge KS, Subedi B (2017) A review of the occurrence of pharmaceuticals and personal care products in Indian water bodies. Ecotoxicol Environ Saf. https://doi.org/10.1016/j.ecoenv.2016.11.014

Behera SK, Kim HW, Oh JE, Park HS (2011) Occurrence and removal of antibiotics, hormones and several other pharmaceuticals in wastewater treatment plants of the largest industrial city of Korea. Sci Total Environ 409:4351–4360. https://doi.org/10.1016/j.scitotenv.2011.07.015

Bisesi JH, Bridges W, Klaine SJ (2014) Reprint of: effects of the antidepressant venlafaxine on fish brain serotonin and predation behavior. Aquat Toxicol 151:88–96. https://doi.org/10.1016/j.aquatox.2014.02.015

Blair B, Nikolaus A, Hedman C, Klaper R, Grundl T (2015) Evaluating the degradation, sorption, and negative mass balances of pharmaceuticals and personal care products during wastewater treatment. Chemosphere. https://doi.org/10.1016/j.chemosphere.2015.04.078

Boleda MR, Galceran MT, Ventura F (2011) Behavior of pharmaceuticals and drugs of abuse in a drinking water treatment plant (DWTP) using combined conventional and ultrafiltration and reverse osmosis (UF/RO) treatments. Environ Pollut 159:1584–1591. https://doi.org/10.1016/j.envpol.2011.02.051

Boy-Roura M, Mas-Pla J, Petrovic M, Gros M, Soler D, Brusi D, Menció A (2018) Towards the understanding of antibiotic occurrence and transport in groundwater: findings from the Baix

Fluvià alluvial aquifer (NE Catalonia, Spain). Sci Total Environ 612:1387–1406. https://doi.org/10.1016/j.scitotenv.2017.09.012
Cantwell MG, Katz DR, Sullivan JC, Shapley D, Lipscomb J, Epstein J, Juhl AR, Knudson C, O'Mullan GD (2018) Spatial patterns of pharmaceuticals and wastewater tracers in the Hudson River Estuary. Water Res. https://doi.org/10.1016/j.watres.2017.12.044
Carmona E, Andreu V, Picó Y (2014) Occurrence of acidic pharmaceuticals and personal care products in Turia River Basin: from waste to drinking water. Sci Total Environ. https://doi.org/10.1016/j.scitotenv.2014.02.085
Chang X, Meyer MT, Liu X, Zhao Q, Chen H, Chen J a, Qiu Z, Yang L, Cao J, Shu W (2010) Determination of antibiotics in sewage from hospitals, nursery and slaughter house, wastewater treatment plant and source water in Chongqing region of Three Gorge Reservoir in China. Environ Pollut. https://doi.org/10.1016/j.envpol.2009.12.034
Chew CM, Aroua MK, Hussain MA (2018) Advanced process control for ultrafiltration membrane water treatment system. J Clean Prod. https://doi.org/10.1016/j.jclepro.2018.01.075
Chollom MN, Pikwa K, Rathilal S, Pillay VL (2017) Fouling mitigation on a woven fibre microfiltration membrane for the treatment of raw water. S Afr J Chem Eng. https://doi.org/10.1016/j.sajce.2016.12.003
Chon K, Kyong Shon H, Cho J (2012) Membrane bioreactor and nanofiltration hybrid system for reclamation of municipal wastewater: removal of nutrients, organic matter and micropollutants. Bioresour Technol 122:181–188. https://doi.org/10.1016/j.biortech.2012.04.048
Chon K, Cho J, Shon HK (2013) A pilot-scale hybrid municipal wastewater reclamation system using combined coagulation and disk filtration, ultrafiltration, and reverse osmosis: removal of nutrients and micropollutants, and characterization of membrane foulants. Bioresour Technol. https://doi.org/10.1016/j.biortech.2013.03.198
Comerton AM, Andrews RC, Bagley DM, Yang P (2007) Membrane adsorption of endocrine disrupting compounds and pharmaceutically active compounds. J Membr Sci. https://doi.org/10.1016/j.memsci.2007.07.025
Comerton AM, Andrews RC, Bagley DM, Hao C (2008) The rejection of endocrine disrupting and pharmaceutically active compounds by NF and RO membranes as a function of compound and water matrix properties. J Membr Sci 313:323–335. https://doi.org/10.1016/j.memsci.2008.01.021
Dai G, Wang B, Huang J, Dong R, Deng S, Yu G (2015) Occurrence and source apportionment of pharmaceuticals and personal care products in the Beiyun River of Beijing, China. Chemosphere. https://doi.org/10.1016/j.chemosphere.2014.08.056
de Souza DI, Dottein EM, Giacobbo A, Siqueira Rodrigues MA, de Pinho MN, Bernardes AM (2018) Nanofiltration for the removal of norfloxacin from pharmaceutical effluent. J Environ Chem Eng 6:6147–6153. https://doi.org/10.1016/j.jece.2018.09.034
Deshmukh SS, Childress AE (2001) Zeta potential of commercial RO membranes: influence of source water type and chemistry. Desalination. https://doi.org/10.1016/S0011-9164(01)00357-5
Dodgen LK, Ueda A, Wu X, Parker DR, Gan J (2015) Effect of transpiration on plant accumulation and translocation of PPCP/EDCs. Environ Pollut 198:144–153. https://doi.org/10.1016/j.envpol.2015.01.002
Dolar D, Vuković A, Ašperger D, Košutić K (2011) Effect of water matrices on removal of veterinary pharmaceuticals by nanofiltration and reverse osmosis membranes. J Environ Sci. https://doi.org/10.1016/S1001-0742(10)60545-1
Dukhin AS, Parlia S (2012) Studying homogeneity and zeta potential of membranes using electro-acoustics. J Membr Sci. https://doi.org/10.1016/j.memsci.2012.05.053
Emnet P, Gaw S, Northcott G, Storey B, Graham L (2015) Personal care products and steroid hormones in the Antarctic coastal environment associated with two Antarctic research stations, McMurdo Station and Scott Base. Environ Res 136:331–342. https://doi.org/10.1016/j.envres.2014.10.019

Esplugas S, Bila DM, Krause LGT, Dezotti M (2007) Ozonation and advanced oxidation technologies to remove endocrine disrupting chemicals (EDCs) and pharmaceuticals and personal care products (PPCPs) in water effluents. J Hazard Mater. https://doi.org/10.1016/j.jhazmat.2007.07.073

Fernández-López C, Guillén-Navarro JM, Padilla JJ, Parsons JR (2016) Comparison of the removal efficiencies of selected pharmaceuticals in wastewater treatment plants in the region of Murcia, Spain. Ecol Eng. https://doi.org/10.1016/j.ecoleng.2016.06.093

Fonseca Couto C, Lange LC, Santos Amaral MC (2018) A critical review on membrane separation processes applied to remove pharmaceutically active compounds from water and wastewater. J Water Process Eng 26:156–175. https://doi.org/10.1016/j.jwpe.2018.10.010

Foureaux AFS, Reis EO, Lebron Y, Moreira V, Santos LV, Amaral MS, Lange LC (2019) Rejection of pharmaceutical compounds from surface water by nanofiltration and reverse osmosis. Sep Purif Technol 212:171–179. https://doi.org/10.1016/j.seppur.2018.11.018

Fram MS, Belitz K (2011) Occurrence and concentrations of pharmaceutical compounds in groundwater used for public drinking-water supply in California. Sci Total Environ 409:3409–3417. https://doi.org/10.1016/j.scitotenv.2011.05.053

Fujioka T, Hoang AT, Okuda T, Takeuchi H, Tanaka H, Nghiem LD (2018) Water reclamation using a ceramic nanofiltration membrane and surface flushing with ozonated water. Int J Environ Res Public Health 15. https://doi.org/10.3390/ijerph15040799

Gao J, O'Brien J, Du P, Li X, Ort C, Mueller JF, Thai PK (2016) Measuring selected PPCPs in wastewater to estimate the population in different cities in China. Sci Total Environ. https://doi.org/10.1016/j.scitotenv.2016.05.216

Gao Q, Blum KM, Gago-Ferrero P, Wiberg K, Ahrens L, Andersson PL (2019) Impact of on-site wastewater infiltration systems on organic contaminants in groundwater and recipient waters. Sci Total Environ. https://doi.org/10.1016/j.scitotenv.2018.10.016

Garcia-Ivars J, Durá-María J, Moscardó-Carreño C, Carbonell-Alcaina C, Alcaina-Miranda MI, Iborra-Clar MI (2017) Rejection of trace pharmaceutically active compounds present in municipal wastewaters using ceramic fine ultrafiltration membranes: effect of feed solution pH and fouling phenomena. Sep Purif Technol 175:58–71. https://doi.org/10.1016/j.seppur.2016.11.027

Gardner M, Comber S, Scrimshaw MD, Cartmell E, Lester J, Ellor B (2012) The significance of hazardous chemicals in wastewater treatment works effluents. Sci Total Environ. https://doi.org/10.1016/j.scitotenv.2012.07.086

Gmurek M, Olak-Kucharczyk M, Ledakowicz S (2017) Photochemical decomposition of endocrine disrupting compounds – a review. Chem Eng J. https://doi.org/10.1016/j.cej.2016.05.014

Gonzalez B, Heijman SGJ, Rietveld LC, van Halem D (2019) As(V) rejection by NF membranes using high temperature sources for drinking water production. Groundw Sustain Dev 8:198–204. https://doi.org/10.1016/j.gsd.2018.11.011

Grabicova K, Lindberg RH, Östman M, Grabic R, Randak T, Joakim Larsson DG, Fick J (2014) Tissue-specific bioconcentration of antidepressants in fish exposed to effluent from a municipal sewage treatment plant. Sci Total Environ. https://doi.org/10.1016/j.scitotenv.2014.04.052

Grabicova K, Grabic R, Fedorova G, Fick J, Cerveny D, Kolarova J, Turek J, Zlabek V, Randak T (2017) Bioaccumulation of psychoactive pharmaceuticals in fish in an effluent dominated stream. Water Res. https://doi.org/10.1016/j.watres.2017.08.018

Gur-Reznik S, Koren-Menashe I, Heller-Grossman L, Rufel O, Dosoretz CG (2011) Influence of seasonal and operating conditions on the rejection of pharmaceutical active compounds by RO and NF membranes. Desalination. https://doi.org/10.1016/j.desal.2011.04.029

Hossain A, Nakamichi S, Habibullah-Al-Mamun M, Tani K, Masunaga S, Matsuda H (2018) Occurrence and ecological risk of pharmaceuticals in river surface water of Bangladesh. Environ Res 165:258–266. https://doi.org/10.1016/j.envres.2018.04.030

Huerta B, Rodriguez-Mozaz S, Lazorchak J, Barcelo D, Batt A, Wathen J, Stahl L (2018) Presence of pharmaceuticals in fish collected from urban rivers in the U.S. EPA 2008–2009 National

Rivers and Streams Assessment. Sci Total Environ. https://doi.org/10.1016/j.scitotenv.2018.03.387

Ji YL, An QF, Zhao Q, Sun WD, Lee KR, Chen HL, Gao CJ (2012) Novel composite nanofiltration membranes containing zwitterions with high permeate flux and improved anti-fouling performance. J Membr Sci. https://doi.org/10.1016/j.memsci.2011.11.047

Jones OAH, Voulvoulis N, Lester JN (2005) Human pharmaceuticals in wastewater treatment processes. Crit Rev Environ Sci Technol. https://doi.org/10.1080/10643380590956966

Jurado A, Vàzquez-Suñé E, Carrera J, López de Alda M, Pujades E, Barceló D (2012) Emerging organic contaminants in groundwater in Spain: a review of sources, recent occurrence and fate in a European context. Sci Total Environ 440:82–94. https://doi.org/10.1016/j.scitotenv.2012.08.029

K'oreje KO, Kandie FJ, Vergeynst L, Abira MA, Van Langenhove H, Okoth M, Demeestere K (2018) Occurrence, fate and removal of pharmaceuticals, personal care products and pesticides in wastewater stabilization ponds and receiving rivers in the Nzoia Basin, Kenya. Sci Total Environ 637–638:336–348. https://doi.org/10.1016/j.scitotenv.2018.04.331

Kanakaraju D, Glass BD, Oelgemöller M (2018) Advanced oxidation process-mediated removal of pharmaceuticals from water: a review. J Environ Manag. https://doi.org/10.1016/j.jenvman.2018.04.103

Kapelewska J, Kotowska U, Karpińska J, Kowalczuk D, Arciszewska A, Świrydo A (2018) Occurrence, removal, mass loading and environmental risk assessment of emerging organic contaminants in leachates, groundwaters and wastewaters. Microchem J. https://doi.org/10.1016/j.microc.2017.11.008

Kasprzyk-Hordern B, Dinsdale RM, Guwy AJ (2008) The occurrence of pharmaceuticals, personal care products, endocrine disruptors and illicit drugs in surface water in South Wales, UK. Water Res. https://doi.org/10.1016/j.watres.2008.04.026

Kibuye FA, Gall HE, Elkin KR, Ayers B, Veith TL, Miller M, Jacob S, Hayden KR, Watson JE, Elliott HA (2019) Fate of pharmaceuticals in a spray-irrigation system: from wastewater to groundwater. Sci Total Environ 654:197–208. https://doi.org/10.1016/j.scitotenv.2018.10.442

Kim I, Tanaka H (2009) Photodegradation characteristics of PPCPs in water with UV treatment. Environ Int. https://doi.org/10.1016/j.envint.2009.01.003

Kimura K, Iwase T, Kita S, Watanabe Y (2009) Influence of residual organic macromolecules produced in biological wastewater treatment processes on removal of pharmaceuticals by NF/RO membranes. Water Res. https://doi.org/10.1016/j.watres.2009.05.042

Klavarioti M, Mantzavinos D, Kassinos D (2009) Removal of residual pharmaceuticals from aqueous systems by advanced oxidation processes. Environ Int. https://doi.org/10.1016/j.envint.2008.07.009

Kosma CI, Lambropoulou DA, Albanis TA (2014) Investigation of PPCPs in wastewater treatment plants in Greece: occurrence, removal and environmental risk assessment. Sci Total Environ. https://doi.org/10.1016/j.scitotenv.2013.07.044

Lapworth DJ, Baran N, Stuart ME, Ward RS (2012) Emerging organic contaminants in groundwater: a review of sources, fate and occurrence. Environ Pollut. https://doi.org/10.1016/j.envpol.2011.12.034

Lee CO, Howe KJ, Thomson BM (2012) Ozone and biofiltration as an alternative to reverse osmosis for removing PPCPs and micropollutants from treated wastewater. Water Res 46:1005–1014. https://doi.org/10.1016/j.watres.2011.11.069

Leijon J, Boström C (2018) Freshwater production from the motion of ocean waves – a review. Desalination. https://doi.org/10.1016/j.desal.2017.10.049

Leung HW, Minh TB, Murphy MB, Lam JCW, So MK, Martin M, Lam PKS, Richardson BJ (2012) Distribution, fate and risk assessment of antibiotics in sewage treatment plants in Hong Kong, South China. Environ Int. https://doi.org/10.1016/j.envint.2011.03.004

Li W, Shi Y, Gao L, Liu J, Cai Y (2015) Occurrence, fate and risk assessment of parabens and their chlorinated derivatives in an advanced wastewater treatment plant. J Hazard Mater. https://doi.org/10.1016/j.jhazmat.2015.06.060

Li W, Nanaboina V, Chen F, Korshin GV (2016) Removal of polycyclic synthetic musks and antineoplastic drugs in ozonated wastewater: quantitation based on the data of differential spectroscopy. J Hazard Mater. https://doi.org/10.1016/j.jhazmat.2015.10.035

Li A, Wu Z, Wang T, Hou S, Huang B, Kong X, Li X, Guan Y, Qiu R, Fang J (2018a) Kinetics and mechanisms of the degradation of PPCPs by zero-valent iron (Fe°) activated peroxydisulfate (PDS) system in groundwater. J Hazard Mater. https://doi.org/10.1016/j.jhazmat.2018.06.008

Li C, Yang Y, Liu Y, Hou L a (2018b) Removal of PhACs and their impacts on membrane fouling in NF/RO membrane filtration of various matrices. J Membr Sci 548:439–448. https://doi.org/10.1016/j.memsci.2017.11.032

Licona KPM, Geaquinto LR d O, Nicolini JV, Figueiredo NG, Chiapetta SC, Habert AC, Yokoyama L (2018) Assessing potential of nanofiltration and reverse osmosis for removal of toxic pharmaceuticals from water. J Water Process Eng 25:195–204. https://doi.org/10.1016/j.jwpe.2018.08.002

Lin YL (2017) Effects of organic, biological and colloidal fouling on the removal of pharmaceuticals and personal care products by nanofiltration and reverse osmosis membranes. J Membr Sci 542:342–351. https://doi.org/10.1016/j.memsci.2017.08.023

Lin YL (2018) In situ concentration-polarization-enhanced radical graft polymerization of NF270 for mitigating silica fouling and improving pharmaceutical and personal care product rejection. J Membr Sci 552:387–395. https://doi.org/10.1016/j.memsci.2018.02.033

Lin Y-L, Lee C-H (2014) Elucidating the rejection mechanisms of PPCPs by nanofiltration and reverse osmosis membranes. Ind Eng Chem Res. https://doi.org/10.1021/ie500114r

Lin YL, Chiou JH, Lee CH (2014) Effect of silica fouling on the removal of pharmaceuticals and personal care products by nanofiltration and reverse osmosis membranes. J Hazard Mater 277:102–109. https://doi.org/10.1016/j.jhazmat.2014.01.023

Lin H, Chen L, Li H, Luo Z, Lu J, Yang Z (2018a) Pharmaceutically active compounds in the Xiangjiang River, China: distribution pattern, source apportionment, and risk assessment. Sci Total Environ. https://doi.org/10.1016/j.scitotenv.2018.04.267

Lin YL, Tsai CC, Zheng NY (2018b) Improving the organic and biological fouling resistance and removal of pharmaceutical and personal care products through nanofiltration by using in situ radical graft polymerization. Sci Total Environ 635:543–550. https://doi.org/10.1016/j.scitotenv.2018.04.131

Liu C (2019) Enhancement of dewaterability and heavy metals solubilization of waste activated sludge conditioned by natural vanadium-titanium magnetite-activated peroxymonosulfate oxidation with rice husk. Chem Eng J. https://doi.org/10.1016/j.cej.2018.11.139

Liu JL, Wong MH (2013) Pharmaceuticals and personal care products (PPCPs): a review on environmental contamination in China. Environ Int 59:208–224. https://doi.org/10.1016/j.envint.2013.06.012

Liu X, Lu S, Guo W, Xi B, Wang W (2018) Antibiotics in the aquatic environments: a review of lakes, China. Sci Total Environ 627:1195–1208. https://doi.org/10.1016/j.scitotenv.2018.01.271

Liu Y l, Wang X m, Yang H w, Xie YF, Huang X (2019) Preparation of nanofiltration membranes for high rejection of organic micropollutants and low rejection of divalent cations. J Membr Sci 572:152–160. https://doi.org/10.1016/j.memsci.2018.11.013

Loos R, Carvalho R, António DC, Comero S, Locoro G, Tavazzi S, Paracchini B, Ghiani M, Lettieri T, Blaha L, Jarosova B, Voorspoels S, Servaes K, Haglund P, Fick J, Lindberg RH, Schwesig D, Gawlik BM (2013) EU-wide monitoring survey on emerging polar organic contaminants in wastewater treatment plant effluents. Water Res. https://doi.org/10.1016/j.watres.2013.08.024

López-Serna R, Jurado A, Vázquez-Suñé E, Carrera J, Petrović M, Barceló D (2013) Occurrence of 95 pharmaceuticals and transformation products in urban groundwaters underlying the metropolis of Barcelona, Spain. Environ Pollut 174:305–315. https://doi.org/10.1016/j.envpol.2012.11.022

Luo J, Wan Y (2011) Effect of highly concentrated salt on retention of organic solutes by nanofiltration polymeric membranes. J Membr Sci. https://doi.org/10.1016/j.memsci.2011.01.066

Luo Y, Guo W, Ngo HH, Nghiem LD, Hai FI, Zhang J, Liang S, Wang XC (2014) A review on the occurrence of micropollutants in the aquatic environment and their fate and removal during wastewater treatment. Sci Total Environ 473–474:619–641. https://doi.org/10.1016/j.scitotenv.2013.12.065

Ma C, Yu S, Shi W, Heijman SGJ, Rietveld LC (2013) Effect of different temperatures on performance and membrane fouling in high concentration PAC-MBR system treating micro-polluted surface water. Bioresour Technol. https://doi.org/10.1016/j.biortech.2013.02.025

Ma R, Wang B, Lu S, Zhang Y, Yin L, Huang J, Deng S, Wang Y, Yu G (2016) Characterization of pharmaceutically active compounds in Dongting Lake, China: occurrence, chiral profiling and environmental risk. Sci Total Environ 557–558:268–275. https://doi.org/10.1016/j.scitotenv.2016.03.053

Ma L, Liu Y, Zhang J, Yang Q, Li G, Zhang D (2018) Impacts of irrigation water sources and geochemical conditions on vertical distribution of pharmaceutical and personal care products (PPCPs) in the vadose zone soils. Sci Total Environ. https://doi.org/10.1016/j.scitotenv.2018.01.168

Mailler R, Gasperi J, Coquet Y, Deshayes S, Zedek S, Cren-Olivé C, Cartiser N, Eudes V, Bressy A, Caupos E, Moilleron R, Chebbo G, Rocher V (2014) Study of a large scale powdered activated carbon pilot: removals of a wide range of emerging and priority micropollutants from wastewater treatment plant effluents. Water Res. https://doi.org/10.1016/j.watres.2014.10.047

Martin Ruel S, Esperanza M, Choubert JM, Valor I, Budzinski H, Coquery M (2010) On-site evaluation of the efficiency of conventional and advanced secondary processes for the removal of 60 organic micropollutants. Water Sci Technol. https://doi.org/10.2166/wst.2010.989

McClellan K, Halden RU (2010) Pharmaceuticals and personal care products in archived U.S. biosolids from the 2001 EPA national sewage sludge survey. Water Res. https://doi.org/10.1016/j.watres.2009.12.032

Meffe R, de Bustamante I (2014) Emerging organic contaminants in surface water and groundwater: a first overview of the situation in Italy. Sci Total Environ. https://doi.org/10.1016/j.scitotenv.2014.02.053

Nakada N, Komori K, Suzuki Y, Konishi C, Houwa I, Tanaka H (2007) Occurrence of 70 pharmaceutical and personal care products in Tone River basin in Japan. Water Sci Technol. https://doi.org/10.2166/wst.2007.801

Nakada N, Hanamoto S, Jürgens MD, Johnson AC, Bowes MJ, Tanaka H (2017) Assessing the population equivalent and performance of wastewater treatment through the ratios of pharmaceuticals and personal care products present in a river basin: application to the River Thames basin, UK. Sci Total Environ. https://doi.org/10.1016/j.scitotenv.2016.09.180

Narbaitz RM, Rana D, Dang HT, Morrissette J, Matsuura T, Jasim SY, Tabe S, Yang P (2013) Pharmaceutical and personal care products removal from drinking water by modified cellulose acetate membrane: field testing. Chem Eng J 225:848–856. https://doi.org/10.1016/j.cej.2013.04.050

Neale PA, Schäfer AI (2012) Quantification of solute-solute interactions in steroidal hormone removal by ultrafiltration membranes. Sep Purif Technol. https://doi.org/10.1016/j.seppur.2012.02.011

Nghiem LD, Hawkes S (2007) Effects of membrane fouling on the nanofiltration of pharmaceutically active compounds (PhACs): mechanisms and role of membrane pore size. Sep Purif Technol. https://doi.org/10.1016/j.seppur.2007.04.002

Nghiem LD, Manis A, Soldenhoff K, Schäfer AI (2004) Estrogenic hormone removal from wastewater using NF/RO membranes. J Membr Sci. https://doi.org/10.1016/j.memsci.2003.12.034

Nie Y, Qiang Z, Zhang H, Ben W (2012) Fate and seasonal variation of endocrine-disrupting chemicals in a sewage treatment plant with A/A/O process. Sep Purif Technol. https://doi.org/10.1016/j.seppur.2011.01.030

Nikolaou A, Meric S, Fatta D (2007) Occurrence patterns of pharmaceuticals in water and wastewater environments. Anal Bioanal Chem. https://doi.org/10.1007/s00216-006-1035-8

Nödler K, Licha T, Barbieri M, Pérez S (2012) Evidence for the microbially mediated abiotic formation of reversible and non-reversible sulfamethoxazole transformation products during denitrification. Water Res. https://doi.org/10.1016/j.watres.2012.01.028

Ogutverici A, Yilmaz L, Yetis U, Dilek FB (2016) Triclosan removal by NF from a real drinking water source – effect of natural organic matter. Chem Eng J. https://doi.org/10.1016/j.cej.2015.07.065

Ouyang Z, Huang Z, Tang X, Xiong C, Tang M, Lu Y (2019) A dually charged nanofiltration membrane by pH-responsive polydopamine for pharmaceuticals and personal care products removal. Sep Purif Technol 211:90–97. https://doi.org/10.1016/j.seppur.2018.09.059

Papageorgiou M, Kosma C, Lambropoulou D (2016) Seasonal occurrence, removal, mass loading and environmental risk assessment of 55 pharmaceuticals and personal care products in a municipal wastewater treatment plant in Central Greece. Sci Total Environ. https://doi.org/10.1016/j.scitotenv.2015.11.047

Parolini M, Pedriali A, Binelli A (2013) Application of a biomarker response index for ranking the toxicity of five pharmaceutical and personal care products (PPCPs) to the bivalve Dreissena polymorpha. Arch Environ Contam Toxicol. https://doi.org/10.1007/s00244-012-9847-3

Peng X, Yu Y, Tang C, Tan J, Huang Q, Wang Z (2008) Occurrence of steroid estrogens, endocrine-disrupting phenols, and acid pharmaceutical residues in urban riverine water of the Pearl River Delta, South China. Sci Total Environ. https://doi.org/10.1016/j.scitotenv.2008.02.059

Peng X, Ou W, Wang C, Wang Z, Huang Q, Jin J, Tan J (2014) Occurrence and ecological potential of pharmaceuticals and personal care products in groundwater and reservoirs in the vicinity of municipal landfills in China. Sci Total Environ 490:889–898. https://doi.org/10.1016/j.scitotenv.2014.05.068

Pereira AMPT, Silva LJG, Laranjeiro CSM, Meisel LM, Lino CM, Pena A (2017) Human pharmaceuticals in Portuguese rivers: the impact of water scarcity in the environmental risk. Sci Total Environ. https://doi.org/10.1016/j.scitotenv.2017.07.200

Petrie B, Barden R, Kasprzyk-Hordern B (2014) A review on emerging contaminants in wastewaters and the environment: current knowledge, understudied areas and recommendations for future monitoring. Water Res. https://doi.org/10.1016/j.watres.2014.08.053

Pothitou P, Voutsa D (2008) Endocrine disrupting compounds in municipal and industrial wastewater treatment plants in Northern Greece. Chemosphere. https://doi.org/10.1016/j.chemosphere.2008.09.037

Prasse C, Schlüsener MP, Schulz R, Ternes TA (2010) Antiviral drugs in wastewater and surface waters: a new pharmaceutical class of environmental relevance? Environ Sci Technol. https://doi.org/10.1021/es903216p

Radjenović J, Petrović M, Ventura F, Barceló D (2008) Rejection of pharmaceuticals in nanofiltration and reverse osmosis membrane drinking water treatment. Water Res. https://doi.org/10.1016/j.watres.2008.05.020

Rana D, Scheier B, Narbaitz RM, Matsuura T, Tabe S, Jasim SY, Khulbe KC (2012) Comparison of cellulose acetate (CA) membrane and novel CA membranes containing surface modifying macromolecules to remove pharmaceutical and personal care product micropollutants from drinking water. J Membr Sci 409–410:346–354. https://doi.org/10.1016/j.memsci.2012.04.005

Reis-Santos P, Pais M, Duarte B, Caçador I, Freitas A, Vila Pouca AS, Barbosa J, Leston S, Rosa J, Ramos F, Cabral HN, Gillanders BM, Fonseca VF (2018) Screening of human and veterinary pharmaceuticals in estuarine waters: a baseline assessment for the Tejo estuary. Mar Pollut Bull. https://doi.org/10.1016/j.marpolbul.2018.08.036

Roberts J, Kumar A, Du J, Hepplewhite C, Ellis DJ, Christy AG, Beavis SG (2016) Pharmaceuticals and personal care products (PPCPs) in Australia's largest inland sewage treatment plant, and its contribution to a major Australian river during high and low flow. Sci Total Environ. https://doi.org/10.1016/j.scitotenv.2015.03.145

Sacher F, Lange FT, Brauch HJ, Blankenhorn I (2001) Pharmaceuticals in groundwaters: analytical methods and results of a monitoring program in Baden-Württemberg, Germany. J Chromatogr A. https://doi.org/10.1016/S0021-9673(01)01266-3

Schaep J, Vandecasteele C (2001) Evaluating the charge of nanofiltration membranes. J Membr Sci. https://doi.org/10.1016/S0376-7388(01)00368-4

Schäfer AI, Nghiem LD, Meier A, Neale PA (2010) Impact of organic matrix compounds on the retention of steroid hormone estrone by a "loose" nanofiltration membrane. Sep Purif Technol. https://doi.org/10.1016/j.seppur.2010.03.023

Schaider LA, Rudel RA, Ackerman JM, Dunagan SC, Brody JG (2014) Pharmaceuticals, perfluorosurfactants, and other organic wastewater compounds in public drinking water wells in a shallow sand and gravel aquifer. Sci Total Environ. https://doi.org/10.1016/j.scitotenv.2013.08.067

Schlüsener MP, Bester K (2006) Persistence of antibiotics such as macrolides, tiamulin and salinomycin in soil. Environ Pollut. https://doi.org/10.1016/j.envpol.2005.10.049

Shanmuganathan S, Johir MAH, Nguyen TV, Kandasamy J, Vigneswaran S (2015) Experimental evaluation of microfiltration-granular activated carbon (MF-GAC)/nano filter hybrid system in high quality water reuse. J Membr Sci 476:1–9. https://doi.org/10.1016/j.memsci.2014.11.009

Sharma A, Ahmad J, Flora SJS (2018) Application of advanced oxidation processes and toxicity assessment of transformation products. Environ Res. https://doi.org/10.1016/j.envres.2018.07.010

Sharma BM, Bečanová J, Scheringer M, Sharma A, Bharat GK, Whitehead PG, Klánová J, Nizzetto L (2019) Health and ecological risk assessment of emerging contaminants (pharmaceuticals, personal care products, and artificial sweeteners) in surface and groundwater (drinking water) in the Ganges River Basin, India. Sci Total Environ 646:1459–1467. https://doi.org/10.1016/j.scitotenv.2018.07.235

Sheng C, Nnanna AGA, Liu Y, Vargo JD (2016) Removal of Trace Pharmaceuticals from Water using coagulation and powdered activated carbon as pretreatment to ultrafiltration membrane system. Sci Total Environ 550:1075–1083. https://doi.org/10.1016/j.scitotenv.2016.01.179

Shrivastava A, Rosenberg S, Peery M (2015) Energy efficiency breakdown of reverse osmosis and its implications on future innovation roadmap for desalination. Desalination 368:181–192. https://doi.org/10.1016/j.desal.2015.01.005

Snyder SA, Westerhoff P, Yoon Y, Sedlak DL (2003) Pharmaceuticals, personal care products, and endocrine disruptors in water: implications for the water industry. Environ Eng Sci. https://doi.org/10.1089/109287503768335931

Spongberg AL, Witter JD, Acuña J, Vargas J, Murillo M, Umaña G, Gómez E, Perez G (2011) Reconnaissance of selected PPCP compounds in Costa Rican surface waters. Water Res 45:6709–6717. https://doi.org/10.1016/j.watres.2011.10.004

Stamatis NK, Konstantinou IK (2013) Occurrence and removal of emerging pharmaceutical, personal care compounds and caffeine tracer in municipal sewage treatment plant in Western Greece. J Environ Sci Heal – Part B Pestic Food Contam Agric Wastes. https://doi.org/10.1080/03601234.2013.781359

Stuart M, Lapworth D, Crane E, Hart A (2012) Review of risk from potential emerging contaminants in UK groundwater. Sci Total Environ 416:1–21. https://doi.org/10.1016/j.scitotenv.2011.11.072

Subedi B, Balakrishna K, Sinha RK, Yamashita N, Balasubramanian VG, Kannan K (2015) Mass loading and removal of pharmaceuticals and personal care products, including psychoactive and illicit drugs and artificial sweeteners, in five sewage treatment plants in India. J Environ Chem Eng 3:2882–2891. https://doi.org/10.1016/j.jece.2015.09.031

Sui Q, Cao X, Lu S, Zhao W, Qiu Z, Yu G (2015) Occurrence, sources and fate of pharmaceuticals and personal care products in the groundwater: a review. Emerg Contam 1:14–24. https://doi.org/10.1016/j.emcon.2015.07.001

Tang J, Shi T, Wu X, Cao H, Li X, Hua R, Tang F, Yue Y (2015) The occurrence and distribution of antibiotics in Lake Chaohu, China: seasonal variation, potential source and risk assessment. Chemosphere. https://doi.org/10.1016/j.chemosphere.2014.11.032

Tappin AD, Loughnane JP, McCarthy AJ, Fitzsimons MF (2016) Unexpected removal of the most neutral cationic pharmaceutical in river waters. Environ Chem Lett 14:455–465. https://doi.org/10.1007/s10311-016-0582-2

Tarpani RRZ, Azapagic A (2018) A methodology for estimating concentrations of pharmaceuticals and personal care products (PPCPs) in wastewater treatment plants and in freshwaters. Sci Total Environ. https://doi.org/10.1016/j.scitotenv.2017.12.059

Terzić S, Senta I, Ahel M, Gros M, Petrović M, Barcelo D, Müller J, Knepper T, Martí I, Ventura F, Jovančić P, Jabučar D (2008) Occurrence and fate of emerging wastewater contaminants in Western Balkan Region. Sci Total Environ. https://doi.org/10.1016/j.scitotenv.2008.03.003

Tixier C, Singer HP, Oellers S, Müller SR (2003) Occurrence and fate of carbamazepine, clofibric acid, diclofenac, ibuprofen, ketoprofen, and naproxen in surface waters. Environ Sci Technol. https://doi.org/10.1021/es025834r

Tran N, Drogui P, Brar SK (2015) Sonochemical techniques to degrade pharmaceutical organic pollutants. Environ Chem Lett 13:251–268. https://doi.org/10.1007/s10311-015-0512-8

Tsui MMP, Leung HW, Lam PKS, Murphy MB (2014) Seasonal occurrence, removal efficiencies and preliminary risk assessment of multiple classes of organic UV filters in wastewater treatment plants. Water Res. https://doi.org/10.1016/j.watres.2014.01.014

Tsuru T, Izumi S, Yoshioka T, Asaeda M (2000) Temperature effect on transport performance by inorganic nanofiltration membranes. AICHE J. https://doi.org/10.1002/aic.690460315

Urtiaga AM, Pérez G, Ibáñez R, Ortiz I (2013) Removal of pharmaceuticals from a WWTP secondary effluent by ultrafiltration/reverse osmosis followed by electrochemical oxidation of the RO concentrate. Desalination 331:26–34. https://doi.org/10.1016/j.desal.2013.10.010

Verliefde ARD, Cornelissen ER, Heijman SGJ, Verberk JQJC, Amy GL, Van Der Bruggen B, Van Dijk JC (2008) The role of electrostatic interactions on the rejection of organic solutes in aqueous solutions with nanofiltration. J Membr Sci. https://doi.org/10.1016/j.memsci.2008.05.022

Vita NA, Brohem CA, Canavez ADPM, Oliveira CFS, Kruger O, Lorencini M, Carvalho CM (2018) Parameters for assessing the aquatic environmental impact of cosmetic products. Toxicol Lett. https://doi.org/10.1016/j.toxlet.2018.01.015

Vona A, di Martino F, Garcia-Ivars J, Picó Y, Mendoza-Roca JA, Iborra-Clar MI (2015) Comparison of different removal techniques for selected pharmaceuticals. J Water Process Eng 5:48–57. https://doi.org/10.1016/j.jwpe.2014.12.011

Vymazal J, Březinová T, Koželuh M (2015) Occurrence and removal of estrogens, progesterone and testosterone in three constructed wetlands treating municipal sewage in the Czech Republic. Sci Total Environ. https://doi.org/10.1016/j.scitotenv.2015.07.077

Wang D, Sui Q, Lu SG, Zhao WT, Qiu ZF, Miao ZW, Yu G (2014) Occurrence and removal of six pharmaceuticals and personal care products in a wastewater treatment plant employing anaerobic/anoxic/aerobic and UV processes in Shanghai, China. Environ Sci Pollut Res 21:4276–4285. https://doi.org/10.1007/s11356-013-2363-9

Wang Z, Zhang XH, Huang Y, Wang H (2015) Comprehensive evaluation of pharmaceuticals and personal care products (PPCPs) in typical highly urbanized regions across China. Environ Pollut. https://doi.org/10.1016/j.envpol.2015.04.021

Wang C, Qian Y, Zhang X, Chen F, Zhang Q, Li Z, Zhao M (2016) A metabolomic study of fipronil for the anxiety-like behavior in zebrafish larvae at environmentally relevant levels. Environ Pollut 211:252–258. https://doi.org/10.1016/j.envpol.2016.01.016

Wegst-Uhrich SR, Navarro DAG, Zimmerman L, Aga DS (2014) Assessing antibiotic sorption in soil: a literature review and new case studies on sulfonamides and macrolides. Chem Cent J. https://doi.org/10.1186/1752-153X-8-5

Wei X, Shi Y, Fei Y, Chen J, Lv B, Chen Y, Zheng H, Shen J, Zhu L (2016) Removal of trace phthalate esters from water by thin-film composite nanofiltration hollow fiber membranes. Chem Eng J 292:382–388. https://doi.org/10.1016/j.cej.2016.02.037

Wei X, Bao X, Wu J, Li C, Shi Y, Chen J, Lv B, Zhu B (2018) Typical pharmaceutical molecule removal behavior from water by positively and negatively charged composite hollow fiber nanofiltration membranes. RSC Adv 8:10396–10408. https://doi.org/10.1039/C8RA00519B

Wenten IG, Khoiruddin (2016) Reverse osmosis applications: prospect and challenges. Desalination 391:112–125. https://doi.org/10.1016/j.desal.2015.12.011

Wray HE, Andrews RC, Bérubé PR (2014) Surface shear stress and retention of emerging contaminants during ultrafiltration for drinking water treatment. Sep Purif Technol. https://doi.org/10.1016/j.seppur.2013.11.003

Wu C, Huang X, Witter JD, Spongberg AL, Wang K, Wang D, Liu J (2014) Occurrence of pharmaceuticals and personal care products and associated environmental risks in the central and lower Yangtze river, China. Ecotoxicol Environ Saf 106:19–26. https://doi.org/10.1016/j.ecoenv.2014.04.029

Wu C, Liu S, Wang Z, Zhang J, Wang X, Lu X, Jia Y, Hung WS, Lee KR (2016) Nanofiltration membranes with dually charged composite layer exhibiting super-high multivalent-salt rejection. J Membr Sci. https://doi.org/10.1016/j.memsci.2016.05.033

Xing J, Wang H, Cheng X, Tang X, Luo X, Wang J, Wang T, Li G, Liang H (2018) Application of low-dosage UV/chlorine pre-oxidation for mitigating ultrafiltration (UF) membrane fouling in natural surface water treatment. Chem Eng J. https://doi.org/10.1016/j.cej.2018.03.052

Xu R, Zhang P, Wang Q, Wang X, Yu K, Xue T, Wen X (2019) Influences of multi influent matrices on the retention of PPCPs by nanofiltration membranes. Sep Purif Technol 212:299–306. https://doi.org/S1383586618329733

Yang Y, Ok YS, Kim KH, Kwon EE, Tsang YF (2017) Occurrences and removal of pharmaceuticals and personal care products (PPCPs) in drinking water and water/sewage treatment plants: a review. Sci Total Environ 596–597:303–320. https://doi.org/10.1016/j.scitotenv.2017.04.102

Yang M, Liu S, Hu L, Zhan J, Lei P, Wu M (2018a) Effects of the antidepressant, mianserin, on early development of fish embryos at low environmentally relevant concentrations. Ecotoxicol Environ Saf 150:144–151. https://doi.org/10.1016/j.ecoenv.2017.12.024

Yang Y, Li C, Hou L an (2018b) Impact of dead cells on biofouling and pharmaceutically active compounds retention by NF/RO membranes. Chem Eng J. https://doi.org/10.1016/j.cej.2017.12.081

Yangali-Quintanilla V, Maeng SK, Fujioka T, Kennedy M, Li Z, Amy G (2011) Nanofiltration vs. reverse osmosis for the removal of emerging organic contaminants in water reuse. Desalin Water Treat 34:50–56. https://doi.org/10.5004/dwt.2011.2860

Yao M, Yan D, Kabat P, Huang H, Hutjes RWA, Werners SE (2016) Analysing monthly sectorial water use and its influence on salt intrusion induced water shortage in urbanized deltas. Sustain Cities Soc. https://doi.org/10.1016/j.scs.2016.06.020

Yao L, Wang Y, Tong L, Deng Y, Li Y, Gan Y, Guo W, Dong C, Duan Y, Zhao K (2017) Occurrence and risk assessment of antibiotics in surface water and groundwater from different depths of aquifers: a case study at Jianghan Plain, central China. Ecotoxicol Environ Saf 135:236–242. https://doi.org/10.1016/j.ecoenv.2016.10.006

Yao L, Zhao JL, Liu YS, Zhang QQ, Jiang YX, Liu S, Liu WR, Yang YY, Ying GG (2018) Personal care products in wild fish in two main Chinese rivers: bioaccumulation potential and human health risks. Sci Total Environ 621:1093–1102. https://doi.org/10.1016/j.scitotenv.2017.10.117

Ye W, Bernstein NJ, Lin J, Jordens J, Zhao S, Tang CY, Van der Bruggen B (2018) Theoretical and experimental study of organic fouling of loose nanofiltration membrane. J Taiwan Inst Chem Eng. https://doi.org/10.1016/j.jtice.2018.08.029

Yoon Y, Westerhoff P, Snyder SA, Wert EC (2006) Nanofiltration and ultrafiltration of endocrine disrupting compounds, pharmaceuticals and personal care products. J Membr Sci 270:88–100. https://doi.org/10.1016/j.memsci.2005.06.045

Yoon Y, Westerhoff P, Snyder SA, Wert EC, Yoon J (2007) Removal of endocrine disrupting compounds and pharmaceuticals by nanofiltration and ultrafiltration membranes. Desalination 202:16–23. https://doi.org/10.1016/j.desal.2005.12.033

Yu H, Cao W (2016) Assessment of pharmaceutical and personal care products (PPCPs) of Dalong Lake in Xuzhou by concentration monitoring and bio-effects monitoring process. Environ Toxicol Pharmacol 43:209–215. https://doi.org/10.1016/j.etap.2016.03.015

Yu Y, Wu L, Chang AC (2013) Seasonal variation of endocrine disrupting compounds, pharmaceuticals and personal care products in wastewater treatment plants. Sci Total Environ. https://doi.org/10.1016/j.scitotenv.2012.10.001

Yuan Y, Kilduff JE (2018) Mass transport modeling of natural organic matter (NOM) and salt during Nanofiltration of inorganic colloid-NOM mixtures. Desalination. https://doi.org/10.1016/j.desal.2017.12.002

Yuan S, Li J, Zhu J, Volodine A, Li J, Zhang G, Van Puyvelde P, Van der Bruggen B (2018) Hydrophilic nanofiltration membranes with reduced humic acid fouling fabricated from copolymers designed by introducing carboxyl groups in the pendant benzene ring. J Membr Sci. https://doi.org/10.1016/j.memsci.2018.06.038

Zepon Tarpani RR, Azapagic A (2018) Life cycle environmental impacts of advanced wastewater treatment techniques for removal of pharmaceuticals and personal care products (PPCPs). J Environ Manag 215:258–272. https://doi.org/10.1016/j.jenvman.2018.03.047

Zhang Y, Fu Q (2018) Algal fouling of microfiltration and ultrafiltration membranes and control strategies: a review. Sep Purif Technol. https://doi.org/10.1016/j.seppur.2018.04.040

Zhang Q, Ji C, Yan L, Lu M, Lu C, Zhao M (2016) The identification of the metabolites of chlorothalonil in zebrafish (Danio rerio) and their embryo toxicity and endocrine effects at environmentally relevant levels. Environ Pollut 218:8–15. https://doi.org/10.1016/j.envpol.2016.08.026

Zhang Q, Zhang Y, Du J, Zhao M (2017) Environmentally relevant levels of Λ-cyhalothrin, fenvalerate, and permethrin cause developmental toxicity and disrupt endocrine system in zebrafish (Danio rerio) embryo. Chemosphere 185:1173–1180. https://doi.org/10.1016/j.chemosphere.2017.07.091

Zhao K, Jia J (2012) Dielectric analysis of multi-layer structure of nanofiltration membrane in electrolyte solutions: ion penetrability, selectivity, and influence of pH. J Colloid Interface Sci 386:16–27. https://doi.org/10.1016/j.jcis.2012.07.022

Zhao Y ying, Wang X mao, Yang, H wei, Xie Y feng F (2018) Effects of organic fouling and cleaning on the retention of pharmaceutically active compounds by ceramic nanofiltration membranes. J Membr Sci. https://doi.org/10.1016/j.memsci.2018.06.047

Zhou C, Shi Y, Sun C, Yu S, Liu M, Gao C (2014) Thin-film composite membranes formed by interfacial polymerization with natural material sericin and trimesoyl chloride for nanofiltration. J Membr Sci. https://doi.org/10.1016/j.memsci.2014.08.033

Zuccato E, Castiglioni S, Bagnati R, Chiabrando C, Grassi P, Fanelli R (2008) Illicit drugs, a novel group of environmental contaminants. Water Res. https://doi.org/10.1016/j.watres.2007.09.010

Chapter 6
Hydrodynamic Enhancement by Dynamic Filtration for Environmental Applications

Xiaomin Xie, Wenxiang Zhang, Luhui Ding, Philippe Schmitz, and Luc Fillaudeau

Contents

Abstract In this communication, we reviewed various dynamic filtration (DF) modules and their hydrodynamics and applications in wastewater treatment. Firstly, the configuration, operation parameter, and antifouling capacity for different dynamic filtration modules including rotating disk/rotor, rotating membrane, and

X. Xie
Institute of Environmental & Ecological Engineering, School of Environmental Science of Engineering, Guangdong University of Technology, Guangzhou, China

W. Zhang (✉)
Institute of Environmental & Ecological Engineering, School of Environmental Science of Engineering, Guangdong University of Technology, Guangzhou, China

Department of Civil and Environmental Engineering, Faculty of Science and Technology, University of Macau, Macau, China

L. Ding
Sorbonne University, Université de Technologire de Compiègne, ESCOM, EA 4297 TIMR, Centre de Recherch Royallieu, CS 60319, Compiègne Cedex, France

P. Schmitz · L. Fillaudeau
TBI, Université de Toulouse, CNRS UMR5504, INRA UMR792, INSA, 31055, 135, avenue de Rangueil, Toulouse, France

FERMAT, Université de Toulouse, CNRS, INPT, INSA, UPS, Toulouse, France

Z. Zhang et al. (eds.), *Membranes for Environmental Applications*, Environmental Chemistry for a Sustainable World 42, https://doi.org/10.1007/978-3-030-33978-4_6

vibratory systems were introduced. However, local hydrodynamics which could better diagnose the filtration performance were often neglected by the lack of knowledge on local measurement. To complete the knowledge on hydrodynamics, experiments were thus carried out by particle image velocimetry (PIV) technique. The velocity field and velocity profile were presented. Computational fluid dynamics (CFD) simulation was developed with the same working condition as PIV experiments and further discussed the velocity field. Moreover, the applications of dynamic filtration for water treatment were also evaluated. In the food processing wastewater treatment, dynamic filtration exhibited the high membrane permeability and excellent antifouling capacity at 12 times protein concentration process; afterwards most proteins in wastewater was recycled. This work provides guidance for the hydrodynamic mechanism and application in terms of dynamic filtration.

Keyword Dynamic filtration · Hydrodynamics · Water treatment · Environmental application

Abbreviations

CCRSM	Central composite response surface methodology
CFD	Computational fluid dynamics
CIP	Clean in place
COD	Chemical oxygen demand (mg O_2 L^{-1})
LDA	Laser doppler anemometry
LDV	Laser doppler velocimetry
LIF	Laser-induced fluorescence
MBR	Membrane bioreactor
MF	Microfiltration
MWCO	Molecular weight cutoff
MTV	Molecular tagging velocimetry
NF	Nanofiltration
PIV	Particle image velocimetry
PLIF	Planar laser-induced fluorescence
RDM	Rotating disk membrane
RO	Reverse osmosis
RVF	Rotating and vibrating filtration
UF	Ultrafiltration
VSEP	Vibratory shear-enhanced system
VRR	Volume reduction rate

6.1 Introduction

As there is continuous depletion of freshwater resources, the focus has been shifted more towards wastewater recovery and recycling, which require advanced wastewater treatment technologies. It has been proved that membrane filtration is an environmentally friendly technique, leading to a considerably effective, flexible (greater flexibility in design and scale-up), and economical process (energy saving and no additives and chemicals required). Coupled with other processes and operations, membrane filtration has been applied in the advanced process such as clarification, purification, dewatering, and so on such as membrane bioreactor, seawater desalination process, and so on. Depending on the membrane pore size, it can be classified as microfiltration (MF), ultrafiltration (UF), nanofiltration (NF), and reverse osmosis (RO), which are widely in demand especially in the field of wastewater treatment (wastewater in power plant, pulp and paper industry, dyeing industry, petrochemical industry, food processing and pharmaceutical industry). Dead-end filtration (DEF) and cross-flow filtration (CFF) are traditional configurations defined by the configurations of filtration modules and operating conditions. The control of flux decline and filtration resistance is mainly determined by increasing feeding flow rate and transmembrane pressure (TMP), which requires much energy and causes nonoptimal membrane utilization. Dynamic filtration appears as an alternative to alleviate the blocking up of filtration process. Dynamic filtration modules have been proven to reduce filtration resistance and flux decline by imposing high shear rates and perturbation on membrane surface. In comparison with traditional modules, dynamic filtration modules do not only increase substantially the permeate flux without a much larger inlet flow rate but also have a favorable effect on membrane selectivity (Zhang et al. 2015; Jaffrin 2008; Ding et al. 2015).

6.1.1 Commercial Dynamic Filtration Modules

In recent decades, various commercial dynamic filtration modules have been developed and applied in various industries (Jaffrin 2008, 2012). Dynamic filtration modules can produce high shear rate on membrane surface by a moving part such as a rotating membrane or a disk rotating near a fixed circular membrane or vibrating the membrane either longitudinally or torsionally around a perpendicular axis. In wastewater treatment by NF and RO (Akoum et al. 2004), it is important to have the highest possible rejection. Because dynamic filtration module reduces concentration polarization, the concentration of rejected solutes on membrane surface is lowered, decreasing the concentration gradient and diffusive solute transfer through the membrane, thence enhancing solute rejection rate. Conversely, concentrating a protein solution by UF (Akoum et al. 2006) and clarification of a suspension by MF (Beier et al. 2006) require a high micro-solute transmission, and this transmission increases in dynamic filtration module. The high shear rate caused by strong shear effect reduces cake formation, thereby ensuring the micro-solute penetration. At the same time, permeate fluxes keep increasing with transmembrane pressure, because the limiting flux is extended by the reduction of concentration polarization and keeps at a high level for the long-term operation, even at a high concentration

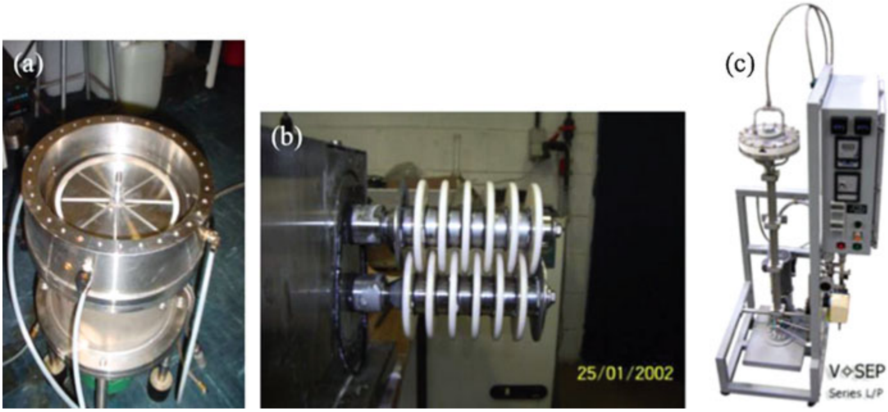

Fig. 6.1 Laboratory pilot module (**a**) rotating disk module in Technological University of Compiegne (membrane area: 460 cm^2), (**b**) multi-shaft rotating ceramic disk membrane system from Westfalia Separator (total membrane area: 121 cm^2) (Jaffrin 2008), and (**c**) VSEP module from New Logic Research, Inc. (membrane area: 500 cm^2) (Jaffrin 2012)

protein solution, which shortens greatly the concentration time and is important for keeping protein freshness (Jaffrin 2008).

Typical dynamic filtration systems are of three types: rotating disk/rotor (Fig. 6.1a), rotating membrane (Fig. 6.1b), and vibratory systems (Fig. 6.1c). Rotating disk/rotor module can create a high shear rate on the membrane by a disk rotating near a fixed circular membrane (Ding and Jaffrin 2014; Chen et al. 2019). The performance depends upon the rotating speed and disk/rotor geometry. In rotating membrane systems, rotating ceramic membranes generate a high shear rate that is orders of magnitude greater than conventional filtration system and provides a high and very stable flow rate on the membrane (Ding et al. 2006). The powerful rotational shear prevents fouling and provides high and very stable system throughput (Ding and Jaffrin 2014). The VSEP (vibratory shear-enhanced system, New Logic Research, Inc., CA, USA) involves a stack of circular organic membranes separated by gaskets and permeate collectors, installed on a vertical torsion shaft spun in azimuthal oscillations by a vibrating base (Beier et al. 2006). The shear rate on the membrane is created by the inertia of the retentate which moves at 180° out of phase and varies sinusoidally with time controlling concentration polarization and preventing membrane fouling. The critical parameter is the azimuthal displacement of the membrane rim (Akoum et al. 2002). The use of resonance permits to minimize the power necessary to produce the vibration, which is only 9 kW, even for large units of 150 m^2 membrane area (Jaffrin 2008). The critical flux was highest at the maximum degree of vibration, and the permeability could keep constant when operating below the critical flux for a 4.5-h test (Beier et al. 2006). Besides, Fane et al. (Li et al. 2013; Zamani et al. 2013) revealed that a small looseness or swing of vibration fibers could reduce the membrane fouling, due mainly to the additional lateral movement of the fibers induced by the looseness. Unlike the rotating

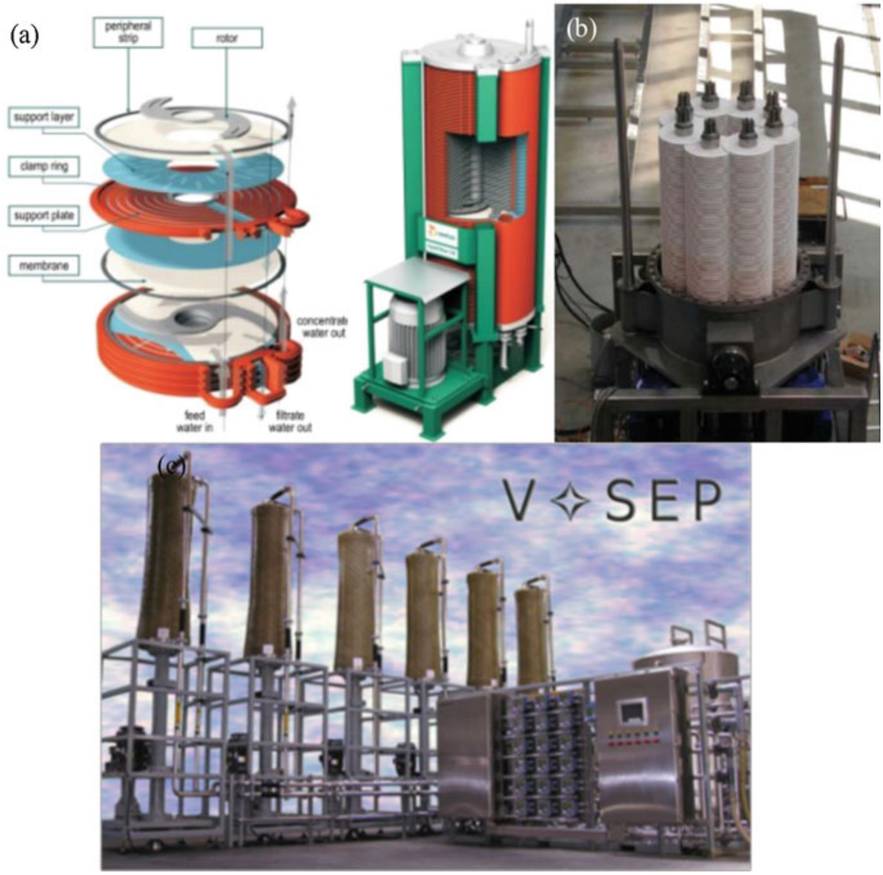

Fig. 6.2 Industrial dynamic filtration module: (**a**) rotating disk (OptiFilter CR, Metso paper), (**b**) rotating membranes (multi-shaft disk module (Westfalia Separator) (Jaffrin 2012), and (**c**) VSEP (Courtesy of New Logic Research, Inc.) (Jaffrin 2008)

membrane or disk system, the pressure of vibrating systems can sustain a pressure of 40 bar and permit efficient NF and RO (Jaffrin 2008).

Nowadays, numerous dynamic filtration modules have achieved commercialization, such as rotating disk/rotor, rotating membrane, and vibratory systems. The industrial rotating rotor module OptiFilter CR is made of flat membranes fastened on both sides of filter cassettes (Fig. 6.2a), which are stacked on top of each other. The rotor between each cassette produces turbulence and enhances filtration capacity and decreases the fouling effect. The OptiFilter CR is efficient for treating water effluents and producing recycled water in the paper industry (Luo 2012). The multi-shaft disk module (Westfalia Separator) (Fig. 6.2b) with eight parallel shafts and 31.2 cm ceramic disks is another commercial application of a rotating membrane system. Overlapping membrane disks did not much enhance permeate flux, due to the high concentration between two adjacent and overlapping membranes (Ding et al. 2006).

With the modification of replacing the ceramic disk on one shaft by metal disks with vanes, it can avoid local overconcentration, increase permeate flux, and save energy and cost (He et al. 2007). The most widely used VSEP system is the series i84 (Fig. 6.2c). With up to 150 m^2 of membrane area in each filter pack, the i84 is the ideal module size to process larger flow rates (Luo 2012). More than 400 large industrial VSEPs with a membrane area of up to 150 m^2 of the membrane have been installed worldwide since 1992 in a large variety of applications (treatment of landfill leachates, biogas effluents, ethanol silage, etc.). Sarker designed and developed the rotating disk membrane (RDM) module (Sarkar et al. 2011) and spinning basket membrane (SBM) module (Sarkar et al. 2012). The module has the facility to rotate membrane and the stirrer in the opposite direction to provide maximum shear in the vicinity of the membrane. However, their rotating speed is less than 300 rpm for the stirrer and less than 100 rpm for the membrane, which is too low for industrial application. The biggest problems of dynamic filtration system industrialization are the small membrane area for some modules and high equipment cost; thus, further studies should be directed towards solving these problems.

6.1.2 Advantages and Drawbacks

As an alternative to dead-end filtration and cross-flow filtration, dynamic filtration does not only increase substantially the permeate flux but has a favorable effect on membrane selectivity and concentration factor, which allows very viscous concentrates and high water recovery during wastewater recycle. It also permits to decouple membrane shear rate from the inlet flow rate into the module, which can be varied independently and does not need to be much larger than the filtration rate, thus avoiding pressure drop appearing in the tubular or spiral-wound modules. Clarification of a suspension by MF requires a high micro-solute transmission, and this transmission is increased in dynamic filtration, which reduces cake formation by combining a high shear rate with a low transmembrane pressure. Moreover, in wastewater treatment by NF and RO, since dynamic filtration reduces concentration polarization, the concentration of rejected solutes at the membrane is lowered, reducing the concentration gradient and diffusive solute transfer through the membrane and therefore increasing solute rejection rate and improving permeate quality. At the same time, permeate fluxes keep increasing until high pressures, as the pressure-limited regime is extended by the reduction of concentration polarization and very high fluxes can be obtained at high transmembrane pressure (Jaffrin 2008).

The drawbacks are the complexity and limitations in membrane area for some systems, such as cylindrical rotating membranes or multi-compartment rotating disk systems, which raise the equipment cost. Moreover, the energy cost for dynamic filtration also needs further optimization.

For recycling industrial wastewater by dynamic filtration, there are very few investigations in both academic research and industrial applications, especially for dynamic filtration NF process. Although the cake fouling is minimized by high shear rate, flux decline and membrane fouling cannot be avoided in this process. The investigations about flux and fouling behavior and mechanism for dynamic filtration are quite necessary, in order to promote the applications of this powerful tool in environment and energy aspects.

6.2 Hydrodynamic Study in Dynamic Filtration Module: Simulation and Local Study

In dynamic filtration system, fouling limitation and reduction highly depends on the complex hydrodynamics which is generated by the geometrical configuration of cell, mixing device, and operating conditions as well as the rheological behavior of the fluid. Therefore, gaining insight into local and global hydrodynamics will highlight the process performances.

6.2.1 Brief Overview of the Accesses to Local Hydrodynamics

Global hydrodynamic investigation refers to the study of liquids in general motion, since it can partly explain the influence on hydrodynamic parameters, e.g., pressure, temperature, flow rate, and residence time distribution. However, local hydrodynamics, e.g., flow pattern and behaviors, which could better diagnose the system performance, were often hidden by the lack of knowledge on local measurement. From the experiment point of view, the optical visualization technique is recently becoming more and more popular for accurate and reliable local measurement. Further information such as velocity distribution, local shear, concentration field, and temperature field could be provided by using optical measurement. These kinds of imaging methods capture two-dimensional or three-dimensional images of the particles at two or more instants; the velocity is calculated from the particle displacements of the images. These techniques are based on tracking the motion of seeded particle groups (particle image velocimetry) or individual particles (particle tracking velocimetry) (Dan-Xun et al. 2013). Molecular tagging velocimetry (MTV) and planar laser-induced fluorescence imaging (PLIF) are methods for determining the velocity of currents in fluids by tagging specific molecules and tracking its displacement by image technique. There are three optical ways via which these tagged molecules can be visualized: fluorescence, phosphorescence, and laser-induced fluorescence (LIF) (Gendrich et al. 1997). Laser Doppler velocimetry (LDV), also known as laser Doppler anemometry (LDA), is one of the techniques of using the Doppler shift in a laser beam to measure the velocity in the transparent or semitransparent fluid or the linear or vibratory motion of opaque, or reflecting, surfaces (Kilander and Rasmuson 2005).

6.2.2 Study of Local Hydrodynamics by Applying PIV Within RVF Module

In this chapter, a case study of a local hydrodynamic investigation by PIV measurement is presented within a dynamic filtration module called rotating and vibrating filtration (RVF) (Xie 2017). The RVF laboratory module consists of two identical filtration cells (Fig. 6.3a shows one filtration cell, volume 0.2 L per cell, 1.5 L in total) in series, including two flat disk membranes fixed onto porous plates which drain the permeate and impeller-shaped rotating bodies attached to a central shaft (Fillaudeau et al. 2007). It can install four membranes in total (two for each filtration cell), with filtration area 0.048 m^2. Each cell (Fig. 6.3b) includes a three-blade impeller (flat blade, diameter = 138 mm, thickness = 8 mm) driven by a central shaft continuously rotating (up to 50 Hz) in a 14 mm gap between two porous substrate plates (membrane support in metal) which drains the permeate. This configuration gives a 3 mm gap between the impeller and the membrane surface. This simple mechanical device runs continuously and generates high shear stress as well as a hydrodynamic perturbation in the small membrane-to-impeller gap transmembrane pressure (up to 300 kPa), and rotation frequency can be adjusted to optimize the operating conditions.

In this case study, hydrodynamics in the cell was investigated by particle image velocimetry (PIV) in laminar flow for the first study. To achieve laminar flow regime, 40% (w/w) diluted BREOX solution was chosen as a test fluid (μ = 0.81–0.85 Pa·s, Cp = 3274 J/(kg·°C) and ρ = 1067 kg/m^3 at T = 20 °C);

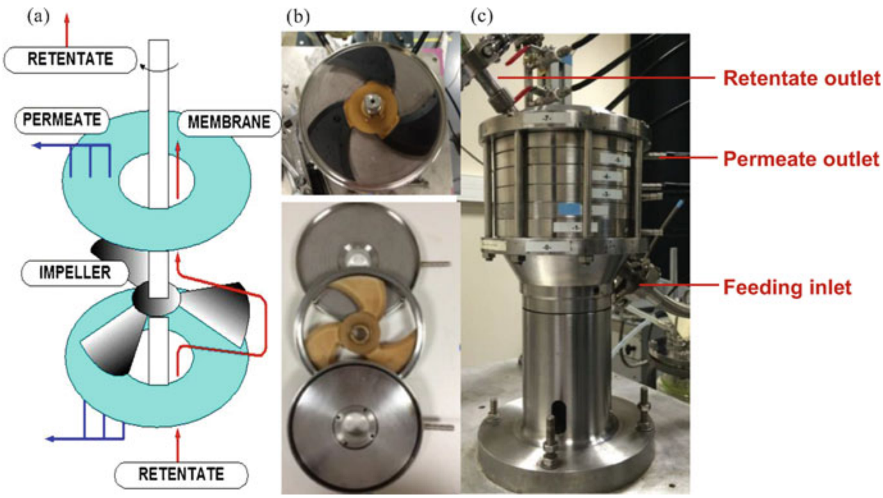

Fig. 6.3 The filtration cells and the RVF (rotating and vibrating filtration) module, mixing rate: 0 < N < 50 Hz, filtration area: S = 0.048 m^2 (4 membranes), diameter of the membrane: D = 62/135 mm, thickness of impeller = 8 mm (Xie 2017). (**a**) Schematic diagram of the filtration cell. (**b**) Filtration cell with the matte impeller. (**c**) The RVF module

rotation speed was controlled at $N = 2$ Hz. The temperature of the feeding tank was controlled at 20 °C by adjusting the thermostat; the room temperature was air controlled at 20 ± 1 °C. By analyzing the PIV raw images, the instantaneous velocity fields (from single images pair) and time-averaged mean velocity fields (from 1000 image pairs) were computed at horizontal plane (6 $x-y$ plane within membrane–impeller gap). To acquire the mean velocity fields in this rotating system, the optical trigger plays a key role in these measurements because it synchronizes and governs the laser generator and the camera with the position of one specific blade.

Figure 6.4 provides an overview of the magnitude of velocity fields. In our experimental conditions, maximal impeller velocity was equal to 0.87 m/s at $R = 69$ mm ($N = 2$ Hz, $d_m = 138$ mm). Raw PIV images (Fig. 6.4a, d) show the constant position of the impeller and the homogeneous surface density of fluorescent particles for $z_1 = 0.25$ (close to membrane) and $z_6 = 2.75$ (close to impeller) mm.

In terms of flow pattern, instantaneous (Fig. 6.4b, e) and mean (Fig. 6.4c, f) velocity fields could be compared. Figure 6.4b, c presents the lowest velocity magnitudes, whereas Fig. 6.4e, f exhibits the highest values (close to the impeller velocity). As expected, mean velocity fields present a uniform and regular flow pattern. Jiang et al. (2013) also introduced a PIV measurement by using pine pollen tracing in water (turbulent flow) with a rotating membrane bioreactor. This membrane module was consisted of nine identical flat sheets vertically in a cylindrical reactor, with an internal diameter of 240 mm and an effective volume of 13 L. Under these conditions, mean velocity fields showed a clear and stable velocity gradient in the radial direction with time-averaged velocity plot. In our study, similar observations were found:

- The velocity around the central shaft was organized and close to zero. Feeding fluid went through the RVF module along the central shaft vertically (z direction) from the bottom to the top, and governing velocity vector was at the z direction, so velocity close to the central shaft in the horizontal ($x-y$) plane was almost zero.
- Velocity gradient increased in the radial direction from inner to outer diameters, but velocity remained nearly equal to zero at the maximum diameter $R = 70$ mm (fluid was stationary close to the surrounding wall, no-slip boundary conditions at the fluid–solid interface). This observation was verified for both positions, $z_1 = 0.25$ and $z_6 = 2.75$ mm.
- Velocity magnitude close to the inner diameter, $R = 25$ mm, remained inferior to 0.1 m/s, whereas shaft velocity was equal to 0.31 m/s.
- Velocity fields likely had periodic movements generated by the specific shape of the impeller. Maximum fluid velocities (Fig. 6.4c, f) were found near the leading edge of the blade. At $R = 65$ mm, the maximum values were 0.15 and 0.45 m/s for $z_1 = 0.25$ and $z_6 = 2.75$ mm, respectively, while the impeller velocity was 0.82 m/s. However, the maximum value of the velocity fields $z_1 = 0.25$ and $z_6 = 2.75$ mm was at $R = 55$–60 mm, with 0.21 and 0.58, respectively.
- At the surrounding wall ($R > 65$ mm to the surrounding wall), velocity decrease from 0.35 to 0.2 was observed.

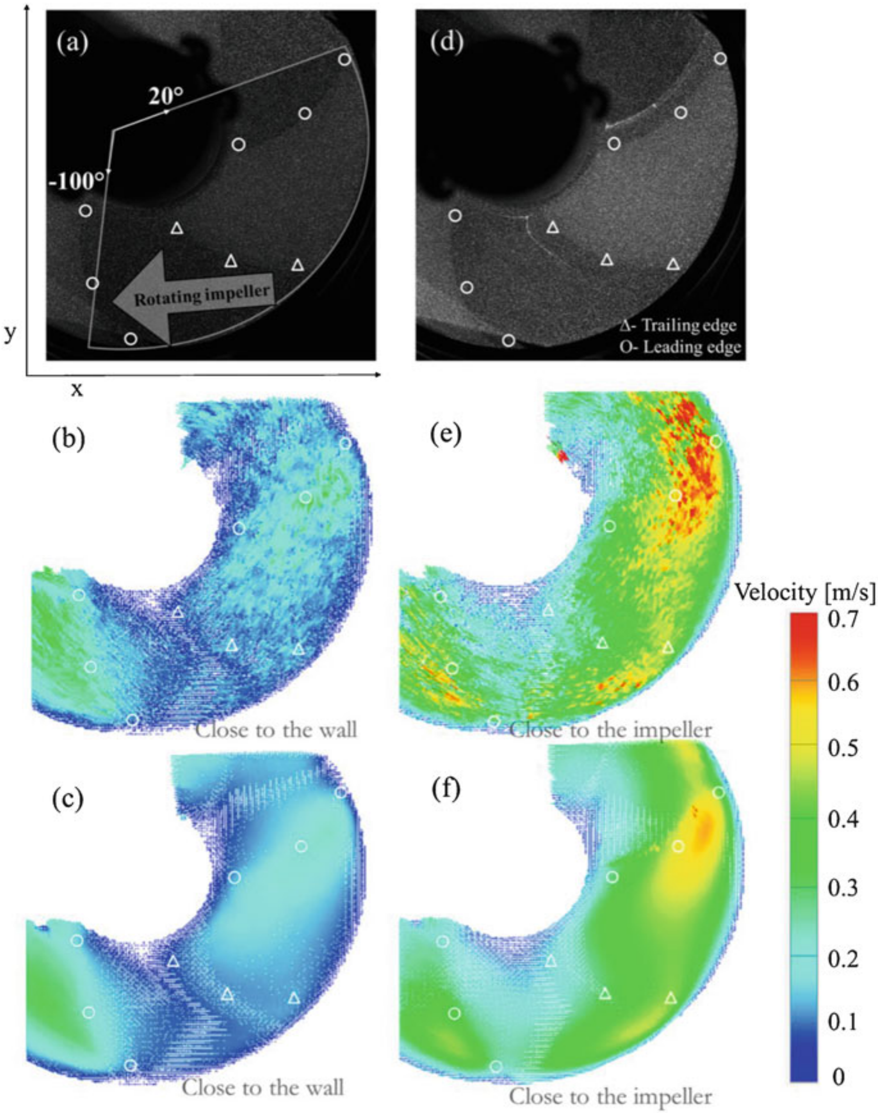

Fig. 6.4 Illustration of PIV raw images in horizontal measurement (**a** and **d**), instantaneous velocity fields (**b** and **e**, issued from single image pair), and time-averaged velocity fields (**c** and **f**, averaged of 1000 image pairs) in the RVF module. Slice positions: z_1 close to the wall (**a**, **b** and **c**) and z_6 close to the impeller (**d**, **e** and **f**); operating conditions: $Q_f = 45$ L/h, $N = 2$ Hz; $\mu = 0.85$ Pa·s and $T = 20$ °C. Symbols: ○, leading edge and Δ, trailing edge of the blade (Xie et al. 2018)

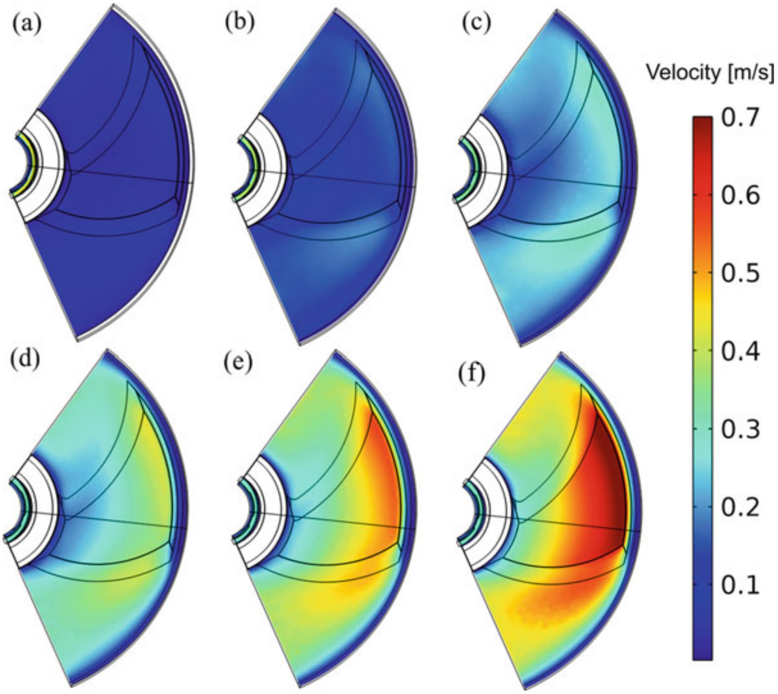

Fig. 6.5 Velocity fields in CFD simulation with six slices, from z_1 (**a**) to z_6 (**f**). Operating conditions: $Q_f = 45$ L/h, $N = 2$ Hz; BREOX solution, $\mu = 0.85$ Pa·s and $T = 20$ °C (Xie 2017)

6.2.3 Hydrodynamic Investigation by CFD

Navier–Stokes equations can be easily and rigorously solved in the laminar regime without any approximation. On the contrary, it is not possible to perform DNS (direct numerical simulations) in turbulent regime except for very simplified geometries. Even if there exist a number of models for turbulent flow generally based on Reynolds decomposition, such as the commonly used k-eps model, we restrict the numerical study to laminar flow. In this case, CFD gives access to velocity in x, y, and z coordinate; result present in this part is velocity magnitude in the x–y plane associated with PIV measurements.

In Fig. 6.5, velocity fields at six slices are plotted to appreciate velocity magnitude and deviation. A first qualitative approach (Figs. 6.4 and 6.5) is presented to compare the simulated and experimental velocity fields:

- Velocities were nearly equal to zero when the flow layers were close to the wall (z_1), while the closest to the impeller present the highest values (z_6).
- Velocity was nearly zero close to the central shaft and the surrounding wall ($R = 70$ mm) of the filtration cell.

- Maximum velocities occurred at leading edge at $R = 55$–60 mm of the impeller for (a), (b), (c), and (d) which has been found also in Fig. 6.4, but for (e) and (f), it was found above the blade body.
- Differences between PIV and CFD might come from the precision and uncertainty of measurement, and as we have described, adjusting the measuring plane might have ± 0.25 mm error due to the thickness of the laser sheet.

To conclude this part of the PIV experiment and CFD simulation which were conducted under a certain condition, they both gave the velocity distribution at slices. Velocity maps of PIV measurements were favorably in agreement with CFD simulations, which not only verified the simulation process but also gave us the possibility to further study the major factor of fouling removal (mean shear stress, wall shear stress, flow pattern, etc.). In the future study, research would be focused on investigating the wall shear on the membrane (wall shear) and flow motion in the filtration cell.

6.3 Applications in Food Processing Wastewater Treatment

Generally speaking, wastewater from food processing plant contains some nutritional matters. Membrane separation treating food processing wastewater could recover these nutritional matters, produce reusable water, and recycle wastewater. For example, dairy wastewater and alfalfa wastewater, from the production processes of milk and leaf proteins, contain plentiful milk proteins and leaf proteins. Using membrane technology, milk and leaf proteins can be separated and recovered. However, during the filtration process, these proteins caused serious membrane fouling, whereas it was difficult to maintain the high flux by the traditional cross-flow module for a long term. Dynamic filtration has been applied for the treatment of food processing wastewater and protein recycling. The results showed that with high shear effect, foulants could be controlled effectively, and flux was sustained at a high level.

6.3.1 Alfalfa Wastewater Treatment

Alfalfa is an important vegetable protein for animals and human consumption industrially obtained from alfalfa juice. The alfalfa processing factory, just as many other food process industries, can generate plenty of wastewater (Firdaous et al. 2009; Volenec et al. 2002; Zhu et al. 2017). This alfalfa wastewater, including diluted alfalfa juice and machine cleaning agents, results in both nutrient loss and water eutrophication, if it is discarded without effective treatment. In fact, with the high content of leaf protein and high nutritive value (absence of animal cholesterol and 50% hydrophilic proteins) (Xie et al. 2008; Lamsal et al. 2007), alfalfa

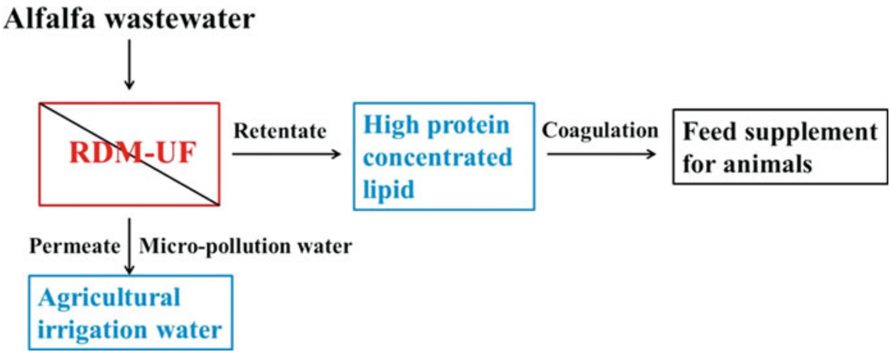

Fig. 6.6 Schematic diagram of a UF process for alfalfa wastewater treatment and resource recycling (Zhang et al. 2017b)

wastewater can be recognized as resource recovery for agricultural irrigation water production and protein recycling.

Zhang et al. (2017a, b) used shear-enhanced dynamic filtration (RDM) to pretreat alfalfa wastewater to realize protein recovery and agricultural irrigation water production. As showed in Fig. 6.6, the leaf proteins in alfalfa wastewater were rejected by RDM-UF and concentrated into retentate. This high protein concentrated lipid could be used to prepare feed supplement for animals with coagulation. At the same time, the permeate with low micro-pollutant concentration was suitable for agricultural irrigation. In order to study the effect of operational conditions, the rotating speed, temperature, and mean transmembrane pressure on filtration behavior were investigated using full recycling tests. Six UF membranes (5, 10, 20, 30, 50, and 100 kDa) with various MWCOs (molecular weight cutoffs) were compared. Flux, pollutant removal (COD, TN, °Brix, NTU, dry matter, ash, and permeability recovery (after membrane cleaning) were utilized to estimate the filtration performance. Ultrafiltration (30 kDa), with good separation performance, excellent flux behavior and high permeability recovery, was a good option for alfalfa wastewater pretreatment. Besides, there was a threshold flux in all flux-transmembrane pressure profiles. Below it, fouling rate kept at a low rate and flux increased with transmembrane pressure linearly. Exceeding it, fouling rate enhanced and flux tended to become a stable value. Furthermore, rotating speed (500–2500 rpm) and temperature (25~55 °C) reinforced flux behavior and productivity, however decreased separation efficiency. Afterwards, a series of concentration tests for long-term filtration was performed at various operating conditions, and the filtration behavior was studied. In this process, 12 L alfalfa wastewater was concentrated to 1 L, and leaf proteins were concentrated to 12 times. As displayed in Fig. 6.7, great concentration polarization was formed, but flux could still maintain at a high level (larger than 90 L m^{-2} h^{-1}), because of shear effect on the membrane. In addition, high temperature could improve flux behavior and productivity significantly. As shown in Table 6.1, 30 kDa UF membrane only took 2.22 h to get 12 times concentration effects and

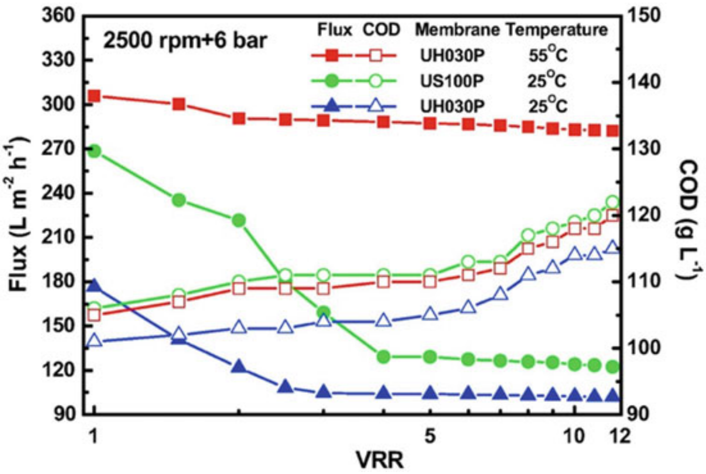

Fig. 6.7 Flux behavior and COD in permeate with VRR at different transmembrane pressure (Zhang et al. 2017b)

Table 6.1 Operation time and productivity for concentration tests at 6 bar and 2500 rpm (Zhang et al. 2017b)

VRR = 12 (concentrated volume = 12 L)	Operation time (h)	Productivity (L h^{-1} m^{-2} bar^{-1})
UH030P + 55 °C	2.22	9.36
US100P + 25 °C	3.25	5.96
UH030P + 25 °C	4.88	4.26

the productivity reached 9.36 L h^{-1} m^{-2} bar^{-1}. Thus, dynamic filtration can effectively pretreat alfalfa wastewater and recover wasteful proteins.

Hermia's blocking model was also utilized to study the fouling process and identify the main fouling mechanism. Internal pore blocking, intermediate pore blocking, and cake formation occurred simultaneously in alfalfa wastewater pretreatment. During this filtration processes, the intermediate pore blocking was dominant at the beginning, because some small leaf proteins entered the membrane pores and narrowed them. After that, more large proteins, lipids, and cleaning agents deposited on the membrane surface, sealing membrane pores, and membrane pores were further narrowed, producing internal pore blocking. At last, because of narrow pore sizes, more foulants accumulated on the membrane surface and formed cake layer, increasing hydraulic resistance.

Central composite response surface methodology (CCRSM) was used to analyze the effect and interaction of operation conditions (feed flow rate (A), mean trans-membrane pressure (B), shear rate (C), and temperature (D)) on pollution reduction and protein recovery, membrane fouling behavior, and energy cost evaluation. Then their fitting models were established as follows:

$$\begin{aligned}\text{COD rejection} =& 25.39 - 0.33\text{A} + 0.68\text{B} - 0.75\text{C} + 1.37\text{D} + 3.36\text{AB} - 0.14\text{AC} \\ &+ 4.92\text{AD} + 1.24\text{BC} + 0.93\text{BD} + 0.99\text{CD}\end{aligned} \tag{6.1}$$

$$\begin{aligned}\text{Crude protein rejection} =& 66.18 - 0.93\text{A} - 0.74\text{B} + 0.17\text{C} + 0.47\text{D} + 2.00\text{AB} \\ &- 0.48\text{AC} + 2.50\text{AD} + 0.89\text{BC} + 0.12\text{BD} + 0.63\text{CD}\end{aligned} \tag{6.2}$$

$$\begin{aligned}\text{Flux} =& 110.48 - 1.19\text{A} + 40.39\text{B} + 17.10\text{C} + 5.35\text{D} + 0.58\text{AB} \\ &+ 2.06\text{AC} + 0.94\text{AD} + 1.05\text{BC} + 1.33\text{BD} - 0.82\text{CD}\end{aligned} \tag{6.3}$$

$$\begin{aligned}\text{Fouling resistance} =& 1.56^{10} + 1.24^{9}\text{A} + 3.7^{9}\text{B} - 2.03^{9}\text{C} + 1.15^{10}\text{D} + 1.26^{10}\text{AB} \\ &- 3.96^{8}\text{AC} + 8.64^{9}\text{AD} + 1.76^{9}\text{BC} + 2.72^{9}\text{BD} - 2.56^{9}\text{CD}\end{aligned} \tag{6.4}$$

$$\begin{aligned}\text{Permeability recovery} =& 73.90 + 1.20\text{A} - 1.52\text{B} + 6.52\text{C} - 0.88\text{D} + 0.21\text{AB} \\ &+ 0.21\text{AC} - 0.21\text{AD} + 0.21\text{BC} - 0.21\text{BD} - 0.21\text{CD}\end{aligned} \tag{6.5}$$

$$\begin{aligned}\text{Energy cost} =& 201.34 - 2.12\text{A} + 109.30\text{B} - 91.39\text{C} + 9.42\text{D} - 0.54\text{AB} \\ &- 3.72\text{AC} - 22.18\text{AD} - 20.56\text{BC} + 4.28\text{BD} - 3.07\text{CD}\end{aligned} \tag{6.6}$$

Moreover, the optimized operation conditions calculated by CCRSM were $Q = 60$ L h^{-1}, $\gamma = 220 \times 10^3$ s^{-1}, transmembrane pressure = 5.61 bar, and $T = 25$ °C. In addition, as illustrated in Table 6.2, the concentration test was conducted with these parameters, and the results showed that experimental and predicted values of the response at optimized operation conditions were similar.

6.3.2 Dairy Wastewater Treatment

The dairy industry, like most other food industries, produces a large volume of wastewater, essentially composed of diluted milk, which is responsible for a 1–3% loss in milk components (lactose and proteins) (Vourch et al. 2008). Moreover, dairy wastewater also contains much chemicals (acids, alkalis, and detergents), most of which coming from clean in place (CIP) systems (Fernández et al. 2010). This effluent results in water eutrophication and is hazardous to aquatic life and soils, causing significant environmental problems when it is discarded without treatment. Dairy wastewater can be separated by membrane technology to produce reusable water, and the concentrates could be reutilized as a feed supplement for animals or substrate for biofuel production. However, for traditional membrane module, serious membrane fouling caused by various foulants, especially for milk proteins, limited

Table 6.2 Experimental and predicted values of the response at optimized operating conditions

Variable				Pollution reduction and protein recovery				Membrane fouling behavior						Energy cost evaluation	
Q	*TMP*	γ	*T*	COD rejection (%)		Crude protein rejection (%)		Flux (L m^{-2} h^{-1})		Fouling resistance (m^{-1})		Permeability recovery (%)		Energy cost (kWh m^{-3})	
L/h	Bar	$\times 10^3$ s^{-1}	°C	E	P	E	P	E	P	E	P	E	P	E	P
60	5.61	220	25	22.77	25.35 ± 0.54	67.58	66.89 ± 0.68	155.71	155 ± 0.89	2.22E+06	2.32E+06	78.39	78.96	215.2	215.9

E experimental value, *P* predicted value
TMP transmembrane pressure

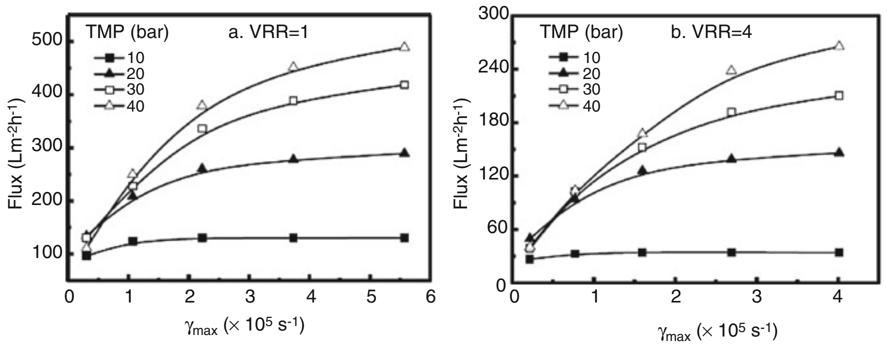

Fig. 6.8 Effect of shear rate and transmembrane pressure on permeate flux (**a**) at VRR = 1, (**b**) at VRR = 4 (35 °C) (Luo et al. 2010)

Fig. 6.9 Comparison of permeate flux between the model solution and real effluents with different pH. Transmembrane pressure = 40 bar; rotating speed = 2000 rpm; $T = 35$ °C (Luo et al. 2010)

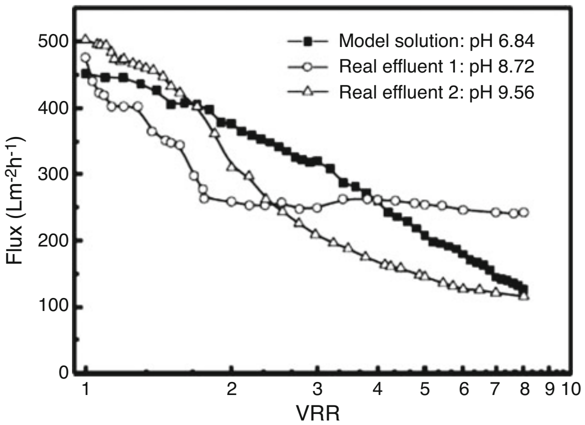

its further concentration. Dynamic filtration was used to overcome concentration polarization and membrane fouling to achieve higher concentration times and greater flux.

In order to improve the process efficiency, the feasibility for operating at extreme hydraulic conditions was studied. As shown in Fig. 6.8, since dynamic filtration produced very high shear rate to reduce concentration polarization, permeate flux could increase continuously along transmembrane pressure rise from 10 to 40 bars. Under extreme hydraulic conditions of highest transmembrane pressure (40 bars) with high shear rate (2000 rpm), as displayed in Fig. 6.9 and Table 6.3, the dynamic filtration system could produce an excellent quality permeate and save energy, due to its very high permeate flux. As showed in Fig. 6.10, the pH variation of dairy wastewater had a large effect on the separation rate of NF. Operating at acid pH resulted in low salt removal, and for alkaline pH, membrane fouling could be alleviated, but permeate flux decreased due to severe concentration polarization.

Table 6.3 Comparison of treatment results between the model solution and industrial effluent (Luo et al. 2010)

Index	Model solution	Batch 1	Batch 2
		Feed/permeate	
Turbidity (NTU)	NA/0.57	101/0.56	100/0.57
COD (mg O2 L − 1)	36,000/54	297/<15	580/<15
Conductivity (μS cm − 1)	2170/685	1084/525	1516/317
pH	6.84/6.62	8.72/7.90	9.56/9.00
Operation time (h)	1.717	1.867	2.083
IF (%)	21.88	26.87	13.40

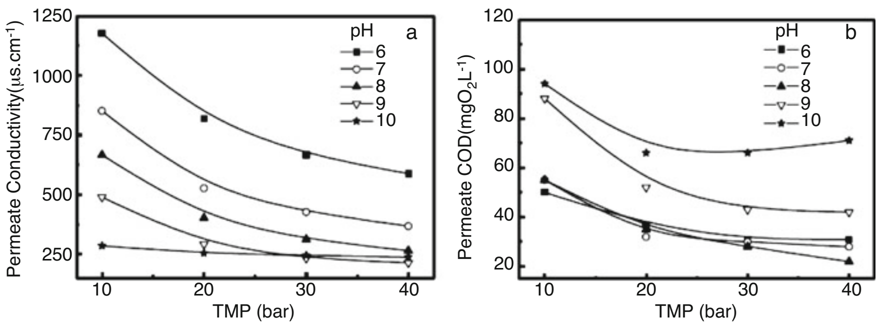

Fig. 6.10 Variation of permeate conductivity (**a**) and permeate COD (**b**) with transmembrane pressure at different pH values (Luo et al. 2010)

Therefore, at alkaline pH, the extreme hydraulic conditions could be used to improve the process efficiency of dynamic filtration for dairy wastewater treatment.

For the long-term filtration process, dynamic filtration process under extreme hydraulic conditions, as illustrated in Fig. 6.11, after the stable flux period, a slow flux decline for NF process caused by surface adsorption of foulants (lactose, multivalent salt ions, and their aggregates) occurs. In this adsorption fouling stage, pore narrowing and blocking governed by foulant–membrane interaction is the main fouling mechanism. In the absence of chemical cleaning, this adsorption fouling can induce cake fouling formation by inorganic–organic aggregates, resulting in severe flux decline.

For the foulants produced by the components in dairy effluents, Fig. 6.12 presents that casein micelles can bind heavy metal; whey proteins are dominant foulant for cake formation as “backbone”; calcium ions are the “bond” for fouling layer; lactose is the dominant foulant for pore adsorption and plugging, as “substrate” of fouling layer.

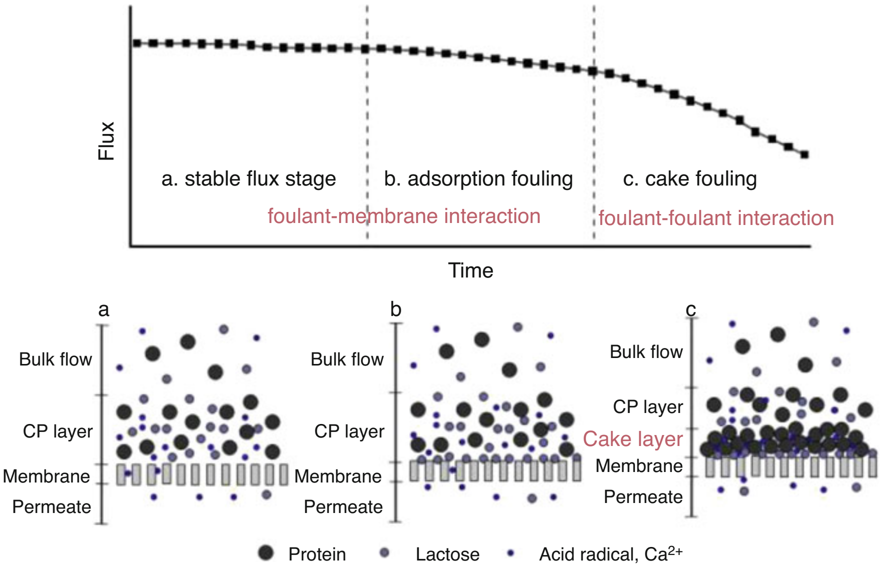

Fig. 6.11 Schematic diagram of the fouling mechanism for wastewater treatment by BF under extreme hydraulic conditions (Luo et al. 2012a)

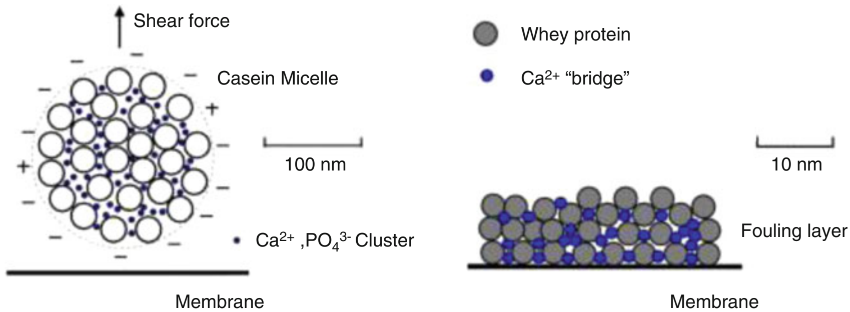

Fig. 6.12 Schematic of foulant behavior on NF membrane when (**a**) with casein (Kruif et al. 2012), (**b**) without casein (Luo et al. 2012b)

6.4 Conclusion

Some dynamic filtration modules, including rotating disk/rotor, rotating membrane, and vibratory systems and other derivative types, have been introduced in this study. Firstly, a brief overview of popular dynamic filtration modules was proposed.

Compared to the traditional filtration modes, dynamic filtration modules generated more complex hydrodynamics in the filtration cell, and membrane fouling and cake layer were likely reduced during the process.

To give insight to this hydrodynamics, a study by PIV experiment and CFD simulation under laminar flow was carried out to investigate the flow behaviors in the dynamic filtration module. Maximum velocity occurred close to the impeller blade, and the fluid was almost stationary close to the membrane surface and the surrounding wall. It can therefore be assumed that high value of shear stress could be generated due to the large deviation of the velocity distribution. A very limited set of publications are available that reported the help of hydrodynamics. Further study might include velocity, shear stress, streamline, and the effect of mechanical damage on microbial substrate.

Applications in wastewater treatment in food process industry were thereafter presented for two purposes: (i) water purification and (ii) waste recycling. For example, the dairy wastewater treatment and alfalfa juice filtration, dynamic filtration was able to overcome the high protein fouling and keep at a great permeability even for very high protein concentration; thus, most of the protein could be cycled by dynamic filtration.

The recent development of the membrane filtration highlights the combination of biochemical, thermochemical, or other water processing. It was found that process combinations (membrane–hybrid process) give more enhanced removal efficiency than the single process. For example, MBR (membrane bioreactor) is with a membrane module coupled with (or submerged in) a bioreactor, which combines biological/chemical substance removal utilizing activated sludge and membrane separation at the same time, and it has been widely used in the wastewater treatment process. As well as novel membrane materials and module configurations, it might significantly improve process productivity and reduce energy consumption.

Acknowledgments The authors acknowledge the financial support from National Natural Science Foundation of China (No. 51908136), Pearl River Talent Program (2017GC010139), Science and Technology Project of Guangzhou of China (No. 201904010122), and Guangdong Natural Science Foundation of China (No. 2017A030310540 and 2018A0303130036).

References

Akoum OA, Jaffrin MY, Ding L, Paullier P, Vanhoutte C (2002) An hydrodynamic investigation of microfiltration and ultrafiltration in a vibrating membrane module. J Membr Sci 197:37–52

Akoum O, Jaffrin MY, Lu HD, Frappart M (2004) Treatment of dairy process waters using a vibrating filtration system and NF and RO membranes. J Membr Sci 235:111–122

Akoum O, Richfield D, Jaffrin MY, Ding LH, Swart P (2006) Recovery of trypsin inhibitor and soy milk protein concentration by dynamic filtration. J Membr Sci 279:291–300

Beier SP, Guerra M, Garde A, Jonsson G (2006) Dynamic microfiltration with a vibrating hollow fiber membrane module: filtration of yeast suspensions. Desalination 199:499–500

Chen W, Mo J, Du X, Zhang Z, Zhang W (2019) Biomimetic dynamic membrane for aquatic dye removal. Water Res 151:243–251

Dan-Xun LI, Zhong Q, Ming-Zhong YU, Wang XK (2013) Large-scale particle tracking velocimetry with multi-channel CCD cameras. Int J Sediment Res 28:103–110

Ding L, Jaffrin MY (2014) Benefits of high shear rate dynamic nanofiltration and reverse osmosis: a review. Sep Sci Technol 49:1953–1967

Ding LH, Jaffrin MY, Mellal M, He G (2006) Investigation of performances of a multishaft disk (MSD) system with overlapping ceramic membranes in microfiltration of mineral suspensions. J Membr Sci 276:232–240

Ding L, Jaffrin MY, Luo J (2015) Chapter two–dynamic filtration with rotating disks, and rotating or vibrating membranes. Prog Filtr Sep:27–59

Fernández P, Riera FA, Álvarez R, Álvarez S (2010) Nanofiltration regeneration of contaminated single-phase detergents used in the dairy industry. J Food Eng 97:319–328

Fillaudeau L, Boissier B, Moreau A, Blanpain-Avet P, Ermolaev S, Jitariouk N, Gourdon A (2007) Investigation of rotating and vibrating filtration for clarification of rough beer. J Food Eng 80:206–217

Firdaous L, Dhulster P, Amiot J, Gaudreau A, Lecouturier D, Kapel R, Lutin F, Vézina LP, Bazinet L (2009) Concentration and selective separation of bioactive peptides from an alfalfa white protein hydrolysate by electrodialysis with ultrafiltration membranes. J Membr Sci 329:60–67

Gendrich CP, Koochesfahani MM, Nocera DG (1997) Molecular tagging velocimetry and other novel applications of a new phosphorescent supramolecule. Exp Fluids 23:361–372

He G, Ding LH, Paullier P, Jaffrin MY (2007) Experimental study of a dynamic filtration system with overlapping ceramic membranes and non-permeating disks rotating at independent speeds. J Membr Sci 300:63–70

Jaffrin MY (2008) Dynamic shear-enhanced membrane filtration: a review of rotating disks, rotating membranes and vibrating systems. J Membr Sci 324:7–25

Jaffrin MY (2012) Dynamic filtration with rotating disks, and rotating and vibrating membranes: an update. Curr Opin Chem Eng 1:171–177

Jiang T, Zhang H, Qiang H, Yang F, Xu X, Du H (2013) Start-up of the anammox process and membrane fouling analysis in a novel rotating membrane bioreactor. Desalination 311:46–53

Kilander J, Rasmuson A (2005) Energy dissipation and macro instabilities in a stirred square tank investigated using an LE PIV approach and LDA measurements. Chem Eng Sci 60:6844–6856

Kruif CGD, Huppertz T, Urban VS, Petukhov AV (2012) Casein micelles and their internal structure. Adv Colloid Interf Sci 99:36–52

Lamsal BP, Koegel RG, Gunasekaran S (2007) Some physicochemical and functional properties of alfalfa soluble leaf proteins. LWT Food Sci Technol 40:1520–1526

Li T, Law WK, Cetin M, Fane AG (2013) Fouling control of submerged hollow fibre membranes by vibrations. J Membr Sci 427:230–239

Luo J (2012) Traitement d'effluents industriels par filtration membranaire dynamique à fort cisaillement. Bibliogr

Luo J, Ding L, Wan Y, Paullier P, Jaffrin MY (2010) Application of NF-RDM (nanofiltration rotating disk membrane) module under extreme hydraulic conditions for the treatment of dairy wastewater. Chem Eng J 163:307–316

Luo J, Ding LH, Wan Y, Paullier P, Jaffrin MY (2012a) Fouling behavior of dairy wastewater treatment by nanofiltration under shear-enhanced extreme hydraulic conditions. Sep Purif Technol 88:79–86

Luo J, Cao W, Ding LH, Zhu Z (2012b) Treatment of dairy effluent by shear-enhanced membrane filtration: the role of foulants. Sep Purif Technol 96:194–203

Sarkar D, Datta D, Sen D, Bhattacharjee C (2011) Simulation of continuous stirred rotating disk-membrane module: an approach based on surface renewal theory. Chem Eng Sci 66:2554–2567

Sarkar A, Sarkar D, Bhattacharjee C (2012) Design and performance characterization of a new shear enhanced module with inbuilt cleaning arrangement. J Chem Technol Biotechnol 87:1121–1130

Volenec JJ, Cunningham SM, Haagenson DM, Berg WK, Joern BC, Wiersma DW (2002) Physiological genetics of alfalfa improvement: past failures, future prospects. Field Crop Res 75:97–110

Vourch M, Balannec B, Chaufer B, Dorange G (2008) Treatment of dairy industry wastewater by reverse osmosis for water reuse. Desalination 219:190–202

Xie X (2017) Investigation of local and global hydrodynamics of a dynamic filtration module (RVF technology) for intensification of industrial bioprocess. INSA-Toulouse

Xie Z, Huang J, Xu X, Jin Z (2008) Antioxidant activity of peptides isolated from alfalfa leaf protein hydrolysate. Food Chem 111:370

Xie X, Le Men C, Dietrich N, Schmitz P, Fillaudeau L (2018) Local hydrodynamic investigation by PIV and CFD within a dynamic filtration unit under laminar flow. Sep Purif Technol 198:38–51

Zamani F, Law AWK, Fane AG (2013) Hydrodynamic analysis of vibrating hollow fibre membranes. J Membr Sci 429:304–312

Zhang W, Luo J, Ding L, Jaffrin MY (2015) A review on flux decline control strategies in pressure-driven membrane processes. In: Proceedings of the 4th international conference on foundations of software science and computation structures, pp 303–317

Zhang W, Grimi N, Jaffrin MY, Ding L, Tang B, Zhang Z (2017a) Optimization of RDM-UF for alfalfa wastewater treatment using RSM. Environ Sci Pollut Res 25:1–9

Zhang W, Ding L, Grimi N, Jaffrin MY, Tang B (2017b) A rotating disk ultrafiltration process for recycling alfalfa wastewater. Sep Purif Technol 188

Zhu Z, Wu Q, Di X, Li S, Barba FJ, Koubaa M, Roohinejad S, Xiong X, He J (2017) Multistage recovery process of seaweed pigments: investigation of ultrasound assisted extraction and ultra-filtration performances. Food Bioprod Process 104

Chapter 7
Membrane Preparation for Unconventional Desalination by Membrane Distillation and Pervaporation

Wenwei Zhong, Qiyuan Li, Xiaodong Zhao, and Shunquan Chen

Contents

W. Zhong (✉)
Guangzhou Institute of Advanced Technology, Chinese Academy of Sciences, Guangzhou, China

UNESCO Centre for Membrane Science and Technology, School of Chemical Engineering, The University of New South Wales (UNSW), Kensington, NSW, Australia
e-mail: ww.zhong@giat.ac.cn

Q. Li
UNESCO Centre for Membrane Science and Technology, School of Chemical Engineering, The University of New South Wales (UNSW), Kensington, NSW, Australia

School of Mechanical and Manufacturing Engineering, The University of New South Wales (UNSW), Kensington, NSW, Australia

X. Zhao
Guangzhou Institute of Advanced Technology, Chinese Academy of Sciences, Guangzhou, China

S. Chen (✉)
Guangzhou Institute of Advanced Technology, Chinese Academy of Sciences, Guangzhou, China

Shenzhen Institutes of Advanced Technology, Chinese Academy of Sciences, Shenzhen, China

Z. Zhang et al. (eds.), *Membranes for Environmental Applications*, Environmental Chemistry for a Sustainable World 42, https://doi.org/10.1007/978-3-030-33978-4_7

Abstract The treatment of concentrated saline effluent has been a great challenge in the industry, where traditional desalination techniques and membrane processes can be energy-intensive with high operational cost. In the past decade, research and development into alternative membrane processes and technologies that are energy-efficient for desalination purposes have been thoroughly explored. For example, membrane distillation and pervaporation are driven by the temperature gradient across the membrane. This special feature has shed lights on the potential utilization of low-grade energy as the driving force of these membrane processes and suggested a prospective application of concentrated saline effluents treatment. The desirable characteristics of the membranes dedicated to membrane distillation and pervaporation have very distinctive features than membranes for traditional membrane processes. Herein, we present a comprehensive review on the current state of unconventional desalination scenarios, along with their obstacles. This chapter will explore the desired characteristics of membranes, the preparation of membranes, and surface engineering, in order to serve the special requirements of membrane distillation and pervaporation. In the end, we will share some perspectives into the future trend of membrane distillation and pervaporation, regarding the design and preparation of the membranes specific to these technologies, as well as other potential applications as concentration technology in food engineering and pharmaceutical industries.

Keywords Unconventional desalination · Membrane distillation · Pervaporation · Food engineering · Pharmaceutical industry

7.1 Introduction

Conventional desalination applications are usually referred as the treatment of seawater and brackish water. Most abundant ions present in seawater are sodium (Na^+), chloride (Cl^-), sulfate ($SO_4{}^{2-}$), magnesium (Mg^{2+}), and calcium (Ca^{2+}), with total dissolved solids (TDS) level roughly around 35,000 ppm. The desalination of seawater by reverse osmosis has now become a robust membrane process with the best energy efficiency among all the other traditional desalination techniques. On the other hand, unconventional desalination is usually referred to the treatment of saline effluents and brine from multiple sources, such as oil and gas produced water, and the concentrated brine from previous membrane discharge, which reverse osmosis is unable to cope with due to its high salinity and complex nature.

Membrane distillation and pervaporation are the two emerging membrane technologies. Even though they have higher specific energy consumption than conventional desalinations (Gopi et al. 2019; Miladi et al. 2019), they can utilize low-grade heat (e.g., industrial surplus heat, solar thermal, geothermal heat) as the energy input (Li et al. 2019c). Their unique features offer great potential in treating highly concentrated saline effluents that are difficult to be handled by conventional desalination operations. While these two processes show similar operating conditions and configurations, the mass transfer mechanism can be considerably different, leading to distinctive design criteria of the membranes. Nonetheless, several issues still need to be addressed for these two processes, hindering their deployment for real brine treatment.

To the best of the author's knowledge, there has not been a review article emphasizing on the preparation of membranes particularly regarding unconventional desalination application by membrane distillation and pervaporation processes. Herein, we present a critical review on the current state of these two processes on the treatment of saline effluent, by briefing the current choices and limitations for unconventional desalination by membrane technology to start with, particularly focusing on the treatment of produced water from the oil and gas industry. Then we proceed to the introduction of membrane distillation and pervaporation technologies, outlining their similarities as well as their differences in terms of transport mechanism. The current state of the treatment of hypersaline effluent and produced water by these two technologies will be elucidated, alongside with their limitations. Then we underline some specific design criteria on the preparation and modification of the membranes for membrane distillation and pervaporation technology. Last but not least, inspired by the special features from these two processes, some perspectives on the future application other than desalination will be highlighted.

7.2 Characteristics of Water from Unconventional Desalination Applications and Current Choices of Membrane Treatment Processes

The scope of this chapter will focus on the characteristic of saline effluent other than seawater and brackish water, such as produced water from oil and gas industry, and RO brine. The characteristics of the saline effluents differ greatly from their types, sources, and geological locations. This review paper focuses on the discussion of the characteristics for the unconventional saline effluents, regardless of their geographical locations, as well as their current membrane treatment choices.

Produced water is a coproduct in the petroleum industry where water is injected into porous reservoir media of oil and gas, maintaining the hydraulic pressure (Igunnu and Chen 2012), which is also known as oilfield brine. The treatment of produced water is critical, considering the toxic nature of it, with a large quantity (Igunnu and Chen 2012). Produced water is generally treated by the removal of suspended solids and particulates, followed by the removal of organic substances and inorganic dissolved mineral ions. The removal of suspended solids could be achieved by screening and gravity assisted sedimentation at ease.

Organics that exist in the produced water could contain polar and nonpolar compounds. Oil and grease are present in the produced water in the form of either dispersed, emulsified or dissolved, with the presence of additives such as surfactants. Dissolved oil is the polar component in the produced water, which is mostly comprised of BTEX (benzene, toluene, ethylbenzene and xylene), phenols and low-molecular-weight aromatic compounds (Hayes and Arthur 2004, Khosravi and Alamdari 2009). High-molecular-weight alkyl phenols and polycyclic aromatic hydrocarbons are the source of dispersed oil.

Salinities of oil and gas produced water could range from 1000 to 400,000 ppm, with coal seam gas produced water generally recorded below 30,000 ppm and shale gas produced water at more than 400,000 ppm (Benko and Drewes 2008; Li et al. 2014). Sodium and chloride are the major contributors to the high salinity level of produced water, while the existence of other ions such as CO_3^{2-}, Ca^{2+}, Mg^{2+}, and Fe^{2+} can cause scaling.

The removal of suspended solids, some hydrocarbons, and colloidal organics can be achieved by microfiltration and ultrafiltration technology (Han et al. 2010), while ultrafiltration with the pore size ranging from 0.01 to 0.1 μm (He and Jiang 2008) could remove dissolved oil. The choice of membranes for microfiltration and ultrafiltration could be ranging from ceramic to polymeric, whereas ceramic ones were more often seen as part of the treatment processes of produced water. Ceramic membranes are known to have a longer life span than polymeric ones, largely due to its strong resistance to chemicals and excellent mechanical strength that can withstand harsh environment and vigorous cleaning. Some studies reported the use of in-air hydrophilic and underwater oleophobic microfiltration membranes for the treatment of produced water (Zarghami et al.2019). The formation of hydro-layer near the membrane surface could effectively prevent oil content from penetrating the membrane. Microfiltration and ultrafiltration can be feasible pretreatment processes for produced water treatment (Rezakazemi et al. 2018), while others argue centrifugation can be more economically sensible for large-scale oily saline effluent treatment.

For the removal of inorganic ions that exist in produced water, the available membrane treatment choices have usually known to be nanofiltration and reverse osmosis (Alzahrani et al. 2013; Riley et al. 2018). Although some reported the use of complexation–ultrafiltration coupled process to removal heavy metal (Garba et al. 2019), ultrafiltration as a stand-alone treatment cannot realize the removal of inorganic substances from the feed. Nanofiltration is most effective when the feed salinity ranges between 500 and 25,000 ppm. Nanofiltration cannot be a stand-alone treatment process of the produced water as it has a low rejection rate of monovalent ions. On the other hand, reverse osmosis is capable of removing all inorganic ions in the saline feed. Yet, for produced water exceeding a certain limit, also known as the osmotic pressure limit, reverse osmosis can be economically unfavorable and beyond which the process could require excessive amount of energy to recover the same quantity of water; some reported the value to be approximately 70,000 ppm (Arnal et al. 2005).

Another concern regarding the use of nanofiltration and reverse osmosis technology in the produced water treatment process is that if the membranes can have a high enough temperature thresholds to withstand the hot produced water. Produced water usually have a relatively high temperature, some recorded over 100 °C (Li et al. 2010, 2014). This has provided valuable insights into the design of treatment process with membrane technology, implying that the membrane material should be high-temperature bearing and the process might be able to benefit from the waste heat carried by the wastewater itself. In line with the abovementioned perspectives, the emerging desalination technologies that can utilize low-grade heat (i.e., membrane distillation and pervaporation) have attracted much attention regarding the application and membrane preparation (Ray et al. 2018), which will be presented in the next section.

7.3 Transport Mechanism of Membrane Distillation and Pervaporation

7.3.1 Transport Mechanism of Membrane Distillation

The transport of membrane distillation is governed by the saturated partial vapor pressure gradient of the volatile components across the microporous hydrophobic membrane. The actual driving force of membrane distillation is usually provided by the temperature difference across the membrane. The temperature on the feed side is elevated to create a higher saturated vapor pressure, and the permeate is cooled at room temperature or lower. This has ensured that the vapor pressure difference is sufficient for the occurrence of water evaporation on the membrane surface (Essalhi and Khayet 2015). Water vapor is then transported through the non-wetted pores of the membrane and condensed in the permeate stream (shown in Fig. 7.1).

Hydrophobic membranes are applied in membrane distillation where the dominating rate limiting steps of desalination by membrane distillation are the rate of water evaporation on the membrane surface and the migration of water vapor through the pores. The evaporation of water vapor is controlled by heat transfer of the process, whereas the migration of water vapor through the pores is dominated by the characteristics of the membrane. Knudsen diffusion model, molecular diffusion model, and viscous flow model are the dominating mass transfer mechanism within membrane distillation. While the combined model can be used to describe membrane distillation process of desalination, assumptions can be made to simplify the mass transfer model according to the type of membrane, operating conditions, and membrane distillation configuration. It is also worthy of mentioning that surface diffusion is negligible during membrane distillation process.

Fundamentally there are four classic configurations in membrane distillation, namely, they are direct contact membrane distillation (DCMD), air-gap membrane distillation (AGMD), sweep gas membrane distillation (SGMD), and vacuum membrane distillation (VMD). DCMD (shown in Fig. 7.2) is the most widely

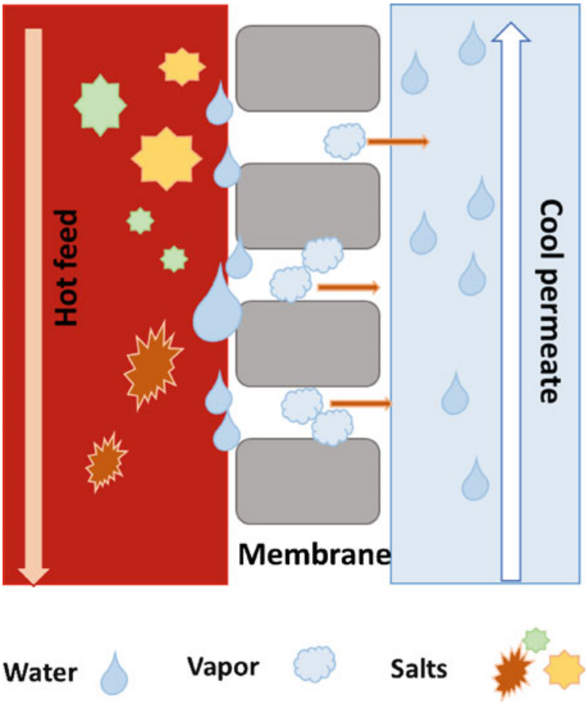

Fig. 7.1 A schematic illustration of desalination process by membrane distillation. The saline feed is heated, providing a gradient of saturated water vapor pressure across the membrane. Water evaporates on the hydrophobic porous membrane pores, while salt compounds remain in the feed side

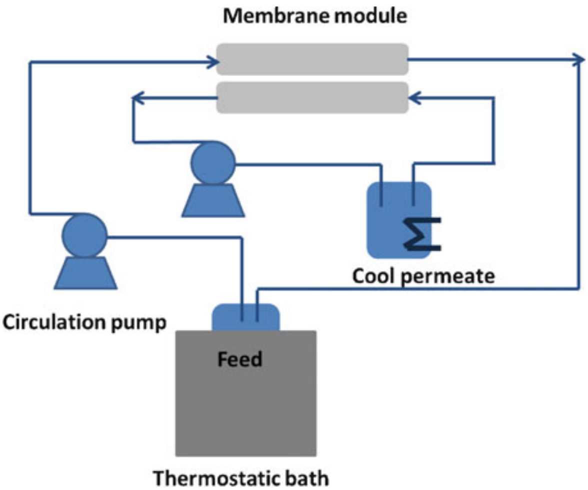

Fig. 7.2 A general configuration of a cross-flow direct contact membrane distillation. The feed temperature is elevated by the thermostatic bath or other heat source and pumped into the membrane module by the circulation pump. The generated permeate is pumped out of the membrane module and transferred into the cold permeate tank for condensation purpose. Then cool permeate is recirculated into the membrane module

implemented configuration of membrane distillation process in research and pilot-scale testing. Other attempts on the innovation in membrane process and configurations will not be discussed in this review.

7.3.2 Transport Mechanism of Pervaporation

Pervaporation is driven by the chemical potential gradient of the component in the feed across the membrane. Conventionally, operating condition for pervaporation is assumed to be set at constant pressure and temperature for convenience (Crespo and Brazinha 2015). Thus the driving force can be simply viewed as the concentration difference of the component across the membrane. Membranes with dense selective layers are commonly applied in pervaporation process, where a sorption-diffusion transport model is suggested. Each component in the feed will have a sorption coefficient (denoted as S_i), to describe its affinity to the membrane surface, which can be tuned by altering membrane material. Beyond the adsorption of the component on the membrane surface, the component diffuses through the dense layer of the membrane at a certain rate, quantified by diffusion coefficient D_i, which is correlated with the component's molecular size and geometry as well as the material characteristics of the dense layer. Both sorption and diffusion processes are the major rate limiting steps for pervaporation. The component then desorbs from the permeate side of the membrane into the permeate stream. Therefore flux J for the component i of this process can be described as the equation below, where δ denotes the thickness of the dense layer for the membrane and C denotes the concentration of i:

$$J_i = \frac{P_i}{\delta}\left(C_{i,\text{feed}} - C_{i,\text{permeate}}\right) \text{ where } P_i = S_i \times D_i \tag{7.1}$$

The transport of one component in the feed involves with the competition of selectivity for other components and flux. The component with higher affinity with the membrane material is expected to have a higher separation selectivity factor. This has allowed the precise separation of azeotropic mixtures with ease when simple distillation process cannot achieve. In the case of desalination application by pervaporation process, it is widely accepted that the driving force is the difference in saturated partial pressure of the evaporative components (i.e., water and other possible volatile organics) on the feed and permeate side of the membrane, leaving dissolved salts and other substances on the feed side. A schematic diagram of the desalination transport mechanism for pervaporation is provided in Fig. 7.3. Although it has been widely accepted that solution–diffusion model is the dominating mass transfer mechanism for pervaporation using membranes with dense active layer, a more sophisticated and in-depth model was proposed particularly based on graphene oxide membrane, attempting to decipher the phase change of water and how the material can influence the process (Li et al. 2019b).

In most desalination applications by pervaporation process, thermopervaporation with the aid of vacuum is often observed (Chaudhri et al. 2017; Li et al. 2017, 2019b) (shown in Fig. 7.4). The use of a vacuum pump is to guarantee the low partial pressure on the permeate side and the thermal treatment of the feed is to elevate the temperature for creating a sufficiently high partial water vapor pressure on the feed side. Innovative process design and configurations such as air-purging aided thermopervaporation desalination (Naim et al. 2015) have been witnessed in recent

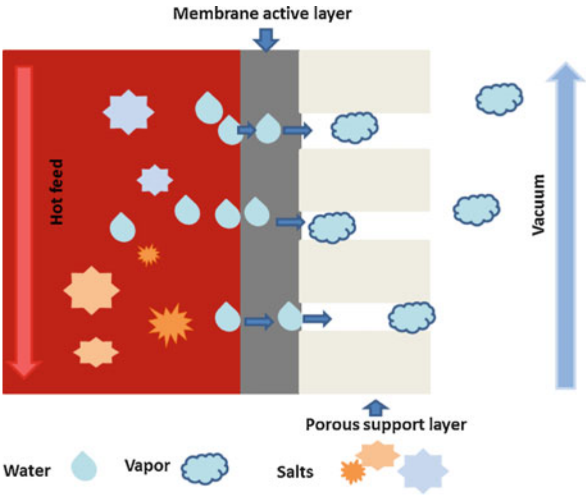

Fig. 7.3 A general schematic illustration of the desalination transport mechanism for pervaporation through a membrane with dense active layer and porous support. Liquid water adsorbs into the membrane active layer. It was suggested that liquid water might undergo phase change into water vapor, resulting in the water desorption from the active layer

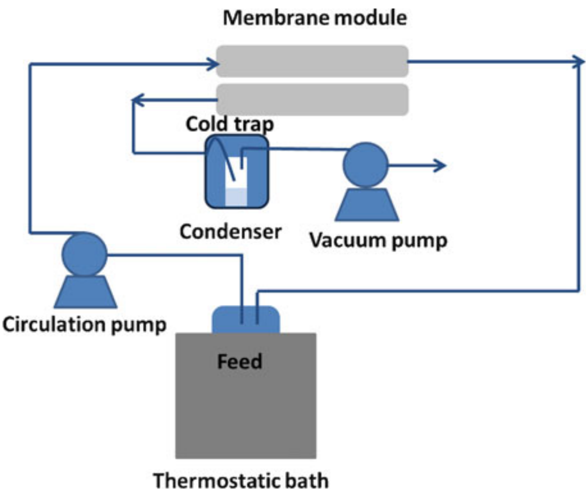

Fig. 7.4 A general configuration of thermopervaporation with the aid of vacuum. A nitrogen cold trap is generally placed before the vacuum pump

studies. Notwithstanding it is beyond the scope of this review to discuss the attempts on module and process optimization for desalination application by pervaporation.

7.4 Current State of Unconventional Desalination by Membrane Distillation and Pervaporation

7.4.1 Unconventional Desalination by Membrane Distillation

Since the increase in feed concentration is not directly proportional to the driving force, the treatment of concentrated brine and saline effluent by membrane distillation can be a favorable option. In the past decades, membrane distillation has drawn a great deal of attention on the treatment of complex produced water from oil and gas industries, as well as handling concentrated brine produced from traditional desalination processes. Table 7.1 presents an overview on the current study for the treatment of produced water by membrane distillation. Most studies were conducted with commercially available hydrophobic membranes without post-modification, which can suffer greatly from fouling, and wetting issues during the treatment of saline effluent with the existence of surfactants. Wetting of the membrane pores could lead to the deterioration of water quality as liquid directly penetrates through the membrane pores with other nonvolatile components.

Most studies were carried out using commercial membrane modules with no post-membrane modification treatment. Not until recently, numbers of studies which reported the testing of superhydrophobic and omniphobic modified membranes for unconventional desalination have been spotted on the rise. Superhydrophobic membranes exhibited improved wetting resistance as compared to the commercial membrane during the treatment of concentrated saline effluent (Zhong et al. 2017); however even superhydrophobic membranes could not tolerate the existence of surfactant, and the wetting of membrane progressively took place (Huang et al. 2017). The development and preparation of omniphobic membranes has become a readily progressing area of interests in research in membrane distillation.

Even though omniphobic membranes showed enhanced wetting resistance, inconsistent results have been reported. For the treatment of saline effluent of 1 M sodium chloride with sodium dodecyl sulfate (SDS, a type of surfactant), PVDF membranes were used in both studies (Boo et al. 2016; Du et al. 2018), which were modified by the similar materials (i.e., silica nanoparticles and low surface energy material). However it was observed that the resultant membranes could have different wetting properties even with the same coating materials. The membrane from the study of Du et al. underwent wetting, while the other remained stable. It was speculated the coating procedures could be the main cause of this minor inconsistency. The details on membrane preparation, selection, and modification specifically for membrane distillation treatment of unconventional saline effluent will be elaborated in the next section.

At an industrial scale, there already have been unconventional desalination demonstrations via membrane distillation technology. For example, membrane distillation from Memsys® and GE Power & Water firm paired with vapor compression was implemented at a shale gas wastewater treatment plant in Texas, USA (Memsys Water Technologies GmbH 2013). The average TDS of inlet feed reported in this case was approximately 190,000 mg/L, while the maximum recorded could reach 290,000 mg/L from time to time. No significant flux decline was observed, while no cleaning was conducted during the 200 h of operation with a recovery ratio of 80%. However, it was suggested that for saline feed with high level of calcium and magnesium ions in the feed, a softening pretreatment procedure should be introduced. At another pilot demonstration of coal-to-chemical saline effluent treatment by Memsys®, the initial feed was softened at a concentration of 40, 000 mg/L. The final feed concentration could only reach 270,000 mg/L since membrane flux drastically declined and the operation was terminated even though most calcium and

Table 7.1 Overview of current study on unconventional desalination by stand-alone membrane distillation processes

Feedwater	Characteristics	Final concentration	Configuration	Membranes	Cause for termination of experiment	Reference
Reverse osmosis brine from sweater desalination	50,200 mg/L	280,000 mg/L	Direct contact membrane distillation	Polypropylene	Fouling	Ji et al. (2010)
					Significant flux drop	
Thermal desalination brine	70,000 mg/L	Between 108,000 and 140,000 mg/L	Air gap membrane distillation and vacuum membrane distillation	Not specified	11 days stable flux at 4.5 $L/m^2 h$	Hussain et al. (2015)
Synthetic coal seam gas produced water	37,200 mg/L	37,200 mg/L	Vacuum membrane distillation	Polypropylene	Wetting and fouling	Zhong et al. (2016)
	With 200 ppm silica				Minor flux drop	
Synthetic shale gas produced water 150,000 mg/L	150,000 mg/L	250,000 mg/L	Direct contact membrane distillation	Polytetrafluoroethylene	Wetting and fouling	Kim et al. (2017)
	With 18 ppm oil and grease				Drastic flux drop to 0	
Real shale gas produced water	30,000 mg/L microfiltration pretreated	187,500 mg/L	Direct contact membrane distillation	Polypropylene	Wetting and fouling	Kim et al. (2018)
					Drastic flux drop to 0	

Synthetic shale gas produced water 58,400 mg/L	58,400 mg/L	NA	Direct contact membrane distillation	Omniphobic modified polyvinylidene fluoride	Slight decrease in flux	Boo et al. (2016)
	With mineral oil and Tween-80® (nonionic surfactant)					
Oily saline feed 35,000 mg/L	35,000 mg/L	NA	Direct contact membrane distillation	Janus omniphobic polyvinylidene fluoride	No observation of flux decline or wetting	Huang et al. (2017)
	Major NaCl					
	1000 ppm crude oil					
Real shale gas produced water	40,000 mg/L	85,600 mg/L	Direct contact membrane distillation	Omniphobic modified polyvinylidene fluoride	Fouling and wetting	Du et al. (2018)
	Complex produced water from a production site in Colorado				Significant flux drop	
Biologically pretreated coke water	2400 μS/cm	NA	Direct contact membrane distillation	Omniphobic modified polyvinylidene fluoride	Insignificant flux drop	Li et al. (2019a)
	COD 127 mg/L					
	Bio-refractory organics (phenolic and nitrogen-heteroatomic compounds)					

magnesium were removed. This observation could be contradictory with the abovementioned results of the shale gas produced water treatment plant, implying that feed compositions and history of the feed chemistry significantly influence the membrane performance in membrane distillation. It was reported elsewhere that feed history could be responsible for the size and structure of the crystals formed on the membrane surface, eventually leading to the deterioration of membrane performance (Julian et al. 2016). Therefore, careful tuning for the right operating condition as well as selecting the appropriate pretreatment processes where feed compositions are evaluated. Apart from the recovery of water resources from hypersaline effluent, the recovery of valuable minerals can also be achieved in membrane distillation coupled with a crystallizer (Tun et al. 2005; Pantoja et al. 2015; Lu et al. 2017; Zhong et al. 2018; Zou et al. 2019).

7.4.2 Unconventional Desalination by Pervaporation

The ability of treating hypersaline effluent exceeding 100 g/L can be an attractive feature of pervaporation, which is viewed as a newly emerging desalination technology to fill the inability and void of reverse osmosis and membrane distillation. Previously, most research and application of pervaporation have been performed on the removal of organics and the separation of azeotropic mixtures; not until recently, the advantages of pervaporation for hypersaline desalination have been reexamined. There have already been reviews and research papers looking into the energy footprint and economic consideration of its projected application in the desalination industry, in particular treating hypersaline effluent (Kaminski et al. 2018; Wang et al. 2016) as an alternative solution as compared to reverse osmosis and membrane distillation. A comprehensive overview of pervaporation technology in the application of desalination is provided in Table 7.2. In terms of fouling, crystals on the membrane surface can be easily removed by rinsing. Furthermore, the wetting of the membrane does not cause a concern for pervaporation, which can be an exceptional advantage as compared to membrane distillation. On the other hand, while pervaporation could be attractive for some features, the rise of concentration in membrane distillation does not pose significant impact on the mass transfer (Meng et al. 2015), while the flux value declined substantially with the rise of concentration in the feed (Yang et al. 2017).

Yet there has been little study on the treatment of complex produced water or brine by pervaporation technology. The research on the desalination by pervaporation is mainly restricted for the treatment of single salt solution (i.e., predominately sodium chloride), some at a concentration exceeding 100,000 mg/L (Huth et al. 2014). It has been noticed that most of the present studies stress on the membrane preparation based, and the process optimization and mass transfer mechanism of desalination by pervaporation have not been properly addressed. The lack of commercially available pervaporation membranes with high performance can be the main cause for such little attention paid on the implementation of pervaporation

Table 7.2 Overview on hypersaline desalination by pervaporation processes

Feed	Membrane type	Feed temperature (°C)	Flux (L/m^{2}h)	Reference
38 g/L synthetic seawater	Silicalite zeolite active layer on α-Al_2O_3 support (0.2 μm)	80	0.72	Duke et al. (2009)
NaCl 14 g/L	Natural zeolite membranes	93	0.39	Swenson et al. (2012)
NaCl 50 g/L	Electrospun polyacrylonitrile – polyethylene terephthalate non-woven on polyvinyl alcohol support	Room temperature	5.81	Liang et al. (2014)
NaCl 70 g/L	Cellulose asymmetric membrane	80	Approx. 4.5	Naim et al. (2015)
NaCl at various concentration	Graphene oxide selective layer on commercial polyacrylonitrile ultrafiltration membrane (40 kDa molecular weight cutoff)	30	16.8 (2 g/L)	Liang et al. (2015)
			14.3 (35 g/L)	
			13.6 (50 g/L)	
			11.2 (100 g/L)	
NaCl 100 g/L	Polyvinyl alcohol active layer on polyvinylidene fluoride support	80	13.7 (Polyvinyl alcohol 0.2 μm)	Li et al. (2017)
			12.1 (Polyvinyl alcohol 0.8 μm)	
			8.1 (Polyvinyl alcohol 2.0 μm)	
NaCl 70 g/L	Commercial PERVAP 2210 from Sulzer	80	Approx.16	Kaminski et al. (2018)
	Hydrophilic activate layer with polyvinyl alcohol support	60	Approx. 8	
		40	Approx. 6	
NaCl 100 g/L	Synthesized graphene oxide active layer on 0.2 μm polyvinylidene fluoride	70	28.6	Li et al. (2019b)
		70	20.9	
	Graphene oxide active layer on 100 kDa polyvinylidene fluoride support	70	42.4	
	Graphene oxide active layer on polycarbonate support			

(continued)

Table 7.2 (continued)

Feed	Membrane type	Feed temperature (°C)	Flux (L/m^{2}h)	Reference
NaCl 150 g/L	Hybrid carbon-silica active layer	60	9.2	Yang et al. (2017)
	By vacuum calcined			
	On tubular α-Al_2O_3 support			
NaCl 20 g/L	Hybrid polyvinyl alcohol/maleic acid/tetraethyl orthosilicate membrane	65	11.7	Xie et al. (2018)
Heavy metal solution (zinc, copper, lithium, arsenic and lead)	Thin polyether block amide polymer coated on dense polyvinyl alcohol support layer	40	Approx. 0.8–1.2	Nigiz (2019)
		50	Approx. 0.9–1.4	
		60	Approx. 1.1–1.5	

in unconventional desalination. Furthermore, the varying desalination performance by pervaporation can be largely attributed to the random choice of membranes with different materials and structures. The details on the attempts and trend of membrane development particularly for desalination by pervaporation technology will be elaborated in the next section. It is believed that with further research and development in membrane fabrication and preparation, pervaporation is expected to be more appropriate when tackling with extremely challenging saline effluent than membrane distillation.

7.5 Membrane Characteristics and Preparations

7.5.1 Development of Membrane Distillation Membranes

Membrane Characteristics

Hydrophobic membranes are generally applied in membrane distillation process to prevent liquid direct intrusion to the membrane and wetting. The pore sizes of the membranes usually range from 0.1 to 0.5 μm, which lies in the range of microfiltration membranes. Therefore, most membrane distillation membranes have been directly purchased from commercial microfiltration membranes. Generally, to achieve lower mass transfer resistance and higher mass transfer rate, membranes with larger pores are desired. However, liquid entry pressure (LEP) of a hydrophobic porous membrane is usually governed by the pore size of the membrane, described in Young–Laplace Equation (Franken et al. 1987). Larger pores are more prone to wetting issues. For optimized desalination process, membranes with uniform narrow pore size are recommended. Since water vapor transports through the membrane pores, a lower membrane thickness will indicate shorter path to travel and subsequently a lower mass transfer resistance (Francis et al. 2013). To balance the trade-off between thermal conduction through the membrane material and membrane permeability, Deshmukh et al. applied numerical simulation to find out that a thickness of 70 to 100 μm can be the optimal membrane thickness for now (Deshmukh et al. 2018). For scale-up operations, thin membranes suffer more severely from the increase of length (Ali et al. 2016), consequently resulting in flux reduction. Ongoing research and case studies regarding the design of appropriate membrane structures and module are still underway, particularly on the manufacturing of membranes with high porosities, to realize the scale-up membrane distillation deployment.

Most membranes used in membrane distillation process are commonly fabricated from polymeric materials such as PVDF, polypropylene, and PTFE (Kim et al. 2017; Zhong et al. 2016; Adnan et al. 2012; Kim et al. 2018). Although PTFE showed superior resistance to strong chemical such as acids and bases, wetting of the membrane in saline feed with surfactants is still inevitable (Eykens et al. 2017). Inorganic membranes have also been seen applied for the desalination by membrane distillation processes. Yet most inorganic membranes exhibit hydrophilic features, indicating grafting low surface energy material to render hydrophobic property is necessary (Chen et al. 2018; Fang et al. 2012). It is commonly accepted that improving the wetting resistance of the membrane plays a critical role on the realization of robust treatment process for hypersaline effluent by membrane distillation (Deshmukh et al. 2018). The current state of the preparation of superhydrophobic and omniphobic membranes will be discussed in the next section.

Superhydrophobic and Omniphobic Membranes

Unconventional desalination is challenging for membrane distillation process due to the existence of surfactants, oil, and other low surface tension compounds in the saline feed as previously stated. These can be detrimental in membrane distillation process, subsequently resulting in wetting of the membrane pores and contamination of the permeate quality. It is therefore, critical to obtain a superhydrophobic or omniphobic membrane that can withstand the traceable amount of oil in the feed with enhanced wetting resistance.

To achieve superhydrophobicity, generally there are two approaches that are deployed in most studies, namely they are, blending of nanoparticles in the dope solution (Roshani et al. 2018) for membrane fabrication and post-membrane surface modification. Yet, the addition of nanoparticles to the dope solution could suffer from the poor dispersion and incorporation of the particles, resulting in particles aggregations and alteration of membrane pore structures. Generally, superhydrophobic and omniphobic surface modification requires either the addition of reentrant structure and roughness (Zhu et al. 2017) or grafting low surface energy material on the designated surface (Boban et al. 2018). Often, wettability of the surface is subjected to the synergistic effect of the surface chemistry and structure. Razmjou et al. found that with the introduction of titanium dioxide particles of hierarchical structure followed by fluorosilanization, the hydrophobicity and fouling repellence were greatly improved as compared to membranes with fluorosilanization only (Razmjou et al. 2012).

Recent advances in surface modification for membrane distillation membranes are not limited for the preparation of superhydrophobic membranes. The ultimate goal is to develop membranes with omniphobic surfaces that have the ability to repel any liquid with robust thermal, mechanical, and chemical stability that are appropriate for membrane distillation process. It is expected that the omniphobic functionalization could help to form a thin gas film near the membrane surface in the aqueous environment, implying a minimized contact area of liquid with the membrane surface. An overview on some recent representative progress achieved on superhydrophobic and omniphobic membranes for membrane distillation process are listed in Table 7.3. Although some studies reported promising results for the omniphobic membrane preparation and their performances in the real unconventional desalination deployment, the critical criteria of rendering omniphobic function in the saline effluent with oil and surfactants are still unclear, particularly regarding the varying choices of membrane coating material and feed characteristics.

Although the modified membranes were able to withstand a small amount of surfactants in the produced water feed, the results could be quite different. Du et al. (Du et al. 2018) reported that the membrane underwent severe wetting whereas the membrane performances remained steady in the study conducted by Boo et al. (2016), both treating the same feed. While the coating materials used in both studies were similar, the procedure of which could be varying. This attributed to the formation of nanoparticles with different sizes (20 nm in the study of Du et al. and 100 nm in the study of Boo et al.), along with their influence on the change of membrane pore sizes. Eventually the membranes from Boo et al. exhibited improved wetting resistance in the feedwater with surfactant. It was reported elsewhere that the grafting procedure could also greatly affect the omniphobicity of the membrane even with the same coating materials (Li et al. 2019a). Grafting via chemical bonding is preferable as it provides greater forces between silica nanoparticles and the membrane surface as compared to electrostatic adsorption of the membrane.

It is believed that the addition of micro- and nanostructure could increase the ability to repel liquids (Razmjou et al. 2012). However, the impact posed by the scale and structure of the micro- and nanoparticles has yet to be confirmed; some argued the introduction of microstructure could be harmful to some oil/water separation (Zhong et al. 2013). Future study should stress on understanding the mechanism of scale and structure of the particle added to the membrane surface on the transformation of hydrophobic to omniphobic property.

Table 7.3 Superhydrophobic and omniphobic modification for membrane distillation membranes

Type of membrane	Material	Contact angle	Membrane performances	Reference
Superhydrophobic	TiO_2 by dip coating and 1H, 1H, 2H, 2H-perfluorododecyltrichlorosilane as low surface energy decoration	163° (water)	No immediate wetting when 15 wt% ethanol was injected in the feed. Gradual decline of flux was observed indicating wetting	Razmjou et al. (2012)
		166° (glycerol)		
		150° (30 wt% mono-ethanol-amine)		
Omniphobic	Sodium hydroxide hydroxyl preparation	Slightly higher than 150° (water)	No wetting observed within 8 h of operation in the feed contained up to 0.01%v/v oil or 0.2 mM SDS	Boo et al. (2016)
	(3-Aminopropyl)triethoxysilane hydrophilic alteration	Higher than 130° (0.1 mM sodium dodecyl sulfate and mineral oil)		
	Silica nanoparticles			
	Perfluorodecyltrichlorosilane			
Omniphobic	NaOH hydroxyl preparation	168–176° (water)	Gradual flux decline observed for all membranes in saline effluent with oil emulsion	Zheng et al. (2018)
	APTES hydrophilic alteration			
	SiNPs @ cationic polystyrene (PS) spheres with polymer P (A174) as bonding agent			
	17-FAS (fluoroalkanesilane)	118–133° (Diiodomethane)	Most presented water contact angle decreased after operation	
		103–149° (4% sodium dodecyl sulfate)		
Omniphobic	Poly(diallyldimethylammonium chloride) to render positive charges	154–177° (water)	No fouling or wetting observed for 72 h operation in the brine from coal seam gas produced water	Woo et al. (2018)
	Silica nanoparticles aerogel with negative charge on poly(diallyldimethylammonium chloride)	Approx. 160° (mineral oil)		
	1H, 1H, 2H, 2H-perfluorododecyltrichlorosilane as low surface energy decoration	>150° (methanol)		

(continued)

Table 7.3 (continued)

Type of membrane	Material	Contact angle	Membrane performances	Reference
Superhydrophobic	Sodium hydroxide hydroxyl preparation	159° (water)	Fouling observed for all membranes when treating real shale oil and gas produced water	Du et al. (2018)
	(3-Aminopropyl)triethoxysilane hydrophilic alteration			
	Silica nanoparticles		Gradual permeate conductivity increased for both pristine and modified membranes	
	FAS (not specific)			

7.5.2 Design and Development of Pervaporation Membranes for Desalination Purpose

Membranes with dense selective layer are often deployed in pervaporation technology, where mass transfer is subjected to the adsorption and diffusion of the permeating species. As previously introduced, adsorption rate of the permeating species can be precisely controlled by tuning the physical and chemical characteristics of the dense layer membrane, and desorption rate is determined by the properties of the species (i.e., geometry, size, etc.), as well as the thickness of the dense selective layer and the material of the supporting layer (Li et al. 2019b). There are usually two types of membranes used in pervaporation application, namely, they are symmetric homogeneous dense membranes and asymmetric membranes. Most of the membranes developed for desalination purpose in pervaporation are asymmetric or composites membranes with an active layer of dense film or small pores on top of the microporous support layer. The material of the active layer can therefore be specifically tailored to benefit water permeation. Therefore, the current state of fabricating composites membranes with a selective layer and porous support layer will be elucidated in this section.

Active Layer

Selecting a material for the active layer with high affinity to the permeating species and considerably low affinity to other existing components in the feed is critical for the design and fabrication of membranes, particularly for pervaporation processes. It is beyond the scope of this review paper to discuss the preparation of membranes for the separation of organic mixtures. This section will stress on the material selection for desalination purpose only.

Water permeation is desired in the case of desalination. Therefore, material with high water selectivity is favored, exhibiting hydrophilic property (Koops and Smolders 1991). Although polymers like polypropylene and polyethylene are often used in the separation of polar/nonpolar in pervaporation process, the implementation of polymer as active layer with the lack of functional groups desalination application by pervaporation is fairly rare. Glass polymers exhibiting hydrophilic properties such as polyvinyl alcohol (PVA) (Li et al. 2017) and cellulose (Naim et al. 2015) or cellulose acetate can be a viable option for the desalination in pervaporation. Although the thickness of the active layer can be tailored as an approach to alter the mass transfer rate of water (Li et al. 2017), the micro-defect of ultrathin PVA film during fabrication process could still be the bottleneck for the development of this particular membrane.

Apart from hydrophilic polymeric materials, inorganic materials such as zeolite in particular can be another viable option for the active layer for pervaporation membranes. To start with, membranes with zeolite as their active layer are found to be favorable in the early period of the desalination by pervaporation (Duke et al. 2009).

The pores of zeolite appeared to be narrow with tailorable size, and it was proven to be able to efficiently reject ions in aqueous solution by size exclusion, which helped to unravel its ability to treat saline effluent in pervaporation process (Lin and Murad 2001). Zeolite membranes have been extensively used (Duke et al. 2009; Khajavi et al. 2010; Cho et al. 2011; Swenson et al. 2012) during the early stages of the development of pervaporation membranes for desalination. However, low water permeation has been the bottleneck. Latest attempt on the synthesis of ZSM-5 nanosheets has provided higher water permeation rate of 10.4 L/m^2 h as compared to the conventional preparation approach to ZSM-5 membrane, which only produced 1.22 L/m^2 h in the same study (Cao et al. 2018), both tested in 3.0 wt% of NaCl solution.

Recently, owing to the innovation in material science, graphene oxide has emerged as a popular research area for the membrane material selection for desalination by pervaporation. Graphene and graphene oxide were first deployed in the preparation of membrane for nanofiltration due to their ability to precisely control pore sizes (Hu and Mi 2014; Han et al. 2015; Goh et al. 2015), which later was demonstrated via the simulation of molecular dynamics that tailoring the interlayer spacing of the nanosheets of graphene oxide could significantly improve the rate of water adsorption without compromising the rejection rate of ions (Chen et al. 2017; Lian et al. 2017; Lian et al. 2018). This has allowed the application of grapheme oxide for the preparation of pervaporation process (Feng et al. 2016; Li et al. 2019b). The major issue associated with graphene oxide as the selective layer is that possible swelling and exfoliation could take place during long-term operation due to the weak adhesion between the material and support layer. The ongoing research on the fine-tuning of the graphene oxide material characteristics can be of great benefit for the fabrication of pervaporation membranes applied in hypersaline desalination.

Support Layer

As previously listed in Table 7.2, the characteristics of the support layer could play a key role in the rate of water collection in the permeate stream. It was found that support layer with higher porosity and larger pore size could benefit the transport of water due to the decreased transport resistance (Sun et al. 2016; Li et al. 2018, 2019b), which is consistent with the observation in membrane distillation process.

Nevertheless, there has been little study to date reported on the effects of the support layer's nature (hydrophobic vs. hydrophilic), regarding the specific water diffusion rate. The use of hydrophobic and hydrophilic as support layer in pervaporation membranes particularly for desalination can be rather random. Yang et al. suggested that hydrophobic material could benefit the desorption of water (Yang et al. 2017), indicating a faster water transport through the support layer. Future work on the preparation of membranes for desalination still requires a systematic analysis on the correlation between the wettability of the support layer and the promotion of water desorption on the permeate side.

7.6 Perspectives on Future Trend

7.6.1 Membrane Distillation and Pervaporation in Food Engineering and Processing

The dewatering and concentration process can be a critical procedure in food processing industry for improved product stability. Most widely applied technology for dewatering and concentration in food processing is multistage vacuum evaporation (Nene et al. 2008), while it could lead to the loss of aroma. Since membrane distillation and pervaporation are capable of dewatering effluent with insignificant impact from the buildup of concentration, this feature has helped to shed lights in the food industry as a stand-alone concentration technology or a hybrid process with other membrane technologies. Most applications of these two technologies were implemented for the realization of fruit juice volume reduction (Bagger-Jørgensen et al. 2011; Onsekizoglu Bagci 2015; Kujawa et al. 2015; Alves and Coelhoso 2006; Karlsson and Tragardh 1996). Other applications such as dealcholization by pervaporation for the production of nonalcoholic beverages have also been witnessed (Castro-Muñoz 2019).

The associated concerns with the utilization of membrane distillation and pervaporation in food processing industries have been identified as low flux and membrane fouling by high-molecular-weight naturally existing polymers in the fruit juice, which will result in the drastic decline in flux over long-term operation. There are attempts on the fouling mitigation for this specific application of membrane distillation; a pretreatment unit of ultrafiltration (Brinck et al. 2000) and additional enzymatic deproteinization (Lukanin et al. 2003) step were included to remove the majority of polysaccharides and proteins and to decrease the viscosity of the feed for improved hydrodynamic conditions near the membrane.

Apart from membrane fouling, the loss of aroma is also associated with membrane distillation processes. Membrane distillation applies a microporous hydrophobic membrane with minimal selectivity of the vapor permeation across the membrane; this inability can be fulfilled by the integration of pervaporation unit to selectively reduce the transport of aroma into the permeate stream. Thus the combination of osmotic distillation and pervaporation was suggested for the concentration process of ethanol–water extract of *Echinacea* plant (Johnson et al. 2002). Since osmotic distillation can be viewed as a similar process to membrane distillation for its mass and heat transfer mechanism, the combination of pervaporation and membrane distillation technologies for fruit juice volume reduction and other food processing applications can be envisaged; osmotic distillation appears to be more favorable for the production of food concentrates although it suffers significantly from a lower mass transfer rate than membrane distillation (Johnson and Nguyen 2017). Pervaporation was also used as an approach to deodorize the food product for its ability to fine-tune the adsorption rate of aroma (Souchon et al. 2002). In terms of the choice for process selection and design, product integrity as well as productivity should be evaluated.

7.6.2 Pharmaceutical Industries

The most exciting aspect of membrane distillation that has been recognized in the past decade besides the special desalination purposes is its potential application in the pharmaceutical industries, in particular its implementation in the concentration technology for traditional Chinese medicine (TCM) extract. The conventional approach for concentrating the extract can usually be achieved by evaporation technology involving conventional and vacuum evaporation, which requires a considerable amount of energy. The application of membrane distillation apart from its environmental aspect had been overlooked. Not until recently, the possibility of concentrating TCM extract by membrane distillation was explored (Nian et al. 2013; Yu et al. 2008; Ding et al. 2008), and a concentration factor of 16 times was achieved. Since the rise in concentration of the extract will not pose significant impact on the driving force for membrane distillation, it was observed that permeate flux did not suffer from a substantial drop. Membrane distillation is expected to show extraordinary potential in the advancement of TCM extract concentration and purification.

Moreover, although there has not yet been a single study on the demonstration of implementing pervaporation technology in the concentration technology for TCM, the ability of pervaporation to dehydrate and separate solvent from water had been shown elsewhere in the food processing sector (Paz et al. 2017; Smuleac et al. 2010). It is worth pointing out that some TCM extract could contain valuable volatile contents and organic solvents. Concentration of these extract solutions can be problematic for membrane distillation as it does not show a precise control over the selectivity of volatile substances (Yao et al. 2018), in which it was reported the existance of a traceable amount of volatile organic contents in the permeate stream after the treatment by membrane distillation. As previous section suggested, pervaporation could fill the void and inability of membrane distillation when it comes to the preservation of volatile compounds in the extract concentration process and potentially exhibit a lower fouling tendency. When design with careful consideration, the membrane for pervaporation can be tuned to favor the removal of organic solvents while limit the transport of the designated volatile compounds in the extract. Similar to the application of membrane distillation and pervaporation in food processing industry, future study on the design and application of these technologies in TCM extract concentration should also consider the effect of membrane fouling by starch and other hydrosol.

7.7 Conclusions

The unconventional desalination requires treatment process that can handle high salinity at reasonable energy consumption which the traditional desalination technique by reverse osmosis cannot offer. Membrane distillation and pervaporation possess excellent potential in treating hypersaline solution, mostly due to that fact that their driving forces show minor impact imposed by the fluctuation in feed salinity and the utilization of low-grade heat can be realized for these two processes. This review presents the opportunities and challenges for membrane distillation and pervaporation implementation for unconventional desalination.

While the two membrane technologies share similarities with elevating the temperature of the feed for the removal of salt from the aqueous solution, their transport mechanisms are different. Membrane distillation process is driven by the temperature difference across a hydrophobic membrane, whereas pervaporation is driven by the concentration difference through adsorption–diffusion approach. Membrane distillation and pervaporation are both prospective solutions to unconventional desalination. Limitations exist within these two technologies which could hinder their large-scale application. Issues such as wetting and fouling for membrane distillation still need to be addressed. Membranes specifically designed for the desalination application for membrane distillation and pervaporation are lacking, particularly for pervaporation process.

To tackle the wetting issue, modifications on the hydrophobic membranes for membrane distillation are often deployed, rendering the membranes to show superhydrophobicity or omniphobicity. Most approaches involved are to increase surface roughness and the grafting of low surface energy material simultaneously on the membrane. Yet the results are not always promising even for the same coating material. There exists knowledge gap between understanding the fundamental of achieving an omniphobic surface and the characteristics of the real saline feed that contains low surface tension compounds such as oil and surfactants. More studies are required to fill the void on indicating the limit of membrane distillation for the treatment of saline effluent and brine; especially in terms of the oil contents, membrane distillation can withstand from the material and process perspectives.

Future recommendation on the prospective applications for membrane distillation and pervaporation such as beverages production and traditional Chinese medicine extract processing was suggested. While membrane distillation can be a genuine technology for concentrating the liquid extracts, the high selectivity of pervaporation process can be valuable in some cases where the removal or retaining of some substances is desired.

Acknowledgments The authors greatly appreciate the financial support of the Tip-top Scientific and Technical Innovative Youth Talents of Guangdong special support program (Grant No. 2016TQ03C478), the Nansha Science and Technology Program (Grant No. 2017CX012), and the Science and Technology Program of Guangzhou (Grant No. 201904010054). Q. Li gratefully acknowledges support from the Australian Research Council's ARC Linkage program – ARC LP160100622.

References

Adnan S, Hoang M, Wang H, Xie Z (2012) Commercial PTFE membranes for membrane distillation application: effect of microstructure and support material. Desalination 284:297–308. https://doi.org/10.1016/j.desal.2011.09.015

Ali A, Quist-Jensen CA, Macedonio F, Drioli E (2016) On designing of membrane thickness and thermal conductivity for large scale membrane distillation modules. J Membr Sci Res 2:179–185. https://doi.org/10.22079/JMSR.2016.21948

Alves VD, Coelhoso IM (2006) Orange juice concentration by osmotic evaporation and membrane distillation: a comparative study. J Food Eng 74(1):125–133. https://doi.org/10.1016/j.jfoodeng.2005.02.019

Alzahrani S, Mohammad AW, Hilal N, Abdullah P, Jaafar O (2013) Comparative study of NF and RO membranes in the treatment of produced water—Part I: Assessing water quality. Desalination 315:18–26. https://doi.org/10.1016/j.desal.2012.12.004

Arnal JM, Sancho M, Iborra I, Gozálvez JM, Santafé A, Lora J (2005) Concentration of brines from RO desalination plants by natural evaporation. Desalination 182(1):435–439. https://doi.org/10.1016/j.desal.2005.02.036

Bagger-Jørgensen R, Meyer AS, Pinelo M, Varming C, Jonsson G (2011) Recovery of volatile fruit juice aroma compounds by membrane technology: sweeping gas versus vacuum membrane distillation. Innov Food Sci Emerg Technol 12:388–397. https://doi.org/10.1016/j.ifset.2011.02.005

Benko KL, Drewes JE (2008) Produced water in the Western United States: geographical distribution, occurrence, and composition. Environ Eng Sci 25(2):239–246. https://doi.org/10.1089/ees.2007.0026

Boban M, Golovin K, Tobelmann B, Gupte O, Mabry JM, Tuteja A (2018) Smooth, all-solid, low-hysteresis, omniphobic surfaces with enhanced mechanical durability. ACS Appl Mater Interfaces 10(14):11406–11413. https://doi.org/10.1021/acsami.8b00521

Boo C, Lee J, Elimelech M (2016) Omniphobic Polyvinylidene Fluoride (PVDF) membrane for desalination of shale gas produced water by membrane distillation. Environ Sci Technol 50 (22):12275–12282. https://doi.org/10.1021/acs.est.6b03882

Brinck J, Jönsson A-S, Jönsson B, Lindau J (2000) Influence of pH on the adsorptive fouling of ultrafiltration membranes by fatty acid. J Membr Sci 164(1-2):187–194. https://doi.org/10.1016/S0376-7388(99)00212-4

Cao Z, Zeng S, Xu Z, Arvanitis A, Yang S, Gu X, Dong J (2018) Ultrathin ZSM-5 zeolite nanosheet laminated membrane for high-flux desalination of concentrated brines. Sci Adv 4(11):eaau8634. https://doi.org/10.1126/sciadv.aau8634

Castro-Muñoz R (2019) Pervaporation-based membrane processes for the production of non-alcoholic beverages. J Food Sci Technol 56(5):2333–2344. https://doi.org/10.1007/s13197-019-03751-4

Chaudhri SG, Chaudhari JC, Singh PS (2017) Fabrication of efficient pervaporation desalination membrane by reinforcement of poly(vinyl alcohol)–silica film on porous polysulfone hollow fiber. J Appl Polym Sci 135(3):45718. https://doi.org/10.1002/app.45718

Chen L, Shi G, Shen J, Peng B, Zhang B, Wang Y, Bian F, Wang J, Li D, Qian Z, Xu G, Liu G, Zeng J, Zhang L, Yang Y, Zhou G, Wu M, Jin W, Li J, Fang H (2017) Ion sieving in graphene oxide membranes via cationic control of interlayer spacing. Nature 550:380. https://doi.org/10.1038/nature24044

Chen X, Gao X, Fu K, Qiu M, Xiong F, Ding D, Cui Z, Wang Z, Fan Y, Drioli E (2018) Tubular hydrophobic ceramic membrane with asymmetric structure for water desalination via vacuum membrane distillation process. Desalination 443:212–220. https://doi.org/10.1016/j.desal.2018.05.027

Cho CH, Oh KY, Kim SK, Yeo JG, Sharma P (2011) Pervaporative seawater desalination using NaA zeolite membrane: Mechanisms of high water flux and high salt rejection. J Membr Sci 371 (1):226–238. https://doi.org/10.1016/j.memsci.2011.01.049

Crespo JG, Brazinha C (2015) 1 - Fundamentals of pervaporation. In: Basile A, Figoli A, Khayet M (eds) Pervaporation, vapour permeation and membrane distillation. Woodhead Publishing, Oxford, pp 3–17

Deshmukh A, Boo C, Karanikola V, Lin S, Straub AP, Tong T, Warsinger DM, Elimelech M (2018) Membrane distillation at the water-energy nexus: limits, opportunities, and challenges. Energy Environ Sci 11(5):1177–1196. https://doi.org/10.1039/C8EE00291F

Ding Z, Liu L, Yu J, Ma R, Yang Z (2008) Concentrating the extract of traditional Chinese medicine by direct contact membrane distillation. J Membr Sci 310(1):539–549. https://doi.org/10.1016/j.memsci.2007.11.036

Du X, Zhang Z, Carlson KH, Lee J, Tong T (2018) Membrane fouling and reusability in membrane distillation of shale oil and gas produced water: effects of membrane surface wettability. J Membr Sci 567:199–208. https://doi.org/10.1016/j.memsci.2018.09.036

Duke MC, O'Brien-Abraham J, Milne N, Zhu B, Lin JYS, Diniz da Costa JC (2009) Seawater desalination performance of MFI type membranes made by secondary growth. Sep Purif Technol 68(3):343–350. https://doi.org/10.1016/j.seppur.2009.06.003

Essalhi M, Khayet M (2015) 10 – Fundamentals of membrane distillation. In: Basile A, Figoli A, Khayet M (eds) Pervaporation, vapour permeation and membrane distillation. Woodhead Publishing, Oxford, pp 277–316

Eykens L, De Sitter K, Dotremont C, De Schepper W, Pinoy L, Van Der Bruggen B (2017) Wetting resistance of commercial membrane distillation membranes in waste streams containing surfactants and oil. Appl Sci 7(118). https://doi.org/10.3390/app7020118

Fang H, Gao JF, Wang HT, Chen CS (2012) Hydrophobic porous alumina hollow fiber for water desalination via membrane distillation process. J Membr Sci 403–404:41–46. https://doi.org/10.1016/j.memsci.2012.02.011

Feng B, Xu K, Huang A (2016) Covalent synthesis of three-dimensional graphene oxide framework (GOF) membrane for seawater desalination. Desalination 394:123–130. https://doi.org/10.1016/j.desal.2016.04.030

Francis L, Ghaffour N, Alsaadi AA, Amy GL (2013) Material gap membrane distillation: a new design for water vapor flux enhancement. J Membr Sci 448:240–247. https://doi.org/10.1016/j.memsci.2013.08.013

Franken ACM, Nolten JAM, Mulder MHV, Bargeman D, Smolders CA (1987) Wetting criteria for the applicability of membrane distillation. J Membr Sci 33(3):315–328. https://doi.org/10.1016/S0376-7388(00)80288-4

Garba MD, Muhammad Usman MA, Mazumder J, Al-Ahmed A, Inamuddin (2019) Complexing agents for metal removal using ultrafiltration membranes: a review. Environ Chem Lett. https://doi.org/10.1007/s10311-019-00861-5

Goh K, Setiawan L, Wei L, Si R, Fane AG, Wang R, Chen Y (2015) Graphene oxide as effective selective barriers on a hollow fiber membrane for water treatment process. J Membr Sci 474:244–253. https://doi.org/10.1016/j.memsci.2014.09.057

Gopi G, Arthanareeswaran G, Af I (2019) Perspective of renewable desalination by using membrane distillation. Chem Eng Res Des 144:520–537. https://doi.org/10.1016/j.cherd.2019.02.036

Han R, Zhang S, Xing D, Jian X (2010) Desalination of dye utilizing copoly(phthalazinone biphenyl ether sulfone) ultrafiltration membrane with low molecular weight cut-off. J Membr Sci 358(1):1–6. https://doi.org/10.1016/j.memsci.2010.03.036

Han Y, Jiang Y, Gao C (2015) High-flux graphene oxide nanofiltration membrane intercalated by carbon nanotubes. ACS Appl Mater Interfaces 7(15):8147–8155. https://doi.org/10.1021/acsami.5b00986

Hayes T, Arthur D (2004) Overview of emerging produced water treatment technologies. In: The 11th annual international petroleum environmental conference, Albuquerque, NM

He Y, Jiang Z-W (2008) Technology review: treating oilfield wastewater. Filtr Sep 45(5):14–16. https://doi.org/10.1016/S0015-1882(08)70174-5

Hu M, Mi B (2014) Layer-by-layer assembly of graphene oxide membranes via electrostatic interaction. J Membr Sci 469:80–87. https://doi.org/10.1016/j.memsci.2014.06.036
Huang Y-X, Wang Z, Jin J, Lin S (2017) Novel janus membrane for membrane distillation with simultaneous fouling and wetting resistance. Environ Sci Technol 51:13304–13310. https://doi.org/10.1021/acs.est.7b02848
Hussain A, Minier-Matar J, Janson A, Adham S (2015) Treatment of produced water from oil and gas operations by membrane distillation. In: Al-Marri MJ, Eljack FT (eds) Proceedings of the 4th international gas processing symposium. Elsevier, Oxford, pp 285–292
Huth E, Muthu S, Ruff L, Brant JA (2014) Feasibility assessment of pervaporation for desalinating high-salinity brines. J Water Reuse Desalin 4(2):109–124. https://doi.org/10.2166/wrd.2014.038
Igunnu ET, Chen GZ (2012) Produced water treatment technologies. Int J Low-Carbon Technol 9 (3):157–177. https://doi.org/10.1093/ijlct/cts049
Ji X, Curcio E, Al Obaidani S, Di Profio G, Fontananova E, Drioli E (2010) Membrane distillation-crystallization of seawater reverse osmosis brines. Sep Purif Technol 71(1):76–82. https://doi.org/10.1016/j.seppur.2009.11.004
Johnson RA, Nguyen MH (2017) Theoretical aspects of osmotic distillation. In: Understanding membrane distillation and osmotic distillation. Wiley, Hoboken
Johnson RA, Sun JC, Sun J (2002) A pervaporation–microfiltration–osmotic distillation hybrid process for the concentration of ethanol–water extracts of the Echinacea plant. J Membr Sci 209 (1):221–232. https://doi.org/10.1016/S0376-7388(02)00322-8
Julian H, Meng S, Li H, Ye Y, Chen V (2016) Effect of operation parameters on the mass transfer and fouling in submerged vacuum membrane distillation crystallization (VMDC) for inland brine water treatment. J Membr Sci 520:679–692. https://doi.org/10.1016/j.memsci.2016.08.032
Kaminski W, Marszalek J, Tomczak E (2018) Water desalination by pervaporation – comparison of energy consumption. Desalination 433:89–93. https://doi.org/10.1016/j.desal.2018.01.014
Karlsson HOE, Tragardh G (1996) Applications of pervaporation in food processing. Trends Food Sci Technol 7(3):78–83. https://doi.org/10.1016/0924-2244(96)81301-X
Khajavi S, Jansen JC, Kapteijn F (2010) Production of ultra pure water by desalination of seawater using a hydroxy sodalite membrane. J Membr Sci 356(1):52–57. https://doi.org/10.1016/j.memsci.2010.03.026
Khosravi J, Alamdari A (2009) Copper removal from oil-field brine by coprecipitation. J Hazard Mater 166(2):695–700. https://doi.org/10.1016/j.jhazmat.2008.11.079
Kim J, Kwon H, Lee S, Lee S, Hong S (2017) Membrane distillation (MD) integrated with crystallization (MDC) for shale gas produced water (SGPW) treatment. Desalination 403:172–178. https://doi.org/10.1016/j.desal.2016.07.045
Kim J, Kim J, Hong S (2018) Recovery of water and minerals from shale gas produced water by membrane distillation crystallization. Water Res 129:447–459. https://doi.org/10.1016/j.watres.2017.11.017
Koops GH, Smolders CA (1991) Pervaporation membrane separation process. In: Huang RYM (ed) Membrane science and technology series. Elsevier, Amesterdam, pp 249–273
Kujawa J, Guillen-Burrieza E, Arafat HA, Kurzawa M, Wolan A, Kujawski W (2015) Raw juice concentration by osmotic membrane distillation process with hydrophobic polymeric membranes. Food Bioprocess Technol 8(10):2146–2158. https://doi.org/10.1007/s11947-015-1570-4
Li L, Ezeokonkwo CI, Lin L, Eliseeva L, Kallio W, Boney CL, Howard P, Samuel MM (2010) Well treatment fluids prepared with oilfiled produced water: Part II. In: SPE annual technical conference and exhibition, Florence, Italy
Li L, Sun H, Qu Q, Mehle MP, Ault MG, Morse A, Zhou J, Smith DD (2014) High-temperature fracturing fluids using produced water with extremely high TDS and hardness. In: International petroleum technology conference, Kuala Lumpur, Malaysia, 2014/12/10/

Li L, Hou J, Ye Y, Mansouri J, Chen V (2017) Composite PVA/PVDF pervaporation membrane for concentrated brine desalination: salt rejection, membrane fouling and defect control. Desalination 422:49–58. https://doi.org/10.1016/j.desal.2017.08.011

Li Q, Cao B, Li P (2018) Fabrication of high performance pervaporation desalination composite membranes by optimizing the support layer structures. Ind Eng Chem Res 57 (32):11178–11185. https://doi.org/10.1021/acs.iecr.8b02505

Li J, Guo S, Xu Z, Li J, Pan Z, Zhiping D, Cheng F (2019a) Preparation of omniphobic PVDF membranes with silica nanoparticles for treating coking wastewater using direct contact membrane distillation: electrostatic adsorption vs. chemical bonding. J Membr Sci 574:349–357. https://doi.org/10.1016/j.memsci.2018.12.079

Li L, Hou J, Chen V (2019b) Pinning down the water transport mechanism in graphene oxide pervaporation desalination membranes. Ind Eng Chem Res 58(10):4231–4239. https://doi.org/10.1021/acs.iecr.8b06081

Li Q, Beier L-J, Tan J, Brown C, Lian B, Zhong W, Wang Y, Ji C, Pan D, Li T, Le Clech P, Tyagi H, Liu X, Leslie G, Taylor RA (2019c) An integrated, solar-driven membrane distillation system for water purification and energy generation. Appl Energy 237:534–548. https://doi.org/10.1016/j.apenergy.2018.12.069

Lian B, Deng J, Leslie G, Bustamante H, Sahajwalla V, Nishina Y, Joshi RK (2017) Surfactant modified graphene oxide laminates for filtration. Carbon 116:240–245. https://doi.org/10.1016/j.carbon.2017.01.102

Lian B, De Luca S, You Y, Alwarappan S, Yoshimura M, Sahajwalla V, Smith SC, Leslie G, Joshi RK (2018) Extraordinary water adsorption characteristics of graphene oxide. Chem Sci 9:5106–5111. https://doi.org/10.1039/c8sc00545a

Liang B, Pan K, Li L, Giannelis EP, Cao B (2014) High performance hydrophilic pervaporation composite membranes for water desalination. Desalination 347:199–206. https://doi.org/10.1016/j.desal.2014.05.021

Liang B, Wu Z, Qi G, Lin S, Nan Q, Liu Y, Cao B, Pan K (2015) High performance graphene oxide/polyacrylonitrile composite pervaporation membranes for desalination applications. J Mater Chem A 3(9):5140–5147. https://doi.org/10.1039/C4TA06573E

Lin J, Murad S (2001) A computer simulation study of the separation of aqueous solutions using thin zeolite membranes. Mol Phys 99(14):1175–1181. https://doi.org/10.1080/00268970110041236

Lu D, Pan L, Wu X, He G, Jiang X (2017) Simultaneous recovery and crystallization control of saline organic wastewater by membrane distillation crystallization. AIChE J 63(6):2187–2197. https://doi.org/10.1002/aic.15581

Lukanin OS, Gunko SM, Bryk MT, Nigmatullin RR (2003) The effect of content of apple juice biopolymers on the concentration by membrane distillation. J Food Eng 60(3):275–280. https://doi.org/10.1016/S0260-8774(03)00048-7

Memsys Water Technologies GmbH (2013) Case study of Memsys plant for shale gas wastewater treatment in US. Accessed April 4th. https://www.memsys.eu/markets/oil-gas-and-ctx.html

Meng S, Hsu Y-C, Ye Y, Chen V (2015) Submerged membrane distillation for inland desalination applications. Desalination 361:72–80. https://doi.org/10.1016/j.desal.2015.01.038

Miladi R, Frikha N, Kheiri A, Gabsi S (2019) Energetic performance analysis of seawater desalination with a solar membrane distillation. Energy Convers Manag 185:143–154. https://doi.org/10.1016/j.enconman.2019.02.011

Naim M, Elewa M, El-Shafei A, Moneer A (2015) Desalination of simulated seawater by purge-air pervaporation using an innovative fabricated membrane. Water Sci Technol 72(5):785–793. https://doi.org/10.2166/wst.2015.277

Nene S, Patil G, Raghavarao KSMS (2008) Membrane distillation in food processing. In: Pabby AK, Rizvi SSH, Requena AMS (eds) Handbook of membrane separations. CRC Press, Boca Raton, pp 513–551

Nian L-J, Han Y-Z, Lu Y-Y, Kong P, Gao R-C (2013) Concentration of traditional chinese medicine extraction by multiple-effect membrane distillation. Chin J Pharm 44(1):76–80

Nigiz FU (2019) Preparation and performance of ultra-thin surface coated pervaporation membranes for seawater purification. Water Supply. https://doi.org/10.2166/ws.2019.053

Onsekizoglu Bagci P (2015) Potential of membrane distillation for production of high quality fruit juice concentrate. Crit Rev Food Sci Nutr 55(8):1098–1113. https://doi.org/10.1080/10408398.2012.685116

Pantoja CE, Nariyoshi YN, Seckler MM (2015) Membrane distillation crystallization applied to brine desalination: a hierarchical design procedure. Ind Eng Chem Res 54(10):2776–2793. https://doi.org/10.1021/ie504695p

Paz AI, Blanco CA, Andrés-Iglesias C, Palacio L, Prádanos P, Hernández A (2017) Aroma recovery of beer flavors by pervaporation through polydimethylsiloxane membranes. J Food Process Eng 40(6):e12556. https://doi.org/10.1111/jfpe.12556

Ray SS, Chen S-S, Sangeetha D, Chang H-M, Thanh CND, Le QH, Hong-Ming K (2018) Developments in forward osmosis and membrane distillation for desalination of waters. Environ Chem Lett 16(4):1247–1265. https://doi.org/10.1007/s10311-018-0750-7

Razmjou A, Arifin E, Dong G, Mansouri J, Chen V (2012) Superhydrophobic modification of TiO_2 nanocomposite PVDF membranes for applications in membrane distillation. J Membr Sci 415–416:850–863. https://doi.org/10.1016/j.memsci.2012.06.004

Rezakazemi M, Khajeh A, Mesbah M (2018) Membrane filtration of wastewater from gas and oil production. Environ Chem Lett 16(2):367–388. https://doi.org/10.1007/s10311-017-0693-4

Riley SM, Ahoor DC, Oetjen K, Cath TY (2018) Closed circuit desalination of O&G produced water: an evaluation of NF/RO performance and integrity. Desalination 442:51–61. https://doi.org/10.1016/j.desal.2018.05.004

Roshani R, Ardeshiri F, Peyravi M, Jahanshahi M (2018) Highly permeable PVDF membrane with PS/ZnO nanocomposite incorporated for distillation process. RSC Adv 8:23499–23515. https://doi.org/10.1039/C8RA02908C

Smuleac V, Wu J, Nemser S, Majumdar S, Bhattacharyya D (2010) Novel perfluorinated polymer-based pervaporation membranes for separation of solvent/water mixtures. J Membr Sci 352 (1–2):41–49. https://doi.org/10.1016/j.memsci.2010.01.058

Souchon I, Pierre FX, Athes-Dutour V, Marin M (2002) Pervaporation as a deodorization process applied to food industry effluents: recovery and valorisation of aroma compounds from cauliflower blanching water. Desalination 148(1):79–85. https://doi.org/10.1016/S0011-9164(02)00657-4

Sun D, Yang Q-C, Sun H-L, Liu J-M, Xing Z-L, Li B-B (2016) Effects of PES support layer structure on pervaporation performances of PDMS/PES hollow fiber composite membranes. Desalin Water Treat 57(20):9123–9135. https://doi.org/10.1080/19443994.2015.1028458

Swenson P, Tanchuk B, Gupta A, An W, Kuznicki SM (2012) Pervaporative desalination of water using natural zeolite membranes. Desalination 285:68–72. https://doi.org/10.1016/j.desal.2011.09.035

Tun CM, Fane AG, Matheickal JT, Sheikholeslami R (2005) Membrane distillation crystallization of concentrated salts—flux and crystal formation. J Membr Sci 257(1):144–155. https://doi.org/10.1016/j.memsci.2004.09.051

Wang Q, Li N, Bolto B, Hoang M, Xie Z (2016) Desalination by pervaporation: a review. Desalination 387:46–60. https://doi.org/10.1016/j.desal.2016.02.036

Woo YC, Kim Y, Yao M, Tijing LD, Choi J, Lee S, Kim S, Shon H (2018) Hierarchical composite membranes with robust omniphobic surface using layer-by-layer assembly technique. Environ Sci Technol 52(4):2186–2196. https://doi.org/10.1021/acs.est.7b05450

Xie Z, Ng D, Hoang M, Zhang J, Gray S (2018) Study of hybrid PVA/MA/TEOS pervaporation membrane and evaluation of energy requirement for desalination by pervaporation. Int J Environ Res Public Health 15(9):1913. https://doi.org/10.3390/ijerph15091913

Yang H, Elma M, Wang DK, Motuzas J, Diniz da Costa JC (2017) Interlayer-free hybrid carbon-silica membranes for processing brackish to brine salt solutions by pervaporation. J Membr Sci 523:197–204. https://doi.org/10.1016/j.memsci.2016.09.061

Yao M, Woo YC, Tijing LD, Choi J-S, Shon HK (2018) Effects of volatile organic compounds on water recovery from produced water via vacuum membrane distillation. Desalination 440:146–155. https://doi.org/10.1016/j.desal.2017.11.012

Yu JF, Ding ZW, Long BW, Liu LY, Yang ZR (2008) Concentration of a traditional Chinese medicine extract by direct contact membrane distillation. J Beijing Univ Chem Technol 35 (2):10–13

Zarghami S, Mohammadi T, Sadrzadeh M (2019) Preparation, characterization and fouling analysis of in-air hydrophilic/underwater oleophobic bio-inspired polydopamine coated PES membranes for oily wastewater treatment. J Membr Sci 582:402–413. https://doi.org/10.1016/j.memsci.2019.04.020

Zheng R, Chen Y, Wang J, Song J, Li X-M, He T (2018) Preparation of omniphobic PVDF membrane with hierarchical structure for treating saline oily wastewater using direct contact membrane distillation. J Membr Sci 555:197–205. https://doi.org/10.1016/j.memsci.2018.03.041

Zhong Z, Xing W, Zhang B (2013) Fabrication of ceramic membranes with controllable surface roughness and their applications in oil/water separation. Ceram Int 39(4):4355–4361. https://doi.org/10.1016/j.ceramint.2012.11.019

Zhong W, Li H, Ye Y, Chen V (2016) Evaluation of silica fouling for coal seam gas produced water in a submerged vacuum membrane distillation system. Desalination 393:52–64. https://doi.org/10.1016/j.desal.2016.03.004

Zhong W, Hou J, Yang H-C, Chen V (2017) Superhydrophobic membranes via facile bio-inspired mineralization for vacuum membrane distillation. J Membr Sci 540:98–107. https://doi.org/10.1016/j.memsci.2017.06.033

Zhong W, Ji C, Li H, Hou J, Chen V (2018) Fouling mitigation in submerged VMD for the treatment of brackish groundwater concentrates with transverse vibration and crystallizer. Desalination 426:32–41. https://doi.org/10.1016/j.desal.2017.10.024

Zhu P, Kong T, Tang X, Wang L (2017) Well-defined porous membranes for robust omniphobic surfaces via microfluidic emulsion templating. Nat Commun 8:15823. https://doi.org/10.1038/ncomms15823

Zou T, Kang G, Zhou M, Li M, Cao Y (2019) Submerged vacuum membrane distillation crystallization (S-VMDC) with turbulent intensification for the concentration of NaCl solution. Sep Purif Technol 211:151–161. https://doi.org/10.1016/j.seppur.2018.09.072

Chapter 8
Role and Characterization of Nano-Based Membranes for Environmental Applications

Oluranti Agboola, Rotimi Sadiku, Patricia Popoola, Samuel Eshorame Sanni, Peter Adeniyi Alaba, Daniel Temitayo Oyekunle, Victoria Oluwaseun Fasiku, and Mukuna Patrick Mubiayi

Contents

O. Agboola (✉)
Department of Chemical Engineering, Covenant University, Ota, Ogun State, Nigeria

Department of Chemical, Metallurgical and Materials Engineering, Tshwane University of Technology, Pretoria, South Africa

R. Sadiku · P. A. Alaba
Department of Chemical, Metallurgical and Materials Engineering, Tshwane University of Technology, Pretoria, South Africa

P. Popoola · V. O. Fasiku
Department of Pharmaceutical Sciences, University of KwaZulu-Natal, Durban, South Africa

S. E. Sanni · D. T. Oyekunle
Department of Chemical Engineering, Covenant University, Ota, Ogun State, Nigeria

M. P. Mubiayi
Department of Mechanical Engineering Science, University of Johannesburg, Johannesburg, South Africa

Z. Zhang et al. (eds.), *Membranes for Environmental Applications*, Environmental Chemistry for a Sustainable World 42, https://doi.org/10.1007/978-3-030-33978-4_8

Abstract Environmental issues emerge as a result of the harmful effects of human activities from different points of sources on biophysical environment. Lots of environmental damages can be rectified. The prevention of further damage can be achieved through the utilization of membrane separation processes. The utilization of membrane separation process to combat environmental pollution illustrates the application of membrane materials to effectively prevent environmental pollution in a sustainable manner. Nano-based membranes usually fabricated from organic polymer-based nanocomposites have proven to be promising membrane separation technology for environmental issues. In this report, we reviewed the role and characterizations of nano-based membranes for environmental applications. Thus, the major points are, firstly, factors influencing nano-based membranes performance and, secondly, important characterization techniques commonly used in characterizing the surface of membranes fabricated with the incorporation of nanomaterials. Thirdly, we reviewed the models used in characterizing the transport properties across nano-based membranes since these properties are principally controlled by the surface layer, thickness, porosity, and pore size. Finally, the environmental applications of nano-based membranes are reviewed.

Keywords Nano-based membranes · Gas separation · Desalination · Solid pollution · Air pollution · Solution diffusion model · Extended Nernst–Planck model · Pathogens · Transport properties · membrane self-cleaning

Nomenclature

NF	Nanofiltration
V_p	Permeate volume
RO	Reverse osmosis
$\%R$	Percentage rejection
SEM	Scanning electron microscopy
J	Flux
AFM	Atomic force microscopy
$C_{i,\ m}$	Bulk feed concentration
CNT	Carbon nanotube

$C_{i,\,p}$	Permeate concentration
DE	Dielectric exclusion
z_i	Valence of ion (i)
DSPM	Donnan–steric partitioning pore model
$D_{i,\,p}$	Hindered diffusivity (m^2/s)
TEM	Transmission electron microscope
γ_{SV}	Solid–vapor interfacial energy
XRD	X-ray powder diffractometer
γ_{SL}	Solid–liquid interfacial energy
PSCF	Preferential sorption/capillary flow
γ_{LV}	Liquid–vapor interfacial energy
FTIR	Fourier-transform infrared
θ_γ	Equilibrium contact angle
T	Absolute temperature (K)
$K_{i,\,c}$	Convection hindrance factor
c_i	Concentration of ions in the membrane (mol/m^3)
F	Faraday constant (C/mol)
ϕ	Equilibrium partition coefficient
ψ	Electrical potential (V)
R	Universal gas constant (J/mol.K)
D_{sm}	Diffusion coefficient
c_T	Total molar concentration
x	Membrane thickness
K_s	Solute distribution coefficient
APAN	Aminated polyacrylonitrile
MWCNTs	Multi-walled carbon nanotubes
X_d	Effective charge density
r_P	Pore radius
e	Electronic charge
ε_b	Dielectric constant of the bulk
YSZ	yttrium-stabilized zirconia
ε_m	Dielectric constant of the membrane material
GO	Graphene oxide
ε_p	Dielectric constant inside the pores
CM	ceramic membranes
DSPM-DE	Donnan–steric partitioning pore model with dielectric exclusion

8.1 Introduction

The developments in nanoscale investigations have made a promising invention of nano-based membranes that is economically feasible and environmentally stable for effective environmental applications (Amin and Alazba 2014). Nanomaterials possess exceptional, physical, chemical, biological, and size-dependent properties connected to their structure and higher specific surface area to volume. These properties give fast dissolution, strong sorption, high reactivity, and discontinuous features such as localized surface plasmon resonance, super-paramagnetism and quantum confinement effect. These explicit nano-based features enable the advancement of new high-technology materials such as adsorption materials, nano-catalysts, functionalized surfaces, coatings, reagents, and membranes for more efficient environmental applications (Kanagalakshmi et al. 2018). Nano-based membranes separate chemical species through filtration mechanism by employing nano-sized porous structure of membrane materials. There are lots of investigation regarding the use of organic polymeric materials for the synthesis and modification of nano-based membranes such as nanofiltration (NF). However, the integration of nanofillers like nanoparticles, such as graphene and carbon nanotubes in the polymeric materials for the synthesis of nano-based membranes, gives excellent properties. Nanoparticles are types of nanofillers (Verdejo et al. 2011). Hence, nano-based membranes are thin and flexible materials that can be fabricated out of polymeric materials and the combinations of polymeric material with nanofillers. These nanofillers are promoting the advancement of more efficient nano-based membranes for environmental applications. Thus, nano-based membranes are organic polymer-based nanocomposites that possess nanoscale thickness across microscopic dimensions (approximately 1 to over 100 μm) with a thickness less than 100 nm, and they are effective filters functioning at the high molecular level. They are not only ultra-lightweight but also robust and flexible. From the mechanical viewpoint, these nano-membranes can exhibit low flexural rigidity; however, they have extremely high toughness, with reported elastic moduli of 1–10 GPa and ultimate strengths of up to 100 MPa (Jiang et al. 2005, 2006). Apart from the theoretical and experimental interest, nano-based membranes have, without a doubt, combined these mechanical characteristics with structural and morphological features leading to a broad spectrum of environmental applications in desalination, solid pollution control, and air pollution control (Cheng et al. 2009). The outline of the environmental applications of nano-based membranes is illustrated in Fig. 8.1. Furthermore, there are several contributing factors responsible for the separation performance of nano-based membranes for different environmental applications. The next subsection discussed the important contributing factors influencing for the separation performance of nano-based membranes.

8.1.1 Factors Influencing Nano-Based Membranes Performance

The accomplishment of using membranes is strictly associated with the essential properties of the membranes. To a larger magnitude, interfacial interactions between the surfaces of the membrane, surrounding environment and solute, control the

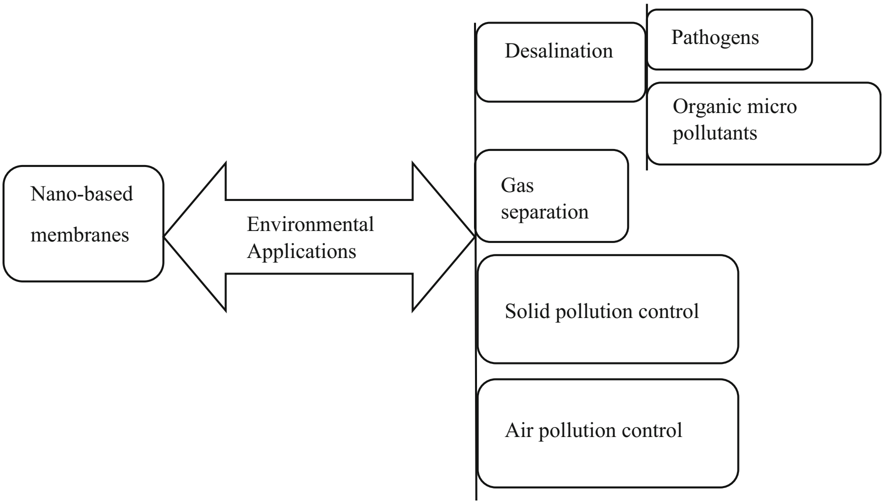

Fig. 8.1 An outline of environmental applications of nano-based membranes

performance of the membrane. These interactions have significant influence on transport characteristics, selectivity, fouling tendency, and bio- and hemo-compatibility of the membrane (Van Rijn 2004). Porous and nonporous nanofillers are the major inorganic materials used for the fabrication of nano-based membranes (Chung et al. 2007). For porous membranes, transport takes place by convective flow with sieving mechanism such as size/shape sieving or adsorption (Baker 2004). The interactions of solutes with the pore surface may significantly affect the performance of nano-based membrane (Li et al. 2012). Hence, porous nanofillers usually enhance the filtering property of the polymeric membranes owing to their structure and pore size. The ability to fabricate membranes with a desired pore size and a narrow pore size distribution will allow a defined control over molecular transport (Li et al. 2012). Nonetheless, nonporous nanofillers increase the permeability by splitting the packing of the polymer chain and increasing the polymer free volume (Aroon et al. 2010). The choice of both nanofillers and polymer matrix is of great importance in determining the separation performance of nano-based membranes (Najari et al. 2015). The appropriate choice of material or surface functionalization of current membrane will be advantageous to the performance of membrane by reducing the possibility of concentration polarization and membrane fouling (Li et al. 2012). Hence, the technical performance of nano-based membranes is characterized by calculating the flux (J) which is measured from the permeate volume (V_p) divided by the surface area (A) of membrane at particular time (t), represented by Eq. (8.1). Furthermore, the performance of nano-based membranes is also characterized by the percentage rejection ($\%R$) of contaminants, which is the membrane's ability to retain contaminants; it is calculated by Eq. (8.2), where C_f and C_p are the concentrations in the feed and permeate, respectively (Izadpanah and Javidnia 2012). In common with other membrane processes, the summary of critical membrane characteristics that

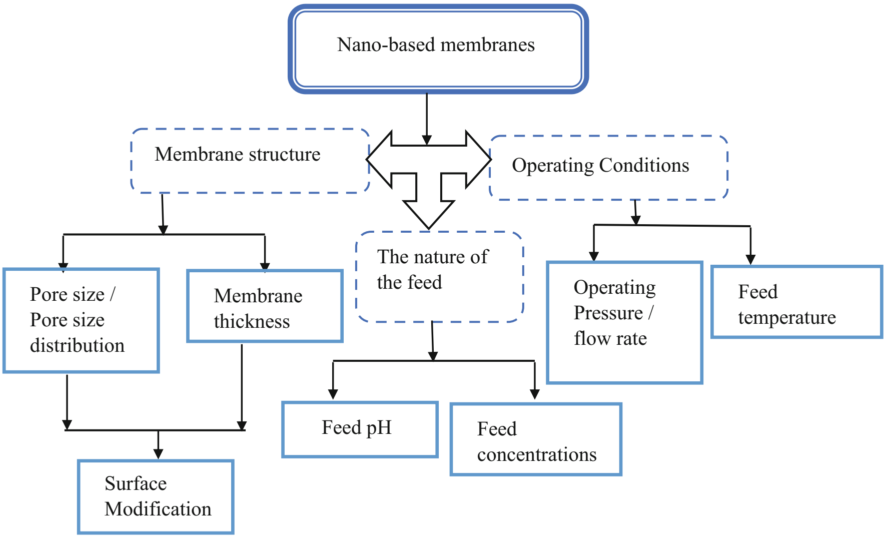

Fig. 8.2 A summary of critical membrane characteristics that affect the performance

determine performance of membranes required in various applications is shown in Fig. 8.2, and they are discussed in the following subsections.

$$J = \frac{V_p}{A \times t} \tag{8.1}$$

$$\%R = \frac{C_f - C_p}{C_f} \times 100 \tag{8.2}$$

Membrane Structure

Polymeric membranes and membranes fabricated with the integration of nano-based materials display a broad range in their physical structure and the material they are made from (Strathmann 2011). These membranes can be classified according to their morphology: dense homogeneous polymer membranes and porous membranes. The dense homogeneous membranes only have a practical usefulness when they are fabricated from a highly permeable polymer such as silicone. Usually, the permeate flow across the membrane is relatively low, since a minimal thickness is needed to offer the membrane mechanical stability (Ladewig and Al-Shaeli 2017). Porous membranes are divided according to their pore diameter (d_p): microporous ($d_p <$ 2 nm), mesoporous (2 nm $< d_p >$ 50 nm), and macroporous ($d_p >$ 50 nm) (Gallucci et al. 2011). Nonetheless, the performance and efficiency of porous membranes is in a greater extent, determined by their internal structure rather than by the material. Hence, the selectivity of porous membranes mostly depends on the pore structure and the pore size distribution such as the mean pore size and the polydispersity (Marrufo-Hernández et al. 2018). Furthermore, the changes in the performance of the membranes have been associated with the structural changes using the Donnan–steric partitioning pore model developed by Bowen and coworkers. This model was founded on the extended Nernst–Plank equation and has frequently been used to describe commercial NF membranes (Bowen and Mukhtar 1996). The features that describe nano-based membranes structure are discussed in the following subsections.

Pore Size and Pore Size Distribution

Dense and nonporous inorganic membranes are made of either solid layers of metals (palladium, silver, alloys) or solid electrolytes. The electrolyte layer permits the diffusion of hydrogen and oxygen, and it also permits the transfer of ions across the membrane pores. Dense membrane can also have a support layer of immobilized liquid such as molten state immobilized in porous steel or ceramic supports. This fills the membrane pores by creating a semipermeable layer. However, the pore structure of the dense membranes is subject to the procedure of fabrication (Fard et al. 2018). The pore size and pore size distribution of nano-based membrane are closely associated with membrane performance. Pore size of membrane is a determinant of membrane rejection level on uncharged contaminant (Mulyanti and Susanto 2018). Variation in pore sizes has been found to significantly influence membrane performance. For example, Mehta and Zydney (2005) investigated the effect of pore size distribution in track-etched membranes on the permeability–selectivity characteristics of ultrafiltration membranes. Kanani et al. (2010) studied the impact of pore geometry on the trade-off between the selectivity and permeability for membranes with pore size below 100 nm. Their results clearly demonstrated that membranes with slit-shaped pores have higher performance, i.e., greater selectivity at a given value of the permeability, than membranes with cylindrical pores. Furthermore, theoretical calculations indicated that this improved performance becomes much less pronounced as the breadth of the pore size distribution increases. However, the pore size and the pore size distribution of the nano-based membranes depend on the application for which it would be used.

Membrane Thickness

A membrane is called a symmetric or isotropic membrane when the separation layer of the membrane cannot be distinguished in the direction of the membrane thickness. Hence, the support layer in the symmetric membrane is designed to offer mechanical robustness for the membrane (Fard et al. 2018). Contrarily, composite or asymmetric (anisotropic) membranes are membranes with a clearly distinguishable top layer and a supporting layer. The majority of the flow resistance (or pressure drop) for these types of membranes occurs primarily in the thin separation layer. Since both

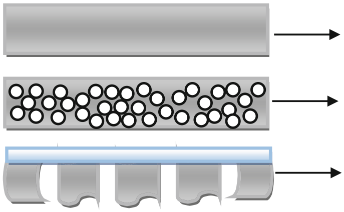

Fig. 8.3 Schematic diagrams of different types of membranes structure and thickness

selectivity and permeability are important for the separation process, the properties of the separation layer with regard to membrane thickness are of utmost importance (Fard et al. 2018).

However, the performance of nano-based membrane thickness depends on the method of fabrication. Hence, both porous and nonporous membranes can be symmetrical or asymmetrical. Figure 8.3 gives the schematic illustration of different types of membranes structure and thickness. A dense skin layer offers selectivity, and a much more open bulk structure affords mechanical support without greatly increasing flow resistance (Paul and Jons 2016). The thickness of the dense skin for nano-based phase-inverted membranes is not at all times measurable or even well-defined, and the thickness clearly varies between membranes. However, the dense selective layer at the top surface is typically thicker than it would usually be, when obtained by interfacial polymerization for nano-based membranes (10–200 nm). At the same time, the discriminating layer of phase-inverted membranes is usually thinner than most free-standing coatings which is without defects and can easily be applied. Lower than this selective layer, pore size speedily increases as one moves into the bulk structures. As a result of this large asymmetry, the majority of resistance to flow for immersion precipitation membranes is occasionally attributed to the region near the thin selective layer (Paul and Jons 2016). Nonetheless, closer analysis has often shown otherwise (Valadez-Blanco and Livingston 2009), and prospects could further exist in order to optimize and decrease contributions to flow resistance from within the bulk or lower surface (Paul and Jons 2016). However, the total resistance of a membrane mass transfer depends on the total thickness of membranes. Hence, a decrease in membrane thickness results in an increased permeation rate (Ladewig and Al-Shaeli 2017). Mansourpanah and Gheshlaghi (2012) used different ethanol amines at various concentrations to produce membranes. The effects of adding these ethanol amines on the performance and morphology of membranes at 200 μm and 280 μm thick were investigated. The results showed that membrane performance in the presence of these additives is strongly related to the thickness of the casting film as well as the type of ethanol amine added. Furthermore, surface modifiers are used to enhance membrane performance. The quantity of the deposited modifier determines the thickness of the membrane layer; hence, the thickness of the modified membrane can easily be adjusted by varying the quantity/concentration of the modifier (Ariono and Wenten 2017).

Surface Modification

The correct choice of the membrane material and surface modification of membranes play a significant role in reducing the adsorption of feed components for nano-based membranes (Dewettinck et al. 2018). Polyamide thin film composite membranes are becoming more extensively used for water desalination both in industrial and experimental plants. Furthermore, these membranes are used in reverse osmosis process as a result of their superior properties. However, trade-off between the permeability and the salt rejections, fouling, and chlorination are seriously limiting their superior operational functions (El-Arnaouty et al. 2018). Thus, several strategies have been explored to solve these problems. Among such strategies is the surface modifications by grafting, and nanoparticles incorporations have been identified to be the most effective ones (Dihua et al. 2010; Balta et al. 2012; Isawia et al. 2016). Dihua et al. (2010) presented the surface modification of the commercial aromatic polyamide thin-film composite-reverse osmosis membranes with thermo-responsive copolymers poly(N-isopropylacrylamide-co-acrylamide) for improved membrane properties. Their results showed that thermo-responsive copolymer poly (N-isopropylacrylamide-co-acrylamide) can be successfully deposited on the surface of the commercial aromatic polyamide thin-film composite-reverse osmosis membrane by dip-coating method, under certain conditions. An increased surface hydrophilicity was observed which would compensate for the reduction in membrane permeability. In addition, the surface coating layer of copolymer poly (N-isopropylacrylamide-co-acrylamide) had little influence on the salt rejection of the modified thin-film composite membrane. Balta et al. (2012) reported a new outlook on the enhancement of membranes with nanoparticles by proposing the use of zinc oxide as an alternative to titanium dioxide. They investigated the synthesis of zinc oxide enhanced membranes and evaluated the performance of mixed-matrix membranes with zinc oxide nanoparticles. It was shown that the new membrane materials embedded with zinc oxide nanoparticles have significantly improved the membrane features. The results showed an overall improvement compared to the neat membranes in terms of permeability, dye rejection, and fouling resistance by adding zinc oxide nanoparticles even in small and ultralow concentrations. Konruang et al. (2014) examined the surface modification of polysulfone membrane by UV irradiation. They reported that FTIR analysis revealed the formations of polar functional groups such as hydroxyl and carbonyl groups. Accordingly, the surface of asymmetric polysulfone membranes was changed from slightly hydrophobic to hydrophilic by UV irradiation, leading to an improvement of the water flux. Isawia et al. (2016) also reported a new approach for the modification of polyamide thin film composite membrane by using synthesized zinc oxide nanoparticles in order to enhance the membrane performances for reverse osmosis water desalination. The zinc oxide nanoparticles modified polymerization of hydrophilic methacrylic acid-g-polyamide thin film composite membrane showed salt rejection of 97% (which is the total of groundwater salinity), 99% of dissolved bivalent ions (Ca^{2+}, SO_4^{2-}, and Mg^{2+}), and 98% of monovalent ions constituents

(Cl^- and Na^+). Furthermore, antifouling performance of the membranes was determined using *E. coli* as a potential foulant. This demonstrated that the zinc oxide nanoparticles modified through polymerization of hydrophilic methacrylic acid-g-polyamide thin film composite membrane can significantly improve the membrane performances. This modification should be favorable to handle the nature of the feedwater for improved selectivity, permeability, water flux, mechanical properties, and the bio-antifouling properties of membranes for water desalination. Hence, it is essential to modify the surface properties of membranes in order to handle the nature of the feedwater.

The Nature of the Feedwater

The nature of the feedwater properties, such as the pH of solution, ionic strength, solute charge, hydrophilicity of solute feed concentration, and the viscous nature of feed (liquid viscosity), significantly influences the performance of membrane. The ionic strength, pH, and solute charge of the feedwater influence the charge of both membrane surface and particles and the geometry and stability of molecules (Cassano 2017). The influence of pH on nano-based membrane performance is relatively complex, because the properties of membrane and solutes mainly differ with pH, and these differences are reliant on membrane material and solute type (Luo and Wan 2013). Furthermore, the surface material of numerous nano-based membranes made from polymer is hydrophilic and susceptible to be hydrated and ionized in the aqueous solution. The geometry and ionization of these polymer chains will change under different surrounding conditions, particularly at different pH and ionic strength. Even a minor change in the pore size or charge pattern would have a strong influence on the membrane permeability and the passage of molecules. This is as a result of the nanoscale pore dimensions ($\sim$1 nm) and electrically charged materials of these membranes. Hence, manipulating and putting the influence of pH and salt into consideration could enhance the nano-based membrane filtration process, through the improvement of the separation performance (in terms of permeate flux and salt rejection) and reducing membrane fouling (Luo and Wan 2013).

The permeate flux and the salt rejection are the two parameters that are generally used to evaluate the performance of membranes (Hoang et al. 2010). Hence, the feed pH during membrane separation is an important factor that affects the performance of membranes because the feed pH can influence membrane charge and it can even change it. Changing the feed pH could alter the membrane surface charge, which can consequently influence the performance of the membrane (Tanninen and Nystrom 2002). Changing the feed pH will change the electrical charge or zeta potential of the solution. The change in pH will modify the electrostatic interaction among the molecules and the membranes. In contrast to the feed composition which is fundamental to the product, the feed pH can be changed by simply adding an acid such as hydrochloric acid or a base such as sodium hydroxide. Depending on the feed properties and the type of the nano-based membrane, either an increase or decrease of feed pH will enhance the performance of a nano-based membrane (Dewettinck et al. 2018). Dalwani et al. (2011) studied the effect of pH on the performance of thin film composite nanofiltration membranes at the relevant pH conditions, in the range of pH 1–13. At extremely alkaline conditions (pH greater than 11), an increase in molecular weight cutoff and a reduction in membrane flux was observed. However, according to the Donnan–steric partitioning pore model, the change in performance in alkaline conditions originates from a larger effective average pore size and a larger effective membrane thickness as compared to the other pH conditions.

Another confounding factor in the use of membranes for water filtration is the reliance of the feed viscosity on particle concentration. The liquid viscosity is usually taken as a constant in models of filtration; however, in practice, the liquid viscosity depends on various properties of the fluid such as fluid temperature, density of the fluid, and the shear rate of the fluid (Herterich et al. 2014). The viscosity of feedwater can also be influenced by the feed concentration. Herterich et al. (2014) studied and analyzed the effects of a concentration dependence of the viscosity of the fluid. They considered the pressures required for a constant inlet fluid flux due to the concentration-dependent viscosity. They found that the addition of particles increases the viscosity of the fluid and the increase in the fluid viscosity resulted in increased hydrodynamic pressure. Furthermore, they observed less variation to the flow due to the concentration-dependent viscosity.

Hence, with the design of membrane performance, which depends on the nature of the feedwater, the basic comprehension of the diffusion mechanisms together with the mass transfer has revealed the importance of science required to select optimal working conditions for membrane processes. However, the working conditions will be influenced by the different geometries and ionization of polymer chains (Camacho et al. 2013). The following section reviewed different working conditions influencing the performance of membrane.

Working Conditions

The separation performance of nano-based membranes depends on multiple working conditions. The working conditions such feed temperature, operating pressure, flow rate, etc. are effective factors that influence the performance of membrane in terms of permeability, water recovery, and rejection of solutes. These working conditions are discussed in the next subsection.

Feed Temperature

The feed temperature is a significant factor controlling mass transfer in membrane separation process. Permeate flux increases together with an increase in temperature because when temperature increases, the viscosity and the level of concentration polarization will decline (Agashichev 2009). Hence, as the feed temperature decreases, the performance of a nano-based membrane characterized by permeability naturally decreases as a result of an increase in water viscosity (Yoon 2016). This is described by Eq. 8.3. Nonetheless, with the presence of fouling, flux will decline in spite of the increase in temperature (Beril et al. 2011). Temperature change also results in the variation of diffusion coefficient and component absorption which in turn influences the flux. Goosen et al. (2002) reported that polymeric membrane rapidly responds to changes in the feed temperature. They presented an increase close to 60% in the permeate flux when the feed temperature was elevated from 20 to 40 °C. In addition, the capability to change or modify the performance characteristics of a membrane by controlling the temperature is a captivating idea which has been pursued to a limited extent (Moll et al. 1997). The movement of the penetrant molecules in nano-based membranes is reliant on thermally activated chain motion. Furthermore, the solubility is tied to the interactions of polymer-penetrant and penetrant condensability. Hence, the properties of polymer/nanofiller material like chain stiffness, free volume, and polymer-penetrant interactions will have a strong impact on the effect of temperature on separation performance (Rowe et al. 2010):

$$J_v = \frac{\Delta P_T}{\mu\left(R_m + R_c + R_f\right)} \tag{8.3}$$

where J_v is the permeate flux (m/s), ΔP is transmembrane pressure (Pa or kg/m/s), μ is the permeate viscosity (kg/m/s), R_m is membrane resistance (/m), R_c is the cake resistance (/m), and R_f is irreversible fouling resistance (/m).

The impact of water temperature was investigated on both permeate flux and rejection of ion; and a linear correlation between temperature and permeate flux by nanofiltration performances was presented in the temperature range from 10 °C to 30 °C (Schaep et al. 1998). The influences of the concentration of poly (phthalazine ether sulfone ketone), the type and additives concentration in the casting solution on membrane permeation flux and rejection were also assessed by using orthogonal array of the strategy of experiments in the separation of polyethyleneglycol. The permeation flux greatly increased by raising the working temperature and the pressure without any significant change on rejection (Jian et al. 1999). The transport property of water on the permeation characteristics of nanofiltration was presented by Sharma et al. (2003). It was concluded that increasing the temperature increased the mean pore radii and the molecular weight cutoff of the membrane. This suggested that the changes in the structure and morphology of the polymer matrix consist of a membrane barricade stratum. Based on the free volume theory of activated gas transport, activation energies of neutral solute permeability in aqueous systems also increased with Stokes radius and molecular weight demonstrating their hindered diffusion in membrane pores (Sharma et al. 2003). Experiments were also done to examine the performance of membranes by varying the seawater temperature from 10 °C to 60 °C. The increase in the permeate flux with an increase in the feed temperature was elucidated as the alteration of water viscosity and the membrane itself. Furthermore, the increase of permeate flux could be predicted by the viscosity alteration in case of nano-based membrane (Kim et al. 2014). These studies have shown that increase in the permeate flux with an increase in temperature attributes to the thermal expansion of the membrane, the structure of membrane, and alteration in water viscosity. However, temperature stability is an important factor for any membrane to stand elevated feed operating temperatures and avoid damage (Fard et al. 2018). Furthermore, a higher temperature increases osmotic pressure and lowers the viscosity of water. Nonetheless, the influence of temperature on viscosity is far more than its influence on osmotic pressure.

Operating Pressure

Nano-based filtration uses rough membranes; as a result, the operating pressure of the nano-based filtration system is usually lesser to reverse osmosis systems. Furthermore, the rate of fouling is lesser in comparison to reverse osmosis systems. Operating at increasing pressure is ultimately directly proportional to an increase in permeate flux. However, when the process reaches a definite point, the proportional relationship between increasing pressure and an increase in permeate flux does not apply due to fouling and concentration polarization occurrence (Susanto 2011). Shaaban et al. (2016) did a parametric study of a nano-based separation process of dye in order to characterize the effects of the operating variables, and transmembrane pressure is one of the operating variables. The authors found that the linear increase in dye concentrate flux declines with a precise pressure. The mechanism of proportional relationship between increasing pressure and increase in permeate flux is defined as a pressure controlling region and mass transfer region. Furthermore, the mechanism of decline in a linear increase in flux going beyond a precise pressure is also defined as a pressure controlling region and mass transfer region. In the mass transfer region, increasing the operating pressure only results in a buildup of a solute stratum. The buildup of a solute stratum will later repel and subsequently delay the increase in the transport rate of components with an increasing pressure. This type of limiting pressure should be taken into account in order to allow suitable design applications that will give assurance of optimum fixed and operating costs. However, the study shows that increased operation pressure increased the dye rejection. Abidi et al. (2016) presented the retention of ions by nanofiltration of synthetic solutions containing phosphate salts with a Nanomax-50 charged membrane. The effects of pressure, ionic strength, and pH on the retention of phosphate anions were examined. The results revealed that the membrane experienced a hydraulic permeability around 24.6 10^{-12} m s^{-1} Pa^{-1}. The values of the rejection rate of the phosphate anions are about 93% for HPO_4^- and 98% for HPO_4^{2-}. The rejection rate of phosphate anions, mainly monovalent, rests on chemical parameters and the transmembrane pressure. Hence, operating pressure affects both rejection of ions and flow rates during membrane separation process.

Flow Rate

For any membrane filtration process, the flow path of the fluid is orthogonal to the membrane surface; hence flow rate is also a contributing factor that influences the performance of nano-based membranes. Studies have shown that the permeation flux of a NF membrane increased with increasing flow rates (Shahtalebi et al. 2011). In the investigation done by Shaaban et al. (2016), greater feed flow rates resulted in higher permeation flux, concentrate flow, and declined salt passage. Their investigation revealed that the permeation flux was increased almost linearly with increasing cross-flow velocity. Increasing cross-flow velocities resulted in the following processes: (i) elevating the system mass transfer, (ii) enhancing the magnitude of mixing close to the surface of the membrane, (iii) elevating the tangential and radial velocities of the fluid that can break down the boundary stratum and result in the failure of resistivity to diffusing species, (iv) expediting an ideal turbulence with favorable flow pattern, and (v) minimizing the magnitude of concentration polarization and osmotic pressure on the membrane surface (He et al. 2008; Shaaban et al. 2016). Hence, the influence of flow rate on the performance of nano-based membranes can be attributed to the likely decrease of concentration polarization effect. The concentration polarization is literally correlated to the boundary stratum thickness, which is highly important for a successful separation.

In addition to all the membrane working conditions, nano-based membranes fabricated should be subjected to characterization because the durability of these membranes in the operational environment depends on diverse characterization. By characterizing these membranes, membrane users would be able to expediently select the membranes that satisfy some specific requirements; hence, decide the working conditions under which the membranes would be operated (Khulbe et al. 2008). The different approaches and techniques such as atomic force microscopy, scanning electron microscopy, transmission electron microscopy, contact angle measurement, Fourier-transform infrared spectroscopy, etc. used for characterizing nano-based membranes are described in the next section.

8.2 Characterizations of Nano-Based Membranes

Several properties demonstrated by nano-based membrane separation are as a result of the contact reactions at the interface with their environment (Johnson et al. 2018). The life span and stability of the nano-based membrane in different operational environment is governed by the chemical, thermal, and mechanical characteristics of the membrane (Khulbe et al. 2008). In an effort to comprehend and interpret how such contact reactions influence their performance, especially when fabricating novel nano-based membranes with enhanced properties, a detailed understanding of their surface properties is very important. Hence, the performance of a nano-based membrane is subjected to the membrane characterization which offers a useful source of information (Hilal et al. 2017) on the environment in which the membrane can be operated. The following subsections describe some important characterization techniques usually used to characterize the surface of membranes fabricated with the incorporation of nanomaterials.

8.2.1 Atomic Force Microscopy (AFM)

Atomic force microscopy is an elevated scanning probe microscopy which demonstrates resolution on the order of fractions of a nanometer by providing pictures of atoms on or in the surfaces. Atomic force microscopy tool is used for imaging, measuring, and manipulation of surfaces of different types of data such as polymer, composite, ceramic, and biological samples, at the nanoscale level. Furthermore, atomic force microscopy does not need a vacuum environment, but it can, thus, be used in either an ambient or liquid environment. Hence, atomic force microscopy has the capability of measuring topography, surface energy, and elasticity of samples at the nanometer scale and molecular scale (Elnashaie et al. 2015). Atomic force microscopy has been used to examine membrane surfaces as a result of its capacity to measure surface roughness (Boussu et al. 2005), measurement of interaction forces between membrane surfaces and foulant particles (Thwala et al. 2013), pore size and pore size distribution (Hilal et al. 2005). However, identifying pores and allocating pore sizes requires careful consideration. The first thing to do is to always remember that the atomic force microscopy can only provide the sizes of the openings of the pores and does not provide any data about the membranes' interior sizes. This results in a possible reason for any discrepancies in values obtained from other methods studying flow through the membrane (Johnson et al. 2012).

Atomic force microscopy is known to be one of the most powerful tools used for the analysis of surface morphologies since it creates three-dimensional images at angstrom and nano-scale. Atomic force microscopy technique has been thoroughly used to analyze the dispersion of nanometric components in nanocomposites membranes (de Sousa et al. 2014). Recently, atomic force microscopy has also been used to characterize novel nano-based membranes with the integration of nanofillers. Abdallah et al. (2015) prepared manganese (III) acetylacetonate nanoparticles by a simple and environmentally benign route based on hydrolysis of potassium–permanganate followed by reaction with acetylacetone in continuous stirring rate. The nanoparticle powder prepared was dissolved in polymer solution mixture to produce reverse osmosis-polyethersulfone with manganese (III) acetylacetonate as metalorganic nanoparticle blend membrane, without any treatment of polyethersulfone membrane surface. The membrane morphology and properties were reported. Atomic force microscopy images demonstrated exceptional pores size distribution of membrane blend and lower the surface roughness compared to bare polyethersulfone. Al-Sheetan et al. (2015) fabricated reverse osmosis membranes modified with tin dioxide nanoparticles of varied concentrations (0.001–0.1 wt. %) through in situ interfacial polymerization of trimesoyl chloride and m-phenylenediamine on nanoporous polysulfone supports. The nanoparticles dispersed in the dense nodular polyamide on the polysulfone side. The effects of interfacial polymerization reaction time and tin dioxide loading on membrane were used to examine the separation performance. The modified reverse osmosis membranes were characterized by atomic force microscopy and several characterization techniques. The synthesized tin dioxide nanoparticles size varies between 10 and 30 nm. The atomic force microscopy analysis showed that the membrane exhibited a smooth membrane surface and average surface roughness from 31 to 68 nm. The results revealed that an interfacial polymerization reaction time was vital to form a denser tin dioxide–polyamide layer for higher salt rejection. Amouamouha and Gholikandi (2017) deposited different thicknesses of silver nanoparticles with proper adhesion on poly(vinylidene fluoride) and polyethersulfone surfaces by physical vapor deposition. Atomic force microscopy analyses were used to study the surface morphology and the bacteria anti-adhesion property of the membranes. The morphology measurements established that after silver grafting, the surface became more hydrophobic, the homogeneity increased, and the flux decreased after coating.

8.2.2 Transmission Electron Microscopy (TEM)

The transmission electron microscope is a powerful tool used in characterizing materials. An elevated energy beam of electrons is shone across a very thin material, and the correlations between the electrons and the atoms can be employed to observe characteristics like the crystal structure and features in the structure such as dislocations and grain boundaries. Chemical analysis and the study of the microstructure and growth of layers and their composition can also be performed using transmission electron microscope (WARWICK 2018). Furthermore, the basic building blocks of membrane can be studied by transmission electron microscope. The quantitative data of particle, size distribution, morphology, and grain size can be attained through transmission electron microscope. The transmission electron microscope can also be used to give the key microstructural features of nano-based membranes.

In order to understand the microstructure of nano-based membranes, the transport mechanism through these membranes has been theoretically studied using models that are related to the dry membrane microstructure (Patterson et al. 2009). Such models are the pore flow model (Vandezande et al. 2008) and the solution diffusion models (Wijmans and Baker 1995). However, the physiochemical properties of the membrane are required in order to elucidate the relationship between microstructure and transport mechanism. Hence, the microstructure of the membranes must be imaged and characterized to achieve the physiochemical properties. Patterson et al. (2009) characterized microstructures of polyimide membranes in different media, such as dry and wet solvent, by transmission electron microscopy, scanning electron microscopy, and environmental scanning electron microscopy, where suitable. The transmission electron microscope imaging of dry membranes showed that the polyimide membrane has three microstructurally distinct polyimide layers.

Furthermore, the transmission electron microscope images disclose nano-sized pore-like topographies in the polyimide structure, which pointed out that the transport mechanism is probably neither only solution–diffusion nor only pore flow. Hence, the transmission electron microscope method of characterization transmitted electron that gives information about the size of nanoparticles (Mokhtari et al. 2017). However, the constraint of transmission electron microscope technique is that it characterizes only thin film samples rather than whole membrane (Zahid et al. 2018), though higher resolution can be attained with the use of transmission electron microscopy. The principle of transmission electron microscope is a little bit different from scanning electron microscope (Zahid et al. 2018). The principle of scanning electron microscope will be discussed in the next subsection.

8.2.3 Scanning Electron Microscopy (SEM)

A scanning electron microscope, similar to a transmission electron microscope, is made up of a vacuum system, an electron optical column, electronics, and a software. The optical column is considerably shorter since the only lenses required are those directly above the specimen which is used to give attention to the narrow beam electrons across the membrane surface and deep inside the membrane. The application of scanning electron microscope needs minimum sample preparation that includes drying of samples and coating of sample with conductive material such as carbon and gold. Depending on the type of equipment available, the resolution of scanning electron microscope is in the range of 10 and 50 nm. The micro-marker on the scanning electron microscope micrographs is used in the estimation of the pore size (diameter) (Agboola et al. 2014). Elia et al. (2016) reported a method for measuring the mean pore size and the determination of the porosity of porous silicon (PSi) layers, which involves image processing of top view by using scanning electron microscope. The processing program could be used to measure the total area of the pores and estimate its proportion to the total scanned area. Agboola et al. (2017) examined the pore sizes of two nanofiltration (Nano-pro-3012 and NF90) membranes using the micro-marker on the scanning electron microscope. The smoothness and the dense nature of Nano-pro-3012 was observed with visible pores, while NF90 membrane exhibited larger pores and an intertwining fibrous network structure with several pores of different sizes.

Apart from the application of micro-marker on the SEM, for the estimation of the pore size, scanning electron microscope is a commonly used tool for the determination of morphology and topography of membrane surface (Zahid et al. 2018). Rajabi et al. (2015) investigated the synthesis of two different kinds of nano-zinc oxide (nanoparticle and nanorod), characterized and embedded in a polyethersulfone membrane matrix in order to study the effects of a nanofiller shape on the mixed-matrix membrane characteristics and the antifouling capability. The characterization of the membranes done by using SEM revealed that bulk porosity measurements obtained from the scanning electron microscope microphotographs for the prepared membranes have a suitable porosity in the range of 61 and 77% and approximately regularly arrayed fingerlike micro voids. Jang et al. (2015) prepared patterned membranes with nano-scale hexagonally packed arrays using nanoimprint lithography and micro-scale structured membranes. In order to confirm the deposition tendency of smaller particles on the structured membranes in Region 1, the scanning electron microscope images of particles on the structures were studied. It was found that most particles with a size of 0.1 μm were mainly deposited in the valley between 2 μm microstructures, whereas the upper regions were sparsely fouled. The authors proposed that the influence of the structures on particle detachment could be too small to detach particles from the membrane surface as a result of the lower shear stress in valleys under the Region 1 condition. The particle deposition was well mitigated in Region 2. It is physically impossible for particles in this region to be placed in the lower shear region and to be trapped between structures because the size of the particles is larger than the valley or spacing between structures. Hence, the particles could deposit only on the upper or top position of dome-shaped structures (Jang et al. 2015).

8.2.4 Gas Adsorption–Desorption Technique (Brunauer–Emmett–Teller, BET) Method

Gas adsorption–desorption technique is used for estimating pore size, pore size distribution, and the surface area using the Brunauer–Emmett–Teller method, primarily for inorganic membranes; it can however be also used for organic membranes (Prádanos et al., 1996). This technique is a pore characterization technique that can measure pore size from 0.3 to 300 nm via the physical adsorption of gas molecules on a solid surface (Hasanuzzaman et al., 2017). Thus, gas adsorption offers a quick and quantitative technique for specific surface area, and it is used to establish other textural properties of a solid such as pore size, total pore volume, pore volume distribution, and adsorption energy distribution. Prádanos et al. (1996) investigated the adsorption isotherms in conjunction with the Brunauer–Emmett–Teller theory for multilayer adsorption which permitted them to attain the internal surface area of the membrane. The volume, surface, and pore number distributions were calculated from the Kelvin equation both in the adsorption and desorption processes. Nitrogen is usually utilized for the adsorbent gas, though other adsorbents like argon and benzene are also used. In this technique, adsorption–isotherm (amount of adsorbed gas versus relative pressure (pressure/saturation vapor pressure of the adsorbent)) is drawn, and the data are analyzed based on the assumption of capillary condensation (Khulbe et al. 2010). The nitrogen adsorption Brunauer–Emmett–Teller analysis is very useful in evaluating the surface area and pore size distribution of ceramic membranes typically in the pore range of micro- and meso-size. However, the nitrogen adsorption Brunauer–Emmett–Teller analysis is rarely used for conventional dense polymer membranes, known as "nonporous" (Tylkowski and Tsibranska 2015).

8.2.5 X-Ray Powder Diffraction (XRD)

X-ray powder diffractometer is made up of an X-ray source (mainly an X-ray tube), a sample stage, a detector, and a method of varying angle θ (see Fig. 8.4). The X-ray is concentrated on the sample at some angle θ, while the detector opposite the source reads the intensity of the X-ray it obtains at 2θ away from the source path. Then the incident angle is increased with time, while the detector angle always remains 2θ above the source path. X-ray powder diffraction is a non-destructive analytical technique principally used for studying the structure, composition, and physical properties of materials. Amouamouha and Gholikandi (2017) used X-ray diffraction technique to appraise the structure of all pure and nanocomposite membranes during deposition process and assess if silver presence could make any difference in the structure of nanocomposite membranes or not. It is also used for identifying phase of a crystalline polymer or nano-composite membrane, and it can provide information on unit cell dimensions. The scattering of X-rays from atoms produces a diffraction pattern, which contains information about the atomic arrangement within the crystal of polymer or nano-composite membranes. Lee, Yoo, and Lee (2015) used X-ray powder diffraction to study the various morphological analyses of the Nafion

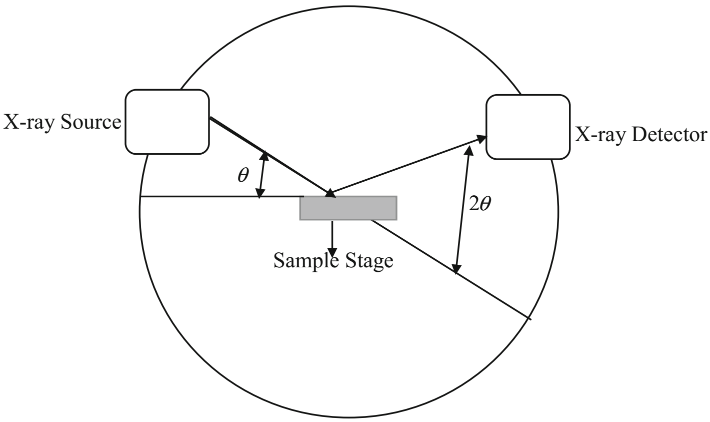

Fig. 8.4 Schematic representation of a powder X-ray diffractometer. X-ray diffractometer is used for recognizing phase of a crystalline of polymer or nano-composite membrane. Hence, a diffraction pattern is used to determine and refine the lattice parameters of a crystal structure

nanocomposite membranes in the states swollen by water. Crystallinity was determined via peak deconvolution of the characteristic X-ray powder diffraction peak (10–24° of 2θ) using Gaussian function. The authors concluded that the right deconvoluted peak can be assigned to the crystalline part due to the close proximity to the crystalline peak of polytetrafluoroethylene.

8.2.6 Fourier-Transform Infrared Spectroscopy (FTIR)

A Fourier-transform infrared spectroscopy technique simultaneously collects high-spectral resolution data over a wide spectral range in order to obtain an infrared spectrum of absorption or emission of a solid, liquid, or gas. Fourier-transform infrared spectroscopy is basically employed in order to get information about composition of membranes or presence of different functional groups on the membrane surface (Homayoonfal et al. 2015; Amouamouha and Gholikandi 2017). FTIR spectroscopy technique is used to identify the cross-linking on a membrane surface and to study the chemical structure of the membrane. In Fourier-transform infrared spectroscopy technique, the molecular vibrations are analyzed when infrared radiations relate with the membrane sample. This provides information about the presence of functional groups on the surface of newly fabricated membranes (Mago et al. 2008) and modified membranes (Battirola et al. 2012). The most commonly mode used for Fourier-transform infrared spectroscopy for the characterization of membrane is attenuated total reflection (Zahid et al. 2018). Tayefeh et al. (2015) investigated the effects of magnetite and titania dioxide nanoparticles by loading in trimesoyl chloride organic solution and in metaphenylene diamine aqueous solutions on the surface characteristics of polyamide membrane. Among other characterization techniques, dispersion of nanoparticles, surface bonds of magnetite and titania nanoparticles with polyamide, and hydrophilicity of magnetic nanocomposite reverse osmosis membrane were taken into account in each method by attenuated total reflection Fourier-transform infrared spectroscopy. Their result revealed the functional group of neat PA layer and thin film nanocomposite membranes which contained of magnetite and titania dioxide nanoparticles. Three typical characteristic peaks of formation of the polyamide layer were seen in spectrums: in 1654 cm^{-1} which corresponds to C=O bonds stretching vibration (amide I), 1545 cm^{-1} which corresponds to N–H bonds of amide group (amide II), and 1612 and 1488 cm^{-1} which correspond to aromatic ring breathing in terms of C=C bond vibrations. Furthermore, in specimen containing magnetite nanoparticles, as a result of the decrease in specific bonds of polyamide as a barrier effect, there was a lower number of bonds, and in the most of the regions, absorbance of membrane was lower. Again, there are characteristic peaks which corresponded to Fe–O bonds: 635 cm^{-1} for magnetite nanoparticles which was related to symmetrical tensional vibration of Fe–O bond (Tayefeh et al. 2015).

8.2.7 Contact Angle Measurement

The contact angle measurement is the measurement of an angle at which a liquid or vapor interface reaches the surface of a solid. Hence, the term contact angle "θ" is a estimative measure of the wettability of a material surface through Young's equation which describes the balance at the three-phase contact of solid, liquid, and gas. Young's equation is given in Eq. 8.4 (Agboola et al. 2014). The surface free energies between the liquid, solid, and surrounding vapor result in the contact angle. γ_{SV} is the solid–vapor interfacial energy, γ_{SL} is the solid–liquid interfacial energy, γ_{LV} is the liquid–vapor interfacial energy, and θ_{γ} is an equilibrium contact angle which the liquid makes with the surface. The interfacial energies form the equilibrium contact angle of wetting. A wetting liquid is the liquid that forms a contact angle lesser than 90° with the solid, and a non-wetting liquid is the liquid that forms a contact angle between 90° and 180° with the solid. The accepted techniques for measuring contact angle are the sessile drop and captive bubble. Hence, the ability of liquids to form boundary surfaces with solid is known as wetting (Agboola et al. 2014). The contact line on a material can be observed as a point object on which the force balances are made in two and dimensional representations (see Fig. 8.5a and b):

$$\gamma_{SV} = \gamma_{SL} + \gamma_{LV} \cos \theta_{\gamma} \tag{8.4}$$

The contact angle measurement is usually used to describe the relative hydrophobicity/hydrophilicity of a membrane surface. Generally, membrane surfaces exhibiting water contact angle higher than 90° are considered hydrophobic, while membrane surfaces exhibiting water contact angle lower than 90° are considered hydrophilic. Ghaemi et al. (2011) measured the water contact angles of

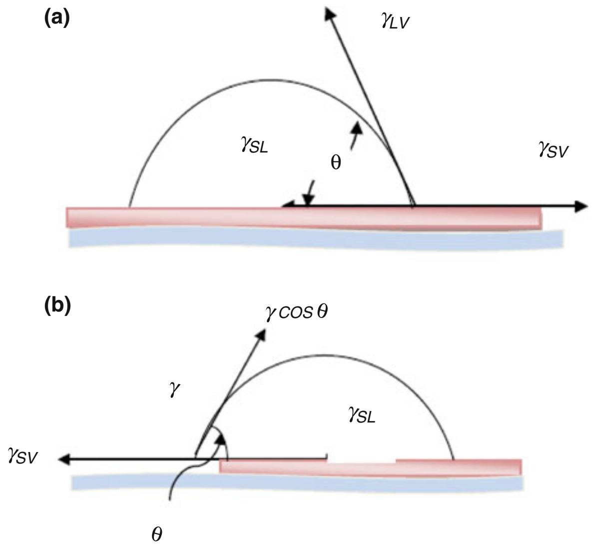

Fig. 8.5 (**a**) Three-dimensional representation of a drop on a surface describing the surface energies; here, the surface tensions can be observed as surface energies; (**b**) two-dimensional representation of a drop on a surface describing the interfacial tension as forces balanced along the x-axis (Agboola et al. 2014)

nanocomposite membranes containing polyethersulfone and organically modified montmorillonite, prepared by a combination of solution dispersion and wet-phase inversion methods. The authors found that the highest contact angle belongs to polyethersulfone which shows the lowest hydrophilicity. When the concentration of organically modified montmorillonite was increased, the contact angle intensely decreased and a more hydrophilic membrane was fabricated. The organically modified montmorillonite$_{10}$ membrane showed the lowest contact angle demonstrating the highest hydrophilicity. The strong change in hydrophilicity of the membranes prepared with organically modified montmorillonite can be attributed to the fact that the organically modified clay is hydrophilic which further carries very hydrophilic polar ammonium moieties. Huang et al. (2010) used the plasma-induced grafting of acrylic acid to enhance the wettability of the electrospun poly(vinylidene fluoride) nanofiber membranes. The surface contact angle of the nanofiber membrane was 91.2° which is in agreement with the strong hydrophobicity of poly(vinylidene fluoride) material to water. A significant decrease in the contact angle on the grafted poly(vinylidene fluoride) membrane was observed, which may be attributed to the grafting of hydrophilic radical, -COOH.

Superhydrophobic surfaces which is usually defined as surfaces with a water contact angle of $\geq$150° and sliding angle of $\leq$10° has found increased attention as a result of lotus effect mechanism reported by Barthlott and Neinhuis (1997). The lotus effect was ascribed to the amalgamation of two characteristics which are a low surface energy waxy layer and hierarchical surface roughness with micro- and nano-scale structures (Li et al. 2017a, b). Artificial superhydrophobic surfaces are normally synthesized in two stages: (1) fabrication of hierarchical micro-/nanostructures in order to enhance the surface roughness and (2) modification of surface chemistry in order to reduce the surface free energy (Hamzah and Leo 2017). Ávila et al. (2013) studied the synthesis of superhydrophobic nano modified membranes using an adjustable micropipette (0.1 μL–1.0 μL). Large variations on water contact angle measurements were observed. The authors concluded that the large variations on water contact angle measurements can be ascribed to the random distribution of fibers that creates a very rough surface. The interface between the beginning of the water droplet and the end of the surfaces becomes more defined as the hydrophobicity increases, and the standard deviation on water contact angle measurements decreases. Furthermore, a smaller fiber diameters increase the surface roughness and consequently the water contact angle (Carré 2007). Shahabadi and Brant (2019) investigated superhydrophobic of nano-fibrous membranes fabricated by having hierarchical surface roughness made of carbon black nanoparticles. The membrane support had an average θ_{H2O} of 139 $\pm$ 0.9° indicating that it was highly hydrophobic. This was due to a combination of the hydrophobic nature of polyvinylidene fluoride-co-hexafluoropropylene polymer and the micro-scale surface roughness made by the randomly arranged and stacked nanofibers. Literature has reported that for the same polymer, non-woven nanofibrous membranes display higher hydrophobicity compared to membranes prepared by traditional approaches as a result of the hierarchical structure of the erratically deposited nanofibers (Kang et al. 2008). Hence, when tested for surface wettability, the prepared membrane showed water contact angle, sliding angle, and contact angle hysteresis values of 160.8°, 7.0°, and 5.3°, respectively. Nonetheless, liquids with surface tensions ≤36.6 mN/m had zero contact angle on the membrane surface (superoleophilicity).

Apart from characterizing nano-based membranes in terms of wettability, surface roughness, pore size distribution, structure, and functional group, it is necessary to characterize membranes based on transport properties in order to know what particular membrane to be used in a particular process. Hence, the relationship between the membrane structure and the actual performance depend the transport mechanism.

8.3 Transport Properties for Nano-Based Membranes

Membranes are thin layers with the capacity of controlling the transport of chemical species in contact with them (Baker 2004). The restriction of the transport rate of molecules through polymeric membranes is due to their micrometer-scale thickness, pore size, and porosity which limit their appropriateness for more practical application (Nguyen et al. 2015). Hence, the transport of solute across nano-based membranes is principally controlled by the surface layer, thickness, porosity, and pore size. Generally, nano-based membranes are seen as a bundle of capillaries with active structural characteristics such as membrane thickness, pore size, and porosity ratio and electrical characteristics like their active volume charge density. The unification of pore diameters of about few nanometers with electrically charged materials indicates that solute exclusion results from a compound mechanism containing several phenomena (Szymczyk and Fievet 2005). Hence, the main aim of theoretical characterization is to predict the performance of a membrane from its morphological features. Theoretical characterization requires the use of pore size of the membrane to model the performance of the membrane.

Various models such as preferential sorption/capillary flow, solution diffusion, Donnan–steric partitioning pore model/dielectric exclusion, and extended Nernst–Planck have been developed to predict the phenomena of solute particles transport across the membranes (Ho and Sirkar 1992). However, the most widely adopted models for nano-based membranes such as nanofiltration are established on the extended Nernst–Planck equation which is use to describe the mass transfer and an equilibrium partitioning in describing the distribution of ions at the pore inlet and outlet (Tsuru et al. 1991; Mohammed et al. 2002). The initial descriptions of the mass transfer process in nanofiltration were based on irreversible thermodynamics; however, another method used in describing mass transfer through nanofiltration membranes was the space-charge modeling system. Most of these models have shown that nanofiltration membranes offer excellent selectivity between neutral solutes, which are rejected based on their size. Monovalent ions, which are rather well transmitted, are mostly rejected by nanofiltration membranes (Lanteri et al. 2009). These sections will discuss the models used in characterizing the transport properties of nano-based membranes.

8.3.1 Preferential Sorption/Capillary Flow (PSCF)

Preferential sorption/capillary flow model is an old model proposed by Sourirajan (1970). This model anticipated that the mechanism of separation is determined by both surface phenomena and fluid transport across the pores. Based on the mechanism of preferential sorption, separation is the joint result of preferential sorption of one of the constituents of the fluid mixture at the boundary membrane–solution and the permeation of fluid across the microporous membrane. The model states that the membrane barrier layer has suitable chemical properties having a preferential sorption for solvent or a preferential repulsion for solute of the feed solution (Ho and Sirkar 1992). In this context, the term "preferential sorption" refers to the existence of a steep concentration gradient at the membrane-solution interface, and the terms "pore" and "capillary" refer to any void space linking the high pressure and low pressure sides of the membrane, with the occurrence of fluid permeation and material transport during the separation process (Sourirajan 1978). Hence, preferential sorption at the boundary of membrane–solution is a dependent on solute–solvent membrane material interactions coming from steric, nonpolar, polar, and/or ionic character of each one of the components (Sourirajan 1978). However, for the separation to occur, one of the constituents of the feed solution must be preferentially sorbed at the membrane–solution interface. Thus, the physicochemical principles responsible for preferential sorption at fluid–solid interfaces constitute a fundamental part of this mechanism. Furthermore, effective molecular size of the permeants, pore size and its distribution in the membrane, the specific interaction between the permeant and the membrane material controls the separation (Roy and Singha 2017). According to this model, the water flux is given as:

$$N_w = A\left\{\Delta p - \left[\pi\left(y_s'\right) - \pi\left(y_s''\right)\right]\right\} \tag{8.5}$$

where A is the pure water permeability constant, Δp is the applied pressure difference, $\pi(y_s)$ is the osmotic pressure of a solution with solute mole fraction of y_s. y_s' and y_s'' are, respectively, the mole fraction of solute in the permeate and the feed solutions. The solute flux is given as:

$$N_s = \frac{c_T K_s D_{sm}}{x}\left(y_s' - y_s''\right) \tag{8.6}$$

where c_T is the total molar concentration, D_{sm} is the diffusion coefficient of the solute in the membrane, K_s is the solute distribution coefficient, and x is the membrane thickness.

For the preferential sorption/capillary rejection, the membrane is heterogeneous and microporous. Furthermore, electrostatic repulsion takes place as a result of different electrostatic constants of the solution and the membrane (Shon et al. 2013). With respect to nano-based membrane, sorption surface–capillary flow characterizes the preferential sorption of molecules of water in the membrane and desorption of multivalent ions which occurs via dielectric forces, instigating exclusion of charged solutes through the assumption of cylindrical pores (Abhang et al. 2013). Nonetheless, the assumption of cylindrical pores, influence of the size, and its distribution restrict its suitability in describing the separation characteristics. Furthermore, the model cannot justify the inverse relation of flux and membrane thickness, membrane swelling, and trade-off relationship of the flux and the separation factor (Roy and Singha 2017).

8.3.2 Solution Diffusion Model

Solution diffusion model is the one of the earliest model proposed for reverse osmosis which is however now applicable to nano-based membranes (Hidalgo et al. 2013). This model is founded on the principle of membrane diffusion of molecule across a dense polymer layer. The component needed to be transported requires to be first dissolved in the membrane. The common procedure used in developing solution-diffusion model is to presume that the chemical potential of permeate and feed fluids are in equilibrium alongside with the membrane surface. The pressure, temperature, and composition of the fluid on either side of the membrane determine the concentration of diffusing species at the membrane surface when in equilibrium with the fluid (Baker 2004). Hence, the suitable expressions for the chemical potential in the fluid and membrane phases can be equated at the solution–membrane interface. The solution diffusion model can be written as:

$$J_w = \left[\left(\frac{D_{mw} \times C_{mw} \times V_m}{RT\delta}\right) * (\Delta P - \Delta\pi)\right] \tag{8.7}$$

$$= A_w(\Delta P - \Delta\pi) \tag{8.8}$$

where D_{mw} is membrane water diffusivity (m^2/s), C_{mw} membrane water concentration (kg solvent/m^3), V_m is molar volume of solvent, A_w is water permeability (constant), and δ is the effective thickness of membrane. $\Delta P = P_1 - P_2$ is the hydrostatic pressure difference with P_1 exerted on the feed and P_2 exerted on the product, and $\Delta\pi = \pi_1 - \pi_2$ is the osmotic pressure difference of the feed solution to that of the permeate solution. However, the model will fail to predict the flux behavior for dilute organics with negligible osmotic pressure. The flux equation for the diffusion of solute through the membrane is written as:

$$J_s = \left[\left(\frac{D_{ms}K_s}{\delta}\right) * (c_1 - c_2)\right] \tag{8.9}$$

$$= A_s(c_1 - c_2) \tag{8.10}$$

where $A_s = \frac{D_{ms}K_s}{\delta}$ is the solute permeability constant (m/s), J_s is the solute flux (kg solvent/s m^2), D_{ms} is the diffusivity of solute in membrane (m^2/s), and K_s is the distribution coefficient. With respect to steady-state condition, the solute diffusing across the membrane must be equal to the amount of solute leaving the permeate solution (kg solvent/m^3):

$$J_s = \frac{J_w c_2}{c_{w2}} \tag{8.11}$$

where c_{w2} is the concentration of solvent in permeate stream.

In conclusion, for a solution diffusion model, the membrane is made of homogeneous and nonporous material. Solute and solvent dissolve in the active layer of the membrane, and the transport of the solvent occurs due to the diffusion through the layer (Shon et al. 2013). The chemical potential gradient regulates the transportation of matters across the membrane. In addition, the chemical potential gradients of the solvent and the solute are influenced by the concentration of species and pressure differences across the membrane (Abdel-Fatah 2018).

8.3.3 Dielectric Exclusion (DE)/Donnan–Steric Partitioning Pore Model (DSPM)

Dielectric exclusion model is known to be one essential mechanism used for the separation of ion in membranes having fixed charges in the active layer of nano-based membranes such as nanofiltration membranes. Nano-based membranes are fabricated to selectively reject a specific ion or group of ions, which was attained by the addition of functional groups (charges) in the membrane active layer. These charges yield an extra rejection as a result of electrostatic phenomena that prevent the movement of charges across the membrane. Furthermore, nanofiltration membranes permit the rejection of ions when their size is lower than the pore size. The rejection of the target compounds take place in two main mechanisms. (1) partitioning mechanisms that take place as a result of steric effect, Donnan equilibrium, and dielectric exclusion, which come about in the interfaces of the active layer, and (2) transport mechanisms that take place as a result of convection, diffusion, and electrokinetic effects, which ensue via the length of the active layer thickness (Silva 2015). In addition, Nano-based membranes are fabricated for adsorption of charged species from the solution onto the membrane surface (Labbez et al. 2002). Hence, the electric charge of a nano-based membrane plays a significant role in the charge separation during a filtration process owing to the formation of electrical double layers that are comparable or bigger than the membrane pore size (Kotrappanavar et al. 2011).

The dielectric effects are made of two different contributions. Firstly, the dielectric effect is related to the reduction of the dielectric constant of a fluid in the nanoporous media (Senapati and Chandra 2001). This effect is known as the Born effect. The effect correlates to the variation of the solvation energy of an ion transported from the bulk solution to the nano pores of the membrane. Even when the effective dielectric constant of the solution compacted inside the pores is lower than the effective dielectric constant of the bulk solution, the excess solvation energy remains positive and hence the ions are rejected by the membrane pores (Fadaei et al. 2012). Secondly, the dielectric effect arises as a result of the difference between the effective dielectric constant of the solution inside the pores and of the membrane (Yaroshchuk 2000). The dielectric Born energy equation is given by Eq. 8.12, and the dielectric image forces energy is given by Eq. 8.13. This effect depends on the geometry of the pores:

$$\Delta W_{i,Born} = \frac{(z_i e)^2}{8\pi\varepsilon_0 k_B T r_i}\left(\frac{1}{\varepsilon_p} - \frac{1}{\varepsilon_b}\right) \tag{8.12}$$

$$\Delta W_{i,image(0-/0+)} = -\alpha_i\, ln\left[1 - \left(\frac{\varepsilon_p - \varepsilon_m}{\varepsilon_p - \varepsilon_m}\right)\exp\left(-2\mu_{(0-/0+)}\right)\right] \times (silt - like\ pores) \tag{8.13}$$

where 0+ is the effect just inside the membrane in the feed interface, 0− is the effect just outside the membrane in the feed interface, i is the ion, z_i is the ion valence, and e is the electronic charge. The subscripts b, m, and p are bulk, membrane, and pores, respectively, ε_b is the dielectric constant of the solution in the bulk (dimensionless), ε_m is the dielectric constant of the membrane material (dimensionless), and ε_p is the dielectric constant inside the pores (dimensionless). $\Delta W_{i,\ image}$ is the energy difference due to image forces effects (J).

Donnan–steric partitioning pore model is the conventional method in modeling the transport across nanofiltration membranes. In 1996, Donnan–steric partitioning pore model was proposed by Bowen and Mukhtar (Bowen and Mukhtar 1996). This model has been utilized to investigate the rejection properties of a variety of nanofiltration membranes. Donnan–steric partitioning pore model has proven to be very effective in modeling the nanofiltration behavior for aqueous solutions of sodium chloride and sodium sulfate (Vezzani and Bandini 2002). The Donnan–steric partitioning pore model uses three main parameters: the pore radius r_p, the effective charge density of the membrane X_d, and the effective ratio of membrane thickness to porosity $\Delta x/A_k$. The equation that describes the ionic transport across the membrane is the Nernst–Planck equation (Eq. 8.14). The hindered nature of ion across the pores is used to account for the ratio λ_i of the solute radii to the membrane pore radius that determines the steric hindrance factors $K_{i,\ d}$ and $K_{i,\ p}$. The electroneutrality conditions of each solution are given in Eq. (8.15). The concentration gradient in Eq. (8.16) can be gotten by combining Eq. (8.14) and Eq. (8.15). The relations between the boundary conditions for the concentrations in the membrane and the concentrations in the solutions are established through the application of Donnan–steric partitioning equation (Eq. 8.17). The volumetric flux Jv is calculated using the Hagen–Poiseuille equation (Eq. 8.18) (Gozálvez-Zafrilla et al. 2005):

$$j_i = -K_{i,p} D_{i,\infty} \frac{dc_i}{dx} - \frac{F z_i c_i K_{i,p} D_{i,\infty}}{RT} \frac{d\psi}{dx} + K_{i,c} c_i V \tag{8.14}$$

$$\begin{gathered} \sum_i z_i C_i = 0 \\ \sum_i z_i c_i + X_d = 0 \end{gathered} \tag{8.15}$$

$$\frac{dc_i}{dx} = J_v \left[\frac{K_{i,c} c_i - C_{i,p}}{K_{i,p} D_{i,\infty}} - z_i c_i \frac{\sum_i z_i \frac{K_{i,c} c_i - C_{i,p}}{K_{i,p} D_{i,\infty}}}{\sum_i z_i^2 c_i} \right] \tag{8.16}$$

$$\frac{c_{i,w}}{C_{i,w}} = (1 - \lambda_i)^2 \exp\left(-z_i \frac{F}{RT} \Delta\Psi_D\right) \tag{8.17}$$

$$J_V = VA_k = \frac{r_p^2}{8\mu\left(\frac{\Delta x}{A_k}\right)} (\Delta P - \Delta\Pi) \tag{8.18}$$

where, $D_{i,\ p}$ is the hindered diffusivity (m^2/s), c_i is the concentration of ions in the membrane (mol/m^3), z_i is the valence of ion (i), $K_{i,\ c}$ is the hindrance factor for convection in the structure of nano-based membrane, R is the universal gas constant (J/mol.K), T is the absolute temperature (K), F is the Faraday constant (C/mol), and ψ is the electrical potential (V) in the pores.

However, the Donnan–steric partitioning pore model and other related models such as dielectric exclusion, based on a steric/electric exclusion mechanism, have several shortcomings (Lanteri et al. 2009). One of the shortcomings is that these models are incapable of fitting the rates of experimental rejection of various electrolytes with a single value of the ratio of the membrane thickness-to-porosity (Bowen and Mukhtar 1996; Schaep et al. 1999). Another shortcoming is that the steric/electric exclusion theory fails to characterize the high rejection rates detected with some NF membranes with respect to ionic solutions containing divalent counterions (Szymczyk and Fievet 2005). Furthermore, Donnan–steric partitioning pore model is not suitable for the prediction of rejection of divalent counterions like calcium chloride (Vezzani and Bandini 2002). The studies of Schaep et al. (2001) and Szymczyk and Fievet (2005) have shown that the Donnan exclusion is not enough to describe the strong rejection rates measured for multivalent counterions. The limitation was as a result of the insufficient combination of Donnan equilibrium and steric effects to predict the solute partitioning at the membrane–feed and the membrane–permeate boundaries (Fadaei et al. 2012). Very much unlike the Donnan exclusion, which is repulsive for co-ions and attractive for counterions, the dielectric exclusion is usually not favorable for any ion, irrespective of its charge sign (Lanteri et al. 2009).

8.3.4 Extended Nernst–Planck Model

The Donnan–steric partitioning pore model employs the extended Nernst–Planck equation to explain the transport of ion inside the pores under the influence of drag forces (Gozálvez-Zafrilla and Santafé-Moros 2008). The model employs structural and electrical parameters, namely, pore radius, r_P; effective ratio of membrane thickness to porosity, $\Delta x/A_k$; and the effective charge density, X_d. When the ranges of these parameters are known, the use of numerical predictive method to choose the membrane best suited to a particular process becomes more possible (Bowen and Mohammad 1998). The fitting of the rejection data of uncharged solutes and simple salts can be used to attain these parameters. After the attainment of these parameters, the model can be utilized to predict the capacity of separating ions or charged solutes in the system (Mohammed et al. 2002). The basis for the description of the transport of ions/solutes inside the membranes is founded based on the extended Nernst–Planck equation. The extended Nernst–Planck equation can be written as:

$$j_i = -D_{i,p}\frac{dc_i}{dx} - \frac{z_i c_i D_{i,p}}{RT}F\frac{d\psi}{dx} + K_{i,c}c_i V \tag{8.19}$$

The term on the left-hand side, j_i, is the flux of ion i, and the terms on the right-hand side signify transport of ions as a result of diffusion, electric field gradient, and convection, respectively. $D_{i,\,p}$ is the hindered diffusivity (m^2/s), c_i is the concentration of ions in the membrane (mol/m^3), z_i is the valence of ion (i), $K_{i,\,c}$ is the hindrance factor for convection in the structure of nano-based membrane, R is the universal gas constant (J/mol.K), T is the absolute temperature (K), F is the Faraday constant (C/mol), and ψ is the electrical potential (V) in the pores (Kowalik-Klimczak et al. 2016). The solution of this model also needs three parameters: the pore radius, r_P; effective ratio of membrane thickness to porosity, $\Delta x/A_k$; and the effective charge density, X_d. The first two parameters can be attained by utilizing rejection data for uncharged solutes, while X_d is attained by utilizing salts data. For uncharged solutes, only the diffusive and convective flows affect the transport of solutes inside the membrane. The solute flux can thus be expressed as:

$$j_i = -D_{i,p}\frac{dc_i}{dx} + K_{i,c}c_i V \tag{8.20}$$

In order to develop an expression for rejection of the solute, Eq. (8.6) is integrated through the membrane with the solute concentrations in the membrane at the upper ($x = 0$) and lower ($x = \Delta x$) surfaces written in terms of the external concentrations ($C_{i,\ m}$ *and* $C_{i,\ p}$) using the equilibrium partition coefficient, ϕ:

$$\phi = \frac{c_{i,x=0}}{C_{i,w}} = \frac{c_{i,x=\Delta x}}{C_{i,p}} = \left(1 - \frac{r_s}{r_p}\right)^2 \tag{8.21}$$

where $C_{i,\ m}$ *and* $C_{i,\ p}$ are bulk feed concentration and permeate concentration, respectively, and these concentrations can also be measured experimentally (Mohammed et al. 2002).

Furthermore, the Donnan–steric partitioning pore model with dielectric exclusion (DSPM-DE) is an extensive model used in predicting the mechanism of nanofiltration. The hybridized model solves the extended Nernst–Planck equation for each solute species across the membrane and applies boundary conditions at the membrane surfaces to account for the Donnan exclusion, dielectric exclusion, and steric exclusion effects. The hybridized model describes the mechanism of dielectric exclusion, which is very important for a correct prediction of the rejection of multivalent ions by the nanofiltration membrane (Roy et al. 2015). Omar et al. (2017) adopted the DSPM-DE model to predict the softening performance of cross-linked NF membranes and to elucidate the observed rejection trends which include negative rejection and their underlying multi-ionic interactions. A method founded on sensitivity analysis demonstrated that the membrane pore dielectric constant and the pore size are principally responsible for the high rejections of the NF membranes to multivalent ions. Their findings show that the distinctive capability of these membranes to completely separate multivalent ions from the solution, while allowing monovalent ions to permeate, is a strategy to making this low-pressure softening process realizable (Omar et al. 2017).

8.4 Environmental Applications of Nano-Based Membranes

Environmental remediation comprises of degradation, sequestration, and other related methods which led to a minimized hazard to human and the environment. The benefits, which originate from the application of nanomaterials for remediation, would be more swift or cost-effective for treating wastes (Mansoori et al. 2008). Environmental applications of nano-based membranes such as nanofiltration and nanocomposite membranes fabricated with the integration of nanofillers address the advanced solutions to the existing environmental problems. The applications further address the advanced preventive measures needed for future challenges resulting from the interactions of wastewater/energy and materials with the environment. There are several promising environmental applications of nano-based membranes;

however, this section focused on researches done on desalination, gas separation, solid pollution control, air pollution control, energy storage, and water technologies.

8.4.1 Nano-Based Membrane Operation for Efficient Desalination

As insufficient available freshwater resources become increasingly scarce to meet the demand of water usage, researchers now consider seawater as an alternative source of freshwater. In order to address the need of pure water, several water treatment technologies have been offered and applied at experimental and field levels (Das et al. 2014). Most of the world's water supply has too much salt for human consumption, and desalination is an option from the several water treatment technologies. However, the cost of desalination method is expensive for the removal of salt to provide new sources of drinking water. Hence, low-cost desalination technique with high efficiency and productivity should be established. In addition, nanofillers such as carbon nanotube and nanoparticles can be used to remediate groundwater and surface water polluted with hazardous chemicals and substances (Mansoori et al. 2008). The application of nanocomposite membranes is an optimistic substitute for water desalination that will continue to be used based on the proof of the increasing number of published articles on the subject matter, demonstrating the growing research in the field. Figure 8.6 shows the articles that focused on the fabrication and development of nanocomposite membranes for wastewater treatment.

Recently, carbon nanotube has stimulated much attention as a result of its exceptional optical, electronic, thermal, and mechanical properties (Razmkhah et al. 2017). As a result of its exceptional properties, carbon nanotube has the

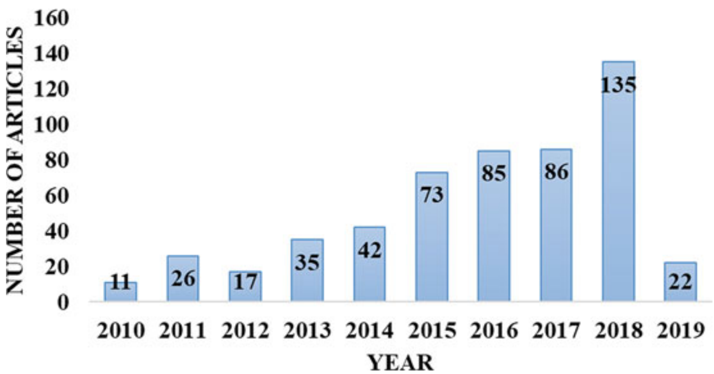

Fig. 8.6 Publications related to the fabrication of nano-based membranes for wastewater treatment during the period of 2010 to 2019 based on literature search using Scopus. (Date of access: 3rd of January 2019)

prospective capability to transform desalination and demineralization. This is due to its capability to remove aromatic compounds, salts, and heavy metals without significant influence on the flow rate of water molecules (Pourzamani et al. 2012). Carbon nanotube membranes have the ability to lessen the cost of desalination (Mansoori et al. 2008). Base on the recent fabrication schemes, there are two types of carbon nanotube membranes: they are (1) vertically aligned (VA) and (2) mixed-matrix carbon nanotube membranes (Ahn et al. 2012). The vertically aligned carbon nanotube membranes can be fabricated by aligning perpendicular carbon nanotubes with supportive filler contents such as silicon nitride, epoxy, etc. between the tubes (Hinds et al. 2004). A mixed-matrix carbon nanotube membrane is made up of a number of layers of polymers or other composite materials. These membranes consume low energy due to carbon nanotube's frictionless water transport ability across nanotube hydrophobic hollow cavity. The membrane is extremely sensitive towards the multiple water contaminants and salts. Furthermore, as a result of the carbon nanotube cytotoxicity, the carbon nanotube membrane has antifouling and self-cleaning abilities with high recrudescence and reusability facilities (Das 2017). Despite the excellent properties that carbon nanotube membranes exhibit, it is important for desalination process to demonstrate proper selection of appropriate parameters in order to ensure a very high level of the process controllability. Hence, the importance of a sophisticated control, tailoring of the growth structure, and morphology of the carbon nanotube arrays (Levchenko et al. 2013).

Controlling the morphology of nano-based membrane components at the nanometer scale is essential to next-generation technologies in water desalination, fuel cell, and gas separation applications (Song et al. 2009). In order to endorse the requirements of desalination and water purification, the membrane should have an appropriate porosity and pore size distribution. Due to the controllable pore size and rational easy aligning process (Yamada et al. 2006), carbon nanotube has revealed a novel space to the application involving desalination process (Razmkhah et al. 2017). Hence, membranes that have carbon nanotubes as pores can be possibly used in desalination and demineralization (Raval and Gohil 2009). A well-aligned carbon nanotube can be used as robust pores in membranes for the applications of water desalination and decontamination (Elimelech and Phillip 2011). Suitable pore diameters can form energy barriers at the channel entries, rejecting salt ions, thus allowing water through the nanotube hollows (Corry 2008). Furthermore, the modification of carbon nanotube pores is possible in order to selectively sense and reject ions (Bakajin et al. 2009). Hence, carbon nanotube membrane could be utilized as a "gate keeper" for size controlled separation of multiple pollutants. The modification of the exterior surfaces of carbon nanotube can enhance the trapping of filler materials into carbon nanotube interstitial spaces. The mixtures of organic and inorganic fillers could also keep individual nanotube in well-aligned carbon nanotube membrane (Das et al. 2014).

A self-standing network of aligned multi-walled carbon nanotubes can appropriately function as an ultrafiltration media. However, there are countless prospects to functionalize carbon nanotubes (Tasis et al. 2006; Hussain et al. 2012). The prospects are grouped as (a) the endohedral filling of carbon nanotubes inner empty

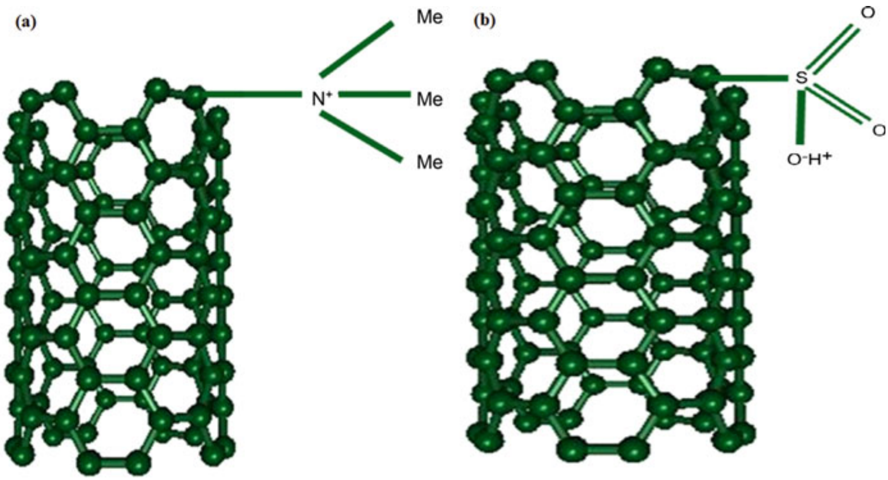

Fig. 8.7 **(a)** Pictorial representation of functionalization of CNT tip with quaternary ammonium group for development of positively charged nanofiltration membrane; **(b)** pictorial representation of functionalization of carbon nanotube tip with sulfonic acid group for development of negatively charged nanofiltration membrane (Kar et al. 2012)

cavity, (b) the addition of covalent chemical groups via reactions onto the π-conjugated skeleton of carbon nanotube, and (c) the adsorption of noncovalent or wrapping of several functional molecules (MingJian et al. 2009). The tips of carbon nanotubes can be suitably functionalized to yield positively charged and negatively charged membranes, in order to be used for water desalination. The functionalization of carbon nanotube tip can present the essential physicochemical features into the surface of the membrane. These features could result in a highly selective elimination of contaminants centered on physicochemical interaction of species with the availability of the functional group over the carbon nanotube tip (Kar et al. 2012). Kar et al. (2012) respectively presented pictorial illustrations of positively charged (quaternary ammonium group) functionalized single-walled carbon nanotube and negatively charged (sulfonic acid group) moieties (see Fig. 8.7). This presentation can serve as a building block towards the development of charged nano-based membrane applications that will facilitate desalination. Hence, functionalization also controls pore size and diameter which are appropriate for synthesizing even carbon nanotube membranes for optimum water desalination (Das et al. 2014).

Nano-Based Membrane Operation for Efficient Removal of Pathogens

Similar to all surface water sources and some groundwater sources, there could be contamination by pathogenic viruses and diverse of chemical contaminants from human actions (World Health Organization 2011). It's been known that there is a need to remove pathogens from potable water supplies due to its negative impact on the community. Desalination process generally offers a substantial barrier to pathogens and chemical contaminants. This barrier might not be absolute, and a number of concerns might possibly have an effect on public health (World Health Organization 2011). Pathogenic contaminations of water result in epidemic diseases. This contributes to the rates of background disease around the world which extremely have negative impact on most developing countries. The detrimental effects from pathogens range from mild acute illness, via chronic severe sickness, to fatality. Vital waterborne (transmission through the consumption of unclean water), water-washed (where the quality of used cleansing water doesn't have much consideration itself, acts as a pathogen source), and water-based (where the pathogen or an intermediate host uses part of its life cycle in water) diseases annually kill millions of people. However, the most common transmission route is the oral consumption route of pathogens, resulting from human feces and urine present in contaminated water, including cleansing/washing water (Clarity 2009). Hence, these pathogens need to be removed from contaminated water.

A variety of water treatment methods can enhance the safety of potable water with respect to pathogenic contamination. The removal of pathogen processes of conventional water treatment plants could have influence on the quality of effluent water (turbidity, pH, temperature) and decrease the capability of sensing pathogen (Das et al. 2014). There has been an increase in the applications of membrane technology, in newly built water treatment plants and existing water treatment plants. In the past two decades, the importance of membrane filtration as a sustainable wastewater treatment technology approach has enhanced membrane variability, system dependability, and cost-effectiveness. The capabilities of microfiltration and ultrafiltration membrane size exclusion have shown their potential for removal of concurrent pathogen (Clarity 2009). Most importantly, the application of ultrafiltration membrane technology can efficiently eliminate pathogens to the very high degree. This is achieved through chemical oxidative disinfection, and it is without any accompanying problems together with the costs of storing and using corrosive agents. However, substantial problems would come up if membrane integrity, such as fiber tear and membrane scratched fail, as the efficiency removal of pathogen can intensely deteriorate.

Therefore, it is necessary to develop strapping membrane materials in order to overcome problems that could affect membrane integrity. It is also important to effectively monitor the effluent in order to identify integrity problems that remains an essential component of a microfiltration/ultrafiltration treatment system (Clarity 2009). However, the nanoporous surfaces of carbon nanotube membranes are appropriate for rejecting micropollutants and ions in liquid phase. The hydrophobic hollow structures motivate the frictionless movement of water molecules without any need for energy-driven force to drive water molecules across hollow tubes. The cytotoxic effects of carbon nanotube membranes decrease biofouling and increase membrane life by killing and removing pathogens (Das et al. 2014). Brady-Estévez et al. (2008) investigated a novel, highly permeable single-walled carbon nanotube filter for effective removal of bacterial and viral pathogen from water at low pressure.

The filter was developed by using a poly (vinylidine fluoride)-based microporous membrane covered with a thin layer of single-walled nanotubes. Their result revealed that *E.coli* bacteria were completely retained on the single-walled nanotube filter and are effectively inactivated upon contact with the single-walled nanotubes. The viruses could also be completely eliminated by a depth-filtration mechanism.

Nano-Based Membrane Operation for Efficient Removal Organic Micropollutants in Drinking Water

Micropollutants are defined as contaminants detected in trace concentrations, in water bodies that are insistent and bioactive. They are not totally biodegradable and cannot be eliminated by conventional water treatment methods (Silva et al. 2017), hence the existence of emerging microcontaminants such as endocrine disrupting compounds in contaminated water. This has made existing conventional wastewater treatment plants noneffective, and they are unable to meet the environmental standards (Amin et al. 2014). When these compounds are discharge into the aquatic environment, they have effect on all living organisms. The traditional materials and treatment technologies like activated carbon, oxidation, and activated sludge are not very effective to treat complicated contaminated waters comprising of pharmaceuticals, surfactants, personal care products, diverse industrial additives, and numerous chemicals claimed. The conventional water treatment processes do not have the capability of adequately addressing the removal of a wide spectrum of toxic chemicals and pathogenic microorganisms in raw water (Amin et al. 2014).

In order to develop efficient techniques that will eliminate these micropollutants, it is important to comprehend their physicochemical properties and the available treatment types and conditions (Silva et al. 2017). Membrane processes are regarded as unconventional methods used for removing massive amounts of organic micropollutants (Kiso et al. 2001; Bodzek et al. 2004). The developed pressure-driven filtration membrane processes such as microfiltration, ultrafiltration, nanofiltration, and reverse osmosis are considered as some new highly effective processes for efficient removal organic micropollutants in drinking water (Adams et al. 2002; Ahmad et al. 2004; Qin et al. 2007). Nanofiltration and reverse osmosis have proven to be relatively efficient filtration technologies for the removal of micropollutants (Yoon et al. 2006; Kegel et al. 2010). It is granted that reverse osmosis and nanofiltration membrane processes are reasonably efficient in removing massive loads of micropollutants (Bolong et al. 2009); however, enhanced materials and treatment approaches are necessary in order to treat newly emerging micropollutants.

Diverse types of materials are used in fabricating membranes; however, polymers are most commonly used for the elimination of micropollutants from wastewaters and sewage. This is because these membranes are not very expensive and they are versatile with respect to conformation and they have high separation performance (Baker 2004; Li et al. 2008). Wang et al. (2018) studied the application of joining membrane bioreactor treatment with reverse osmosis or nanofiltration membrane treatment for the elimination of pharmaceuticals and personal care products in municipal wastewater. Twenty-seven pharmaceuticals and personal care products were studied and analyzed in real influent with lowest average concentration being trimethoprim (7.12 ng/L) and the highest being caffeine (18.4 ng/L). The outcome of their investigation proposed that the membrane bioreactor system effectively removes the pharmaceuticals and personal care products with efficiency between 41.08% and 95.41%. They found that the integrated membrane systems, membrane bioreactor–nanofiltration/reverse osmosis, can achieve even higher removal rates of above 95% for most of pharmaceuticals and personal care products. The study has shown that the combination of membrane bioreactor–nanofiltration resulted in the elimination of 13 compounds below detection limits and membrane bioreactor–reverse osmosis attained better results with elimination of 20 compounds below detection limits.

8.4.2 Nano-Based Membrane Operation for Gas Separation

Natural gas is a vital global energy source, and high carbon dioxide concentrations must be reduced to less than 2% in order to meet pipeline transportation specifications (Baker and Lokhandwala 2008). Majority of industrial gas companies have not overlooked the competition from membrane separation. On the contrary and without doubt, they have made this noncryogenic system a serious part of their process technology for gas separation and recovery. The separation of gas mixtures can be effectively achieved by synthetic membranes fabricated from polymers like polyamide or cellulose acetate or from ceramic materials (Frank 2007). Hence, compared with traditional gas separation techniques such as amine absorption, pressure swing adsorption, and cryogenic distillation, membrane separation processes are principally attractive as a result of the flexible design, compactness, and the efficiency of the membrane units (Nasab and Zahmatkesh 2017).

Innovative membrane materials with outstanding selectivity are needed for a controllable separation process of gas purifications (Xu et al. 2015). From the several nanomaterials, carbon nanomaterials such as carbon nanotube and graphene have drawn incredible attentions in the advanced materials applications. Contingent on the quantity of the shell of graphene, carbon nanotube can be grouped as single-walled carbon nanotube with single shell of graphene, double-walled carbon nanotube, and multi-walled carbon nanotubes. Furthermore, graphene is a one-atom-thick sheet of graphite made of sp2-hybridized carbon atoms well arranged in the hexagonal honeycomb lattices (Mondal 2017). Graphene oxide nanosheets are known to be oxygen functional groups made of graphene which could be attained by treating graphite with strong oxidizer (Xu et al. 2015; Sun et al. 2015). Nano-based membrane with high porosity can be synthesized by arranging graphene or graphene oxide with precise design and size. Graphene and graphene oxide-based membrane can be synthesized by deposition of graphene on a substrate as reinforcing graphene/graphene oxide in the polymeric membrane matrix (Zahri et al. 2016). Just as the

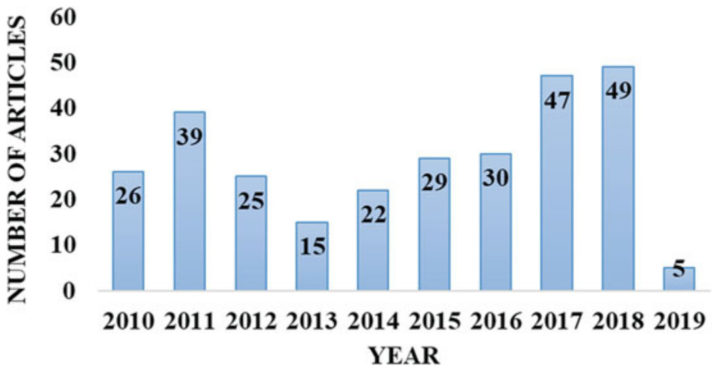

Fig. 8.8 Publications related to the fabrication of nano-based membranes for gas separation during the period of 2010 to 2019 based on literature search using Scopus. (Date of access: 3rd of January 2019

application of nanocomposite membranes is an optimistic substitute for water desalination, it is also a promising alternative for gas separation. It will also continue to be used based on the few evidence of the increasing number of published articles in the field. Figure 8.8 shows the articles that focused on the fabrication and development of nanocomposite membranes for gas separation.

One of the principal applications of the carbon nanotube membranes for gas separation is reinforcing materials in the matrix such as fabrication of nanocomposite membranes as a result of their exceptional physical, mechanical, and functional properties. Li et al. (2017a, b) fabricated carbon/carbon nanotubes hybrid membranes by pyrolyzing poly amic acid precursors incorporated with carbon nanotubes. Their results showed that the combination of carbon molecular sieve membranes with carbon nanotubes brings into play a significantly advantageous influence on the improvement of gas separation performance. Carbon membrane incorporated by multi-walled carbon nanotubes displayed higher permeabilities but lower selectivities than that embedded by single-walled carbon nanotubes. Afsari et al. (2017) investigated the separation performance of supported carbon membranes fabricated from Novolac Phenolic resin as the key precursor and carbon nanotubes as nanofiller for separation of carbon dioxide from nitrogen and methane. Supports were made by carbonization of Novolac Phenolic resin-activated carbon mixture, and selective layer was prepared by dipping the coating of prepared supports into solutions at different concentrations of Novolac Phenolic resin/carbon nanotubes. They observed that the best proportion of Novolac Phenolic resin/activated carbon was 40/60 wt% which was used to make a defect-free and applicable support; most pores of which had sizes less than 10 nm. Membranes were tested at different pressures, and the results revealed that carbon dioxide permeability increased with an increasing pressure. Hence, gas separation driving force is the partial pressure gradient which is the product of total pressure and mole fraction.

Properties of the nanocomposite membranes are hinged on numerous factors such as the dimensions of nanomaterials, distribution, dispersion, and interfacial interaction of nanofillers with the matrix (Michael et al. 2013). However, the mechanism for gas separation is independent of any membrane configuration but depends only on the simple principle of physics that certain gases permeate more rapidly than others (Frank 2007). De et al. (2009) investigated the permeability and selectivity of graphene sheets with designed subnanometer pores using first principle density functional theory calculations. They found that high selectivity was on the order of 10^8 for hydrogen/methane with a high hydrogen permeance for a nitrogen-functionalized pore. Furthermore, they found that extremely high selectivity was on the order of 10^{23} for hydrogen/methane for an all-hydrogen passivated pore whose small width (at 2.5 A) offers a formidable obstruction (1.6 eV) for methane but easily attainable for hydrogen (0.22 eV). These results suggested that these pores are far superior to traditional polymer and silica membranes, with the domination of the transport of gas molecules through the material by bulk solubility and diffusivity. Du et al. (2011) designed a series of nanoporous graphene for separating nitrogen and hydrogen and discovered that there were different mechanisms for hydrogen and nitrogen to permeate through the nanoporous graphene membrane. The flux of the hydrogen was linear with reference to the pore size of nanoporous graphene, while nitrogen flux was not. This showed that the hydrogen and nitrogen permeation across the porous graphene have different mechanisms. Hence, they observed more permeation events of nitrogen than that of hydrogen molecules. This is as result of the van der Waals interactions with the graphene membrane which make the nitrogen molecules to accumulate on the surface of graphene. Thus, gas separation occurs according to the morphology of the membrane which is dependent on different transport mechanisms and forces of interactions.

8.4.3 Nano-Based Membrane Operation for Air Pollution Control

Air pollution is another potential area where nanotechnology has great promise. Numerous types of volatile air pollutants, either organic or inorganic, could be found in waste gases. However, the buildup of intermediate metabolites can occasionally occur under high load conditions (Kennes et al. 2009). Air pollution is usually affected by the emission of pollution spawned from industry, power plants, municipal waste, car transport, and agricultural (Mulder 1994). One of the problems of air pollution is the generation of vast volumes of gases, which adds to the creation of the effect of greenhouse–carbon dioxide while burning carbon-derived fuels and simultaneous emission of methane and carbon dioxide from solid waste dumps (Bodzek 2000). In regard to the case of simultaneous emission of methane and carbon dioxide from solid waste dumps, the process will be beneficial to recover methane because it is a valuable source of energy (Rautenbach and Welsch 1993; Prabhudessai et al. 2013) and is regarded as higher global greenhouse factor than carbon dioxide (Dickinson and Cicerone 1986; Muller and Muller 2017). Filtration techniques using polymeric membranes similar to the water purification methods described in Sect. 8.4.1 can be used in buildings, for the purification of indoor air volumes.

Polymeric membranes have recently found a new potential application such as contact separation surface of two phases (gas phase and aqueous phase), commonly used in membrane bioreactors. In the application of membrane bioreactors for air pollution control, both a gas phase and an aqueous phase are fed to the reactor. The two phases are separated by a membrane. The polluted air (i.e., the volatile pollutant), usually containing a carbon source, is considered the gas phase, while the aqueous phase gives nutrients to the biofilm growing on the aqueous side of the surface of the membrane. The membranes are inserted inside the reactor by either tubular configuration or flat sheets. More often than not, the gas phase flows through the lumen, while the aqueous phase is fed through the shell side (Kennes et al. 2009). In order to separate water phase from gas phase or from another water phase, the membrane must have hydrophobic character. As a result of the hydrophobic character, it is possible to carry out a process similar to extraction, and the absorption of gases with the use of membrane units. Hence, most of the absorbents used in the conventional absorption process are also applicable in membrane absorbers (Aravind and Kathirasen 2017). Throughout the application of porous membranes for gas absorbers, the liquid phase must not be mixed with the gas phase. However, the process depends on pore sizes, pressure difference and the liquid absorption affinity with the membrane material. Furthermore, with the occurrence of fast chemical reactions in the presence of membranes, the transport of matter is limited by diffusion stage in the gas phase; hence, depends on hydrodynamic conditions over the membrane surface, its properties such as porosity, thickness, morphology, and transport properties such as diffusion index (Aravind and Kathirasen 2017).

Nano-based filters could be used for air pollution control. Hence, another gray area for air pollution control is the application of nanostructured membranes that have pores small enough to separate different pollutants from exhaust. Investigations now concentrate on the enhancement and optimization of nanostructured membranes to capture several gas pollutants (Mohamed 2017). Particularly, filtration by nanostructured membranes is suitable for several volatile organic compounds vapors (Scholten et al. 2011). Scholten et al. (2011) developed electrospun polyurethane fibers for the removal of volatile organic compounds from air with fast volatile organic compound absorption and desorption. It is known that activated carbon possessed a many-fold higher surface area than polyurethane fiber meshes. The sorption capacity of the polyurethane fibers was however, found to be comparable to that of activated carbon, and specifically designed for vapor adsorption. Furthermore, the polyurethane fibers established a completely reversible absorption and desorption with respect to desorption gotten by simple purging with nitrogen at room temperature. Hence, the selectivity of the polyurethane fibers towards different types of vapor, together with the ease of regeneration, make them attractive materials for volatile organic compound filtration (Scholten et al. 2011).

Nano-based membrane filters could be used in automobile tailpipes and factory smokestacks to separate out contaminants and inhibit them from entering the atmosphere (Mansoori et al. 2008). The design of nanoparticle embedded nano-membrane-filter was proposed by (Muralikrishnan et al. 2014) to reduce air pollution from the vehicular exhaust. During the design, the pores of the nano-membrane filters are very essential and should be designed based on the requirement. The membrane would be inserted in the exhaust system of the vehicle, which traps the harmful gases thereby reduces air pollution (Muralikrishnan et al. 2014). Furthermore, nano-sensors could be developed to discover toxic gas leaks at very low concentrations (Mansoori et al. 2008). In addition, particulate matter can be successfully captured in nanomembranes, in relation to microfibers as a result of its small fiber diameter, small pore size and high specific surface area. Electrospun nanomembranes have recently been used to filter gaseous pollutants due to their capability of active surface modification (Kadam et al. 2016). Hence, the utilization of nano-based membrane filters for air pollution control has the potential to improve air quality that are presently of concern to scientists globally.

8.4.4 Nano-Based Membrane Operation for Solid Pollution Control

Solid wastes are regarded as any garbage, sludge, and refuse from wastewater treatment plant; discarded materials such as liquid, solid, semi-solid, and gaseous materials; and hazardous materials from mining activities and other industrial activities. The hazardous wastes are the elements which causes hazard to human beings, plants, and animals. Some of the common hazardous wastes are radioactive substances, flammable and explosives wastes, chemicals, and biological wastes. Solid wastes have the capacity of polluting air, water, and soil, thus resulting in various environmental impacts and causing health hazard, as a result of improper handling and transportation (Chadar and Chadar 2017), hence the need to control solid waste. Control of solid pollution is commonly done through a sanitary landfill or through incineration. A modern sanitary landfill is dispersed in an impermeable soil layer, lined with an impermeable membrane. In it, solid waste is positioned in a properly selected and prepared landfill site, in a recommended method. The waste material is spread out and condensed with suitable heavy machinery (Chadar and Chadar 2017).

One way of controlling solid waste pollution is through incineration and the process of incineration is done for different reasons. Incineration is the burning of unwanted or waste materials from processes where they are being generated. For example, incineration is the burning of hospital medical waste and the burning of domestic garbage. Finally, some incinerators burn only tires. Hence, all incinerators were developed as a substitute for burying solid waste in the ground. However, the process produced air pollution and soil pollution (Griffin, Product Manager, Tetratec 2018). With an enhanced operation of incinerators and waste segregation, woven fiberglass with a stretched polytetrafluoroethylene membrane, and in a couple of cases Ryton®, has proven to work perfectly, especially in medical waste (Griffin, Product Manager, Tetratec 2018). Nanotechnology has the capability to control matter at the nanoscale and fabricate materials that have specific properties with a specific function (Roco et al. 2000). Nanomaterial is very small and has high ratio of surface area to volume ratio that can be used to detect very sensitive contaminants (Lu and Zhao 2004). Owing to the properties of nanomaterials, nano-based membranes could also perfectly enhance operation of incinerators and waste segregation.

8.5 Development and Applications of Nano-Based Membranes in Environmental Chemistry

Environmental chemistry is the study of chemical processes such as sources, reactions, and the effect of chemical species that take place in the environment (water, air, and soil) which are influenced by human and biological activities. In order to combat the effects of human and biological activities in the environment, scientists and researchers have developed and applied nano-based membranes. The development of nano-based membranes for environmental chemistry applications provides the fundamental physicochemical characterizations of recently employed integration of nanocomposites, such as nanoparticle, graphene, graphene oxide, carbon nanotubes, and other nano-sized carbon allotropes in membrane materials such as polymer. This section reviewed the development and applications of nano-based membranes for environmental chemistry applications.

Titanium dioxide has been extensively utilized for wastewater treatment (Kumar and Bansal 2013), water splitting (Gellé and Moores 2017), air purification (Paz 2010; Binas et al. 2017), and self-cleaning of surfaces (Banerjee et al. 2015) due to its exceptional photocatalytic property. TiO_2 has also been integrated in several membrane matrices in order to offer photocatalytic activities (Pandey et al. 2017). The integration of membrane filtration with photocatalysis offers multifunction that involves filtration and photocatalytic degradation for the removal of pollutants from water. Wang et al. (2015) designed and developed a TiO_2/carbon/Al_2O_3 membrane through sequentially depositing graphitic carbon layer with good electroconductivity and TiO_2 nanoparticle layer with photocatalytic activity on Al_2O_3 membrane support for improved water treatment application. Membrane performance tests pointed out that the photoelectrocatalytic membrane filtration showed improved removal of natural organic matters and permeate flux with increasing voltage supply. Furthermore, the photoelectrocatalytic membrane process demonstrated special improvement in removing organic chemicals, such as rhodamine B. Zhang et al. (2018) built a photo-assisted multifunctional NF membrane assembled with g-C_3N_4, TiO_2, CNTs, and graphene oxide (GO), in which CNTs not only increase the interlayer space between neighbored graphene sheets but also improve the stability and the strength of GO layer. The NF membranes demonstrated an improved water flux of $\sim$16 L m^{-2} h^{-1} bar^{-1} while maintaining a high dye rejection of $\sim$100% for methyl orange. The photo-assisted NF membranes further show good rejection ratio for salt ions (i.e., 67% for Na_2SO_4) as a result of the layer-by-layer sieving. Simultaneously, the NF membrane integrated with photocatalysis displays a multifunctional characteristic for the effective removal of ammonia (50%), antibiotic (80%), and bisphenol A (82%) in water.

Apart from the integration of titanium dioxide in several membrane matrices for water treatment applications, polyacrylonitrile (PAN) alone and silver nanoparticle/CNT/PAN membranes have been employed for the filtration of *E. coli*-contaminated water (Pandey et al. 2017). Gunawan et al. (2011) developed an alternative and safe water disinfection system consisting of silver nanoparticle/multi-walled carbon nanotubes (AgNP/MWCNTs) coated on PAN hollow fiber membrane. In the continuous filtration test using *E. coli* feedwater, the relative flux drop over AgNP/MWCNTs/PAN was 6%, and the relative flux drop over the pristine PAN was 55% at 20 h of filtration. The results showed that AgNP/CNT coating has considerably improved antimicrobial activity and antifouling properties of the membranes. Kumar and Gopinath (2016) developed silver nanoparticle (AgNP)-incorporated carboxylated multi-walled carbon nanotube (MWCNT)-grafted aminated polyacrylonitrile (APAN)-based nanofibrous membrane appropriate for the removal of toxic heavy metals and bacteria present in wastewater. The nanofibrous membrane was found to have exceptional antibacterial properties and a filtration capability. These nano-based membranes can be applied for water treatment at industrial level.

The characteristics of nano-based membranes for industrial scale water treatment application are based on the fabrication of tailored membranes with high selectivity, competitive flux, and self-cleaning properties. These characteristics put into consideration the sustainability conditions in terms of environmental impacts, easy application, flexibility, and adaptability (Ursino et al. 2018). Kim et al. (2013) evaluated membrane systems for the removal of the extractable organic fraction from oil sands process-affected water. They developed membranes with and without multi-walled carbon nanotubes. The MWCNTs were modified with strong acid in order to enhance dispersion in an organic solvent. Dispersion of the MWCNTs and physicochemical properties of the membranes were characterized by microscopic and spectroscopic methods. The results revealed that acid-modified MWCNTs developed surface functional groups that increased their hydrophilicity, increased the rejection of hydrophobic pollutants, increased the permeate flux of oil sands process-affected water, and considerably reduced membrane fouling. Zhang et al. (2013) used polysulfone membranes with phosphorylated TiO_2–SiO_2 particles for oily wastewater treatment. Their results revealed that TiO_2–SiO_2 particles are uniformly dispersed in the TiO_2–SiO_2/polysulfone composite membrane and the water contact angle of the membrane declines from 78.0° to 45.5°, which demonstrated the good hydrophilic nature of TiO_2–SiO_2 particles. TiO_2–SiO_2 particles improved the polysulfone membrane hydrophilicity, antifouling capacity, and mechanical strength significantly. Hence, TiO_2–SiO_2/polysulfone composite membranes are desirable for treating wastewater containing oil. Zhang and Liu (2015) developed and combined silica nanotubes and SO_4^{2-}/TiO_2 solid to fabricate sulfated TiO_2 deposited on SiO_2 nanotubes for treating wastewater containing oil. Compared with polysulfone membranes, SiO_2/polysulfone membranes, and phosphorylated Zr-doped hybrid silica (SZP)/polysulfone membranes, SiO_2 nanotubes/polysulfone composite membranes demonstrated stronger antifouling and anti-compaction performance. Hence, SiO_2 nanotubes/polysulfone composite membranes are appropriate for the treatment of wastewater containing oil. Therefore, the development of novel nanocomposite membranes has been established to be successfully utilized in water treatment, due to their antifouling and antibacterial properties, with the aim of improving the membrane lifetime and its separation performance (Ursino et al. 2018).

8.6 State of the Art of Nano-Based Membranes

Membranes that are based on nanofillers (polymer/inorganic nanoparticles, polymer/carbon nanotubes, and polymer/graphene membranes) are nanocomposite membranes. Nanocomposites are usually related to inorganic, i.e., porous and nonporous, nanoparticles distributed within a continuous phase of organic polymers. These nanofillers have the capacity to make exclusive permeation pathways for selective transport, at the same time posing barrier for unwanted transport. The progress in carbon nanotubes and graphene-based materials has resulted in the fabrication of polymer/carbon nanotubes and polymer/graphene membranes. This section reviews the current state of the art in the polymer/inorganic nanoparticles, polymer/carbon nanotubes, and polymer/graphene-based nanofiller nanocomposite membranes with special emphasis on environmental chemistry.

8.6.1 Inorganic Nanoparticles in Polymeric Membranes

The integration of inorganic nanoparticles as fillers within a polymer matrix has extended prospects to fabricate multifunctional nanocomposite membranes that have the capability of performing tasks beyond separation alone (Goh et al. 2014). Composite materials which contain polymeric and inorganic units have been extensively used for various applications as a result of their improved and more practical performance properties (Ma et al. 2010). In the past two decades, inorganic micromaterials such as alumina, zirconia, and silica were mostly being used as fillers in order to improve the performance of membrane process by enhancing the permeate flux, increasing the salt rejection and improving the thermal, chemical, and mechanical stabilities (Genne et al. 1996; Sekuliċ et al. 2002). The application of resultant membranes was restricted to microfiltration and ultrafiltration because the size of the particles is in micrometer range, having pore sizes of ca. 0.1 μm and ca. 0.01 μm, respectively (Jhaveri and Murthy 2016). As a result of the progress, which is based on the use of novel materials with at least one dimension in nanometer range (nanoparticles), the prospect of applying inorganic materials was extended nanocomposite membranes (Jhaveri and Murthy 2016).

Most of the modification of nano-based membrane involves the use of inorganic nanoparticles such as metal or metal oxide (Jhaveri and Murthy 2016). These nanomaterials are either mixed in the membrane matrix or coated on the membrane surface, usually with the aid of tethering chemicals (Dong et al. 2015). However, there are some exceptions, such as NaA-type zeolite NPs (Xu et al. 2018), $CaCO_3$ and $CaCO_4$ (Ray et al. 2017), and Mg $(OH)_2$ (Zhao et al. 2006). The most widely used metal oxide for the fabrication and modification of membrane for applications in water treatment and desalination are alumina (Al_2O_3), titania (TiO_2), zirconia (ZrO_2), and silica (SiO_2) (Fard et al. 2018). TiO_2 nanoparticles have successfully mitigated fouling of organic matter onto PES. Al_2O_3 and most recently ZrO_2 nanoparticles have proven to reduce the fouling rate of polyethersulfone membranes in wastewater. However, ZrO_2 nanoparticles also showed lower flux decline of the composite membrane (Richards et al. 2012).

Membrane Integrated with Alumina-Based Nanoparticle

Alumina as a material is mostly used for water treatment and desalination as a result of the economical consideration together with its capability to resist in high trans-membrane pressures (TMP) (Elaine Fung and Wang 2013). There has recently been a growing interest in the use of inorganic membranes, mainly alumina (Al_2O_3) ceramic membranes (CMs) (Younssi et al. 2018). In addition, Al_2O_3 has two important characteristics which are hydrophilic and covalent bonding characteristics. Ceramic nano-based membranes are characterized by a very high chemical, thermal, and mechanical stability, combined with good separation characteristics and long lifetime (Rezaei Hosseinabadi et al. 2014). However, nano Al_2O_3 have also been introduced in polymeric membrane for the purpose of enhancing the performance of organic membranes to form new generation of membranes (composite membranes) with new performances that combine organic and CM proprieties (Younssi et al. 2018). Saleh and Gupta (2012) reported polyamide nanocomposite membrane containing alumina nanoparticles synthesized via in situ interfacial polymerization. The nanocomposite membrane was cured at 80 °C for 5 min. They found that the nanocomposite membrane performed better than a pristine membrane. The introduction of alumina nanoparticles in the membrane enhances the permeate flux and maintains the salt rejection. The introduction of alumina nanoparticles in the membrane also resulted in enhanced hydrophilicity of the membranes proved by decreased in water contact angle. Ghaemi (2016) used γ-Al_2O_3 nanoparticles to improve the copper removal efficiency of polyethersulfone membranes. The results they obtained showed higher water permeation compared with the pristine polyethersulfone membrane just by the addition of small amounts of nanoparticles ($\leq$1.0 wt. %). This is as a result of increasing the membrane porosity and hydrophilicity after the addition of alumina nanoparticles into the membrane matrix. Hence, adding an appropriate amount of nano-sized Al_2O_3 particles to a polymeric membrane can enhance the membrane's hydrophilicity properties. Like alumina oxide nanoparticles, titanium-based nanoparticles also have properties which could increase the performance of membranes when integrated into the membrane during fabrication (see sect. 8.5). Zirconia (ZrO_2) is another metal oxide that possess the properties which could increase the performance of membranes when impregnated into the membrane during fabrication.

Membrane Integrated with Zirconia (ZrO_2)-Based Nanoparticle

Numerous researchers have employed a variety of inorganic particles to fabricate organic-inorganic membranes; nonetheless, the investigations on the application of zirconia particles in the preparation of organic–inorganic hybrid membranes are not sufficient. Furthermore, the fabrication of organic–inorganic membranes impregnated with zirconia particles with grain sizes in nanometer range is not much (Kim and Van der Bruggen 2010). However, research has shown that zirconia membranes are known to be chemically more stable than titania and alumina membranes, hence more suitable for liquid phase applications under harsh conditions (Maximous et al. 2010). Zirconia (ZrO_2) have been used by Zhang et al. (2011) as doping materials for the poly (ether sulfone) membrane for treating wastewater containing oil. The results obtained showed that the oil concentration in the permeation is 0.67 mg/L, which meets the recycle standard of the Chinese oil field (SY/T 5329-94, oil concentration). Thuyavan et al. (2014) also studied the removal of humic acid from groundwater using zirconia embedded in poly (ether sulfone) mixed-matrix membranes. For this study, the authors used chemical precipitation method to prepare nano zirconia (ZrO_2). The modified poly (ether sulfone) membrane with nano ZrO_2 of 2.5 and 5 wt% was studied. The addition of nano ZrO_2 altered the morphology of the membrane and improved pure water permeability. Chen et al. (2018) fabricated a carbon composite membrane on a hollow yttrium-stabilized zirconia (YSZ) tube with a porous wall. Yttrium-stabilized zirconia (YSZ) is a very stable ceramic, while carbon is also chemically inert, so the composition of the carbon composite membrane on a hollow yttrium-stabilized zirconia was very stable. In order to confirm the stability of its functionality, the membrane was tested under the forward osmosis process at 80 °C for an extended period of 168 h. The authors found that the membrane property was very stable. Their research showed that nanoporous carbon composite membranes can exhibit 100% desalination and a freshwater flux that is 3–20 times higher than existing polymeric membranes. The carbon composite membrane showed improved hydrophilicity in terms of the freshwater flux.

8.7 Future Direction of Nano-Based Membranes in Environmental Applications

It is well-known that membrane technology has its own advantages and disadvantages. The integration of inorganic nanoparticles and carbon nanotubes in polymeric membranes has, however, advanced in terms of ideal innovation in environmental applications. Membranes based on nanomaterials have shown innovatory performances, and they have a commercially viable prospect in the near future. However, the commercial accessibility of the carbon nanotube membranes and nano-based membranes embedded with inorganic nanoparticles must meet certain standards such as the capacity of desalination, water permeability, antifouling, solute selectivity, robustness, energy savings, material costs, scalability, and compatibility with industrial settings (Das et al. 2014). In addition, most of the carbon nanotube-based membranes are presently assembled on a ceramic or polymeric membrane that may have negative impact on the properties of carbon nanotubes. It is therefore necessary to focus more on the synthesis of freestanding membrane in order to completely exploit the exceptional features of carbon nanotubes. As a result of the limitations of the current applications of carbon nanotube-based membrane to improve the performance of pressure driven membrane, it is important to carry out an extensive study in order to explore the other potential applications of carbon nanotube-based membranes such as membrane distillation and capacitive deionization (Ihsanullah 2019).

Furthermore, fouling on polymeric membrane surfaces is considered the most severe problem on membrane performance during filtration process. Polymeric membranes are less chemically stable and low fouling-resistant when compared to ceramic membranes, in many water treatment applications (Pendergast and Hoek 2011). Irregular pore size, poisonous micropollutants, influent water quality, and pH variations always have negative influence on membrane capacities (Das et al. 2014). Thus, fouling has the capacity to intensely diminish the effectiveness and economic benefits of a membrane process during the filtration of wastewater. Certain aspects of the economic have to be taken into consideration, and different strategies in combating membrane fouling have to be considered. The two basic tools that can be used to combat fouling are permeate flux and transmembrane pressure.

The best indicators of membrane fouling are permeate flux and transmembrane pressure. Membrane fouling results to a significant increase in hydraulic resistance, demonstrated as permeate flux decline or increase in transmembrane pressure when the process is operated under constant transmembrane pressure or constant flux conditions. In a system where the permeate flux is maintained by increasing transmembrane pressure, the energy needed to achieve filtration also increases (Abdelrasoul et al. 2013). Membrane fouling is not completely reversible by backwashing for an extended period of operation. Increase in the number of filtration cycles results to an increase in irreversible fraction of membrane fouling. Hence, chemical cleaning is required for the purpose of achieving the desired production rate for membrane to recover most of its permeability. However, the elevated cost that resulted from chemical cleaning makes membranes economically less feasible for many separation processes. There are also worries that repeated chemical cleaning might shorten the membrane life span (Abdelrasoul et al. 2013). However, the development of self-cleaning membranes can be a way to reduce the fouling as well as maintain the membrane water permeation (Ursino et al. 2018). Nano-based membranes with self-cleaning features provide a critically required solution to combating the problem of fouling. It is therefore important for researchers to carry out extensive investigations that will explore the potential of carbon nanotubes and inorganic nanoparticles in fabricating self-cleaning membranes for the treatment of wastewater and purification of water. Such membranes can easily clean themselves when fouled; this could make pressure-driven membrane filtration systems employed in treating and desalinating wastewater more energy and economic efficient.

8.8 Conclusion

This report has summarized and discussed the role and characterization of nano-based membranes for environmental applications. It was found that membrane structure, surface modification, nature of feed, and operating conditions play significant roles in the membrane performance. The separation mechanisms of membranes for most pollutants depend on the pore size and porosity, dielectric exclusion surface phenomena, fluid transport across the pores, effective charge density, and solution diffusion. The environmental applications of nano-based membranes synthesized with the integration of nanofillers address the cutting-edge solutions to the existing and prevention of environmental problems. As a result of the unique selectivity of nano-based membrane, it has been successful in efficient desalination and in the efficient removal of pathogens and organic micropollutants in drinking water and gas separation. Furthermore, the application of membrane technology for air pollution and solid pollution control was discussed. Separation of gases and vapors has been reviewed for removal of volatile organics from air in relation to the membrane absorption process. The application of nano-based membrane filters for air pollution control has the prospect of improving air quality; in addition, nano-based membranes can effectively improve the operation of incinerators and waste segregation. The fabrication self-cleaning membranes for the treatment of wastewater and purification of water also have the prospect of combating membrane fouling.

References

Abdallah H, Shalaby MS, Shaban AMH (2015) Performance and characterization for blend membrane of PES with Manganese (III) Acetylacetonate as metalorganic nanoparticles. Int J Chem Eng:1–9. https://doi.org/10.1155/2015/896486

Abdel-Fatah MA (2018) Nanofiltration systems and applications in wastewater treatment: review article. Ain Shams Eng J 9(4):3077–3092

Abdelrasoul A, Doan H, Lohi A (2013) Fouling in membrane filtration and remediation methods. In: Mass transfer – advances in sustainable energy and environment oriented numerical modeling. Intech, Rijeka

Abhang RM, Wani KS, Patil VS, Pangarkar BL, Parjane SB (2013) Nanofiltration for recovery of heavy metal ions from waste water - a review. Int J Res Environ Sci Technol 3(1):29–34

Abidi A, Gherraf N, Ladjel S, Rabiller-Baudry M, Bouchami T (2016) Effect of operating parameters on the selectivity of nanofiltration phosphates transfer through a Nanomax-50 membrane. Arabian J Chem 9:S334–S341. https://doi.org/10.1016/j.arabjc.2011.04.014

Adams C, Wang Y, Loftin K, Meyer M (2002) Removal of antibiotics from surface and distilled water in conventional water treatment processes. J Environ Eng 128(3):253–260

Afsari M, Asghari M, Moghaddam PM (2017) Synthesis and characterization of supported Phenolic resin/Carbon nanotubes Carbon membranes for gas separation. Int J Nano Dimens 8 (4):316–328

Agashichev SP (2009) Modeling the influence of temperature on gel-enhanced concentration polarization in reverse osmosis. Desalination 236(1–3):252–258. https://doi.org/10.1016/j.desal.2007.10.074

Agboola O, Maree J, Mbaya R (2014) Characterization and performance of nanofiltration membranes: review. Environ Chem Lett 12:241–255. https://doi.org/10.1007/s10311-014-0457-3

Agboola O, Mokrani T, Sadiku ER, Kolesnikov A, Olukunle OI, Maree JP (2017) Characterization of two nanofiltration membranes for the separation of ions from acid mine Water. Mine Water Environ 36:401–408. https://doi.org/10.1007/s10230-016-0427-z

Ahmad AL, Ooi BS, Mohammad AW, Choudhury JP (2004) Development of a highly hydrophilic nanofiltration membrane for desalination and water treatment. Desalination 168(1-3):215–221

Ahn CH, Baek Y, Lee C, Kim SO, Kim S, Lee S, Kim S-H, Bae SS, Park J, Yoon J (2012) Carbon nanotube-based membranes: fabrication and application to desalination. J Ind Eng Chem 18 (5):1551–1559

Al-Sheetan KM, Shaik MR, AL-Hobaib AS, Alandis NM (2015) Characterization and evaluation of the improved performance of modified reverse osmosis membranes by incorporation of various organic modifiers and SnO_2 nanoparticles. J Nanomater 2015:1–11. https://doi.org/10.1155/2015/363175

Amin MT, Alazba AA (2014) A review of nanomaterials based membranes for removal of contaminants from polluted waters. Membr Water Treat 5(2):123–146. https://doi.org/10.12989/mwt.2014.5.2.123

Amin TA, Alazba AA, Manzoor U (2014) A review of removal of pollutants from water/wastewater using different types of nanomaterials. Adv Mater Sci Eng 2014:1–24

Amouamouha M, Gholikandi GB (2017) Characterization and antibiofouling performance investigation of hydrophobic silver nanocomposite membranes: a comparative study. Membranes (Basel) 7(64):1–16. https://doi.org/10.3390/membranes7040064

Aravind SV, Kathirasen R (2017) Air pollution control using membrane technique. Int J Adv Res Civil, Struct, Environ Infrast Eng Dev 3(1):322–327

Ariono KD, Wenten SIG (2017) Surface modification of ion-exchange membranes: Methods, characteristics, and performance. J Appl Polym Sci 2017:1–13

Aroon MA, Ismail AF, Matsuura T, Montazer-Rahmati MM (2010) Performance studies of mixed matrix membranes for gas separation: a review. Sep Purif Technol 75:229–242. https://doi.org/10.1016/j.seppur.2010.08.023

Ávila AF, de Oliveira AM, Lacerda GRDS, Munhoz VC, Santos MCG, Santos PF, Triplett M (2013) A nano-modified superhydrophobic membrane. Mater Res 16(3):609–613. https://doi.org/10.1590/S1516-14392013005000028

Bakajin O, Noy A, Fornasiero F, Grigoropoulus JK, Holt JB, Kim IS, Park HG (2009) Nanofluidic carbon nanotube membranes: applications for water purification and desalination. In: Savage et al (eds) . Willian Andrew Inc./Elsevier, New York, pp 77–93

Baker RW (2004) Membrane technology and applications, 2nd edn. John Wiley & Sons Ltd, Chichester

Baker RW, Lokhandwala K (2008) Natural gas processing with membranes: an overview. Ind Eng Chem Res 47:2109–2121

Balta S, Sotto A, Luis P, Benea L, Van der Bruggen B, Kim J (2012) A new outlook on membrane enhancement with nanoparticles: the alternative of ZnO. J Membr Sci 389:155–161. https://doi.org/10.1016/j.memsci.2011.10.025

Banerjee S, Dionysiou DD, Pillai SC (2015) Self-cleaning applications of TiO_2 by photo-induced hydrophilicity and photocatalysis. Appl Catal B Environ 176–177:396–428

Barthlott W, Neinhuis C (1997) Purity of the sacred lotus, or escape from contamination in biological surfaces. Planta 202:1–8

Battirola LC, Gasparotto LHS, Rodrigues-Filho UP, Tremiliosi-Filho G (2012) Poly(imide)/organically-modified montmorillonite nanocomposite as a potential membrane for alkaline fuel cells. Membranes (Basel) 2:430–439. https://doi.org/10.3390/membranes2030430

Beril Gonder Z, Arayici S, Barlas H (2011) Advanced treatment of pulp and paper mill wastewater by nanofiltration process: effects of operating conditions on membrane fouling. Sep Purif Technol 76:292–302. https://doi.org/10.1016/j.seppur.2010.10.018

Binas V, Venieri D, Kotzias D, Kiriakidis G (2017) Modified TiO_2 based photocatalysts for improved air and health quality. J Materiomics 3:3–16

Bodzek M (2000) Mebrane techniques in air cleaning. Polish J Environ Studies 9(1): 1–12

Bodzek M, Dudziak M, Luks-Betlej K (2004) Application of membrane techniques to water purification. Removal of phthalates. Desalination 162(1–3):121–128

Bolong N, Ismail AF, Salim MR, Matsuura T (2009) A review of the effects of emerging contaminants in wastewater and options for their removal. Desalination 238(1–3):229–246

Boussu K, Van der Bruggen B, Volodin A, Snauwaert J, Van Haesendonck C, Vandecasteele C (2005) Roughness and hydrophobicity studies of nanofiltration membranes using different modes of AFM. J Colloid Interface Sci 286:632–638. https://doi.org/10.1016/j.jcis.2005.01.095

Bowen WR, Mohammad AW (1998) A theoretical basis for specifying nanofiltration membranes-dye/salt/water streams. Desalination 8(1-3):257–264. https://doi.org/10.1016/S0011-9164(98)00112-X

Bowen WR, Mukhtar H (1996) Characterisation and prediction of separation performance of nanofiltration membranes. J Membr Sci 112:263–274. https://doi.org/10.1016/0376-7388(95)00302-9

Brady-Estévez AS, Kang S, Elimelech M (2008) A single-walled-carbon-nanotube filter for removal of viral and bacterial pathogens. Small 4(4):481–484. https://doi.org/10.1002/smll.200700863

Camacho LM, Dumée L, Zhang J, Li JD, Duke M, Gomez J, Gray S (2013) Advances in membrane distillation for water desalination and purification applications. Water 5:94–196

Carré A (2007) Polar interactions at liquid/polymer interfaces. J Adhes Sci Technol 21(10):961–981. https://doi.org/10.1163/156856107781393875

Cassano A (2017) Recovery technologies for water-soluble bioactives: advances in membrane-based processes. In: Engineering foods for bioactives stability and delivery, Food engineering series. Springer Science+Business Media, New York, p 64

Chadar SN, Chadar K (2017) Solid waste pollution: a hazard to environment. Recent Adv Petrochem Sci 2(3):1–3

Chen W, Chen S, Liang T, Zhang Q, Fan Z, Yin H, Huang K-W, Zhang X, Lai Z, Sheng P (2018) High-flux water desalination with interfacial salt sieving effect in nanoporous carbon composite membranes. Nat Nanotechnol 13:345–350

Cheng W, Campolongo MJ, Tan SJ, Luo D (2009) Freestanding ultrathin nano-membranes via self-assembly: review. Nano Today 4:482–493. https://doi.org/10.1016/j.nantod.2009.10.005

Chung T-S, Jiang LY, Li Y, Kulprathipanja S (2007) Mixed matrix membranes (MMMs) comprising organic polymers with dispersed inorganic fillers for gas separation. Prog Polym Sci 32:483–507. https://doi.org/10.1016/j.progpolmsci.2007.01.008

Clarity AB (2009) Pathogen removal from water technologies and techniques. Filtration + separation: water and wastewater: Dexmet corporation. http://www.filtsep.com/water-and-wastewater/features/pathogen-removal-from-water-technologies-and/. Assessed 20 Oct 2018

Corry B (2008) Designing carbon nanotube membranes for efficient water desalination. J Phys Chem B112(5):1427–1434

Dalwani M, Benes NE, Bargeman G, Stamatialis D, Wessling M (2011) Effect of pH on the performance of polyamide/polyacrylonitrile based thin film composite membranes. J Membr Sci 372:228–238. https://doi.org/10.1016/j.memsci.2011.02.012

Das R (2017) Nanohybrid catalyst based on carbon nanotube: a step by step guideline from preparation to demonstration. Springer International Publishing, Cham, p 41

Das R, Ali ME, Hamid SBA, Ramakrishna S, Chowdhury ZZ (2014) Carbon nanotube membranes for water purification: A bright future in water desalination. Desalination 336:97–109

de Sousa FDB, de Engenharia CHSC, Aplicadas MCS (2014) The use of atomic force microscopy as an important technique to analyze the dispersion of nanometric fillers and morphology in nanocomposites and polymer blends based on elastomers. Polímeros 24(6):661–672. https://doi.org/10.1590/0104-1428.1648

De J, Cooper VR, Dai S (2009) Porous graphene as the ultimate membrane for gas separation. Nano Lett 9(12):4019–4024. https://doi.org/10.1021/nl9021946

Dewettinck K, Le TT, Nguyen VB (2018) Membrane separations. In: Alternatives to conventional food processing, 2nd edn. Royal Society of Chemistry, London

Dickinson RE, Cicerone RJ (1986) Future global warning from atmospheric trace gases. Nature 319:109–115

Dihua W, Xuesong L, Sanchuan Y, Meihong L, Congjie G (2010) Modification of aromatic polyamide thin-film composite reverse osmosis membranes by surface coating of thermo-responsive copolymers P(NIPAM-co-Am). I: preparation and characterization. J Membr Sci 352:76–85. https://doi.org/10.1016/j.memsci.2010.01.061

Dong L-X, Yang H-W, Liu S-T, Wang X-M, Xie YF (2015) Fabrication and anti-biofouling properties of alumina and zeolite nanoparticle embedded ultrafiltration membranes. Desalination 365:70–78

Du H, Li J, Zhang J, Su G, Li X, Zhao Y (2011) Separation of hydrogen and nitrogen gases with porous graphene membrane. J Phys Chem C 115(47):23261–23266. https://doi.org/10.1021/jp206258u

Elaine Fung Y-L, Wang H (2013) Investigation of reinforcement of porous alumina by nickel aluminate spinel for its use as ceramic membrane. J Membr Sci 444:252–258. https://doi.org/10.1016/j.memsci.2013.05.025

El-Arnaouty MB, Abdel Ghaffar AM, Eid M, Aboulfotouh ME, Taher NH, Soliman E-S (2018) Nano-modification of polyamide thin film composite reverse osmosis membranes by radiation grafting. J Radiation Res Appl Sci:1–13. https://doi.org/10.1016/j.jrras.2018.01.005

Elia P, Nativ-Roth E, Zeiri Y, Porat Z (2016) Determination of the average pore-size and total porosity in porous silicon layers by image processing of SEM micrographs. Microporous Mesoporous Mater 225:465–471. https://doi.org/10.1016/j.micromeso.2016.01.007

Elimelech M, Phillip WA (2011) The future of seawater desalination: energy, technology, and the environment. Science 333(6043):712–717

Elnashaie SS, Danafar F, Rafsanjani HH (2015) Nanotechnology for chemical engineers. Springer, Singapore, p 104

Fadaei F, Hoshyargar V, Shirazian S, Ashrafizadeh AN (2012) Mass transfer simulation of ion separation by nanofiltration considering electrical and dielectrical effects. Desalination 284:316–323

Fard AK, McKay G, Buekenhoudt A, Al Sulaiti H, Motmans F, Khraisheh M, Atieh M (2018) Inorganic membranes: preparation and application for water treatment and desalination-review. Materials 11(74):1–47. https://doi.org/10.3390/ma11010074

Frank GK (2007) Industrial gas handbook: gas separation and purification. CRC Press, New York, pp 275–280

Gallucci F, Basile A, Hai FI (2011) Introduction-a review of membrane reactors. In: Membranes for membrane reactors: preparation, optimization and selection. Wiley, Chichester

Gellé A, Moores A (2017) Water splitting catalyzed by titanium dioxide decorated with plasmonic nanoparticles. Pure Appl Chem 89(12):1817–1827

Genne I, Kuypers S, Leysen R (1996) Effect of the addition of ZrO_2 to polysulfone based UF membranes. J Membr Sci 113:343–350

Ghaemi N (2016) A new approach to copper ion removal from water by polymeric nanocomposite membrane embedded with γ-alumina nanoparticles. Appl Surf Sci 364:221–228. https://doi.org/10.1016/j.apsusc.2015.12.109

Ghaemi N, Madaeni SS, Alizadeh A, Rajabi H, Daraei P (2011) Preparation, characterization and performance of polyethersulfone/organically modified montmorillonite nanocomposite membranes in removal of pesticides. J Membr Sci 382:135–147. https://doi.org/10.1016/j.memsci.2011.08.004

Goh PS, Ng BC, Lau WJ, Ismail AF (2014) Inorganic nanomaterials in polymeric ultrafiltration membranes for water treatment. Sep Purif Rev 44(3):216–249

Goosen MFA, Sablani SS, Al-Maskari SS, Al-Belushi RH, Wilf M (2002) Effect of feed temperature on permeate flux and mass transfer coefficient in spiral-wound reverse osmosis systems. Desalination 144:367–372. https://doi.org/10.1016/S0011-9164(02)00345-4

Gozálvez-Zafrilla JM, Santafé-Moros A (2008) Nanofiltration modeling based on the extended nernst-planck equation under different physical modes. In: Excerpt from the proceedings of the COMSOL conference 2008 Hannover, Germany

Gozálvez-Zafrilla JM, Gómez-Martínez B, Santafé-Moros A (2005) Evaluation of nanofiltration processes for brackish water treatment using the dspm model. In: European symposium on computer aided process engineering – 15

Griffin JW (Product Manager, Tetratec) (2018) High temperature filtration media in incineration. http://www.seas.columbia.edu/earth/wtert/sofos/nawtec/nawtec07/nawtec07-07.pdf. Accessed 7 Nov 2018

Gunawan P, Guan C, Song X, Zhang Q, Leong SSJ, Tang C, Chen Y, Chan-Park MB, Chang MW, Wang K, Xu R (2011) Hallow fiber membrane decorated with Ag/MWCNTs: toward effective water disinfection and biofouling control. ACS Nano 5(12):10033–10040

Hamzah N, Leo CP (2017) Membrane distillation of saline with phenolic compound using superhydrophobic PVDF membrane incorporated with TiO_2 nanoparticles: separation, fouling and self-cleaning evaluation. Desalination 418:79–88

Hasanuzzaman M, Rashid ARMH, Olabi AG (2017) Characterization of porous glass and ceramics by mercury intrusion porosimetry. Ref Mod Mater Sci Mater Eng. https://doi.org/10.1016/B978-0-12-803581-8.09266-3

He Y, Li G, Wang H, Zhao J, Su H, Huang Q (2008) Effect of operating conditions on separation performance of reactive dye solution with membrane process. J Membr Sci 321(2):183–189. https://doi.org/10.1016/j.memsci.2008.04.056

Herterich JG, Griffiths IM, Field RW, Vella D (2014) The effect of a concentration-dependent viscosity on particle transport in a channel flow with porous walls. AIChE J 60(5):1891–1904

Hidalgo AM, Leòn G, Gòmez M, Murcia MD, Barbosa DS, Blanco P (2013) Application of the solution-diffusion model for the removal of atrazine using a nanofiltration membrane. Desalin Water Treat 51(10–12):2244–2252. https://doi.org/10.1080/19443994.2012.734720

Hilal N, AI-Zoubi H, Darwish NA, Mohammad AW (2005) Characterisation of nanofiltration membranes using atomic force microscopy. Desalination 177:187–199. https://doi.org/10.1016/j.desal.2004.12.008
Hilal N, Ismail AF, Matsuura T, Oatley-Radcliffe D (2017) Membrane characterization, 1st edn. Elsevier, Amsterdam
Hinds BJ, Chopra N, Rantell T, Andrews R, Gavalas V, Bachas LG (2004) Aligned multiwalled carbon nanotube membranes. Science 303(5654):62–65
Ho WSW, Sirkar KK (1992) Membrane handbook, vol 1. Springer Science, New York
Hoang T, Stevens G, Kentish S (2010) The effect of feed pH on the performance of a reverse osmosis membrane. Desalination 261:99–103. https://doi.org/10.1016/j.desal.2010.05.024
Homayoonfal M, Mehrnia MR, Shariaty-Niassar M, Akbari A, Sarrafzadeh MH, Ismail AF (2015) Fabrication of magnetic nanocomposite membrane for separation of organic contaminant from water. Desalin Water Treat 54(13):3603–3609
Huang FL, Wang QQ, Wei QF, Gao WD, Shou HY, Jiang SD (2010) Dynamic wettability and contact angles of poly(vinylidene fluoride) nanofiber membranes grafted with acrylic acid. Express Polym Lett 4(9):551–558. https://doi.org/10.3144/expresspolymlett.2010.69
Hussain S, Amade R, Jover E, Bertran E (2012) Functionalization of carbon nanotubes by water plasma. Nanotechnology 23(38):385604
Ihsanullah (2019) Carbon nanotube membranes for water purification: Developments, challenges, and prospects for the future. Sep Purif Technol 209:307–337
Isawia H, El-Sayeda MH, Xianshe F, Hosam S, Abdel Mottaleb MS (2016) Surface nanostructuring of thin film composite membranes via grafting polymerization and incorporation of ZnO nanoparticles. Appl Surf Sci 385:268–281. https://doi.org/10.1016/j.apsusc.2016.05.141
Izadpanah AA, Javidnia A (2012) The ability of a nanofiltration membrane to remove hardness and ions from diluted seawater. Water 4:283–294
Jang JH, Lee J, Jung S-Y, Choi D-C, Won Y-J, Ahn KY, Park PY, Lee CH (2015) Correlation between particle deposition and the size ratio of particles to patterns in nano- and micro-patterned membrane filtration systems. Sep Purif Technol 156:608–616. https://doi.org/10.1016/j.seppur.2015.10.056
Jhaveri JH, Murthy ZVP (2016) A comprehensive review on anti-fouling nanocomposite membranes for pressure driven membrane separation processes. Desalination 379:137–154
Jian X, Dai Y, He G, Chen G (1999) Preparation of UF and NF poly (phthalazine ether sulfone ketone) membranes for high temperature application. J Membr Sci 161(1-2):185–191. https://doi.org/10.1016/S0376-7388(99)00112-X
Jiang CY, Rybak BM, Markutsya S, Kladitis PE, Tsukruk VV (2005) Self-recovery of stressed nanomembranes. Appl Phys Lett 86(12):121912–121913. https://doi.org/10.1063/1.1889239
Jiang C, Kommireddy DS, Tsukruk VV (2006) Gradient array of freely suspended nanomembranes. Adv Funct Mater 16:27–32. https://doi.org/10.1002/adfm.200500326
Johnson DJ, Al Malek SA, Al-Rashdi BAM, Hilal N (2012) Atomic force microscopy of nanofiltration membranes: effect of imaging mode and environment. J Membr Sci 389:486–498. https://doi.org/10.1016/j.memsci.2011.11.023
Johnson DJ, Oatley-Radcliffe DL, Hilal N (2018) State of the art review on membrane surface characterization: visualisation, verification and quantification of membrane properties. Desalination 434:12–36. https://doi.org/10.1016/j.desal.2017.03.023
Kadam VV, Wang L, Padhye R (2016) Electrospun nanofibre materials to filter air pollutants - a review. J Ind Text 47(8):2253–2280
Kanagalakshmi AS, Sharankumar A, Shenbagavalli E, Tamilpriya S, Durga P (2018) Nanotechnology in water purification. J Mech Civil Eng 15(1):47–52. https://doi.org/10.9790/1684-1501024752
Kanani DM, Fissell WH, Roy S, Dubnisheva A, Fleischman A, Zydney AL (2010) Permeability-selectivity analysis for ultrafiltration: effect of pore geometry. J Membr Sci 349:405–410. https://doi.org/10.1016/j.memsci.2009.12.003

Kang M, Jung R, Kim HS, Jin HJ (2008) Preparation of superhydrophobic polystyrene membranes by electrospinning. Colloid Surf A 313:411–414

Kar S, Bindal RC, Tewari PK (2012) Carbon nanotube membranes for desalination and water purification: challenges and opportunities. Nano Today 7(5):385–389. https://doi.org/10.1016/j.nantod.2012.09.002

Kegel FS, Rietman BM, Verliefde ARD (2010) Reverse osmosis followed by activated carbon filtration for efficient removal of organic micropollutants from river bank filtrate. Water Sci Technol 6(10):2603–2610. https://doi.org/10.2166/wst.2010.166

Kennes C, Rene ER, Veiga MC (2009) Bioprocesses for air pollution control. J Chem Technol Biotechnol 84(10):1419–1436. https://doi.org/10.1002/jctb.2216

Khulbe KC, Feng CY, Matsuura TS (2008) Synthetic polymeric membranes characterization by atomic force microscopy. Springer, Berlin, p 17

Khulbe CK, Feng CY, Matsuura T (2010) Membrane characterization. In: Desalination and water resources: membrane processes, vol II. Eolss Publishers/UNESCO, Oxford, p 140

Kim J, Van der Bruggen B (2010) The use of nanoparticles and nanotubes in polymeric and ceramic membrane structures: review of envisaged performance improvements for water treatment. Environ Pollut 158(7):2335–2349. https://doi.org/10.1016/j.envpol.2010.03.024

Kim ES, Liu Y, Gamal El-Din M (2013) An in-situ integrated system of carbon nanotubes nanocomposite membrane for oil sands process-affected water treatment. J Membr Sci 429:418–427

Kim KS, Moon DS, Kim HJ, Lee SW, Ji H, Jung HJ, Won HJ (2014) The effect of feed temperature on permeate flux during membrane separation. J Korean Soc Mar Environ Energy 17(1):13–19. https://doi.org/10.7846/JKOSMEE.2014.17.1.13

Kiso Y, Kon T, Kitao T, Nishimura K (2001) Rejection properties of alkyl phthalates with nanofiltration membranes. J Membr Sci 182(1-2):205–214

Konruang S, Chittrakarn T, Sirijarukul S (2014) Surface modification of asymmetric polysulfone membrane by UV irradiation. J Teknol 70:55–60. https://doi.org/10.11113/jt.v70.3435

Kotrappanavar NS, Hussain AA, Abashar MEE, Al-Mutaz IS, Aminabhavi TM, Nadagouda MN (2011) Prediction of physical properties of nanofiltration membranes for neutral and charged solutes. Desalination 3:174–181

Kowalik-Klimczak A, Zalewski M, Gierycz P (2016) Removal of Cr(III) ions from salt solution by nanofiltration: experimental and modelling analysis. Polish J Chem Technol 18(3):10–16. https://doi.org/10.1515/pjct-2016-0042

Kumar J, Bansal A (2013) Photocatalysis by nanoparticles of titanium dioxide for drinking water purification: a conceptual and state-of-art review. Mater Sci Forum 764:30–150

Kumar SR, Gopinath P (2016) Dual applications of silver nanoparticles incorporated functionalized MWCNTs grafted surface modified PAN nanofibrous membrane for water purification. RSC Adv 6:109241–109252

Labbez C, Fievet P, Szymczyk A, Vidonne A, Foissy A, Pagetti J (2002) Analysis of the salt retention of a titania membrane using the 'DSPM' model: effect of pH, salt concentration and nature. J Membr Sci 208(3):15–3290

Ladewig B, Al-Shaeli MNZ (2017) Fundamentals of membrane processes. In: Fundamentals of membrane bioreactors. Springer Nature Singapore, Singapore

Lanteri Y, Fievet P, Szymczyk A (2009) Evaluation of the steric, electric, and dielectric exclusion model on the basis of salt rejection rate and membrane potential measurements. J Colloid Interface Sci 331:148–155

Lee J-W, Yoo Y-T, Lee JY (2015) Characterization of nafion nanocomposites with spheric silica, layered silicate, and amphiphilic organic molecule and their actuator application. Macromol Res 23(2):167–176. https://doi.org/10.1007/s13233-015-3029-x

Levchenko I, Han Z-J, Kumar S, Yick S, Fang J, Ostrikov K (2013) Large arrays and networks of carbon nanotubes: morphology control by process parameters. In: Syntheses and applications of carbon nanotubes and their composites. Intech, Rijeka

Li NN, Fane AG, Winston WS, Matsuura T (2008) Advanced membrane technology and applications. John Wiley & Sons, Inc., Hoboken

Li L, Sokol N, Eigil JG, Etchells VM (2012) Nanoporous polymers for membrane applications. Department of Chemical Engineering, Technical University of Denmark, Kgs.Lyngby

Li L, Song C, Jiang D, Wang T (2017a) Preparation and enhanced gas separation performance of carbon/carbon nanotubes (C/CNTs) hybrid membranes. Sep Purif Technol 188:73–80

Li SH, Huang JY, Chen Z, Chen GQ, Lai YK (2017b) A review on special wettability textiles: theoretical models, fabrication technologies and multifunctional applications. J Mater Chem A 5:31–55

Lu GQ, Zhao XS (2004) Nanoporous materials - science and engineering. In: Nanoporous Materials-an Overview. World Scientific, Singapore

Luo J, Wan Y (2013) Effects of pH and salt on nanofiltration—a critical review. J Membr Sci 438:18–28

Ma N, Zhang Y, Quan X, Fan X, Zhao H (2010) Performing a microfiltration integrated with photocatalysis using an Ag-TiO_2/HAP/Al_2O_3 composite membrane for water treatment: Evaluating effectiveness for humic acid removal and anti-fouling properties. Water Res 44:6104–6114

Mago G, Kalyon DM, Fisher FT (2008) Membranes of polyvinylidene fluoride and PVDF nanocomposites with carbon nanotubes via immersion precipitation. J Nanomater:1–8. https://doi.org/10.1155/2008/759825

Mansoori GA, Bastami TR, Ahmadpour A, Eshaghi Z (2008) Environmental application of nanotechnology. Annual Rev Nano Res 2:439–493

Mansourpanah Y, Gheshlaghi A (2012) Effects of adding different ethanol amines during membrane preparation on the performance and morphology of nanoporous PES membranes. J Polym Res 19(13):1–7. https://doi.org/10.1007/s10965-012-0013-4

Marrufo-Hernández NA, Hernández-Guerrero M, Nápoles-Duarte JM, Palomares-Báez JP, Chávez-Rojo MA (2018) Prediction of the filtrate particle size distribution from the pore size distribution in membrane filtration: Numerical correlations from computer simulations. AIP Adv 8(035308):1–15. https://doi.org/10.1063/1.5009568

Maximous N, Nakhla G, Wan W, Wong K (2010) Performance of a novel ZrO_2/PES membrane for wastewater filtration. J Membr Sci 352(1–2):222–230

Mehta A, Zydney AL (2005) Permeability and selectivity analysis for ultrafiltration membranes. J Membr Sci 249:245–249. https://doi.org/10.1016/j.memsci.2004.09.040

Michael FL, Volder D, Tawfick SH, Baughman RH, Hart AJ (2013) Carbon nanotubes: present and future commercial applications. Science 339:535–539

MingJian L, XianBao W, Rong T, Li W, ShaoQing L, Qin L (2009) Carbon nanotubes periodically decorated by high density polyethylene crystalline using solution crystallization. Sci China Ser B-Chem 52(7):905–910

Mohamed EF (2017) Nanotechnology: future of environmental air pollution control. Environ Manage Sustainable Dev 6(2):439–454

Mohammed A, Pei L, Kadhum MA (2002) Characterization and identification of rejection mechanisms in nanofiltration membranes using extended Nernst-Plank model. Clean Technol Environ Policy 4:151–156

Mokhtari S, Rahimpour A, Shamsabadi AA, Habibzadeh S, Soroush M (2017) Enhancing performance and surface antifouling properties of polysulfone ultrafiltration membranes with salicylate-alumoxane nanoparticles. Appl Surf Sci 393:93–102. https://doi.org/10.1016/j.apsusc.2016.10.005

Moll DJ, Burmester AF, Young TC, McReynolds KB, Clark JE, Hotz CZ, Wessling RA, Quarderer GJ, Lacher RM (1997) Gas separations utilizing glassy polymer membranes at sub-ambient temperatures. European Patent number: EP 0 529 052 B1

Mondal S (2017) Carbon nanomaterials based membranes. J Membr Sci Technol 6(4):1–3

Mulder M (1994) The use of membrane processes in environ mental problems. An introduction. In: Crepso JG, Boddeker KW (eds) Membrane processes in separation and purification. Kluwer Academic Publishers, Dordrecht-Boston-London, pp 229–262

Muller RA, Muller EA (2017) Fugitive methane and the role of atmospheric half-life: an overview. Geoinfor Geostat 5(3):1–7. https://doi.org/10.4172/2327-4581.1000162

Mulyanti R, Susanto H (2018) Wastewater treatment by nanofiltration membranes. IOP Conf Ser Earth Environ Sci 142(012017):1–6. https://doi.org/10.1088/1755-1315/142/1/012017

Muralikrishnan R, Swarnalakshmi M, Nakkeeran E (2014) Nanoparticle-membrane filtration of vehicular exhaust to reduce air pollution - a review. Int Res J Environ Sci 3(4):82–86

Najari S, Omidkhah M, Hosseini SS (2015) An investigation on the factors affecting the properties and performance of polymeric nanocomposite membranes for olefin/paraffin Separation. In: 5th International biennial conference on ultrafine grained and nanostructured materials, UFGNSM15, 11–12th Nov 2015, Iran, pp 1–6

Nasab SS, Zahmatkesh S (2017) Preparation, structural characterization, and gas separation properties of functionalized zinc oxide particle filled poly(ether-amide) nanocomposite films. J Plast Film Sheet 33(1):92–113

Nguyen QH, Ali M, Nasir S, Ensinger W (2015) Transport properties of track-etched membranes having variable effective pore-lengths. Nanotechnology 26(48):485502

Omar L, Liu C, Chong TH, Lienhard JHV (2017) Fundamentals of low-pressure nanofiltration: membrane characterization, modeling, and understanding the multi-ionic interactions in water softening. J Membr Sci 521:18–32

Pandey N, Shukla SK, Singh NB (2017) Water purification by polymer nanocomposites: an overview. J Nanocompos 3(2):47–66

Patterson DA, Havill A, Costello S, See-Toh YH, Livingston AG, Turner A (2009) Membrane characterisation by SEM, TEM and ESEM: the implications of dry and wetted microstructure on mass transfer through integrally skinned polyimide nanofiltration membranes. Sep Purif Technol 66:90–97. https://doi.org/10.1016/j.seppur.2008.11.022

Paul M, Jons SD (2016) Chemistry and fabrication of polymeric nanofiltration membranes: a review. Polymer 103:417–456

Paz Y (2010) Application of TiO_2 photocatalysis for air treatment: patents' overview. Appl Catal B Environ 99:448–460

Pendergast MM, Hoek EMV (2011) A review of water treatment membrane nanotechnologies. Energy Environ Sci 4:1946–1971. https://doi.org/10.1039/c0ee00541j

Pourzamani H, Bina B, Amin MM, Rashidi A (2012) Monoaromatic pollutant removal by carbon nanotubes from aqueous solution. Adv Mater Res 488–489:934–939

Prabhudessai V, Ganguly A, Mutnuri A (2013) Biochemical methane potential of agro wastes. J Energy 2013:1–7

Prádanos P, Rodríguez-Méndez ML, Calvo JI, Hernández A, Tejerina F, De Saja JA (1996) Structural characterization of an UF membrane by gas adsorption-desorption and AFM measurements. J Membr Sci 117(1):291–302

Qin J-J, Oo MH, Kekre KA (2007) Nanofiltration for recovering wastewater from a specific dyeing facility. Sep Purif Technol 56(2):199–203

Rajabi H, Ghaemi N, Madaeni SS, Daraei P, Astinchap B, Zinadini S, Razavizadeh SH (2015) Nano-ZnO embedded mixed matrix polyethersulfone (PES) membrane: Influence of nanofiller shape on characterization and fouling resistance. Appl Surf Sci 349:66–77. https://doi.org/10.1016/j.apsusc.2015.04.214.

Rautenbach R, Welsch K (1993) Treatment of landfill gas by gas permeation - pilot plant results and comparison to alternatives. Desalination 90(1-3):193–207. https://doi.org/10.1016/0011-9164(93)80176-N

Raval HD, Gohil JM (2009) Carbon nanotube membrane for water desalination. Int J Nuclear Desalin 3(4):360–368

Ray JR, Wong W, Jun YS (2017) Antiscaling efficacy of $CaCO_3$ and $CaSO_4$ on polyethylene glycol (PEG)-modified reverse osmosis membranes in the presence of humic acid: interplay of membrane surface properties and water chemistry. Phys Chem Chem Phys 19(7):5647–5657

Razmkhah M, Ahmadpour A, Mosavian ATH, Moosavi F (2017) What is the effect of carbon nanotube shape on desalination process? a simulation approach. Desalination 407:103–115

Rezaei Hosseinabadi S, Wyns K, Meynen V, Carleer R, Adriaensens P, Buekenhoudt A, Van der Bruggen B (2014) Organic solvent nanofiltration with Grignard functionalised ceramic nanofiltration membranes. J Membr Sci 454:496–504. https://doi.org/10.1016/j.memsci.2013.12.032

Richards HL, Baker PGL, Iwuoha E (2012) Metal nanoparticle modified polysulfone membranes for use in wastewater treatment: a critical review. J Surf Eng Mater Adv Technol 2:183–193

Roco MC, Williams S, Alivisatos P (2000) IWGN workshop report. Nanotechnology research directions: Vision for nanotechnology in the next decade. Kluwer Academic Publishers, Dordrecht

Rowe BW, Robeson LM, Freeman BD, Paul DR (2010) Influence of temperature on the upper bound: theoretical considerations and comparison with experimental results. J Membr Sci 360:58–69. https://doi.org/10.1016/j.memsci.2010.04.047

Roy S, Singha NR (2017) Polymeric nanocomposite membranes for next generation pervaporation process: strategies, challenges and future prospects. Membranes (Basel) 7(53):1–64

Roy Y, Sharqawy MH, John H, Lienhard V (2015) Modeling of flat-sheet and spiral-wound nanofiltration configurations and its application in seawater nanofiltration. J Membr Sci 493:360–372

Saleh TA, Gupta VK (2012) Synthesis and characterization of alumina nano-particles polyamide membrane with enhanced flux rejection performance. Sep Purif Technol 89:245–251

Schaep J, Van der Bruggen B, Uytterhoeven S, Croux R, Vandecasteele C, Wilms D, Van Houtte E, Vanlerberghe F (1998) Removal of hardness from groundwater by nanofiltration. Desalination 119(1–3):295–302. https://doi.org/10.1016/S0011-9164(98)00172-6

Schaep J, Vandecasteele C, Mohammad AW, Bowen WR (1999) Analysis of salt retention of nanofiltration membranes using the Donnan-Steric Partitioning Pore Model. Sep Sci Technol 34 (15):3009–3030

Schaep J, Vandecasteele C, Mohammad AW, Bowen WR (2001) Modelling the retention of ionic components for different nanofiltration membranes. Sep Purif Technol 22-23(1-3):169–179

Scholten E, Bromberg L, Rutledge GC, Hatton TA (2011) Electrospun polyurethane fibers for absorption of volatile organic compounds from air. ACS Appl Mater Interface 3 (10):3902–3909. https://doi.org/10.1021/am200748y

Sekulić J, Luiten MWJ, ten Elshof JE, Benes NE, Keizer K (2002) Microporous silica and doped silica membrane for alcohol dehydration by pervaporation. Desalination 148(1–3):19–23

Senapati S, Chandra A (2001) Dielectric constant of water confined in a nanocavity. J Phys Chem B 105:5106–5109

Shaaban AMF, Hafez AI, Abdel-Fatah MA, Abdel-Monem NM, Mahmoud MH (2016) Process engineering optimization of nanofiltration unit for the treatment of textile plant effluent in view of solution diffusion model. Egypt J Pet 25:79–90. https://doi.org/10.1016/j.ejpe.2015.03.018

Shahabadi SMS, Brant JA (2019) Bio-inspired superhydrophobic and superoleophilic nanofibrous membranes for non-aqueous solvent and oil separation from water. Sep Purif Technol 210:587–599

Shahtalebi A, Sarrafzadeh MH, Montazer Rahmati MM (2011) Application of nanofiltration membrane in the separation of amoxicillin from pharmaceutical wastewater. Iran J Environ Health Sci Eng 8(2):109–116

Sharma RR, Agrawal R, Chellam S (2003) Temperature effects on sieving characteristics of thin-film composite nanofiltration membranes: pore size distributions and transport parameters. J Membr Sci 223:69–87. https://doi.org/10.1016/S0376-7388(03)00310-7

Shon HK, Phuntsho S, Chaudhary DS, Vigneswaran S, Cho J (2013) Nanofiltration for water and wastewater treatment – a mini review. Drink Water Eng Sci 6:47–53

Silva V (2015) Dielectric excusion model in membranes. In: Drioli E, Giorno L (eds) Encyclopedia of membranes. Springer, Berlin, Heidelberg

Silva LLS, Moreira CG, Curzio BA, da Fonseca FV (2017) Micropollutant removal from water by membrane and advanced oxidation processes-a review. J Water Resourc Protect 9:411–431

Song C, Kwon T, Han J-E, Shandell M, Strano MS (2009) Controllable synthesis of single-walled carbon nanotube framework membranes and capsules. Nano Lett 9(12):4279–4284

Sourirajan S (1970) Reverse osmosis. Academic Press, New York

Sourirajan S (1978) The science of reverse osmosis – mechanisms, membranes, transport and applications. Pure Appl Chem 50:593–615

Strathmann H (2011) Introduction to membrane science and technology. Wiley-VCH, Weinheim

Sun CZ, Wen B, Bai BF (2015) Recent advances in nanoporous graphene membrane for gas separation and water purification. Sci Bull 60:1807–1823

Susanto H (2011) Teknologi Membran. Badan Penerbit Universitas Diponegoro, Semarang

Szymczyk A, Fievet P (2005) Investigating transport properties of nanofiltration membranes by means of a steric, electric and dielectric exclusion model. J Membr Sci 252:77–88. https://doi.org/10.1016/j.memsci.2004.12.002

Tanninen J, Nystrom M (2002) Separation of ions in acidic conditions using NF. Desalination 147:295–299. https://doi.org/10.1016/S0011-9164(02)00555-6

Tasis D, Tagmatarchis N, Bianco A, Prato M (2006) Chemistry of carbon nanotubes. Chem Rev 106(3):1105–1136. https://doi.org/10.1021/cr050569o

Tayefeh A, Mousavi SA, Wiesner M, Poursalehi R (2015) Synthesis and surface characterization of magnetite-titania nanoparticles/polyamide nanocomposite smart RO membrane. 5th International Biennial Conference on Ultrafine Grained and Nanostructured Materials, UFGNSM15. Proc Mater Sci 11:342–346

Thuyavan YL, Anantharaman N, Arthanareeswaran G (2014) Adsorptive removal of humic acid by zirconia embedded in poly (ether sulfone) membrane. Ind Eng Chem Res 53(28):11355–11364. https://doi.org/10.1021/ie5015712

Thwala JM, Minghua L, Wong MSY, Kang S, Hoek EMV, Mamba BB (2013) Bacteria-polymeric membrane interactions: atomic force microscopy and XDLVO predictions. Langmuir 29 (45):13773–13782. https://doi.org/10.1021/la402749y

Tsuru T, Nakao SI, Kimura S (1991) Calculation of ion rejection by extended Nernst-Planck equation with charged reverse osmosis membranes for single and mixed electrolyte solutions. J Chem Eng Jpn 24:511–517

Tylkowski B, Tsibranska T (2015) Overview of main techniques used for membrane characterization. J Chem Technol Metal 50(1):3–12

Ursino C, Castro-Muñoz R, Drioli E, Gzara L, Albeirutty MH, Figoli A (2018) Progress of nanocomposite membranes for water treatment: review. Membranes (Basel) 8(18):1–40

Valadez-Blanco R, Livingston AG (2009) Solute molecular transport through polyimide asymmetric organic solvent nanofiltration (OSN) membranes and the effect of membrane-formation parameters on mass transfer. J Membr Sci 326(2):332–342

Van Rijn CJM (2004) Nano and macro engineered membrane technology, Membrane science and technology series 10. Elsevier, Amsterdam, p 4

Vandezande P, Gevers LEM, Vankelecom IFJ (2008) Solvent resistance nanofiltration: separating on a molecular level. Chem Soc Rev 37:365–405. https://doi.org/10.1039/B610848M

Verdejo R, Bernal MM, Romasanta LJ, Tapiador FJ, Lopez-Manchado MA (2011) Reactive nanocomposite foams. Cellular Polym 30(2):45–61

Vezzani D, Bandini S (2002) Donnan equilibrium and dielectric exclusion for characterization of nanofiltration membranes. Desalination 149:477483

Wang G, Chen S, Yu H, Quan X (2015) Integration of membrane filtration and photoelectrocatalysis using a TiO_2/carbon/Al_2O_3 membrane for enhanced water treatment. J Hazard Mater s 299:27–34

Wang Y, Wang X, Li M, Dong J, Sun C, Chen G (2018) Removal of pharmaceutical and personal care products (PPCPs) from municipal waste water with integrated membrane systems, MBR-RO/NF. Int J Environ Res Public Health 15(269):1–12

WARWICK (2018) warwick.ac.uk/fac/sci/physics/current/postgraduate/regs/mpagswarwick/ex5/techniques/structural/tem/. Assessed 23 Aug 2018

Wijmans JG, Baker RW (1995) The solution-diffusion model: a review. J Membr Sci 107:1–21. https://doi.org/10.1016/0376-7388(95)00102-I

World Health Organization (2011) Safe drinking water from desalination. WHO/HSE/WSH/11.03. http://www.who.int/water_sanitation_health/publications/2011/desalination_guidance_en.pdf. Assessed 21 Oct 2018

Xu Q, Xu H, Chen J, Lv Y, Dong C, Sreeprasad TS (2015) Graphene and graphene oxide: Advanced membranes for gas separation and water purification. Inorg Chem Front 2:417–424

Xu YY, Wei XL, Liang S, Sun YL, Chao ZS (2018) Synthesis of a ZSM-5/NaA hybrid zeolite membrane using kaolin as a modification layer. New J Chem 42:6664–6672

Yamada T, Namai T, Hata K, Futaba DN, Mizuno K, Fan J, Yudasaka M, Yumura M, Iijima S (2006) Size-selective growth of double-walled carbon nanotube forests from engineered iron catalysts. Nat Nanotechnol 1:131–136

Yaroshchuk AE (2000) Dielectric exclusion of ions from membranes. Adv Colloid Interface Sci 85:193–230

Yoon S-H (2016) Membrane bioreactor processes: principles and applications, Advances in water and wastewater transport and treatment, 1st edn. CRC Press, Taylor and Francis, London

Yoon Y, Westerhoff P, Snyder SA, Wert EC (2006) Nanofiltration and ultrafiltration of endocrine disrupting compounds, pharmaceuticals and personal care products. J Membr Sci 270 (1–2):88–100

Younssi SA, Breida M, Achiou B (2018) Alumina membranes for desalination and water treatment. Intech, Rijeka

Zahid M, Rashid A, Akram S, Rehan ZA, Razzaq W (2018) A comprehensive review on polymeric nano-composite membranes for water treatment. J Membr Sci Technol 8(1):1–20. https://doi.org/10.4172/2155-9589.1000179

Zahri K, Goh PS, Ismail AF (2016) The incorporation of graphene oxide into polysulfone mixed matrix membrane for CO_2/CH_4 separation. Earth Environ Sci 36:012007

Zhang Y, Liu P (2015) Polysulfone(PSF) composite membrane with micro-reaction locations (MRLs) made by doping sulfated TiO_2 deposited on SiO_2 nanotubes (STSNs) for cleaning wastewater. J Membr Sci 493:275–284

Zhang Y, Shan X, Jin Z, Wang Y (2011) Synthesis of sulfated Y-doped zirconia particles and effect on properties of polysulfone membranes for treatment of wastewater containing oil. J Hazard Mater 192(2):559–567

Zhang Y, Liu F, Lu Y, Zhao L, Song L (2013) Investigation of phosphorylated TiO_2-SiO_2 particles/polysulfone composite membrane for wastewater treatment. Desalination 324:118–126

Zhang Q, Chen S, Fan X, Zhang H, Yu H, Quan X (2018) A multifunctional graphene-based nanofiltration membrane under photo assistance for enhanced water treatment based on layer-by-layer sieving. Appl Catal B Environ 224:204–213

Zhao Y, Tan Y, Wong FS, Fane A, Xu N (2006) Formation of $Mg(OH)_2$ dynamic membranes for oily water separation: Effects of operating conditions. Desalination 191:344–350

Chapter 9
Membrane Technologies for Sustainable and Eco-Friendly Microbial Energy Production

Haixing Chang, Nianbing Zhong, Xuejun Quan, Xueqiang Qi, Ting Zhang, Rui Hu, Yahui Sun, and Chengyang Wang

Contents

Abstract Environmental deterioration and energy crisis caused by ever-increasing exploitation of traditional fossil fuels are urgent problems that need to be addressed. Microbial energy conversion technologies have attracted wide attentions since they can convert chemical energy contained in wastes, like solid wastes and wastewater, into biofuels or bioelectricity, realizing environmental remediation and energy

H. Chang · X. Quan (✉) · X. Qi · R. Hu · C. Wang
School of Chemistry and Chemical Engineering, Chongqing University of Technology, Chongqing, China
e-mail: hengjunq@cqut.edu.cn

N. Zhong (✉)
Chongqing Key Laboratory of Fiber Optic Sensor and Photodetector, Chongqing Key Laboratory of Modern Photoelectric Detection Technology and Instrument, Chongqing University of Technology, Chongqing, China

T. Zhang
School of Intellectual Property, Chongqing University of Technology, Chongqing, China

Y. Sun
School of Energy and Mechanical Engineering, Nanjing Normal University, Nanjing, China

Z. Zhang et al. (eds.), *Membranes for Environmental Applications*, Environmental Chemistry for a Sustainable World 42, https://doi.org/10.1007/978-3-030-33978-4_9

production at the same time. But the conventional methods have many limitations, like low mass transfer rate, uneven energy distribution, and strong product or by-product inhibition. The introduction of membranes in the reaction system can effectively relieve these technical bottlenecks by regulating the transfer and distribution properties of mass, heat, and energy, which play important roles on bioenergy productivity and quality.

We review (1) membrane application on liquid biofuels production, mainly on biomass cultivation and harvesting, liquid biofuels generation, and liquid products refining; (2) membrane application on gaseous biofuels production, mainly on photo-dependent biohydrogen production, dark-fermentative biohydrogen production, and gaseous products purification; (3) membrane application on microbial fuel cell; (4) membrane biofouling; and (5) antibiofouling technologies. The membranes mainly act as physical barrier, internal bridge, inhibitors separator, or products extractor in microbial energy production processes, which varies according to the detailed occasions. In overall, the membrane can effectively enhance microbial energy productivity and quality. But biofouling is the vital problem for all cases. Further researches and development on antifouling of membranes are still necessary.

Keywords Microbial biofuels · Membrane · Bioethanol · Biolipids · Microbial fuel cell · Biohydrogen · Bioreactor · Biofouling · Fermentation · Recovery

9.1 Introduction

Currently, traditional fossil fuels like coal, natural gas, and petroleum are still predominant fuel types for human beings. But limited reservoir, depleting supply, and random consumption hinder the dependency on traditional fossil fuels as major energy sources (Chang et al. 2018). In addition, vast utilization of fossil fuels has caused many problems, such as global warming, energy crisis, and environmental destruction (Fu et al. 2018; Guo et al. 2018; Tian et al. 2010). There are pressing needs to develop renewable and environmental-friendly energy sources which are derived from non-fossil sources in ways that can be replenished (Chang et al. 2018). Renewable energy mainly includes solar, wind, hydro, geothermal, and biofuels. Among these different renewable energy types, the biofuels produced via microbial energy conversion are considered as one of the most promising energy types due to its high energy conversion efficiency, mild operating conditions, and environmental remediation ability (Chang et al. 2016a; Li et al. 2017; Liao et al. 2014; Lu et al. 2018).

A variety of materials can be used as feedstocks for biofuels production, and based on that, the biofuels production can be mainly classified into first-, second-, and third-generation biofuels (Nigam and Singh 2011), as shown in Table 9.1. The first-generation biofuels are mainly generated from oil crops or starch-based food

Table 9.1 Various generations of biofuel (Correa et al. 2017; Leong et al. 2018; Nigam and Singh 2011; Kumari and Singh 2018)

Biofuels generations	Feedstocks	Advantages and disadvantages
The first generation	Soybean, sunflower, sugarcane, corn, etc.	Advantages:
		Simple pretreatment process, pure products, and high conversion rate of feedstocks
		Disadvantages:
		Food and freshwater competition with human beings, low economic efficiency
The second generation	Agricultural and forestry residues, like wheat and maize crops, sawdust, and sugarcane bagasse	Advantages:
		Abundant feedstocks, without competition with human beings for arable land, waste utilization
		Disadvantages:
		Sophisticated pretreatment process, low conversion rate, high energy cost, impure products
The third generation	Biofuels or electricity generation with microorganisms, like microalgae and microbes	Advantages:
		High conversion rate, less by-products, high products quality
		Disadvantages:
		High economy investment

crops. For example, the oleaginous crops including soybean and sunflower can be used as feedstocks for biolipid extraction through transesterification, and the starch-containing grains like corn, sorghum, and sugarcane are used as substrates for bioethanol and biohydrogen production through fermentation for the first-generation biofuels. The advantages of the first-generation biofuels are relatively simple pretreatment technologies since the starch and fats contained in food crops have simpler structure which are easier to be decomposed than lignocellulose. But the competition of arable land and freshwater for biofuels production with human beings' food demand strongly restricted its application (Correa et al. 2017). The second-generation biofuel fulfills the impractical gap of the first-generation biofuel due to its utilization of nonedible substrates from forestry and agricultural lignocellulose, like wheat and maize crops, sawdust, and sugarcane bagasse (Tian et al. 2009). Through hydrolysis and fermentation of this lignocellulosic biomass, biofuels like bioethanol and biohydrogen are produced in forms which can be utilized as energy sources. However, due to the tightly connected structure of lignin–cellulose association and crystalline structure of cellulose which resist enzymatic hydrolysis, sophisticated processes are necessary to achieve potential biofuels outcome, greatly increasing the energy cost of the second-generation biofuels (Kumari and Singh 2018; Raman et al. 2015). The third-generation biofuels which are derived from microorganisms, like microalgae and microbes, are considered as promising alternative energy sources since they can avoid the major disadvantages of food competition for the first-generation biofuels and non-degradability for the second-generation liquid biofuels (Zhu et al. 2018). Many microorganism species have abilities to accumulate fatty acids in the cells, like microalgae, yeast, and fungi (Leong et al. 2018; Liao et al. 2014; Mathimani and Pugazhendhi 2019). The intracellular fatty acids can be used as substrates for biodiesel production through downstream processing of the microbial biomass.

Biofuels production mainly experiences three steps: feedstocks pretreatment, biofuels generation, and biofuels refining. Until now, the biofuels productivity and quality are still poor attributing to many technical limitations despite the feedstock materials. The limitations are mainly confined to low pretreatment efficiency of the feedstock, poor biomass to biofuels conversion efficiency, and hardness on products separation and purification (Rodionova et al. 2017). Environmental conditions like temperature, humidity, and pH; operating parameters like material proportion, retention time, and inoculum density; and some other intrinsic properties like material composition, yeast activity, and bioreactor structure have important roles on biofuels productivity and quality (Srivastava et al. 2018; Liao et al. 2015; Pei et al. 2017).

During biofuels production processes, transfer characteristic of mass, heat, and energy determines its distribution in the system, which ultimately affects direction and rate of the chemical reactions, like lignocellulose hydrolysis to produce sugars and sugar fermentation to produce bioethanol or biohydrogen. Therefore, regulations on mass, heat, and energy transfer and distribution can greatly improve effectiveness of biomass to biofuels conversion. But conventional methods paid few attentions on transfer regulation attributing to rough system structure, resulting in low biofuels productivity and poor quality. The introduction of membrane modules in microbial energy conversion system can significantly reduce the technological limitations by acting as physical barrier, internal bridge, inhibitors separator, or products extractor. The functions of membrane vary with its utilizing occasions. Major applications of membranes on microbial energy production processes, i.e., liquid biofuels, gaseous biofuels, and microbial fuel cell, are illustrated in Fig. 9.1 and discussed in the following parts in detail.

9.2 Membrane Application on Liquid Biofuels Production

Liquid biofuels, like biolipids and bioethanol, are favored types of biofuels since they can blend with petroleum for combustion, realizing partly replacement of fossil energy by eco-friendly ways without sacrificing power output. In particular, the bioethanol has gained wide attentions since it satisfies the necessities of clean technology, like sustainability, biodegradability, abundant substrate, and reduction in greenhouse gas emissions, and is suitable to be used in most diesel engines with little or no modification (Enagi et al. 2018). In many countries, vehicles using bioethanol and gasoline mixture for transportation have been successfully realized, reducing greenhouse gas emissions to a large extent ranging from 20% to 85% (Wei

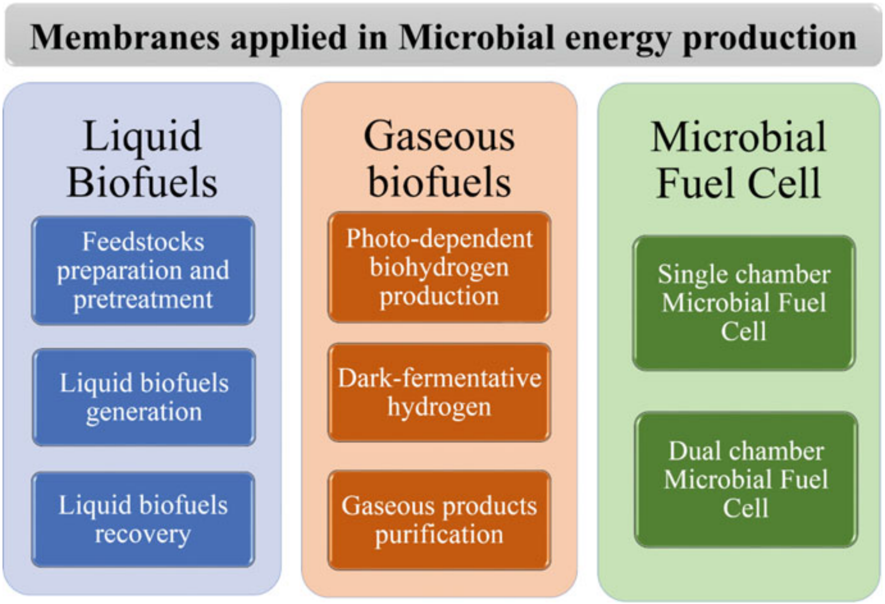

Fig. 9.1 Major application of membranes on microbial energy production processes

et al. 2014). Therefore, developing liquid biofuel technologies are promising approaches for environmental and energy sustainability in the present.

The process of liquid biofuels production mainly includes feedstocks preparation like microalgae cultivation and harvesting, liquid biofuels generation like fermentation and the related processes, and products refining like bioethanol and biodiesel recovery (Carrillo-Nieves et al. 2019). Among these steps, membrane can play an important role on enhancement of liquid biofuels productivity over the traditional technologies. Major applications of membranes in liquid biofuels production process and its advantages are shown in Table. 9.2.

9.2.1 Membranes Used for Microalgae Cultivation and Harvesting

Abundant biodegradable feedstocks are prerequisites for economically feasible liquid biofuels production. Among different materials like corn, sugarcane, lignocellulosic biomass, and microorganisms, microalgae biomass is a promising type attributing to its intrinsic merits (Chang et al. 2018). Microalgae can be cultivated on nonarable lands using CO_2 as carbon source, wastewater as nutrients source, and solar light as energy source to produce intracellular fatty acids and carbohydrates at a photosynthetic efficiency over tenfold than terrestrial plants, realizing energy production, carbon mitigation, and wastewater remediation at the same time

Table 9.2 Major application of membranes in liquid biofuels production process and its advantages

Process	Examples	Advantages
Feedstocks preparation and pretreatment	Microalgae biomass cultivation and harvesting	For carbon supply: higher CO_2 transfer rate with membrane module, like hollow fiber membrane For nutrients supply: effective separation of microalgae with inhibitors in wastewater, like ion-exchange membrane For biomass harvesting: cost-effective microalgae biomass harvesting, like microfiltration or ultrafiltration membrane
Liquid biofuels generation	Fermentation for liquid biofuels generation (bioethanol, biolipids, etc.)	For enzyme recovery: enzyme recovery without damaged enzymatic activity, like microfiltration or ultrafiltration membrane For sugar concentration and inhibitor removal: simultaneously realize sugar concentration and inhibitors removal with low energy cost, like ultrafiltration, nanofiltration, reverse osmosis, and membrane distillation
Liquid biofuels recovery	Liquid products concentrating for downstream processing or utilization	Membrane distillation or pervaporation: low energy cost, pure products, and mild operating conditions, like the porous membrane for distillation and nonporous membrane for pervaporation Hybrid membrane process: realize more functions at the same time, like distillation–pervaporation system

(Georgianna and Mayfield 2012; Guo et al. 2018). It was reported that the lipid content of many microalgae species are over 50 times of the terrestrial oil crops (Chisti 2007). However, there are still many drawbacks that need to be addressed for the traditional approaches of microalgae biomass production, like poor light penetration, low carbon transfer rate, and inappropriate nutrients feeding, and from these aspects, membranes are useful to enhance the performance of the microalgae cultivation system (Chang et al. 2017; Fu et al. 2016).

Carbon is an important element for microalgae biomass, accounting for more than 50% of the microalgal dry cell weight (Chang et al. 2016b). However, the CO_2 transfer rate was usually very low, resulting in low carbon availability in microalgae culture and thus limiting microalgae growth and carbon fixation. To enhance CO_2 transfer efficiency in microalgae cultivation system, hollow fiber membrane (Mortezaeikia et al. 2016), selective CO_2 transfer membrane (Rahaman et al. 2011), and integrated alkali-absorbent membrane system (Ibrahim et al. 2018; Li et al. 2018b, 2018c; Zheng et al. 2016) were successfully adopted in their works. Results demonstrated that the carbon availability in microalgae suspensions was effectively improved and microalgae biomass was enhanced to some extents.

Besides carbon source, light and nutrients are also key factors influencing microalgal biomass concentration (Liao et al. 2018; Sun et al. 2016a, 2018). To exploit inorganic salts in wastewater as nutrients for microalgae cultivation, Chang et al. (2016a) designed an annular photobioreactor based on ion-exchange membranes for selectively transferring cations and anions from wastewater chamber to microalgae cultivation chamber but preventing transport of suspended solids in wastewater, ensuring high light penetration and proper nutrients availability in microalgae culture. The biomass concentration was increased to 4.24, 3.15, and 2.04 g/L in the membrane photobioreactor from 2.34, 2.15, and 0 g/L in the membraneless photobioreactor when using simulated agricultural, municipal, and industrial wastewater as nutrients source. Besides, a scalable membrane-based tubular photobioreactor was used in microalgae biomass and biofuels production, which effectively enhanced economic and technical feasibility of microalgae cultivation with membrane photobioreactor (Chang et al. 2019).

In addition to microalgae biomass cultivation, membrane is also used in microalgae harvesting for downstream fermentation or fatty acids extraction. As is known, microalgae suspension contains more than 99% of water in weight ratio. Recovery of biomass from microalgae suspension was estimated to contribute 20%–30% of total energy cost for biomass production (Huang et al. 2019; Wei et al. 2018). In contrast, membrane filtration with microfiltration or ultrafiltration membrane is known as an energy saving method for microalgae biomass harvesting than other methods like centrifugation or drying, since energy cost on transmembrane pressure for membrane filtration is much lower than conventional methods. But the membrane fouling is an inescapable problem for microalgae harvesting with membrane filtration. To cope with the fouling problem of filtering membrane, many approaches were proposed, like nanofiber membrane (Bilad et al. 2018), rotational-dynamic filtration membrane (Hapońska et al. 2018), axial vibration membrane (Zhao et al. 2016), and composite membrane (Khairuddin et al. 2019). However, the antifouling performance of the existing technologies is limited, which is not capable of greatly reducing the energy cost. Further researches on membrane fouling control are still necessary.

9.2.2 Membranes Used for Fermentation

Saccharification and fermentation are important steps for biomass conversion to liquid biofuels, directly determining biofuels productivity and quality. During these processes, membranes play important roles on enzyme recovery from hydrolysis solution, sugar enrichment, and detoxification of the fermentation broth.

Before fermentation, the macromolecular organic matters in the biomass should be firstly hydrolyzed into simple sugars by enzyme for fermentation. In detail, the hexose sugar monomer contained in cellulose and the pentose sugar monomer contained in hemicellulose should be released and hydrolyzed into simple sugars like glucose, and the complex lipids- and proteins-containing organic matters in microalgae biomass should be hydrolyzed into simple structures like long-chain fatty acids, glycerol, and amino acids (Kang et al. 2018). Then, the simple organics can be utilized by microorganisms for fermentation to produce liquid biofuels like bioethanol. Compared with chemical process for hydrolysis of cellulose like dilute acid catalyzed, enzymatic hydrolysis of cellulose has many advantages, including mild operation conditions, low energy cost, and low inhibitors formation (Li et al. 2019). But the cost on enzyme utilization is very high, accounting to almost half of the total cost on hydrolysis process (Wooley et al. 1999).

Recovery and reuse of the hydrolysis enzyme can effectively reduce energy cost on enzymatic hydrolysis process. Membrane-based technology, using various membranes like microfiltration and ultrafiltration membrane as physical barrier, is regarded as a promising approach for enzyme recovery from hydrolysis solution since it can retain the catalytic activity of the enzyme, ensuring high efficiency and low cost of biomass conversion to fermentative sugars (Saha et al. 2017). Membranes used for enzyme recovery are mainly divided into microfiltration and ultrafiltration membranes according to the pore size. Microfiltration membranes are usually made of cellulose acetate, nylon, or polysulfone, which can efficiently remove most of the remaining biomass in hydrolysis solution (Singh and Purkait 2019). And the ultrafiltration membranes which are made of polyethersulfone or polysulfone are frequently used in enzyme separation and extraction from the hydrolysis solution (Enevoldsen et al. 2007).

The fermentative sugar concentration in hydrolysate is usually low mainly due to low hydrolysis efficiency, limiting bioethanol production. In addition, many inhibitors for bioethanol fermentation are produced along with the hydrolysis process, which also plays negative effects on bioethanol output (Nguyen et al. 2018). Therefore, sugar enrichment and inhibitors removal of the hydrolysate are important steps to improve bioethanol productivity and reduce cost on downstream processing. Some conventional methods for sugar concentration and inhibitors removal include physical adsorption, thermal evaporation, solvent extraction, and ion exchange (Sambusiti et al. 2016; Tanaka et al. 2019; Zhang et al. 2018a). But these methods are energy intensive and cannot simultaneously realize sugar concentration and inhibitors removal. The application of membrane process can greatly reduce the energy cost and deal with the technological problems, like incompatible operation of sugar concentration and inhibitors removal. Nowadays, the commonly used membrane technologies for sugar concentration and inhibitors removal are ultrafiltration, nanofiltration, reverse osmosis, and membrane distillation. The characteristics of different membrane technologies have been reviewed by previous authors (Wei et al. 2014; Zabed et al. 2017). Although membrane technologies have many advantages for fermentation process, membrane fouling is still a troublesome problem which limits economic feasibility. Works to conquer the problem of membrane fouling is vital to reduce cost of hydrolysate pretreatment.

9.2.3 Membranes Used for Liquid Biofuels Recovery

The final liquid biofuels concentration is influenced by many factors, such as feedstock compositions, fermentative sugar concentration in hydrolysate, activity of the fermentative yeast, and operating parameters like pH and temperature. Taking bioethanol as an example, the final bioethanol concentration in a fermenter is usually low when using lignocellulose as feedstocks than that with food as feedstocks (Ferreira et al. 2018). In general, the bioethanol concentration is lower than 5% (in w/w) when using cellulose as feedstocks, meaning that the produced bioethanol must be firstly concentrated to a higher concentration for downstream processing. Besides, the products are usually inhibitive to yeast cells for continuous production. Therefore, separation and recovery of the bioethanol from a fermenter are significant for economical production of bioethanol at continuous mode. Among different biofuels recovery processes, membrane-assisted bioethanol recovery has particularly advantages of low energy requirement, pure products, and mild operating conditions over the traditional processes like distillation (Balat et al. 2008). The known membrane-based bioethanol recovery technologies include ultrafiltration, reverse osmosis, membrane distillation, pervaporation, and hybrid process; among them membrane distillation and evaporation are the two well-established methods nowadays (Bayrakci Ozdingis and Kocar 2018).

The working mechanism of membrane distillation is based on the differential vapor pressure at microporous hydrophobic membrane surface, which acts as the driving force for biofuels separation. For example, the ethanol partial pressure is higher than water; thus, ethanol vapor can transfer across the membrane in priority, and based on that, the separation of bioethanol from broth can be realized (Tomaszewska and Białończyk 2013). The commonly used membrane types for membrane distillation are prepared from low surface energy hydrophobic polymer like polypropylene, polytetrafluorethylene, and polyvinylidene fluoride (Saha et al. 2017). And a nonporous membrane is usually used in the pervaporation process to recover biofuels from solution by partial vaporization based on the solution–diffusion model (Trinh et al. 2019). During pervaporation, permeation of a component from solution to membrane and evaporation of the specific component from the membrane to vapor stream successively happen. In this way, the biofuels in solution can be selectively separated and recovered. Pervaporation membrane can be roughly classified into two types, i.e., hydrophilic membrane and hydrophobic membrane. The hydrophilic membrane is mainly used to remove water from the mixed solution, while the hydrophobic membrane is mainly used to extract biofuels from the liquid stream (Huang et al. 2008). Therefore, the hydrophobic membrane is more energy efficient for biofuels recovery when biofuels concentration in liquid is low, especially in the case for bioethanol recovery from digestate in which bioethanol concentration is usually less than 10% w/w.

In recent years, the hybrid processes have attracted wide attentions since it can fulfill the requirements for high-efficiency continuous biofuels production. The hybrid process integrates various units together for some specific functions. For example, the hybrid fermentation–pervaporation process can remove the produced bioethanol in situ to offset product inhibition and avoid yeast cells washout by holding back the yeast biomass with the membrane module (Santos et al. 2018). A hybrid system integrating membrane fermentation and cogeneration was proposed by Lopez-Castrillon et al. (2018), which effectively improved energy output efficiency of the fermentation system with possibility of additional electricity generation (275 kWh/t of cane). A hybrid extractive distillation column with high selectivity pervaporation was implemented in alcohol dehydration process, which demonstrated that the hybrid system could save up to 25%–40% of the total annual cost and energy (Novita et al. 2018).

9.3 Membrane Application on Gaseous Biofuels Production

Gaseous biofuels, like biohydrogen and methane, are also important renewable energy types which have been widely and practically used. For example, the biogas digester is commonly constructed in medium or small size dispersedly for household cases attributing to simple digester configuration and low investment (Chen et al. 2017). The bioreactors with sophisticated structure, like membrane-based bioreactors, are not suitable to be used in rural places attributing to their high cost but are frequently used in hydrogen production. Hydrogen is a clean energy than traditional fossil fuels, which generates only water as a by-product with zero greenhouse gas emissions during combustion while embracing larger energy content per unit mass (142 kJ/g) over other fuel types (Di Paola et al. 2015; Zhong et al. 2017). Compared with hydrogen production via thermochemical method like steam reforming and electrochemical method like electrolysis, biological hydrogen production has attracted particular interests due to its mild operating conditions, low energy consumption, and abundant feedstocks (Aslam et al. 2018a). However, biohydrogen productivity in large-scale application is still very low, hindering the commercialization of biohydrogen.

Many process parameters and environmental factors have significant influences on biohydrogen productivity, such as pH, temperature, substrate and nutrients availability, by-product and product concentration, microbial competition, and other hazardous materials (Liao et al. 2013; Prabakar et al. 2018). Researches are necessary to solve the remaining bottlenecks to practical applications of biohydrogen energy. Among many emerging approaches for high-efficiency biohydrogen production, membrane-integrated biohydrogen production system is for sure a promising technology allowing for dealing with various kinetic inhibitions in biohydrogen production, like biomass washout and substrate or product inhibition, as shown in Table. 9.3 (Aslam et al. 2018a).

Biological hydrogen production is a technology that produces hydrogen gas with microorganisms. It can be roughly classified into photo-dependent biohydrogen production via photolysis of water by algae and cyanobacteria or photo-fermentation by decomposing organic matters with photosynthetic bacteria and dark fermentation

Table 9.3 Major application of membranes in gaseous biofuels production process

Process	Target of membranes	Characteristics
Photo-dependent biohydrogen	Algae, cyanobacteria, or photo-fermentation with photosynthetic bacteria	Membrane application mainly focused on downstream products refining
Dark-fermentative biohydrogen	Anaerobic conditions that avoid oxygen inhibition and light inhibition	Submerged membrane bioreactor: low energy cost but high membrane area Side-stream membrane bioreactor: small membrane area but high transmembrane pressure, high energy cost
Products purification	Remove impurities for quality upgrading of gaseous biofuels	Gas transfer mechanisms of the membrane: (1)viscous flow, (2) surface diffusion, (3) Knudsen diffusion, (4) capillary condensation, (6) molecular sieving, (7) solution diffusion, (8) facilitated transport, etc. (Bakonyi et al. 2018; Li et al. 2015a; Lundin et al. 2017) Key criteria for the membrane: (1) permeability and (2) selectivity

for hydrogen production with facultative or obligate anaerobic bacteria (Trchounian et al. 2017).

9.3.1 *Membranes Used for Photo-dependent Biohydrogen Production*

During photolysis, which is the first case of the photo-dependent biohydrogen production, some oxygenic photosynthetic microorganisms like algae or cyanobacteria strains absorb solar energy and convert it into chemical energy by splitting water to proton (H^+) and molecular oxygen (O_2) with intracellular pigments (Yilanci et al. 2009). Then the generated H^+ acts as electron acceptor for H_2 production in the downstream combination with excessive electrons assisted by intracellular enzyme of algal or cyanobacterial cells (He et al. 2017). Besides H_2 generation, the technology also realizes high-efficiency carbon mitigation since the growth and metabolism of algae or cyanobacteria can absorb ambient CO_2 as carbon source at solar energy conversion efficiency of tenfold than terrestrial plants (Khetkorn et al. 2017). Thus, biohydrogen production via photolysis is regarded as the cleanest way of hydrogen production, but its application is severely inhibited by low hydrogen productivity, oxygen inhibition, and strict light requirement (Argun and Kargi 2011). Many works were reported on enhancement of photolysis biohydrogen production. Ban et al. (2018) found that Ca^+ was capable of decreasing the rate of chlorophyll reduction, maintaining the protein content at high level, and scavenging most of reactive oxygen species, which improve direct and indirect photolysis H_2 production, with the maximum value of 306 ml/L H_2 under Ca^+

adding amount of 5 mM. Rashid et al. (2013) applied mechanical agitation of culture medium in the photobioreactor to enhance oxygen escape from suspensions to reduce inhibiting effect of oxygen on biohydrogen production in microalgae system.

Unlike photolysis with algae or cyanobacteria, photo-fermentation with photosynthetic bacteria like non-sulfur purple photosynthetic bacterium, which is regarded as the second case of photo-dependent biohydrogen production, is unable to derive electrons from water. Photo-fermentation bacteria usually use simple sugars and volatile fatty acids as feedstocks (Zhang et al. 2018b). And many problems like high energy demand, low light conversion efficiency, and uneven light distribution in bioreactors still need to be addressed for photo-fermentation. To enhance the light conversion efficiency and improve the uneven light distribution in reactors, two kinds of optical fibers with high surface luminous intensity have been developed by using the polymer optical fiber and hollow quartz optical fiber (Xin et al. 2017; Zhong et al. 2016, 2019), respectively, and the prepared fibers have been applied in the photoreactors (Zhong et al. 2019). Tian et al. (2010) adopted a cell immobilization technique to a biofilm-based photobioreactor to enhance light conversion efficiency and biohydrogen production rate with photosynthetic bacteria *Rhodopseudomonas palustris CQK 01*. By cultivating photosynthetic bacteria on the surface of packed glass beads in the work by Tian et al. (2010), the maximum biohydrogen production rate was improved to 38.9 mL/L/h and the light conversion efficiency was enhanced to 56%. Fu et al. (2017) adopted light guide plate in photo-fermentation system to realize uniform light distribution in the system and enhance biohydrogen production. In the system, light was supplied from one side of the light guide plate and then emitted from the surface of the plate, in which way the light was elaborately dispersed in the culture. As a result, the hydrogen production rate was improved to 11.6 mmol/h/m^2.

Unfortunately, applications of membrane technology on photo-dependent biohydrogen production system are relatively scarce up to date, which are mainly focused on downstream purification of hydrogen products (Lin et al. 2018). Since some membranes have the ability to selectively separate gas and liquid components as well as regulate mass and heat transfer, membrane integrated photobioreactors for biohydrogen production are expected to enhance photo-biohydrogen production.

9.3.2 Membranes Used for Dark-Fermentative Biohydrogen Production

Compared with biohydrogen production via photolysis or photo-fermentation, dark-fermentative biohydrogen production occupies more predominant status nowadays. Dark fermentation presents many advantages over photo-fermentation. Since light is unnecessary for dark fermentation process, reactors design is more flexible for dark fermentation, and the volume utilization of the bioreactors can be fully exploited (Łukajtis et al. 2018). In addition, oxygen inhibition is no longer a problem in anaerobic conditions; dark-fermentative biohydrogen production shows more reliable and faster hydrogen production rate.

For conventional dark fermentation process, continuous stirred-tank reactor (CSTR) is widely used due to its simple construction, effective mixing, and ease of operation. But low biomass density in fermentative broth of the CSTR caused by high biomass washout rate and by-product and product inhibitions are crucial shortcomings for feedstocks conversion and hydrogen production (Kariyama et al. 2018). The membrane modules in anaerobic membrane bioreactor (AnMBR) typically assist the biochemical conversion processes of feedstocks to hydrogen by ensuring high solid retention time (SRT) and selectively removal of inhibiting products (Shin and Bae 2018). In detail, membranes can separate liquid stream from biomass and thus retain biomass in the bioreactor, in which way long SRT required for efficient wastewater treatment and short hydraulic retention time (HRT) for cost-effectiveness are satisfied at the same time (Aslam et al. 2018b). In addition, membranes in the bioreactors can retain the metabolites in the system for further conversion to produce biohydrogen, enhancing the substrate conversion efficiency (Park et al. 2017). For example, Nielsen et al. (2001) used a heated palladium–silver membrane reactor to separate hydrogen from the gas stream, in order to eliminate the inhibiting effects of products (H_2) on H_2 generation. Teplyakov et al. (2002) integrated active polyvinyl-trimethyl-silane membrane system with dark-fermentative bioreactor for hydrogen removal to reduce partial pressure of hydrogen in the gaseous units.

In general, the membrane bioreactor can be mainly classified into two types: submerged membrane bioreactor and side-stream membrane bioreactor (as shown in Fig. 9.2). Membrane modules are usually submerged in the liquid phase of the reactor for the submerged membrane bioreactor, while they are set outside of the reactor as a separate unit for the side-stream membrane bioreactor (Łukajtis et al.

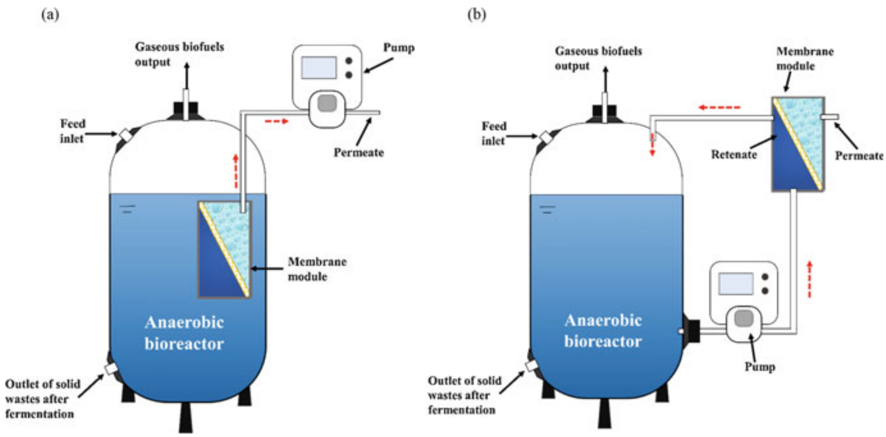

Fig. 9.2 Configurations of (**a**) the submerged membrane bioreactor (MBR) and (**b**) the side-stream MBR for gaseous biofuels production

2018). The side-stream membrane bioreactor is characterized by small exchange area of the membrane and easy conduction of membrane washing. However, a high energy cost is required to supply enough transmembrane pressure for the filtration of fermentative broth. On the contrary, the energy cost in the submerged membrane bioreactor is much lower than the side-stream membrane bioreactor, but larger membrane exchange area is necessary (Aslam et al. 2018a). Recently, many derived types of membrane bioreactor are proposed for high-efficiency biohydrogen production. Bakonyi et al. (2015) established a double-membrane bioreactor, in which a commercial microfiltration membrane module was added into a membrane hydrogen fermenter, which realized simultaneous biohydrogen production and purification. A dynamic membrane bioreactor integrating a self-forming dynamic membrane with a continuous fermenter was constructed by Park et al. (2017). In the dynamic membrane bioreactor, the membrane module successfully retained effective hydrogen-producing–bacterial consortia, resulting in a maximum hydrogen production rate of 51.38 L/L/day. Saleem et al. (2018) adopted a side-stream dynamic membrane bioreactor using dynamic membrane as a solid–liquid separation media and significantly improved the dark-fermentative biohydrogen production under mesophilic conditions.

9.3.3 Membranes Used for Biohydrogen Purification

Another important role of membrane in biohydrogen production system is purification of the gaseous products to obtain high-quality hydrogen fuel. During biohydrogen production via photo- or dark fermentation, large quantities of by-products are generated along with hydrogen gas, like CO_2, CO, SO_x, and NO_x, which have great negative effects on combustion property of biohydrogen as fuel (Khan et al. 2018). It is important to remove the impurities with CO_2 as a major target for gas upgradation. Membrane technology for biohydrogen purification is a feasible approach because it avoids chemical conversion of the mixed gas.

In general, a membrane is a semipermeable separator which acts as a selective mass transfer barrier to realize separation of different compositions (Bakonyi et al. 2018). According to membrane type (porous or nonporous membrane), gas transfer mechanisms of the membrane mainly include (1) viscous flow, (2) surface diffusion, (3) Knudsen diffusion, (4) capillary condensation, (6) molecular sieving, (7) solution diffusion, and (8) facilitated transport, which are elaborately described in the previous paper (Bakonyi et al. 2018; Li et al. 2015a; Lundin et al. 2017). Superior permeability and selectivity are two key criteria for the membrane applied in gas purification, but it is unfortunate that these two factors are usually not compatible with each other. This limits application of most available membrane types in industrial production of biohydrogen. Many researchers have been dedicating so much effort to enhance the gas separation characteristics of membranes for biohydrogen purification. Ahmad et al. (2016) constructed a nearly superhydrophobic and microporous membrane by blending amorphous poly-

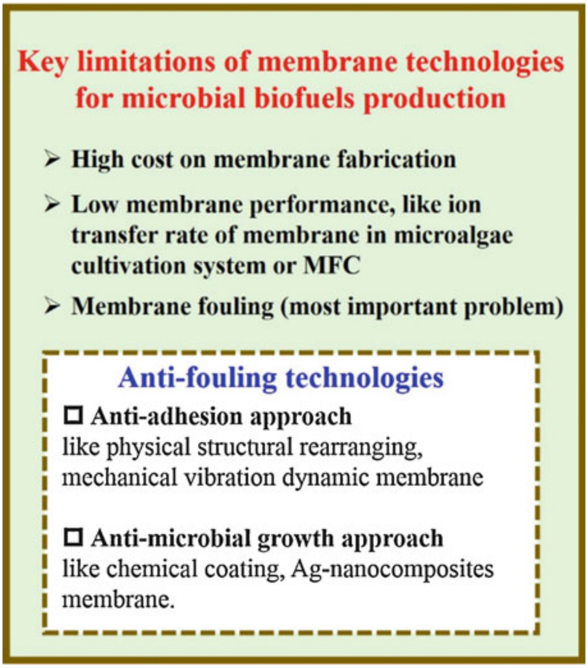

Fig. 9.3 Key limitations of membrane application in microbial biofuels production process (Buitrón et al. 2019)

benzimidazole and semicrystalline polyvinylidene fluoride, which removed 67% of CO_2 in gas mixture of H_2 and CO_2 at highest CO_2 flux of 4.16×10^{-4} mol/m^2/s across the membrane. Wu et al. (2017a) synthesized a membrane made of glassy polymers, polyetherimide-coated bio-cellulose nanofibers, and a coconut shell active carbon as adsorbent carriers for CO_2 separation in dark-fermentative gas mixture. The synthesized membrane was convinced to have CO_2 permeability of 16.72 Barrer and corresponding CO_2/H_2 selectivity of 0.15. Abd. Hamid et al. (2019) proposed a synthesized polysulfone–polyimide membrane with the highest permeability of 348 GPU (gas permeation unit, 1 GPU equal to 1×10^{-6} cm^3(STP)/(cm^2•s•cm Hg)) for H_2 and 86 GPU for CO_2, H_2/CO_2 selectivity of 4.4, and H_2 purification efficiency of 80%.

However, many previous literatures also reported that the equipment cost, reliability, and energy efficiency of the membrane bioreactor are unable to compete with the traditional CSTR. Among various influencing factors, membrane fouling is one of the most important problems, as seen in Fig. 9.3 (Buitrón et al. 2019). During microorganism growth and metabolism, a quantity of soluble microbial products and extracellular polymeric substances which consists of complex biopolymer mixtures like proteins, polysaccharides, lipopolysaccharides, and lipoproteins, is produced in the cultures (Zhang et al. 2015). With assistance of the excretive soluble microbial products and extracellular polymeric substances, the biomass flocs are easily attached and accumulated on membrane surface since the biomass flocs are usually

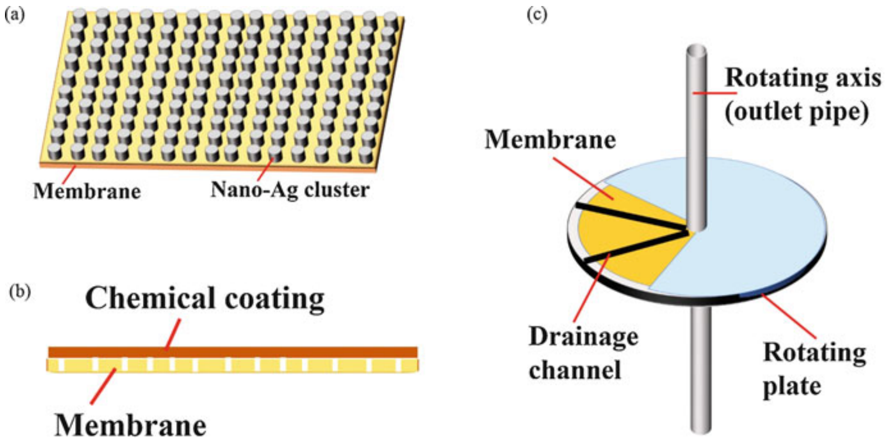

Fig. 9.4 Typical antifouling membrane system. (**a**) Membrane surface modification with nano-Ag cluster, (**b**) chemical coating of membrane and (**c**) dynamic membrane system with rotating unit (Qin et al. 2018)

larger than the membrane pore size, resulting in pore blocking and membrane fouling (Khan et al. 2019; Zhang et al. 2015).

In this regard, enhancement of physical–chemical properties of the membrane to reduce foulant attaching on the membrane surface is a primary objective to prevent membrane fouling. Membrane modifications with physical structural rearranging, chemical coating, and functional material embedding are promising approaches for antifouling membrane development (López-Cázares et al. 2018; Qin et al. 2018; Shan et al. 2018). Schematic of some typical membrane modification methods for antifouling technology is shown in Fig. 9.4, like physical structural modification with nano-Ag cluster (Fig. 9.4a) and chemical solvents coating on the membrane (Fig. 9.4b). For example, López-Cázares et al. (2018) enhanced the anti(bio)fouling of cation exchange membranes (Nafion and Ultrex membranes) by immobilizing nanocomposites of nanoparticles on graphene oxide as a thin film using a polydopamine adhesive. Shan et al. (2018) explored a facile and biomimetic method of amphiphobic surface with special structure and controllable wettability, which enhanced the flux and antifouling performances of the membrane. Li et al. (2018a) grafted thermo-responsive polymer chains on the surface of polyethersulfone, developing a modified membrane with rich porosity and well antifouling property.

Another important antifouling approach is dynamic membrane technology which uses a physical barrier to prevent formation of cake layer on the membrane surface (Yang et al. 2018). Compared with the conventional approaches to control membrane fouling by air bubbling, the dynamic membranes can provide stronger shear force on the phase interface of the liquid and membrane by mechanical vibration, like rotating, vibrating, and oscillating (Bagheri and Mirbagheri 2018; Qin et al. 2018). The typical dynamic membrane system, like membrane rotating system, is shown in Fig. 9.4c. Ruigómez et al. (2017) proposed a physical cleaning strategy based on membrane rotation in a submerged anaerobic membrane bioreactor and improved the fouling removal effectiveness, achieving a stable net permeate flux of 6.7 L/m^2 h. Chatzikonstantinou et al. (2015) employed high-frequency powerful vibration technique in both hollow fiber and flat sheet modules to prevent membrane fouling. They reported that the strategy of high-frequency powerful vibration is capable of reducing membrane fouling and is promising with respect to energy savings. These emerging antifouling technologies provide great potential to reduce membrane manufacturing and operating costs, which then enhance the commercial feasibility of biohydrogen application as energy sources.

9.4 Membrane Application in Microbial Fuel Cells

Microbial fuel cells (MFCs), which are bioelectrochemical devices, have attracted a particular interest in the energy field due to its environmental-friendly characteristic by using microorganism as electrocatalyst to conduct an oxidation–reduction reaction and convert chemical energy in wastewater into electrical energy (Leong et al. 2013; Zhong et al. 2018). The configuration of MFCs generally contains three parts, anode, cathode, and electrolyte layer, in which the MFCs can be roughly classified into two types, i.e., dual chamber MFC and single chamber MFC (as shown in Fig. 9.5). The dual chamber MFC contains an anode and a cathode chamber, which are separated by a proton exchange membrane that acts as electrolyte bridge. In contrast, the single chamber MFC contains only anode chamber, with air as the cathode of the system. The MFC has dual advantages of simultaneous electricity generation and treating wastewater, but commercialization of this technology is still hindered by high cost (Tender et al. 2008) and low power density (Tender et al. 2002).

The membrane is a major part of the MFC acting as separator that physically divides the anode and cathode but keeping them chemically and ionically connected, which significantly influences the MFCs' overall investment and power density.

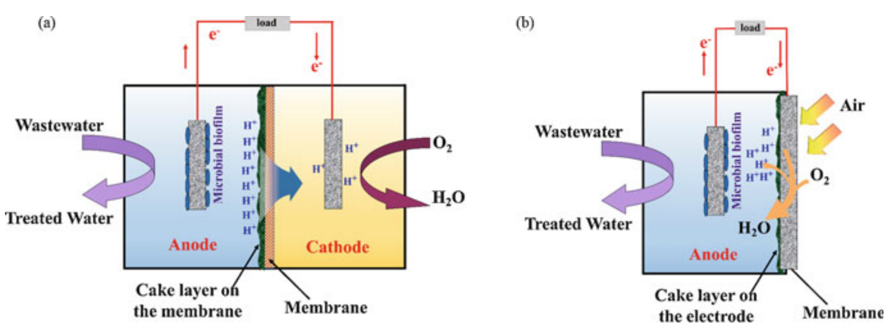

Fig. 9.5 Schematic diagram of (**a**) the dual chamber microbial fuel cell (MFC) and (**b**) the single chamber MFC

Until now, the possible types of membranes that can be used in the MFC include cation exchange membrane (Daud et al. 2018), anion exchange membrane (Elangovan and Dharmalingam 2017), porous membrane (Li et al. 2015b), polymer/composite membrane (Ahilan et al. 2018), etc. Each type of membrane has its advantages and disadvantages. For example, cation exchange membrane is the preferential separator used in MFC since it directly conducts H^+ from anode to cathode, which enhances coulombic efficiency of the MFC (Chaudhuri and Lovley 2003). pH splitting between the anode and cathode chamber of the MFC easily happened, attributing to transfer competition of other cations (like K^+, Na^+, NH_4^+, and Ca^{2+}) with H^+ across the cation exchange membrane, which may cause H^+ accumulation in anolyte (Chae et al. 2008). The anion exchange membrane can effectively diminish pH splitting since the AEM conduct OH^- or carbonate anions transfer from cathode to anode, promoting H^+ transfer by acting as H^+ carrier (Varcoe et al. 2014; Ye and Logan 2018). However, the substrate crossover through the AEM is a major drawback for MFC performance (Hernández-Flores et al. 2017). Though the internal resistance of porous membrane is low, it is not a good candidate for the MFC, attributing to high crossover rate of oxygen and substrate through the pores, except for cases when aerobic bacterium in anode is intended to be cultivated for removal of some specific organic matters, like azo bonds during azo dyes treatment (Slate et al. 2019). Polymer/composite membrane is a newly emerging type which combines merits of polymers and inorganic or organic fillers to realize more abundant functions, but it is in cost of larger surface roughness, resulting in higher possibility of biofouling (Antolini 2015). In general, the membrane affects MFCs' performance and cost from aspects of membrane internal resistance, oxygen diffusion, substrate loss across the membrane, pH splitting, and membrane biofouling (Dharmalingam et al. 2019; Leong et al. 2013).

The membrane with high resistance is not conducive to proton diffusion from anode to cathode due to low ion-exchange capacity of the membrane, resulting in poor MFC performance, while low resistance membrane with porosity like microfiltration membrane can also reduce the power density of the MFC, attributing to high crossover rate of oxygen and substrate through the pore on the membrane (Zhao et al. 2009). Therefore, the membrane with low internal resistance and low oxygen and substrate crossover rate is an ideal type for improving coulombic efficiency and power density of the MFC (Ji et al. 2011). Gao et al. (2018) developed a novel carbon-based conductive membrane that had a lower internal resistance (752 Ω) relative to the proton exchange membrane (937 Ω) and enhanced the power density of the MFC to 228 mW/m^3. Wu et al. (2017b) adopted an electroconductivity aerated membrane (EAM) as biocathode in the MFC to enhance power density and wastewater treatment. The EAM had superior property in controlling oxygen and substrate diffusion as well as proton transfer, resulting in a power density of 4.20 ± 0.13 W/m^3 at a current density of 4.10 ± 0.11 A/m^2.

Oxygen and substrate diffusion across the membrane are important issues for MFC which can significantly reduce MFC's power density and coulombic efficiency (Do et al. 2018). Oxygen transfers from cathode to anode and then competes with the anode to accept electrons since oxygen is a more favorable electron acceptor. In contrast, the substrate transfers across the membrane from anode to cathode chamber, which is in opposite direction of oxygen diffusion. The substrate is then oxidized by aerobic bacteria, and extra electrons are generated for the oxygen reduction reaction at the cathode, leading to an internal short circuit inside the MFC and reducing coulombic efficiency (Kim et al. 2013). Thus, the occurrence of oxygen and substrate diffusion across the membrane diminishes the power density of the MFC. The membrane in the MFC acts as a physical barrier for oxygen and substrate diffusion during operation. From this view, the performance of the MFC with membrane is usually better than the membraneless MFC. For example, it was reported that the coulombic efficiency of the MFC with membrane was 20% higher than the membraneless one (Li et al. 2018b; Slate et al. 2019). Unfortunately, a membrane that can totally avoid oxygen and substrate diffusion is still not yet developed. Some auxiliary approaches are necessary to minimize negative effects of oxygen and substrate crossover on MFC performance. For example, Ahilan et al. (2018) modified ceramic membrane with montmorillonite–$H_3PMo_{12}O_{40}/SiO_2$ composite to reduce the oxygen mass transfer coefficient to 5.62×10^{-4} cm/s, which is near the commercia polymeric Nafion membrane. Logan et al. (2005) used chemical oxygen scavenger, i.e., cysteine, in the anode chamber to remove the oxygen by reacting with oxygen to form disulfide dime (cystine). Yousefi et al. (2018) assembled a chitosan/montmorillonite nanocomposite film layer-by-layer over the surface of commercial unglazed wall ceramics to be utilized as the separator of MFC, in which the oxygen diffusion coefficient was one-sixth of the blank ceramic membrane. To avoid substrate diffusion, a membrane which is nonporous and has high selectivity for cations but does not allow anions transfer is the preferred approach (Leong et al. 2013).

The oxygen and substrate diffusion can also induce biofouling of the membrane and pH splitting of the MFC, which cause negative effects on MFC performance. The membrane biofouling usually occurs on the membrane surface facing the anode chamber due to the attachment of microbial and organic matter as a biofilm (Chae et al. 2008). Besides, oxygen near the membrane in the anode side that transferred from the cathode triggered biofilm formation of aerobic bacteria, which acts as barrier for proton diffusion between the anode and cathode (Li et al. 2018b). Thus, the produced H^+ in the anode accumulates in the anolyte, making the anolyte more acidic and the catholyte more alkaline. The phenomenon of pH splitting may deteriorate bacterial growth and metabolism and then reduce power density and coulombic efficiency. To ensure high performance of the MFC, the fouled membrane must be replaced with new one for proton diffusion, but this dramatically improved operating investment of the MFC. In recent years, researchers proposed some approaches to reduce membrane biofouling, like antimicrobial approach and anti-adhesion approach (Chatterjee and Ghangrekar 2014; Noori et al. 2018; Sun et al. 2016b; Yang et al. 2016). Chatterjee and Ghangrekar (2014) constructed antifouling MFC using vanillin as biocide. Yang et al. (2016) coated the membrane with a silver nanoparticle–polydopamine to mitigate biofouling of the membrane by taking advantage of antimicrobial effect of nano-Ag particle. Sun et al. (2016b) used well-ordered multi-walled carbon nanotubes and its derivative modified with the carboxyl-modified to prevent microbial adhesion. However, the effectiveness of these antifouling methods drastically reduced after a certain period of operation. Until now, biofouling is still one of the biggest limitations for membrane application in MFC field, which will deteriorate membrane performance and durability and then negatively affect the power output and operational cost (Do et al. 2018; Gajda et al. 2018).

In conclusion, the membrane is a very important component for the MFC. The properties of mass transfer like H^+, oxygen, and substrate; energy transfer like thermal, chemical, and electrical; and energy conversion between chemical, electrical, and thermal power in the MFC system are closely related to the function and structure of the membrane modules, which ultimately affects MFC's performance. Among various available membranes, the choice of an ideal type for the MFC requires certain criteria, including internal resistance; ion conductivity; permeability; physical, chemical, and thermal stability; biofouling; and cost (Dharmalingam et al. 2019; Rabaey and Verstraete 2005). A superior membrane with characteristics of high ionic conductivity and high antibiofouling property but with low internal resistance, low oxygen, low substrate diffusion rate, and low cost is needed to be developed for large-scale application of MFC.

9.5 Conclusions

Microbial energy conversion technology is a potential method for simultaneous realization of environmental remediation and energy production. Membranes play very important roles in bioenergy production processes for enhancement of bioenergy productivity and quality. This chapter presents a review on the roles and mechanisms of membranes on bioenergy production processes, and the important influencing factors are discussed. For liquid biofuels production, membranes can enhance microalgae biomass productivity, concentrate sugar concentration, remove inhibitors from the hydrolysate, and recover liquid biofuels from solution. For gaseous biofuels production, the membranes can enhance bioenergy output by ensuring high solid retention time (SRT) and purify the produced biogas for high-quality fuel generation. For the microbial fuel cell, the membrane can avoid internal short circuit and increase power density by acting as physical barrier and electrolyte bridge. But biofouling of membrane caused by microbial attachment is a vital problem that needs to be addressed. Antifouling technologies, like anti-adhesion approach or antimicrobial growth approach, are discussed in the work. For future prospect, antifouling technology of membranes is still the primary target to reduce membrane cost. Some versatile membrane types coated with functionalized groups or materials should be developed to fulfill various occasions. In addition, further application of membrane on microbial energy conversion should be explored, like membrane application on photo-dependent hydrogen production.

Acknowledgments The authors are grateful for the financial support provided by the National Natural Science Funds for Young Scholar (No. 51806026), National Natural Science Foundation of China (51876018), National Social Sciences Founding Project (17CGJ003), Foundation and Frontier Research Project of Chongqing of China (cstc2018jcyjAX0608), Science and Technology Research Program of Chongqing Municipal Education Commission (KJQN201801130), and Foundation and Frontier Research Project of Chongqing of China (cstc2018jcyjAX0513).

References

Abd. Hamid MA, Chung YT, Rohani R, Mohd. Junaidi MU (2019) Miscible-blend polysulfone/polyimide membrane for hydrogen purification from palm oil mill effluent fermentation. Sep Purif Technol 209:598–607. https://doi.org/10.1016/j.seppur.2018.07.067

Ahilan V, Wilhelm M, Rezwan K (2018) Porous polymer derived ceramic (PDC)-montmorillonite-$H_3PMo_{12}O_{40}/SiO_2$ composite membranes for microbial fuel cell (MFC) application. Ceram Int 44(16):19191–19199. https://doi.org/10.1016/j.ceramint.2018.07.138

Ahmad NA, Leo CP, Ahmad AL, Mohammad AW (2016) Separation of CO_2 from hydrogen using membrane gas absorption with PVDF/PBI membrane. Int J Hydrog Energy 41(8):4855–4861. https://doi.org/10.1016/j.ijhydene.2015.11.054

Antolini E (2015) Composite materials for polymer electrolyte membrane microbial fuel cells. Biosens Bioelectron 69:54–70. https://doi.org/10.1016/j.bios.2015.02.013

Argun H, Kargi F (2011) Bio-hydrogen production by different operational modes of dark and photo-fermentation: An overview. Int J Hydrog Energy 36(13):7443–7459. https://doi.org/10.1016/j.ijhydene.2011.03.116

Aslam M, Ahmad R, Yasin M, Khan AL, Shahid MK, Hossain S, Khan Z, Jamil F, Rafiq S, Bilad MR, Kim J, Kumar G (2018a) Anaerobic membrane bioreactors for biohydrogen production: recent developments, challenges and perspectives. Bioresour Technol 269:452–464. https://doi.org/10.1016/j.biortech.2018.08.050

Aslam M, Yang P, Lee P-H, Kim J (2018b) Novel staged anaerobic fluidized bed ceramic membrane bioreactor: energy reduction, fouling control and microbial characterization. J Membr Sci 553:200–208. https://doi.org/10.1016/j.memsci.2018.02.038

Bagheri M, Mirbagheri SA (2018) Critical review of fouling mitigation strategies in membrane bioreactors treating water and wastewater. Bioresour Technol 258:318–334. https://doi.org/10.1016/j.biortech.2018.03.026

Bakonyi P, Nemestóthy N, Lankó J, Rivera I, Buitrón G, Bélafi-Bakó K (2015) Simultaneous biohydrogen production and purification in a double-membrane bioreactor system. Int J Hydrog Energy 40(4):1690–1697. https://doi.org/10.1016/j.ijhydene.2014.12.002

Bakonyi P, Kumar G, Belafi-Bako K, Kim SH, Koter S, Kujawski W, Nemestothy N, Peter J, Pientka Z (2018) A review of the innovative gas separation membrane bioreactor with mechanisms for integrated production and purification of biohydrogen. Bioresour Technol 270:643–655. https://doi.org/10.1016/j.biortech.2018.09.020

Balat M, Balat H, Öz C (2008) Progress in bioethanol processing. Prog Energy Combust Sci 34 (5):551–573. https://doi.org/10.1016/j.pecs.2007.11.001

Ban S, Lin W, Luo J (2018) Ca^{2+} enhances algal photolysis hydrogen production by improving the direct and indirect pathways. Int J Hydrog Energy. https://doi.org/10.1016/j.ijhydene.2018.11.075

Bayrakci Ozdingis AG, Kocar G (2018) Current and future aspects of bioethanol production and utilization in Turkey. Renew Sust Energ Rev 81:2196–2203. https://doi.org/10.1016/j.rser.2017.06.031

Bilad MR, Azizo AS, Wirzal MDH, Jia Jia L, Putra ZA, Nordin NAHM, Mavukkandy MO, Jasni MJF, Yusoff ARM (2018) Tackling membrane fouling in microalgae filtration using nylon 6,6

nanofiber membrane. J Environ Manag 223:23–28. https://doi.org/10.1016/j.jenvman.2018.06.007
Buitrón G, Muñoz-Páez KM, Hernández-Mendoza CE (2019) Biohydrogen production using a granular sludge membrane bioreactor. Fuel 241:954–961. https://doi.org/10.1016/j.fuel.2018.12.104
Carrillo-Nieves D, Rostro Alanís MJ, de la Cruz Quiroz R, Ruiz HA, Iqbal HMN, Parra-Saldívar R (2019) Current status and future trends of bioethanol production from agro-industrial wastes in Mexico. Renew Sust Energ Rev 102:63–74. https://doi.org/10.1016/j.rser.2018.11.031
Chae KJ, Choi M, Ajayi FF, Park W, Chang IS, Kim IS (2008) Mass transport through a proton exchange membrane (Nafion) in microbial fuel cells. Energy Fuel 22(1):169–176. https://doi.org/10.1021/ef700308u
Chang HX, Fu Q, Huang Y, Xia A, Liao Q, Zhu X, Zheng YP, sun CH (2016a) An annular photobioreactor with ion-exchange-membrane for non-touch microalgae cultivation with wastewater. Bioresour Technol 209:668–676. https://doi.org/10.1016/j.biortech.2016.08.032
Chang HX, Huang Y, Fu Q, Liao Q, Zhu X (2016b) Kinetic characteristics and modeling of microalgae *Chlorella vulgaris* growth and CO_2 biofixation considering the coupled effects of light intensity and dissolved inorganic carbon. Bioresour Technol 206:231–238. https://doi.org/10.1016/j.biortech.2016.01.087
Chang H, Fu Q, Huang Y, Xia A, Liao Q, Zhu X (2017) Improvement of microalgae lipid productivity and quality in an ion-exchange-membrane photobioreactor using real municipal wastewater. Int J Agric Biol Eng 10(1):97–106. https://doi.org/10.3965/j.ijabe.20171001.2706
Chang H, Quan X, Zhong N, Zhang Z, Lu C, Li G, Cheng Z, Yang L (2018) High-efficiency nutrients reclamation from landfill leachate by microalgae *Chlorella vulgaris* in membrane photobioreactor for bio-lipid production. Bioresour Technol 266:374–381. https://doi.org/10.1016/j.biortech.2018.06.077
Chang H, Fu Q, Zhong N, Yang X, Quan X, Li S, Fu J, Xiao C (2019) Microalgal lipids production and nutrients recovery from landfill leachate using membrane photobioreactor. Bioresour Technol 277:18–26. https://doi.org/10.1016/j.biortech.2019.01.027
Chatterjee P, Ghangrekar M (2014) Preparation of a fouling-resistant sustainable cathode for a single-chambered microbial fuel cell. Water Sci Technol 69(3):634–639. https://doi.org/10.2166/wst.2013.760
Chatzikonstantinou K, Tzamtzis N, Pappa A, Liodakis S (2015) Membrane fouling control using high-frequency power vibration, in an SMBR pilot system—preliminary studies. Desalin Water Treat 57(25):11550–11560. https://doi.org/10.1080/19443994.2015.1048309
Chaudhuri SK, Lovley DR (2003) Electricity generation by direct oxidation of glucose in mediatorless microbial fuel cells. Nat Biotechnol 21(10):1229. https://doi.org/10.1038/nbt867
Chen Y, Hu W, Chen P, Ruan R (2017) Household biogas CDM project development in rural China. Renew Sust Energ Rev 67:184–191. https://doi.org/10.1016/j.rser.2016.09.052
Chisti Y (2007) Biodiesel from microalgae. Biotechnol Adv 25(3):294–306. https://doi.org/10.1016/j.biotechadv.2007.02.001
Correa DF, Beyer HL, Possingham HP, Thomas-Hall SR, Schenk PM (2017) Biodiversity impacts of bioenergy production: microalgae vs. first generation biofuels. Renew Sust Energ Rev 74:1131–1146. https://doi.org/10.1016/j.rser.2017.02.068
Daud SM, Daud WRW, Kim BH, Somalu MR, Bakar MHA, Muchtar A, Jahim JM, Lim SS, Chang IS (2018) Comparison of performance and ionic concentration gradient of two-chamber microbial fuel cell using ceramic membrane (CM) and cation exchange membrane (CEM) as separators. Electrochim Acta 259:365–376. https://doi.org/10.1016/j.electacta.2017.10.118
Dharmalingam S, Kugarajah V, Sugumar M (2019) Chapter 1.7: Membranes for microbial fuel cells. In: Mohan SV, Varjani S, Pandey A (eds) Microbial electrochemical technology. Elsevier, pp 143–194. https://doi.org/10.1016/b978-0-444-64052-9.00007-8
Di Paola L, Russo V, Piemonte V (2015) Chapter 9: membrane reactors for biohydrogen production and processing. In: Basile A, Di Paola L, Hai FL, Piemonte V (eds) Membrane reactors for

energy applications and basic chemical production. Woodhead Publishing, Amsterdam, pp 267–286. https://doi.org/10.1016/B978-1-78242-223-5.00009-1

Do MH, Ngo HH, Guo WS, Liu Y, Chang SW, Nguyen DD, Nghiem LD, Ni BJ (2018) Challenges in the application of microbial fuel cells to wastewater treatment and energy production: a mini review. Sci Total Environ 639:910–920. https://doi.org/10.1016/j.scitotenv.2018.05.136

Elangovan M, Dharmalingam S (2017) Application of polysulphone based anion exchange membrane electrolyte for improved electricity generation in microbial fuel cell. Mater Chem Phys 199:528–536. https://doi.org/10.1016/j.matchemphys.2017.07.038

Enagi II, Al-attab KA, Zainal ZA (2018) Liquid biofuels utilization for gas turbines: a review. Renew Sust Energ Rev 90:43–55. https://doi.org/10.1016/j.rser.2018.03.006

Enevoldsen AD, Hansen EB, Jonsson G (2007) Electro-ultrafiltration of amylase enzymes: process design and economy. Chem Eng Sci 62(23):6716–6725. https://doi.org/10.1016/j.ces.2007.08.040

Ferreira JA, Brancoli P, Agnihotri S, Bolton K, Taherzadeh MJ (2018) A review of integration strategies of lignocelluloses and other wastes in 1st generation bioethanol processes. Process Biochem 75:173–186. https://doi.org/10.1016/j.procbio.2018.09.006

Fu Q, Chang HX, Huang Y, Liao Q, Zhu X, Xia A, Sun YH (2016) A novel self-adaptive microalgae photobioreactor using anion exchange membranes for continuous supply of nutrients. Bioresour Technol 214:629–636. https://doi.org/10.1016/j.biortech.2016.04.081

Fu Q, Li Y, Zhong N, Liao Q, Huang Y, Xia A, Zhu X, Hou Y (2017) A novel biofilm photobioreactor using light guide plate enhances the hydrogen production. Int J Hydrog Energy 42(45):27523–27531. https://doi.org/10.1016/j.ijhydene.2017.05.182

Fu Q, Xiao S, Li Z, Li Y, Kobayashi H, Li J, Yang Y, Liao Q, Zhu X, He X, Ye D, Zhang L, Zhong M (2018) Hybrid solar-to-methane conversion system with a faradaic efficiency of up to 96%. Nano Energy 53:232–239. https://doi.org/10.1016/j.nanoen.2018.08.051

Gajda I, Greenman J, Ieropoulos IA (2018) Recent advancements in real-world microbial fuel cell applications. Current Opinion Electrochem 11:78–83. https://doi.org/10.1016/j.coelec.2018.09.006

Gao C, Liu L, Yu T, Yang F (2018) Development of a novel carbon-based conductive membrane with in-situ formed MnO2 catalyst for wastewater treatment in bio-electrochemical system (BES). J Membr Sci 549:533–542. https://doi.org/10.1016/j.memsci.2017.12.053

Georgianna DR, Mayfield SP (2012) Exploiting diversity and synthetic biology for the production of algal biofuels. Nature 488(7411):329–335. https://doi.org/10.1038/nature11479

Guo C-L, Wang W, Duan D-R, Zhao C-Y, Guo F-Q (2018) Enhanced CO_2 biofixation and protein production by microalgae biofilm attached on modified surface of nickel foam. Bioprocess Biosyst Eng. https://doi.org/10.1007/s00449-018-2055-4

Hapońska M, Clavero E, Salvadó J, Torras C (2018) Application of ABS membranes in dynamic filtration for *Chlorella sorokiniana* dewatering. Biomass Bioenergy 111:224–231. https://doi.org/10.1016/j.biombioe.2017.03.013

He S, Fan X, Luo S, Katukuri NR, Guo R (2017) Enhanced the energy outcomes from microalgal biomass by the novel biopretreatment. Energy Convers Manag 135:291–296. https://doi.org/10.1016/j.enconman.2016.12.049

Hernández-Flores G, Poggi-Varaldo HM, Romero-Castañón T, Solorza-Feria O, Rinderknecht-Seijas N (2017) Harvesting energy from leachates in microbial fuel cells using an anion exchange membrane. Int J Hydrog Energy 42(51):30374–30382. https://doi.org/10.1016/j.ijhydene.2017.08.201

Huang H-J, Ramaswamy S, Tschirner UW, Ramarao BV (2008) A review of separation technologies in current and future biorefineries. Sep Purif Technol 62(1):1–21. https://doi.org/10.1016/j.seppur.2007.12.011

Huang Y, Wei C, Liao Q, Xia A, Zhu X, Zhu X (2019) Biodegradable branched cationic starch with high C/N ratio for *Chlorella vulgaris* cells concentration: regulating microalgae flocculation performance by pH. Bioresour Technol 276:133–139. https://doi.org/10.1016/j.biortech.2018.12.072

Ibrahim MH, El-Naas MH, Zhang Z, Van der Bruggen B (2018) CO_2 capture using hollow fiber membranes: a review of membrane wetting. Energy Fuel 32(2):963–978. https://doi.org/10.1021/acs.energyfuels.7b03493

Ji E, Moon H, Piao J, Ha PT, An J, Kim D, Woo JJ, Lee Y, Moon SH, Rittmann BE, Chang IS (2011) Interface resistances of anion exchange membranes in microbial fuel cells with low ionic strength. Biosens Bioelectron 26(7):3266–3271. https://doi.org/10.1016/j.bios.2010.12.039

Kang S, Fu J, Zhang G (2018) From lignocellulosic biomass to levulinic acid: a review on acid-catalyzed hydrolysis. Renew Sust Energ Rev 94:340–362. https://doi.org/10.1016/j.rser.2018.06.016

Kariyama ID, Zhai X, Wu B (2018) Influence of mixing on anaerobic digestion efficiency in stirred tank digesters: a review. Water Res 143:503–517. https://doi.org/10.1016/j.watres.2018.06.065

Khairuddin NFM, Idris A, Hock LW (2019) Harvesting Nannochloropsis sp. using PES/MWCNT/LiBr membrane with good antifouling properties. Sep Purif Technol 212:1–11. https://doi.org/10.1016/j.seppur.2018.11.013

Khan MA, Ngo HH, Guo W, Liu Y, Zhang X, Guo J, Chang SW, Nguyen DD, Wang J (2018) Biohydrogen production from anaerobic digestion and its potential as renewable energy. Renew Energy 129:754–768. https://doi.org/10.1016/j.renene.2017.04.029

Khan MA, Ngo HH, Guo W, Liu Y, Nghiem LD, Chang SW, Nguyen DD, Zhang S, Luo G, Jia H (2019) Optimization of hydraulic retention time and organic loading rate for volatile fatty acid production from low strength wastewater in an anaerobic membrane bioreactor. Bioresour Technol 271:100–108. https://doi.org/10.1016/j.biortech.2018.09.075

Khetkorn W, Rastogi RP, Incharoensakdi A, Lindblad P, Madamwar D, Pandey A, Larroche C (2017) Microalgal hydrogen production - a review. Bioresour Technol 243:1194–1206. https://doi.org/10.1016/j.biortech.2017.07.085

Kim K-Y, Chae K-J, Choi M-J, Yang E-T, Hwang MH, Kim IS (2013) High-quality effluent and electricity production from non-CEM based flow-through type microbial fuel cell. Chem Eng J 218:19–23. https://doi.org/10.1016/j.cej.2012.12.018

Kumari D, Singh R (2018) Pretreatment of lignocellulosic wastes for biofuel production: a critical review. Renew Sust Energ Rev 90:877–891. https://doi.org/10.1016/j.rser.2018.03.111

Leong JX, Daud WRW, Ghasemi M, Liew KB, Ismail M (2013) Ion exchange membranes as separators in microbial fuel cells for bioenergy conversion: a comprehensive review. Renew Sust Energ Rev 28:575–587. https://doi.org/10.1016/j.rser.2013.08.052

Leong W-H, Lim J-W, Lam M-K, Uemura Y, Ho Y-C (2018) Third generation biofuels: a nutritional perspective in enhancing microbial lipid production. Renew Sust Energ Rev 91:950–961. https://doi.org/10.1016/j.rser.2018.04.066

Li P, Wang Z, Qiao Z, Liu Y, Cao X, Li W, Wang J, Wang S (2015a) Recent developments in membranes for efficient hydrogen purification. J Membr Sci 495:130–168. https://doi.org/10.1016/j.memsci.2015.08.010

Li Y, Liu L, Yang F, Ren N (2015b) Performance of carbon fiber cathode membrane with C–Mn–Fe–O catalyst in MBR–MFC for wastewater treatment. J Membr Sci 484:27–34. https://doi.org/10.1016/j.memsci.2015.03.006

Li Y, Zhong N, Liao Q, Fu Q, Huang Y, Zhu X, Li Q (2017) A biomaterial doped with LaB_6 nanoparticles as photothermal media for enhancing biofilm growth and hydrogen production in photosynthetic bacteria. Int J Hydrog Energy 42(9):5793–5803. https://doi.org/10.1016/j.ijhydene.2017.01.082

Li D, Niu X, Yang S, Chen Y, Ran F (2018a) Thermo-responsive polysulfone membranes with good anti-fouling property modified by grafting random copolymers via surface-initiated eATRP. Sep Purif Technol 206:166–176. https://doi.org/10.1016/j.seppur.2018.05.046

Li M, Zhou M, Tian X, Tan C, McDaniel CT, Hassett DJ, Gu T (2018b) Microbial fuel cell (MFC) power performance improvement through enhanced microbial electrogenicity. Biotechnol Adv 36(4):1316–1327. https://doi.org/10.1016/j.biotechadv.2018.04.010

Li Y, Wang L, Zhang Z, Hu X, Cheng Y, Zhong C (2018c) Carbon dioxide absorption from biogas by amino acid salt promoted potassium carbonate solutions in a hollow fiber membrane

contactor: a numerical study. Energy Fuel 32(3):3637–3646. https://doi.org/10.1021/acs.energyfuels.7b03616
Li Y-J, Li H-Y, Sun S-N, Sun R-C (2019) Evaluating the efficiency of γ-valerolactone/water/acid system on Eucalyptus pretreatment by confocal Raman microscopy and enzymatic hydrolysis for bioethanol production. Renew Energy 134:228–234. https://doi.org/10.1016/j.renene.2018.11.038
Liao Q, Zhong NB, Zhu X, Chen R, Wang YZ, Lee DJ (2013) Enhancement of hydrogen production by adsorption of *Rhodoseudomonas palustris* CQK 01 on a new support material. Int J Hydrog Energy 38(35):15730–15737. https://doi.org/10.1016/j.ijhydene.2013.04.146
Liao Q, Li L, Chen R, Zhu X (2014) A novel photobioreactor generating the light/dark cycle to improve microalgae cultivation. Bioresour Technol 161:186–191. https://doi.org/10.1016/j.biortech.2014.02.119
Liao Q, Zhong N, Zhu X, Huang Y, Chen R (2015) Enhancement of hydrogen production by optimization of biofilm growth in a photobioreactor. Int J Hydrog Energy 40(14):4741–4751. https://doi.org/10.1016/j.ijhydene.2015.02.040
Liao Q, Chang HX, Fu Q, Huang Y, Xia A, Zhu X, Zhong N (2018) Physiological-phased kinetic characteristics of microalgae *Chlorella vulgaris* growth and lipid synthesis considering synergistic effects of light, carbon and nutrients. Bioresour Technol 250:583–590. https://doi.org/10.1016/j.biortech.2017.11.086
Lin C-Y, Nguyen TM-L, Chu C-Y, Leu H-J, Lay C-H (2018) Fermentative biohydrogen production and its byproducts: a mini review of current technology developments. Renew Sust Energ Rev 82:4215–4220. https://doi.org/10.1016/j.rser.2017.11.001
Logan BE, Murano C, Scott K, Gray ND, Head IM (2005) Electricity generation from cysteine in a microbial fuel cell. Water Res 39(5):942–952. https://doi.org/10.1016/j.watres.2004.11.019
Lopez-Castrillon C, Leon JA, Palacios-Bereche MC, Palacios-Bereche R, Nebra SA (2018) Improvements in fermentation and cogeneration system in the ethanol production process: hybrid membrane fermentation and heat integration of the overall process through pinch analysis. Energy 156:468–480. https://doi.org/10.1016/j.energy.2018.05.092
López-Cázares MI, Pérez-Rodríguez F, Rangel-Méndez JR, Centeno-Sánchez M, Cházaro-Ruiz LF (2018) Improved conductivity and anti(bio)fouling of cation exchange membranes by AgNPs-GO nanocomposites. J Membr Sci 565:463–479. https://doi.org/10.1016/j.memsci.2018.08.036
Lu L, Guest JS, Peters CA, Zhu X, Rau G, Ren Z (2018) Wastewater treatment for carbon capture and utilization. Nat Sustain 1:750–758. https://doi.org/10.1038/s41893-018-0187-9
Łukajtis R, Hołowacz I, Kucharska K, Glinka M, Rybarczyk P, Przyjazny A, Kamiński M (2018) Hydrogen production from biomass using dark fermentation. Renew Sust Energ Rev 91:665–694. https://doi.org/10.1016/j.rser.2018.04.043
Lundin, S.-T.B., Patki, N.S., Fuerst, T.F., Ricote, S., Wolden, C.A., Way, J.D. 2017. Dense inorganic membranes for hydrogen separation. Membranes for gas separations, 1, 271. DOI: https://doi.org/10.1142/9789813207714_0007
Mathimani T, Pugazhendhi A (2019) Utilization of algae for biofuel, bio-products and bio-remediation. Biocatal Agric Biotechnol 17:326–330. https://doi.org/10.1016/j.bcab.2018.12.007
Mortezaeikia V, Yegani R, Tavakoli O (2016) Membrane-sparger vs. membrane contactor as a photobioreactors for carbon dioxide biofixation of Synechococcus elongatus in batch and semi-continuous mode. J CO2 Util 16:23–31. https://doi.org/10.1016/j.jcou.2016.05.009
Nguyen DTT, Praveen P, Loh K-C (2018) Zymomonas mobilis immobilization in polymeric membranes for improved resistance to lignocellulose-derived inhibitors in bioethanol fermentation. Biochem Eng J 140:29–37. https://doi.org/10.1016/j.bej.2018.09.003
Nielsen AT, Amandusson H, Bjorklund R, Dannetun H, Ejlertsson J, Ekedahl L-G, Lundström I, Svensson BH (2001) Hydrogen production from organic waste. Int J Hydrog Energy 26(6):547–550. https://doi.org/10.1016/S0360-3199(00)00125-7
Nigam PS, Singh A (2011) Production of liquid biofuels from renewable resources. Prog Energy Combust Sci 37(1):52–68. https://doi.org/10.1016/j.pecs.2010.01.003

Noori MT, Tiwari BR, Mukherjee CK, Ghangrekar MM (2018) Enhancing the performance of microbial fuel cell using AgPt bimetallic alloy as cathode catalyst and anti-biofouling agent. Int J Hydrog Energy 43(42):19650–19660. https://doi.org/10.1016/j.ijhydene.2018.08.120

Novita FJ, Lee H-Y, Lee M (2018) Energy-efficient and ecologically friendly hybrid extractive distillation using a pervaporation system for azeotropic feed compositions in alcohol dehydration process. J Taiwan Inst Chem Eng 91:251–265. https://doi.org/10.1016/j.jtice.2018.05.023

Park J-H, Anburajan P, Kumar G, Park H-D, Kim S-H (2017) Biohydrogen production integrated with an external dynamic membrane: a novel approach. Int J Hydrog Energy 42 (45):27543–27549. https://doi.org/10.1016/j.ijhydene.2017.05.145

Pei H-S, Guo C-L, Zhang G-F, Tang Q-Y, Guo F-Q (2017) Dynamic behavior of bubble forming at capillary orifice in methane oxidizing bacteria suspension. Int J Heat Mass Transf 110:872–879. https://doi.org/10.1016/j.ijheatmasstransfer.2017.03.094

Prabakar D, Manimudi VT, Suvetha KS, Sampath S, Mahapatra DM, Rajendran K, Pugazhendhi A (2018) Advanced biohydrogen production using pretreated industrial waste: outlook and prospects. Renew Sust Energ Rev 96:306–324. https://doi.org/10.1016/j.rser.2018.08.006

Qin L, Zhang Y, Xu Z, Zhang G (2018) Advanced membrane bioreactors systems: new materials and hybrid process design. Bioresour Technol 269:476–488. https://doi.org/10.1016/j.biortech.2018.08.062

Rabaey K, Verstraete W (2005) Microbial fuel cells: novel biotechnology for energy generation. Trends Biotechnol 23(6):291–298. https://doi.org/10.1016/j.tibtech.2005.04.008

Rahaman MSA, Cheng L-H, Xu X-H, Zhang L, Chen H-L (2011) A review of carbon dioxide capture and utilization by membrane integrated microalgal cultivation processes. Renew Sust Energ Rev 15(8):4002–4012. https://doi.org/10.1016/j.rser.2011.07.031

Raman S, Mohr A, Helliwell R, Ribeiro B, Shortall O, Smith R, Millar K (2015) Integrating social and value dimensions into sustainability assessment of lignocellulosic biofuels. Biomass Bioenergy 82:49–62. https://doi.org/10.1016/j.biombioe.2015.04.022

Rashid N, Rehman MSU, Memon S, Ur Rahman Z, Lee K, Han J-I (2013) Current status, barriers and developments in biohydrogen production by microalgae. Renew Sust Energ Rev 22:571–579. https://doi.org/10.1016/j.rser.2013.01.051

Rodionova MV, Poudyal RS, Tiwari I, Voloshin RA, Zharmukhamedov SK, Nam HG, Zayadan BK, Bruce BD, Hou HJM, Allakhverdiev SI (2017) Biofuel production: challenges and opportunities. Int J Hydrog Energy 42(12):8450–8461. https://doi.org/10.1016/j.ijhydene.2016.11.125

Ruigómez I, González E, Guerra S, Rodríguez-Gómez LE, Vera L (2017) Evaluation of a novel physical cleaning strategy based on HF membrane rotation during the backwashing/relaxation phases for anaerobic submerged MBR. J Membr Sci 526:181–190. https://doi.org/10.1016/j.memsci.2016.12.042

Saha K, UM R, Sikder J, Chakraborty S, da Silva SS, dos Santos JC (2017) Membranes as a tool to support biorefineries: applications in enzymatic hydrolysis, fermentation and dehydration for bioethanol production. Renew Sust Energ Rev 74:873–890. https://doi.org/10.1016/j.rser.2017.03.015

Saleem M, Lavagnolo MC, Spagni A (2018) Biological hydrogen production via dark fermentation by using a side-stream dynamic membrane bioreactor: effect of substrate concentration. Chem Eng J 349:719–727. https://doi.org/10.1016/j.cej.2018.05.129

Sambusiti C, Monlau F, Antoniou N, Zabaniotou A, Barakat A (2016) Simultaneous detoxification and bioethanol fermentation of furans-rich synthetic hydrolysate by digestate-based pyrochar. J Environ Manag 183(Pt 3):1026–1031. https://doi.org/10.1016/j.jenvman.2016.09.062

Santos ELI, Rostro-Alanis M, Parra-Saldivar R, Alvarez AJ (2018) A novel method for bioethanol production using immobilized yeast cells in calcium-alginate films and hybrid composite pervaporation membrane. Bioresour Technol 247:165–173. https://doi.org/10.1016/j.biortech.2017.09.091

Shan H, Liu J, Li X, Li Y, Tezel FH, Li B, Wang S (2018) Nanocoated amphiphobic membrane for flux enhancement and comprehensive anti-fouling performance in direct contact membrane distillation. J Membr Sci 567:166–180. https://doi.org/10.1016/j.memsci.2018.09.038
Shin C, Bae J (2018) Current status of the pilot-scale anaerobic membrane bioreactor treatments of domestic wastewaters: a critical review. Bioresour Technol 247:1038–1046. https://doi.org/10.1016/j.biortech.2017.09.002
Singh R, Purkait MK (2019) Chapter 4: microfiltration membranes. In: Ismail AF, Rahman MA, Othman MHD, Matsuura T (eds) Membrane separation principles and applications. Elsevier, Amsterdam, pp 111–146. https://doi.org/10.1016/B978-0-12-812815-2.00004-1
Slate AJ, Whitehead KA, Brownson DAC, Banks CE (2019) Microbial fuel cells: An overview of current technology. Renew Sust Energ Rev 101:60–81. https://doi.org/10.1016/j.rser.2018.09.044
Srivastava N, Srivastava M, Mishra PK, Gupta VK, Molina G, Rodriguez-Couto S, Manikanta A, Ramteke PW (2018) Applications of fungal cellulases in biofuel production: advances and limitations. Renew Sust Energ Rev 82:2379–2386. https://doi.org/10.1016/j.rser.2017.08.074
Sun Y, Huang Y, Liao Q, Fu Q, Zhu X (2016a) Enhancement of microalgae production by embedding hollow light guides to a flat-plate photobioreactor. Bioresour Technol 207:31–38. https://doi.org/10.1016/j.biortech.2016.01.136
Sun Y, Lang Y, Sun Q, Liang S, Liu Y, Zhang Z (2016b) Effect of anti-biofouling potential of multi-walled carbon nanotubes-filled polydimethylsiloxane composites on pioneer microbial colonization. Colloids Surf B: Biointerfaces 145:30–36. https://doi.org/10.1016/j.colsurfb.2016.04.033
Sun Y, Huang Y, Liao Q, Xia A, Fu Q, Zhu X, Fu J (2018) Boosting Nannochloropsis oculata growth and lipid accumulation in a lab-scale open raceway pond characterized by improved light distributions employing built-in planar waveguide modules. Bioresour Technol 249:880–889. https://doi.org/10.1016/j.biortech.2017.11.013
Tanaka K, Koyama M, Pham PT, Rollon AP, Habaki H, Egashira R, Nakasaki K (2019) Production of high-concentration bioethanol from cassava stem by repeated hydrolysis and intermittent yeast inoculation. Int Biodeterior Biodegradation 138:1–7. https://doi.org/10.1016/j.ibiod.2018.12.007
Tender LM, Reimers CE, Stecher Iii HA, Holmes DE, Bond DR, Lowy DA, Pilobello K, Fertig SJ, Lovley DR (2002) Harnessing microbially generated power on the seafloor. Nat Biotechnol 20:821. https://doi.org/10.1038/nbt716
Tender LM, Gray SA, Groveman E, Lowy DA, Kauffman P, Melhado J, Tyce RC, Flynn D, Petrecca R, Dobarro J (2008) The first demonstration of a microbial fuel cell as a viable power supply: powering a meteorological buoy. J Power Sources 179(2):571–575. https://doi.org/10.1016/j.jpowsour.2007.12.123
Teplyakov VV, Gassanova LG, Sostina EG, Slepova EV, Modigell M, Netrusov AI (2002) Lab-scale bioreactor integrated with active membrane system for hydrogen production: experience and prospects. Int J Hydrog Energy 27(11):1149–1155. https://doi.org/10.1016/S0360-3199(02)00093-9
Tian X, Liao Q, Liu W, Zhong WY, Zhu X, Li J, Wang H (2009) Photo-hydrogen production rate of a PVA-boric acid gel granule containing immobilized photosynthetic bacteria cells. Int J Hydrog Energy 34:4708–4717. https://doi.org/10.1016/j.ijhydene.2009.03.042
Tian X, Liao Q, Zhu X, Wang Y, Zhang P, Li J, Wang H (2010) Characteristics of a biofilm photobioreactor as applied to photo-hydrogen production. Bioresour Technol 101(3):977–983. https://doi.org/10.1016/j.biortech.2009.09.007
Tomaszewska M, Białończyk L (2013) Production of ethanol from lactose in a bioreactor integrated with membrane distillation. Desalination 323:114–119. https://doi.org/10.1016/j.desal.2013.01.026
Trchounian K, Sawers RG, Trchounian A (2017) Improving biohydrogen productivity by microbial dark- and photo-fermentations: novel data and future approaches. Renew Sust Energ Rev 80:1201–1216. https://doi.org/10.1016/j.rser.2017.05.149

Trinh LTP, Lee Y-J, Park CS, Bae H-J (2019) Aqueous acidified ionic liquid pretreatment for bioethanol production and concentration of produced ethanol by pervaporation. J Ind Eng Chem 69:57–65. https://doi.org/10.1016/j.jiec.2018.09.008

Varcoe JR, Atanassov P, Dekel DR, Herring AM, Hickner MA, Kohl PA, Kucernak AR, Mustain WE, Nijmeijer K, Scott K (2014) Anion-exchange membranes in electrochemical energy systems. Energy Environ Sci 7(10):3135–3191. https://doi.org/10.1039/C4EE01303D

Wei P, Cheng L-H, Zhang L, Xu X-H, Chen H-l, Gao C-j (2014) A review of membrane technology for bioethanol production. Renew Sust Energ Rev 30:388–400. https://doi.org/10.1016/j.rser.2013.10.017

Wei C, Huang Y, Liao Q, Fu Q, Xia A, Sun Y (2018) The kinetics of the polyacrylic superabsorbent polymers swelling in microalgae suspension to concentrate cells density. Bioresour Technol 249:713–719. https://doi.org/10.1016/j.biortech.2017.10.066

Wooley R, Ruth M, Sheehan J, Ibsen K, Majdeski H, Galvez A (1999) Lignocellulosic biomass to ethanol process design and economics utilizing co-current dilute acid prehydrolysis and enzymatic hydrolysis current and futuristic scenarios. Off Sci Tech Inf Tech Rep. https://doi.org/10.2172/12150

Wu S-Y, Hsiao IC, Liu C-M, Mt Yusuf NY, Wan Isahak WNR, Masdar MS (2017a) A novel bio-cellulose membrane and modified adsorption approach in CO2/H2 separation technique for PEM fuel cell applications. Int J Hydrog Energy 42(45):27630–27640. https://doi.org/10.1016/j.ijhydene.2017.05.148

Wu Y, Yang Q, Zeng Q, Ngo HH, Guo W, Zhang H (2017b) Enhanced low C/N nitrogen removal in an innovative microbial fuel cell (MFC) with electroconductivity aerated membrane (EAM) as biocathode. Chem Eng J 316:315–322. https://doi.org/10.1016/j.cej.2016.11.141

Xin X, Zhong N, Liao Q, Cen Y, Wu R, Wang Z (2017) High-sensitivity four-layer polymer fiber-optic evanescent wave sensor. Biosens Bioelectron 91:623–628. https://doi.org/10.1016/j.bios.2017.01.019

Yang E, Chae K-J, Alayande AB, Kim K-Y, Kim IS (2016) Concurrent performance improvement and biofouling mitigation in osmotic microbial fuel cells using a silver nanoparticle-polydopamine coated forward osmosis membrane. J Membr Sci 513:217–225. https://doi.org/10.1016/j.memsci.2016.04.028

Yang T, Liu F, Xiong H, Yang Q, Chen F, Zhan C (2018) Fouling process and anti-fouling mechanisms of dynamic membrane assisted by photocatalytic oxidation under sub-critical fluxes. Chin J Chem Eng., in press. https://doi.org/10.1016/j.cjche.2018.10.019

Ye Y, Logan BE (2018) The importance of OH^- transport through anion exchange membrane in microbial electrolysis cells. Int J Hydrog Energy 43(5):2645–2653. https://doi.org/10.1016/j.ijhydene.2017.12.074

Yilanci A, Dincer I, Ozturk HK (2009) A review on solar-hydrogen/fuel cell hybrid energy systems for stationary applications. Prog Energy Combust Sci 35(3):231–244. https://doi.org/10.1016/j.pecs.2008.07.004

Yousefi V, Mohebbi-Kalhori D, Samimi A (2018) Application of layer-by-layer assembled chitosan/montmorillonite nanocomposite as oxygen barrier film over the ceramic separator of the microbial fuel cell. Electrochim Acta 283:234–247. https://doi.org/10.1016/j.electacta.2018.06.173

Zabed H, Sahu JN, Suely A, Boyce AN, Faruq G (2017) Bioethanol production from renewable sources: current perspectives and technological progress. Renew Sust Energ Rev 71:475–501. https://doi.org/10.1016/j.rser.2016.12.076

Zhang Z, Wang Y, Leslie GL, Waite TD (2015) Effect of ferric and ferrous iron addition on phosphorus removal and fouling in submerged membrane bioreactors. Water Res 69:210–222. https://doi.org/10.1016/j.watres.2014.11.011

Zhang Q, Wei Y, Han H, Weng C (2018a) Enhancing bioethanol production from water hyacinth by new combined pretreatment methods. Bioresour Technol 251:358–363. https://doi.org/10.1016/j.biortech.2017.12.085

Zhang Q, Zhang Z, Wang Y, Lee D-J, Li G, Zhou X, Jiang D, Xu B, Lu C, Li Y, Ge X (2018b) Sequential dark and photo fermentation hydrogen production from hydrolyzed corn Stover: a pilot test using 11 m^3 reactor. Bioresour Technol 253:382–386. https://doi.org/10.1016/j.biortech.2018.01.017

Zhao F, Slade RC, Varcoe JR (2009) Techniques for the study and development of microbial fuel cells: an electrochemical perspective. Chem Soc Rev 38(7):1926–1939. https://doi.org/10.1039/B819866G

Zhao F, Chu H, Su Y, Tan X, Zhang Y, Yang L, Zhou X (2016) Microalgae harvesting by an axial vibration membrane: the mechanism of mitigating membrane fouling. J Membr Sci 508:127–135. https://doi.org/10.1016/j.memsci.2016.02.007

Zheng Q, Martin GJ, Kentish SE (2016) Energy efficient transfer of carbon dioxide from flue gases to microalgal systems. Energy Environ Sci 9(3):1074–1082. https://doi.org/10.1039/c5ee02005k

Zhong N, Zhao M, Zhong L, Liao Q, Zhu X, Luo B, Li Y (2016) A high-sensitivity fiber-optic evanescent wave sensor with a three-layer structure composed of Canada balsam doped with GeO_2. Biosens Bioelectron 85:876–882. https://doi.org/10.1016/j.bios.2016.06.002

Zhong N, Zhao M, Zhong L, Li S, Luo B, Tang B, Song T, Shi S, Hu X, Xin X, Wu R, Cen Y, Wu Z (2017) Luminous exothermic hollow optical elements for enhancement of biofilm growth and activity. Opt Express 25(6):5876–5890. https://doi.org/10.1364/OE.25.005876

Zhong D, Liao X, Liu Y, Zhong N, Xu Y (2018) Quick start-up and performance of microbial fuel cell enhanced with a polydiallyldimethylammonium chloride modified carbon felt anode. Biosens Bioelectron 119:70–78. https://doi.org/10.1016/j.bios.2018.07.069

Zhong N, Chen M, Luo Y, Wang Z, Xin X, Rittmann BE (2019) A novel photocatalytic optical hollow-fiber with high photocatalytic activity for enhancement of 4-chlorophenol degradation. Chem Eng J 355:731–739. https://doi.org/10.1016/j.cej.2018.08.167

Zhu C, Zhai X, Wang J, Han D, Li Y, Xi Y, Tang Y, Chi Z (2018) Large-scale cultivation of Spirulina in a floating horizontal photobioreactor without aeration or an agitation device. Appl Microbiol Biotechnol 102(20):8979–8987. https://doi.org/10.1007/s00253-018-9258-0

Chapter 10
Membrane Reactors for Renewable Fuel Production and Their Environmental Benefits

Sanaa Hafeez, S. M. Al-Salem, and Achilleas Constantinou

Contents

Abstract In this communication, we discuss various production methods as potential venues targeted towards alternative fuel generation. These will revolve around the Fischer–Tropsch (FT) process and biodiesel and hydrogen generation techniques. The implementation of membrane reactors in the production of fuels will be shown and discussed; and their advantages will be detailed. The main routes of hydrogen production are also detailed, which include autothermal reforming and biological process. This was done to compare the main advantages of various

S. Hafeez
Division of Chemical & Petroleum Engineering, School of Engineering, London South Bank University, London, UK

S. M. Al-Salem
Environment & Life Sciences Research Centre, Kuwait Institute for Scientific Research, Safat, Kuwait

A. Constantinou (✉)
Division of Chemical & Petroleum Engineering, School of Engineering, London South Bank University, London, UK

Department of Chemical Engineering, University College London, London, UK
e-mail: constaa8@lsbu.ac.uk

Z. Zhang et al. (eds.), *Membranes for Environmental Applications*, Environmental Chemistry for a Sustainable World 42, https://doi.org/10.1007/978-3-030-33978-4_10

techniques for the production of hydrogen, as it is noted to be the most desired utility fuel that can serve various purposes. The application of membranes also facilitates an increase in the conversion of desired products while shifting the equilibrium of the reaction and reducing undesired by-products. Membrane reactors also overcome immiscibility issues that hinder conventional reactor processes. Membrane reactors are also demonstrated to reduce the difficulty in separating and purifying impurities, as they couple separation and reaction in one process. This shows drastic economic and energy requirement reductions in the amount of wastewater treatment associated with conventional fuel production reactor. Emphasis is also paid to catalytic membranes used for the production of biodiesel, which can also remove glycerol from the product line as an added advantage.

Keywords Countercurrent membrane · Fischer–Tropsch · Hydrogen · Pyrolysis · Transesterification

Abbreviations

CH_4	Methane
CO	Carbon monoxide
CO_2	Carbon dioxide
FAME	Fatty acid methyl esters
FT	Fischer–Tropsch
GHGs	Greenhouse gases
HC	Hydrocarbon
ML-CMR	Monolith loop catalytic membrane reactor
Ni	Nickel (-based catalyst)
O_2	Oxygen
PSA	Pressure swing absorption
PVA	Poly(vinyl alcohol)
Rh	Rhodium (-based catalyst)
SMR	Steam methane reforming
SO_2	Sulfur dioxide
SPVA	Sulfonated poly(vinyl alcohol)
TCT	Thermochemical treatment

10.1 Introduction

The increase in the global population has led to greater fossil fuel consumption and, as a result, a significant increase of greenhouse gases (GHGs) in the atmosphere. This poses a serious threat to the worldly environment and subsequently impacts climate change. Fossil fuels are the slowest growing source of energy, and their supplies are dwindling daily (Barreto 2018). The price of fossil fuel resources is also increasing due to their heightened demand. The increasing emissions of carbon dioxide (CO_2), sulfur dioxide (SO_2), hydrocarbons (HCs), and volatile hydrocarbons from the burning of fossil fuels lead to significant amount of air pollution and global warming (Shuit et al. 2012). Recent fuel production technologies have focused on utilizing renewable resources, in order to be more sustainable and environmentally friendly. Alternative fuels such as biodiesel and hydrogen and the products from Fischer–Tropsch (FT) process are now commercially produced to offer a solution towards the aforementioned problems.

Hydrogen is a promising fuel for the environment as its only waste product is water. It can be produced from any primary energy resource and can be used for direct combustion in an internal combustion engine or in a fuel cell (Marbán and Valdés-Solís 2007). Furthermore, hydrogen is the only carbon-free fuel and has the highest energy content among all fuel types. It is also deemed globally as an environmentally benign form of renewable energy as opposed to conventional fossil fuels. Moreover, hydrogen can be used for domestic purposes because it has the potential to be transported by typical means, and for it to be fed to stationary fuel cells, it can be stored as a solid hydride, compressed gas, or cryogenic liquid (Nikolaidis and Poullikkas 2017). Hydrogen fuel can be produced from fossil fuels by using methods such as steam reforming, partial oxidation, and autothermal reforming. It can also be produced from nonrenewable resources such as thermochemical treatment (TCT) and biological processes and water splitting methods.

Biodiesel as a source of energy has received a lot of attention due to the fact that it is renewable and biodegradable and can deliver better quality of exhaust gas emissions (Lu et al. 2007; Wang et al. 2009). Biodiesel is a mixture of monoalkyl esters of long-chain fatty acids derived from renewable lipid feedstocks, for example, vegetable oils and animal fats. Biodiesel has demonstrated superiority over conventional diesel fuel, due to its higher combustion efficiency, cleaner emissions, higher cetane number, biodegradability, higher flash point, and better lubrication (Shuit et al. 2012). A variety of methods such as dilution, microemulsion, pyrolysis, and transesterification have been utilized to reduce the viscosity of vegetable oil so that it is suitable for use as a fuel. Transesterification is the most common route used to produce biodiesel, and the reactions include homogeneous catalyzed transesterification, heterogeneous catalyzed transesterification, enzymatic catalyzed transesterification, and supercritical technology.

Membrane reactors have successfully been employed to intensify the renewable fuel production processes (Gutiérrez-Antonio et al. 2018; Pal et al. 2018; Tian et al. 2018). One of the most prominent advantages of the membrane reactor is the fact that the reaction and separation aspects of the process are combined into one single unit. This prevents the need for additional separation and recycling units, and as a result, the process becomes greener and environmentally sustainable. Moreover, membrane reactors can improve the conversion and selectivity of the reactions, reduce mass transfer limitations, and have a greater thermal stability, as opposed to the conventional reactors (Zhang et al. 2018).

In this communication, we will discuss renewable fuel production routes and technologies in detail, which include biofuels, hydrogen, and the FT process. The advantages of membrane reactors will then be highlighted and elaborated and then compared to conventional reactors and their environmental benefits. An in-depth review of membrane reactors for renewable fuel production will then be conducted to assess how conventional processes are intensified.

10.2 Fuel Production Routes

Membrane technology has been applied to biofuels and hydrogen fuels and for FT synthesis. Biofuels are most commonly produced by transesterification; this consists of homogeneous catalytic transesterification and heterogeneous catalytic transesterification (Cannilla et al. 2018). Hydrogen can be produced by using fossil fuels as the feedstock (Wen et al. 2018). This includes steam reforming, partial oxidation, and autothermal reforming. In addition, hydrogen can be produced by biological processes and TCT, such as pyrolysis, gasification, and water splitting operations.

10.2.1 Biofuels Production

There are many well-established methods and technologies for producing biodiesel fuel. It has been found that vegetable oils and animal fats are suitable for alteration to reduce their viscosities so that they can be used as diesel engine fuels (Abbaszaadeh et al. 2012). Typically, biofuels can be obtained by direct use and blending (Keskin et al. 2008), microemulsions (Ramadhas et al. 2004), pyrolysis (Yusuf et al. 2011), and transesterification (Aca-Aca et al. 2018). However, transesterification is commonly used to produce biofuels in membrane reactors.

The transesterification of oils (triglycerides) with alcohol produces biodiesel (fatty acid alkyl esters, FAAE) as the main product and glycerine as the by-product. Figure 10.1 illustrates the transesterification reaction. The conversion of triglycerides to diglycerides takes place first, which is subsequently followed by

CH_2-OOC-R_1				R_1-COO-R'		CH_2-OH
CH_2-OOC-R_2	+	3R'OH	Catalyst ⇄	R_2-COO-R'	+	CH_2-OH
CH_2-OOC-R_3				R_3-COO-R'		CH_2-OH
Glyceride		Alcohol		Esters		Glycerol

Fig. 10.1 Transesterification reaction of glyceride with alcohol (Ma and Hanna 1999). (Reprinted with permission of Elsevier from Ma and Hanna 1999)

the conversion of diglycerides to monoglycerides and then of monoglycerides to glycerol, and this yields one methyl ester molecule from each glyceride at each step (Ma and Hanna 1999). The transesterification reaction can take place with a homogeneous or heterogeneous catalyst. A homogeneous catalyst has the same phase as the reactants used, which in this case is liquid. On the contrary, if the catalyst is present in a different phase, then it is a heterogeneous catalytic reaction. Commercial biodiesel is typically produced by homogeneous catalyzed transesterification; this is because it has a lower production cost (Sharma et al. 2009).

Homogeneous Catalytic Transesterification

Homogeneous catalysts for transesterification can be classified into basic and acidic catalysts (Bing and Wei 2019). The transesterification reaction using basic catalysts often needs raw materials of a high purity and requires an additional separation of the catalyst, products, and side products at the end of the reaction. Biodiesel is typically produced using a homogeneous base catalyst such as alkaline metal alkoxides and hydroxides and sodium or potassium carbonates. Mainly sodium or potassium hydroxides have been used for the basic methanolysis reaction, within a concentration range of 0.4–2% w/w of oil. Homogeneous base catalysts are often preferred to be used in industry due to their high conversions and catalytic activity and the fact that they are widely available and economical to use (Abbaszaadeh et al. 2012; Aransiola et al. 2014). Transesterification reactions using base catalysts are conducted at low temperatures and pressures (333–338 K and 1.4–4.2 bar) with catalyst concentrations of (0.5–2 wt%) (Abbaszaadeh et al. 2012; Lotero et al. 2006).

Homogeneous base catalysts limit the process because of the sensitivity to the purity of the reactants, free fatty acid content, as well as to the water concentration of the sample. When there is a substantial amount of free fatty acids and water present in the oil, the oil is converted to soap as opposed to biodiesel. The free fatty acids present in the oil will react with the base catalyst to aid the production of soaps, which inhibits the separation of biodiesel, glycerine, and wash water (Meher et al. 2006). The presence of water makes the reaction change slightly to saponification, and as a result, the base catalyst is used to produce the soap and so the catalyst efficiency decreases. The accumulation of soap leads to an increase in viscosity and gel formation, which diminishes the ester yield and makes the removal of glycerol challenging. Hence, the side reactions such as hydrolysis and saponification should be kept to a minimum, in order to enhance catalyst productivity (Enweremadu and Mbarawa 2009).

Another type of homogeneous catalyst for the transesterification reaction is an acid catalyst. This type of catalyst is well suited for feedstocks which have a high free fatty acid content which are of a lower grade and inexpensive. The types of acid catalysts typically used are sulfuric, hydrochloric, sulfonic, and phosphoric acids. These types of catalysts can produce customized biodiesel, as the properties of the fuel can be modified based on the fatty acids existing in the feed and subsequently the fatty esters found in the product (Kiss 2009). Acid-catalyzed homogeneous transesterification begins by mixing the oil directly with the acidified alcohol, which allows separation and transesterification to occur simultaneously in one single step, with the alcohol playing the role of both solvent and esterification reagent (Cerveró et al. 2008). Using excel alcohol in the reaction leads to a reduction in the reaction time needed for the acid catalyzed homogeneous reaction. Therefore, Bronsted acid catalyzed transesterification requires the use of high catalyst concentration and a high molar ratio so as to shorten the reaction time (Enweremadu and Mbarawa 2009).

Acid catalyzed homogeneous transesterification demonstrates superiority over base catalyzed transesterification due to its low susceptibility to the presence of free fatty acids in the feedstock. On the other hand, acid catalyzed transesterification is highly sensitive to the presence of water. For example, it has been observed that 0.1 wt% of water in the reaction mixture can affect the ester product yields in the transesterification of vegetable oil with methanol, with the reaction nearly fully inhibited at 5 wt.% water concentration (Cerveró et al. 2008). In addition, acid catalyzed homogeneous transesterification can lead to equipment corrosion, issues with recycling, formation of by-products, increased reaction temperatures, long reaction times, slow rate of reaction, and a weak catalytic activity (Di Serio et al. 2007; Goff et al. 2004).

Heterogeneous Catalytic Transesterification

Heterogeneous catalysts demonstrate superiority over homogeneous catalysts due to their ease of separation from the reaction mixture and reuse. In addition, using heterogeneous catalysts for transesterification reactions does not cause the production of soap (Wang and Yang 2007). Lower production costs and higher efficiencies can be achieved with the use of these catalysts due to the elimination of several process steps such as washing/recovery of biodiesel/catalyst. The heterogeneous catalytic transesterification process can operate in extreme reaction conditions, between 70 and 200 °C to obtain a product yield of greater than 95% using MgO, CaO, and TiO_2 catalysts (Singh and Fernando 2007). An economic assessment of homogeneous and heterogeneous processes in large-scale biodiesel production plants has previously demonstrated the benefits of heterogeneous catalytic processes with regard to higher biodiesel yields and higher glycerine purities, as well as low catalyst costs and maintenance (Kiss et al. 2010).

Heterogeneous catalysts for transesterification can be classified into solid base or solid acid. Majority of the heterogeneous solid catalysts are base or basic oxides, as they are more active than the solid acid catalysts. Basic zeolites, alkaline earth metal oxides, and hydrotalcites are the most prominent solid base catalysts used for the transesterification reaction (Kouzu and Hidaka 2012). Solid base catalysts have demonstrated higher activity than the solid acid catalysts (Abbaszaadeh et al. 2012). Metal oxide catalysts such as CaO and MgO are relatively cheap, and if they have a high catalytic activity and stability, utilizing them as catalysts would be economically desirable to produce biodiesel. Nevertheless, CaO has been found to leach into the reaction mixture, and as a result the metal ions would have to be extracted from the product by water washing, and so the benefits of using a heterogeneous catalyst would be gone. Despite this, CaO is still predominantly used as a solid base catalyst and has shown a long catalyst lifetime, high activity, and low methanol solubility and does not require extreme operating conditions (Liu et al. 2008).

Heterogeneous solid acid catalysts have a variety of acid sites with varying strengths of Bronsted or Lewis acidity, as opposed to homogeneous acid catalysts. Solid acid catalysts are unaffected by free fatty acid content, allow simultaneous esterification and transesterification (Dalai et al. 2006) and easy catalyst removal from product stream, and prevent corrosion (Patil and Deng 2009). Typical solid acid catalysts used for the transesterification reaction are Nafion NR50, sulfated zirconia, and tungstated zirconia due to the acidic strength of the active sites. The catalyst which depicts a higher selectivity towards methyl esters and glycerol is Nafion as it has the strongest acid strength (Abbaszaadeh et al. 2012).

10.2.2 Hydrogen Production

Hydrogen can be produced from a primary energy source, such as fossil fuels, and can then be used as a fuel either for direct combustion in an internal combustion engine or in a fuel cell. Another method of producing hydrogen is from renewable resources, which can be from biomass or water (Edrisi and Abhilash 2016). If biomass is used as the feedstock, then hydrogen can be obtained by means of thermochemical and biological processes. Thermochemical processes largely consist of pyrolysis, gasification, combustion, and liquefaction, whereas biological processes consist of direct and indirect bio-photolysis, dark fermentation, photo-fermentation, and sequential dark and photo-fermentation. More recent hydrogen production methods consist of electrolysis, thermolysis, and photo-electrolysis, which require water as the only raw material. The various routes for hydrogen production are depicted in Fig. 10.2 (Nikolaidis and Poullikkas 2017).

Production of Hydrogen from Fossil Fuels

The main method of producing hydrogen from fossil fuels is hydrocarbon reforming and pyrolysis. Until now, hydrogen was produced from 48% natural gas, 30% from heavy oils and naphtha, and 18% from coal. The production of hydrogen from fossil fuels has remained as the dominant method in the world hydrogen supply because the production costs are strongly correlated to the fuel prices which are maintained at an acceptable level (Nikolaidis and Poullikkas 2017).

The steam reforming method essentially consists of an HC and steam reacting together to form hydrogen and carbon oxides by using a catalyst. The main steps in this reaction are synthesis gas (syngas) production, water–gas shift (WGS), and

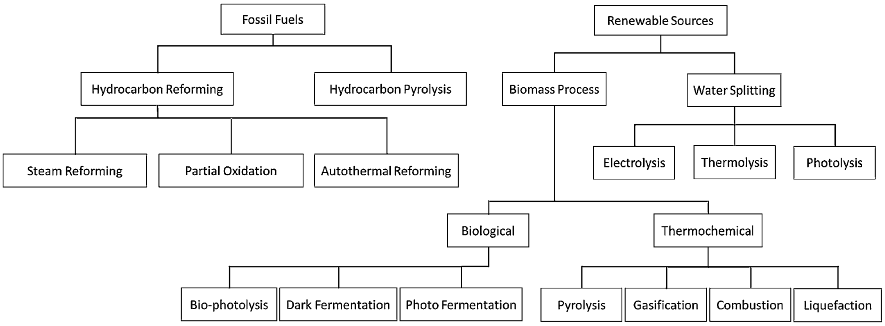

Fig. 10.2 Hydrogen production routes (Nikolaidis and Poullikkas 2017). (Reprinted with permission of Elsevier from Nikolaidis and Poullikkas 2017)

methanation or gas purification. The raw materials used for this reaction can be methane, natural gas, combinations of light hydrocarbons, and light and heavy naphtha (Balthasar 1984). The steam reforming reaction conditions are high temperatures, pressures (up to 3.5 MPa), and steam-to-carbon ratios of 3.5. This is so that the desired hydrogen purity can be achieved, as well as reducing the coke formation on the solid catalyst surface (Ersöz 2008). Once reforming is complete, the product stream is passed into a WGS reactor and a heat recovery step where the CO reacts with the steam to produce more hydrogen. Finally, the mixture is taken through CO_2 removal and methanation, or through pressure swing absorption (PSA), which allows a hydrogen purity of approximately 100% to be obtained (Steinberg and Cheng 1989). The main chemical reactions that take place for steam reforming are depicted below with respect to each unit operation as follows (Holladay et al. 2009; Nikolaidis and Poullikkas 2017):

$$\text{Reformer}: C_nH_m + nH_2O \rightarrow nCO + \left(n + \frac{1}{2}m\right)H_2 \quad (10.1)$$

$$\text{WGS reactor}: CO + H_2O \rightarrow CO_2 + H_2 \quad (10.2)$$

$$\text{Methanator}: CO + 3H_2 \rightarrow CH_4 + H_2O \quad (10.3)$$

Steam methane reforming (SMR) is the most widely used method for hydrogen production, with a conversion efficiency of approximately 74–85%. Steam and methane are reacted at 850–900 °C in the presence of a nickel-based catalyst to produce syngas, and a hydrogen purity of 99.99% can be achieved when PSA is utilized to remove the hydrogen (Chen et al. 2008).

Partial oxidation method is another route for converting steam, oxygen, and hydrocarbons to hydrogen and carbon oxides. The non-catalytic partial oxidation of hydrocarbons usually occurs with flame temperatures of around 1300–1500 °C to ensure that complete conversion and prevention of soot formation is achieved (Rostrup-Nielsen 2003). The catalytic process operates at 950 °C, with the feedstock ranging from methane to naphtha (Steinberg and Cheng 1989). Once sulfur has been removed from the HC feedstock, pure oxygen (O_2) is required to partially oxidize the HCs, and the resultant syngas product is upgraded in the same way as the steam reforming product (Balthasar 1984). Although using catalysts for partial oxidation can lead to lower reaction temperatures, there are issues with temperature control due to coke and hot spot formation because of the exothermic nature of the reactions. When using natural gas as the feedstock, the catalysts of choice tend to be nickel (Ni) or rhodium (Rh). However, Ni catalysts have a strong tendency to coke, and the cost of Rh has increased over the years (Holladay et al. 2009). The catalytic and non-catalytic reactions are depicted below (Nikolaidis and Poullikkas 2017):

$$\text{Reformer (catalytic)} : C_nH_m + \frac{1}{2}nO_2 \rightarrow nCO + \frac{1}{2}mH_2 \tag{10.4}$$

$$\text{Reformer (non}-\text{catalytic)} : C_nH_m + nH_2O \rightarrow nCO + \left(n + \frac{1}{2}m\right)H_2 \tag{10.5}$$

$$\text{WGS reactor} : CO + H_2O \rightarrow CO_2 + H_2 \tag{10.6}$$

$$\text{Methanator} : CO + 3H_2 \rightarrow CH_4 + H_2O \tag{10.7}$$

The autothermal reforming (ATR) method combines the exothermic partial oxidation reaction with the endothermic steam reforming reaction to enhance hydrogen production. The reforming and oxidation reactions happen simultaneously in the ATR reactor (Eq. 10.8) (Nikolaidis and Poullikkas 2017):

$$C_nH_m + \frac{1}{2}nH_2O + \frac{1}{4}nO_2 \rightarrow nCO + \left(\frac{1}{2}n + \frac{1}{2}m\right)H_2 \tag{10.8}$$

The oxygen-to-fuel ratio and the steam-to-carbon ratio must be carefully controlled in order to control the reaction temperature and product gas composition while preventing soot formation (Holladay et al. 2009). Using methane (CH_4) as the HC fuel for the ATR process, thermal efficiencies of 60–75% can be achieved, while the optimum reaction conditions are around 700 °C for a steam-to-carbon ratio of 1.5 and an oxygen-to-carbon ratio of 0.45 where a maximum hydrogen yield of 2.5 can be achieved (Ersöz 2008; Holladay et al. 2009). This process can be expected to be favorable with the gas-to-liquid industry because of the desirable gas composition for the FT process, the lower capital cost, and the potential for economies of scale (Wilhelm et al. 2001).

The production of hydrogen from the pyrolysis of HC is also another common process, where the HC is subjected to thermal decomposition to produce hydrogen. The general reaction follows the route shown below:

$$\text{Hydrocarbon species } (C_nH_m) \rightarrow nC + \frac{1}{2}mH_2 \tag{10.9}$$

The pyrolysis process eliminates the WGS reaction and CO_2 separation step, and as a result, the capital investment of these large-scale plants is lower when compared to the steam reforming or partial oxidation methods. This leads to an approximately 25–30% reduction in the hydrogen production cost (Muradov 1993).

Production of Hydrogen from Renewable Resources

Even though HCs are the most common feedstock for hydrogen generation, it is imperative to investigate renewable and sustainable technologies due to the numerous environmental benefits of doing so. The depletion of fossil fuels and the increase of GHGs emissions have led to the increase of finding alternative methods to produce hydrogen. Hydrogen production from biomass and water splitting will be briefly discussed.

Biomass can undergo thermochemical processes to produce hydrogen; these processes are mainly pyrolysis and gasification. These processes are environmentally sustainable as they have zero GHG emissions (Fremaux et al. 2015). The pyrolysis of biomass consists of thermal degradation of the feedstock in the absence of oxygen under reaction conditions of 650–800 K and 0.1–0.5 MPa, to produce bio-oil, solid char, and gaseous products. Pyrolysis of biomass can be categorized further into fast pyrolysis and slow pyrolysis. Slow pyrolysis is often not conducted because the main product of this process tends to be solid charcoal. In fast pyrolysis, the biomass feedstock is heated very quickly under anaerobic conditions to produce a vapor and a dark-brownish bio-oil product. The gaseous products contain H_2, CH_4, CO, CO_2, and other gases depending on the biomass feedstock used (Jalan and Srivastava 1999; Ni et al. 2006). Hydrogen can be produced directly using fast or flash pyrolysis, if high temperatures and a sufficient volatile phase residence time are given as follows (Ni et al. 2006):

$$\text{Biomass} + \text{heat} \rightarrow H_2 + CO + CH_4 + \text{other products} \tag{10.10}$$

The CH_4 produced can be further upgraded by SMR to produce additional hydrogen:

$$CH_4 + H_2O \rightarrow CO + 3H_2 \tag{10.11}$$

To enhance the hydrogen production, the WGS reaction can be applied as follows:

$$CO + H_2O \rightarrow CO_2 + H_2 \tag{10.12}$$

Biomass gasification is another thermochemical route for producing hydrogen. Here, the biomass can be gasified at high temperatures in excess of 1000 K; the partial oxidation of biomass will take place to produce gas and solid char. The charcoal will subsequently be reduced to H_2, CO, CO_2, and CH_4. This can be expressed as:

$$\begin{aligned}\text{Biomass} + \text{heat} + \text{steam} \rightarrow\ & H_2 + CO + CO_2 + CH_4 \\ & + \text{light and heavy hydrocarbons} + \text{char}\end{aligned} \tag{10.13}$$

The gasification of biomass takes place in the presence of oxygen (O_2) gas, as opposed to the pyrolysis of biomass reaction. Furthermore, the main aim of the gasification process is to produce predominantly gaseous products, and these products can then be further upgraded to produce hydrogen by steam reforming, and the process can be further improved by using the WGS reaction. Biomass feedstock which has a moisture content of less than 35% is well suited to the gasification process (Demirbaş 2002).

In addition to thermochemical processes, biological processes have also been developed to minimize waste and to enhance environmental sustainability. Majority of these processes operate at standard conditions, and so they are deemed to be more environmentally friendly and sustainable. In addition, these processes make use of renewable energy resources, and they contribute to waste recycling as the feedstocks they often require are waste materials (Das and Veziroğlu 2001). The main biological processes for hydrogen generation are direct and indirect photolysis, photo- and dark fermentations, and multistage or sequential dark and photo-fermentation.

10.2.3 *Fischer–Tropsch (FT) Synthesis*

The FT process converts synthetic gas to HCs. Figure 10.3 shows how the FT process can be utilized to produce liquid fuels (Hafeez et al. 2018). Essentially, any carbon source can be used as the feedstock for the FT process to obtain alternative fuels. The FT process can produce a wide range of products which can then be upgraded to obtain the desired hydrocarbon fractions. The FT reaction is highly exothermic and makes use of heterogeneous catalysts with reaction conditions of 300–350 °C and high pressures (Guettel et al. 2008).

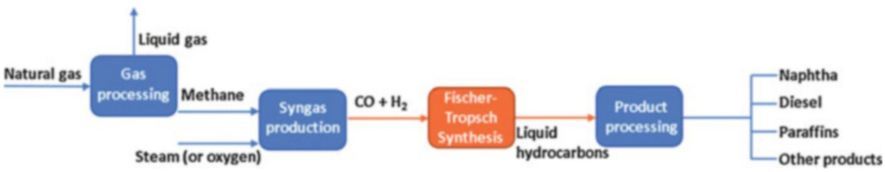

Fig. 10.3 Schematic showing how liquid fuels can be obtained via FT synthesis (Hafeez et al. 2018). (Reprinted with permission of Royal Society of Chemistry from Hafeez et al. 2018)

Current FT operates at low temperature for the production of liquid fuels. The basic FT reaction produces paraffinic or olefinic chains:

$$nCO + (2n + 1)H_2 \rightarrow C_nH_{2n+2} + nH_2O \tag{10.14}$$

$$nCO + 2nH_2 \rightarrow C_nH_{2n} + nH_2O \tag{10.15}$$

Equation 10.14 is highly exothermic and has a reaction enthalpy of −150 kJ per mole of converted CO. The CO product can be converted to CO_2 and hydrogen by the WGS reaction as seen in Eq. 10.12 (Guettel et al. 2008). Typical catalysts used for the FT process are iron, cobalt, and ruthenium. However, the high cost of ruthenium means that iron and cobalt are most commonly used. One limitation of using an iron catalyst is its inhibition by the side product of water. On the contrary, its activity for the WGS reaction permits the use of CO_2-containing gases or hydrogen exhausted syngas mixtures. Cobalt catalysts are found to have higher activity and longer catalyst lifetime when compared to iron catalysts. On the other hand, cobalt tends to be more expensive than iron (Guettel et al. 2008; Van Der Laan and Beenackers 1999).

10.3 Membrane Reactors Versus Conventional Systems for Environmental Applications

A membrane reactor can be defined as a device that couples reaction and separation within one single unit. Due to the significant problems faced with regard to the separation and purification of fatty acid methyl esters (FAME) from impurities, novel research into membrane reactors has been conducted in order to circumvent this costly problem, as well as optimize the production of biodiesel. According to a research carried out by Cao et al. (2008b) on methanol recycling a membrane reactor for the production of biodiesel, it was found that using an inorganic membrane in the membrane reactor could remove the desired constituents during the reaction from the oil. The addition of a membrane also facilitates an increase in conversion, as the products permeate through the membrane and can be removed. This shifts the equilibrium in the forward reaction resulting in a higher yield of FAME while reducing the amount of undesired side products. In addition, membrane reactors attain high conversion rates when compared to conventional ones due to the removal of undesired by-products (Baroutian et al. 2011).

The issue of immiscibility of methanol and oil arises in a conventional reactor as it leads to limited mass transfer (Dubé et al. 2007). And the two-phase nature of the mixture between the respective compounds is fundamental for the success of the membrane reactor. This is because the membrane acts as a barrier allowing methanol to permeate through while preventing the oil droplets that were emulsified in the methanol from passing through due to its larger molecular size relative to the pore size of the membrane (Baroutian et al. 2011). As a result of this separation via a membrane, the mass transfer is not limited as was the case with the conventional reactor.

Using conventional reactors for biodiesel production requires a purification stage as the biodiesel produced must be of a certain purity. The primary method of purifying FAME is by water washing the nonpolar phase, which involves the removal of any residual catalyst and small quantities of glycerol, as well as other impurities which are soluble in water. However, the nonpolar phase of FAME is not easily removed from the water layer. Therefore, it requires more expenditure on separation equipment. This leads to the production of a significant amount of wastewater that will need further treatment. In contrast, the membrane reactor was found to have greatly reduced the difficulty in separating and purifying FAME from impurities, as evidenced by the research of Cao et al. (2008b) showing a drastic reduction in the amount of water washing to purify FAME (Atadashi et al. 2011).

The use of a membrane reactor is more economically viable than conventional ones. This is linked to the fact that such processes are intensified by combining the reaction and separation aspects in one unit. This can allow for the potential reductions in separation and recycling units, which would result in the process becoming less energy intensive. Therefore, efficiency increase is also anticipated. Furthermore, the intrinsic properties of inorganic membranes make them possess a high thermal threshold. Due to their thermal stability, membrane reactors can be used for reactions that are highly exothermic (Dubé et al. 2007).

As a result of the biodiesel production process being intensified with the operation of a catalytic membrane reactor, the energy consumption has been significantly reduced. An experiment conducted by Dubé et al. (2007) stated that the highest reported reaction temperature used in the membrane reactor was 70 °C; in comparison with using a solid basic catalyst or solid acid catalyst for transesterification, the reaction temperatures are in the ranges of 180–200 °C (Jitputti et al. 2006; Di Serio et al. 2006) and 200–300 °C (Chen et al. 2007; Furuta et al. 2004; Jitputti et al. 2006). This shows that less electricity is required to be generated for energy for the membrane reactor by burning fossil fuels, which is detrimental to the welfare of the environment. Burning fossil fuels are notorious for producing undesired particulates into the air, such as carbon dioxide and sulfur dioxide; these emissions play a direct role in the production of acid rain which go on to have negative effects on plants and aquatic animals and damage infrastructures. With the use of membrane reactors, these harmful effects on the environment are minimized (Kampa and Castanas 2008).

The issue of large amounts of wastewater produced due to the separation and purification stages is an environmental concern. The increase of wastewater effluents could potentially lead to an increase in the quantity of chemicals and solvents that are toxic to the environment (Shuit et al. 2012). However, if 20 million tons per year of biodiesel is produced (Licht and Agra 2007) with a density of 900 kg/m^3 (Knothe et al. 2005), the amount of wastewater that is produced by conventional separation methods would be 59 billion gallons. On the other hand, by using a membrane reactor, the amount of wastewater will significantly reduce to 12 billion gallons. Therefore, a membrane reactor could potentially make the purification step and the water washing procedure redundant as using a catalytically active membrane would not require water washing for purification. Therefore, the problem of wastewater can be dealt with. This in turn would drastically decrease the probability of chemicals and solvents harming the environment, due to the contaminants that come with wastewater. Furthermore, glycerol removal can be done via the use of a membrane reactor separating it from the FAME phase during the reaction which makes the requirement of water washing all the more unnecessary (Shuit et al. 2012).

10.4 Membrane Reactors for Renewable Fuel Production

Typically, a membrane reactor can be classified into four distinct parts. These are the design of the reactor (e.g., distributor, extractor, or contactor), type of membrane used (e.g., porous, organic, or inorganic), catalyst presence in the membrane, and finally, the reaction that is taking place inside the membrane reactor (Mueller et al. 2008). Furthermore, this type of reactor configuration has been proven to enhance the product yield and selectivity of the reaction (Marcano and Tsotsis 2002). Figure 10.4 represents a schematic comparing conventional reaction system with a combined membrane and reactor system (Lipnizki et al. 1999). The main benefit of using the combined membrane and reactor system is the fact that the capital and operating costs are significantly reduced because an intermediate separation step is not required (Marcano and Tsotsis 2002). Membrane technology has recently been applied to the production of renewable fuels due to its advantages over the conventional reactors.

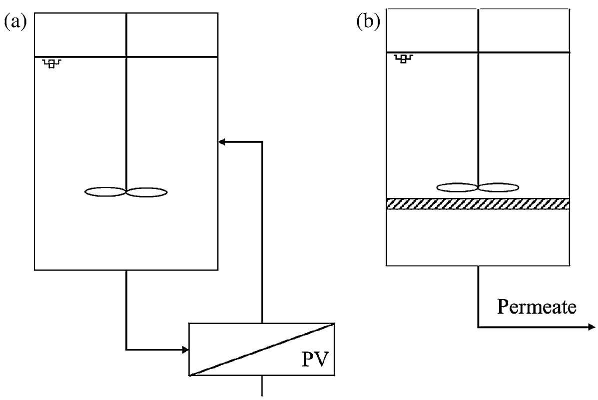

Fig. 10.4 Schematic showing a membrane reactor; (**a**) a conventional system; and (**b**) a combined membrane reactor system (Lipnizki et al. 1999). (Reprinted with permission of Elsevier from Lipnizki et al. 1999)

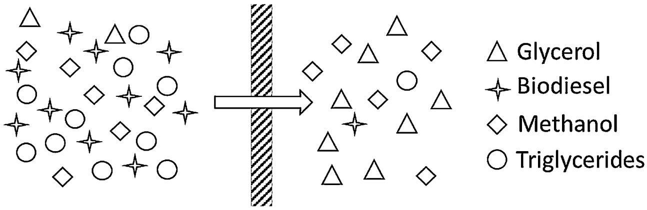

Fig. 10.5 Diagram showing how a membrane can remove glycerol from the product stream (Shuit et al. 2012). (Reprinted with permission of Elsevier from Shuit et al. 2012)

10.4.1 Membrane Reactors for Biofuels Production

For biodiesel production, the most important role of the membrane is to either remove the glycerol from the product (Guerreiro et al. 2006; Saleh et al. 2010) or to preserve the unreacted glycerides in the membrane (Baroutian et al. 2011; Dubé et al. 2007). The two main methods of producing biodiesel using membrane reactors is separation by oil droplet size (Cao et al. 2008a, 2008b) and by utilizing catalytic membranes (Guerreiro et al. 2006, 2010; Shao and Huang 2007). Membrane separation based on oil droplet size involves a microporous membrane which is typically a ceramic or microporous membrane (Fig. 10.5) (Shuit et al. 2012). A study conducted by Baroutian et al. (2010) has demonstrated this particular separation. Methanol recovery during the transesterification of palm oil in a ceramic membrane reactor using TiO_2/Al_2O_3 catalyst was also demonstrated. The methanol molecules were able to pass through the membrane with the products because of its small molecular size. It is necessary to recover the methanol as it is one of the most essential reactants needed for transesterification. The ceramic membrane was therefore attached to a simple distillation unit to remove the methanol from the membrane permeate stream. In a further study conducted by Baroutian et al. (2011), a packed-bed membrane reactor was used for the production of biodiesel using a potassium hydroxide catalyst supported on palm shell activated carbon. The results showed that the highest conversion of palm oil to biodiesel in the reactor was found at 70 °C utilizing 157.04 g of catalyst per unit volume of the reactor and a cross-flow circulation velocity of 0.21 cm/s. The biodiesel product obtained was compared with standard specifications based on the physical and chemical properties. It was concluded that high-quality palm oil diesel was obtained by using this membrane reactor configuration.

Dubé et al. (2007) developed a two-phase membrane reactor to produce biodiesel from canola oil and methanol. The transesterification reaction of canola oil was achieved via acid or base catalysis. The results showed that increasing the temperature, catalyst concentration and the feed flow rate would significantly increase the conversion of oil to biodiesel. Furthermore, the two-phase membrane reactor was highly useful in separating the unreacted canola oil from the biodiesel product which resulted in biodiesel of a high purity and maintained the reaction equilibrium to the product side.

Cao et al. (2008a) conducted a high-purity fatty acid methyl ester production from different lipids such as canola, soybean, palm, and yellow grease lipids, combined with methanol using a membrane reactor. The membrane system consisted of reaction and separation within one single unit, which allowed a continuous mixing of the raw materials, and kept a desirable molar ratio of methanol to lipid in the reaction loop while maintaining two phases during the reaction. The biodiesel was analyzed using GC, and it was found that the product quality was high. In addition, the quality of biodiesel was significantly affected by the composition of the fatty acids in the feedstock. Cao et al. (2008a) further utilized a membrane reactor to produce a permeate stream which readily phase separates at room temperature into a fatty acid methyl ester (FAME)-rich nonpolar phase and a methanol- and glycerol-rich polar phase. The results showed that the highest recycle ratio of 100% produced a FAME concentration of between 85.7 and 92.4 wt% in the FAME-rich nonpolar phase. Furthermore, decreasing the methanol/oil ratio to 10:1 in the reaction system while keeping a FAME production rate of 0.04 kg/min resulted in a FAME product with a high purity.

Another method of producing biodiesel is by using a catalytic membrane. This involves a dense nonporous polymer membrane, for example, poly(vinyl alcohol) (PVA). This type of configuration works based on the interaction between the target component and the polymer functional groups of the membrane (Shuit et al. 2012). Guerreiro et al. (2006) investigated the transesterification of soybean oil over sulfonic acid (functionalized) polymeric membranes using solid catalysts at 60 °C and atmospheric pressure. The catalytic membrane used for the transesterification studies was a Nafion one with ion-exchange resins and poly(vinyl alcohol) membranes containing sulfonic groups. The results showed that PVA polymers cross-linked with sulfosuccinic acid and are more active than the commercial Nafion membranes used due to the higher content of sulfonic groups. A further study conducted by Guerreiro et al. (2010) showed that the most desirable results were obtained with a hydrophilic membrane using solid base catalysts. In addition, the same sample of the membrane was utilized in seven consecutive runs to assess the catalyst stability. It was found that these catalysts were most active in the transesterification of soybean oil with methanol and can also be reused for many runs without the risk of further reactivation.

Shi et al. (2010) developed a novel organic–inorganic hybrid membrane as a heterogeneous acid catalyst for biodiesel production prepared from zirconium sulfate ($Zr(SO_4)_2$) and sulfonated poly(vinyl alcohol) (SPVA). It was found that the $Zr(SO_4)_2$ particles were better dispersed in SPVA matrix as a result of the stronger interaction between $Zr(SO_4)_2$ and SPVA compared with $Zr(SO_4)_2$/poly(vinyl alcohol) (PVA) hybrid membrane. It was found that the conversions of free fatty acid (FFA) in acidified oil were 94.5% and 81.2% for $Zr(SO_4)_2$/SPVA and $Zr(SO_4)_2$/PVA catalytic membranes, respectively. Furthermore, the $Zr(SO_4)_2$/SPVA catalytic membrane has a higher performance to the $Zr(SO_4)_2$/PVA catalytic membrane.

Aca-Aca et al. (2018) conducted a catalytic performance study for biodiesel production by a novel catalytically active membrane from polyacrylic acid (PAAc) cross-linked with 4,40-diamino-2,20-biphenyl sulfonic acid (PAAc-BDSA). It was found that the methyl ester yield follows the order 90, 92, and 73% for PVA-88-SSA, PVA-99-SSA, and PAAc-BDSA, respectively. Higher diffusion coefficients and sorption of methanol and glycerol by PAAc-BDSA membrane make it suitable to use in membrane reactors for biodiesel production and glycerol separation simultaneously.

Zhu et al. (2010) prepared poly(styrene sulfonic acid) (PSSA)/poly(vinyl alcohol) (PVA) blend membranes by solution casting and were employed as heterogeneous acid catalysts for biodiesel production from acidic oil obtained from waste cooking oil (WCO). The membranes were annealed at varying temperatures in order to increase their stability. The results of esterification of acidic oil show that the conversion was higher with the PVA content in the membrane at a constant PSSA content. Furthermore, the catalytic membrane thickness had negligible effect on the conversion at the end. The membrane annealed at 120 °C exhibited superior catalytic performance among the membranes, with a stable conversion of 80% with the runs.

Catalytic membranes possess the ability to incorporate a catalyst depending on its formulations and functionality. A membrane without the incorporated catalyst can also be referred to as a catalytically *inert* membrane where the catalyst is added to the reactants, but not implanted inside the membrane (Buonomenna et al. 2010). The main catalytically inert membranes found in biodiesel production are the filtanium ceramic membranes (Cao et al. 2008a, b), $Ti/O_2/Al_2O_3$ in ceramic membrane (Baroutian et al. 2010, 2011), and carbon membrane (Dubé et al. 2007) with the separation principle based on the oil droplet sizes. The pore sizes of these membranes can vary from 0.02 to 0.05 μm (Baroutian et al. 2010). The catalysts used for the membranes without the incorporated catalyst include sulfuric acid (H_2SO_4) (Dubé et al. 2007) and potassium hydroxide/sodium hydroxide solution (KOH/NaOH) (Baroutian et al. 2010). Firstly, a predetermined quantity of oil and a homogeneous mixture of methanol/KOH are passed into a mixing vessel for premixing. The reaction mixture is then heated to the target reaction temperature, before being passed into the membrane reactor. The permeate stream is comprised of biodiesel, methanol, glycerol, and catalysts (Baroutian et al. 2010; Dubé et al. 2007). Oil droplets which have a pore size larger than the membrane pore size (12 μm) (DeRoussel et al. 2001) are trapped on the retentate side and are subsequently recycled back to the mixing vessel (Cao et al. 2008b). The permeate stream can be separated into polar and nonpolar phases. The nonpolar phase is made up of methanol, trace amounts of diglycerides, and catalysts (Cao et al. 2008a, b). On the other hand, the polar phase is comprised of glycerol, methanol, catalysts, and biodiesel (Cao et al. 2008b). It has been observed that this type of catalytic membrane reactor is able to achieve an oil-to-biodiesel conversion of $\geq$90% for both H_2SO_4 and KOH catalysts (Dubé et al. 2007). In addition, using activated carbon as a catalyst support resulted in an increase in conversion by 93.5% (Rahimpour 2015). The methanol that permeates through the membrane is recycled back to the reactor to lessen the overall methanol-to-oil molar ratio (Cao et al. 2007). Methanol can be recycled back to the reactor by distilling the methanol from the nonpolar phase and direct recycling of the polar phase (Rahimpour 2015).

Baroutian et al. (2011) used a packed-bed membrane reactor, which utilized activated carbon as the catalyst support to prevent the permeation of catalysts through the membrane. The catalyst was prepared by adding activated carbon into a potassium hydroxide (KOH) solution. The mixture was then agitated for a period of 24 h and a temperature of 25 °C. The catalysts were then packed inside the TiO_2/Al_2O_3 membrane reactor. It was reported that for this particular configuration, the oil conversion obtained was higher than that of the membrane reactor with the addition of H_2SO_4 or KOH catalysts (Baroutian et al. 2011).

A membrane which incorporates the catalyst has the catalyst immobilized in the polymeric matrix and is more commonly referred to as a catalytically active membrane. The membrane can be made catalytically active by the heterogenization of the homogeneous catalysts or the incorporation of heterogeneous catalysts inside the polymeric matrix. This particular type of membrane combines the reaction and separation in a single step, which is essentially the same principle of reactive separation (Buonomenna et al. 2010); thus. the membrane can be regarded as a separative reactor (Stankiewicz 2003). Until now, poly(vinyl alcohol) (PVA) membranes are the only conveyed polymer membranes that have been used for biodiesel production (Sarkar et al. 2010). This is due to their high hydrophilicity, good thermal properties, and good chemical resistance (Guan et al. 2006).

10.4.2 Membrane Reactors for Hydrogen Production

Recently, membrane reactors for hydrogen production have gained increasing attention due to their superiority over the conventional reaction systems. Typically, packed-bed membrane reactors (PBMR) have been used for hydrogen production. However, novel systems such as fluidized-bed membrane reactors (FBMR) and micro membrane reactors (MMR) have now been employed due to their better mass and heat transfer (Gallucci et al. 2013).

In a packed-bed membrane reactor, the catalyst is packed in a fixed-bed configuration and is in contact with a permselective membrane. The most popular and widely used configuration is the tubular one, where the catalyst can be packed in the membrane tube (Fig. 10.6a) or in the shell side (Fig. 10.6b) (Gallucci et al. 2013). For multi-tubular membrane reactor configurations, packing the catalyst within the tube is preferred due to construction issues and for bed-to-wall mass and heat transfer limitations which can have damaging effects if the catalyst is placed within the shell side. It is common to use a sweep gas in the permeation side of the membrane to ensure that the permeation hydrogen partial pressure is at the lowest for minimizing the membrane area needed for hydrogen removal. The use of a sweep gas in the permeation side can allow the packed-bed membrane reactor to be used in both cocurrent and countercurrent modes. The countercurrent mode configuration

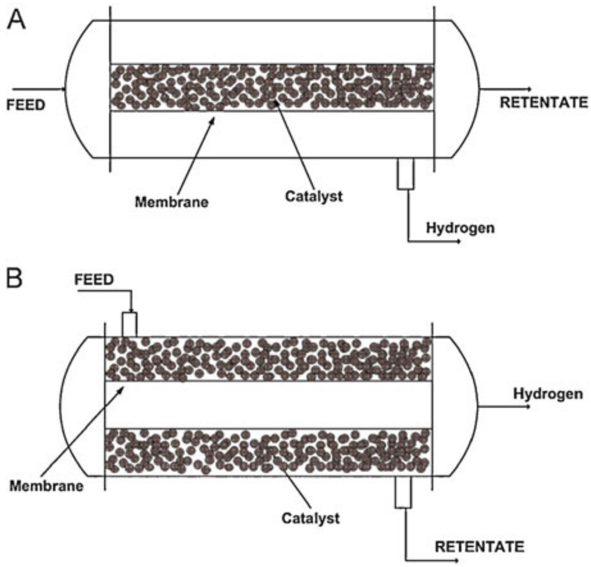

Fig. 10.6 Schematic showing (**a**) catalyst packed in tube and (**b**) catalyst packed in shell (Gallucci et al. 2013). (Reprinted with permission of Elsevier from Gallucci et al. 2013)

can lead to different partial pressure profiles in reaction and permeation sides when compared to the cocurrent mode (Gallucci et al. 2008).

Gallucci et al. (2008) created a mathematical model for a palladium membrane reactor packed with a co-based catalyst. The results were obtained for both co- and countercurrent modes in terms of ethanol conversion and molar fraction versus temperature, pressure, the molar feed flow rate ratio, and axial coordinate. The results demonstrated that cocurrent mode membrane reactor configuration generated higher ethanol conversions as opposed to the countercurrent mode; however, the countercurrent mode allows a larger amount of hydrogen to be extracted from the reaction zone. Basile et al. (2008) studied the steam reforming of methanol by using a dense Pd–Ag membrane reactor and a fixed-bed reactor, and a constant sweep gas flow rate in countercurrent mode was employed. Both reactors were packed with a catalyst based on $CuOAl_2O_3ZnOMgO$ and had an upper temperature limit of around 350 °C. It was found that the catalyst showed high activity and selectivity towards the CO_2 and H_2 formation in the range of temperatures used. It was concluded that the membrane reactor demonstrated higher conversions than the fixed-bed reactor under the same operating conditions. In addition, at an operating temperature of 300 °C and a H_2O/CH_3OH molar ratio greater than 5:1, the membrane reactor achieved a 100% methanol conversion.

The application of a tube in shell configuration is noted to be one of the main methods of increasing the membrane area in the packed bed (Tosti et al. 2008). This has been demonstrated by Buxbaum (2002) where the catalyst is loaded in the shell side of the reactor while the membrane tubes are connected to a collector for the pure hydrogen. Furthermore, it is possible to use a catalyst in a separate chamber, in which case the chamber acts as a pre-reforming zone where the largest temperature profiles are found. This means that the membranes can operate almost isothermally.

Another method of increasing the membrane area per volume of reactor is by using a hollow fiber configuration. Kleinert et al. (2006) conducted the partial oxidation of methane for hydrogen production in a hollow fiber membrane reactor. A phase inversion spinning technique was used to produce the perovskite membranes made from Ba(Co,Fe,Zr)$O_{3\text{-}d}$ (BCFZ) powder. The results demonstrated that a methane conversion and CO selectivity of 82% and 83% were achieved, respectively. Furthermore, the membrane proved to be quite stable under the reaction conditions used. In addition, Maneerung et al. (2016) used a triple-layer hollow fiber catalytic membrane reactor (T-HFCMR) consisting of (1) Ni-based catalyst (outer) layer, (2) porous inorganic support (middle) layer, and (3) ultrathin Pd-based membrane (inner) layer, for the production of hydrogen. It was observed that the high hydrogen permeability of the ultrathin Pd-based membrane led to 84% of the total hydrogen to be separated from the reaction side. Furthermore, the continuous permeation of hydrogen from the reaction side significantly enhanced the reaction conversion. Since the membrane is not exposed directly to the external surface, mechanical damages of the Pd–Ag membrane can be prevented which is beneficial for practical applications.

A more recent approach to produce hydrogen is using fluidized-bed membrane reactors. This consists of a bundle of hydrogen-selective membranes, which are submerged to a catalytic bed and demonstrate a bubble or turbulent flow regime. Fluidized-bed membrane reactors are found to reduce bed-to-wall mass transfer limitations but also enable the reactor to function isothermally. This type of configuration can be used for performing the autothermal reforming of hydrocarbons to produce hydrogen.

A fluidized-bed membrane reactor schematic is shown in Fig. 10.7 to produce hydrogen and methanol (Rahimpour and Bayat 2011). The production of methanol occurs in the inner tube and provides heat to the endothermic side. The cyclohexane dehydrogenation to benzene takes place in the second tube which is coated by a Pd–Ag membrane layer. The hydrogen produced from the dehydrogenation of cyclohexane diffuses into the outer tube/permeation side. The results from this study were compared to those obtained from a thermally coupled membrane reactor at the same reaction operating conditions. It was found that the hydrogen recovery yield and benzene production of the fluidized-bed membrane reactor were 5.6% and 8.52% greater to that of the thermally coupled membrane reactor. This is due to the low pressure drop and the negligible mass and heat transfer limitations in the fluidization process. It was concluded that this membrane reactor configuration is feasible for the production of pure hydrogen (Rahimpour and Bayat 2011). In addition, Spallina et al. (2018) utilized Pd-based membranes for the production of pure hydrogen in a fluidized-bed catalytic reactor for the autothermal reforming of ethanol. It was concluded that the reactor concept is feasible for the production of hydrogen, especially because a hydrogen recovery factor of 70% can be achieved.

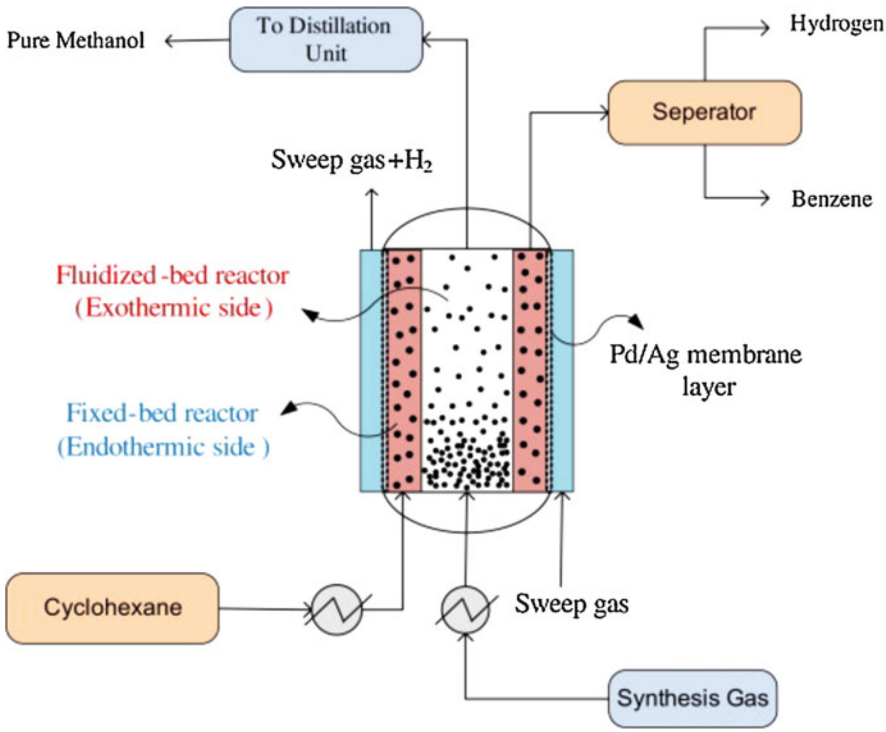

Fig. 10.7 Configuration of a fluidized-bed thermally coupled membrane reactor in cocurrent mode of operation (Rahimpour and Bayat 2011). (Reprinted with permission of Elsevier from Rahimpour and Bayat 2011)

Micro membrane reactors have recently been developed for hydrogen production. This is because membrane microreactors have enhanced mass and heat transfer (Constantinou et al. 2014) because of the shortened length of the microchannels, removal of mass transfer limitations (concentration polarization), and heightened process intensification by integrating various process steps in small-scale process unit (Gallucci et al. 2013). Mejdell et al. (2009a, b, c) compared the performance of the same membrane in varying configurations. It was observed that by using the tubular configuration, the extent of concentration polarization is the limiting step for hydrogen permeation. On the other hand, the same membrane applied in a microreactor configuration, the concentration polarization effect can be totally ignored (Mejdell et al. 2009c). Figure 10.8 shows a depiction of the microchannel reactor configuration used by Bredesen and coworkers (Mejdell et al. 2009b). The reactor is comprised of s-shaped microchannels which have a length of 13 mm and a section of 1 mm × 1 mm. The membranes used are Pd based which have a thickness of less than 3 μm; this type of membrane configuration is able to tolerate differential pressures of greater than 470 kPa.

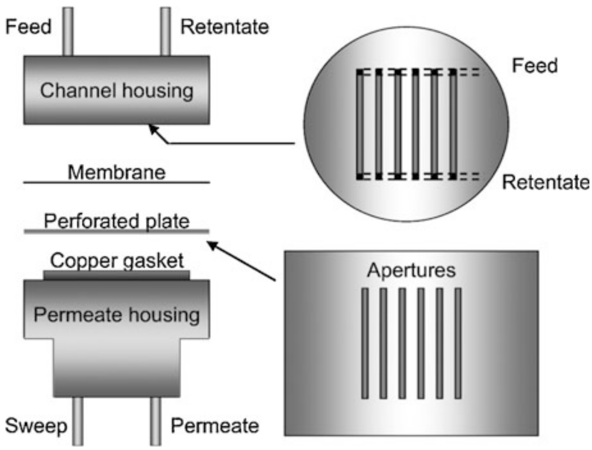

Fig. 10.8 Schematic of the microreactor configuration used by Bredesen for the Pd-based membrane runs (Mejdell et al. 2009b). (Reprinted with permission of Elsevier from Mejdell et al. 2009b)

10.4.3 Membrane Reactors for Fischer–Tropsch Synthesis

Recently, membrane reactors for FT synthesis have gained an increasing attention due to their advantageous properties. Membrane reactors for FT synthesis have the potential to be used in small or medium plants for future offshore or biomass-to-liquid applications (Guettel et al. 2008). There are four concepts of using membranes for FT synthesis: distributed feed of reactants, in situ removal of water, forced-through membrane contactor, and zeolite encapsulated catalysts (Fig. 10.9) (Rohde et al. 2005b).

A catalytic membrane has the potential to offer a defined reaction zone, while the reactants are forced through the membrane by means of a pressure gradient. High gas–liquid mass transfer rates can be observed depending on the properties of the membrane; this leads to higher volume-specific production rates. In a more recent concept, the products from the FT process are passed through a catalytic membrane which results in an altered product distribution. Therefore, the driving forces for applying membrane technology to FT synthesis are longer catalyst lifetime, higher product selectivity, and higher specific production rates (Rohde et al. 2005b).

The distributed feed of reactants through a membrane can enable better temperature control, and the selectivity of methane can be affected, by changing the H_2/CO ratio. Since the activity and product selectivity rely heavily on the H_2/CO ratio when using Co-based catalysts, distributed feeding can affect the gas phase composition positively (Rohde et al. 2005b).

Water is a side product formed during the FT process, and its accumulation in the gas phase can decrease the partial pressure of the reactants. This particular type of membrane configuration because high water partial pressures can result in re-oxidation and shorter catalyst lifetime. It has been observed that water can adversely affect the reaction rate and can encourage the formation of CO_2 by the WGS reaction. By integrating the in situ removal of water membrane into the FT process, the rate of reaction can be enhanced and shift the equilibrium in favor of CO

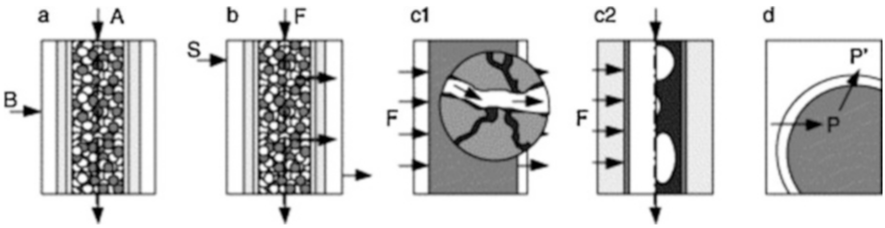

Fig. 10.9 Membrane applications for Fischer–Tropsch synthesis: (**a**) distributed feed of reactants, (**b**) in situ removal of water, (**c**) forced-through membranes, (**d**) encapsulated catalysts (Rohde et al. 2005b). (Reprinted with permission of Elsevier from Rohde et al. 2005b)

production (Espinoza et al. 2000; Rohde et al. 2005a; Zhu et al. 2005). Espinoza et al. (2000) conducted a series of permeation experiments with silicalite-1/ZSM-5 and mordenite (on a-Al_2O_3/stainless steel support) under nonreactive conditions typical for FT (200–300 °C and 2 MPa). The results showed that mordenite membranes demonstrated high water fluxes ($PH_2O = 2 \times 10^{-7}$ mol/(s Pa m^2), 250 °C) and desirable permselectivities. Rohde et al. (2005a) carried out experiments in a packed-bed reactor with an integrated silica membrane. Although the membrane was found to show low permselectivities regarding the water under the FT reaction conditions, the shortcomings of the permselectivities can be overcome by the choice of H_2 and H_2/CO_2 as the sweep gas. It was concluded that the increase in conversion of CO_2 to long-chain hydrocarbons via the CO_2 shift and FT process can be enhanced by the in situ removal of water, which results in higher product yields.

A study conducted by Khassin et al. (2005) investigated the concept of forced-through flow membrane for FT synthesis by using thermally conductive contactor modules (plug-through contactor membrane, PCM). The synthesis gas enters through the internal void space and then passes through the membrane which has a thickness of 2.5 mm. In order to improve the thermal conductivity, copper can be applied during membrane production. It was observed that PCMs can offer lower pressure drops, high space–time yields at flat temperature profiles, larger reactor capacities, high gas–liquid mass transfer rates, and low diffusive constraints. Furthermore, Bradford et al. (2005) utilized a monolith loop catalytic membrane reactor (ML-CMR) concept for Fischer–Tropsch synthesis (FTS) to evaluate the performance of a P/Pt–Co/γ-Al_2O_3catalyst in a prototype, tubular CMR and in a tubular, fixed-bed reactor. The synthesis gas was fed from the shell side to the alumina carrier material and passed through the membrane to the catalyst. The membrane allowed the produced hydrocarbons to be collected from the tube side.

The catalysts used for the FT process can be combined with acidic zeolites, for example, in physical mixtures or by the dispersion of Co on zeolite. The purpose of this is to alter the distribution of FT products by the hydrocracking and isomerization as soon as the products are formed (Rohde et al. 2005b). He et al. (2005) prepared a catalyst in the form of a capsule by coating a HZSM5 membrane on a preshaped Co/SiO_2 catalyst pellet. The capsule catalyst with HZSM5 membrane displayed brilliant selectivity for light hydrocarbon synthesis, particularly for isoparaffin synthesis from syngas ($CO + H_2$). Long-chain hydrocarbon production was totally repressed by the zeolite membrane. The adjustment of membrane and core catalyst significantly enhanced the catalytic properties of these novel types of capsule catalysts.

10.5 Conclusions

The various applications of membrane reactors in biofuels, hydrogen, and the FT process have been presented in this work. Membrane reactors offer promising opportunities for process intensification to improve the alternative fuel production processes. They offer the combination of reaction and separation into one single unit and so eliminating the need for additional separation and recycling units. As a result, the fuel production process becomes less energy intensive which makes it greener and environmentally sustainable, as well as reducing capital costs. Furthermore, membrane reactors can enhance conversion and selectivity, reduce mass transfer limitations, and have a greater thermal stability when compared to the conventional reactors. Membrane reactors have been mainly applied to homogeneous catalytic transesterification and heterogeneous catalytic transesterification to produce biodiesel. Membrane technology can be applied to this process based on the separation of oil droplet size and based on catalytic membranes. It has also been found that membranes can be incorporated with catalysts or by using a catalytically inert membrane for the biodiesel production process. The production of biodiesel by utilizing a catalytically inert membrane needs further purification because the permeate stream comprises of catalysts, glycerol, methanol, and FAME. Therefore, the membranes with the incorporated catalyst are more desirable for this process as less separation and purification are required. Recent advances for the hydrogen production process highlight the use of packed-bed membrane reactors, fluidized-bed membrane reactors, membrane microreactors, and membrane bioreactors. Due to the fact that fluidized membrane reactors are superior to the packed-bed membrane configuration, this type of reactor is most likely to be applied in industry as well as the membrane microreactors. The concept of distributed feeding, water removal, forced-through flow membrane, and encapsulated catalyst have all been applied to membrane technology for the FT process. The application of forced-through flow membrane is capable for small-/medium-scale FT reactors. The large reactor capacities, novel concepts for heat removal, and a well-defined and fixed reaction zone ensure a safe and economically feasible process. The membrane reactors discussed in this paper can be applied to methane reforming and bioethanol reforming on a large commercial scale. Future applications of membrane reactors could include thermochemical treatment, such as pyrolysis of biomass and plastic waste. It can be incorporated to compliment the processing of plastic waste and biomass. On the other hand, membrane technology can also be applied to obtain higher-quality distillates and fuel products from solid waste. This could be achieved by incorporating the technology downstream of processes aimed at producing gasoline, gas–oil, or heavy oil from solid waste thermolysis. In addition, more research could be performed to analyze the effects of fouling and stability of the membranes, for the production of renewable fuels. The production and development of novel membrane materials, and reactor configurations, can potentially result in improvements in reactor productivity and the economics of the renewable fuel production process. Furthermore, optimization framework studies that incorporate membrane reactor technologies are very scant. Such work can be conducted to help understand the overall yield and process intensification strategies that could take place on industrial scale. Such mathematical platforms can also aid in conducting economic analysis that will render membrane technology more viable for the commercial market.

References

Abbaszaadeh A, Ghobadian B, Omidkhah MR, Najafi G (2012) Current biodiesel production technologies: a comparative review. Energy Convers Manag 63:138–148

Aca-Aca G, Loría-Bastarrachea MI, Ruiz-Treviño FA, Aguilar-Vega M (2018) Transesterification of soybean oil by PAAc catalytic membrane: sorption properties and reactive performance for biodiesel production. Renew Energy 116:250–257

Aransiola E, Ojumu T, Oyekola O, Madzimbamuto T, Ikhu-Omoregbe D (2014) A review of current technology for biodiesel production: state of the art. Biomass Bioenergy 61:276–297

Atadashi I, Aroua M, Aziz AA (2011) Biodiesel separation and purification: a review. Renew Energy 36(2):437–443

Balthasar W (1984) Hydrogen production and technology: today, tomorrow and beyond. Int J Hydrog Energy 9(8):649–668

Baroutian S, Aroua MK, Raman AAA, Sulaiman NMN (2010) Methanol recovery during transesterification of palm oil in a TiO2/Al2O3 membrane reactor: experimental study and neural network modeling. Sep Purif Technol 76(1):58–63

Baroutian S, Aroua MK, Raman AAA, Sulaiman NM (2011) A packed bed membrane reactor for production of biodiesel using activated carbon supported catalyst. Bioresour Technol 102 (2):1095–1102

Barreto RA (2018) Fossil fuels, alternative energy and economic growth. Econ Model 75:196–220

Basile A, Parmaliana A, Tosti S, Iulianelli A, Gallucci F, Espro C, Spooren J (2008) Hydrogen production by methanol steam reforming carried out in membrane reactor on Cu/Zn/Mg-based catalyst. Catal Today 137(1):17–22

Bing W, Wei M (2019) Recent advances for solid *basic catalysts*: structure design and catalytic performance. J Solid State Chem 269:184–194

Bradford MC, Te M, Pollack A (2005) Monolith loop catalytic membrane reactor for Fischer–Tropsch synthesis. Appl Catal A Gen 283(1–2):39–46

Buonomenna M, Choi S, Drioli E (2010) Catalysis in polymeric membrane reactors: the membrane role. Asia Pac J Chem Eng 5(1):26–34

Buxbaum RE (2002) U.S. patent no. 6,461,408. U.S. Patent and Trademark Office, Washington, DC

Cannilla C, Bonura G, Costa F, Frusteri F (2018) *Biofuels* production by esterification of oleic acid with ethanol using a *membrane* assisted *reactor* in vapour permeation configuration. Appl Catal A Gen 566:121–129

Cao P, Tremblay AY, Dubé MA, Morse K (2007) Effect of membrane pore size on the performance of a membrane reactor for biodiesel production. Ind Eng Chem Res 46(1):52–58

Cao P, Dubé MA, Tremblay AY (2008a) High-purity fatty acid methyl ester production from canola, soybean, palm, and yellow grease lipids by means of a membrane reactor. Biomass Bioenergy 32(11):1028–1036

Cao P, Dubé MA, Tremblay AY (2008b) Methanol recycling in the production of biodiesel in a membrane reactor. Fuel 87(6):825–833

Cerveró JM, Coca J, Luque S (2008) Production of biodiesel from vegetable oils. Grasas Aceites 59 (1):76–83

Chen H, Peng B, Wang D, Wang J (2007) Biodiesel production by the transesterification of cottonseed oil by solid acid catalysts. Front Chem Eng China 1(1):11–15

Chen HL, Lee HM, Chen SH, Chao Y, Chang MB (2008) Review of plasma catalysis on hydrocarbon reforming for hydrogen production—interaction, integration, and prospects. Appl Catal B Environ 85(1–2):1–9

Constantinou A, Ghiotto F, Lam KF, Gavriilidis A (2014) Stripping of acetone from water with microfabricated and membrane gas–liquid contactors. Analyst 139(1):266–272

Dalai A, Kulkarni M, Meher L (2006) Biodiesel productions from vegetable oils using heterogeneous catalysts and their applications as lubricity additives. In: EIC climate change technology, 2006 IEEE. IEEE, pp 1–8. https://doi.org/10.1109/EICCCC.2006.277228

Das D, Veziroğlu TN (2001) Hydrogen production by biological processes: a survey of literature. Int J Hydrog Energy 26(1):13–28

Demirbaş A (2002) Hydrogen production from biomass by the gasification process. Energy Sources 24(1):59–68

DeRoussel P, Khakhar D, Ottino J (2001) Mixing of viscous immiscible liquids. Part 2: overemulsification—interpretation and use. Chem Eng Sci 56(19):5531–5537

Di Serio M, Ledda M, Cozzolino M, Minutillo G, Tesser R, Santacesaria E (2006) Transesterification of soybean oil to biodiesel by using heterogeneous basic catalysts. Ind Eng Chem Res 45(9):3009–3014

Di Serio M, Cozzolino M, Tesser R, Patrono P, Pinzari F, Bonelli B, Santacesaria E (2007) Vanadyl phosphate catalysts in biodiesel production. Appl Catal A Gen 320:1–7

Dubé M, Tremblay A, Liu J (2007) Biodiesel production using a membrane reactor. Bioresour Technol 98(3):639–647

Edrisi SA, Abhilash PC (2016) Exploring marginal and degraded lands for *biomass* and bioenergy production: an Indian scenario. Renew Sust Energ Rev 54:1537–1551

Enweremadu C, Mbarawa M (2009) Technical aspects of production and analysis of biodiesel from used cooking oil—a review. Renew Sust Energ Rev 13(9):2205–2224

Ersöz A (2008) Investigation of hydrocarbon reforming processes for micro-cogeneration systems. Int J Hydrog Energy 33(23):7084–7094

Espinoza R, Du Toit E, Santamaria J, Menendez M, Coronas J, Irusta S (2000) Use of membranes in Fischer-Tropsch reactors. In: Studies in surface science and catalysis, vol 130. Elsevier, pp 389–394. https://doi.org/10.1016/S0167-2991(00)80988-X

Fremaux S, Beheshti S-M, Ghassemi H, Shahsavan-Markadeh R (2015) An experimental study on hydrogen-rich gas production via steam gasification of biomass in a research-scale fluidized bed. Energy Convers Manag 91:427–432

Furuta S, Matsuhashi H, Arata K (2004) Biodiesel fuel production with solid superacid catalysis in fixed bed reactor under atmospheric pressure. Catal Commun 5(12):721–723

Gallucci F, De Falco M, Tosti S, Marrelli L, Basile A (2008) Co-current and counter-current configurations for ethanol steam reforming in a dense Pd–Ag membrane reactor. Int J Hydrog Energy 33(21):6165–6171

Gallucci F, Fernandez E, Corengia P, van Sint Annaland M (2013) Recent advances on membranes and membrane reactors for hydrogen production. Chem Eng Sci 92:40–66

Goff MJ, Bauer NS, Lopes S, Sutterlin WR, Suppes GJ (2004) Acid-catalyzed alcoholysis of soybean oil. J Am Oil Chem Soc 81(4):415–420

Guan H-M, Chung T-S, Huang Z, Chng ML, Kulprathipanja S (2006) Poly (vinyl alcohol) multilayer mixed matrix membranes for the dehydration of ethanol–water mixture. J Membr Sci 268(2):113–122
Guerreiro L, Castanheiro J, Fonseca I, Martin-Aranda R, Ramos A, Vital J (2006) Transesterification of soybean oil over sulfonic acid functionalised polymeric membranes. Catal Today 118(1–2):166–171
Guerreiro L, Pereira P, Fonseca I, Martin-Aranda R, Ramos A, Dias J, Oliveira R, Vital J (2010) PVA embedded hydrotalcite membranes as basic catalysts for biodiesel synthesis by soybean oil methanolysis. Catal Today 156(3–4):191–197
Guettel R, Kunz U, Turek T (2008) Reactors for Fischer-Tropsch synthesis. Chem Eng Technol: Ind Chem-Plant Equip-Process Eng-Biotechnol 31(5):746–754
Gutiérrez-Antonio C, Ornelas MLS, Gómez-Castro FI, Hernández S (2018) *Intensification* of the hydrotreating *process* to produce *renewable* aviation *fuel* through reactive distillation. Chem Eng Process – Process Intensif 124:122–130
Hafeez S, Manos G, Al-Salem SM, Aristodemou E, Constantinou A (2018) Liquid fuel synthesis in microreactors. React Chem Eng 3(4):414–432. https://doi.org/10.1039/C8RE00040A
He J, Yoneyama Y, Xu B, Nishiyama N, Tsubaki N (2005) Designing a capsule catalyst and its application for direct synthesis of middle isoparaffins. Langmuir 21(5):1699–1702
Holladay JD, Hu J, King DL, Wang Y (2009) An overview of hydrogen production technologies. Catal Today 139(4):244–260
Jalan R, Srivastava V (1999) Studies on pyrolysis of a single biomass cylindrical pellet—kinetic and heat transfer effects. Energy Convers Manag 40(5):467–494
Jitputti J, Kitiyanan B, Rangsunvigit P, Bunyakiat K, Attanatho L, Jenvanitpanjakul P (2006) Transesterification of crude palm kernel oil and crude coconut oil by different solid catalysts. Chem Eng J 116(1):61–66
Kampa M, Castanas E (2008) Human health effects of air pollution. Environ Pollut 151(2):362–367
Keskin A, Gürü M, Altiparmak D, Aydin K (2008) Using of cotton oil soapstock biodiesel–diesel fuel blends as an alternative diesel fuel. Renew Energy 33(4):553–557
Khassin AA, Sipatrov AG, Chermashetseva GK, Yurieva TM, Parmon VN (2005) Fischer–Tropsch synthesis using plug-through contactor membranes based on permeable composite monoliths. Selectivity control by porous structure parameters and membrane geometry. Top Catal 32 (1–2):39–46
Kiss AA (2009) Novel process for biodiesel by reactive absorption. Sep Purif Technol 69 (3):280–287
Kiss FE, Jovanović M, Bošković GC (2010) Economic and ecological aspects of biodiesel production over homogeneous and heterogeneous catalysts. Fuel Process Technol 91 (10):1316–1320
Kleinert A, Feldhoff A, Schiestel T, Caro J (2006) Novel hollow fibre membrane reactor for the partial oxidation of methane. Catal Today 118(1–2):44–51
Knothe G, Krahl J, Van Gerpen J (2005) The biodiesel handbook. AOCS Press, Champaign, p 2005
Kouzu M, Hidaka J-s (2012) Transesterification of vegetable oil into biodiesel catalyzed by CaO: a review. Fuel 93:1–12
Licht F, Agra C (2007) World biodiesel markets: the outlook to 2010. Agra Informa Ltd, Kent
Lipnizki F, Field RW, Ten P-K (1999) Pervaporation-based hybrid process: a review of process design, applications and economics. J Membr Sci 153(2):183–210
Liu X, He H, Wang Y, Zhu S, Piao X (2008) Transesterification of soybean oil to biodiesel using CaO as a solid base catalyst. Fuel 87(2):216–221
Lotero E, Goodwin JG, Bruce DA, Suwannakarn K, Liu Y, Lopez DE (2006) The catalysis of biodiesel synthesis. Catalysis 19(1):41–83
Lu G, Da Costa JD, Duke M, Giessler S, Socolow R, Williams R, Kreutz T (2007) Inorganic membranes for hydrogen production and purification: a critical review and perspective. J Colloid Interface Sci 314(2):589–603
Ma F, Hanna MA (1999) Biodiesel production: a review. Bioresour Technol 70(1):1–15

Maneerung T, Hidajat K, Kawi S (2016) Triple-layer catalytic hollow fiber membrane reactor for hydrogen production. J Membr Sci 514:1–14

Marbán G, Valdés-Solís T (2007) Towards the hydrogen economy? Int J Hydrog Energy 32 (12):1625–1637

Marcano JGS, Tsotsis TT (2002) Catalytic membranes and membrane reactors. Wiley-VCH Verlag GmbH. https://doi.org/10.1002/3527601988

Meher LC, Kulkarni MG, Dalai AK, Naik SN (2006) Transesterification of karanja (Pongamia pinnata) oil by solid basic catalysts. Eur J Lipid Sci Technol 108(5):389–397

Mejdell A, Jøndahl M, Peters T, Bredesen R, Venvik H (2009a) Effects of CO and CO2 on hydrogen permeation through a∼ 3 μm Pd/Ag 23 wt.% membrane employed in a microchannel membrane configuration. Sep Purif Technol 68(2):178–184

Mejdell A, Jøndahl M, Peters T, Bredesen R, Venvik H (2009b) Experimental investigation of a microchannel membrane configuration with a 1.4 μm Pd/Ag23 wt.% membrane—effects of flow and pressure. J Membr Sci 327(1–2):6–10

Mejdell A, Peters T, Stange M, Venvik H, Bredesen R (2009c) Performance and application of thin Pd-alloy hydrogen separation membranes in different configurations. J Taiwan Inst Chem Eng 40(3):253–259

Mueller U, Schubert M, Yaghi O, Ertl G, Knözinger H, Schüth F, Weitkamp J (2008) Handbook of heterogeneous catalysis, vol 1. Wiley-VCH, Weinheim, pp 247–262

Muradov N (1993) How to produce hydrogen from fossil fuels without CO2 emission. Int J Hydrog Energy 18(3):211–215

Ni M, Leung DY, Leung MK, Sumathy K (2006) An overview of hydrogen production from biomass. Fuel Process Technol 87(5):461–472

Nikolaidis P, Poullikkas A (2017) A comparative overview of hydrogen production processes. Renew Sust Energ Rev 67:597–611

Pal P, Kumar R, Ghosh AK (2018) Analysis of *process intensification* and performance assessment for fermentative continuous *production* of bioethanol in a multi-staged *membrane*-integrated bioreactor system. Energy Convers Manag 171:371–383

Patil PD, Deng S (2009) Optimization of biodiesel production from edible and non-edible vegetable oils. Fuel 88(7):1302–1306

Rahimpour M (2015) Membrane reactors for biodiesel production and processing. In: Membrane reactors for energy applications and basic chemical production. Elsevier, pp 289–312. https://doi.org/10.1016/C2013-0-16489-6

Rahimpour M, Bayat M (2011) Production of ultrapure hydrogen via utilizing fluidization concept from coupling of methanol and benzene synthesis in a hydrogen-permselective membrane reactor. Int J Hydrog Energy 36(11):6616–6627

Ramadhas A, Jayaraj S, Muraleedharan C (2004) Use of vegetable oils as IC engine fuels—a review. Renew Energy 29(5):727–742

Rohde MP, Unruh D, Schaub G (2005a) Membrane application in Fischer− Tropsch synthesis to enhance CO2 hydrogenation. Ind Eng Chem Res 44(25):9653–9658

Rohde MP, Unruh D, Schaub G (2005b) Membrane application in Fischer–Tropsch synthesis reactors—overview of concepts. Catal Today 106(1–4):143–148

Rostrup-Nielsen J (2003) Encyclopedia of catalysis, vol 6. Wiley, New York

Saleh J, Tremblay AY, Dubé MA (2010) Glycerol removal from biodiesel using membrane separation technology. Fuel 89(9):2260–2266

Sarkar B, Sridhar S, Saravanan K, Kale V (2010) Preparation of fatty acid methyl ester through temperature gradient driven pervaporation process. Chem Eng J 162(2):609–615

Shao P, Huang R (2007) Polymeric membrane pervaporation. J Membr Sci 287(2):162–179

Sharma Y, Singh B, Upadhyay S (2009) Response to the comments on "Advancements in development and characterization of biodiesel: A review". Sharma YC, Singh B, Upadhyay SN. Fuel 2008; 87: 2355–73 by Clifford Jones. Fuel 4(88):768–769

Shi W, He B, Ding J, Li J, Yan F, Liang X (2010) Preparation and characterization of the organic–inorganic hybrid membrane for biodiesel production. Bioresour Technol 101(5):1501–1505

Shuit SH, Ong YT, Lee KT, Subhash B, Tan SH (2012) Membrane technology as a promising alternative in biodiesel production: a review. Biotechnol Adv 30(6):1364–1380

Singh AK, Fernando SD (2007) Reaction kinetics of soybean oil transesterification using heterogeneous metal oxide catalysts. Chem Eng Technol: Ind Chem-Plant Equip-Process Engi-Biotechnol 30(12):1716–1720

Spallina V, Matturro G, Ruocco C, Meloni E, Palma V, Fernandez E, Melendez J, Tanaka AP, Sole JV, van Sint AM (2018) Direct route from ethanol to pure hydrogen through autothermal reforming in a membrane reactor: experimental demonstration, reactor modelling and design. Energy 143:666–681

Stankiewicz A (2003) Reactive separations for process intensification: an industrial perspective. Chem Eng Process Process Intensif 42(3):137–144

Steinberg M, Cheng HC (1989) Modern and prospective technologies for hydrogen production from fossil fuels. Int J Hydrog Energy 14(11):797–820

Tian Y, Demirel SE, Hasan MMF, Pistikopoulos EN (2018) An overview of *process* systems engineering approaches for *process intensification*: state of the art. Chem Eng Process Process Intensif 133:160–210

Tosti S, Basile A, Bettinali L, Borgognoni F, Gallucci F, Rizzello C (2008) Design and process study of Pd membrane reactors. Int J Hydrog Energy 33(19):5098–5105

Van Der Laan GP, Beenackers A (1999) Kinetics and selectivity of the Fischer–Tropsch synthesis: a literature review. Catal Rev 41(3–4):255–318

Wang L, Yang J (2007) Transesterification of soybean oil with nano-MgO or not in supercritical and subcritical methanol. Fuel 86(3):328–333

Wang Y, Wang X, Liu Y, Ou S, Tan Y, Tang S (2009) Refining of biodiesel by ceramic membrane separation. Fuel Process Technol 90(3):422–427

Wen M, Mori K, Kuwahara Y, An T, Yamashita H (2018) Design and architecture of metal organic frameworks for visible light enhanced *hydrogen* production. Appl Catal B Environ 218:555–569

Wilhelm D, Simbeck D, Karp A, Dickenson R (2001) Syngas production for gas-to-liquids applications: technologies, issues and outlook. Fuel Process Technol 71(1–3):139–148

Yusuf N, Kamarudin SK, Yaakub Z (2011) Overview on the current trends in biodiesel production. Energy Convers Manag 52(7):2741–2751

Zhang G, Jin W, Xu N (2018) Design and fabrication of ceramic catalytic *Membrane Reactors* for green chemical engineering applications. Engineering 4(6):848–860

Zhu W, Gora L, Van den Berg A, Kapteijn F, Jansen J, Moulijn J (2005) Water vapour separation from permanent gases by a zeolite-4A membrane. J Membr Sci 253(1–2):57–66

Zhu M, He B, Shi W, Feng Y, Ding J, Li J, Zeng F (2010) Preparation and characterization of PSSA/PVA catalytic membrane for biodiesel production. Fuel 89(9):2299–2304

Chapter 11
Waste Management and Conversion to Pure Hydrogen by Application of Membrane Reactor Technology

Majid Saidi, Mohammad Hossein Gohari, and Ali Talesh Ramezani

Contents

Abstract Waste conversion has an essential role in the development of environmental-friendly methods to obtain efficient and clean energy. Due to increasing rate of waste production, waste management policy has become a very crucial issue in recent years. The main aim of the waste management is the increase of material and energy recovery from waste, which can reduce the landfill disposal and minimize the environmental impact. These goals can be achieved by developing and

M. Saidi (✉) · M. H. Gohari · A. T. Ramezani
School of Chemistry, College of Science, University of Tehran, Tehran, Iran
e-mail: majid.saidi@khayam.ut.ac.ir; majid.saidi@ut.ac.ir

Z. Zhang et al. (eds.), *Membranes for Environmental Applications*, Environmental Chemistry for a Sustainable World 42, https://doi.org/10.1007/978-3-030-33978-4_11

applying novel technologies such as membrane technology for waste recovery. Membrane technology is introduced as an applicable method for waste conversion to pure hydrogen which can be integrated with a high efficiency energy conversion system. In this study, different waste conversion techniques such as incineration, pyrolysis, gasification, and anaerobic digestion are reviewed, with focus on waste gasification to produce syngas and subsequently pure hydrogen production using membrane reactor. The potential and suitability of these configurations are discussed. Considering the related previous researches indicated that the membrane technology is a viable candidate for combined energy and material valorization. Finally, the continued advances that are being made in waste conversion, membrane durability, process control, and process efficiency of membrane reactor are expected to improve the commercial viability of waste conversion technologies to pure hydrogen, in the future.

Graphical Abstract

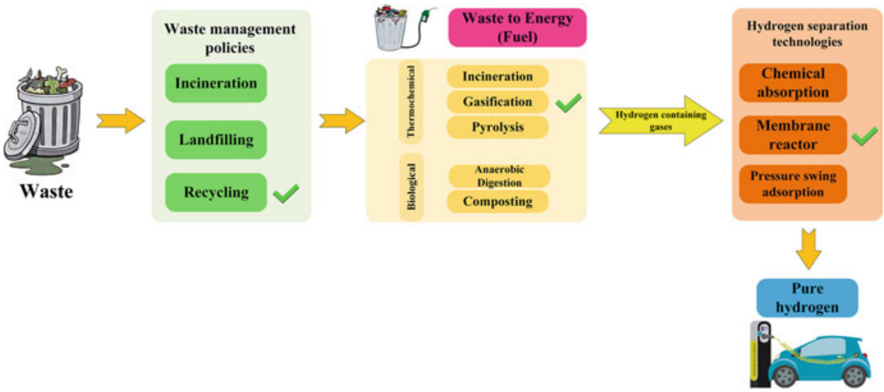

Keywords Waste management · Gasification · Membrane reactor · Hydrogen · Syngas

11.1 Introduction

Due to strict environmental regulations, efforts to replace fossil fuels with more environmental-friendly fuels have been raised (Sánchez et al. 2014); effective utilization of waste can be taken into account to meet environmental regulation goals (Nishioka et al. 2007). To meet these goals, producing hydrogen as a green fuel from different sources is a matter of debate these days. Hydrogen can be used both as energy carrier and energy storage mean (Dincer 2011). The concept of using hydrogen to decrease greenhouse gas emission is growing slowly because of hydrogen gas unavailability and obstacles in its production, storage, and utilization technology (Chen et al. 2017b). The importance of replacing fossil fuels with hydrogen will be significantly notable, if hydrogen is obtained from waste.

Significant amount of waste is produced in large industrialized countries. About 2600 Mton (10^6 metric ton) of waste was made in the EU27 in 2008 (Van Caneghem et al. 2012). Waste can be defined differently depending on the regions. For example, Wen et al. (2014) classified waste in China as substances in solid, semi-solid, or gaseous state in containers that are the result of production, living, and other activities. Indeed, wastes have lost their original use though have not lost use values; these substances are included into the management of solid wastes upon the strength of administrative regulations (Wen et al. 2014). While Thürer et al. (2017), mentioned the definition of waste as the result of misusing something valuable that occurs because too much of it being used or because it is being used in a way that is not necessary or effective; an action or use that results in the unnecessary loss of something valuable; a situation in which something valuable is not being used or is being used in a way that is not appropriate or effective. Waste has different forms and can be divided in a variety of types based on waste sources notably including municipal waste, industrial waste, and special hazardous waste. However, it should be noted that the waste types mentioned above are not exclusive and they may have slight overlap with each other.

Waste management policies are based on dealing with waste in a manner that is less harmful to the environment. Decreasing waste quantity, reusing materials, recycling them, incinerating to gain energy, and at last landfilling wastes are the ways to treat waste. The last two policies are not considered environmental friendly and have some disadvantages. Incineration is a process of burning waste through a controlled way in an aerobic condition at high temperature (above 800 °C). High emission of greenhouse gases and high operating cost are considered as major disadvantages of incineration method, while cost of waste transportation to the landfilling area and polluting the soil are related to landfilling method.

There are two processes to convert waste to energy including biological and thermochemical processes. Biological processes include fermentation, while thermochemical processes can be divided into pyrolysis, combustion, and gasification (Widjaya et al. 2018). Among thermochemical processes, gasification process is investigated in this review article as an effective thermochemical process. To obtain high-purity hydrogen via gasification, separation and purification are inevitable. Indeed, separation process is a critical step to reach pure hydrogen, because carbon dioxide and carbon monoxide are produced through synthesis gas (syngas) formation process, water–gas shift reactions or obtained as the products of steam reforming (Sánchez et al. 2014). Among different separation methods, membrane technology is introduced as an applicable, efficient technology to produce pure hydrogen.

11.1.1 Waste Types

As discussed above, waste can be categorized into three main classes, including municipal waste, industrial waste, and special hazardous waste.

Municipal Wastes

Municipal waste can be classified into household waste, commercial waste (related to waste produced in trade, business, etc.), and demolition waste (produced by destruction of roads, buildings, etc.). Agricultural waste (animal waste, slaughtering waste and etc.) may also be inserted into this category. Municipal waste or to be more specific municipal solid waste (MSW) can be defined as substances that seem to have no usage and discarded in urban and suburban zones. In Europe, municipal solid waste only corresponds to about 10% of the total waste generated (Van Caneghem et al. 2012). In the United States, municipal solid waste generation was about 351 Mton in 2008 (Van Caneghem et al. 2012). Figure 11.1 represents MSW generation rates from 1960 until 2015 in the United States (EPA 2015). Characteristics of some common municipal solid wastes are represented in Table 11.1 (Jocelyn et al. 2014; Muhammad et al. 2016). About 254 million tons municipal solid waste were generated in 2013, among which about 34% was recycled according to US Environmental Protection Agency (US EPA) (Chen et al. 2016).

Municipal solid waste generation is predicted to reach 2.2 billion tons/year in 2025 (Beyene et al. 2018). In developing nations, the total municipal solid waste generation rate will also grow rapidly in the coming years (Beyene et al. 2018). According to Intergovernmental Panel on Climate Change (IPCC), municipal solid waste is composed of food waste (25–70%), plastic, metal, glass, textiles, wood, rubber, leather, paper, biomass, fossil fuel derivatives, and others (Beyene et al. 2018). The composition of MSW differs with the topographical site, life smartness,

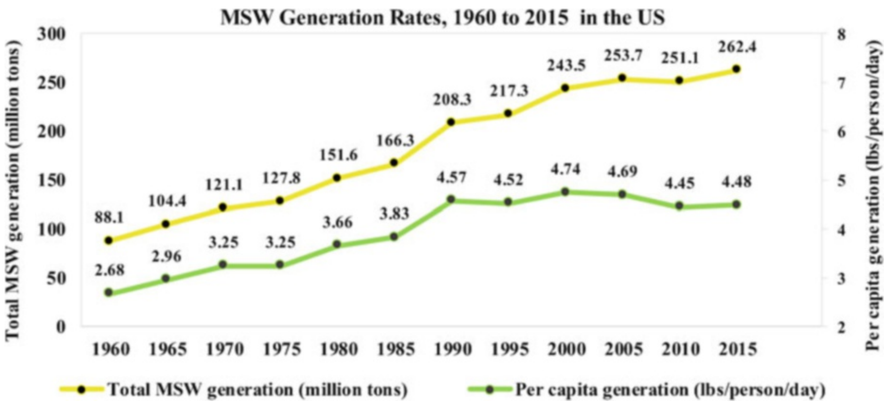

Fig. 11.1 MSW generation rates from 1960 until 2015 in the United States (EPA 2015)

Table 11.1 Characteristics of some common municipal solid wastes

Waste type	Density (Kg/m^3)	Moisture content (%)	Volatile matter (%)	Ash content (%)	Ultimate analysis %					References
					C	H	O	S	N	
MSW- meat	450	27.7	60.3	10.8	51.12	7.77	17.42	0.88	12.0	Jocelyn et al. (2014)
MSW- paper	200	3.2	85.7	11.7	47.75	7.40	33.62	0.00	0.13	Jocelyn et al. (2014)
Mixed MSW	197	8.6	52.21	24.48	22.78	5.92	46.73	0.07	0.28	Muhammad et al. (2016)

the standard of living, the population of city, etc. (Beyene et al. 2018). Both inorganic and organic matters are found in municipal solid waste, and by applying proper technologies and methods (waste-to-energy processes), the energy within their organic matter can be liberated. Besides this energy acquirement, there are other benefits that can be achieved by this conversion including (Patil et al. 2014):

- Reduction in environmental pollution
- Reduction of municipal solid waste quantity up to 90% (depending on waste composition and the technology applied)
- Reduction in waste transportation and management cost to landfilling area
- Less area requirement for landfilling

Industrial Wastes

Industrial waste is produced and discarded in any factories and industries. This type of waste generators may be categorized into chemical manufacturers (reactive waste), petroleum refining manufacturing (sludge and exhausted gases from refining process), etc. (EPA 1986). Annual worldwide production of municipal solid waste ranges from 350 to 1200 kg MSW/capita in high-income countries, from 250 to 550 kg MSW/capita in medium-income countries and from 150 to 250 kg/capita/year in low-income countries (Van Caneghem et al. 2012).

Special Hazardous Waste

This type may include biomedical waste, electronic waste (E-waste), explosive waste (from explosive compounds that should be destructed, not disposed), and radioactive waste (generally a nuclear power generation by-product). Biomedical waste is recognized as a hazardous type which may include clinical (medical) waste. World Health Organization (WHO) defined medical waste as "generated waste in the diagnosis, treatment or immunization of human beings or animals." Inefficiency in medical waste sorting is due to insufficient information on guidance as to which objects are classed as infectious (Windfeld and Brooks 2015). At the present time, there are some ways to treat this type of waste such as incineration (between 49% and 60%), autoclaving (between 20% and 37%), and other technologies (between 4% and 5%) (Weber and Rutala 2001). Incineration disadvantages were discussed before, while autoclaving is a process whereby dry heat or steam is added to the wastes to increase the temperature to an extent in which pathogens are killed (Lee et al. 2004).

E-waste is generally referred to equipment that once has used electricity and now is discarded (by any reason). Computers, cellphones, and televisions are examples of this category. Waste Electrical and Electronic Equipment (WEEE) refers to traditionally non-electronic devices like refrigerators and ovens. With the advent of smart devices, electronic boards are used in both electronic and traditional electrical devices. The distinction between e-waste and WEEE is less sharp as the result (Robinson 2009). Reusing, remanufacturing, recycling, landfilling, and incineration are the options available for e-waste treatment.

11.2 Waste Conversion and Management

Waste-to-energy technology can be divided into two treatment methods, thermal treatment (incineration, gasification, pyrolysis) and the biological treatment (anaerobic digestion, composting) (Maisarah et al. 2018). The main final method to get rid of waste in most countries is controlled and uncontrolled landfill of waste. According to Van Caneghem et al., until 2012, 69% of the municipal solid waste is landfilled, 24% is recycled and composted, and 7% is incinerated in the United States (Van Caneghem et al. 2012). Also according to Chen et al., in 2013, 134.3 million tons of municipal solid waste went to landfills, and 32.7 million tons were combusted for energy recovery worldwide *(*Chen et al. 2016*)*. Japan is ranked first in using thermal waste treatment in the world (40 Mton/year) (Van Caneghem et al. 2012). Municipal solid waste treatment methods and their distributions in some European countries are reported in Fig. 11.2 (Van Caneghem et al. 2012).

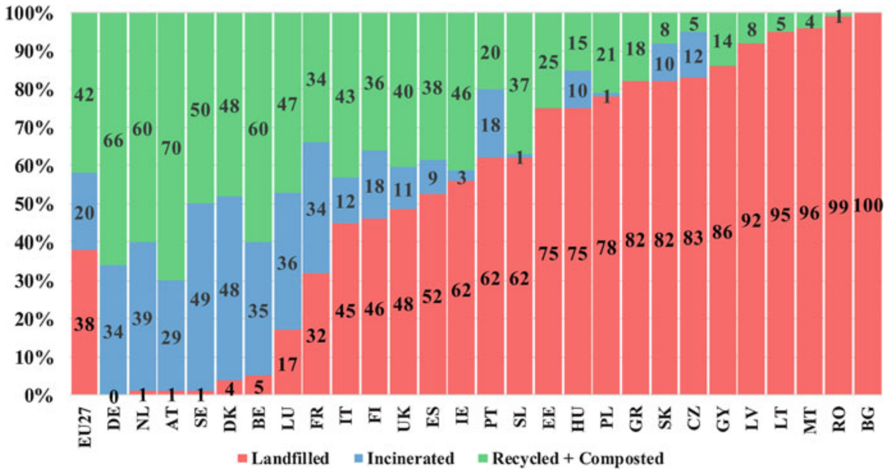

Fig. 11.2 Municipal solid waste treatment methods and their distributions in some European countries (Van Caneghem et al. 2012)

11.2.1 Landfilling

Landfilling is a traditional approach to get rid of bio-waste. Landfilling is the most common municipal solid waste disposal method worldwide probably because it is the most economical option and does not require skilled operators (Gerçel 2011). As a result, it is especially suitable for developing countries where low capital and maintenance cost depression or closed mining sites are commonly used for landfills (Daskalopoulos et al. 1998). The third largest source of methane emissions in the United States is landfill. It has huge influence on global warming (EPA 2013).In the United States, modern landfills are well-engineered facilities. These modern landfills are designed, operated, and monitored in acquiescence with federal regulations. Potentially harmful landfill gases (LFG) are collected in some of these new landfills and are then converted into energy. Although landfilling is a low-cost method, it is potentially a serious threat to the environment. Landfilling is a process in which waste is transferred from one place to landfilling area, rather than be used as an energy resource. The biodegradable content in waste is gradually biodegraded in the landfills, resulting in liquid leachate and landfill gas. The main disadvantage of landfilling is that liquid leachate causes pollution of groundwater and landfill gases composed largely of methane and carbon dioxide result in greenhouse effect. The number of US landfills has declined consistently, which may be due to the strict EPA regulations regarding waste landfills. In the United States, governments are determined to reduce the generation and increase recycling of waste. Attempt to generate electricity from landfill leachate by using microbial fuel cells has also been reported by Damiano et al. (2014).

11.2.2 Pyrolysis

The term “pyrolysis” is derived from the Greek word “pyro” (fire) and “lysis” (break/decomposition) (Bukkarapu et al. 2018). Pyrolysis is a thermal process for converting waste to energy. It is an endothermic reaction that breakdowns the long chain of polymer molecules into smaller, less complex molecules at temperatures higher than 400 °C in the absence of oxygen (Lombardi et al. 2015). There are several reviews on characterization and development of pyrolysis process in many aspects, for example, in terms of product characterization and reactor improvement (Sannita et al. 2012; Williams 2013; Yang et al. 2013); in terms of oil characterization and enhancement and oil production operating conditions (Quek and Balasubramanian 2013); parameters affecting pyrolysis process and its products (Martínez et al. 2013); and the kinetics modelling of the pyrolysis process or mechanism investigation of the process (Al-Salem et al. 2010; Quek and Balasubramanian 2012). The feedstock, temperature range, heating rate, and type of reactor used affect the pyrolysis products yield and composition of waste (Beyene et al. 2018). For example, as the pyrolysis temperature varies, change in product

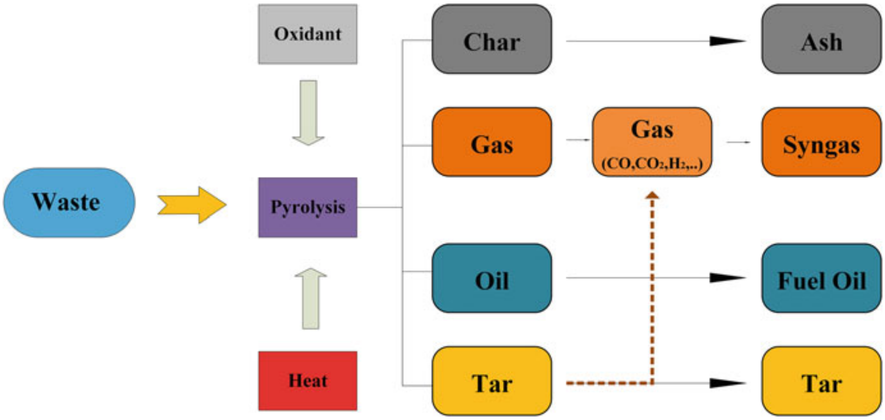

Fig. 11.3 A schematic representation of waste pyrolysis process (Beyene et al. 2018)

spreading pattern occurs. Lower pyrolysis temperatures usually produce more liquid products, and higher pyrolysis temperatures usually produce more gaseous products. When converting waste into energy using pyrolysis process, there are disadvantages including air pollution due to exhaust gas emission such as HCl, H_2S, NH_3, SO_x, NO_x, and odor impacts (Beyene et al. 2018). Pyrolysis process can be generally classified into slow (550–900 K), fast (850–1250 K), and flash (1050–1300 K) pyrolysis (Beyene et al. 2018; Chen et al. 2016). The main products of pyrolysis are oil, gas, and char, which are valuable for the production and refineries of the industries (Arena et al. 2010). Reactions in a pyrolysis process can be expressed as (Chen et al. 2015):

$$C_xH_yO_z + \text{Heat} \rightarrow \text{Char} + \text{Liquid} + \text{Gas} + \text{Water} \tag{11.1}$$

A schematic representation of waste pyrolysis process is shown in Fig. 11.3 (Beyene et al. 2018) and operating parameters of the pyrolysis process are reported in Table 11.2 (Ruiz et al. 2013).

Sharuddin et al. reported that pyrolysis is a flexible process (Sharuddin et al. 2016). It is due to the fact that process parameters can be manipulated to optimize the product yield (Sharuddin et al. 2016). Producing high amount of liquid oil up to 80% wt at temperatures around 500 °C was the reason that this process is chosen by many researchers (FakhrHoseini and Dastanian 2013). The liquid oil produced can be used for different purposes, e.g., for boiler, furnace, turbines, and diesel engine without upgrading (Sharuddin et al. 2016). The pyrolytic gases produce different hydrocarbons: straight, branched, cyclic aliphatic, and cyclic aromatic (Bukkarapu et al. 2018). There are two main sections in pyrolysis process of biomass, the furnace/reactor and the condensing system. The furnace/reactor converts biomass to vapor, non-condensable gas, and char (Bamdad and Hawboldt 2016; Bamdad et al. 2017; Demirbas 2007; Papari and Hawboldt 2015, 2017; Pütün et al. 2005). The common pyrolysis reactors are fixed-bed, rotary kiln, fluidized-bed, and tubular reactors but at

Table 11.2 Operating parameters of the pyrolysis process

Pyrolysis	Rate of heating ($K.s^{-1}$)	Time of residence (s)	Temperature (°C)	Size of particles (mm)	Main products
Slow	< 1	300–1800	400	5–50	Char
			600		Gas, oil, and char
Fast	500–10^5	0.5–5	500–650	< 1	70% oil
					15% char
					15% gas
Flash	> 10^5	< 1	< 650	< 0.2	Oil
		< 1	> 650		Gas
		< 0.5	1000		Gas

large-scale rotary kilns and tubular reactors are conveniences (Beyene et al. 2018). Condensing system recovers condensable gases (Papari and Hawboldt 2018). Cracking is a phenomenon that occurs during pyrolysis producing hydrocarbons of shorter chain lengths from longer ones. Four types of cracking are thermal cracking, catalytic cracking, steam cracking, and hydrocracking (Bukkarapu et al. 2018).

A cleaner way of obtaining energy can be accomplished in a pyrolysis-involved process compared to conventional municipal solid waste incineration plants because lower amounts of nitrogen oxides (NO_x) and sulfur oxides (SO_2) are produced as the result of the inert atmosphere in the pyrolysis processes. Another advantage is the opportunity to wash syngas before its combustion. Besides reduced gas emissions, higher quality of solid residues can be also obtained from pyrolysis-involved process for municipal solid waste (Saffarzadeh et al. 2006).

11.2.3 Incineration

Incineration is a process that includes the combustion and conversion of waste materials that can produce heat and energy at a temperature about 800 °C. Baran et al. reported that energy generation by incineration is environmentally sustainable waste management process (Baran et al. 2016). However, Yay (2015) reported that incineration is not always sustainable because of high operating cost of the process and high cost of maintenance. The notion of dealing with rising volumes of waste by incineration and recovering the energy available in the substances of waste streams was emerged during last quarter of the nineteenth century (Makarichi et al. 2018). Historically, the first municipal solid waste incinerator in the United Kingdom was built in 1870 (Lu et al. 2017). The same incinerator (without energy recovery) was built in 1885 in New York City (Makarichi et al. 2018). Incineration with heat recovery was built before the twentieth century in Europe. In the United States, incineration with heat recovery was not built until halfway through the twentieth century. Rise in oil prices was a driving force to use heat from the incinerators to produce steam and therefore electricity (Makarichi et al. 2018).

Until 2018, there are about 1179 municipal solid waste incineration plants around the world. The total capacity is more than excess of 700,000 metric tons per day (Lombardi et al. 2015). Incineration is used in different countries like 74% of municipal solid waste generated in Japan and 54% in Denmark, and 50% of Switzerland and Sweden are being treated using this method (Psomopoulos et al. 2009).

In the incinerator, the waste is combusted and the heat is used to generate high-pressure steam. The steam is then expanded in a turbine coupled to a generator, and electricity is produced as the result. Gases containing pollutants like sulfur oxides and nitrogen oxides are treated in scrubbers and finally liberated into the atmosphere (Liu et al. 2015). The ash produced as the result of combustion (about 15–25% by weight of the municipal solid waste) is sent to landfills (Chen et al. 2016).

Incineration reduces the volume of municipal solid waste by 90% and the weight by 70%. Incineration causes less pollution to the groundwater or the air than landfills. For high calorific value waste, incineration is fruitful; it can be located within city, while for landfilling it is not possible. It has lower transportation costs compared to landfilling and is operated as continuous process (Jha et al. 2011). Large-scale incinerators include the municipal waste combustors (MWC), medical waste combustors (MWI), hazardous waste incinerators (HWI), boiler and industrial furnaces (BIF), cement kiln (CK), and biomass combustor (BC) (Arena 2012). Bubbling, circulating, and rotating fluidized beds have been applied growingly within incineration method (Van Caneghem et al. 2012). Thermal, kinetic, and hydrodynamic considerations are needed in designing of a fluidized bed waste incinerator (Van Caneghem et al. 2012). While municipal solid waste is suitable for incineration with energy recovery due to its 70% combustible organic contents, industrial waste mostly includes inorganic contents that makes recycling and landfilling more fruitful options compared to incineration (Van Caneghem et al. 2012). Mass-burn incineration is the most common applied technology in incineration. Municipal solid waste combustion with little or no separation or pre-screening is carried out (Van Caneghem et al. 2012). Combustion can be done in a grate furnace incinerator, rotary kiln, or a fluidized bed incinerator. Three types of fluidized bed reactors are used for waste incineration: the traditional bubbling fluidized bed (BFBC), the rotating fluidized bed (RFBC), and the (external) circulating fluidized bed (CFBC).

Yet, these two approaches suffer from two disadvantages, landfilling release organic and nitrogen-containing compounds, which pollute aquifers (Bove et al. 2015; Lema et al. 1988), though it is a cheap approach to get biogas. In terms of incineration, this method associates with high operational costs (Patil et al. 2014) and produces ash as a by-product which has high concentration of toxic metal (Gao et al. 2015).

In contrast with the old approaches to handle bio-waste, gasification has some benefits including reliability in method to treat bio-waste, flexibility and adoptability to different types of waste (Heidenreich and Foscolo 2015), greenhouse gas emissions decrease, and energy security enhancement (Watson et al. 2018). According to Widjaya et al., non-woody biomass, having a lower lignin content than woody materials, is a common waste material found in agricultural processing plants and fields *(*Widjaya et al. 2018*)*. Appropriate pretreatments are crucial before gasification of non-woody biomass, because of its heterogeneous nature.

In biochemical waste conversion processes, microorganisms such as bacteria and enzymes are used to decompose biomass. Biochemical waste conversion is an outstanding and environmental-friendly method for gaining energy from waste. The commonly applied biochemical methods that use microorganisms for converting waste to energy are anaerobic digestion and fermentation (Eddine and Salah 2012).

11.2.4 Anaerobic Digestion

Anaerobic digestion (AD) is considered as a biological method that decays organic matter in the absence of oxygen to produce biogas mainly containing methane and carbon dioxide. In these days, feedstock may contain bio-solids, livestock manure, and wet organic materials and municipal solid waste (Rogoff and Screve 2011; Thi Phuong et al. 2014). Anaerobic digestion process may have three common steps. The first step is the decomposition of waste by bacteria; subsequently, the complex organic species is converted to simple soluble substances such as amino acids, monosaccharides, and fatty acids. The second step is the generation of materials such as volatile fatty acids (VFA), H_2, and CO_2. Conversion of organic acid to CH_4 by methanogenesis is the third step of anaerobic digestion. Figure 11.4 represents a schematic diagram of digestive conversion.

Biogas produced from anaerobic digestion may be used in solid oxide fuel cells, gas turbines, and gas engines or even can be modified to produce chemicals (Lee 2017). Anaerobic digestion of sewage sludge has been investigated by many

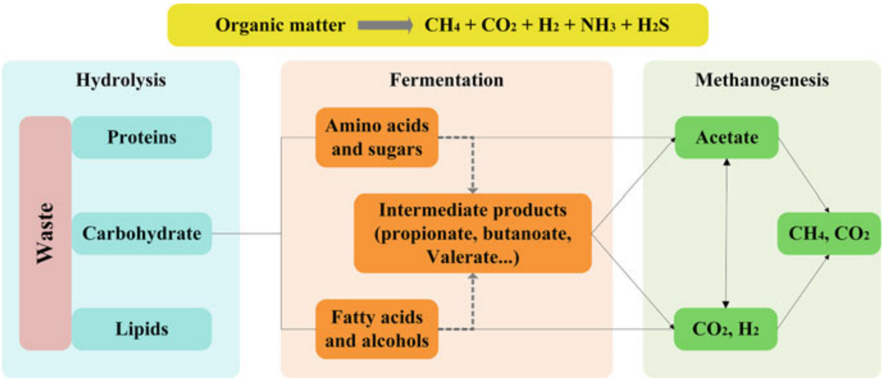

Fig. 11.4 A schematic diagram of digestive conversion (Beyene et al. 2018)

researchers (Wang et al. 2018) (Safari and Dincer 2019). In anaerobic digestion of sewage sludge, low portion of dry matter is the main source in biogas production since sewage sludge has a high portion of water (almost 95 wt%). The digestion process generates biogas and digestate as the main products. CO_2 and CH_4 are usually the major gases found in biogas. The digestate may be used for agricultural purposes or gas production via gasification (Safari and Dincer 2019). Recently coproduction of biohydrogen and bio-methane via anaerobic digestion process was reported by Qin et al. (Qin et al. 2019). Anaerobic co-digestion of paper waste or municipal solid waste containing paper waste with sewage sludge, manure, etc. has also been reported (Hartmann and Ahring 2005) (Li et al. 2018). Anaerobic gasification is the prior method to recover bioenergy in paper waste because moisture content of food waste makes direct incineration inappropriate for paper waste (Gonzalez-Estrella et al. 2017). Recently, biogas production from food waste via anaerobic digestion with wood chips was investigated by Oh et al. (2018). They found that utilization of wood chips can enhance the yield of methane production by 640% via anaerobic digestion of food waste. They concluded that the optimal ratio of food waste to the wood chips (w/w) is 0.5.

11.3 Membrane Reactor Technology

The most common conventional technologies for hydrogen separation from streams include chemical absorption (e.g., CO_2 removal by amine solvents), pressure swing adsorption (PSA), and membrane technology (without using an integrated membrane reactor). Absorption of carbon dioxide onto different amine-based solvents is carried out at large scales. CO_2 capture in flue gas using hollow fiber membrane is reviewed by Zhang et al. (Zhang et al. 2014, 2018b). The main disadvantages of this method are related to solvent recovery and operating cost. It is necessary to mention that CO_2 removal using chemical solvents does not lead to a high-purity hydrogen production (Jordal et al. 2015). Pressure swing adsorption is used to exclude desired gas species from gas mixtures under pressure at near-ambient temperatures. Industrial application of pressure swing adsorption started in the 1970s (Barelli et al. 2008). This technology is used for removal of carbon dioxide in large-scale hydrogen production.

Membrane reactor is an efficient technology where the fuel conversion reaction, mostly over a catalytic, fluidized, or packed bed, is accomplished and product separation is performed at the same time (Saidi 2017, 2018; Saidi and Jahangiri 2018). This technology has been applied for reactions limited by thermodynamic equilibria. The selective permeability of membranes shifts the equilibrium towards the products. Traditional technologies were limited by thermodynamic barriers, while this technology coped with these barriers successfully (Gallucci et al. 2017). So producing high-purity hydrogen via membrane reactors has been dramatically ascended. Figure 11.5 represents number of researches done on membrane reactors

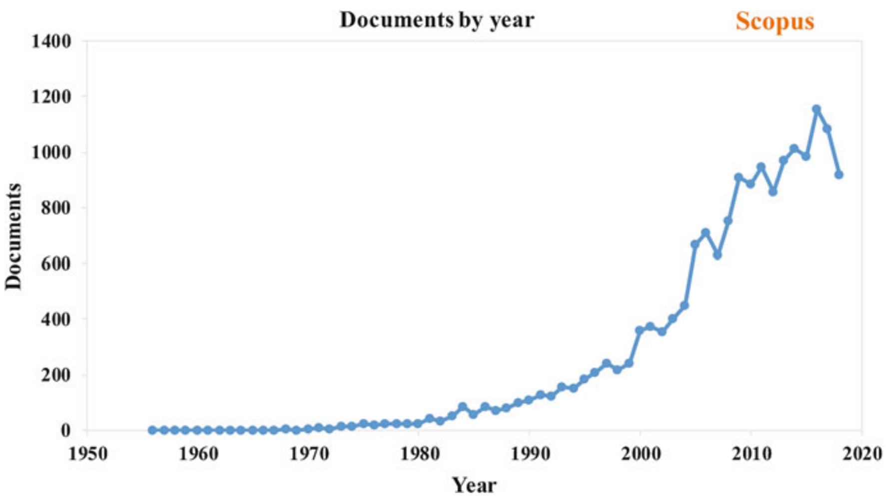

Fig. 11.5 Number of researches done on membrane reactors per year

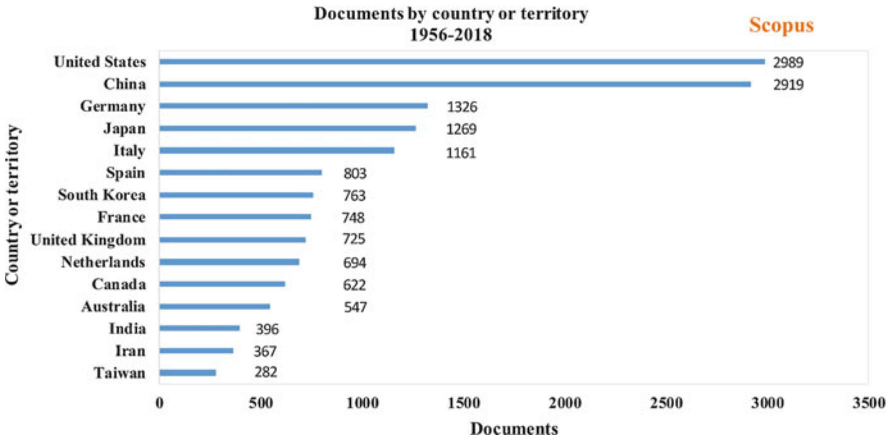

Fig. 11.6 Pioneer countries of doing researches on membrane reactors

per year, and Fig. 11.6 represents pioneer countries of doing researches on membrane reactors.

Palladium and palladium alloy membranes are considered as a promising technology for hydrogen separation (Sánchez et al. 2014). In 1866, the first investigation of hydrogen absorption and diffusion through Pd membranes was reported by Graham (1866) and the comprehensive concept of membrane reactors (MRs) was introduced in the 1950s (Iulianelli et al. 2014). In EU FP6 project CACHET, integrated Pd alloy membrane reactors were investigated for power production (Beavis 2011). Contrary to pressure swing adsorption systems, palladium-based membranes can operate at high temperatures (around 573 K compared to near-ambient temperatures in pressure swing adsorption). They also have the ability to keep hydrogen at high pressures, hence saving operating costs for compression (Anderson et al. 2009). In fact, membrane reactors integrate two unit operations, that is, hydrogen production and separation processes, in only one unit. It has not only economic advantages over conventional methods but also avoids application of further hydrogen separation systems (Drioli et al. 2003). Membranes can be combined with catalysts to be utilized the equilibrium-limited reactions and hydrogen separation in a catalytic membrane reactor (CMR) which leads to a compact, high-efficient integrated system (Basile et al. 2008; Ma 2007). Among different types of palladium-based membrane reactors, dense metal palladium-based membranes are used in reactors for water–gas shift and reforming reactions to produce high-purity hydrogen via different feedstock such as flare gas, waste gasification products, alcohols, etc. (Basile et al. 2001; Lin et al. 2003; Saidi 2018; Shu et al. 1994; Tong et al. 2005a).

Membrane reactors are used to produce hydrogen for different purposes such as fuel cells. Yet, there are several problems that restrict utilization of this method to produce hydrogen in large scale. Industrial scale production of hydrogen (more than 80%) is still via reforming of natural gas due to incomplete development of membrane reactors for high temperature applications and also lack of assurance in stability of membranes during long-term utilization, which leads to constant maintenance costs (Gallucci et al. 2017). In a membrane reactor, reforming and water–gas shift reaction occur, and simultaneous stripping of the produced hydrogen increases the conversion yield of the reactions. Steam reforming process takes place in large multi-tubular fixed-bed reactors. For bench scale production, there are other methods besides steam reforming: partial oxidation reaction, autothermal reforming (ATR), and dry reforming (DR). In autothermal reforming, the partial oxidation (exothermic) and steam reforming (endothermic) take place in the same reactor (Gallucci et al. 2013). Table 11.3 represents reactions of different types of reforming methods.

The practical configuration of a membrane reactor can be mainly classified into either packed (fixed) bed or fluidized bed reactor. Packed beds have advantages like simplicity in construction and keeping catalyst in a fixed position which leads to avoidance of damaging membrane caused by erosion. In contrast the disadvantages of this type of reactors are the temperature differences that the reactor (and so the

Table 11.3 Reactions of different type of reforming methods

Steam reforming (SR)	
Reaction	Main reaction: $C_nH_m + nH_2O \leftrightarrow nCO + (n + m/2)H_2$ Water–gas shift reaction: $CO + H_2O \leftrightarrow CO_2 + H_2$
Partial oxidation reforming (POR)	
Reaction	$C_nH_m + (n/2)O_2 \leftrightarrow nCO + (m/2)H_2$
Autothermal reforming (ATR)	
Reaction	$C_nH_m + (m/4)O_2 + 2(n - m/4)H_2O \leftrightarrow nCO + 2nH_2$ $C_nH_m + ((n - 1)/2)O_2 + CO_2 \leftrightarrow (n + 1)CO + (m/2)H_2$
Dry reforming (DR)	
Reaction	$C_nH_m + nCO_2 \leftrightarrow 2nCO + (m/2)H_2$

membrane) experiences in endothermic or exothermic reactions, and also mass transfer limitation is another problem, yet these issues are less notable in fluidized beds. Disadvantages of those conventional methods mentioned above are equilibrium restriction and gaseous by-products production, even in total fuel conversion. Microstructured reactors are another type of membrane that also have been studied because of their good heat and mass transfer features (Arratibel Plazaola et al. 2017). There are some characteristics that should be taken into account for choosing membrane to obtain stripped hydrogen: considerable selectivity towards hydrogen, economic feasibility, high stability (both mechanical and chemical), and high flux (Gallucci et al. 2013). H_2-selective membranes can be classified into different types depending on type of materials including polymeric membranes, dense metal membranes, and proton conducting membranes. To compare these membranes, different critical parameters such as permeated flux, operating condition range, and permselectivity must be considered. Dense metal membranes (palladium alloys) and dense ceramic membranes are the best materials to gain high-purity hydrogen, due to their high selectivity towards hydrogen. Pd alloys are useful to descend the embrittlement and decrease the catalyst poisons like CO and H_2S. Selectivity restriction is inevitable in these membranes compared to inorganic membranes due to their separation process which is size exclusion-based (Gallucci et al. 2013). Among dense metal membranes, Pd-based membranes can be sorted into two groups: unsupported and supported. Unsupported membranes have some disadvantages like high cost of production and mass transfer resistance (bulk diffusion) that result in low hydrogen permeability. To obtain hydrogen with ultra-purity, these processes are taken place into reactors (Gallucci et al. 2013; Saidi 2017). Hydrogen permeation through palladium-based membranes is a complex process. Hydrogen molecule adsorption on the surface followed by dissociation into atomic hydrogen, diffusion of atomic hydrogen from surface into the bulk metal, diffusion through the bulk metal, and recombination of atomic hydrogen on the surface before they desorb as hydrogen molecules are the noteworthy steps in this complex process (Ward and Dao 1999). A conceptual figure of hydrogen separation is illustrated in Fig. 11.7. A membrane reactor consists of two concentric tubes (Mardanpour et al. 2012). The inner and the outer tubes are the catalytic reaction and permeation sides, respectively (Brunetti et al. 2007). The stream containing the components that permeate through the membrane is called permeate, and the stream containing the retained components is called retentate. The overall membrane performance depends on various parameters: mainly porosity and supporting material, operating conditions (temperature and pressure), composition of feedstock, and membrane thickness. The difference in hydrogen partial pressures between the reaction side and the permeation side is the driving force that the generated hydrogen permeates through the membrane. Mass transfer driving forces is the result of:

1. Sweeping an inert gas on the side that permeation happens (e.g., N_2, He, etc.).
2. Pressure in the retentate should be higher than the permeate channel (by evacuation of permeate, if necessary).
3. Sweeping a reactive gas to use the permeated hydrogen (e.g., O_2, air, CO, etc.) (Dittmeyer et al. 2001).

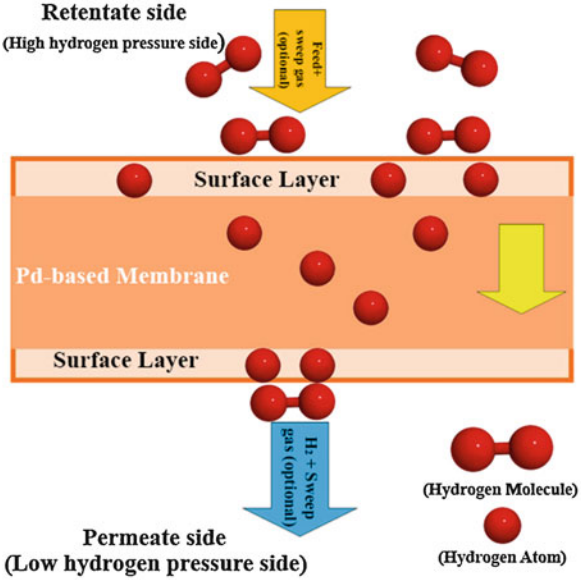

Fig. 11.7 A conceptual figure of hydrogen separation in a palladium-based membrane reactor

Some opportunities are available to enhance Pd-based membrane reactor efficiency. Common Pd-based membrane reactors have self-supporting films with thickness ranging from 25 to 100 μm (Saeidi et al. 2017). However, high cost and having a low hydrogen flux are the main challenges for improvement. Decrease in thickness increases chemical performance but decreases mechanical strength. Metallic membranes are deposited on supports in order to achieve high selectivity, good permeability, and mechanical strength (Saeidi et al. 2017). The presence of other gases coexisting with hydrogen in mixture can decrease hydrogen permeation through membrane due to polarization phenomenon. Unemoto et al. reported that presence of CO, CO_2, and H_2O can reduce hydrogen flux (Unemoto et al. 2007b). In general, the hydrogen flux permeating through a membrane may be expressed as the below equation (Iulianelli et al. 2014):

$$J_{\mathrm{H}_2} = \frac{\mathrm{Pe}_{\mathrm{H}_2} \cdot \left[\left(P^{c}_{\mathrm{H}_2} \right)^{n} - \left(P^{c}_{\mathrm{H}_2} \right)^{n} \right]}{\delta} \tag{11.2}$$

where J_{H2} is the hydrogen flux permeating through the membrane, Pe_{H2} is the hydrogen permeability, and n is the dependence factor of the hydrogen flux on the hydrogen partial pressure (variable from 0.5 to 1). δ and $P_{H2retentate}$ and $P_{H2permeate}$ are the membrane thickness and the hydrogen partial pressures in the retentate and permeate side, respectively. For membranes with thickness greater than 5 μm, the n value is 0.5, and where the hydrogen–hydrogen interactions in the bulk are not negligible at high pressures, n equals to 1. If the hydrogen permeability is described as an Arrhenius-like equation, Sieverts–Fick law becomes the Richardson's relation:

Table 11.4 Hydrogen separation efficiency of some pd-based membranes

Membrane	Thickness (μm)	Temperature (°C)	Driving force (MPa)	H_2 flux (mol/m^2.s)	References
Pd/PG	13	500	0.202	0.189	Uemiya et al. (1988)
Pd–Ag/PG	21.6	400	0.202	0.067	Uemiya et al. (1988)
Pd/Al_2O_3	0.5–1	30–4500	0.1	0.05–0.1	Xomeritakis and Lin (1996)
Pd–Cu/Al_2O_3	3.5	350	0.1	0.056	Roa and Way (2003)
Pd–Cu/Al_2O_3	1.5	350	0.1	0.499	Tong et al. (2006)
Pd/MPSS	6	550	0.1	0.300	Tong et al. (2006)
Pd–Ag/MPSS	4	500	0.1	0.280	Tong et al. (2006)
Pd/HF	3–4	430	0.1	0.136	Liang and Hughes (2005)
Pd/MPSS	10	480	0.1	0.089	Iulianelli et al. (2010)
Pd/MPSS	19–20	500	0.101	0.0150–0.030	Mardilovich et al. (1998)
Pd–Ag/MPSS	15	500	0.202	0.103	Iliuta et al. (2003)
Pd–Ag	50	500	0.1	0.010	Gallucci et al. (2004)
Pd–CeO_2/MPSS	13	500	0.2	0.275	Tong et al. (2005b)

$$J_{H_2} = \frac{\mathrm{Pe}_0.\exp\left(\frac{-E_a}{\mathrm{RT}}\right)\left[\sqrt{P_{H_2}^{c}} - \sqrt{P_{H_2}^{s}}\right]}{\delta} \tag{11.3}$$

Hydrogen separation efficiency of some pd-based membranes is shown in Table 11.4 (Gallucci et al. 2004; Iliuta et al. 2003; Iulianelli et al. 2010; Liang and Hughes 2005; Roa and Way 2003; Tong et al. 2005b, 2006; Uemiya et al. 1988; Xomeritakis and Lin 1996).

Due to high cost of palladium-group metals (PGMs) and their high usage in unsupported membrane production, manufacturing cost highly depends on thickness of membranes. According to Morreale et al., the membrane permeability increases at high temperatures due to the dominance of endothermic activation energy for diffusion over exothermic hydrogen adsorption (Morreale et al. 2003). The effect of nitrogen on hydrogen permeability is investigated by Li et al. (2000), Augustine et al. (2011), Peters et al. (2008), and Sánchez et al. (2014). Polarization concentration is the reported reason for reduction of hydrogen permeation. Alsom Wang et al. reported the blockage of permeation area due to formation of nitrogen species (NH_x, x = 0–2) (Wang et al. 2007). Nitrogen inhibition followed a linear trend regarding its quantity in mixture, and carbon dioxide followed a higher inhibition. Some researchers concluded that steam could dissociate on the active sites and permeate through the membrane (Gao et al. 2004). However, Li et al. (2000) used steam to improve hydrogen permeation by regenerating deactivated membranes. Steam showed diverse behavior depending on its concentration in the feed gas. Inhibition by steam was even stronger than that of nitrogen and carbon dioxide when mixture was rich in hydrogen (higher than 50%), while in steam-rich mixtures (hydrogen concentration lower than 50%), inhibition was nearly independent of steam quantity. The effect of carbon monoxide is noteworthy. Carbon monoxide can deactivate palladium-based membranes. Flanagan et al. reported that carbon monoxide adsorbs strongly on the membrane surface which leads to deactivating and blocking hydrogen dissociation sites (Flanagan et al. 2000). The effect of carbon monoxide is dependent on its quantity in mixture and temperature (Li et al. 2007). At higher temperatures, milder deactivation was reported by Galluci et al. (2007) and Chabot et al. (1988). However, Pd/Ag alloy membranes was founded to be less deactivated by carbon monoxide (Khan et al. 2006; Sakamoto et al. 1996). The interesting part is that at 723 K carbon monoxide has no strong inhibition influence as Sánchez et al. reported in their research. Beside carbon monoxide, sulfur also blocks the hydrogen dissociation sites in pd alloy membranes (Amandusson et al. 2000; Catalano et al. 2010; Gallucci et al. 2007; Mejdell et al. 2009; Nguyen et al. 2009; Peters et al. 2008; Unemoto et al. 2007a, b). Thus in case of coal and waste gasification, sulfur removal is necessary for achieving the highest efficiency when using pd alloy membranes (Jordal et al. 2015). Jordal et al. mentioned that H_2S concentration should be preferably less than 2–3 ppm depending on temperature and H_2 concentration (Jordal et al. 2015). Arsenic, thiophene, unsaturated hydrocarbons, Hg vapor, chlorine carbon from organic materials, etc. may contaminate dense Pd-based membranes which results their irreversible poisoning (Iulianelli et al. 2014).

11.4 Waste Gasification

Waste gasification can be defined as a thermochemical conversion of organic waste materials into H_2, CO, CO_2, and CH_4 in the presence of a gasification agent and catalyst. Gasification process is known as an excellent method to treat waste as it produces less greenhouse gas (GHG) emissions comparing to other methods. Another advantage of gasification process is its flexibility towards different types of feedstock. Gasification conditions can be modified to separate desired gaseous products. The desired products can be used for heating, power generation, and transportation. In conclusion, economic and environmental considerations beside green energy generation are the main reasons to select waste gasification over other methods to treat waste (Watson et al. 2018). An overview of major methods to treat wastes is summarized in Table 11.5 (Maisarah et al. 2018; Münster and Meibom 2011; Verma 2002; Wilson et al. 2013).

Table 11.5 An overview of major methods to treat wastes

Process	Description	Conversion efficiency (MWh/ton MSW)	Service life (year)	Typical MSW input heating value (MJ/Kg)	Max fuel moisture (%)	Input	pH level
Incineration	Incinerating wastes in a boiler in temperature of about 1000–1200 °C	0.5[a]	30[a]	8–10.5[b]	40–50[a]	Mixed MSW	Not important
Gasification	Reacting MSW in a controlled amount of agents to produce desired products, i.e., CO,CO_2, and H_2; and the temperature is above 700 °C	0.9[a]	20[a]	16.5[b]	40–50[a]	Sorted MSW	Not important
Pyrolysis	At the temperature between 200 and 300 °C, organic fractions of MSW will be decomposed	0.3[a]	20[a]		10[a]	Sorted MSW	Not important
Anaerobic digestion	Anaerobic microorganisms work synergistically to break down organic fractions of MSW	0.15[c]	20[a]	2.5[b]	About 97[a]	Sorted MSW	6–8[d]

[a]Wilson et al. (2013)
[b]Münster and Meibom (2011)
[c]Verma (2002)
[d]Maisarah et al. (2018)

The main difference between waste gasification and combustion is that gasification adds hydrogen (H_2) and strips away carbon (C) from the feedstock that result in packing energy into chemical bonds, yet combustion breaks bonds of the matter by oxidizing hydrogen into water and carbon into carbon dioxide (Basu 2010b). In order to use gasification method, some pre-requirements are necessary: like other thermochemical conversion methods, the feedstock must be dry, and its moisture content should be between 10% and 20%, and waste that contain more moisture should be dried (Ahmad et al. 2016). Also homogenizing the waste based on their size and composition should be taken place (Kumar et al. 2009; Molino et al. 2016). Waste gasification methods contain the following steps (Balat 2009; Basu 2010b; Puig-Arnavat et al. 2010; Ruiz et al. 2013):

1. Waste drying at the temperature between 100 and 200 °C to drop its moisture content below 5%.
2. Waste impurity removal.
3. Devolatilizing at 150–400 °C to break down large molecules into smaller one and gas, char, and tar.
4. Syngas production.

The main drawback of traditional gasification methods is the coproduction of residue (tar, char, etc.) besides syngas. In order to improve the produced syngas quality and also decrease contaminants, using proper catalyst and agent is required. Steam as a gasification agent is mostly used not only to minimize the amount of tar but also to produce hydrogen selectively. This process is called steam gasification (Xiao et al. 2013). Since, this method is endothermic, so it needs an energy resource to keep running (Hejazi et al. 2014). Positive and negative aspects of hydrogen production processes are presented in Table 11.6 (Gao et al. 2015; Nikoo et al. 2015).

Waste gasification process is classified based on different criteria, such as used agent like air, steam, oxygen and plasma; thermodynamic concept like endothermic and exothermic; density factor like dense phase reactor and lean phase reactor; etc. *(*Lohri et al. 2017*)*. Dense phase reactors include fixed bed gasifiers (downdraft or co-current fixed bed and updraft or countercurrent fixed bed) and lean phase reactors include fluidized bed gasifiers (bubbling fluidized bed, circulating bed and entrained flow) (Salam et al. 2018). A comparison between using different gasification agents is summarized in Table 11.7 (He et al. 2009c; Niu et al. 2014; Thamavithya and Dutta 2008). Updraft gasifier can be used for waste conversion with both low and high moisture content in feedstock (Thamavithya and Dutta 2008). An overview of technologies used in gasification process is presented in Table 11.8 (Arena 2012; Basu 2010a; Kramreiter et al. 2008; Puig-Arnavat et al. 2010; Ruiz et al. 2013). Table 11.9 summarized some of the investigations done on gasification technology (Bhavanam and Sastry 2011; Chopra and Jain 2007; Sikarwar et al. 2016; Surjosatyo et al. 2010; Wang et al. 2008).

Table 11.6 Positive and negative aspects of hydrogen production processes

Method of hydrogen production	Advantages	Disadvantages	References
Incineration	Proper for units with high waste input	High cost and not proper to be utilized in cities and environmental hazards	Gao et al. (2015)
Steam gasification	Fuel gas production in high quantity with high-purity and more environmental-friendly than conventional methods	Low efficiency at high moisture content	Gao et al. (2015)
Anaerobic digestion	No need of electrical power and aesthetic view and environmental friendly	Suitable only for wastes with high content of organic matters	Gao et al. (2015)
Plasma gasification	Environmental-friendly and industrialized and good process control	Uses a great amount of electricity and high operating costs and special maintenance is needed	Nikoo et al. (2015)
Pyrolysis	Inexpensive feedstock and able to recover tar and the most inexpensive method to produce H_2	Environmental hazards and production a notable amount of solid substances	Nikoo et al. (2015)
Partial oxidation	Industrial	Greenhouse gas emission and less effective	Nikoo et al. (2015)
Autothermal reforming	Less capital costs and industrial	Greenhouse gas emission and less effective	Nikoo et al. (2015)

Table 11.7 A comparison between using different gasification agents

Characteristic	Steam	Oxygen	Air
Feedstock	MSW	MSW	MSW
Catalyst	Not needed	Not needed	Not needed
Moisture content (%)	–	8.31	7.59
Temperature (°C)	900	800	777
Steam to waste ratio	0.8	–	–
E/R	–	0.2	0.4
H_2 (vol%)	28	11.8	5
CH_4(vol%)	21	10.3	5
CO(vol%)	16.5	30.3	19
CO_2(vol%)	17.5	35.5	15
LHV (MJ/Nm^3)	15.0	8.5	2.4
Tar yield (wt%)	0.2	43.5	11.4 (g/m^3)
Char yield (wt%)	7.9	15.5	–
Dry gas yield (m^3/kg)	0.5	–	14
Carbon conversion efficiency (%)	44.1	–	61

Table 11.8 An overview of technologies used in gasification process

Operational condition	Gasification technology: Updraft	Downdraft	Bubbling fluidized bed	Circulating fluidized bed	Entrained flow bed
Specification of fuel	> 51 mm	> 51 mm	> 6 mm	> 6 mm	> 15 mm
Max. moisture content valid	60%	25%	< 55%	< 55%	< 15%
LHV (MJ/Nm^3)	5–6	4.5–5.0	3.7–8.4	4.5–13	4–6
Temperature of reaction (°C)		1090	800–1000		1990
Ash and other produced particulates	Notable	Ignorable	Notable	Notable	Ignorable
Temperature of exhaust gas (°C)	200–400	700	800–1000		>1260
Tar (g/Nm^3)	30–150	0.015–3.0	3.7–61.9	4–20	0.01–4
Hot gas potency (%)	90–95	85–90	89	89	80
Time of residence	Until complete infusion		Long period	Particles pass through the bed	Few seconds
Melting point of ash (°C)	> 1000	> 1250	> 1000		> 1250
Efficiency of carbon conversion	High	High (carbon aggravation in ash is noticed)	High	High	High
Flexibility of process		Very determinate	More flexible to load than design		Very determined (specially range of size and content of energy)
Temperature profile		High	Almost constant with a slight radial variation (vertical gasifier)	Almost constant (vertical gasifier)	Temperature is higher than the ash melting temperature

Table 11.9 Some of the investigations done on gasification technology

Area of investigation	References
Focusing on using different biomass as the feedstock since it is an environmental-friendly approach	Sikarwar et al. (2016)
Improvement of several factors affecting the process using downdraft gasifier	Bhavanam and Sastry (2011)
Discussing different methods to decrease in residual tar content	Surjosatyo et al. (2010)
Discussing progress and bottlenecks of using biomass as the feedstock of the process	Wang et al. (2008)
Improvement of the process using fixed bed gasifier	Chopra and Jain (2007)

11.4.1 Waste Steam Gasification

According to the Table 11.3, this process produces more amount of hydrogen with more heating value compared to other methods. The gasification agent in this method improves the yield of reactions, i.e., water–gas shift and steam reforming. Oxidation of feed takes place due to water–gas reactions and also decomposition of steam (Watson et al. 2018). There are several parameters that waste gasification process depends on. Feedstock particle size, operating conditions like pressure and temperature, applied materials for bed, catalysts, agents used for gasification, heating rate, amount of feedstock moisture, and steam to waste ratio (S/W) (Radwan 2012; Sikarwar et al. 2016). By increasing steam to waste ratio, the quantity of H_2 and CO_2 increases, while the content of CH_4 and CO decreases (Garcia et al. 1999). The performance of this method will be enhanced by integrating this method and slow pyrolysis steam gasification techniques. By using this method, thermal efficiency and the quality of the produced syngas will be improved, and also the tar yield will be decreased (Dawoud et al. 2007; Parthasarathy and Narayanan 2015; Parthasarathy and Sheeba 2015).

11.4.2 Waste Oxygen and Air Gasification

Oxygen gasification is mostly used for its ability to make medium heating value. Yet, this agent has some drawbacks like high cost of producing pure oxygen and also high cost of separating it from the produced syngas. Due to availability and ease of access, air is the most used agent in gasification. The outcome of this reaction depends on air temperature; as the temperature is increased, higher heating value is resulted (Lucas et al. 2004).

11.4.3 Plasma Gasification

Using plasma is an ideal alternative of using oxygen as the blast agent, as oxygen production is hazardous and also costly. Using plasma increases gasification rate and value heat combustion of produced syngas; furthermore, this method can be used to treat more variant types of waste comparing to other methods (Indarto and Palguandi 2013).

11.4.4 Waste to Syngas

As discussed before, waste can be converted to syngas via gasification. Gasification product is then considered as feedstock for membrane reactor. In membrane reactor, hydrogen content is increased (and separated) via steam reforming and water–gas shift reactions. In fact, any type of waste containing carbon can be gasified leading to syngas. Comparing to traditional incineration, gasification can convert all kinds of carbonaceous solid waste into syngas (CH_4, CO, CO_2, and H_2) besides heat energy recovery, while incineration can just recover heat energy from combustion without considering the possible reuse of feedstock (Maneerung et al. 2016; Ong et al. 2015; Saidi 2018). It must be noted that depending on the waste type, composition of the produced syngas varies. As an example, Lee et al. studied steam gasification of different types of solid waste materials, i.e., municipal solid waste (MSW), used tires, and sewage sludge (Lee et al. 2016). Sewage sludge is considered as a biomass containing a high energy content energy source. The disadvantage of this source is its high nitrogen and sulfur content besides heavy metals and pathogens (He et al. 2009a; Mawioo et al. 2017; Zhang et al. 2016, 2017). The sewage sludge gasification is similar to that of coal and biomass. First sewage sludge is pyrolyzed, and volatile contents are liberated, and subsequently the remaining solid reacts with gasification agents to produce H_2 and CO (Chen et al. 2017a). In their study, tires were used as feedstock since it contains high carbon content. In 2013 in the United States, about 1.8 million tons of used tires were collected. It is about 60% of the total amount of rubber in tires (Gupta and Cichonski 2007). They investigated and compared different syngas compositions derived from different feedstock. All three types of feedstock were gasified in the same conditions (3 g of feedstock gasified, 1000 °C steam, and 5 g/min steam flow rate). In gasification of sewage sludge, concentration of CO was very high at the same time the concentration of H_2 increased with time. The concentration of hydrogen reached around 60% by volume. Methane was produced in the beginning, and reaction with steam produced hydrogen. It was because of the higher temperature condition in the reactor after the initiation where methane was reacted with water vapor. Interestingly, even for rubber and MSW, the similar results were obtained. Except for the rubber as feedstock, CO concentrations are nearly as high as hydrogen concentration, seemingly because of the pyrolysis process happening before the feedstock reacting with steam. In their reactor design, at first the feedstock was put inside the reactor, and subsequently the steam flow was added. In this design, a pyrolysis stage happens before steam–feedstock chemical interaction. During the pyrolysis process, the steam available for gasification is quite restricted, and as a result, CO production is favored since rate of water–gas shift reaction is low. A comparison between the pyrolysis and gasification is reported by Nipattummakul et al. (2010). They concluded that the gasification process leads to a relatively higher hydrogen concentration and lower CO concentration, while in the pyrolysis process, higher CO concentration and lower hydrogen concentration was achieved. In comparison to air gasification, steam gasification produced much higher concentrations of hydrogen and CO. The total energy value was nearly double air gasification, since hydrogen is provided from the steam. It was found that the rubber as feedstock generated more than twice the amount of syngas as compared to the other two types of feedstock. Hydrogen generated by the rubber is three times of that generated by the sewage sludge or MSW. Higher hydrogen production by rubber is because of high carbon content in the rubber shifting the water shift gas reaction to hydrogen production. Umeki et al. (2010) investigated the steam gasification of woody biomass with high temperature steam above 1200 K. The high temperature steam acted both as the gasifying agent and heat carrier to the reactor. The hydrogen concentration was around 35–55 vol. % which was higher in comparison to air gasification. Another example of waste gasification is studied by Zhang et al. (2018a). Gasification system containing food waste and woods chips were studied. Syngas with over 34% of CH_4, H_2, and CO was produced from gasification of wood chips with bio char as a by-product. The results of the in situ analysis showed that syngas composition containing CH_4, H_2, CO_2, and CO was 2.6%, 17.1%, 15.9%, and 15%, respectively. Over 34% syngas (CH_4, H_2, and CO) was effectively generated via woody biomass gasification (Zhang et al. 2018a). Syngas production by steam gasification of sewage sludge was also investigated by Chen et al. (2017a). They found that higher temperature improves the rate of gasification reaction, reforming of CH_4 and cracking of tar. So at a higher temperature, increase in both hydrogen fraction and yield resulted. They also concluded that the addition of metal element Ni and Fe can improve the tar cracking, methane reforming, and char conversion into gases. So the addition of metal elements in gasification of sewage sludge can improve hydrogen production (Chen et al. 2017a). It has been proven by Dudynski that gasification is reliable way to use difficult to handle industrial waste, such as tannery residues and feathers (Dudynski 2018). Gasification found to be effective for converting such hazardous organic waste into energy. Another example of syngas production via MSW gasification was reported by Zheng et al. (2018). In their study, key parameters of gasification, i.e., temperature and CO_2/steam ratio, ranging from 1000 to 1100 °C in temperature and 0.5–3 in CO_2/steam ratio are investigated. Their experiments showed that increasing CO_2/steam ratio ranging from 0.5 to 2.5 increases both H_2 and CO production. Simultaneously, the CO_2 conversion efficiency rises. It was concluded that Boudouard reaction (shown below) and water–gas reaction proceed independently in the gasification process. As predictable, when using only syngas as the gasifying agent, maximum values for H_2 and syngas yield were achieved. In general, there are several researches based on

H_2 or syngas production from MSW or its components using steam as the gasifying agent (Couto et al. 2016a, b; He et al. 2009b, c; Hu et al. 2015; Lee et al. 2014; Zheng et al. 2016). As an example, Ahmed et al. studied syngas production from cardboard gasification beside the pyrolysis and steam gasification of paper (Ahmed and Gupta 2009b, c). They found that gasification of paper was strongly connected to char gasification process. They also investigated the composition of syngas and yield of syngas from CO_2 gasification of cardboard and paper. They noted that further study on CO_2 as a gasifying agent for gasification of wastes is crucial (Ahmed and Gupta 2009a). On the other hand, Castaldi and Dooher studied the gasification of coal by reusing CO_2 in a gasifier (Castaldi and Dooher 2007). Their results indicated that 15% more hydrogen production was resulted when up to 25% of CO_2 reused in the gasifier. The main gasification reactions of wastes are summarized as (Widjaya et al. 2018):

$$\mathrm{C} + \frac{1}{2}\mathrm{O_2} \rightarrow \mathrm{CO} \quad \Delta H = -110.6\ \mathrm{kJ/mol} \tag{11.4}$$

$$\mathrm{C} + \mathrm{O_2} \rightarrow \mathrm{CO_2} \quad \Delta H = -393.6\ \mathrm{kJ/mol} \tag{11.5}$$

$$\mathrm{C} + \mathrm{CO_2} \rightarrow 2\mathrm{CO} \quad \Delta H = +127\ \mathrm{kJ/mol} \tag{11.6}$$

$$\mathrm{C} + \mathrm{H_2O} \rightarrow \mathrm{CO} + \mathrm{H_2} \quad \Delta H = +122.9\ \mathrm{kJ/mol} \tag{11.7}$$

$$\mathrm{C} + 2\mathrm{H_2} \rightarrow \mathrm{CH_4} \quad \Delta H = - + 74.9\ \mathrm{kJ/mol} \tag{11.8}$$

Also, shift reaction (also in reactor to achieve complete CO conversion) occurs as:

$$\mathrm{CO} + \mathrm{H_2O} \leftrightarrow \mathrm{CO_2} + \mathrm{H_2} \quad \Delta H = -41.1\ \mathrm{kJ/mol} \tag{11.9}$$

And steam reforming (also in reactor to achieve complete methane conversion) takes place as:

$$\mathrm{CH_4} + \mathrm{H_2O} \leftrightarrow \mathrm{CO} + 3\mathrm{H_2} \quad \Delta H = - + 206\ \mathrm{kJ/mol} \tag{11.10}$$

11.4.5 Syngas to Pure Hydrogen

To achieve complete CO and methane conversion in syngas, steam reforming and water–gas shift reactions are conducted in membrane reactor. Applying a membrane reactor to carry out the water–gas shift reaction enables the opportunity to replace the traditional two-unit reactor, a unit operated at high temperature (HT) and another unit at low temperature (LT), by a one-unit system to produce high-purity H_2. In addition, further purification such as PSA (pressure swing Adsorption) is not required (Cornaglia et al. 2015). Recently, there have been several researches on the application of membrane reactors to carry out water–gas shift reaction, but only a few of them have investigated the catalyst–membrane interaction (Babita et al. 2011; De Falco et al. 2013; Mendes et al. 2010). Many studies also focused on high-grade hydrogen recovery from a catalytic membrane reactor using dense Pd-based (Augustine et al. 2011; Babita et al. 2011; Basile et al. 2010; Bi et al. 2009; Cornaglia et al. 2015; Hwang et al. 2013) or composite Pd-based (Augustine et al. 2012; Calles et al. 2014; Liguori et al. 2012; Pinacci et al. 2010). Cornaglia et al. (2013, 2014) studied WGS reaction by application a Pd–Ag membrane operating at 400 °C; this temperature was imposed by two parameters: (i) at T < 400 °C the CO adsorption on the membrane increased; thus the hydrogen permeability reduced; and (ii) at T > 450 °C the membrane durability reduced. They inferred that the optimum temperature of a Pd–Ag membrane reactor conducting the WGS reaction should balance a high CO conversion, a high H_2 recovery, and membrane stability. The most important variables of the WGS reaction in reactors are summarized below (Iulianelli et al. 2015):

- Temperature: In higher temperature the catalytic activity increases but conversion of CO decreases. As the result, it is essential to carry out the reaction in two successive steps (i.e., HT and LT).
- Pressure: Increase in pressure leads to an enhanced catalytic activity. In addition, operating at higher pressures enables the opportunity to decrease the size of the equipment.
- Space velocity: Decreasing the reactants' space velocity on the catalyst surface enables the opportunity to increase CO conversion near the equilibrium.
- Steam/gas ratio: An increase in the steam/gas ratio decreases CO content at the equilibrium and also decreases the reagents' contact time.
- Catalysts dimensions: The catalytic activity is highly affected by the catalyst dimension; thus, with smaller catalysts, it is possible to increase the reactor performances.

In order to produce high-purity hydrogen, methane steam reforming (MSR) is conducted in membrane reactor. First, MSR reaction and water–gas shift (WGS) reactions (high temperature shift-HTS and low temperature shift-LTS) happen, and finally purification to separate hydrogen from the reformed stream occurs (Li et al. 2016; Ritter and Ebner 2007). Considering operating conditions, high temperature (>1123 K) is needed in MSR reaction because of the endothermic nature of reaction (LeValley et al. 2014). Several researches investigated the development of advanced technologies for energy enhancement and economic feasibility (Basile et al. 2015; Di Marcoberardino et al. 2016; Murmura et al. 2017; Zheng et al. 2017). Iulianelli et al. investigated H_2 production from bio-methane steam reforming in membrane reactors (Iulianelli et al. 2017). Kim et al. performed MSR reaction in a membrane reactor equipped with commercial Ru/Al_2O_3 catalysts and a tubular Pd-based composite membrane at a temperature of 773 K and pressure difference range of 203–507 kPa (Kim et al. 2018).

11.5 Waste Impurities Removal

As mentioned earlier, several barriers exist in the way of producing pure hydrogen by membrane reactors, one of which is presence of impurities in waste. As a result, the efficiency of process decreases dramatically. Impurities are defined as the chemical substances that are not involved in the hydrogen production processes. Depending on the waste type, impurities may differ. For instance, municipal solid wastes such as paper, textiles, cosmetic products, and e-waste contain siloxanes as the impurity, while industrial units may be the main sources of sulfur impurities such as hydrogen sulfide. The processes leading to CO, CO_2, and H_2O production can also affect efficiency of pure hydrogen production.

11.5.1 Siloxanes Removal

The chemical backbone of siloxanes (Si−O−Si) is stable, so physical adsorption on activated carbon is the most common siloxane removal procedure (Ajhar et al. 2010). It is necessary to mention that the moisture content of the gas containing this type of impurities should be removed; otherwise the activated carbon will be saturated by moisture. Activated carbon performance is mostly influenced by moisture and temperature of the gas used in the process.

11.5.2 Hydrogen Sulfide Removal

H_2S removal methods can be mainly categorized as biological, physical, and chemical processes. Biological processes have the advantage of being both economic and environmental friendly (Fortuny et al. 2008). Physical and chemical processes include chemical absorption, physical adsorption, and chemical oxidation methods, at which their application depends on flow rate of H_2S feed gas. Waste utilization in the membrane reactor needs H_2S removal as it has catalyst poisoning nature which contains notable amounts of sulfur content.

In the waste purification units, H_2S abatement is the first step. Desulfurization is carried out by the reaction with mixed−metal oxides leading to a stable metal sulfide formation. A common method of H_2S removal is impregnation of iron sponge and activated carbon that are catalytic processes used in biogas H_2S removal (Choi et al. 2008; Yan et al. 2004). Chemical reaction on adsorbent surface using supporting material with ferric oxide coated onto is taken place in iron sponge as a catalytic process. The proposed removal mechanism is as follows: H_2S is adsorbed on the catalyst, and by the reaction of hydrated iron oxide with H_2S, iron sulfide will be produced, and H_2S is removed from the feedstock (Cherosky and Li 2013).

By impregnation of activated carbon with certain bases (NaOH, KOH), selectivity of the removal will be increased (Yan et al. 2002). Dissolution of mildly acidic H_2S gas and oxygen is the result of thin basic layer available on the surface of activated carbon and then radicals generated by O_2 react with dissolved hydrosulfide ions.

11.6 Economic and Environmental Investigation

11.6.1 Economic Investigation

Feed and process pressures (compressors), flow rates, operating temperatures, product purity, flexibility, and future expansions capability are the notable factors when a reaction takes place in a membrane reactor. Generally, factors related to economics of membrane reactors are those mentioned above, beside membrane type. In particular, permeability and selectivity of membrane influence the process capacity and purity of the product, respectively. Depending on the material used in membrane, operating conditions may differ, and thus the operating cost of the hydrogen production via different reactors will not be the same (Criscuoli 2006). As mentioned earlier, partial pressure gradient between permeate and retentate side should be made by applying pressure on the feed or sweeping an inert gas like nitrogen or by utilizing vacuum on the permeate side. This factors all influence the efficiency of hydrogen production (Criscuoli 2006). Fixed cost of manufacturing a membrane reactor is mainly based on the amount of palladium that is used in the reactor, and the cost is based on the thickness of the membrane as the cost of palladium varies during the year (Criscuoli 2006). In order to optimize manufacturing cost, application of new techniques to construct a low-thickness palladium-based membrane is crucial. Higher permeation rate is achieved in lower membrane thickness; thus, the desired recovery of hydrogen with lower membrane area is obtained.

Membrane reactor economic issues can mainly be divided to capital and operating costs. Installation costs and catalyst and equipment costs go into capital costs. Raw materials, replacement of membrane (the lifetime of a palladium membrane reactor is estimated about 3 years (Criscuoli et al. 2001)), consuming energy, etc. go into operating cost category (Criscuoli 2006).

Economic analysis of different membrane shows that amount of hydrogen in feedstock affects the economics of the membrane reactor: higher driving force and lower membrane area are needed for removal of hydrogen to desired amount as higher hydrogen is present in feedstock (Criscuoli et al. 2001). Criscuoli et al. have studied the effect of H_2O/CO ratio in several membranes and their effect on the total costs of the membrane. He concluded that by changing the ratio from 9.8 to 2, the efficiency reduces slightly (99.3–94.94%), yet the total costs decrease more than 50% (13.75 M€/year to 6.54 M€/year) (Criscuoli et al. 2001).

Landfilling has some bottlenecks as a waste management policy; transportation cost besides environmental issues is the major ones. Incineration has high operating and transportation cost (which is less than landfilling). In comparison, transportation cost is less considerable in membrane reactor technology and application of waste as raw material in gasification. Using gasification products (mainly syngas) as feed-stock in membrane reactor leads to lower operating cost for membrane reactor technology. Amount of palladium used in membrane can be recovered by various methods which make application of palladium membrane reactor more economically feasible for waste management.

Another advantage of membrane reactor technology over landfilling and incineration is its emerging technology. A lot of optimization is being suggested recently, helping construction cost of membrane reactor decrease, such as new technologies in membrane construction (e.g., reducing the thickness of palladium used in the membrane leading to lower construction cost).

11.6.2 Environmental Investigation

Considering the two main methods to convert waste to energy (chemical and biological), landfilling and incineration as common chemical methods are harmful method for the environment which release greenhouse gases and also produce small solid particles that easily suspend in the air and in polluted area, leading to arithmetic diseases. Pyrolysis and gasification cause indirect soil and groundwater pollution and inappropriate by-product formation. Biological methods such as anaerobic digestion produces lignin that cannot be decomposed soon (Beyene et al. 2018). On the other hand, using membrane technology for converting waste to energy is an efficient technology to manage and recover the waste and also resolves the abovementioned disadvantages.

11.7 Perspective

It is clear that the best solution to waste management is reducing the amount of produced waste, and this can be reached with a little change in life style. Among various thermochemical processes of waste to hydrogen conversion, further researches about integrated gasification in the membrane reactors are necessary. Also, more research and development about economic technologies to convert current types of waste into hydrogen is needed.

Pd/Ag alloy membranes are less sensitive to carbon monoxide as an inhibitor. Hence, developing new Pd/Ag alloy membranes or other types of alloy membranes that resist other inhibitors is inevitable in order to improve the efficiency of producing hydrogen via membrane reactors. Also manufacturing new membrane should be noticed, since cost of membrane manufacturing is highly dependent of the amount of palladium or other kinds of precious metals used. So developing and manufacturing new membranes that have low thickness and low amount of metal persuades

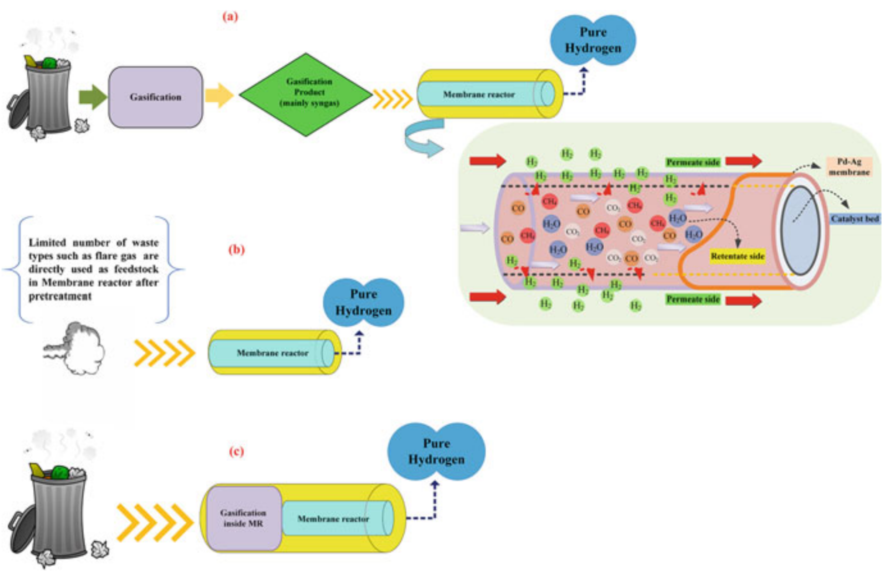

Fig. 11.8 (**a**) Gasification of waste materials and moving the gasification product to a membrane reactor; (**b**) usage of some special types of waste such as flare gas, etc. after pretreatment and moving them to membrane reactor; (**c**) gasification of wastes inside a membrane reactor

researchers and organization to use membrane reactors as a promising method to produce hydrogen, as it is more feasible compared to other technologies.

There may be three concepts in terms of using waste in membrane reactor technology. One is by gasification of waste materials and moving the gasification product to a membrane reactor (Fig. 11.8a). The second concept is the usage of some special types of waste such as flare gas, etc. after pretreatment and utilizing them as feedstock in membrane reactor (Fig. 11.8b). The other concept which seems to be more precious is gasification of wastes inside a membrane reactor which is called integrated configuration (Fig. 11.8c). The latter concept leads to an ultra-compact high-efficient integrated system. It is obvious that pretreatment of waste such as flare gas is necessarily needed when using it directly in the reactor if the lifetime of membrane matters. It is because of the fact that wastes such as flare gas contain notable amount of sulfur and other contaminants which can poison the catalytic portion of the membrane. Integrated systems have the advantages of being compact while not having the gasification issues. At the same time, only limited number of waste types can be used in an integrated system. Also, development of biochemical methods to produce hydrogen from waste due to its advantages such as being environmental friendly and no needs of electricity for the process is recommended. Harsh operating conditions of gasification is harmful to the membrane in the case of integrated configuration; therefore, newer gasification methods with milder operating conditions should be developed. In order to achieve milder gasification operating conditions, more studies on catalytic process development is substantial. However, some new modifications should be done to cope with this method bottleneck, i.e., its application for low organic content wastes.

11.8 Summary

As protecting environment has become a matter of debate these years and will be in the upcoming years, waste management has turned into a critical issue. Replacement of fossil fuels with green and environmental-friendly fuels like hydrogen will support the concept of protecting environment. Developing new methods and modifying the traditional methods to produce hydrogen, especially from waste, is necessary. It has both the benefit of reducing amount of generated waste and producing a green fuel instead of fossil fuels. The present study reviewed conversion technologies of waste to hydrogen. Waste conversion by application of membrane reactor provides the combined valorization of waste as both materials and energy and incorporates the goal to prevent CO_2 and other greenhouse gas emissions and produce hydrogen during gasification and reforming processes. In the future, more investigation is necessary to improve the commercial viability of membrane reactors in order to encourage the implementation of advanced waste conversion approaches.

References

Ahmad AA, Zawawi NA, Kasim FH, Inayat A, Khasri A (2016) Assessing the gasification performance of biomass: a review on biomass gasification process conditions, optimization and economic evaluation. Renew Sust Energ Rev 53:1333–1347

Ahmed I, Gupta A (2009a) Characteristics of cardboard and paper gasification with CO2. Appl Energy 86:2626–2634

Ahmed I, Gupta A (2009b) Evolution of syngas from cardboard gasification. Appl Energy 86:1732–1740

Ahmed I, Gupta A (2009c) Syngas yield during pyrolysis and steam gasification of paper. Appl Energy 86:1813–1821

Ajhar M, Travesset M, Yüce S, Melin T (2010) Siloxane removal from landfill and digester gas–a technology overview. Bioresour Technol 101:2913–2923

Al-Salem S, Lettieri P, Baeyens J (2010) The valorization of plastic solid waste (PSW) by primary to quaternary routes: from re-use to energy and chemicals. Prog Energy Combust Sci 36:103–129

Amandusson H, Ekedahl L-G, Dannetun H (2000) The effect of CO and O_2 on hydrogen permeation through a palladium membrane. Appl Surf Sci 153:259–267

Anderson DH, Evenson CR, Harkins TH, Jack DS, Mackay R, Mundschau MV (2009) Hydrogen separation using dense composite membranes. In: Inorganic membranes for energy and environmental applications. Springer, New York, pp 155–171

Arena U (2012) Process and technological aspects of municipal solid waste gasification. A review. Waste Manag 32:625–639

Arena U, Zaccariello L, Mastellone ML (2010) Fluidized bed gasification of waste-derived fuels. Waste Manag 30:1212–1219

Arratibel Plazaola A, Pacheco Tanaka DA, Van Sint Annaland M, Gallucci F (2017) Recent advances in Pd-based membranes for membrane reactors. Molecules 22:51

Augustine AS, Ma YH, Kazantzis NK (2011) High pressure palladium membrane reactor for the high temperature water–gas shift reaction. Int J Hydrog Energy 36:5350–5360

Augustine AS, Mardilovich IP, Kazantzis NK, Ma YH (2012) Durability of PSS-supported Pd-membranes under mixed gas and water–gas shift conditions. J Membr Sci 415:213–220

Babita K, Sridhar S, Raghavan K (2011) Membrane reactors for fuel cell quality hydrogen through WGSR–review of their status, challenges and opportunities. Int J Hydrog Energy 36:6671–6688

Balat M (2009) Gasification of biomass to produce gaseous products. Energy Sources Part A 31:516–526

Bamdad H, Hawboldt K (2016) Comparative study between physicochemical characterization of biochar and metal organic frameworks (MOFs) as gas adsorbents. Can J Chem Eng 94:2114–2120

Bamdad H, Hawboldt K, MacQuarrie S (2017) A review on common adsorbents for acid gases removal: focus on biochar. Renew Sust Energ Rev

Baran B, Mamis MS, Alagoz BB (2016) Utilization of energy from waste potential in Turkey as distributed secondary renewable energy source. Renew Energy 90:493–500

Barelli L, Bidini G, Gallorini F, Servili S (2008) Hydrogen production through sorption-enhanced steam methane reforming and membrane technology: a review. Energy 33:554–570

Basile A, Chiappetta G, Tosti S, Violante V (2001) Experimental and simulation of both Pd and Pd/Ag for a water gas shift membrane reactor. Sep Purif Technol 25:549–571

Basile A, Gallucci F, Tosti S (2008) Synthesis, characterization, and applications of palladium membranes. Membr Sci Technol 13:255–323

Basile, A., Pinacci, P., Tosti, S., De Falco, M., Evangelisti, C., Longo, T., Liguori, S., Iulianelli, A., 2010. Water gas shift reaction in Pd-based membrane reactors, Advances in science and technology. Stafa-Zuerich Trans Tech Publ, 99–104

Basile A, Liguori S, Iulianelli A (2015) Membrane reactors for methane steam reforming (MSR). In: Membrane reactors for energy applications and basic chemical production. Elsevier, pp 31–59

Basu P (2010a) Biomass gasification and pyrolysis: practical design and theory. Elsevier Science, Burlington

Basu P (2010b) Gasification theory and modeling of gasifiers. In: Biomass gasification and pyrolysis: practical design and theory. Elsevier, Burlington

Beavis R (2011) The EU FP6 CACHET project-final results. Energy Procedia 4:1074–1081

Beyene HD, Werkneh AA, Ambaye TG (2018) Current updates on waste to energy (WtE) technologies: a review. Renew Energy Focus 24:1–11

Bhavanam A, Sastry R (2011) Biomass gasification processes in downdraft fixed bed reactors: a review. Int J Chem Eng Appl 2:425

Bi Y, Xu H, Li W, Goldbach A (2009) Water–gas shift reaction in a Pd membrane reactor over $Pt/Ce_{0.6}Zr_{0.4}O_2$ catalyst. Int J Hydrog Energy 34:2965–2971

Bove D, Merello S, Frumento D, Arni SA, Aliakbarian B, Converti A (2015) A critical review of biological processes and technologies for landfill leachate treatment. Chem Eng Technol 38:2115–2126

Brunetti A, Caravella A, Barbieri G, Drioli E (2007) Simulation study of water gas shift reaction in a membrane reactor. J Membr Sci 306:329–340

Bukkarapu KR, Gangadhar DS, Jyothi Y, Kanasani P (2018) Management, conversion, and utilization of waste plastic as a source of sustainable energy to run automotive: a review. Energy Sources Part A: Recovery, Utilization, and Environmental Effects 40:1681–1692

Calles JA, Sanz R, Alique D, Furones L (2014) Thermal stability and effect of typical water gas shift reactant composition on H_2 permeability through a Pd-YSZ-PSS composite membrane. Int J Hydrog Energy 39:1398–1409

Castaldi MJ, Dooher JP (2007) Investigation into a catalytically controlled reaction gasifier (CCRG) for coal to hydrogen. Int J Hydrog Energy 32:4170–4179

Catalano J, Baschetti MG, Sarti GC (2010) Hydrogen permeation in palladium-based membranes in the presence of carbon monoxide. J Membr Sci 362:221–233

Chabot J, Lecomte J, Grumet C, Sannier J (1988) Fuel clean-up system: poisoning of palladium-silver membranes by gaseous impurities. Fusion Technol 14:614–618

Chen D, Yin L, Wang H, He P (2015) Reprint of: pyrolysis technologies for municipal solid waste: a review. Waste Manag 37:116–136

Chen P, Xie Q, Addy M, Zhou W, Liu Y, Wang Y, Cheng Y, Li K, Ruan R (2016) Utilization of municipal solid and liquid wastes for bioenergy and bioproducts production. Bioresour Technol 215:163–172

Chen S, Sun Z, Zhang Q, Hu J, Xiang W (2017a) Steam gasification of sewage sludge with CaO as CO_2 sorbent for hydrogen-rich syngas production. Biomass Bioenergy 107:52–62

Chen Y-P, Bashir S, Liu JL (2017b) Nanostructured materials for next-generation energy storage and conversion., ISBN 978-3-662-53512-7. Springer-Verlag GmbH Germany, Berlin, Heidelberg

Cherosky P, Li Y (2013) Hydrogen sulfide removal from biogas by bio-based iron sponge. Biosyst Eng 114:55–59

Choi D-Y, Lee J-W, Jang S-C, Ahn B-S, Choi D-K (2008) Adsorption dynamics of hydrogen sulfide in impregnated activated carbon bed. Adsorption 14:533–538

Chopra S, Jain A (2007) A review of fixed bed gasification systems for biomass. Internationale Kommission für Agrartechnik 9

Cornaglia CA, Tosti S, Sansovini M, Múnera J, Lombardo EA (2013) Novel catalyst for the WGS reaction in a Pd-membrane reactor. Appl Catal A Gen 462–463:278–286

Cornaglia CA, Tosti S, Múnera JF, Lombardo EA (2014) Optimal Pt load of a $Pt/La_2O_3SiO_2$ highly selective WGS catalyst used in a Pd-membrane reactor. Appl Catal A Gen 486:85–93

Cornaglia L, Múnera J, Lombardo E (2015) Recent advances in catalysts, palladium alloys and high temperature WGS membrane reactors: a review. Int J Hydrog Energy 40:3423–3437

Couto N, Monteiro E, Silva V, Rouboa A (2016a) Hydrogen-rich gas from gasification of Portuguese municipal solid wastes. Int J Hydrog Energy 41:10619–10630

Couto ND, Silva VB, Rouboa A (2016b) Assessment on steam gasification of municipal solid waste against biomass substrates. Energy Convers Manag 124:92–103

Criscuoli A (2006) Economics associated with implementation of membrane reactors. In: Nonporous inorganic membranes: for chemical processing. Wiley-VCH Verlag GmbH & Co. KGaA, Weinheim

Criscuoli A, Basile A, Drioli E, Loiacono O (2001) An economic feasibility study for water gas shift membrane reactor. J Membr Sci 181:21–27

Damiano L, Jambeck JR, Ringelberg DB (2014) Municipal solid waste landfill leachate treatment and electricity production using microbial fuel cells. Appl Biochem Biotechnol 173:472–485

Daskalopoulos E, Badr O, Probert S (1998) An integrated approach to municipal solid waste management. Resour Conserv Recycl 24:33–50

Dawoud B, Amer EH, Gross DM (2007) Experimental investigation of an adsorptive thermal energy storage. Int J Energy Res 31:135–147

De Falco M, Iaquaniello G, Palo E, Cucchiella B, Palma V, Ciambelli P (2013) Palladium-based membranes for hydrogen separation: preparation, economic analysis and coupling with a water gas shift reactor. In: Handbook of membrane reactors: reactor types and industrial applications. Elsevier, Amsterdam, pp 456–486

Demirbas A (2007) The influence of temperature on the yields of compounds existing in bio-oils obtained from biomass samples via pyrolysis. Fuel Process Technol 88:591–597

Di Marcoberardino G, Gallucci F, Manzolini G, van Sint Annaland M (2016) Definition of validated membrane reactor model for 5 kW power output CHP system for different natural gas compositions. Int J Hydrog Energy 41:19141–19153

Dincer I (2011) Thermal energy storage: systems and applications. Hoboken, Wiley

Dittmeyer R, Höllein V, Daub K (2001) Membrane reactors for hydrogenation and dehydrogenation processes based on supported palladium. J Mol Catal A Chem 173:135–184

Drioli E, Criscuoli A, Curcio E (2003) Membrane contactors and catalytic membrane reactors in process intensification. Chem Eng Technol: Industrial Chemistry-Plant Equipment-Process Engineering-Biotechnology 26:975–981
Dudynski M (2018) Gasification of selected biomass waste for energy production and chemicals recovery. Chem Eng Trans 65:391–396
Eddine BT, Salah MM (2012) Solid waste as renewable source of energy: current and future possibility in Algeria. Int J Energy Environ Eng 3:17
EPA (1986) Solving the hazardous waste problem: EPA's RCRA program. Office of Solid Waste, United States Environmental Protection Agency, Washington, DC
EPA (2013) Inventory of US greenhouse gas emissions and sinks United States Environmental Protection Agency, Office of Land and Emergency Management, Washington, DC
EPA (2015) Advancing sustainable materilas management: 2015 fact sheet. United States Environmental Protection Agency, Office of Land and Emergency Management, Washington, DC
FakhrHoseini SM, Dastanian M (2013) Predicting pyrolysis products of PE, PP, and PET using NRTL activity coefficient model. J Chem 2013:1–5
Flanagan TB, Wang D, Shanahan KL (2000) Inhibition by gaseous impurities of hydrogen absorption by Pd and by internally oxidized Pd–Al alloys. Phys Chem Chem Phys 2:4976–4982
Fortuny M, Baeza JA, Gamisans X, Casas C, Lafuente J, Deshusses MA, Gabriel D (2008) Biological sweetening of energy gases mimics in biotrickling filters. Chemosphere 71:10–17
Gallucci F, Paturzo L, Famà A, Basile A (2004) Experimental study of the methane steam reforming reaction in a dense Pd/Ag membrane reactor. Ind Eng Chem Res 43:928–933
Gallucci F, Chiaravalloti F, Tosti S, Drioli E, Basile A (2007) The effect of mixture gas on hydrogen permeation through a palladium membrane: experimental study and theoretical approach. Int J Hydrog Energy 32:1837–1845
Gallucci F, Fernandez E, Corengia P, van Sint Annaland M (2013) Recent advances on membranes and membrane reactors for hydrogen production. Chem Eng Sci 92:40–66
Gallucci, F., Medrano, J., Fernandez, E., Melendez, J., van Sint Annaland, M., Pacheco, A., 2017. Advances on high temperature Pd-based membranes and membrane reactors for hydrogen purification and production. J Membr Sci Res 3, 142–156
Gao H, Lin Y, Li Y, Zhang B (2004) Chemical stability and its improvement of palladium-based metallic membranes. Ind Eng Chem Res 43:6920–6930
Gao P, Dai Y, Tong Y, Dong P (2015) Energy matching and optimization analysis of waste to energy CCHP (combined cooling, heating and power) system with exergy and energy level. Energy 79:522–535
Garcia L, Salvador M, Arauzo J, Bilbao R (1999) Catalytic steam gasification of pine sawdust. Effect of catalyst weight/biomass flow rate and steam/biomass ratios on gas production and composition. Energy Fuel 13:851–859
Gerçel HF (2011) Bio-oil production from Onopordum acanthium L. by slow pyrolysis. J Anal Appl Pyrolysis 92:233–238
Gonzalez-Estrella J, Asato CM, Stone JJ, Gilcrease PC (2017) A review of anaerobic digestion of paper and paper board waste. Rev Environ Sci Biotechnol 16:569–590
Graham T (1866) XVIII. On the absorption and dialytic separation of gases by colloid septa. Philos Trans R Soc Lond 156:399–439
Gupta A, Cichonski W (2007) Ultra-high temperature steam gasification of biomass and solid wastes. Environ Eng Sci 24:1179–1189
Hartmann H, Ahring BK (2005) Anaerobic digestion of the organic fraction of municipal solid waste: influence of co-digestion with manure. Water Res 39:1543–1552
He M-m, Tian G-m, Liang X-q (2009a) Phytotoxicity and speciation of copper, zinc and lead during the aerobic composting of sewage sludge. J Hazard Mater 163:671–677
He M, Hu Z, Xiao B, Li J, Guo X, Luo S, Yang F, Feng Y, Yang G, Liu S (2009b) Hydrogen-rich gas from catalytic steam gasification of municipal solid waste (MSW): influence of catalyst and temperature on yield and product composition. Int J Hydrog Energy 34:195–203

He M, Xiao B, Liu S, Guo X, Luo S, Xu Z, Feng Y, Hu Z (2009c) Hydrogen-rich gas from catalytic steam gasification of municipal solid waste (MSW): influence of steam to MSW ratios and weight hourly space velocity on gas production and composition. Int J Hydrog Energy 34:2174–2183

Heidenreich S, Foscolo PU (2015) New concepts in biomass gasification. Prog Energy Combust Sci 46:72–95

Hejazi B, Grace JR, Bi X, Mahecha-Botero A (2014) Steam gasification of biomass coupled with lime-based CO_2 capture in a dual fluidized bed reactor: a modeling study. Fuel 117:1256–1266

Hu M, Guo D, Ma C, Hu Z, Zhang B, Xiao B, Luo S, Wang J (2015) Hydrogen-rich gas production by the gasification of wet MSW (municipal solid waste) coupled with carbon dioxide capture. Energy 90:857–863

Hwang K-R, Lee S-W, Ryi S-K, Kim D-K, Kim T-H, Park J-S (2013) Water-gas shift reaction in a plate-type Pd-membrane reactor over a nickel metal catalyst. Fuel Process Technol 106:133–140

Iliuta MC, Grandjean BP, Larachi F (2003) Methane nonoxidative aromatization over Ru− Mo/HZSM-5 at temperatures up to 973 K in a palladium− silver/stainless steel membrane reactor. Ind Eng Chem Res 42:323–330

Indarto A, Palguandi J (2013) Syngas: production, applications and environmental impact. Nova Publishers, New York

Iulianelli A, Liguori S, Calabrò V, Pinacci P, Basile A (2010) Partial oxidation of ethanol in a membrane reactor for high purity hydrogen production. Int J Hydrog Energy 35:12626–12634

Iulianelli A, Ribeirinha P, Mendes A, Basile A (2014) Methanol steam reforming for hydrogen generation via conventional and membrane reactors: a review. Renew Sust Energ Rev 29:355–368

Iulianelli A, Pirola C, Comazzi A, Galli F, Manenti F, Basile A (2015) Water gas shift membrane reactors. In: Membrane reactors for energy applications and basic chemical production. Elsevier, Amsterdam, pp 3–29

Iulianelli A, Dalena F, Basile A (2017) H_2 production from bioalcohols and biomethane steam reforming in membrane reactors. Bioenergy systems for the future. Elsevier, pp 321–344

Jha AK, Singh S, Singh G, Gupta PK (2011) Sustainable municipal solid waste management in low income group of cities: a review. Trop Ecol 52:123–131

Jocelyn D, Jean-Philippe L, Sherif F, Jamal C (2014) Distributed microwave pyrolysis of domestic waste. Waste Biomass Valoriz 5:1–9

Jordal K, Anantharaman R, Peters TA, Berstad D, Morud J, Nekså P, Bredesen R (2015) High-purity H_2 production with CO_2 capture based on coal gasification. Energy 88:9–17

Khan NA, Uhl A, Shaikhutdinov S, Freund H-J (2006) Alumina supported model Pd–Ag catalysts: a combined STM, XPS, TPD and IRAS study. Surf Sci 600:1849–1853

Kim C-H, Han J-Y, Lim H, Lee K-Y, Ryi S-K (2018) Methane steam reforming using a membrane reactor equipped with a Pd-based composite membrane for effective hydrogen production. Int J Hydrog Energy 43:5863–5872

Kramreiter R, Url M, Kotik J, Hofbauer H (2008) Experimental investigation of a 125 kW twin-fire fixed bed gasification pilot plant and comparison to the results of a 2 MW combined heat and power plant (CHP). Fuel Process Technol 89:90–102

Kumar S, Singh SP, Mishra IM, Adhikari DK (2009) Recent advances in production of bioethanol from lignocellulosic biomass. Chem Eng Technol: Industrial Chemistry-Plant Equipment-Process Engineering-Biotechnology 32:517–526

Lee D-H (2017) Evaluation the financial feasibility of biogas upgrading to biomethane, heat, CHP and AwR. Int J Hydrog Energy 42:27718–27731

Lee B-K, Ellenbecker MJ, Moure-Ersaso R (2004) Alternatives for treatment and disposal cost reduction of regulated medical wastes. Waste Manag 24:143–151

Lee U, Chung J, Ingley HA (2014) High-temperature steam gasification of municipal solid waste, rubber, plastic and wood. Energy Fuel 28:4573–4587

Lee U, Dong J, Chung J (2016) Production of useful energy from solid waste materials by steam gasification. Int J Energy Res 40:1474–1488

Lema J, Mendez R, Blazquez R (1988) Characteristics of landfill leachates and alternatives for their treatment: a review. Water Air Soil Pollut 40:223–250

LeValley TL, Richard AR, Fan M (2014) The progress in water gas shift and steam reforming hydrogen production technologies–a review. Int J Hydrog Energy 39:16983–17000

Li A, Liang W, Hughes R (2000) The effect of carbon monoxide and steam on the hydrogen permeability of a Pd/stainless steel membrane. J Membr Sci 165:135–141

Li H, Goldbach A, Li W, Xu H (2007) PdC formation in ultra-thin Pd membranes during separation of H_2/CO mixtures. J Membr Sci 299:130–137

Li B, He G, Jiang X, Dai Y, Ruan X (2016) Pressure swing adsorption/membrane hybrid processes for hydrogen purification with a high recovery. Front Chem Sci Eng 10:255–264

Li Q, Xu M, Wang G, Chen R, Qiao W, Wang X (2018) Biochar assisted thermophilic co-digestion of food waste and waste activated sludge under high feedstock to seed sludge ratio in batch experiment. Bioresour Technol 249:1009–1016

Liang W, Hughes R (2005) The catalytic dehydrogenation of isobutane to isobutene in a palladium/silver composite membrane reactor. Catal Today 104:238–243

Liguori S, Pinacci P, Seelam P, Keiski R, Drago F, Calabrò V, Basile A, Iulianelli A (2012) Performance of a Pd/PSS membrane reactor to produce high purity hydrogen via WGS reaction. Catal Today 193:87–94

Lin Y-M, Liu S-L, Chuang C-H, Chu Y-T (2003) Effect of incipient removal of hydrogen through palladium membrane on the conversion of methane steam reforming: experimental and modeling. Catal Today 82:127–139

Liu A, Ren F, Lin WY, Wang J-Y (2015) A review of municipal solid waste environmental standards with a focus on incinerator residues. Int J Sustain Built Environ 4:165–188

Lohri CR, Diener S, Zabaleta I, Mertenat A, Zurbrügg C (2017) Treatment technologies for urban solid biowaste to create value products: a review with focus on low-and middle-income settings. Rev Environ Sci Biotechnol 16:81–130

Lombardi L, Carnevale E, Corti A (2015) A review of technologies and performances of thermal treatment systems for energy recovery from waste. Waste Manag 37:26–44

Lu J-W, Zhang S, Hai J, Lei M (2017) Status and perspectives of municipal solid waste incineration in China: a comparison with developed regions. Waste Manag 69:170–186

Lucas C, Szewczyk D, Blasiak W, Mochida S (2004) High-temperature air and steam gasification of densified biofuels. Biomass Bioenergy 27:563–575

Ma YH (2007) Palladium membranes for hydrogen separation. Membranes for energy conversion 2, pp 245–261

Maisarah M, Bong CPC, Ho WS, Lim JS, Ab Muis Z, Hashim H, Elagroudy S, Teck GLH, Ho CS (2018) Review on the suitability of waste for appropriate waste-to-energy technology. Chem Eng Trans 63:187–192

Makarichi L, Jutidamrongphan W, Techato K-a (2018) The evolution of waste-to-energy incineration: a review. Renew Sust Energ Rev 91:812–821

Maneerung T, Liew J, Dai Y, Kawi S, Chong C, Wang C-H (2016) Activated carbon derived from carbon residue from biomass gasification and its application for dye adsorption: kinetics, isotherms and thermodynamic studies. Bioresour Technol 200:350–359

Mardanpour MM, Sadeghi R, Ehsani MR, Esfahany MN (2012) Enhancement of dimethyl ether production with application of hydrogen-permselective Pd-based membrane in fluidized bed reactor. J Ind Eng Chem 18:1157–1165

Mardilovich PP, She Y, Ma YH, Rei M-H, (1998) Defect-free palladium membranes on porous stainless-steel support. AICHE J 44:310–322

Martínez JD, Puy N, Murillo R, García T, Navarro MV, Mastral AM (2013) Waste tyre pyrolysis–a review. Renew Sust Energ Rev 23:179–213

Mawioo PM, Garcia HA, Hooijmans CM, Velkushanova K, Simonič M, Mijatović I, Brdjanovic D (2017) A pilot-scale microwave technology for sludge sanitization and drying. Sci Total Environ 601–602:1437–1448

Mejdell A, Jøndahl M, Peters T, Bredesen R, Venvik H (2009) Effects of CO and CO_2 on hydrogen permeation through a ~3 μm Pd/Ag 23 wt.% membrane employed in a microchannel membrane configuration. Sep Purif Technol 68:178–184

Mendes D, Mendes A, Madeira L, Iulianelli A, Sousa J, Basile A (2010) The water-gas shift reaction: from conventional catalytic systems to Pd-based membrane reactors—a review. Asia Pac J Chem Eng 5:111–137

Molino A, Chianese S, Musmarra D (2016) Biomass gasification technology: the state of the art overview. J Energy Chem 25:10–25

Morreale BD, Ciocco MV, Enick RM, Morsi BI, Howard BH, Cugini AV, Rothenberger KS (2003) The permeability of hydrogen in bulk palladium at elevated temperatures and pressures. J Membr Sci 212:87–97

Muhammad SK, Rasool BM, Muhammad AU (2016) Optimization of waste to energy routes through biochemical and thermochemical treatment options of municipal solid waste in Hyderabad, Pakistan. Energy Convers Manag 124:333–343

Münster M, Meibom P (2011) Optimization of use of waste in the future energy system. Energy 36:1612–1622

Murmura MA, Cerbelli S, Annesini MC (2017) An equilibrium theory for catalytic steam reforming in membrane reactors. Chem Eng Sci 160:291–303

Nguyen TH, Mori S, Suzuki M (2009) Hydrogen permeance and the effect of H_2O and CO on the permeability of $Pd_{0.75}Ag_{0.25}$ membranes under gas-driven permeation and plasma-driven permeation. Chem Eng J 155:55–61

Nikoo MK, Saeidi S, Lohi A (2015) A comparative thermodynamic analysis and experimental studies on hydrogen synthesis by supercritical water gasification of glucose. Clean Techn Environ Policy 17:2267–2288

Nipattummakul N, Ahmed II, Kerdsuwan S, Gupta AK (2010) Hydrogen and syngas production from sewage sludge via steam gasification. Int J Hydrog Energy 35:11738–11745

Nishioka K, Taniguchi T, Ueki Y, Ohno KI, Maeda T, Shimizu M (2007) Gasification and reduction behavior of plastics and iron ore mixtures by microwave heating. ISIJ Int 47:602–607

Niu M, Huang Y, Jin B, Wang X (2014) Oxygen gasification of municipal solid waste in a fixed-bed gasifier. Chin J Chem Eng 22:1021–1026

Oh J-I, Lee J, Lin K-YA, Kwon EE, Fai Tsang Y (2018) Biogas production from food waste via anaerobic digestion with wood chips. Energy Environ 29:1365–1372

Ong Z, Cheng Y, Maneerung T, Yao Z, Tong YW, Wang CH, Dai Y (2015) Co-gasification of woody biomass and sewage sludge in a fixed-bed downdraft gasifier. AICHE J 61:2508–2521

Papari S, Hawboldt K (2015) A review on the pyrolysis of woody biomass to bio-oil: focus on kinetic models. Renew Sust Energ Rev 52:1580–1595

Papari S, Hawboldt K (2017) Development and validation of a process model to describe pyrolysis of forestry residues in an auger reactor. Energy Fuel 31:10833–10841

Papari S, Hawboldt K (2018) A review on condensing system for biomass pyrolysis process. Fuel Process Technol 180:1–13

Parthasarathy P, Narayanan S (2015) Effect of combined slow pyrolysis and steam gasification of sugarcane bagasse on hydrogen generation. Korean J Chem Eng 32:2236–2246

Parthasarathy P, Sheeba K (2015) Combined slow pyrolysis and steam gasification of biomass for hydrogen generation—a review. Int J Energy Res 39:147–164

Patil AA, Kulkarni AA, Patil BB (2014) Waste to energy by incineration. J Comput Technol:2278–3814

Peters T, Stange M, Klette H, Bredesen R (2008) High pressure performance of thin Pd–23% Ag/stainless steel composite membranes in water gas shift gas mixtures; influence of dilution, mass transfer and surface effects on the hydrogen flux. J Membr Sci 316:119–127

Pinacci P, Broglia M, Valli C, Capannelli G, Comite A (2010) Evaluation of the water gas shift reaction in a palladium membrane reactor. Catal Today 156:165–172

Psomopoulos C, Bourka A, Themelis NJ (2009) Waste-to-energy: a review of the status and benefits in USA. Waste Manag 29:1718–1724

Puig-Arnavat M, Bruno JC, Coronas A (2010) Review and analysis of biomass gasification models. Renew Sust Energ Rev 14:2841–2851

Pütün AE, Özbay N, Önal EP, Pütün E (2005) Fixed-bed pyrolysis of cotton stalk for liquid and solid products. Fuel Process Technol 86:1207–1219

Qin Y, Li L, Wu J, Xiao B, Hojo T, Kubota K, Cheng J, Li Y-Y (2019) Co-production of biohydrogen and biomethane from food waste and paper waste via recirculated two-phase anaerobic digestion process: bioenergy yields and metabolic distribution. Bioresour Technol 276:325–334

Quek A, Balasubramanian R (2012) Mathematical modeling of rubber tire pyrolysis. J Anal Appl Pyrolysis 95:1–13

Quek A, Balasubramanian R (2013) Liquefaction of waste tires by pyrolysis for oil and chemicals—a review. J Anal Appl Pyrolysis 101:1–16

Radwan AM (2012) An overview on gasification of biomass for production of hydrogen rich gas. Der Chem Sin 3:323–335

Ritter JA, Ebner AD (2007) State-of-the-art adsorption and membrane separation processes for hydrogen production in the chemical and petrochemical industries. Sep Sci Technol 42:1123–1193

Roa F, Way JD (2003) Influence of alloy composition and membrane fabrication on the pressure dependence of the hydrogen flux of palladium− copper membranes. Ind Eng Chem Res 42:5827–5835

Robinson BH (2009) E-waste: an assessment of global production and environmental impacts. Sci Total Environ 408:183–191

Rogoff MJ, Screve F (2011) Waste-to-energy: technologies and project implementation. William Andrew, Norwich

Ruiz J, Juárez M, Morales M, Muñoz P, Mendívil M (2013) Biomass gasification for electricity generation: review of current technology barriers. Renew Sust Energ Rev 18:174–183

Saeidi S, Fazlollahi F, Najari S, Iranshahi D, Klemeš JJ, Baxter LL (2017) Hydrogen production: perspectives, separation with special emphasis on kinetics of WGS reaction: a state-of-the-art review. J Ind Eng Chem 49:1–25

Safari F, Dincer I (2019) Development and analysis of a novel biomass-based integrated system for multigeneration with hydrogen production. Int J Hydrog Energy

Saffarzadeh A, Shimaoka T, Motomura Y, Watanabe K (2006) Chemical and mineralogical evaluation of slag products derived from the pyrolysis/melting treatment of MSW. Waste Manag 26:1443–1452

Saidi M (2017) Performance assessment and evaluation of catalytic membrane reactor for pure hydrogen production via steam reforming of methanol. Int J Hydrog Energy 42:16170–16185

Saidi M (2018) Application of catalytic membrane reactor for pure hydrogen production by flare gas recovery as a novel approach. Int J Hydrog Energy 43:14834–14847

Saidi M, Jahangiri A (2018) Theoretical study of hydrogen production by ethanol steam reforming: technical evaluation and performance analysis of catalytic membrane reactor. Int J Hydrog Energy 43:15306–15320

Sakamoto Y, Chen F, Kinari Y, Sakamoto F (1996) Effect of carbon monoxide on hydrogen permeation in some palladium-based alloy membranes. Int J Hydrog Energy 21:1017–1024

Salam MA, Ahmed K, Akter N, Hossain T, Abdullah B (2018) A review of hydrogen production via biomass gasification and its prospect in Bangladesh. Int J Hydrog Energy 43:14944–14973

Sánchez JM, Barreiro MM, Maroño M (2014) Bench-scale study of separation of hydrogen from gasification gases using a palladium-based membrane reactor. Fuel 116:894–903

Sannita E, Aliakbarian B, Casazza AA, Perego P, Busca G (2012) Medium-temperature conversion of biomass and wastes into liquid products, a review. Renew Sust Energ Rev 16:6455–6475

Sharuddin SDA, Abnisa F, Daud WMAW, Aroua MK (2016) A review on pyrolysis of plastic wastes. Energy Convers Manag 115:308–326
Shu J, Grandjean BP, Kaliaguine S (1994) Methane steam reforming in asymmetric Pd-and Pd-Ag/porous SS membrane reactors. Appl Catal A Gen 119:305–325
Sikarwar VS, Zhao M, Clough P, Yao J, Zhong X, Memon MZ, Shah N, Anthony EJ, Fennell PS (2016) An overview of advances in biomass gasification. Energy Environ Sci 9:2939–2977
Surjosatyo A, Vidian F, Nugroho YS (2010) A review on gasifier modification for tar reduction in biomass gasification. Jurnal Mekanikal 31
Thamavithya M, Dutta A (2008) An investigation of MSW gasification in a spout-fluid bed reactor. Fuel Process Technol 89:949–957
Thi Phuong TP, Rajni K, Ganesh KP, Russell M, Rajasekhar B (2014) Waste Manag 12:4
Thürer M, Tomašević I, Stevenson M (2017) On the meaning of ‘waste’: review and definition. Prod Plan Control 28:244–255
Tong J, Matsumura Y, Suda H, Haraya K (2005a) Experimental study of steam reforming of methane in a thin (6 μM) Pd-based membrane reactor. Ind Eng Chem Res 44:1454–1465
Tong J, Sun J, Chen D, Zhang S (2005b) Geometrical features and wettability of dung beetles and potential biomimetic engineering applications in tillage implements. Soil Tillage Res 80:1–12
Tong J, Su L, Kashima Y, Shirai R, Suda H, Matsumura Y (2006) Simultaneously depositing Pd–Ag thin membrane on asymmetric porous stainless steel tube and application to produce hydrogen from steam reforming of methane. Ind Eng Chem Res 45:648–655
Uemiya S, Kude Y, Sugino K, Sato N, Matsuda T, Kikuchi E (1988) A palladium/porous-glass composite membrane for hydrogen separation. Chem Lett 17:1687–1690
Umeki K, Yamamoto K, Namioka T, Yoshikawa K (2010) High temperature steam-only gasification of woody biomass. Appl Energy 87:791–798
Unemoto A, Kaimai A, Sato K, Otake T, Yashiro K, Mizusaki J, Kawada T, Tsuneki T, Shirasaki Y, Yasuda I (2007a) The effect of co-existing gases from the process of steam reforming reaction on hydrogen permeability of palladium alloy membrane at high temperatures. Int J Hydrog Energy 32:2881–2887
Unemoto A, Kaimai A, Sato K, Otake T, Yashiro K, Mizusaki J, Kawada T, Tsuneki T, Shirasaki Y, Yasuda I (2007b) Surface reaction of hydrogen on a palladium alloy membrane under co-existence of H_2O, CO, CO_2 or CH_4. Int J Hydrog Energy 32:4023–4029
Van Caneghem J, Brems A, Lievens P, Block C, Billen P, Vermeulen I, Dewil R, Baeyens J, Vandecasteele C (2012) Fluidized bed waste incinerators: design, operational and environmental issues. Prog Energy Combust Sci 38:551–582
Verma S (2002) Anaerobic digestion of biodegradable organics in municipal solid wastes. Columbia University, New York
Wang W, Pan X, Zhang X, Yang W, Xiong G (2007) The effect of co-existing nitrogen on hydrogen permeation through thin Pd composite membranes. Sep Purif Technol 54:262–271
Wang L, Weller CL, Jones DD, Hanna MA (2008) Contemporary issues in thermal gasification of biomass and its application to electricity and fuel production. Biomass Bioenergy 32:573–581
Wang G, Li Q, Dzakpasu M, Gao X, Yuwen C, Wang XC (2018) Impacts of different biochar types on hydrogen production promotion during fermentative co-digestion of food wastes and dewatered sewage sludge. Waste Manag 80:73–80
Ward TL, Dao T (1999) Model of hydrogen permeation behavior in palladium membranes. J Membr Sci 153:211–231
Watson J, Zhang Y, Si B, Chen W-T, de Souza R (2018) Gasification of biowaste: a critical review and outlooks. Renew Sust Energ Rev 83:1–17
Weber DJ, Rutala WA (2001) Lessons from outbreaks associated with bronchoscopy. Infect Control Hosp Epidemiol 22:403–408
Wen X, Luo Q, Hu H, Wang N, Chen Y, Jin J, Hao Y, Xu G, Li F, Fang W (2014) Comparison research on waste classification between China and the EU, Japan, and the USA. J Mater Cycles Waste Manage 16:321–334

Widjaya ER, Chen G, Bowtell L, Hills C (2018) Gasification of non-woody biomass: a literature review. Renew Sust Energ Rev 89:184–193

Williams PT (2013) Pyrolysis of waste tyres: a review. Waste Manag 33:1714–1728

Wilson B, Williams N, Liss B, Wilson B (2013) A comparative assessment of commercial technologies for conversion of solid waste to energy. EnviroPower Renewable, Inc., Boca Raton

Windfeld ES, Brooks MS-L (2015) Medical waste management – a review. J Environ Manag 163:98–108

Xiao X, Cao J, Meng X, Le DD, Li L, Ogawa Y, Sato K, Takarada T (2013) Synthesis gas production from catalytic gasification of waste biomass using nickel-loaded brown coal char. Fuel 103:135–140

Xomeritakis G, Lin Y (1996) Fabrication of a thin palladium membrane supported in a porous ceramic substrate by chemical vapor deposition. J Membr Sci 120:261–272

Yan R, Liang DT, Tsen L, Tay JH (2002) Kinetics and mechanisms of H_2S adsorption by alkaline activated carbon. Environ Sci Technol 36:4460–4466

Yan R, Chin T, Ng YL, Duan H, Liang DT, Tay JH (2004) Influence of surface properties on the mechanism of H_2S removal by alkaline activated carbons. Environ Sci Technol 38:316–323

Yang X, Sun L, Xiang J, Hu S, Su S (2013) Pyrolysis and dehalogenation of plastics from waste electrical and electronic equipment (WEEE): a review. Waste Manag 33:462–473

Yay ASE (2015) Application of life cycle assessment (LCA) for municipal solid waste management: a case study of Sakarya. J Clean Prod 94:284–293

Zhang Z, Yan YF, Zhang L, Ju SX (2014) Hollow fiber membrane contactor absorption of CO_2 from the flue gas: review and perspective. Glob NEST J 16:355–374

Zhang J, Zuo W, Tian Y, Chen L, Yin L, Zhang J (2016) Sulfur transformation during microwave and conventional pyrolysis of sewage sludge. Environ Sci Technol 51:709–717

Zhang L, Zeng G, Dong H, Chen Y, Zhang J, Yan M, Zhu Y, Yuan Y, Xie Y, Huang Z (2017) The impact of silver nanoparticles on the co-composting of sewage sludge and agricultural waste: evolutions of organic matter and nitrogen. Bioresour Technol 230:132–139

Zhang J, Kan X, Shen Y, Loh K-C, Wang C-H, Dai Y, Tong YW (2018a) A hybrid biological and thermal waste-to-energy system with heat energy recovery and utilization for solid organic waste treatment. Energy 152:214–222

Zhang Z, Chen F, Rezakazemi M, Zhang W, Lu C, Chang H, Quan X (2018b) Modeling of a CO_2-piperazine-membrane absorption system. Chem Eng Res Des 131:375–384

Zheng X, Chen C, Ying Z, Wang B (2016) Experimental study on gasification performance of bamboo and PE from municipal solid waste in a bench-scale fixed bed reactor. Energy Convers Manag 117:393–399

Zheng Y, Li K, Wang H, Tian D, Wang Y, Zhu X, Wei Y, Zheng M, Luo Y (2017) Designed oxygen carriers from macroporous $LaFeO_3$ supported CeO_2 for chemical-looping reforming of methane. Appl Catal B Environ 202:51–63

Zheng X, Ying Z, Wang B, Chen C (2018) Hydrogen and syngas production from municipal solid waste (MSW) gasification via reusing CO_2. Appl Therm Eng 144:242–247

Chapter 12
Advances in Pd Membranes for Hydrogen Production from Residual Biomass and Wastes

M. Maroño and D. Alique

Contents

Abstract Hydrogen production from residual biomass and wastes is a sustainable approach for reducing their final accumulation in landfills and simultaneously a very promising alternative for the energy recovery. Most developed technologies to produce H_2 from residual biomass and wastes are reviewed in this chapter focusing on the separation/purification of the produced hydrogen. Suitability of both thermochemical and biological technologies for hydrogen production is described, and examples of industrial processes are included. Basics of hydrogen separation/purification with membranes are detailed, and suitable separation technologies for the purification of hydrogen produced from biomass and waste conversion are presented focusing on the most recent advances in Pd-based membranes. The use of membrane reactors in which the traditional chemical reaction is combined to the continuous extraction of the main product with high purity, in this case hydrogen, is particularly interesting, being also addressed the most recent developments in this field.

M. Maroño (✉)
CIEMAT, Combustion and Gasification Division, Madrid, Spain
e-mail: marta.marono@ciemat.es

D. Alique
Department of Chemical, Energy and Mechanical Technology, Rey Juan Carlos University, Móstoles, Spain

Z. Zhang et al. (eds.), *Membranes for Environmental Applications*, Environmental Chemistry for a Sustainable World 42, https://doi.org/10.1007/978-3-030-33978-4_12

Keywords Hydrogen production · Wastes · Residual biomass · Valorization · Palladium · Membrane · Membrane reactor · CO_2 capture

Acronyms

ATR	Autothermal reforming
CCS	Carbon capture and storage
CCU	Carbon capture and utilization
DC	Direct current
DF	Dark fermentation
DOE	Department Of Energy (United States of America)
DOR	Dry oxidation reforming
DR	Dry reforming
EAP	East Asia and Pacific region
ELP	Electroless plating
ELP-PL	Electroless plating with additional protective layer
ELP-PP	Electroless pore-plating
EU	European Union
FBR	Fluidized-bed reactor
GHGs	Greenhouse gases
GHSV	Gas hourly space velocity
HT	High temperature
HRF	Hydrogen recovery factor
IGCC	Integrated gasification combined cycle
LT	Low temperature
MCW	Microwaves
MR	Membrane reactor
MSW	Municipal solid waste
NG	Natural gas
OCDE	Organization for Economic Co-operation and Development
OMW	Olive mill wastewater
OS-ELP	Osmosis-assisted electroless plating
PBR	Packed bed reactor
PCB	Printed circuit board
PF	Pore filling
POR	Partial oxidation reforming
PSA	Pressure swing adsorption
PSS	Porous stainless steel
RDF	Refuse-derived fuel
RF	Refuse fraction
RFR	Radio frequency
SEM	Scanning electron microscopy
SEWGS	Sorption-enhanced water–gas shift
SIP	Steam–iron process

SMR-OG	Steam methane reforming off-gas
SNG	Synthetic natural gas
SR	Steam reforming
SRF	Solid recovered fraction
USA	United States of America
VA-ELP	Vacuum-assisted electroless plating
WGS	Water–gas shift

12.1 Introduction

Anthropogenic emissions of greenhouse gases (GHGs) such as CO_2 and hydrocarbons are acknowledged worldwide as one of the main contributors to global climate change. Pathways limiting global warming to 1.5 °C scenario would require rapid and far-reaching transitions in energy, land, urban and infrastructure (including transport and buildings), and industrial systems that imply deep emissions reductions in all sectors, a wide portfolio of mitigation options, and a significant upscaling of investments in those options (Yue and Gao 2018).

Finite availability of the fossil sources (coal, natural gas, etc.) and insecurity of energy supply are contributing factors to the consolidated idea that transition towards a sustainable energy system requires that energy sources must be carbon-free and renewable to cope with climate change and minimizing dependence on oil/natural gas imports (Nikolaidis and Poullikkas 2017). Energy and chemicals are still mostly being produced from fossil resources which causes the release of more than 80% of the global emissions of CO_2 (37,1 billion tons in 2018) with China and the United States as the two larger emitters (Global Carbon Project n.d.). An emissions reduction target of halving CO_2 emissions by 2050 will require the contribution of all available technologies including carbon capture and storage (CCS) or carbon capture and utilization (CCU) applied to large CO_2 point sources, especially fossil-fired power plants, and the development and deployment of renewable energy forms such as wind, solar, biomass, and H_2 energy which are promising and feasible options (Aldy et al. 2017).

Another significant challenge that society is facing is the accumulation of wastes in the environment. A continuously increasing generation rate of wastes is a consequence of the increase in global population which not only may produce environmental damages and negative health effects but also causes unnecessary losses of materials and energy. A general distribution of the generation of wastes in the different regions of the world can be seen in Fig. 12.1 where the OCDE (Organization for Economic Co-operation and Development) leads the ranking with a 44% of the global waste generation followed by EAP (East Asia and Pacific) with a 29% showing the direct influence that exists between the degree of development of a country/region and the volume of wastes generated (Daniel and Bhada-Tata n.d.).

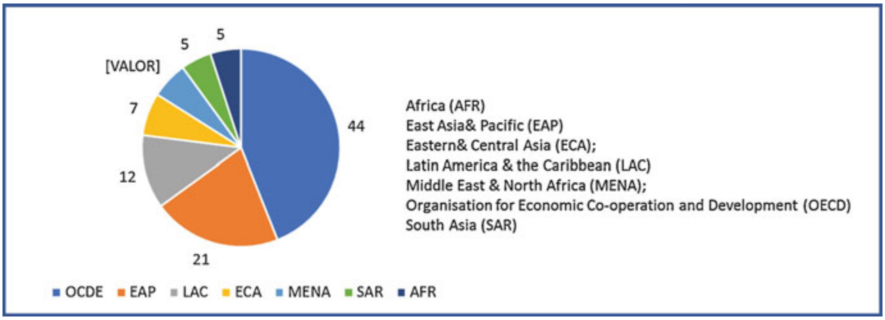

Fig. 12.1 Global waste generation per region (Daniel and Bhada-Tata n.d.)

Waste management strategies include mainly landfilling, composting, incineration, and recycling, having in general concrete national politics a strong influence in the approach followed in each country or region. For example, helped by the European Union (EU) legislation implemented during the last two decades, the landfilling rate of municipal solid wastes (landfilled waste as share of generated waste) compared with municipal waste generation dropped in the EU-28 from 64 to 23% between 1995 and 2017, respectively (European Commission n.d.-a). However, in general, out of different available alternatives, recycling and composting are responsible for the reduction of landfilling rate in most countries. Recyclable materials such as metals, paper, and plastics are used for recycled product manufacture, while the organic fraction (biodegradable) and food waste can be further processed, for example, to convert it to biogas via anaerobic digestion. The remaining fraction or refuse fraction (RF), which cannot be further recycled, can be used to obtain the so-called solid recovery fuel (SRF) and refuse-derived fuel (RDF) which can be both converted into liquid and gaseous biofuels for production of heat and power or to be used as a transport fuel. Moreover, RDF can be transformed thermochemically into heat, electricity, or added-value chemicals as H_2 and fuels (Nowakowski et al. 2018).

All this potential has been especially recognized at EU, where the limit to recyclability was raised to 50% of their municipal waste and 70% of construction waste by 2020 and waste processing for energy and added-value products production is increasing, providing a sustainable method of obtaining a valuable product and simultaneously a way to eliminate a waste storage problem (European Parliament 2018).

However, the term waste not only refers to municipal solid waste. Waste composition is very variable, and depending on its origin, nature, or composition, different classifications are possible, and optimum management strategies can be proposed for its disposal. For example, according to Carioca et al. (2013), wastes can be divided in five groups: agricultural waste, yard and forestry waste, sludge, food processing waste, and organic household waste. Other authors refer to residual biomass as a waste (Otto et al. 2018), which can be defined as any renewable resource derived from organic material of animal or plant origin, existing in nature or generated by man and/or animals that can be used as an alternative source of energy. According to this definition, residual biomass could include biomass deriving from livestock residue (slurries), agricultural waste (residue of grains, cotton, etc.), tree and woody residue (from pruning, changes of variety/species), and industrial residue (rejected wood, dull edges, residual lignin, etc.). The term biowaste is also used in the EU legislation (European Commission 2008) as biodegradable garden and park waste; food and kitchen waste from households, restaurants, caterers, and retail premises; and comparable waste from food processing plants.

More and more the use of biomass to make biofuels and generate electricity is increasing due to its potential valuable source of renewable energy. In general, due to the high volume of residual flows of these types of wastes, their total value is similar to or higher than that of pharma, compost, and unprocessed/basic food products. A recent study has assessed the key factors relating to the sustainability of bioenergy production and suggests global biomass could potentially meet up to one third of the projected global energy demand in 2050 (European Commission n.d.-b).

The use of residual biomass and wastes as a renewable source of energy, fuels, and added-value products such as hydrogen is an open issue today providing a sustainable pathway for the elimination of wastes and recovery of energy. Different approaches, including thermochemical and biological technologies, are available, most of them have been commercially demonstrated for fossil resources, and their suitability is being demonstrated as future new pathways for renewable resources such as residual biomass and wastes.

In this chapter a review of the most developed technologies for H_2 production from biomass and waste is presented, focusing on the separation/purification of the produced H_2 as the final step of the process. Achievements and recent advances of membrane technology for H_2 separation in residual biomass and waste valorization are widely addressed.

12.2 Technologies for Waste and Residual Biomass Valorization to Hydrogen

Energy contained in residual biomass and wastes can be recovered in the form of electricity, heat, fuels, and/or added-value products by using many different technologies. Depending on the form, type, and properties of the available biomass/waste and the final targeted product, different conversion processes can be used which can be generally classified in two main groups, as shown in Fig. 12.2 (Chung 2014), biochemical and thermochemical conversion processes.

In this chapter, focused in the production of hydrogen as fuel and added-value product, four main technologies have been considered for the valorization of biomass-based feedstock, namely, pyrolysis and gasification within the thermochemical processes and anaerobic digestion and fermentation within the biochemical

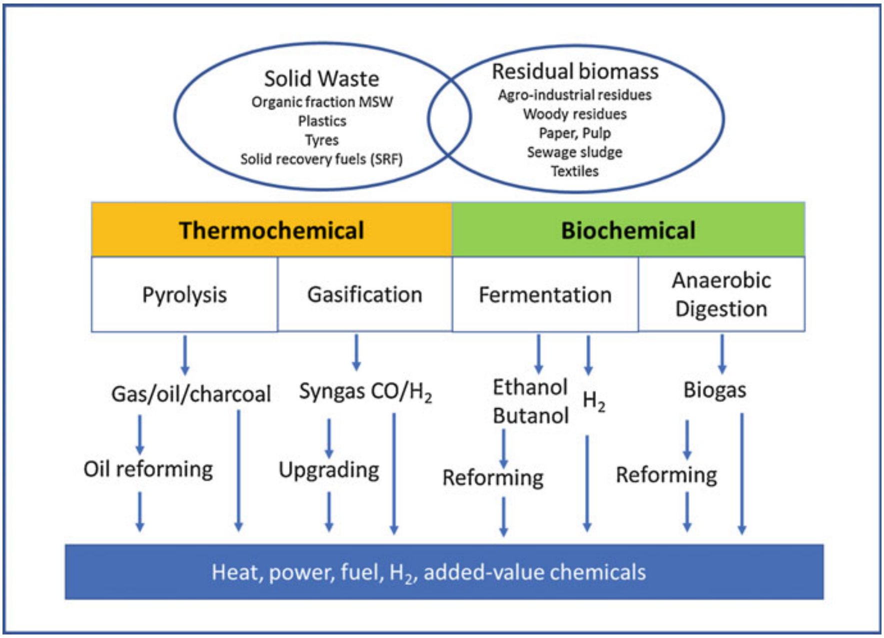

Fig. 12.2 Main conversion processes for waste and residual biomass to different products focusing on hydrogen. (Adapted from (Chung 2014))

ones. Some other biological conversion processes such as some photocatalytic or electrolytic processes which are still in early stages of development have not been considered here (Singh Yadav et al. 2018; Heidrich et al. 2013).

12.2.1 Biochemical Routes

The term biochemical refers to the use of microorganisms to convert organic feedstock (biomass or wastes) into other added-value products such as chemicals or fuels. The interest in producing hydrogen from biomass and wastes by biological routes has increased significantly during the last decades due to a growing attention payed to waste minimization and sustainable development at lower costs (Stephen et al. 2017). Biological processes operate at low–moderate temperature and pressure and therefore are less energy-intensive than other conversion processes. The most common products of microbial conversion of organic fractions include liquid fuels (ethanol) and gaseous fuels (methane and hydrogen). When focusing on hydrogen production, major biochemical conversion processes of biomass or wastes containing carbohydrates include anaerobic digestion followed by reforming of the biogas and dark fermentation.

Anaerobic Digestion/Biogas Reforming

Anaerobic digestion is based on the transformation of organic matter to biogas (consisting essentially of a mixture of 40–70% CH_4 balanced with CO_2 and other minority compounds) using some suitable bacteria such as mixed methanogenic bacterial cultures which grow under anaerobic environment at different temperature ranges (not usually exceeding from 60 °C). Different types of biomass and residual wastes are being used as feedstock in the anaerobic digestion process to produce biogas, and the number of biogas plants in EU has greatly increased during the last decade. In less than 10 years, the total number of biogas plants has tripled reaching more than 17,000 units mostly due to the increase in plants running on agricultural substrates (Matsakas et al. 2015; Nitsos et al. 2015), followed by biogas plants running on sewage sludge, landfill waste, and various other types of waste (European Biogas Association, Statistical report 2017 n.d.). The spectra of suitable wastes to produce biogas are growing including waste textiles (Jeihanipour et al. 2013) and municipal solid waste (MSW) (Alzate-Gaviria et al. 2007). Most common applications of this biogas include its use as fuel in vehicles (Damrongsak and Tippayawong 2010) and burners for producing heat and electricity (Pöschl et al. 2010; Swami Nathan et al. 2010) or to directly inject it into the natural gas grid (Penev et al. 2013).

However, together with CH_4 and CO_2, which are the main constituents of biogas, and depending on the feedstock and the microorganisms used, other gaseous species might be produced during the anaerobic digestion process such as hydrogen sulfide, water, silicon organic compounds (e.g., siloxanes), oxygen, ammonia, dust, and aerosols and also several trace gases such as aldehydes and ketones, carboxylic acids, and aromatic compound (Fachverband Biogas e. V. 2017) whose influence must be taken into consideration prior to final use of the biogas.

Upgrading of biogas to bio-methane is one of its most common pathways for valorization. For this application, biogas cleaning is a crucial step for increasing its heating value and for meeting requirements for gas final application (engines, boilers, fuel cells, vehicles, etc.). The aim of all upgrading technologies is to achieve high methane purity and low losses with low energy consumption. Different available technologies can be grouped in four main types: scrubbing technologies, membrane separation, pressure swing adsorption (PSA), and cryogenic treatment (Fachverband Biogas e. V. 2017). Figure 12.3 shows the distribution of biogas upgrading technologies in Europe in the last decade (European Biogas Association, Statistical report 2017 n.d.): scrubbing technologies account for the greatest proportion of upgrading systems, at 73% share (around 200 facilities), followed by pressure swing adsorption with an 18% share (used at 53 facilities), membrane separation (8%), and finally cryogenic separation which is only used in a few plants in Europe. Total bio-methane production in Europe reached 1.23 billion m^3 in 2015. Each of the abovementioned methods has its advantages and disadvantages, so, in general, the best choice of treatment technology should always be based on local conditions.

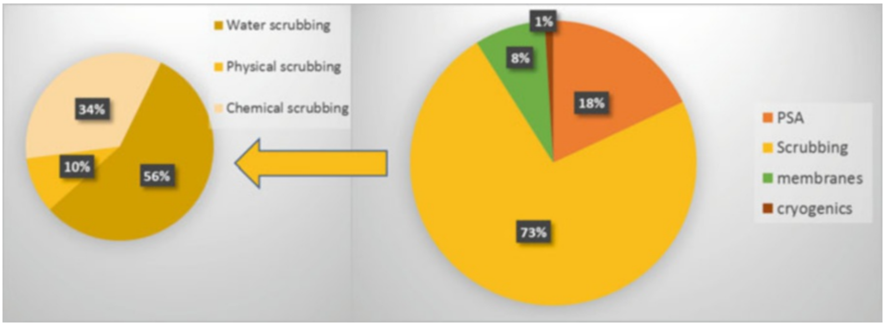

Fig. 12.3 Biogas cleaning technology distribution in Europe (European Biogas Association, Statistical report 2017 n.d.)

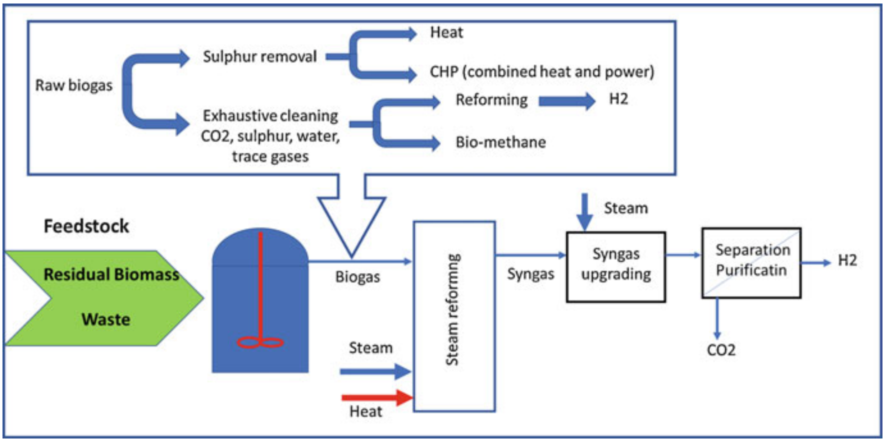

Fig. 12.4 Combined process for hydrogen and biogas production from biomass and wastes

Besides the direct use of biogas as fuel, the interest in using bio-methane as a source of H_2 has been growing during the last decade due to its potential for power generation in fuel cells (Wee 2007; Alves et al. 2013). The most common available technologies to produce hydrogen from biogas include a reforming step using either steam (steam reforming, SR), CO_2 (dry reforming, DR) or autothermal reforming (ATR), partial oxidation reforming (POR), or dry oxidation reforming (DOR) (Basile et al. 2016). Some other novel technologies are still under development such as solar reforming, plasma reforming, or catalytic decomposition (Alves et al. 2013).

The production of hydrogen from biogas by SR involves, in general, three main steps: reforming, shift reaction, and separation unit, usually requiring a previous cleaning treatment of the raw biogas stream. A scheme of the combined process, including some cleaning strategies, is depicted in Fig. 12.4. Using raw biogas in engines for heat or combined heat and power production usually requires a desulfurization step to avoid corrosion problems (Khan et al. 2009), while a deeper cleaning treatment, including removal of concomitant gases such as CO_2, steam, and trace components, is usually required if upgrading of biogas to bio-methane or hydrogen production by steam reforming of biogas is performed (Sun et al. 2015).

Practical demonstration of H_2 production from steam reforming of biogas can be found both in literature, for example, biogas and hydrogen production from wastewater of milk processing industry (Coskun et al. 2012), or at industrial scale with the production of renewable hydrogen from upgraded biogas obtained by anaerobic digestion of agricultural waste and manure from nearby livestock farms at the Shikaoi Hydrogen Farm, a hydrogen production facility in Hokkaido, Japan (World Bioenergy Association, 2019 n.d.).

The gas stream leaving the reformer (syngas) consists of a mixture of CO, CO_2, H_2, H_2O, and traces of non-converted CH_4. Further upgrading of the syngas produced in the reforming step, by means of the water–gas shift (WGS) reaction, allows the CO present in the gas phase leaving the reformer to be fully converted into H_2 and CO_2 reaching final H_2 concentrations that can vary between 50% and 60% v/v depending on the catalyst activity and operating conditions (temperature, space velocity, etc.) (Byron Smith et al. 2010). The separation/purification of H_2 is the final step of the process which is usually performed using commercially available PSA units. However, a growing interest in the use of membranes and membrane reactor (MR) technologies for H_2 production by biogas steam reforming can be found in literature at both lab-scale, using gas mixtures to mimic the biofuel compositions (Sato et al. 2010) or using real biogas from the direct digestion process of residual biomass and wastes (Vásquez Castillo et al. 2015; Silva et al. 2015). Advantages of the application of process intensification strategies have been recently demonstrated in the project BIONICO by the integration of the reforming step with an in situ separation of the produced H_2 using a fluidized-bed membrane reactor achieving a hydrogen production efficiency around 69% at 20 bar (Di Marcoberardino et al. 2018).

Dark Fermentation

In a fermentative process, heterotrophic microorganisms are used to convert the organic carbon sources into simpler compounds producing molecular H_2. The alcoholic fermentation of sugar crops, starch, and more recently lignocellulosic materials can be considered the principal biological process to produce ethanol and butanol which can be further processed to obtain hydrogen (Sarkar et al. 2012). However, the high cost of raw feedstock has promoted the use of residual biomass or waste as substrates which additionally may provide a sustainable approach to reduce waste disposal in landfills (Liu et al. 2011).

As for the direct production of H_2 from biomass/waste feedstock, major biological processes are photo-fermentation (in presence of light) and dark fermentation.

Out of the two types, dark fermentation (DF) represents one of the most promising biological routes due to its faster conversion efficiencies and lower process costs (Gao et al. 2017; Toledo-Alarcón et al. 2018). Different types of wastes and biomasses have demonstrated good properties as feedstock for H_2 production by dark fermentation such as grass, straw and food industry residues (Drljo et al. 2014), marine algae (Shi et al. 2011), or tequila vinasses (Rodríguez-Félix et al. 2018) although most results correspond to laboratory-scale studies. Moreover, dark fermentation has demonstrated significant flexibility to use many renewable complex waste biomasses as feedstock and to produce a wide variety of valuable platform biochemicals of economic interest (Wang and Wan 2009; Ghimire et al. 2015). Recent reviews show a growing interest in the advantages of using hybrid systems based in sequential dark and photo-fermentation processes (Nikolaidis and Poullikkas 2017).

The use of MSW as a source for the direct production of H_2 by dark fermentation has been studied and optimized during the past years focusing on both waste composition and fermentation conditions for optimizing the production of hydrogen. Previous studies had showed that those MSW feedstocks rich in carbohydrates resulted in higher H_2 yields, while predominant presence of oils, fats, and lignocellulosic materials resulted in significantly lower H_2 yields (Kobayashi et al. 2012). Moreover, one of the substrates considered as very good feedstock for producing H_2 by dark fermentation is kitchen waste (Jayalakshmi et al. 2009). The critical role of those fractions in the final H_2 yield is also being investigated by treating municipal solid waste with high pressure and steam, which is then converted into butanol and hydrogen by anaerobic bacteria during a fermentation process (Truus de Vrije 2018).

Industrial application of H_2 produced by dark fermentation is still limited due to the low H_2 yields achieved. Different approaches for improving H_2 yields can be found in literature. One of the most promising methods includes the use of mixed microflora instead of pure cultures, which is favorable in terms of easier process control and substrate conversion efficiencies. However, mixed cultures should be first pretreated in order to select sporulating hydrogen-producing bacteria and suppress nonspore-forming hydrogen consumers. Various inoculum pretreatments have been used to enhance hydrogen production by dark fermentation including heat shock, acid or alkaline treatment, chemical inhibition, aeration, irradiation, and inhibition by long-chain fatty acids (Rafieenia et al. 2018).

Additionally, in order to obtain a highly pure H_2 stream, different cleaning and separation technologies might be necessary. At this stage, all the already described methods for biogas cleaning can be used, being possible to consider scrubbing or PSA as one of the most appropriate ones. The final selection of the best technology must be done after considering both impurities present in the gas stream and final use for hydrogen. However, the use of membranes and membrane reactors could also play an important role in the future due to their multiple possible benefits. More details about the use of membranes with these purposes will be addressed later.

12.2.2 Thermochemical Routes

Thermochemical conversion processes refer to the use of heat to convert feedstock into fuels. Depending on the amount of oxygen used in the reaction, the conversion process goes from combustion, where stoichiometric amount of oxygen or air is generally used to completely oxidize the organic matter to CO_2 producing heat and/or electricity (DemirbaÅŸ 2001) to pyrolysis, where the thermal destruction of the biomass/waste takes place in absence of oxygen or air, converting the biomass/waste into solid substances (coal), liquid (bio-oil), and gas (fuel gas) (Goyal et al. 2008). Finally, gasification is a partial oxidation of the biomass/waste which produces a synthesis gas (syngas), consisting of a mixture of H_2, CO, CO_2, CH_4, etc. that can be further processed to fuels and/or added-value products (Wang et al. 2013).

Compared to biological processes, thermochemical conversion technologies require elevated temperatures, and the conversion rates are generally faster. Thermochemical technologies to produce H_2 from biomass and wastes include two main routes, pyrolysis and gasification, which can be also combined in a unique process. These two routes are economically viable strategies which provide the highest potential to produce hydrogen becoming competitive on a large scale in the near future (Nikolaidis and Poullikkas 2017). Both processes are performed under limited or no oxygen, and the operating conditions and the yield of products vary greatly among them.

Pyrolysis

Pyrolysis is a highly flexible thermochemical process that has demonstrated a high potential in the residual biomass and waste management sector in the last two decades (Czajczyńska et al. 2017; Bridgwater 1996). By regulating substrate composition, temperature, and retention times, the ratio between solid (char), liquid (oils), and gas (syngas) can be adjusted to focus on the desired fraction (Maggi and Delmon 1994). Depending on the maximum heating rate and temperatures used in the process, pyrolysis can be classified as slow, fast, and flash being fast pyrolysis, which has reached a wider deployment at industrial scale (Butler et al. 2011).

Figure 12.5 summarizes the inverse relationship between thermal conditions used in the process (heating rate and temperature) and the production of bio-oils: slow pyrolysis is characterized by relatively low temperatures (<450 °C), low heating rates, and long residence times which lead to maximum yield of char with moderate amounts of tar by-products. Intermediate pyrolysis is characterized by temperatures around 450 °C–500 °C and residence time in the order of few seconds. Fast pyrolysis is characterized by very high heating rates (>1000 °C/s), very short residence time (<2 s), and rapid cooling of the products which may reach bio-oil yields of 60–70% (Onay and Kockar 2003). Moreover, in fast pyrolysis moderate temperatures (up to 550 °C depending on the feedstock) maximize the yield of condensable vapors and

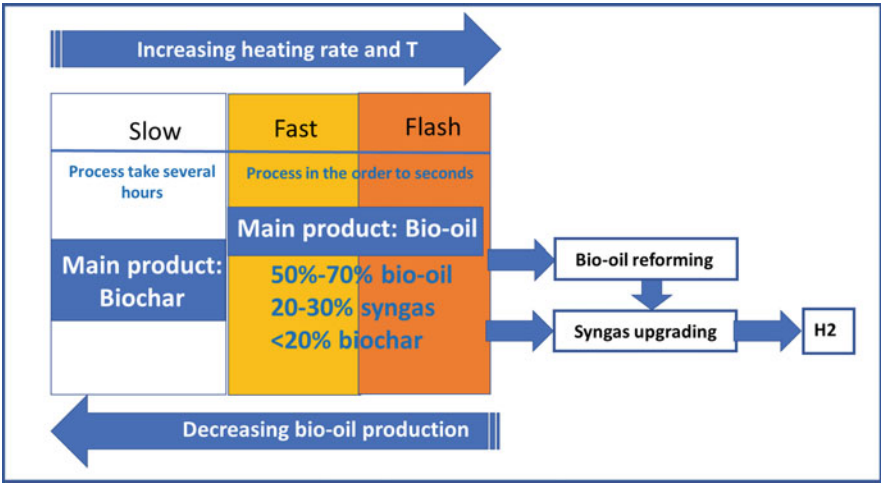

Fig. 12.5 Hydrogen production pathways from pyrolysis of biomass and wastes

therefore bio-oil (about 70% wt), and high temperatures (above 600 °C) maximize pyrolysis gas yields (about 80% wt) (Bridgwater 2012). As shown in Fig. 12.5, maximum syngas yields can be obtained by fast pyrolysis of biomass or wastes (in the range of 20–30%), while bio-oil production can reach up to 70%. For maximizing the production of hydrogen, upgrading of this syngas and further processing of the liquid stream are required. Significant advances reached in fast pyrolysis technologies in the 1990s (Horne and Williams 1996) supported the feasibility of combining the fast pyrolysis with steam reforming of the produced bio-oil which has already been demonstrated in the late 1990s for agriculture and forest biomass reaching hydrogen yields as high as 85% of the stoichiometric value (Bridgwater 1999). Nowadays fast pyrolysis is a relatively mature technology, and significant advances have been achieved at both laboratory and pilot scale regarding the upgrading of bio-oils to H_2, fuels, and other chemicals (Wang et al. 1998).

Suitability of different biomasses and wastes for H_2 production by pyrolysis has been also explored during the last decades, including plastics, municipal solid wastes, or tires.

Plastics accounted in the early 2000s for 8–9% of total waste stream and were already envisaged as potential feedstock able to generate more than six million tons of hydrogen per year following a pyrolysis/reforming concept (Czernik and French 2006). Nowadays, with plastic contents in the MSW around 10% wt (European Environment Agency, Waste-municipal solid waste generation and management n.d.), this approach is fully justified, and the interest in hydrogen production from plastics continues, for example, in the study of co-feeding plastics to the steam pyrolysis/gasification of different biomasses such as sawdust which has showed a production of 36% vol of H_2 when 20% wt of polypropylene was mixed with the biomass (Alvarez et al. 2014).

Pyrolysis of different MSW fractions has also been explored as a feasible pathway to produce hydrogen, and the influence of different types of MSW in the final distribution of pyrolysis products has been investigated (Ateş et al. 2013). More recently, Kabir et al. have investigated the pyrolysis of MSW finding that above 550 °C the quantity of syngas produced reached 30% (Kabir et al. 2015). Moreover, different strategies can be found in literature for increasing H_2 production from MSW pyrolysis including co-feeding different fractions of MSW in the final pyrolysis gas yield (Bridgwater 2012) or the use of by-product char to reform the volatiles fraction towards the production of H_2 (Grieco and Baldi 2012).

Suitability of pyrolysis has also been demonstrated for the treatment of waste tires. During this process, sulfide bonds occurring in the rubber become broken, next carbon chains are bursting, and finally gaseous, liquid, and solid products are formed, which then can be subjected to further processing (Wang et al. 2017). While a wide variety of alkanes, alkenes, and aromatic compounds are usually found in the pyrolysis oil fractions (Ryms et al. 2013), main products in the pyrolysis gases derived from tires consist in aliphatic compounds such as methane, ethane, ethene, propane, propene, butane, butene, pentane, and pentene which can be further processed to obtain hydrogen or added-value chemicals and oxides like carbon monoxide, carbon dioxide, and hydrogen sulfide (Williams et al. 1990). As it also happened for other biomasses or wastes, carbon monoxide is usually the major component of the gas phase, and H_2 content is generally lower than 10% v/v (Januszewicz et al. 2012). As for the enrichment in hydrogen of the gas stream, some approaches that had been followed include co-pyrolysis of waste tire/coal mixtures for production of a hydrogen-rich gas (Bičáková and Straka 2016); plasma pyrolysis of tires with steam injection, used in Israel by Plasma Recycling Ltd, which produces synthesis gas with large quantities of CO and H_2 (Chang et al. 1996); or a steam catalytic pyrolysis–gasification process where the potential H_2 production from waste tires was largely increased up to 13%wt (Elbaba and William 2012).

The great potential of residual biomass and wastes to produce H_2 by pyrolysis is supported by the high hydrocarbon-based elements present in the pyrolytic products which can be further processed to obtain H_2 by catalytic reforming of the bio-oil fractions or upgrading of the syngas. However, prior to the conversion step, the removal of all the contaminants which might negatively affect the activity of the catalyst must be removed. Most common technologies are those that can also be used for the cleaning of biogas such as scrubbing type (water, physical or chemical), but they can also include cold traps, demisters, and filters (Ryms et al. 2013). There is not a general rule; most suitable method must be selected based on the contaminants present in the gas stream and the final use of the hydrogen.

Gasification/Syngas Upgrading

Gasification or “incomplete combustion” is the conversion of solid feedstock, residual biomass, or waste into synthesis gas at both high temperatures and heating rates, which optimize the generation of gas products such as carbon monoxide, carbon dioxide, hydrogen, and lower amounts of methane. Among the different thermochemical conversion processes, gasification can be considered the most suitable technology to produce hydrogen from biomass and wastes where hydrogen yield is influenced by many factors such as feedstock composition, particle size, temperature, and gasifying agent (Sheth and Babu 2010).

Depending on the gasification technology, thermal power of gasifiers may range from values as low as 10 kW to those reaching 1000 MW. Gasifiers smaller than 1 MW are usually low-temperature downdraft or updraft type, and those of capacity higher than 100 MW are usually high-temperature fluidized-bed or entrained flow gasifiers type. For intermediate powers, in the range of 10–100 MW, the most commonly used technology is fluidized bed, both bubbling and circulating, which provides high heat transfer improving net efficiency (Power Technology, Power from waste – the world's biggest biomass power plants 2014).

Gasification of biomass is a mature technology used worldwide to produce electricity in commercial plants operating with thermal power capacities that ranged from 100 to 1000 MW (IEA Bioenergy 2016). However, the produced syngas has multiple applications including its further processing into fuels and added-value chemicals such as Fischer–Tropsch fuels, methanol, hydrogen, mixed alcohols, or biosynthetic natural gas (bio-SNG) (Higman 2013).

Gasification has also been demonstrated to be a technically viable option for the conversion of different solid wastes providing several potential benefits over the conventional combustion process such as the flexibility of both the design and the operation under different operating conditions. Advantages of gasifying municipal solid wastes have been extensively reported in literature as a sustainable and environmentally suitable solution for the reduction of MSW disposal in landfills. However, the deployment of gasification technology for MSW treatment is still very slow with a limited number of plants commercially available worldwide (Arena 2012). Moreover, in literature, it is still an open topic with many researchers and laboratories focusing on the optimization of reaction conditions including temperature, heating rate, or the use of catalysts to improve the yield and the quality of the syngas production together with the reduction of tars and non-desired by-products (Ahmad et al. 2016; Gómez-Barea et al. 2014; Nilsson et al. 2012).

It is well-known that the producer gas or syngas obtained by gasification of different feedstock consists mainly in a mixture of H_2, CO, CO_2, and small amounts of CH_4. However, it is also usually contaminated by some undesirable components such as tars, chloride, alkali metals, sulfur, etc., which need to be removed prior to its subsequent processing and conversion into power, mechanical energy, fuels, or chemical products. In fact, one of the main challenges of gasification technologies is the formation of tars. Tar is a complex mixture of condensable high-molecular-weight hydrocarbons in which its composition depends on both feedstock composition and process conditions (Milne and Evans 1998). Depending on the final application of the syngas, tar contents must be kept below specific limits, for example, <10 mg/Nm^3 of gas for its use in internal combustion engines or as low as <0.1 mg/Nm^3 for methanol synthesis (Kölling et al. 2012).

Therefore, considerable efforts are currently underway to find suitable procedures to remove tars from fuel gas. Both physical methods (scrubbers, filters, wet electrostatic precipitators, etc.) and chemical ones (thermal and catalytic cracking) can be used. This last type is gaining much attention nowadays as they allow the direct gas treatment inside the gasifier (using catalysts or sorbents) avoiding the need for additional downstream treatment of the gas (Neubauer 2011; Shen et al. 2014; Soomro et al. 2018).

When focusing on hydrogen production by gasification of residual biomass and wastes, three main processes are usually required: thermochemical conversion of feedstock into syngas in the gasifier (which may include the direct removal of tars), the upgrading of the syngas to maximize hydrogen contents, and, finally, the separation/purification of the produced H_2. Some details on recent advances on the three mentioned technologies are included in the next paragraphs.

(i) **Advanced Gasification Technologies for H_2 Production**

Two of the most promising gasification-based technologies for H_2 production from biomass and wastes which aim at both increasing H_2 yield and reducing or minimizing the presence of tars are steam gasification and plasma-based gasification system.

– *Steam Gasification*

Steam gasification is a highly endothermic reaction which usually requires high temperatures (above 800 °C) for generating syngas with a high yield of H_2 and low tar contents if no catalysts are present. The oxidizing (or gasifying) agent is usually pure steam or steam-enriched air which enhances the hydrogen contents of the product gas generating a medium–high calorific value gas (>15 MJ/Nm^3) (Xu et al. 2017; Balu et al. 2015).

Optimization of steam gasification of biomass for H_2 production has been extensively investigated, and many studies can be found in literature on different strategies used for increasing H_2 production and for reducing tar formation which usually include increasing temperatures or the use of catalysts for the thermal or catalytic cracking of tars (de Lasa et al. 2011; Delgado et al. 1997). Some of the most common reported approaches include the use of catalysts, sorbents, or the combination of both in the gasification media. Extensive work has been done, for example, on biomass steam gasification, using different types of catalysts for tar removal including Ni-based, dolomite or olivine (Soomro et al. 2018), sorbents such as CaO in the gasifier for increasing the concentration of hydrogen at low–moderate temperatures (600–800 °C) (Delgado et al. 1997). Other authors have reported the advantages of including a pyrolysis step followed by the steam gasification or catalytic steam gasification of the charcoal, which demonstrated a significant reduction of tar production (Wu et al. 2014).

Feasibility of catalytic steam gasification of residual biomass and wastes has also been investigated in the steam gasification of MSW where the use of catalyst has demonstrated to significantly improve the efficiency of tar cracking and the reforming of hydrocarbons to generate valuable gases (Nilsson et al. 2012). Some examples include the use of natural materials such as dolomites (Yang et al. 2008) or Ni-based catalysts (Luo et al. 2012). In the work by Ponzio et al. (2006), MSW was gasified in a packed bed reactor (PBR) by mixtures of air and steam preheated to 1400 °C. The results showed that high gasification temperature is effective in terms of thermal cracking of tar and increase of gas yield. Another example is the production of hydrogen by catalytic steam gasification of waste tires in a two-stage reactor (Elbaba and William 2012). More recently, Lee et al. have obtained a syngas with heating value of 8–10 MJ/Nm^3 by super-high-temperature (1000 °C) steam gasification of different types of wastes including MSW, rubber, plastic, and wood (Lee et al. 2014).

However, most of the available results correspond to laboratory/small pilot scale, and few examples can be found on pre-industrial- or industrial-scale demonstrations. One of the most recent achievements is the UNIQUE gasifier (Heidenreich and Foscolo 2015) developed under the European project UNIfHY (Project UNIfHY 2012) where the production of H_2 from biomass (almond shells) was demonstrated at 1 MW_{th} gasifier scale. Within this project it has been proved at industrial scale the feasibility of producing H_2 from biomass by catalytic steam gasification reaching a significant increase in gas yields (from 1 to 2 Nm^3/kg_{daf}) and water conversion (from 25% to 45%) with a very low contents in methane (2%v), tar (1 g/Nm^3), and ammonia (1500 ppm).

– *Plasma Gasification*

Plasma gasification refers to the use of plasma torches as the source of the heat required to the conversion process, as opposed to conventional fires and furnaces. Plasma torches have the advantage of being one of the most intense heat sources available while being relatively simple to operate. Plasma gasifiers typically operate at temperatures above 1500 °C, and, at those temperatures, materials are subjected to a process called molecular disassociation, meaning their molecular bonds are broken down so all toxins and organic poisons are destroyed (Tang et al. 2013). The interest in the application of plasma technologies to waste management is increasing during the last decade due to their high efficiency in converting organic and carbonaceous materials into syngas, while nonorganic materials are melted and cooled into a vitrified glass (Hassanpour 2017). Plasma torches are commonly used in foundries to melt and cut metals, and they have been used for many years to destroy chemical weapons and toxic wastes, like printed circuit boards (PCBs) and asbestos, but since the late 1980s, these processes have been optimized for energy and fuel production. Several companies such as Alter NRG are running plasma gasifiers at industrial scale for MSW since 2002 in Japan and India, for second-generation ethanol in the United States since 2009, or for converting biomass to energy in China since 2010 (ALTER NRG Corp 2016).

First plasma gasifier designs focused on optimizing the movement of solids into the gasifier such as fixed bed, moving bed, entrained, or spouted bed. More recent designs focus on the plasma discharge technique, which can be mainly direct current (DC), radio frequency (RFR), and microwaves (MCW) (Tang et al. 2013). The power input range reported in most of the studies published on plasma gasification during the last decade is between 0.6 and 118.8 kW with a variety of fuel waste such as municipal solid waste, coal, and some industrial waste, being MCW the most used plasma discharge technology (Sanlisoy and Carpinlioglu 2017).

Although up to now the main application of plasma gasification at industrial scale focuses on the production of energy, recent application of thermal plasma gasification can be found, for example, for the reformation of natural gas or the production of hydrogen and H_2-rich gases (Ismail and Ani 2015). The main advantage of both conventional and modern plasma gasifiers is their ability to provide 100% elimination efficiency for contaminants derived from many different types of biomasses and wastes including MSW, tires, plastics, etc., such as H_2S, COS, SO_2, NH_3, HCN, C_2H, and C (solid) (Bosmans et al. 2013). Alternative processes, such as hybrid system plasma–heterogeneous catalysis are under development due to the great synergy potential that can be gathered by lowering activation energy via the catalyst, enhancing the conversion of reactants, and providing increased selectivity and yield to desirable products (Tu et al. 2017).

Some examples of thermochemical processes used to produce H_2 from different types of biomasses and wastes in the industry are summarized in Table 12.1.

Table 12.1 Hydrogen production by thermochemical conversion of biomass and waste at industrial scale

Company	Process/technology	Feedstock	Product/end use
OEN	Wet slow pyrolysis	Tires, plastic wastes, waste oil, residual biomass	Syngas + char for cogeneration of power and heat
Open MS with Blue Plasma Power S.L.	Catalytic plasma hydrogasification HGCP	Wood chips and waste	Power and liquid fuels
Sierra Energy	FastOx gasification	MSW and other waste resources	H_2 and syngas for fuel cells
	Fixed bed; Steam & O_2		
Eco Energy International (EEI)	Bio-reformation with CO_2 capture with carbonates	MSW, biomass, biogas, landfill gas, methanol, ethanol, and sugars	H_2 for existing H_2 consumer customers
	BFR process		
Northumbrian Water	Microbial electrolytic cells (MICs)	Domestic wastewater	H_2
PowerHouse Energy	ACT system	End-of-life plastics	H_2 for end user
	Distributed modular gasification (DMG)		
Enerkem	Gasification	Nonrecyclable waste including plastics	Eco-methanol
Advanced Plasma Power	Gasplasma®	MSW and mixed wastes	Syngas for further processing
Strebl Energy™	COOL PLASMA™ Gasification	Waste	Syngas for electricity, liquid fuels, and specialized chemicals

(ii) **Syngas Upgrading: WGS Reaction and Advanced Systems**

Depending on fuel and gasification technology, contents of CO and H_2 in the syngas usually range from 60 and 15 to 20 and 45 (vol%), respectively, being the higher H_2 concentrations obtained when steam gasification is used (Rauch et al. 2014). When it is desired an increase in syngas hydrogen content, WGS allows the conversion of the CO present in the syngas into additional H_2 and CO_2 in presence of excess steam and a specific catalyst. This chemical reaction can be expressed as follows:

$$CO + H_2O \leftrightarrow CO_2 + H_2 \left(\Delta H^\circ = -41\,\text{kJ/mol}\right) \qquad (12.1)$$

The common practice in the industry is to carry out the water–gas shift reaction in two consecutive steps. The first one is at high temperature (300–400 °C) using Fe–Cr-based catalysts which allows the reduction of CO contents to 10%–3% vol (HT-WGS), followed by a low-temperature step (200–300 °C) using Cu–Zn-based catalysts to completely convert the CO into H_2 and CO_2 (LT-WGS).

Some traditional examples of processes involving this reaction include coal gasification processes, H_2 production for ammonia synthesis, or other industrial processes such as hydrotreating of petroleum stocks. More recently, it has been used in biomass gasification integrated with CO_2 capture processes for high-purity hydrogen production (Detchusananard et al. 2018). One real example of this one is the IGCC Plant of Elcogás at Puertollano (Spain), which in 2004 launched the construction of a demonstration pilot plant of 14 MW_{th} for the capture of CO_2 with production of H_2. The main gasifier was a Prenflow entrained flow type, and the pilot plant was fed by a 2% slipstream of the main plant. A continuous production of 2 ton/d of H_2 was demonstrated using one-step high-temperature commercial WGS reactor followed by a PSA unit for the final purification of the produced hydrogen (Casero et al. 2014).

For most of the final applications of H_2 produced from biomass gasification, the development of highly active, stable, and sulfur-tolerant catalysts for the WGS reaction is usually required. Iron–chromium oxides are the most often used catalyst for high-temperature WGS reaction, and its suitability for the upgrading of biomass gasification syngas has been demonstrated at pilot scale (Maroño et al. 2010; Rauch et al. 2015). However, the limited resistance to poisoning in presence of sulfur compounds and the environmental and safety problems related to the use of chromium compounds in the catalysts (De Araújo and Do Carmo Rangel 2000) has promoted extensive research and developments during the last decades. Some of the strategies followed since the early 1990s included the use of highly active and sulfur-resistant catalysts based on platinum (Maroño et al. 2008) and platinum-supported bifunctional catalysts (Panagiotopoulou and Kondarides 2007; Haryanto et al. 2007; Querino et al. 2005) or the development of sour WGS catalysts based on cobalt or cobalt–molybdenum (Beavis et al. 2013; Hakkarainen et al. 1993; Mellor et al. 1997), which avoid the need to use a desulfurization unit.

More recent developments focus on integrated approaches that combine the WGS reaction with the separation in situ of one of the products, CO_2 or H_2. Those approaches include the sorption-enhanced WGS (SEWGS) reaction and the water–gas shift membrane reactor (WGS-MR). Main principle underlying those two technologies is the same: to exceed CO conversion rate above the equilibrium by the continuous removal of one of the products from the reaction media. In the case of the SEWGS process, a high-temperature sorbent is used to capture CO_2 and increase CO conversion to H_2. Suitability of different types of solid sorbents has been investigated during the last decade, including dolomites, sepiolites, and pillared clays such as hydrotalcites (Maroño et al. 2014a). Suitability of this technology has been already demonstrated at pilot scale for pre-combustion decarbonization of power production by IGCC using a potassium promoted hydrotalcite material as sorbent, which showed also good catalytic activity for the water–gas shift reaction (van Dijk et al. 2011). Recent approaches include the study of different configurations WGS catalyst/CO_2 capture sorbent (Maroño et al. 2015) or the preparation of sour bifunctional sorbents for their use in SEWGS applicable to H_2 production with CO_2 capture by steam gasification of different biomasses (Torreiro et al. 2017).

The concept of water–gas shift membrane reactor brings together the production of H_2 by a high-temperature WGS catalyst and its simultaneous removal from the reaction media by means of a hydrogen-selective membrane. The presence of the membrane avoids the need of a second WGS reactor at low temperature and the additional hydrogen separation unit reducing equipment costs and increasing process efficiency (Brunetti et al. 2017). Application of WGS-MR technologies to hydrogen production by biomass/waste gasification processes is still under development, and extensive experimental works regarding membrane reactor configurations can be found in literature, which will be described later in detail in a specific section of this chapter.

(iii) **H_2 Separation/Purification**

The final step in the production of hydrogen by biomass and/or waste gasification is the separation/purification of the produced H_2. In general, after the upgrading of the syngas via WGS or the reforming of tars, in order to obtain a pure stream of H_2, it is necessary to selectively separate it from a CO_2-rich gas stream. Different technological approaches can be followed to reach pure H_2 streams. Two main groups can be proposed: adsorbents (generally in PSA units) and membranes.

PSA is a commercially available technology that is employed to separate gas species from a mixture of gases under pressure. The technology dates from the 1950s, and it is based on molecular sieves, where sorbents of specific pore diameter allow the separation of different-sized molecules. This makes the manufacture or selection of tailored sorbents for each targeted molecule the most critical part of the technology (Sircar and Golden 2000; Elseviers et al. 2015; Voss 2005). The principles of performance of PSA consist of a cycling mode of sorption/desorption: by swinging the pressure from high to low, it is possible to adsorb all non-desired molecules at the higher pressure and then release them at the low pressure. This procedure gives the name to the technique.

The main advantage of PSA for the purification of H_2 is that it can remove impurities to a required level providing very high levels of H_2 purity. Nowadays main industrial application of PSA technology for H_2 separation/purification takes place at refineries, which amount for about 65% of the installed PSA systems, followed by steam cracker applications (about 15% of the total) (Grande 2012). Other niche applications such as the production of H_2 with or without a by-product (CO_2 from steam methane reforming off-gas, SMR-OG) or PSA processes for direct production of ammonia synthesis gas (from SMR-OG) are also significant (Boon et al. 2015a). Moreover, in addition to typical integration of PSA units in the plant structures (e.g., combination of steam reformer and H_2–PSA), more complex combinations are possible to optimize the overall process performance flexibility and automation (Baker 2002). An example is demonstrated in its recent application to SEWGS processes (Gupta and Lapalikar 2016).

Membranes and membrane reactors are the other main group of technologies that can be used for the final separation/purification of H_2 produced by biomass or waste gasification. Membranes are physical barriers that allow one specific component from a mixture to selectively pass through to the permeate side retaining the non-permeable components at the retentate side. Membrane separation technology has been extensively applied in many industries including not only separations in gaseous phase (Dhineshkumar and Ramaswamy 2017) but also in water treatment processes (Thanuja et al. 2018), food industry (Scott and Scott 1995), or drug delivery (Perry et al. 2006), among others.

In the specific case of hydrogen, membrane separation systems can be made of different materials including a polymer or a metallic or ceramic material (Yun et al. 2011a). Generally, they use pressure as driving force, and the permeation mechanism through a membrane is strongly dependent on the membrane material and design. In the case of polymeric membranes, for example, which are usually made of microporous materials, the separation of gas species takes place following a molecular diffusion transport mechanism determined by the pore diameter and particle size of the membrane material (Mivechian and Pakizeh 2013). As for the selective separation of H_2, nonporous dense metallic membranes are of special interest as permeation of H_2 takes place following the solution–diffusion mechanism, which means that the molecule of H_2 is dissociated into atoms at the membrane surface and they pass through the metal layer being recombined again into H_2 molecules at the other side of the membrane (Yun et al. 2011a).

Compared to PSA, membranes are easily scalable, and they can operate in continuous mode which has the potential to reduce costs, improve efficiency, and simplify the process achieving high hydrogen recovery and purity at the same time (Maroño et al. 2014b). However, they also present some limitations such as their low tolerance to contaminants present in the gas or their mechanical resistance, which are still open fields of research (Nikoli and Kikkinides 2015). Advanced hydrogen separation systems based on reaction, adsorption, permeation, or a combination of them include the development of hybrid catalyst–sorbent–membrane systems, hybrid PSA–membrane systems, and significant improved membrane reactor configurations (Ruan et al. 2016).

Description of the principles for dense metal membrane performance, advances in membranes and membrane reactors, and main developments towards their application to hydrogen production from biomass and waste thermochemical conversion are detailed in the following sections.

12.3 Pd Membranes in Waste and Residual Biomass Valorization

Most technologies for waste and residual biomass valorization by hydrogen production require some additional purification steps since it is generated usually together with other subproducts such as carbon dioxide, carbon monoxide, methane, or water vapor, among others (Balat and Kırtay 2010; Yin and Yip 2017). In this context, the use of selective membranes represents a very promising alternative for an effective separation of these impurities at reasonable cost, independent of the biorefinery capacity (Coutanceau et al. 2018; Alique 2018; Bakonyi et al. 2018). Usually, these membranes can be selected for high permselectivity towards hydrogen (Adhikari and Fernando 2006; Li et al. 2015) or carbon dioxide (Salehi et al. 2017; Ali et al. 2019) because they are majority in the product stream. Considering all the abovementioned possible impurities, the first option is preferred in case of using this hydrogen for generating electricity in fuel cells in order to guarantee an adequate ultrahigh purity of the product (Zornoza et al. 2013; Mei et al. 2018). These H_2-selective membranes can be formed by a wide variety of materials, including polymers (Zhao et al. 2018a; Rezakazemi et al. 2018), zeolites (Mei et al. 2018; Mabande et al. 2004), metal–organic frameworks (Jin et al. 2016; Adatoz et al. 2015), mixed-complex metal oxides (Hashim et al. 2018; Aykac Ozen and Ozturk 2019) or metals (Zhao et al. 2016; Rahimpour et al. 2017), as well as mixed-matrix structures by combination of diverse materials (Strugova et al. 2018). The selection of an adequate material is still under study, and the best option for any application has not been agreed. Thus, different materials have been proposed for diverse particular applications attending to gas composition, operating conditions (mainly pressure and temperature), and final required purity of hydrogen (Brunetti et al. 2011; Lu et al. 2007). However, Pd-based membranes stand out between their competitors because of their excellent permeability and potential complete selectivity for hydrogen at high temperatures (Arratibel Plazaola et al. 2017; Tosti 2010; Alique et al. 2018), being possible to be used as independent separators (Kiadehi and Taghizadeh 2019; Wang et al. 2006; Martinez-Diaz et al. 2019) or combined with any catalyst just in the reactor, providing additional benefits (Tosti et al. 2008; Rahimpour et al. 2017; Basile et al. 2013).

In the following sections, the most recent advances of Pd-based membranes for hydrogen production have been summarized, including last trends in membrane manufacturing and distinguishing particular applications of these membranes for independent purification units from the use of real membrane reactors for valorization processes.

12.3.1 Recent Trends in Pd Membrane Manufacturing

It is widely known that Pd-based membranes are typically classified into self-supported (Santucci et al. 2013; Moriani et al. 2018) and composite structures, in which a palladium film is deposited onto a porous support (Melendez et al. 2017a; Alique et al. 2016). The second alternative is prevalent in order to achieve important benefits such as material savings and increasing permeate fluxes (Yun et al. 2011b; Deveau et al. 2013) without compromising the mechanical resistance of the membrane (Alique et al. 2018; Al-Mufachi et al. 2015). Theoretically, the preparation of progressively thinner Pd layers helps to save money due to the high cost of palladium, and it simultaneously increases the permeability of the membrane (Peters et al. 2011a). Most researchers have adopted this strategy, although the cost of using complex supporting materials or manufacturing processes could overcome the palladium film itself (Alique 2018; Alique et al. 2018). Thus, selection of adequate supporting materials and development of better membrane compositions and manufacturing process are of key importance to commercialize these membranes in real industrial processes.

Composite Membranes: Support Selection

Diverse materials have been proposed to be used as support for preparation of composite membranes, although two main groups can be distinguished: i) technical ceramics and ii) porous metals. The first group provides excellent properties in terms of chemical and thermal resistance, as well as surface quality with a very smooth surface and narrow pores (García-García et al. 2012; Arratibel et al. 2016). These supports include multiple materials such as alumina (Boon et al. 2015b), silica (Van Gestel et al. 2014), zirconia, or YSZ (Lewis et al. 2013), among others. However, their fragility and thermal expansion coefficient, significantly different to that of palladium, limit their industrial use in practice (Alique et al. 2018). On the contrary, porous metals offer exceptional mechanical resistance and handling, making them very attractive for industrial applications, while simultaneously exhibiting a thermal expansion coefficient very close to that of palladium so the membrane stability against thermal stress is guaranteed (Mateos-Pedrero et al. 2010; Hwang et al. 2017). Despite these benefits, the use of metal supports also presents some relevant drawbacks. The rough surface with presence of large pores that makes difficult the incorporation of thin layers is maybe one of the most relevant ones (Alique et al. 2016), as well as the possible metal interdiffusion between both support and Pd-selective film when the membrane operates at high temperatures for long times

Table 12.2 Main properties of diverse materials frequently used as support for Pd composite membranes

Category	Material	Thermal expansion coefficient (μstrain/°C)	Average porosity (%)	Average pore size (μm)
Technical ceramics	Al_2O_3	4.50–8.30	30–55	$5 \cdot 10^{-3}$–$8 \cdot 10^{-1}$
	SiO_2	0.73–0.76	30–40	$1 \cdot 10^{-3}$–$1 \cdot 10^{-2}$
	TiO_2	8.40–10.80	30–55	$1 \cdot 10^{-3}$–$8 \cdot 10^{-1}$
	ZrO_2	6.00–8.80	30–55	$3 \cdot 10^{-3}$–$1.1 \cdot 10^{-1}$
	YSZ	11.10–11.50	30–55	$3 \cdot 10^{-3}$–$1.1 \cdot 10^{-1}$
Porous metals	AISI 316L SS	15.00–18.00	20–25	$1 \cdot 10^{-1}$–$2 \cdot 10^{2}$
	Hastelloy®	13.70–14.40	20–25	$1 \cdot 10^{-1}$–$1 \cdot 10^{2}$
	Nickel	13.00–15.00	–	–

(Pujari et al. 2014; Han et al. 2017). This group includes diverse sintering metals, mainly 316L stainless steel (SS) (Sanz et al. 2011; Pinacci and Drago 2012; Tarditi et al. 2017), Hastelloy® (Ryi et al. 2010), and nickel (Ryi et al. 2008), with diverse media grade, properties, and cost. Table 12.2 collects some of the most relevant properties for alternative materials reported in the specialized literature for supporting palladium membranes. As it can be deduced, the wide variety of parameters involved in the selection of the material together with multiple particular conditions in which the composite membrane will be used makes the decision really difficult. In fact, a prevalent solution is not reached up to now (Alique et al. 2016).

In many occasions, the raw support is not directly used for the membrane preparation, and different treatments have been previously carried out in order to improve the adherence or the future membrane performance. An initial deep cleaning is always carried out to ensure the complete removal of any dirt, grease, and oil, coming from the sintering of the support material. This first step usually consists of successive washings in diverse solution, including diluted acid and alkaline solutions as well as organic solvents like acetone or alcohols (Alique 2018). After that, a chemical etching with any strong acid solution can be also applied in order to improve the adherence of the palladium film, as suggested in previous works of Mardilovich (1998), Li (2007), and Kim et al. (2015). However, the most frequent treatments are focused on modifying the surface properties of the porous substrates for making the preparation of thin Pd films easier, especially in case of considering a metallic one. Despite being possible to polish the raw surface to achieve this effect (Ryi et al. 2008), the incorporation of any intermediate layer between the porous support and the palladium film is the preferred alternative (Mateos-Pedrero et al. 2010). In this manner, the main benefits of using both technical ceramics and metals as supporting materials can be combined, avoiding fragility, resistance to handling, poor surface properties, and possible metal interdiffusion at the same time (Alique 2018; Alique et al. 2018). In fact, most of technical ceramics considered as potential supports have been also proposed as suitable

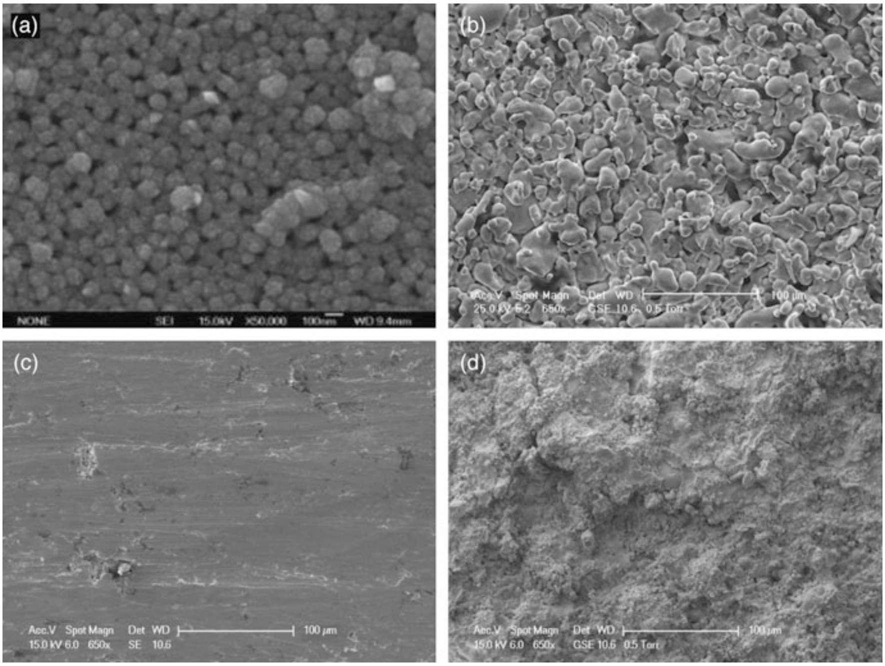

Fig. 12.6 SEM micrographs for different materials and techniques typically used for preparing composite Pd-based membranes: (**a**) raw Al_2O_3 support (reproduced from (Wu et al. 2010)), (**b**) raw PSS support, (**c**) polished PSS support, and (**d**) YSZ intermediate layer onto PSS

interlayers, especially in case of presenting a similar thermal expansion coefficient to that of palladium as occurs for YSZ (Huang and Dittmeyer 2007; Calles et al. 2014) and CeO_2 (Martinez-Diaz et al. 2019; Ryi et al. 2014) materials. Figure 12.6 collects diverse micrographs of the external surface for different materials and techniques typically used for preparing composite Pd-based membranes. As it can be appreciated, a wide variety of morphologies can be found despite most of them having been satisfactorily used as supporting materials. Figure 12.6a, b, corresponding to Al_2O_3 and PSS supports, evidences the abovementioned differences between typical ceramic and metallic substrates. The narrow pore size distribution with small pore mouths obtained on the alumina smooth surface (Fig. 12.6a) clearly differs from the rough one observed for PSS, in which a wide variety of large pores up to a few microns appears (Fig. 12.6b). This irregular surface can be plastically deformed by mechanical polishing (Fig. 12.6c) or modified by incorporating an intermediate ceramic barrier (Fig. 12.6c). In both cases, original porosity and pore size distribution drastically change, being necessary to optimize these parameters in order to maintain a suitable permeability of the porous media, avoiding permeation fluxes below the values defined as technical targets by the Department Of Energy (DOE) for a competitive industrial implementation (Advanced Hydrogen Transport Membranes for Coal Gasification n.d.).

Membrane Composition: Binary and Ternary Alloys

Great efforts are also directed to replace the pure palladium by diverse alloy formulations as selective layer in composite membranes for H_2 separation. This strategy has been mainly applied for years in binary alloy formulations of palladium with silver (Chen et al. 2016), copper (Zhao et al. 2015), or gold (Patki et al. 2016), although new alloying metals and ternary formulations are under investigation in the last years (Conde et al. 2017). All of them can be prepared by diverse techniques, although a final thermal treatment at 500–600 °C for several hours is always required to form the final alloy (Gade et al. 2009a; Zeng et al. 2012; Sumrunronnasak et al. 2017). The concrete conditions for this annealing are crucial to achieve a homogeneous composition of the alloy, especially in radial direction for thickness of several microns.

PdAg alloys are the most widely reported ones in the literature, especially in case of containing around 23% silver. At these conditions, the PdAg alloy exhibits a maximum permeability that doubles the value reached with pure Pd while significantly improving its resistance to suffer hydrogen embrittlement (Wald et al. 2016). This process could cause a dramatic fail of the membrane due to the formation of α- and β-crystalline structures for the H_2–metal hybrids at temperatures lower than 298 °C (Yun and Ted Oyama 2011). Additionally, the partial replacement of a certain amount of palladium by silver in the selective film also contributes to reduce the final cost of the membrane (Tarditi et al. 2017; Chen et al. 2016). Despite the clear advantages of these membranes in the face of pure Pd films, their permeation behavior is almost the same in case of feed streams containing sulfur compounds, as usually occurs in many industrial processes for waste valorization (Arratibel Plazaola et al. 2017; Nayak and Bhushan 2019). Any small sulfur concentration from a few ppm rapidly provokes a drastic reduction on the H_2 flux through the membrane and formation of pinholes that could provoke a structural failure of the membrane with time (Braun et al. 2012). Moreover, in most cases this effect is not reversible. To avoid the membrane deterioration at these conditions, binary alloys of palladium with copper (Zhao et al. 2015; Jia et al. 2017) or gold (Zhao et al. 2016; Patki et al. 2016) have been proposed in the literature. Pd–Cu alloys exhibit a maximum permeability for a copper content of 40%, reaching similar values to the obtained ones for pure Pd films with a significant cost decrease (Zhao et al. 2015; Jia et al. 2017). Moreover, this alloy prevents the irreversible damage of the membrane when operating in presence of sulfur compounds, maintaining a reasonably good mechanical integrity (Zhao et al. 2015). The main drawback of these membranes is the rapid decrease in permeance when some slight deviation from the ideal $Pd_{60}Cu_{40}$ composition is given, even if feed does not contain sulfur compounds. Similar benefits in terms of sulfur tolerance can be reached if palladium is alloyed with gold with an optimal composition not still completely defined. In fact, most researchers obtained suitable H_2 permeabilities with a wide gold content, ranging from 1 to 20%, while it decreases for higher values (Patki et al. 2016; Tarditi et al. 2013). However, the use of gold does not help to reduce the elevated cost of palladium, and these PdAu membranes are still out of market unless the presence of sulfur compounds justifies their use.

Beside the abovementioned binary alloys, other possibilities have been also explored in the past, including the combination of palladium with other metals such as platinum (Lewis et al. 2013) or ruthenium (Gade et al. 2009b), among others. Nevertheless, the formulation of ternary alloys with multiple combination of elements seems to be most promising alternative for the present and coming years, since it combines simultaneously the improvements of each constituent (Braun et al. 2012; Fontana et al. 2018; Tarditi and Cornaglia 2011). However, detailed studies about the synthesis of ternary alloys are still scarce. First works suggest that particular compositions seem to reach an additional improvement on the membrane properties as compared to binary alloys, in terms of increasing hydrogen permeability and/or chemical resistance (Al-Mufachi et al. 2015; Tarditi et al. 2017; Lewis et al. 2014). It is possible to improve not only the membrane permeability but also the mechanical and chemical resistances to sulfur poisons by alloying palladium simultaneously with two or more other metals, while the overall cost of the membrane is simultaneously reduced by using cheap alloying metals (Braun et al. 2014). Some interesting studies can be found in that regard for membranes prepared by electroless plating (ELP) (Fontana et al. 2018) or physical vapor deposition (PVD) (Peters et al. 2011b). Table 12.3 collects some relevant information for key recent studies, including metal incorporation technique, alloy composition, thickness, annealing conditions, and membrane performance. In general, PVD membranes offer a wide variety of possibilities for studying new alloy formulations, being possible to adjust accurately the final composition, at the expense of the costs. On the contrary, ELP technique provides a cheaper alternative to prepare alloyed membranes, but only a few metals can be considered, additionally appearing some problems to ensure a good homogeneity in axial and/or radial dimensions (Alique et al. 2018; Pinacci and Basile 2013).

Innovative Manufacturing Processes

Different routes can be used for incorporating a H_2-selective layer onto a porous substrate, independently of being formed by pure palladium or any Pd-based alloy, mainly including chemical vapor deposition (CVD) (Huang et al. 1997), electrodeposition (EL) (Sumrunronnasak et al. 2017; Chen et al. 2008), physical vapor deposition (PVD) (Navinšek et al. 1999; Mattox and Mattox 2010; Peters et al. 2015), or electroless plating (ELP) (Kiadehi and Taghizadeh 2019; Zhang 2016).

PVD alternative is worth mentioning in case of searching novel alloy compositions, as previously discussed in Sect. 12.3.1.2, although the high cost of this technique and complex equipment limit its use for a potential scale-up for the industry (Alique 2018). PVD technique basically consists of incorporating metal particles onto a substrate from a vapor phase without any chemical reaction (Jayaraman et al. 1995). This metal vapor phase is generated by thermal evaporation at vacuum conditions (Mattox and Mattox 2010) or, more usually, magnetron

Table 12.3 Recent advances on preparation of Pd-based alloys

Metal incorporation	Alloy composition	Thickness (μm)	Annealing conditions	Membrane performance			Ref.
				Permeation	$\alpha_{H2/N2}$	S tolerance test (ppm)	
ELP	$Pd_{77}Ag_{23}$	3.2	500 °C, 2 h (N_2)	$3.1 \cdot 10^{-6a}$	>8000	–	Fernandez et al. (2014)
ELP	Pd_xAg_y	4.0–5.0	n.a.	$1.0 \cdot 10^{-6c}$	>200,000	–	Medrano et al. (2016)
ELP	$Pd_{81}Cu_{19}$	5.0	500 °C, 48 h (N_2)	$1.2 \cdot 10^{-6a}$	1194	Yes (35 ppm)	Zhao et al. (2015)
ELP	$Pd_{98}Ru_2$	6.0	n.a.	$2.1 \cdot 10^{-3a}$	1860	–	El Hawa et al. (2014)
ELP	Pd_xNi_y	7.0	n.a.	$2.7 \cdot 10^{-3a}$	640	–	Lu et al. (2015)
ELP	$Pd_{91.5}Ag_{4.7}Au_{3.8}$	2.7	500 °C, 8 h	$2.3 \cdot 10^{-3a}$	793–4115	Yes (9 ppm)	Melendez et al. (2017b)
ELP	$Pd_{69}Au_{17}Cu_{14}$	14.0	500 °C (H_2)	$6.2 \cdot 10^{-4a}$	n.a.	Yes (100 ppm)	Tarditi et al. (2015)
PVD	Pd_xNi_y	1.0	n.a.	$2.6 \cdot 10^{-6b}$	458	Yes (10 ppm)	Dunbar (2015)
PVD	$Pd_{77}Ag_{23}$	1.9–3.8	n.a.	$1.5 \cdot 10^{-2a}$	2900	–	Peters et al. (2011a)
PVD	$Pd_{70}Cu_{30}$	2.2	n.a.	$3.2 \cdot 10^{-9d}$	10,000	Yes (2–100 ppm)	Peters et al. (2012)
PVD	$Pd_{85}Cu_{15}$	1.9	n.a.	$7.6 \cdot 10^{-9d}$	10,000	Yes (2–100 ppm)	Peters et al. (2012)
PVD	$Pd_{75}Ag_{22}Au_3$	1.9	n.a.	$6.7–9.3 \cdot 10^{-9d}$	n.a.	Yes (20 ppm)	Peters et al. (2013)
PVD	$Pd_{76}Ag_{21}Mo_3$	2.3	n.a.	$3.6–5.8 \cdot 10^{-9d}$	n.a.	Yes (20 ppm)	Peters et al. (2013)
PVD	$Pd_{69}Ag_{27}Y_4$	2.4	n.a.	$8.8–13 \cdot 10^{-9d}$	n.a.	Yes (20 ppm)	Peters et al. (2013)

n.a.= non-available
[a]Permeance ($mol \cdot m^{-2} \cdot s^{-1} \cdot Pa^{-0.5}$)
[b]Permeance ($mol \cdot m^{-2} \cdot s^{-1} \cdot Pa^{-1}$)
[c]Permeate flux ($mol \cdot m^{-2} \cdot s^{-1}$)
[d]Permeability ($mol \cdot m^{-2} \cdot s^{-1} \cdot Pa^{-0.5}$)

sputtering, in which a metal target is bombed with ions of high energy, generating a plasma (Checchetto et al. 2004). Currently, the research group headed by R. Bredesen in SINTEF is the most relevant one in preparing Pd-based membranes by PVD. They have multiple manuscripts and patents describing a unique membrane preparation process in which the selective film is firstly deposited by this technology onto a silicon single crystal substrate and, subsequently, it is removed to be used as an unsupported film or transferred to any other porous support, usually made on stainless steel (Peters et al. 2015; Tucho et al. 2009; Mejdell et al. 2009).

On the other hand, ELP is the most promising one in terms of simplicity and cost, being possible to cover complex geometries of both conducting and nonconducting supports. For this reason, most researchers go for this alternative in their studies, trying to improve the method for reaching very thin and homogeneous layers with high reproducibility (Alique 2018; Alique et al. 2018). During last years, Pacheco-Tanaka et al. developed the so-called pore-filled method, based on the conventional ELP, to prepare mainly PdAg membranes by co-deposition (Tanaka et al. 2008; Plazaola et al. 2017; Arratibel et al. 2018a). This alternative consists on the formation of the H_2-selective film around ceramic particles placed just in the middle of the support thickness. Figure 12.7 represents a simple scheme of the process, including all steps involved for the preparation of a pore-filled membrane onto an alumina support. First, an intermediate layer formed by ceramic particles (in this case, two adjacent layers of TiO_2 and ZrO_2) is generated. These particles are activated with Pd nuclei, and a new external ceramic layer (YSZ) is deposited on the top as protective layer. Finally, the H_2-selective film is deposited by vacuum-assisted ELP (VA-ELP)

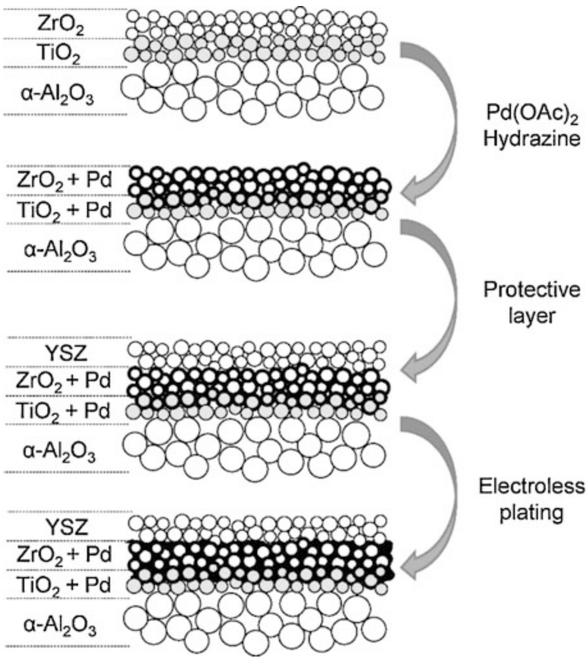

Fig. 12.7 Scheme of the experimental procedure for obtaining pore-filled membranes using a porous α-Al_2O_3 support with diverse intermediate layers of TiO_2 and ZrO_2. (Reproduced with permission from (Arratibel et al. 2018a))

around the previously activated ceramic particles. In general, very thin selective films can be reached with this technique, although some limitations related to the inherent difficulty and cost of the process, as well as limited H_2 permeability, were also found. The number of nanoporous intermediate layers and the applied vacuum level during the ELP were not directly related to the permeation properties reached by these membranes. The authors explained this behavior by considering a non-well-connected network in the palladium film across the ceramic intermediate layers. In this manner, H_2 molecules need to split and recombine several times along the palladium clusters created throughout the porous media, and, consequently, the permeation capacity is affected (Arratibel et al. 2018a).

Despite the limitations of pore-filled membranes, clear advantages are also pointed out in contrast to conventional ELP membranes. In this context, the situation of the H_2-selective layer in the middle of a sandwich structure formed by multiple ceramic layers is especially relevant. Thus, the position of the palladium film provides an additional protection against generation of mechanical stresses, influence of possible pollutants presented in the feed stream, and direct contact of the film with the catalyst particles. The last potential benefit could be certainly interesting in case of operating in fluidized-bed membrane reactors, in which the contact between Pd film and catalyst particles in movement could provoke important damages on the membrane (Arratibel et al. 2018a). In this manner, the preparation of double-skin membranes, in which the Pd-based film is deposited by conventional ELP or VA-ELP between two ceramic porous layers, has been also proposed to achieve similar advantages (Arratibel et al. 2018b, c).

Electroless pore-plating (ELP-PP) is another interesting alternative with an objective quite similar to the pore-filled membranes, based on the formation of the selective film just into the cavities of the porous support (Alique 2018; Alique et al. 2018; Sanz et al. 2012). In this case, the procedure is quite easier, feeding directly both palladium source and reducing agent from opposite sides of the porous media and forcing the chemical reaction to take place just inside the pores, thus avoiding the necessity of incorporating complex or multiple ceramic layers (Sanz et al. 2012). Moreover, this methodology ensures the formation of a fully dense Pd layer with an unnecessary increase of the metal thickness, and it minimizes the number of rejected membranes during the fabrication process. However, the Pd film is not entirely generated inside the pores, and an external layer is also formed onto the side of the porous support in contact with the plating solution. Figure 12.8 represents two basic diagrams for comparison of the H_2-selective film formation when using the conventional ELP or ELP-PP methods.

The characteristics of the H_2-selective film for ELP-PP membranes are determined by hydrazine concentration (Calles et al. 2018) and porous support properties, mainly average porosity, pore size distribution, and external roughness (Martinez-Diaz et al. 2019; Alique et al. 2016; Furones and Alique 2017). In this manner, it is possible to reach diverse Pd thicknesses and metal distribution between top and internal layers. These variations clearly affect the permeation capacity of the membranes, and, despite obtaining an almost complete H_2/N_2 ideal selectivity, it is pointed out the generation of an additional resistance to the H_2 permeation due to

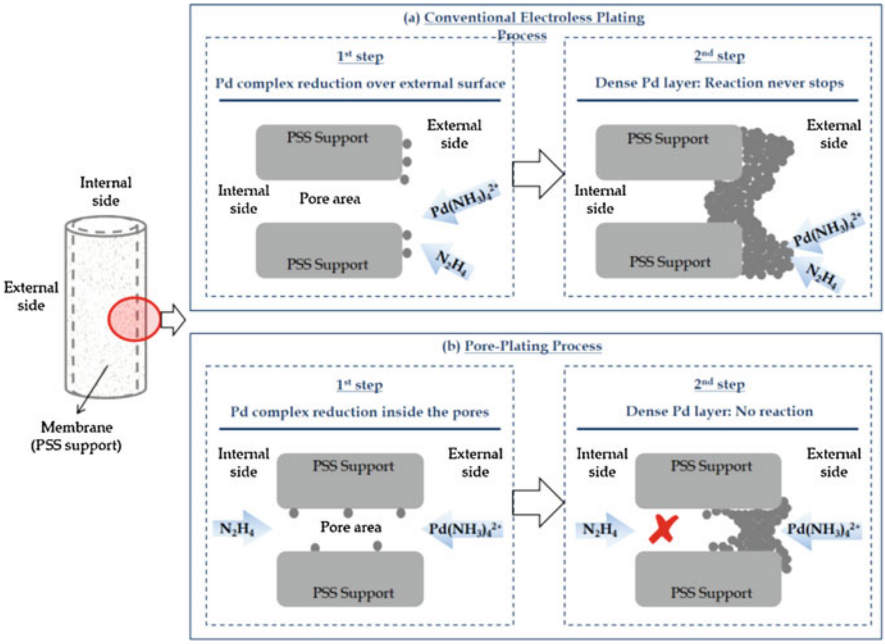

Fig. 12.8 Comparison of the H_2-selective film formation when using conventional ELP (**a**) or ELP-PP (**b**). (Reproduced with permission from (Sanz et al. 2013))

partial infiltration of Pd inside the pores of the support (Sanz et al. 2013; Calles et al. 2018).

A. Goldbach et al. have proposed a new type of Pd-based membranes prepared by ELP, denoted as duplex membranes, in which the porous substrate contains two different H_2-selective layers on each surface on both permeate and retentate sides (Zhao et al. 2018b). The total Pd or Pd–alloy thickness of a traditional fully dense layer is divided into these layers with near a half thickness, thus obtaining a membrane with a similar total amount of palladium but distributed in a very peculiar manner. In fact, it is not required that both layers become fully dense, and they can contain several defects. However, despite the presence of defects, a really high H_2 selectivity is reached, noticeably improving the current capability of traditional membranes and also suppressing the mass transfer resistance caused by sweep gas diffusion into the support of conventional composite membranes. Different paths for permeation of H_2 and N_2 or other gas molecules through the new structure of the membrane provoke this improvement. Figure 12.9 collects some schemes about the membrane structure in comparison with a conventional one, as well as the shortest permeation paths for H_2 and N_2 molecules through these membranes. As it can be seen, permeation of H_2 is almost the same in both cases because of a minimum effective distance between both retentate and permeate sides, of course assuming no additional resistances to the permeation process in gas phases and similar total Pd thickness in both configurations. However, in case of analyzing the permeation of N_2

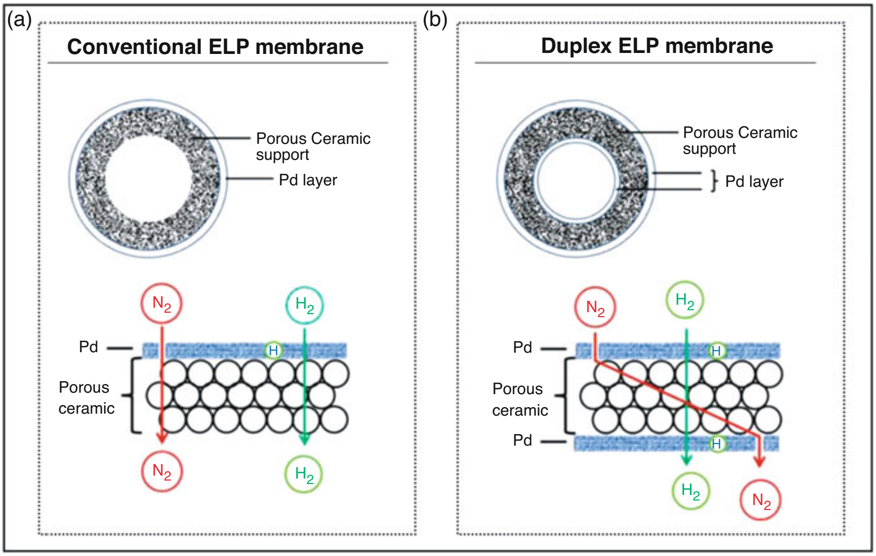

Fig. 12.9 Structure and permeation scheme for (**a**) conventional ELP membranes (with a single Pd layer) and (**b**) duplex membranes with a double Pd layer on both internal and external surfaces of a porous support. (Adapted from original images published in (Zhao et al. 2018b))

through membrane defects, important differences arise in both cases. For conventional membranes with a single Pd layer, the permeation path of N_2 could be similar to that of H_2 if the layer contains any defect. However, proposed by Goldbach et al., the probability of obtaining a similar permeation path for N_2 with the duplex structure drastically decreased, and, hence, the H_2 selectivity is noticeably increased.

12.3.2 Membrane Behavior for Independent Purification Units

Most of the research studies about Pd-based membranes include permeation tests in independent purification units to determine H_2 flux, permeance, H_2 selectivity, or other related parameters. These analyses are very useful to understand the real behavior of the membranes at diverse operating conditions, mainly focused on evaluating the effect of pressure, temperature, or gas feed composition.

Permeation is strongly dependent on pressure which is the driving force of the process. In the case of the permeation of hydrogen using Pd-based membranes the driving force is expressed as the difference between hydrogen partial pressures at both sides of the membrane (retentate and permeate), and the flow of hydrogen through the membrane can be obained following the general expresion:

$$J_{H_2} = \frac{k_{H_2}\left(P^n_{H_{2,ret}} - P^n_{H_{2,perm}}\right)}{t} \quad (12.2)$$

where J_{H2} is the hydrogen flux through the Pd layer, k_{H2} the hydrogen permeability, t the Pd thickness, P_{H2} the hydrogen partial pressure in the retentate (subscript "ret") or the permeate side (subscript "perm"), and n an exponential factor ranging from 0.5 to 1 according to the rate-controlling step. In general, hydrogen diffusion though bulk metal is the limiting step if the Pd film does not contain defects, adopting this parameter the value $n=0.5$ and denoting the expression as Sieverts' law (Alique et al. 2018; Yun and Ted Oyama 2011). On the contrary, some deviations from this ideal value can also arise in case of presence of defects in the Pd film or become relevant additional resistances during transport in the gas phase or molecule dissociation/re-association steps ($n=0.5$–1), and they can be caused by the presence of defects or to the hydrogen permeation process (i.e., problems in the gas phase diffusion or hydrogen dissociation steps) (Caravella et al. 2014).

Recently, a particular deviation from this general trend has been presented for ELP-PP membranes (Sanz et al. 2013; Calles et al. 2018). In these membranes, the palladium is distributed between an external top layer onto a porous support, as usual for most of composite membranes, and inside the pores. Therefore, an additional resistance to the H_2 permeation arises, becoming more important as the infiltration of palladium inside the pore structure of the supports increases (Calles et al. 2018). This effect is collected in Fig. 12.10, in which a simple scheme of the Pd distribution on the porous support together with the permeation behavior of three ELP-PP membranes prepared by using diverse experimental conditions (variation of the reducing agent concentration) is shown. As it can be seen, it is clear that diverse synthesis conditions affect noticeably the additional resistance to the H_2 permeation but the good linearity between permeate and pressure driving force is maintained in all cases, in a similar way to that predicted by Sieverts' law. This additional resistance is presented as a minimum pressure driving force that needs to be overcome to initiate the permeation process. Authors explain in detail this deviation from the ideal permeation behavior of Pd-based membranes by assuming a clear effect of Pd introduction grade into the pores of the support on the abovementioned resistance. Thus, the membrane prepared with the highest hydrazine concentration ($C_{N2H4} = 1.00$ M) contains the thickest Pd top film and a relative low infiltration grade inside the pores, showing the lowest permeation resistance. This fact evidences a slight contribution of diffusional effects derived from the presence of Pd inside the pores. On the contrary, the ELP-PP membrane prepared with the most diluted hydrazine solution ($C_{N2H4} = 0.05$ M) shows a really high infiltration of Pd inside the pores with a top layer significantly thinner than the estimated one by gravimetric analysis. Hence, the real pressure difference between both sides of the palladium film is noticeably different to that of the measured one on both gas phases, and hence the highest resistance is obtained. Taking into account this particular behavior, the authors stated that a hydrazine concentration of $C_{N2H4} = 0.20$ M provides an intermediate situation, allowing the reduction of the amount of Pd used

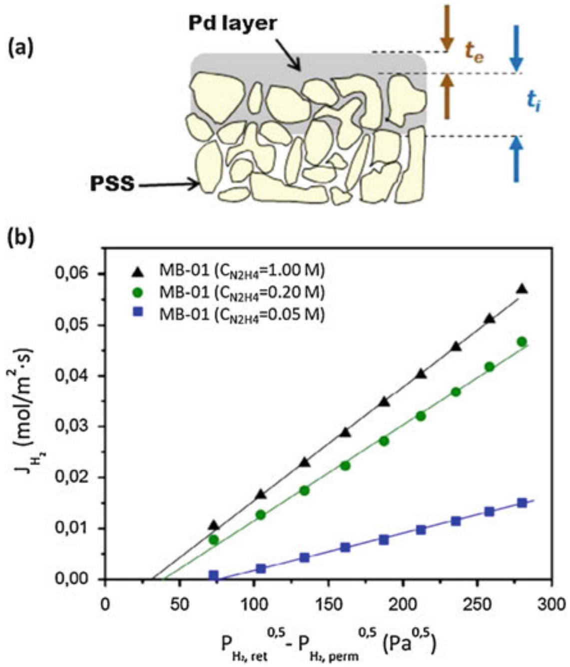

Fig. 12.10 (**a**) Scheme of palladium incorporation on the PSS support by ELP-PP and (**b**) permeation behavior for ELP-PP membranes prepared with diverse hydrazine concentrations. (Adapted from original images published in (Calles et al. 2018))

during the preparation of the membranes while keeping metal infiltration inside the pores within acceptable values.

The hydrogen flux can also be affected by other factors such as permeation mode or gas feed composition. The presence of certain molecules in the feed stream can decrease the permeate flux due to dilution effect of inlet stream, concentration–polarization effect, or competitive adsorption on the membrane surface (Yun and Ted Oyama 2011). The presence of any molecule apart of hydrogen in the feed provokes a dilution of the stream and, hence, a decrease on the driving force obtained. However, this effect can be easily corrected if real hydrogen partial pressures are calculated. The dilution effect is typical for gas mixtures containing inert molecules such as helium, nitrogen, or carbon dioxide, which usually present a minimum interaction with the palladium film (Yun and Ted Oyama 2011). However, despite the absence of interaction between these molecules and the Pd layer, particular operating conditions could make relevant the well-known concentration–polarization effect by which hydrogen concentration in the gas phase near the membrane surface drastically drops in comparison with the bulk gas (Nekhamkina and Sheintuch 2016). Therefore, concentration of non-permeable species increases in the gas volume immediately adjacent to the membrane surface, thus reducing real driving force and overall performance of the permeation process (Catalano et al. 2009; Steil et al. 2017). Despite this effect always occurring, it is especially relevant in case of preparing ultrathin Pd layers and/or reaching inlet gases first the porous substrate and then the selective film (Caravella et al. 2008, 2014). Additionally, certain compounds can also be adsorbed on the metal surface, thus reducing the number of possible active sites in which the hydrogen molecules can be split. It is particularly noticeable in case of gas mixtures containing carbon monoxide, steam water, or sulfur compounds, needing to be correctly addressed when working with real industrial streams (Cornaglia et al. 2015; Kurokawa et al. 2014; Dunbar and Lee 2017). This effect can be partially mitigated by adjusting the operating conditions of the purification unit (pressure, temperature, or residence time), preparing new alloy formulations in which this adsorption is hindered, or incorporating any protective layer that prevents contact between certain molecules and the selective layer surface (Abate et al. 2016).

Temperature has also an important effect on the hydrogen flux due to the membrane permeability (k_{H2}) varying with this parameter following an Arrhenius-type dependence (Dunbar and Lee 2017; Gallucci et al. 2007), as expressed in Eq. 12.3:

$$k_{H_2} = k_{H_2}^0 e^{\left(-\frac{E_a}{R\,T}\right)} \tag{12.3}$$

Typically, the activation energy for palladium membranes ranged from 7 to 30 kJ mol^{-1} (Sanz et al. 2011; Ryi et al. 2010). However, the apparent activation energy can significantly vary in alloy formulations with diverse composition, as suggested by Patki et al. (Patki et al. 2018). They have recently presented a detailed study in which several 4–5-μm-thick PdAu composite membranes with diverse gold content were measured. Although a decrease on the activation energy value from 12.2 kJ mol^{-1} to 7.5 kJ mol^{-1} was observed for increasing contents in gold up to 21%wt, this trend changed for high contents in gold reaching a value of 9 kJmol-1 for 41 %wt Au. Authors attributed this behaviour to the contribution of the partial enthalpy of solution of H into the PdAu alloy (ΔHH) and the activation energy for diffusion of H in the alloy (ED) into the global apparent activation energy value obtained. These two contributions have opposite signs that counteract each other and cause a nonlinear trend with increasing Au compositions (Patki et al. 2018).

Finally, some basic concerns about hydrogen selectivity need to be also addressed in this chapter. Despite in theory only hydrogen can permeate through a dense Pd-based film, it is common that some residual amounts of other gases present in the feed stream reach the permeate side. It can be basically explained by the presence of micro-cracks or defects in the selective layer (Ryi et al. 2011; Zeng et al. 2009) or problems with sealing (Arratibel et al. 2018c; Chen et al. 2010). These problems are usually accounted as hydrogen selectivity, differentiating between ideal separation factor and real H_2 selectivity. The first parameter is obtained from permeate values reached when the membrane is fed with hydrogen and any other gas, typically helium or nitrogen, during independent permeation tests. It reflects the maximum potential of the membrane for reaching pure hydrogen fluxes. This parameter is calculated as follows:

$$\alpha_{ideal} = \frac{J_{H_2}^{perm}}{J_i^{perm}} \tag{12.4}$$

On the other hand, the real selectivity is calculated from the real molar fractions of each compound in both permeate and retentate streams obtained in a single experiment, feeding the membrane with a gas mixture. Thus, this second parameter determines the membrane efficiency at real operation conditions with mixtures.

$$\alpha_{real} = \frac{y_{H_2}^{perm} / y_i^{perm}}{y_{H_2}^{ret} / y_i^{ret}} \tag{12.5}$$

12.3.3 Membrane Reactors for Valorization Processes

One of the most promising technologies to improve the current development of industrial hydrogen production processes is the use of membrane reactors instead the conventional scheme based on consecutive reaction and purification steps. These systems provide separated hydrogen with a really high purity at the same time that it is produced, hence shifting the equilibrium of main reactions involved in hydrogen production towards the products. In this manner, it is possible to increase the yield of these reactions or maintain a concrete value with softer operating conditions. In both cases, it can be achieved significant savings for heating, pumping, or reaction volume requirements, which pose the real implementation of devices with high efficiency for large or limited production rates, equally. This fact, usually known as process intensification, is of key importance to develop a distributed hydrogen production grid against the current big-sized centralized industries. In this context, numerous studies addressing the use of membrane reactors for hydrogen production have been published during last years, also including residual biomass and waste valorization processes (Basile et al. 2013; Sánchez et al. 2011).

Biogas upgrading to H_2 is one of the primary technologies where the use of membrane reactors demonstrated its advantages. The favorable H/C ratio of the feedstock enhances the production of H_2 with respecto to other subproducts as carbon monoxide or carbon dioxide and, consequently, turning the H_2 permeation through the membrane easier (Gao et al. 2018). In this context, Iulianelli et al. presented the use of a membrane reactor, in which a composite Pd/Al_2O_3 membrane partially extracted the generated hydrogen by steam reforming of a synthetic biogas mixture (Iulianelli et al. 2015). At the most favorable operating conditions ($T = 450$ °C, $P = 3.5$ bar, $H_2O{:}CH_4 = 4{:}1$, and $GHSV = 11000\ h^{-1}$), the overall conversion overcomes a 30% with a H_2 recovery of around 70%, although the generation of defects and pinholes on the Pd layer of the composite membranes limited the purity of the permeate stream below 70%. On the contrary, the use of milder operating conditions ($T = 380$ °C, $P = 2.0$ bar, $H_2O{:}CH_4 = 3{:}1$, and

GHSV = 9000 h^{-1}) significantly improved the mechanical resistance of the membrane, reaching H_2 purities of around 96%, although it was detrimental to the reaction performance with modest conversion and hydrogen recovery values (27% and 20%, respectively). A detailed study about temperature and pressure effects on hydrogen production from biogas steam reforming in both conventional and PdAg membrane reactor was also published by Vásquez Castillo et al. (Vásquez Castillo et al. 2015). They observed a higher H_2 production when a membrane reactor was used at the same operating conditions (T, P) than a traditional one. Thus, a maximum hydrogen yield of 80% was reached at T=450 °C and P=0.4 MPa on reaction side, while the hydrogen recovery increased with increasing temperature and pressure in case of testing the membrane reactor. More recently, Chompupun et al. (Ramachandran et al. 2018) have explored the use of membrane reactors to improve the steam methane reforming, also proposing interesting scale-up strategies. After achieving a significant increase of the methane conversion with a MR in comparison with a conventional PBR without any shift effect, different geometries for the process scaling-up were evaluated, selecting a square annular honeycomb monolith arrangement with provision for simultaneous heat supply and hydrogen removal. This design provided the best effectiveness for the MR with a ratio between membrane surface area and catalyst volume of 255 m^2/m^3. Niek de Nooijer et al. also addressed the biogas SR but considering a fluidized-bed membrane reactor with a ceramic-supported PdAg thin-film membrane (De Nooijer et al. 2018). They reached hydrogen purities up to 99.8%, being possible to model the MR behavior if some concentration–polarization effects are considered. Thus, a 0.54-cm-thick stagnant mass transfer boundary layer around the membrane is considered to fit the experimental results performed at temperatures in the range of 435–535 °C, pressures between 2 and 5 bar, and CO_2/CH_4 ratios up to 0.9. On the other hand, Bruni et al. have presented a comparison between a traditional scheme based on a PBR followed by an independent membrane separator and an intensified one in which a MR is considered in terms of both performance and energy efficiency (Bruni et al. 2019). The first configuration presented energy efficiency values in the range of 35–40% with T = 720 °C, S/C = 4, and P = 3–10 bar, finding that hydrogen yield was favored at higher pressures and S/C, although it was not significantly affected by temperature. Very similar values were reached in case of using a membrane reactor configuration but only if pressure overcomes 10 bar. These results confirmed that a PBMR plant only achieves comparable performances to a traditional plant if it is operated at high pressures, being the energy efficiency for both configurations extremely similar. Di Marcoberardino et al. discussed a detailed techno-economic assessment for hydrogen production from biogas in a MR under the umbrella of the European project BIONICO (Di Marcoberardino et al. 2017, 2018). Two different biogas compositions obtained from typical landfill or anaerobic digestion were considered to assess the impact on overall system design, performance, and costs. It was found that the latter alternative presents the lower overall costs as consequence of the higher methane content. Thus, an average hydrogen cost production around 4 €/kg_{H2} was presented, being certainly competitive with the average cost when a reference SR process is considered. In summary, the use of a MR configuration for biogas SR provides lower biogas and capital costs but higher electricity costs. A similar techno-economic study has been presented by Lachén et al. for production of high-purity H_2 from biogas by dry reforming in a fluidized-bed membrane reactor and steam–iron process (SIP) (Lachén et al. 2018). In this way, the integrated process enhances energy efficiencies of every single process allowing values greater than 45% and pure hydrogen yields up to 68% at 575 °C. However, the H_2 production costs were calculated in the range of 4–15 €/kg_{H2}, still certainly far away from the fixed ones by DOE technical targets for year 2020 (2 US$/kg $_{H2}$).

The production of hydrogen from bioethanol in membrane reactors is another alternative widely reported in the literature. Seelam et al. explored this alternative by feeding a MR containing a composite PSS–Pd membrane with $1C_2H_5OH{:}13H_2O{:}0.18CH_3COOH{:}0.04C_3H_8O_3$ (Seelam et al. 2012). After analyzing diverse operating conditions, the best results obtained when using T = 400 °C, P = 12 bar, and GHSV = 800 h^{-1} reach a bioethanol conversion of 94% with hydrogen yield and hydrogen recovery factor (HRF) around 40%. However, the membrane was affected by chemical reactions, and, despite maintaining a hydrogen purity of around 95%, a decrease on the permeate after each reaction test was observed. This effect was explained by deposition of coke on the membrane surface, thus causing a decrease of MR performance, mainly HRF. A similar feedstock was used by Tosti et al. (2013a), also evidencing the potential of MR for producing ultrapure hydrogen via oxidative reforming from liquid wastes of dairy industries. Operating at 450 °C and 200 kPa with a Pt-based catalyst and a self-supported PdAg membrane with a thickness of around 60 μm, it was possible to generate pure hydrogen with a hydrogen yield close to 3, against the maximum theoretical value of 5. Mironova et al. compared different catalysts in both traditional and membrane reactors, remarking that the process intensification allows not only the production of high-purity hydrogen but also an increase in the efficiency of SR process (Muraviev et al. 2014). More recently, the research group headed by Basile has also worked on this topic, publishing some interesting studies about the use of Pd-based membrane reactors for bioethanol reforming (Iulianelli et al. 2016, 2018). In a first study, 98% of ethanol conversion and more than 65% of hydrogen recovered in the permeate side were reached as best results when operating with excess of steam at 400 °C, 3.0 bar, and GHSV = 5000 h^{-1}. These values are slightly greater than the obtained ones by supplying a stoichiometric feed (93% and 60%, respectively) or increasing the GHSV (Iulianelli et al. 2016). A thinner membrane with only 5 μm thick was used in other similar study but feeding a real bioethanol mixture coming from industry (Iulianelli et al. 2018). In that case, an ethanol conversion of 60% was reached at 400 °C, 2.0 bar, and 1900 h^{-1}, recovering almost 70% of the hydrogen generated during the process with a purity improving higher than 99%. In this manner, besides the generation of ultrapure hydrogen for possible PEM fuel cells supplying, the ethanol conversion was increased around 20% with respect to the obtained one in an equivalent traditional PBR. However, also a deterioration of the Pd-based membrane was found due to the surface morphological variations and deposition of coke, as represented in Fig. 12.11 together with a scheme of the MR used for the experimental campaign.

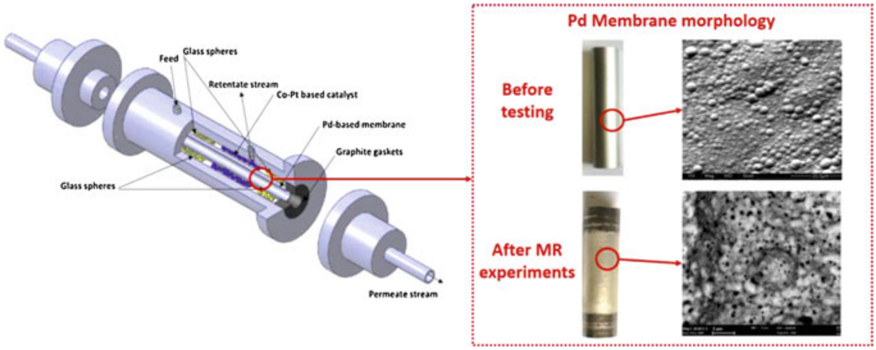

Fig. 12.11 (**a**) Scheme of tubular membrane reactor used for bioethanol SR and external morphology of the membrane before and after being used. (Adapted from original images published in (Iulianelli et al. 2018))

The gasification of a solid feedstock, i.e., residual biomass, in a membrane reactor has been also widely reported in the literature. Thus, Ghasemzadeh et al. have demonstrated in a computational fluid dynamic modeling the better efficiency of a membrane reactor containing a Pd–Ag membrane compared with a traditional system, especially operating in countercurrent mode (Ghasemzadeh et al. 2018). An almost complete biomass conversion was reached in the best operating conditions after analyzing the influence of temperature, pressure, and steam/biomass ratio with a H_2 recovery around 70%. The same authors have also studied the valorization of residual glycerol via steam reforming for producing pure hydrogen in both traditional and membrane reactors, also finding a better performance for the second configuration (Ghasemzadeh et al. 2019). The glycerol conversion was enhanced from 10% to 64% in the MR, while CO selectivity was reduced from 99.0% to 7.5%. Soria et al. compared four types of reactors including a traditional one, a membrane reactor with H_2 separation, a sorption-enhanced reactor with CO_2 sorption, and a sorption-enhanced membrane reactor with simultaneous H_2 and CO_2 extraction for steam reforming of real bio-oils obtained by biomass fast pyrolysis (Soria et al. 2019). The last alternative, shifting the chemical equilibrium by extracting simultaneously both H_2 and CO_2, provided the best results with 97–99% of the maximum theoretical yield for wheat or spruce bio-oil, respectively, and minimizing other subproducts such as CH_4, CO, or coke. Similar studies but also including experiments at lab scale found insights in agreement. For example, Wang et al. demonstrated good fitting between simulated and experimental data for glycerol steam reforming in a PBMR in which different membranes were considered (Wang et al. 2018). In general, the membrane separation promoted the hydrogen production at low temperatures, although the shift effect achieved with the membrane is very sensitive to the temperature variation under different operating conditions. Thus, it is essential to optimize the operating conditions to increase the hydrogen yield maintaining moderate energy consumption derived from increasing temperature or pressure variables.

Some interesting studies addressing novel processes or types of wastes used for the production of hydrogen from wastes are worth to mention. For example, Tosti to be here included some of them due to their novelty or intrinsic problematic of wastes used as feedstock for the generation of hydrogen. In this context, Tosti et al. (Tosti et al. 2013b) employed for the first time a 150-μm-thick Pd–Ag membrane to valorize olive mill wastewater (OMW), reducing original TOC and phenol concentration by about 90% while producing around 2 kg ton_{OMW}^{-1} of pure hydrogen, in addition to a useful syngas in the retentate stream. After improving the catalyst formulation, it was possible to treat the OMW while increasing the hydrogen production up to 3.25 kg ton_{OMW}^{-1} (Tosti et al. 2015). The main problem of these valorizations is the economy of the process due to the large dilution of organic compounds in the OMW. To take advantage of this large water excess, Tosti et al. proposed a simultaneous steam reforming of OMW with methane, reaching a significant savings in the economy of the treatment process (Tosti et al. 2016). Rocha et al. (2017) also addressed this problem suggesting a simultaneous hydrogen and carbon dioxide extraction during the steam reforming. It was stated that, in perspective of valorizing the OMW from waste to energy, the use of a sorption-enhanced membrane reactor with simultaneous H_2 and CO_2 removal provides a hydrogen yield very close to the stoichiometric value at certain operating conditions. These results significantly improved the achieved ones with an equivalent traditional fixed-bed reactor. Saidi suggested a possible hydrogen production in a membrane reactor by flare gas recovery gas processing plant located in Iran (Saidi 2018). The results confirmed that the flare gas conversion and hydrogen recovery improve with increasing the operating temperature, pressure, and sweep ratio because of increasing the driving force for H_2 permeation through the PdAg membrane selected for the membrane reactor. The optimal operating conditions were fixed at 477 °C, 5 bar, 5 as sweep ratio, and 4 as feed molar ratio for producing 12.7 kg/s of pure H_2, while greenhouse gas emission was reduced from 2179 kg/s to 36 kg/s. On the other hand, Hassan and Dincer recently presented a comparative assessment of various gasification fuels with waste tires for hydrogen production (Hasan and Dincer 2019). From this study, they ensured 11.1 kW net power production from the combined cycle when tires are used as the feedstock for the gasifier with energy and exergy efficiencies of the overall system around 55% and 52%, respectively. However, in this study the membrane reactor is only implemented for the WGS system, not directly for the gasifier, although the use of a membrane reactor configuration for this typical syngas upgrading has been also widely reported in many other studies, such as the performed one by Barreiro et al. (2015).

12.4 Conclusions and Future Directions

The limitation of energy resources, the negative environmental impacts of the current energy system, and the increasing amount of wastes are promoting an active search of attractive technological solutions. In this context, hydrogen is playing an increasing role for the transition towards a more sustainable energy system, in which it can be produced from a wide variety of feedstock, thus reducing dependence of unstable regions. Moreover, most European countries include more and more the reduction of the waste accumulation in landfills in their agenda about waste management strategies. The combination of both strategies for waste valorization via hydrogen production has been demonstrated technologically viable by both biological and thermochemical processes, although the scale-up at industrial level is still limited due to economic profitability. Most of these processes generate the final hydrogen by obtaining intermediate biogas or syngas, which could be also considered as final products in specific contexts. The spectra of wastes that can be used as feedstock for their conversion into H_2 are continuously growing up, but cleaning and upgrading tasks required to obtain the target hydrogen purity needed for final applications are still challenging. Pd-based membranes offer the opportunity to cover these demanding requirements in flexible configurations for both small and intensive production capacities with noticeable energy and cost savings with respect to well-stablished technologies such as cryogenic distillation or PSA. Additionally, these membranes can be combined with catalysts in a membrane reactor configuration favouring the application of process intensification principles (i.e, reduction of reaction volume requirements, heating or pumping, among others). Currently, these advantages have been demonstrated by numerous studies in literature that address the use of membranes and membrane reactors for hydrogen production/separation applicable to steam methane reforming or syngas upgrading by WGS-MR. Moreover, significant research efforts are being placed in valorization of residual biomass and diverse wastes through this technology.

The most relevant biochemical processes for hydrogen production, anaerobic digestion, and dark fermentation are still emerging technologies, while biogas upgrading is the most developed one at industrial scale due to their similarities to traditional treatments of natural gas. However, in this case, the gas is generated by anaerobic digestion from diverse wastes, and later this biogas is reformed to generate hydrogen, thus representing a renewable route to be produced. Regarding the production of hydrogen by thermochemical methods, pyrolysis and gasification can be considered as the most developed ones, being commercially demonstrated for a wide variety of feedstock also including residual biomass and wastes. Currently, most of these processes are directed to waste-to-energy or waste-to-heat concepts, thus generating as main products electricity and heat, respectively. However, it is foreseeable to consider hydrogen as target product of some of these processes, i.e., reforming of pyrolysis oils and upgrading of syngas coming from gasification units. In both cases, hydrogen is generated together with other subproducts, so any posttreatments to adjust the hydrogen concentration such as HT-WGS and LT-WGS and consecutive purification steps are always required.

Numerous studies address the advantages of using membrane separators and/or membrane reactors for all these types of processes, thus obtaining a hydrogen stream with a really high purity and reaching significant improvements on the hydrogen yield when traditional reactions are replaced by membrane reactors in both fixed-bed or fluidized-bed configurations. Main difficulty of these processes refers to ensuring the mechanical resistance of the membranes at operating conditions for long time periods, which may reduce the purity of the produced hydrogen due to the formation of defects (pores or cracks) on the surface of the membrane. Development of new alloy formulations and improved membrane preparation methods and their optimization are still under study to achieve resistant membranes with improved permeability. In this context, the formulation of palladium ternary alloys (mainly with silver, copper, or gold, among others) for the selective film seems to be an attractive alternative, as well as the preparation of membranes with multiple intermediate or H_2-selective layers. In this context, the preparation of double-skin membranes has presented excellent mechanical resistances against the selective layer deterioration during operation inside a fluidized-bed membrane reactor, while duplex membranes with a couple of H_2-selective films ensure an extremely high H_2 permselectivity despite the presence of residual defects in any of these films. In recent years, also the so-called electroless pore-plating has appeared as an attractive alternative to ensure a good reproducibility during manufacturing of membranes also with high H_2 selectivity. However, most of these advances need to be applied at industrial scale for detecting any possible additional problem prior to be commercialized. At this point, also the reproducibility during membrane manufacturing processes is a key issue to be addressed in most of the researches. Anyway, a great diversification of hydrogen production processes and production capacities is the most probably future scenario, and, under this perspective, the use of H_2-selective membranes will be especially relevant for independent separators and membrane reactors for process intensification.

Acknowledgments We would express our gratitude to professors Z. Zhang, W. Zhang, and E. Lichtfouse, editors of this book, for the opportunity to prepare a contribution based on the advances in Pd membranes for hydrogen production from residual biomass and wastes. Some words of thanks need also to be dedicated to the Spanish Ministry of Economy and Competitiveness for supporting the research activities of CIEMAT and URJC on this topic through diverse public research projects: PSE-120000-2008-29, ENE2009-08002, IPT-2012-0365-120000 and ENE-2007-66959, CTQ2010-21102-C02-01, CTQ2013-44447-R, and ENE2017-83696-R, respectively. Finally, we also thank all rights for reproducing figures and tables from previous works.

List of Symbols

$\alpha_{H2/N2}$	Ideal separation factor between hydrogen and nitrogen
E_a	Activation energy (kJ mol^{-1})
k_{H2}	Hydrogen permeability (mol m^{-1} s^{-1} Pa$^{-0.5}$)
k'_{H2}	Hydrogen permeance (mol m^{-2} s^{-1} Pa$^{-0.5}$)

K_{int} Intra-particle diffusion coefficient
J_i Permeate flux of component *i* (i.e., hydrogen, nitrogen, etc.) (mol s^{-1})
n Exponent of pressure driving force in Sieverts' law
P Pressure (Pa)
$P_{p,i}$ Pressure of component *i* in the permeate side (Pa)
$P_{r,i}$ Pressure of component *i* in the retentate side (Pa)
η_{mem} Membrane effectiveness factor
T Temperature (°C)
t Thickness (μm)
X_i Chemical conversion of component *i* (%)

References

Abate S, Díaz U, Prieto A, Gentiluomo S, Palomino M, Perathoner S, Corma A, Centi G (2016) Influence of zeolite protective overlayer on the performances of Pd thin film membrane on tubular asymmetric alumina supports. Ind Eng Chem Res 55:4948–4959. https://doi.org/10.1021/acs.iecr.6b00690

Adatoz E, Avci AK, Keskin S (2015) Opportunities and challenges of MOF-based membranes in gas separations. Sep Purif Technol 152:207–237. https://doi.org/10.1016/J.SEPPUR.2015.08.020

Adhikari S, Fernando S (2006) Hydrogen membrane separation techniques. Ind Eng Chem Res 45:875–881. https://doi.org/10.1021/ie050644l

Advanced Hydrogen Transport Membranes for Coal Gasification (n.d.). https://www.netl.doe.gov/

Ahmad AA, Zawawi NA, Kasim FH, Inayat A, Khasri A (2016) Assessing the gasification performance of biomass: A review on biomass gasification process conditions, optimization and economic evaluation. Renew Sustain Energy Rev 53:1333–1347. https://doi.org/10.1016/j.rser.2015.09.030

Aldy JE, Pizer WA, Akimoto K (2017) Comparing emissions mitigation efforts across countries. Clim Policy 17:501–515. https://doi.org/10.1080/14693062.2015.1119098

Ali A, Pothu R, Siyal SH, Phulpoto S, Sajjad M, Thebo KH (2019) Graphene-based membranes for CO_2 separation. Mater Sci Energy Technol 2:83–88. https://doi.org/10.1016/J.MSET.2018.11.002

Alique D (2018) Processing and characterization of coating and thin film materials. In: Zhang J, Jung Y (eds) Advanced ceramic and metallic coating and thin film materials for energy and environmental applications. https://doi.org/10.1007/978-3-319-59906-9

Alique D, Imperatore M, Sanz R, Calles JA, Baschetti MG (2016) Hydrogen permeation in composite Pd-membranes prepared by conventional electroless plating and electroless pore-plating alternatives over ceramic and metallic supports. Int J Hydrog Energy 41:19430–19438. https://doi.org/10.1016/j.ijhydene.2016.06.128

Alique D, Martinez-Diaz D, Sanz R, Calles JA (2018) Review of supported pd-based membranes preparation by electroless plating for ultra-pure hydrogen production. Membranes (Basel). https://doi.org/10.3390/membranes8010005

Al-Mufachi NA, Rees NV, Steinberger-Wilkens R (2015) Hydrogen selective membranes: a review of palladium-based dense metal membranes. Renew Sustain Energy Rev 47:540–551. https://doi.org/10.1016/j.rser.2015.03.026.

ALTER NRG Corp (2016). www.alternrg.com

Alvarez J, Kumagai S, Wu C, Yoshioka T, Bilbao J, Olazar M, Williams PT (2014) Hydrogen production from biomass and plastic mixtures by pyrolysis-gasification. Int J Hydrog Energy 39:10883–10891. https://doi.org/10.1016/j.ijhydene.2014.04.189

Alves HJ, Bley Junior C, Niklevicz RR, Frigo EP, Frigo MS, Coimbra-Araújo CH (2013) Overview of hydrogen production technologies from biogas and the applications in fuel cells. Int J Hydrog Energy 38:5215–5225. https://doi.org/10.1016/j.ijhydene.2013.02.057

Alzate-Gaviria LM, Sebastian PJ, Pérez-Hernández A, Eapen D (2007) Comparison of two anaerobic systems for hydrogen production from the organic fraction of municipal solid waste and synthetic wastewater. Int J Hydrogen Energ 32:3141–3146. https://doi.org/10.1016/j.ijhydene.2006.02.034

Arena U (2012) Process and technological aspects of municipal solid waste gasification. A review. Waste Manag 32:625–639. https://doi.org/10.1016/j.wasman.2011.09.025

Arratibel Plazaola A, Pacheco Tanaka D, Van Sint Annaland M, Gallucci F (2017) Recent advances in Pd-based membranes for membrane reactors. Molecules 22:51. https://doi.org/10.3390/molecules22010051

Arratibel A, Astobieta U, Pacheco Tanaka DA, Van Sint Annaland M, Gallucci F (2016) N_2, He and CO_2 diffusion mechanism through nanoporous YSZ/γ-Al_2O_3 layers and their use in a pore-filled membrane for hydrogen membrane reactors. Int J Hydrog Energy 41:8732–8744. https://doi.org/10.1016/j.ijhydene.2015.11.152

Arratibel A, Pacheco Tanaka DA, Slater TJA, Burnett TL, van Sint Annaland M, Gallucci F (2018a) Unravelling the transport mechanism of pore-filled membranes for hydrogen separation. Sep Purif Technol 203:41–47. https://doi.org/10.1016/j.seppur.2018.04.016

Arratibel A, Medrano JA, Melendez J, Pacheco Tanaka DA, van Sint Annaland M, Gallucci F (2018b) Attrition-resistant membranes for fluidized-bed membrane reactors: double-skin membranes. J Membr Sci 563:419–426. https://doi.org/10.1016/j.memsci.2018.06.012

Arratibel A, Pacheco Tanaka A, Laso I, van Sint Annaland M, Gallucci F (2018c) Development of Pd-based double-skinned membranes for hydrogen production in fluidized bed membrane reactors. J Membr Sci 550:536–544. https://doi.org/10.1016/J.MEMSCI.2017.10.064

Ateş F, Miskolczi N, Borsodi N (2013) Comparision of real waste (MSW and MPW) pyrolysis in batch reactor over different catalysts. part I: product yields, gas and pyrolysis oil properties. Bioresour Technol 133:443–454. https://doi.org/10.1016/j.biortech.2013.01.112

Aykac Ozen H, Ozturk B (2019) Gas separation characteristic of mixed matrix membrane prepared by MOF-5 including different metals. Sep Purif Technol 211:514–521. https://doi.org/10.1016/J.SEPPUR.2018.09.052

Baker RW (2002) Future directions of membrane gas separation technology. Ind Eng Chem Res 41:1393–1411. https://doi.org/10.1021/ie0108088

Bakonyi P, Kumar G, Bélafi-Bakó K, Kim S-H, Koter S, Kujawski W, Nemestóthy N, Peter J, Pientka Z (2018) A review of the innovative gas separation membrane bioreactor with mechanisms for integrated production and purification of biohydrogen. Bioresour Technol 270:643–655. https://doi.org/10.1016/J.BIORTECH.2018.09.020

Balat H, Kırtay E (2010) Hydrogen from biomass e present scenario and future prospects. Int J Hydrog Energy 35:7416–7426. https://doi.org/10.1016/j.ijhydene.2010.04.137

Balu E, Lee U, Chung JN (2015) High temperature steam gasification of woody biomass – a combined experimental and mathematical modeling approach. Int J Hydrogen Energy 40:14104–14115. https://doi.org/10.1016/j.ijhydene.2015.08.085

Barreiro MM, Maroño M, Sánchez JM (2015) Hydrogen separation studies in a membrane reactor system: Influence of feed gas flow rate, temperature and concentration of the feed gases on hydrogen permeation. Appl Therm Eng 74:186–193. https://doi.org/10.1016/j.applthermaleng.2013.12.035

Basile A, Tong J, Millet P (2013) 2 – inorganic membrane reactors for hydrogen production: an overview with particular emphasis on dense metallic membrane materials. In: Basile A (ed) Handb. Membr. React. Woodhead Publishing, pp 42–148. https://doi.org/10.1533/9780857097330.1.42

Basile A, Jokar S, Shariati A, Iulianelli A, Rahimpour M, Dalena F, Vita A, Bagnato G (2016) Pure hydrogen production in membrane reactor with mixed reforming reaction by utilizing waste gas: a case study. Processes 4:33. https://doi.org/10.3390/pr4030033

Beavis R, Forsyth J, Roberts E, Song B, Combes G, Abbott J, Macleod N, Vass E, Davies M, Barton I (2013) A step-change sour shift process for improving the efficiency of IGCC with CCS. Energy Procedia 37:2256–2264. https://doi.org/10.1016/j.egypro.2013.06.106

Bičáková O, Straka P (2016) Co-pyrolysis of waste tire/coal mixtures for smokeless fuel, maltenes and hydrogen-rich gas production. Energy Convers Manag 116:203–213. https://doi.org/10.1016/j.enconman.2016.02.069

Boon J, Cobden PD, van Dijk HAJ, van Sint Annaland M (2015a) High-temperature pressure swing adsorption cycle design for sorption-enhanced water-gas shift. Chem Eng Sci 122:219–231. https://doi.org/10.1016/j.ces.2014.09.034

Boon J, Pieterse JAZ, van Berkel FPF, van Delft YC, van Sint Annaland M (2015b) Hydrogen permeation through palladium membranes and inhibition by carbon monoxide, carbon dioxide, and steam. J Membr Sci 496:344–358. https://doi.org/10.1016/j.memsci.2015.08.061

Bosmans A, Vanderreydt I, Geysen D, Helsen L (2013) The crucial role of Waste-to-Energy technologies in enhanced landfill mining: a technology review. J Clean Prod 55:10–23. https://doi.org/10.1016/j.jclepro.2012.05.032

Braun F, Miller JB, Gellman AJ, Tarditi AM, Fleutot B, Kondratyuk P, Cornaglia LM (2012) PdAgAu alloy with high resistance to corrosion by H_2S. Int J Hydrog Energy 37:18547–18555. https://doi.org/10.1016/j.ijhydene.2012.09.040

Braun F, Tarditi AM, Miller JB, Cornaglia LM (2014) Pd-based binary and ternary alloy membranes: morphological and perm-selective characterization in the presence of H_2S. J Membr Sci 450:299–307. https://doi.org/10.1016/j.memsci.2013.09.026

Bridgwater AV (1996) Production of high grade fuels and chemicals from catalytic pyrolysis of biomass. Catal Today 29:285–295. https://doi.org/10.1016/0920-5861(95)00294-4

Bridgwater AV (1999) Principles and practice of biomass fast pyrolysis processes for liquids. J Anal Appl Pyrolysis 51:3–22. https://doi.org/10.1016/S0165-2370(99)00005-4

Bridgwater AV (2012) Review of fast pyrolysis of biomass and product upgrading. Biomass Bioenergy 38:68–94. https://doi.org/10.1016/j.biombioe.2011.01.048

Brunetti A, Barbieri G, Drioli E (2011) Integrated membrane system for pure hydrogen production : A Pd – Ag membrane reactor and a PEMFC. Fuel Process Technol 92:166–174. https://doi.org/10.1016/j.fuproc.2010.09.023

Brunetti A, Zito PF, Giorno L, Drioli E, Barbieri G (2017) Membrane reactors for low temperature applications: an overview. Chem Eng Process Process Intensif. https://doi.org/10.1016/j.cep.2017.05.002

Bruni G, Rizzello C, Santucci A, Alique D, Incelli M, Tosti S (2019) On the energy efficiency of hydrogen production processes via steam reforming using membrane reactors. Int J Hydrog Energy 44:988–999. https://doi.org/10.1016/j.ijhydene.2018.11.095

Butler E, Devlin G, Meier D, McDonnell K (2011) A review of recent laboratory research and commercial developments in fast pyrolysis and upgrading. Renew Sustain Energy Rev 15:4171–4186. https://doi.org/10.1016/j.rser.2011.07.035

Byron Smith RJ, Loganathan M, Shantha MS (2010) A review of the water gas shift reaction kinetics. Int J Chem React Eng 8:1–32

Calles JA, Sanz R, Alique D, Furones L (2014) Thermal stability and effect of typical water gas shift reactant composition on H_2 permeability through a Pd-YSZ-PSS composite membrane. Int J Hydrog Energy 39:1398–1409. https://doi.org/10.1016/j.ijhydene.2013.10.168

Calles JA, Sanz R, Alique D, Furones L, Marín P, Ordoñez S (2018) Influence of the selective layer morphology on the permeation properties for Pd-PSS composite membranes prepared by electroless pore-plating: experimental and modeling study. Sep Purif Technol 194:10–18. https://doi.org/10.1016/j.seppur.2017.11.014

Caravella A, Barbieri G, Drioli E (2008) Modelling and simulation of hydrogen permeation through supported Pd-alloy membranes with a multicomponent approach. Chem Eng Sci 63:2149–2160. https://doi.org/10.1016/j.ces.2008.01.009

Caravella A, Hara S, Sun Y, Drioli E, Barbieri G (2014) Coupled influence of non-ideal diffusion and multilayer asymmetric porous supports on Sieverts law pressure exponent for hydrogen permeation in composite Pd-based membranes. Int J Hydrog Energy 39:2201–2214. https://doi.org/10.1016/j.ijhydene.2013.11.074

Carioca OB, Reis M, Fava F, Poggi-Varaldo HM, Ferreira BS, Diels L, Totaro G, Duarte J (2013) Biowaste biorefinery in Europe: opportunities and research & development needs. New Biotechnol 32:100–108. https://doi.org/10.1016/j.nbt.2013.11.003

Casero P, Peña FG, Coca P, Trujillo J (2014) ELCOGAS 14 MWth pre-combustion carbon dioxide capture pilot. Technical & economical achievements. Fuel 116:804–811. https://doi.org/10.1016/j.fuel.2013.07.027

Catalano J, Giacinti Baschetti M, Sarti GC (2009) Influence of the gas phase resistance on hydrogen flux through thin palladium–silver membranes. J Membr Sci 339:57–67. https://doi.org/10.1016/j.memsci.2009.04.032

Chang JS, Gu BW, Looy PC, Chu FY, Simpson CJ (1996) Thermal plasma pyrolysis of used old tires for production of syngas. J Environ Sci Health Part A: Environ Sci Eng Toxicol 31:1781–1799. https://doi.org/10.1080/10934529609376456

Checchetto R, Bazzanella N, Patton B, Miotello A (2004) Palladium membranes prepared by r.f. magnetron sputtering for hydrogen purification. Surf Coat Technol 177:73–79. https://doi.org/10.1016/j.surfcoat.2003.06.001

Chen SC, Tu GC, Hung CCY, Huang CA, Rei MH (2008) Preparation of palladium membrane by electroplating on AISI 316L porous stainless steel supports and its use for methanol steam reformer. J Membr Sci 314:5–14. https://doi.org/10.1016/j.memsci.2007.12.066

Chen W, Hu X, Wang R, Huang Y (2010) On the assembling of Pd/ceramic composite membranes for hydrogen separation. Sep Purif Technol 72:92–97. https://doi.org/10.1016/j.seppur.2010.01.010

Chen C-H, Huang Y-R, Liu C-W, Wang K-W (2016) Preparation and modification of PdAg membranes by electroless and electroplating process for hydrogen separation. Thin Solid Films 618:189–194. https://doi.org/10.1016/j.tsf.2016.04.049

Chung JN (2014) A theoretical study of two novel concept systems for maximum thermal-chemical conversion of biomass to hydrogen. Front Energy Res 1:1–10. https://doi.org/10.3389/fenrg.2013.00012

Conde JJ, Maroño M, Sánchez-Hervás JM (2017) Pd-based membranes for hydrogen separation: review of alloying elements and their influence on membrane properties. Sep Purif Rev 46:152–177. https://doi.org/10.1080/15422119.2016.1212379

Cornaglia L, Múnera J, Lombardo E (2015) Recent advances in catalysts, palladium alloys and high temperature WGS membrane reactors: a review. Int J Hydrog Energy 40:3423–3437. https://doi.org/10.1016/j.ijhydene.2014.10.091

Coskun C, Bayraktar M, Oktay Z, Dincer I (2012) Investigation of biogas and hydrogen production from waste water of milk-processing industry in Turkey. Int J Hydrog Energy 37:16498–16504. https://doi.org/10.1016/j.ijhydene.2012.02.174

Coutanceau C, Baranton S, Audichon T (2018) Chapter 2 – Hydrogen production from thermal reforming BT – hydrogen electrochemical production. In: Hydrog. Energy Fuel Cells Prim. Academic Press, pp 7–15. https://doi.org/10.1016/B978-0-12-811250-2.00002-9

Czajczyńska D, Nannou T, Anguilano L, Krzyzyńska R, Ghazal H, Spencer N, Jouhara H (2017) Potentials of pyrolysis processes in the waste management sector. Energy Procedia 123:387–394. https://doi.org/10.1016/j.egypro.2017.07.275

Czernik S, French RJ (2006) Production of hydrogen from plastics by pyrolysis and catalytic steam reform. Energy Fuels 20:754–758. https://doi.org/10.1021/ef050354h

Damrongsak D, Tippayawong N (2010) Experimental investigation of an automotive air-conditioning system driven by a small biogas engine. Appl Therm Eng 30:400–405. https://doi.org/10.1016/j.applthermaleng.2009.09.003
Daniel H, Bhada-Tata P (n.d.) What a waste: a global review of solid waste management, 2012. https://openknowledge.worldbank.org/handle/10986/17388
De Araújo GC, Do Carmo Rangel M (2000) Environmental friendly dopant for the high-temperature shift catalysts. Catal Today 62:201–207. https://doi.org/10.1016/S0920-5861(00)00421-1
de Lasa H, Salaices E, Mazumder J, Lucky R (2011) Catalytic steam gasification of biomass: catalysts, thermodynamics and kinetics. Chem Rev 111:5404–5433. https://doi.org/10.1021/cr200024w
De Nooijer N, Gallucci F, Pellizzari E, Melendez J, Alfredo D, Tanaka P, Manzolini G, Van Sint M (2018) On concentration polarisation in a fl uidized bed membrane reactor for biogas steam reforming: modelling and experimental validation. Chem Eng J 348:232–243. https://doi.org/10.1016/j.cej.2018.04.205
Delgado J, Aznar MP, Corella J (1997) Biomass gasification with steam in fluidized bed: effectiveness of CaO, MgO, and CaO-MgO for hot raw gas cleaning. Ind Eng Chem Res 36:1535–1543. https://doi.org/10.1021/ie960273w
DemirbaÅŸ A (2001) Biomass resource facilities and biomass conversion processing for fuels and chemicals. Energy Convers Manag 42:1357–1378. https://doi.org/10.1016/S0196-8904(00)00137-0
Detchusananard T, Im-orb K, Ponpesh P, Arpornwichanop A (2018) Biomass gasification integrated with CO_2 capture processes for high-purity hydrogen production: process performance and energy analysis. Energy Convers Manag 171:1560–1572. https://doi.org/10.1016/j.enconman.2018.06.072
Deveau ND, Ma YH, Datta R (2013) Beyond Sieverts' law: a comprehensive microkinetic model of hydrogen permeation in dense metal membranes. J Membr Sci 437:298–311. https://doi.org/10.1016/j.memsci.2013.02.047
Dhineshkumar V, Ramaswamy D (2017) Review on membrane technology applications in food and dairy processing. J Appl Biotechnol Bioeng 3:399–407. https://doi.org/10.15406/jabb.2017.03.00077
Di Marcoberardino G, Binotti M, Manzolini G, Viviente JL, Arratibel A, Roses L, Gallucci F (2017) Achievements of European projects on membrane reactor for hydrogen production. J Clean Prod 161:1442–1450. https://doi.org/10.1016/j.jclepro.2017.05.122
Di Marcoberardino G, Foresti S, Binotti M, Manzolini G (2018) Potentiality of a biogas membrane reformer for decentralized hydrogen production. Chem Eng Process – Process Intensif 129:131–141. https://doi.org/10.1016/j.cep.2018.04.023
Drljo A, Wukovits W, Friedl A (2014) HyTIME – combined biohydrogen and biogas production from 2nd Generation Biomass. Chem Eng Trans 39:1393–1398. https://doi.org/10.3303/CET1439233
Dunbar ZW (2015) Hydrogen purification of synthetic water gas shift gases using microstructured palladium membranes. J Power Sources 297:525–533. https://doi.org/10.1016/j.jpowsour.2015.08.015
Dunbar ZW, Lee IC (2017) Effects of elevated temperatures and contaminated hydrogen gas mixtures on novel ultrathin palladium composite membranes. Int J Hydrog Energy 42:29310–29319. https://doi.org/10.1016/j.ijhydene.2017.10.032
El Hawa HWA, Paglieri SN, Morris CC, Harale A, Way JD (2014) Identification of thermally stable Pd-alloy composite membranes for high temperature applications. J Membr Sci 466:151–160. https://doi.org/10.1016/j.memsci.2014.04.029
Elbaba IF, William PT (2012) Hydrogen from waste tyres. Int J Environ Chem Ecol Geol Geophys Eng 6:321–323
Elseviers W, Hassett PF, Navarre J-L, Whysall M (2015) 50 years of PSA technology for H_2 purification, UOP. https://www.uop.com/?document=psa-50-paper&download=1

European Biogas Association, Statistical report 2017 (n.d.). http://european-biogas.eu/wp-content/uploads/2017/12/Statistical-report-of-the-European-Biogas-Association-web.pdf
European Commission (2008) GREEN PAPER. On the management of bio-waste in the European Union. https://eur-lex.europa.eu/legal-content/EN/TXT/PDF/?uri=CELEX:52008DC0811&from=EN
European Commission (n.d.-a) Eurostat. https://ec.europa.eu/eurostat
European Commission (n.d.-b) Science for environment policy. http://ec.europa.eu/environment/integration/research/newsalert/pdf/197na5_en.pdf
European Environment Agency, Waste-municipal solid waste generation and management (n.d.). http://www.eea.europa.eu/soer-2015/countries-comparison/waste
European Parliament (2018) Directive EU 2018/851. https://eur-lex.europa.eu/eli/dir/2018/851/oj
Fachverband Biogas e. V. (2017) Biogas to biomethane. https://www.biogas-to-biomethane.com/Download/BTB.pdf
Fernandez E, Helmi A, Coenen K, Melendez J, Luis J, Alfredo D, Tanaka P, Van Sint M, Gallucci F (2014) Development of thin Pd e Ag supported membranes for fluidized bed membrane reactors including WGS related gases. Int J Hydrog Energy 40:3506–3519. https://doi.org/10.1016/j.ijhydene.2014.08.074
Fontana AD, Sirini N, Cornaglia LM, Tarditi AM (2018) Hydrogen permeation and surface properties of PdAu and PdAgAu membranes in the presence of CO, CO_2 and H_2S. J Membr Sci 563:351–359. https://doi.org/10.1016/j.memsci.2018.06.001
Furones L, Alique D (2017) Interlayer properties of in-situ oxidized porous stainless steel for preparation of composite Pd membranes. Chem Eng 2:1. https://doi.org/10.3390/chemengineering2010001
Gade SK, Payzant EA, Park HJ, Thoen PM, Way JD (2009a) The effects of fabrication and annealing on the structure and hydrogen permeation of Pd–Au binary alloy membranes. J Membr Sci 340:227–233. https://doi.org/10.1016/j.memsci.2009.05.034
Gade SK, Keeling MK, Davidson AP, Hatlevik O, Way JD (2009b) Palladium–ruthenium membranes for hydrogen separation fabricated by electroless co-deposition. Int J Hydrog Energy 34:6484–6491. https://doi.org/10.1016/j.ijhydene.2009.06.037
Gallucci F, De Falco M, Tosti S, Marrelli L, Basile A (2007) The effect of the hydrogen flux pressure and temperature dependence factors on the membrane reactor performances. Int J Hydrog Energy 32:4052–4058. https://doi.org/10.1016/j.ijhydene.2007.03.039
Gao Q, Jansson S, Christakopoulos P, Matsakas L, Rova U (2017) Green conversion of municipal solid wastes into fuels and chemicals. Electron J Biotechnol 26:69–83. https://doi.org/10.1016/j.ejbt.2017.01.004
Gao Y, Jiang J, Meng Y, Yan F, Aihemaiti A (2018) A review of recent developments in hydrogen production via biogas dry reforming. Energy Convers Manag 171:133–155. https://doi.org/10.1016/j.enconman.2018.05.083
García-García FR, Torrente-Murciano L, Chadwick D, Li K (2012) Hollow fibre membrane reactors for high H_2 yields in the WGS reaction. J Membr Sci 405–406:30–37. https://doi.org/10.1016/j.memsci.2012.02.031
Ghasemzadeh K, Khosravi M, Sadati Tilebon SM, Ghaeinejad-Meybodi A, Basile A (2018) Theoretical evaluation of Pd Ag membrane reactor performance during biomass steam gasification for hydrogen production using CFD method. Int J Hydrog Energy 43:11719–11730. https://doi.org/10.1016/j.ijhydene.2018.04.221
Ghasemzadeh K, Ghahremani M, Amiri TY, Basile A (2019) Performance evaluation of Pd–Ag membrane reactor in glycerol steam reforming process: development of the CFD model. Int J Hydrog Energy 44:1000–1009. https://doi.org/10.1016/j.ijhydene.2018.11.086
Ghimire A, Frunzo L, Pontoni L, d'Antonio G, Lens PNL, Esposito G, Pirozzi F (2015) Dark fermentation of complex waste biomass for biohydrogen production by pretreated thermophilic anaerobic digestate. J Environ Manage 152:43–48. https://doi.org/10.1016/j.jenvman.2014.12.049
Global Carbon Project (n.d.). http://www.globalcarbonatlas.org/en/CO2-emissions

Gómez-Barea A, Umeki K, Moilanen A, Kramb J, Konttinen J (2014) Modeling biomass char gasification kinetics for improving prediction of carbon conversion in a fluidized bed gasifier. Fuel 132:107–115. https://doi.org/10.1016/j.fuel.2014.04.014

Goyal HB, Seal D, Saxena RC (2008) Bio-fuels from thermochemical conversion of renewable resources: a review. Renew Sustain Energy Rev 12:504–517. https://doi.org/10.1016/j.rser.2006.07.014

Grande CA (2012) Advances in pressure swing adsorption for gas separation. ISRN Chem Eng 2012:1–13. https://doi.org/10.5402/2012/982934

Grieco EM, Baldi G (2012) Pyrolysis of polyethylene mixed with paper and wood: interaction effects on tar, char and gas yields. Waste Manag 32:833–839. https://doi.org/10.1016/j.wasman.2011.12.014

Gupta RKP, Lapalikar V (2016) Recent advances in membrane based waste water treatment technology: a review. Energy Environ Focus 5:241–267

Hakkarainen R, Salmi T, Keiski RL (1993) Water-gas shift reaction on a cobalt-molybdenum oxide catalyst. Appl Catal A Gen 99:195–215. https://doi.org/10.1016/0926-860X(93)80099-C

Han J-Y, Kim C-H, Lim H, Lee K-Y, Ryi S-K (2017) Diffusion barrier coating using a newly developed blowing coating method for a thermally stable Pd membrane deposited on porous stainless-steel support. Int J Hydrog Energy 42:12310–12319. https://doi.org/10.1016/j.ijhydene.2017.03.053

Haryanto A, Fernando S, Adhikari S (2007) Ultrahigh temperature water gas shift catalysts to increase hydrogen yield from biomass gasification. Catal Today 129:269–274. https://doi.org/10.1016/j.cattod.2006.09.039

Hasan A, Dincer I (2019) Comparative assessment of various gasification fuels with waste tires for hydrogen production. Int J Hydrog Energy. https://doi.org/10.1016/j.ijhydene.2018.11.150

Hashim SS, Somalu MR, Loh KS, Liu S, Zhou W, Sunarso J (2018) Perovskite-based proton conducting membranes for hydrogen separation: a review. Int J Hydrog Energy 43:15281–15305. https://doi.org/10.1016/j.ijhydene.2018.06.045

Hassanpour M (2017) Plasma technology and waste management abstract management. iMedPub J 1:11–13

Heidenreich S, Foscolo PU (2015) New concepts in biomass gasification. Prog Energy Combust Sci 46:72–95. https://doi.org/10.1016/j.pecs.2014.06.002

Heidrich ES, Dolfing J, Scott K, Edwards SR, Jones C, Curtis TP (2013) Production of hydrogen from domestic wastewater in a pilot-scale microbial electrolysis cell. Appl Microbiol Biotechnol 97:6979–6989. https://doi.org/10.1007/s00253-012-4456-7

Higman C (2013) State of the gasification industry – the updated worldwide gasification database. In: Int. Pittsburgh Coal Conf. https://www.globalsyngas.org/uploads/downloads/Higman_-2013_PCC_paper_docx.pdf

Horne PA, Williams PT (1996) Influence of temperature on the products from the flash pyrolysis of biomass. Fuel 75:1051–1059. https://doi.org/10.1016/0016-2361(96)00081-6

Huang Y, Dittmeyer R (2007) Preparation of thin palladium membranes on a porous support with rough surface. J Membr Sci 302:160–170. https://doi.org/10.1016/j.memsci.2007.06.040

Huang L, Chen CS, He ZD, Peng DK, Meng GY (1997) Palladium membranes supported on porous ceramics prepared by chemical vapor deposition. Thin Solid Films 302:98–101. https://doi.org/10.1016/S0040-6090(97)00035-7

Hwang K-R, Oh D-K, Lee S-W, Park J-S, Song M-H, Rhee W-H (2017) Porous stainless steel support for hydrogen separation Pd membrane; fabrication by metal injection molding and simple surface modification. Int J Hydrog Energy 42:14583–14592. https://doi.org/10.1016/j.ijhydene.2017.04.032

IEA Bioenergy (2016) Status report on thermal biomass gasification in countries participating in IEA Bioenergy. https://www.ieabioenergy.com/wp-content/uploads/2017/12/Status-report-Task-33-2016.pdf

Ismail N, Ani FN (2015) A review on plasma treatment for the processing of solid waste. J Teknol 72:41–49. https://doi.org/10.11113/jt.v72.3938

Iulianelli A, Liguori S, Huang Y, Basile A (2015) Model biogas steam reforming in a thin Pd-supported membrane reactor to generate clean hydrogen for fuel cells. J Power Sources 273:25–32. https://doi.org/10.1016/j.jpowsour.2014.09.058

Iulianelli A, Liguori S, Vita A, Italiano C, Fabiano C, Huang Y, Basile A (2016) The oncoming energy vector: Hydrogen produced in Pd-composite membrane reactor via bioethanol reforming over Ni/CeO_2 catalyst. Catal Today 259:368–375. https://doi.org/10.1016/j.cattod.2015.04.046

Iulianelli A, Palma V, Bagnato G, Ruocco C, Huang Y, Veziroğlu NT, Basile A (2018) From bioethanol exploitation to high grade hydrogen generation: steam reforming promoted by a Co-Pt catalyst in a Pd-based membrane reactor. Renew Energy 119:834–843. https://doi.org/10.1016/j.renene.2017.10.050

Januszewicz K, Klein M, Klugmann-Radziemska E (2012) Gaseous products from scrap tires pyrolisis. Ecol Chem Eng S 19:451–460. https://doi.org/10.2478/v10216-011-0035-6

Jayalakshmi S, Joseph K, Sukumaran V (2009) Bio hydrogen generation from kitchen waste in an inclined plug flow reactor. Int J Hydrog Energy 34:8854–8858. https://doi.org/10.1016/j.ijhydene.2009.08.048

Jayaraman V, Lin YS, Pakala M, Lin RY (1995) Fabrication of ultrathin metallic membranes on ceramic supports by sputter deposition. J Membr Sci 99:89–100. https://doi.org/10.1016/0376-7388(94)00212-H

Jeihanipour A, Aslanzadeh S, Rajendran K, Balasubramanian G, Taherzadeh MJ (2013) High-rate biogas production from waste textiles using a two-stage process. Renew Energy 52:128–135. https://doi.org/10.1016/j.renene.2012.10.042

Jia H, Wu P, Zeng G, Salas-Colera E, Serrano A, Castro GR, Xu H, Sun C, Goldbach A (2017) High-temperature stability of Pd alloy membranes containing Cu and Au. J Membr Sci 544:151–160. https://doi.org/10.1016/J.MEMSCI.2017.09.012

Jin H, Wollbrink A, Yao R, Li Y, Caro J, Yang W (2016) A novel CAU-10-H MOF membrane for hydrogen separation under hydrothermal conditions. J Membr Sci 513:40–46. https://doi.org/10.1016/J.MEMSCI.2016.04.017

Kabir MJ, Chowdhury AA, Rasul MG (2015) Pyrolysis of municipal green waste: a modelling, simulation and experimental analysis. Energies 8:7522–7541. https://doi.org/10.3390/en8087522

Khan AA, de Jong W, Jansens PJ, Spliethoff H (2009) Biomass combustion in fluidized bed boilers: potential problems and remedies. Fuel Process Technol 90:21–50. https://doi.org/10.1016/j.fuproc.2008.07.012

Kiadehi AD, Taghizadeh M (2019) Fabrication, characterization, and application of palladium composite membrane on porous stainless steel substrate with NaY zeolite as an intermediate layer for hydrogen purification. Int J Hydrog Energy 44:2889–2904. https://doi.org/10.1016/J.IJHYDENE.2018.12.058

Kim SS, Xu N, Li A, Grace JR, Lim CJ, Ryi SK (2015) Development of a new porous metal support based on nickel and its application for Pd based composite membranes. Int J Hydrog Energy 40:3520–3527. https://doi.org/10.1016/j.ijhydene.2014.08.075

Kobayashi T, Xu KQ, Li YY, Inamori Y (2012) Evaluation of hydrogen and methane production from municipal solid wastes with different compositions of fat, protein, cellulosic materials and the other carbohydrates. Int J Hydrog Energy 37:15711–15718. https://doi.org/10.1016/j.ijhydene.2012.05.044

Kölling A, Zhang W, Neubauer Y, Ul Hai I, Oldenburg H, Schröder P, Liu H, Seilkopf A (2012) Gas cleaning strategies for biomass gasification product gas. Int J Low-Carbon Technol 7:69–74. https://doi.org/10.1093/ijlct/ctr046

Kurokawa H, Yakabe H, Yasuda I, Peters T, Bredesen R (2014) Inhibition effect of CO on hydrogen permeability of Pd-Ag membrane applied in a microchannel module configuration. Int J Hydrog Energy 39:17201–17209. https://doi.org/10.1016/j.ijhydene.2014.08.056

Lachén J, Durán P, Menéndez M, Peña JA, Herguido J (2018) Biogas to high purity hydrogen by methane dry reforming in TZFBR+MB and exhaustion by Steam-Iron Process. Techno–

economic assessment. Int J Hydrog Energy 43:11663–11675. https://doi.org/10.1016/j.ijhydene.2018.03.105
Lee U, Chung JN, Ingley HA (2014) High-temperature steam gasification of municipal solid waste, rubber, plastic and wood. Energy Fuel 28:4573–4587. https://doi.org/10.1021/ef500713j
Lewis AE, Kershner DC, Paglieri SN, Slepicka MJ, Way JD (2013) Pd-Pt/YSZ composite membranes for hydrogen separation from synthetic water-gas shift streams. J Membr Sci 437:257–264. https://doi.org/10.1016/j.memsci.2013.02.056
Lewis AE, Zhao H, Syed H, Wolden CA, Way JD (2014) PdAu and PdAuAg composite membranes for hydrogen separation from synthetic water-gas shift streams containing hydrogen sulfide. J Membr Sci 465:167–176. https://doi.org/10.1016/j.memsci.2014.04.022
Li A, Grace JR, Lim CJ (2007) Preparation of thin Pd-based composite membrane on planar metallic substrate: part I: pre-treatment of porous stainless steel substrate. J Membr Sci 298:175–181. https://doi.org/10.1016/j.memsci.2007.04.016
Li P, Wang Z, Qiao Z, Liu Y, Cao X, Li W, Wang J, Wang S (2015) Recent developments in membranes for efficient hydrogen purification. J Membr Sci 495:130–168. https://doi.org/10.1016/j.memsci.2015.08.010
Liu B, Ren N, Ding J, Guo W, Cao G (2011) Biological hydrogen production by dark fermentation: challenges and prospects towards scaled-up production. Curr Opin Biotechnol 22:365–370. https://doi.org/10.1016/j.copbio.2011.04.022
Lu GQ, da Costa JCD, Duke M, Giessler S, Socolow R, Williams RH, Kreutz T (2007) Inorganic membranes for hydrogen production and purification: a critical review and perspective. J Colloid Interface Sci 314:589–603. https://doi.org/10.1016/j.jcis.2007.05.067
Lu H, Zhu L, Wang W, Yang W, Tong J (2015) Pd and Pd-Ni alloy composite membranes fabricated by electroless plating method on capillary α-Al_2O_3 substrates. Int J Hydrog Energy 40:3548–3556. https://doi.org/10.1016/j.ijhydene.2014.09.121
Luo S, Zhou Y, Yi C (2012) Syngas production by catalytic steam gasification of municipal solid waste in fixed-bed reactor. Energy 44:391–395. https://doi.org/10.1016/j.energy.2012.06.016
Mabande GTP, Pradhan G, Schwieger W, Hanebuth M, Dittmeyer R, Selvam T, Zampieri A, Baser H, Herrmann R (2004) A study of Silicalite-1 and Al-ZSM-5 membrane synthesis on stainless steel supports. Microporous Mesoporous Mater 75:209–220. https://doi.org/10.1016/j.micromeso.2004.07.009
Maggi R, Delmon B (1994) Comparison between 'slow' and 'flash' pyrolysis oils from biomass. Fuel 73:671–677. https://doi.org/10.1016/0016-2361(94)90007-8
Mardilovich PP, She Y, Ma YH, Rei M-H (1998) Defect-free palladium membranes on porous stainless-steel support. AIChE J 44:310–322. https://doi.org/10.1002/aic.690440209
Maroño M, Sánchez-Hervás JM, Ruiz E, Cabanillas A (2008) Study of the suitability of a Pt based catalyst for the upgrading of a biomass gasification syngas stream via the WGS reaction. Catal Lett 126:369–426
Maroño M, Sánchez JM, Ruiz E (2010) Hydrogen-rich gas production from oxygen pressurized gasification of biomass using a Fe-Cr Water Gas Shift catalyst. Int J Hydrog Energy 35:37–45. https://doi.org/10.1016/j.ijhydene.2009.10.078
Maroño M, Torreiro Y, Montenegro L, Sánchez J (2014a) Lab-scale tests of different materials for the selection of suitable sorbents for CO_2 capture with H_2 production in IGCC processes. Fuel 116:861–870. https://doi.org/10.1016/j.fuel.2013.03.067
Maroño M, Barreiro MM, Torreiro Y, Sánchez JM (2014b) Performance of a hybrid system sorbent-catalyst-membrane for CO_2 capture and H_2 production under pre-combustion operating conditions. Catal Today 236:77–85. https://doi.org/10.1016/j.cattod.2013.11.003
Maroño M, Torreiro Y, Cillero D, Sánchez JM (2015) Experimental studies of CO_2 capture by a hybrid catalyst/adsorbent system applicable to IGCC processes. Appl Therm Eng 74:28–35. https://doi.org/10.1016/j.applthermaleng.2014.02.068
Martinez-Diaz D, Sanz R, Calles JA, Alique D (2019) H2 permeation increase of electroless pore-plated Pd/PSS membranes with CeO_2 intermediate barriers. Sep Purif Technol 216:16–24. https://doi.org/10.1016/J.SEPPUR.2019.01.076

Mateos-Pedrero C, Soria MA, Rodríguez-Ramos I, Guerrero-Ruiz A (2010) Modifications of porous stainless steel previous to the synthesis of Pd membranes. In: Stud. Surf. Sci. Catal, pp 779–783. https://doi.org/10.1016/S0167-2991(10)75159-4

Matsakas L, Rova U, Christakopoulos P (2015) Sequential parametric optimization of methane production from different sources of forest raw material. Front Microbiol 6:1–10. https://doi.org/10.3389/fmicb.2015.01163

Mattox DM, Mattox DM (2010) Chapter 6 – Vacuum evaporation and vacuum deposition. In: Handb. Phys. Vap. Depos. Process, pp 195–235. https://doi.org/10.1016/B978-0-8155-2037-5.00006-X

Medrano JA, Fernandez E, Melendez J, Parco M, Tanaka DAP, van Sint Annaland M, Gallucci F (2016) Pd-based metallic supported membranes: high-temperature stability and fluidized bed reactor testing. Int J Hydrog Energy 41:8706–8718. https://doi.org/10.1016/j.ijhydene.2015.10.094

Mei W, Du Y, Wu T, Gao F, Wang B, Duan J, Zhou J, Zhou R (2018) High-flux CHA zeolite membranes for H_2 separations. J Membr Sci 565:358–369. https://doi.org/10.1016/j.memsci.2018.08.025

Mejdell AL, Jøndahl M, Peters TA, Bredesen R, Venvik HJ (2009) Effects of CO and CO_2 on hydrogen permeation through a ~3 μm Pd/Ag 23 wt.% membrane employed in a microchannel membrane configuration. Sep Purif Technol 68:178–184. https://doi.org/10.1016/j.seppur.2009.04.025

Melendez J, Fernandez E, Gallucci F, van Sint Annaland M, Arias PL, Tanaka DAP (2017a) Preparation and characterization of ceramic supported ultra-thin (~1 μm) Pd-Ag membranes. J Membr Sci 528:12–23. https://doi.org/10.1016/j.memsci.2017.01.011

Melendez J, de Nooijer N, Coenen K, Fernandez E, Viviente JL, van Sint Annaland M, Arias PL, Tanaka DAP, Gallucci F (2017b) Effect of Au addition on hydrogen permeation and the resistance to H_2S on Pd-Ag alloy membranes. J Membr Sci 542:329–341. https://doi.org/10.1016/j.memsci.2017.08.029

Mellor JR, Copperthwaite RG, Coville NJ (1997) The selective influence of sulfur on the performance of novel cobalt-based water-gas shift catalysts. Appl Catal A Gen 164:69–79. https://doi.org/10.1016/S0926-860X(97)00158-0

Milne TA, Evans RJ (1998) Biomass gasifier "tars": their nature, formation, and conversion. EEUU, Golden. https://www.nrel.gov/docs/fy99osti/25357.pdf

Mivechian A, Pakizeh M (2013) Performance comparison of different separation systems for H_2 recovery from catalytic reforming unit off-gas streams. Chem Eng Technol 36:519–527. https://doi.org/10.1002/ceat.201200558

Moriani A, Bruni G, Incelli M, Santucci A, Liger K, Troulay M, Tosti S (2018) Innovative joining of Pd-Ag permeator tubes. Fusion Eng Des 136. https://doi.org/10.1016/j.fusengdes.2018.02.075

Muraviev DN, Orekhova NV, Mironova EY, Yaroslavtsev AB, Ermilova MM (2014) Production of high purity hydrogen by ethanol steam reforming in membrane reactor. Catal Today 236:64–69. https://doi.org/10.1016/j.cattod.2014.01.014

Navinšek B, Panjan P, Milošev I (1999) PVD coatings as an environmentally clean alternative to electroplating and electroless processes. Surf Coat Technol 116:476–487. https://doi.org/10.1016/S0257-8972(99)00145-0

Nayak A, Bhushan B (2019) An overview of the recent trends on the waste valorization techniques for food wastes. J Environ Manag 233:352–370. https://doi.org/10.1016/J.JENVMAN.2018.12.041

Nekhamkina O, Sheintuch M (2016) Approximate models of concentration-polarization in Pd-membrane separators. Fast numerical analysis. J Membr Sci 500:136–150. https://doi.org/10.1016/J.MEMSCI.2015.11.027

Neubauer Y (2011) Strategies for tar reduction in fuel-gases and synthesis-gases from biomass gasification. J Sustain Energy Environ 2011:67–71

Nikolaidis P, Poullikkas A (2017) A comparative overview of hydrogen production processes. Renew Sust Energ Rev 67:597–611. https://doi.org/10.1016/j.rser.2016.09.044

Nikoli DD, Kikkinides ES (2015) Modelling and optimization of hybrid PSA/membrane separation processes. Adsorption 21:283–305. https://doi.org/10.1007/s10450-015-9670-z

Nilsson S, Gómez-Barea A, Fuentes-Cano D, Ollero P (2012) Gasification of biomass and waste in a staged fluidized bed gasifier: modeling and comparison with one-stage units. Fuel 97:730–740. https://doi.org/10.1016/j.fuel.2012.02.044

Nitsos C, Matsakas L, Triantafyllidis K, Rova U, Christakopoulos P (2015) Evaluation of mediterranean agricultural residues as a potential feedstock for the production of biogas via anaerobic fermentation. Biomed Res Int 2015. https://doi.org/10.1155/2015/171635

Nowakowski R, Lisowski P, Pieta I, Serwicka E, Kazmierczuk A, Epling W (2018) Waste into fuel—catalyst and process development for MSW valorisation. Catalysts 8:113. https://doi.org/10.3390/catal8030113

Onay O, Kockar OM (2003) Slow, fast and flash pyrolysis of rapeseed. Renew Energy 28:2417–2433. https://doi.org/10.1016/S0960-1481(03)00137-X

Otto RB, De Souza SS, Ferreira LRA, Ando Junior OH, Silva FP, De Souza SNM (2018) Review of the energy potential of the residual biomass for the distributed generation in Brazil. Renew Sust Energ Rev 94:440–455. https://doi.org/10.1016/j.rser.2018.06.034

Panagiotopoulou P, Kondarides DI (2007) A comparative study of the water-gas shift activity of Pt catalysts supported on single (MOx) and composite (MOx/Al_2O_3, MOx/TiO_2) metal oxide carriers. Catal Today 127:319–329. https://doi.org/10.1016/j.cattod.2007.05.010

Patki NS, Lundin S-T, Way JD (2016) Rapid annealing of sequentially plated Pd-Au composite membranes using high pressure hydrogen. J Membr Sci 513:197–205. https://doi.org/10.1016/j.memsci.2016.04.034

Patki NS, Lundin STB, Way JD (2018) Apparent activation energy for hydrogen permeation and its relation to the composition of homogeneous PdAu alloy thin-film membranes. Sep Purif Technol 191. https://doi.org/10.1016/j.seppur.2017.09.047

Penev M, Melaina MW, Antonia O (2013) Blending hydrogen into natural gas pipeline networks: a review of key issues. EEUU, Golden. https://www.nrel.gov/docs/fy13osti/51995.pdf

Perry JD, Nagai K, Koros WJ (2006) Polymer membranes for hydrogen separations. MRS Bull 31:745–749. https://doi.org/10.1557/mrs2006.187

Peters TA, Stange M, Bredesen R (2011a) On the high pressure performance of thin supported Pd–23%Ag membranes—evidence of ultrahigh hydrogen flux after air treatment. J Membr Sci 378:28–34. https://doi.org/10.1016/j.memsci.2010.11.022

Peters TA, Kaleta T, Stange M, Bredesen R (2011b) Development of thin binary and ternary Pd-based alloy membranes for use in hydrogen production. J Membr Sci 383:124–134. https://doi.org/10.1016/j.memsci.2011.08.050

Peters TA, Kaleta T, Stange M, Bredesen R (2012) Hydrogen transport through a selection of thin Pd-alloy membranes: membrane stability, H_2S inhibition, and flux recovery in hydrogen and simulated {WGS} mixtures. Catal Today 193:8–19. https://doi.org/10.1016/j.cattod.2011.12.028

Peters TA, Kaleta T, Stange M, Bredesen R (2013) Development of ternary Pd–Ag–TM alloy membranes with improved sulphur tolerance. J Membr Sci 429:448–458. https://doi.org/10.1016/j.memsci.2012.11.062

Peters TA, Stange M, Bredesen R (2015) 2 – Fabrication of palladium-based membranes by magnetron sputtering. In: Doukelis A, Panopoulos K, Koumanakos A, Kakaras E (eds) Palladium Membr. Technol. Hydrog. Prod. Carbon Capture Other Appl. Woodhead Publishing, pp 25–41. https://doi.org/10.1533/9781782422419.1.25.

Pinacci P, Basile A (2013) 3 – Palladium-based composite membranes for hydrogen separation in membrane reactors BT. In: Handbook of Membrane Reactors, Woodhead Publ. Ser. Energy. Woodhead Publishing, pp 149–182. https://doi.org/10.1533/9780857097330.1.149

Pinacci P, Drago F (2012) Influence of the support on permeation of palladium composite membranes in presence of sweep gas. Catal Today 193:186–193. https://doi.org/10.1016/j.cattod.2012.02.041

Plazaola AA, Tanaka DAP, Annaland MVS, Gallucci F (2017) Recent advances in pd-based membranes for membrane reactors. Molecules 22:1–53. https://doi.org/10.3390/molecules22010051

Ponzio A, Kalisz S, Blasiak W (2006) Effect of operating conditions on tar and gas composition in high temperature air/steam gasification (HTAG) of plastic containing waste. Fuel Process Technol 87:223–233. https://doi.org/10.1016/j.fuproc.2005.08.002

Pöschl M, Ward S, Owende P (2010) Evaluation of energy efficiency of various biogas production and utilization pathways. Appl Energy 87:3305–3321. https://doi.org/10.1016/j.apenergy.2010.05.011

Power Technology, Power from waste – the world's biggest biomass power plants (2014). https://www.power-technology.com/features/featurepower-from-waste-the-worlds-biggest-biomass-power-plants-4205990/

Project UNIfHY (2012). https://hydrogeneurope.eu/project/unifhy

Pujari M, Agarwal A, Uppaluri R, Verma A (2014) Role of electroless nickel diffusion barrier on the combinatorial plating characteristics of dense Pd/Ni/PSS composite membranes. Appl Surf Sci 305:658–664. https://doi.org/10.1016/j.apsusc.2014.03.156

Querino PS, Bispo JRC, Rangel MDC (2005) The effect of cerium on the properties of Pt/ZrO_2 catalysts in the WGSR. Catal Today 107–108:920–925. https://doi.org/10.1016/j.cattod.2005.07.032

Rafieenia R, Lavagnolo MC, Pivato A (2018) Pre-treatment technologies for dark fermentative hydrogen production: current advances and future directions. Waste Manag 71:734–748. https://doi.org/10.1016/j.wasman.2017.05.024

Rahimpour MR, Samimi F, Babapoor A, Tohidian T, Mohebi S (2017) Palladium membranes applications in reaction systems for hydrogen separation and purification: a review. Chem Eng Process Process Intensif 121:24–49. https://doi.org/10.1016/j.cep.2017.07.021

Ramachandran PA, Chompupun T, Kanhari C, Vatanatham T, Limtrakul S (2018) Experiments, modeling and scaling-up of membrane reactors for hydrogen production via steam methane reforming. Chem Eng Process – Process Intensif 134:124–140. https://doi.org/10.1016/j.cep.2018.10.007

Rauch R, Hrbek J, Hofbauer H (2014) Biomass gasification for synthesis gas production and applications of the syngas. Wiley Interdiscip Rev Energy Environ 3:343–362. https://doi.org/10.1002/wene.97

Rauch R, Musmarra D, Malits M, Chianese S, Loipersböck J, Hofbauer H, Molino A (2015) Hydrogen from the high temperature water gas shift reaction with an industrial Fe/Cr catalyst using biomass gasification tar rich synthesis gas. Fuel Process Technol 132:39–48. https://doi.org/10.1016/j.fuproc.2014.12.034

Rezakazemi M, Sadrzadeh M, Matsuura T (2018) Thermally stable polymers for advanced high-performance gas separation membranes. Prog Energy Combust Sci 66:1–41. https://doi.org/10.1016/J.PECS.2017.11.002

Rocha C, Soria MA, Madeira LM (2017) Steam reforming of olive oil mill wastewater with in situ hydrogen and carbon dioxide separation – thermodynamic analysis. Fuel 207:449–460. https://doi.org/10.1016/J.FUEL.2017.06.111

Rodríguez-Félix E, Contreras-Ramos SM, Davila-Vazquez G, Rodríguez-Campos J, Marino-Marmolejo EN (2018) Identification and quantification of volatile compounds found in vinasses from two different processes of Tequila production. Energies 11:12–15. https://doi.org/10.3390/en11030490

Ruan X, Li B, Dai Y, Jiang X, He G (2016) Pressure swing adsorption/membrane hybrid processes for hydrogen purification with a high recovery. Front Chem Sci Eng 10:255–264. https://doi.org/10.1007/s11705-016-1567-1

Ryi S-K, Park J-S, Kim S-H, Kim D-W, Cho K-I (2008) Formation of a defect-free Pd–Cu–Ni ternary alloy membrane on a polished porous nickel support (PNS). J Membr Sci 318:346–354. https://doi.org/10.1016/j.memsci.2008.02.055

Ryi S-K, Xu N, Li A, Lim CJ, Grace JR (2010) Electroless Pd membrane deposition on alumina modified porous Hastelloy substrate with EDTA-free bath. Int J Hydrog Energy 35:2328–2335. https://doi.org/10.1016/j.ijhydene.2010.01.054

Ryi S-K, Park J-S, Hwang K-R, Lee C-B, Lee S-W (2011) Repair of Pd-based composite membrane by polishing treatment. Int J Hydrog Energy. https://doi.org/10.1016/j.ijhydene.2011.07.120

Ryi S-K, Ahn H-S, Park J-S, Kim D-W (2014) Pd–Cu alloy membrane deposited on CeO_2 modified porous nickel support for hydrogen separation. Int J Hydrog Energy 39:4698–4703. https://doi.org/10.1016/j.ijhydene.2013.11.031

Ryms M, Januszewicz K, Lewandowski WM, Klugmann-Radziemska E (2013) Pyrolysis process of whole waste tires as A biomass energy recycling. Ecol Chem Eng S 20:93–107. https://doi.org/10.2478/eces-2013-0007

Saidi M (2018) Application of catalytic membrane reactor for pure hydrogen production by flare gas recovery as a novel approach. Int J Hydrog Energy 43:14834–14847. https://doi.org/10.1016/j.ijhydene.2018.05.156

Salehi M, Søgaard M, Esposito V, Foghmoes SPV, Persoon ES, Schroeder M, Hendriksen PV (2017) Oxygen permeation and stability study of $(La_{0.6}Ca_{0.4})_{0.98}(Co_{0.8}Fe_{0.2})O_{3-\delta}$ membranes. J Membr Sci 542:245–253. https://doi.org/10.1016/j.memsci.2017.07.050

Sánchez JM, Barreiro MM, Maroño M (2011) Hydrogen enrichment and separation from synthesis gas by the use of a membrane reactor. Biomass Bioenergy 35. https://doi.org/10.1016/j.biombioe.2011.03.037

Sanlisoy A, Carpinlioglu MO (2017) A review on plasma gasification for solid waste disposal. Int J Hydrogen Energy 42:1361–1365. https://doi.org/10.1016/j.ijhydene.2016.06.008

Santucci A, Borgognoni F, Vadrucci M, Tosti S (2013) Testing of dense Pd–Ag tubes: effect of pressure and membrane thickness on the hydrogen permeability. J Membr Sci 444:378–383. https://doi.org/10.1016/j.memsci.2013.05.058

Sanz R, Calles JA, Alique D, Furones L, Ordóñez S, Marín P, Corengia P, Fernandez E (2011) Preparation, testing and modelling of a hydrogen selective Pd/YSZ/SS composite membrane. Int J Hydrog Energy 36:15783–15793. https://doi.org/10.1016/j.ijhydene.2011.08.102

Sanz R, Calles JA, Alique D, Furones L (2012) New synthesis method of Pd membranes over tubular PSS supports via "pore-plating" for hydrogen separation processes. Int J Hydrog Energy 37:18476–18485. https://doi.org/10.1016/j.ijhydene.2012.09.084

Sanz R, Calles JA, Ordóñez S, Marín P, Alique D, Furones L (2013) Modelling and simulation of permeation behaviour on Pd/PSS composite membranes prepared by "pore-plating" method. J Membr Sci 446:410–421. https://doi.org/10.1016/j.memsci.2013.06.060

Sarkar N, Ghosh SK, Bannerjee S, Aikat K (2012) Bioethanol production from agricultural wastes: an overview. Renew Energy 37:19–27. https://doi.org/10.1016/j.renene.2011.06.045

Sato T, Suzuki T, Aketa M, Ishiyama Y, Mimura K, Itoh N (2010) Steam reforming of biogas mixtures with a palladium membrane reactor system. Chem Eng Sci 65:451–457. https://doi.org/10.1016/j.ces.2009.04.013

Scott K, Scott K (1995) Membrane materials, preparation and characterisation. Handb Ind Membr:187–269. https://doi.org/10.1016/B978-185617233-2/50005-2

Seelam PK, Piemonte V, De Falco M, Liguori S, Pinacci P, Calabrò V, Iulianelli A, Keiski R, Tosti S, Huuhtanen M, Basile A (2012) Hydrogen production from bio-ethanol steam reforming reaction in a Pd/PSS membrane reactor. Catal Today 193:42–48. https://doi.org/10.1016/j.cattod.2012.01.008

Shen Y, Zhao P, Ma D, Yoshikawa K (2014) Tar in-situ conversion for biomass gasification via mixing simulation with rice husk char-supported catalysts. Energy Procedia 61:1549–1552. https://doi.org/10.1016/j.egypro.2014.12.167

Sheth PN, Babu BV (2010) Production of hydrogen energy through biomass (waste wood) gasification. Int J Hydrog Energy 35:10803–10810. https://doi.org/10.1016/j.ijhydene.2010.03.009

Shi X, Jung KW, Kim DH, Ahn YT, Shin HS (2011) Direct fermentation of Laminaria japonica for biohydrogen production by anaerobic mixed cultures. Int J Hydrog Energy 36:5857–5864. https://doi.org/10.1016/j.ijhydene.2011.01.125

Silva FSA, Benachour M, Abreu CAM (2015) Evaluating hydrogen production in biogas reforming in a membrane reactor. Braz J Chem Eng 32:201–210. https://doi.org/10.1590/0104-6632.20150321s00002820

Singh Yadav V, Vinoth R, Yadav D (2018) Bio-hydrogen production from waste materials: a review. MATEC Web Conf 192:02020. https://doi.org/10.1051/matecconf/201819202020

Sircar S, Golden TC (2000) Purification of hydrogen by pressure swing adsorption. Sep Sci Technol 35:667–687. https://doi.org/10.1081/SS-100100183

Soomro A, Chen S, Ma S, Xiang W (2018) Catalytic activities of nickel, dolomite, and olivine for tar removal and H_2-enriched gas production in biomass gasification process. Energy Environ 29:839–867. https://doi.org/10.1177/0958305X18767848

Soria MA, Barros D, Madeira LM (2019) Hydrogen production through steam reforming of bio-oils derived from biomass pyrolysis: thermodynamic analysis including in situ CO_2 and/or H_2 separation. Fuel 244:184–195. https://doi.org/10.1016/j.fuel.2019.01.156

Steil MC, Fouletier J, Geffroy PM (2017) Surface exchange polarization vs. gas concentration polarization in permeation through mixed ionic-electronic membranes. J Membr Sci 541:457–464. https://doi.org/10.1016/j.memsci.2017.07.028

Stephen AJ, Archer SA, Orozco RL, Macaskie LE (2017) Advances and bottlenecks in microbial hydrogen production. Microb Biotechnol 10:1120–1127. https://doi.org/10.1111/1751-7915.12790

Strugova DV, Zadorozhnyy MY, Berdonosova EA, Yablokova MY, Konik PA, Zheleznyi MV, Semenov DV, Milovzorov GS, Padaki M, Kaloshkin SD, Zadorozhnyy VY, Klyamkin SN (2018) Novel process for preparation of metal-polymer composite membranes for hydrogen separation. Int J Hydrog Energy 43:12146–12152. https://doi.org/10.1016/J.IJHYDENE.2018.04.183

Sumrunronnasak S, Tantayanon S, Kiatgamolchai S (2017) Influence of layer compositions and annealing conditions on complete formation of ternary PdAgCu alloys prepared by sequential electroless and electroplating methods. Mater Chem Phys 185:98–103. https://doi.org/10.1016/j.matchemphys.2016.10.010

Sun Q, Li H, Yan J, Liu L, Yu Z, Yu X (2015) Selection of appropriate biogas upgrading technology-a review of biogas cleaning, upgrading and utilisation. Renew Sust Energ Rev 51:521–532. https://doi.org/10.1016/j.rser.2015.06.029

Swami Nathan S, Mallikarjuna JM, Ramesh A (2010) An experimental study of the biogas-diesel HCCI mode of engine operation. Energy Convers Manag 51:1347–1353. https://doi.org/10.1016/j.enconman.2009.09.008

Tanaka DAP, Tanco MAL, Okazaki J, Wakui Y, Mizukami F, Suzuki TM (2008) Preparation of "pore-fill" type Pd–YSZ–γ-Al_2O_3 composite membrane supported on α-Al_2O_3 tube for hydrogen separation. J Membr Sci 320:436–441. https://doi.org/10.1016/j.memsci.2008.04.044

Tang L, Huang H, Hao H, Zhao K (2013) Development of plasma pyrolysis/gasification systems for energy efficient and environmentally sound waste disposal. J Electrostat 71:839–847. https://doi.org/10.1016/j.elstat.2013.06.007

Tarditi AM, Cornaglia LM (2011) Novel PdAgCu ternary alloy as promising materials for hydrogen separation membranes: synthesis and characterization. Surf Sci 605:62–71. https://doi.org/10.1016/j.susc.2010.10.001

Tarditi A, Gerboni C, Cornaglia L (2013) PdAu membranes supported on top of vacuum-assisted ZrO_2-modified porous stainless steel substrates. J Membr Sci 428:1–10. https://doi.org/10.1016/j.memsci.2012.10.029

Tarditi AM, Imhoff C, Braun F, Miller JB, Gellman AJ, Cornaglia L (2015) PdCuAu ternary alloy membranes: Hydrogen permeation properties in the presence of H_2S. J Membr Sci 479:246–255. https://doi.org/10.1016/j.memsci.2014.12.030

Tarditi AM, Bosko ML, Cornaglia LM (2017) Electroless plating of Pd binary and ternary alloys and surface characteristics for application in hidrogen separation. Elsevier, Oxford, pp 1–24. https://doi.org/10.1016/B978-0-12-803581-8.09166-9

Thanuja MY, Anupama C, Ranganath SH (2018) Bioengineered cellular and cell membrane-derived vehicles for actively targeted drug delivery: so near and yet so far. Adv Drug Deliv Rev 132:57–80. https://doi.org/10.1016/j.addr.2018.06.012

Toledo-Alarcón J, Capson-Tojo G, Marone A, Paillet F, Júnior ADNF, Chatellard L, Bernet N, Trably E (2018) Basics of bio-hydrogen production by dark fermentation BT. In: Liao Q, Chang J, Herrmann C, Xia A (eds) Bioreactors for microbial biomass and energy conversion. Springer Singapore, Singapore, pp 199–220. https://doi.org/10.1007/978-981-10-7677-0_6

Torreiro Y, Maroño M, Sánchez JM (2017) Study of sour water gas shift using hydrotalcite based sorbents. Fuel 187:58–67. https://doi.org/10.1016/j.fuel.2016.09.038

Tosti S (2010) Overview of Pd-based membranes for producing pure hydrogen and state of art at ENEA laboratories. Int J Hydrog Energy 35:12650–12659. https://doi.org/10.1016/j.ijhydene.2010.07.116

Tosti S, Basile A, Bettinali L, Borgognoni F, Gallucci F, Rizzello C (2008) Design and process study of Pd membrane reactors. Int J Hydrog Energy 33:5098–5105. https://doi.org/10.1016/j.ijhydene.2008.05.031

Tosti S, Zerbo M, Basile A, Calabrò V, Borgognoni F, Santucci A (2013a) Pd-based membrane reactors for producing ultra pure hydrogen: oxidative reforming of bio-ethanol. Int J Hydrog Energy 38:701–707. https://doi.org/10.1016/j.ijhydene.2012.04.144

Tosti S, Accetta C, Fabbricino M, Sansovini M, Pontoni L (2013b) Reforming of olive mill wastewater through a Pd-membrane reactor. Int J Hydrog Energy 38:10252–10259. https://doi.org/10.1016/j.ijhydene.2013.06.027

Tosti S, Cavezza C, Fabbricino M, Pontoni L, Palma V, Ruocco C (2015) Production of hydrogen in a Pd-membrane reactor via catalytic reforming of olive mill wastewater. Chem Eng J 275:366–373. https://doi.org/10.1016/j.cej.2015.04.001

Tosti S, Fabbricino M, Pontoni L, Palma V, Ruocco C (2016) Catalytic reforming of olive mill wastewater and methane in a Pd-membrane reactor. Int J Hydrog Energy 41:5465–5474. https://doi.org/10.1016/j.ijhydene.2016.02.014

Truus de Vrije PAMC (2018) Production of butanol and hydrogen by fermentation techniques using steam treated municipal solid waste. www.wur.eu/wfbr

Tu X, Williams PT, Gadkari S, Nahil MA, Gu S, Liu SY, Mei DH (2017) Hybrid plasma-catalytic steam reforming of toluene as a biomass tar model compound over Ni/Al_2O_3 catalysts. Fuel Process Technol 166:269–275. https://doi.org/10.1016/j.fuproc.2017.06.001

Tucho WM, Venvik HJ, Stange M, Walmsley JC, Holmestad R, Bredesen R (2009) Effects of thermal activation on hydrogen permeation properties of thin, self-supported Pd/Ag membranes. Sep Purif Technol 68:403–410. https://doi.org/10.1016/j.seppur.2009.06.015

van Dijk HAJ, Walspurger S, Cobden PD, van den Brink RW, de Vos FG (2011) Testing of hydrotalcite-based sorbents for CO_2 and H_2S capture for use in sorption enhanced water gas shift. Int J Greenhouse Gas Control 5:505–511. https://doi.org/10.1016/j.ijggc.2010.04.011

Van Gestel T, Hauler F, Bram M, Meulenberg WA, Buchkremer HP, Van Gestel T, Hauler F, Bram M, Meulenberg WA, Buchkremer HP (2014) Synthesis and characterization of hydrogen-selective sol–gel SiO_2 membranes supported on ceramic and stainless steel supports. Sep Purif Technol 121:20–29. https://doi.org/10.1016/j.seppur.2013.10.035

Vásquez Castillo JM, Sato T, Itoh N (2015) Effect of temperature and pressure on hydrogen production from steam reforming of biogas with Pd-Ag membrane reactor. Int J Hydrog Energy 40:3582–3591. https://doi.org/10.1016/j.ijhydene.2014.11.053

Voss C (2005) Applications of pressure swing adsorption technology. Adsorption 11:527–529. https://doi.org/10.1007/s10450-005-5979-3

Wald K, Kubik J, Paciulli D, Talukder M, Nott J, Massicotte F, Rebeiz K, Nesbit S, Craft A (2016) Effects of multiple hydrogen absorption/desorption cycles on the mechanical properties of the alloy system palladium/silver (wt% = 10–25). Scr Mater 117:6–10. https://doi.org/10.1016/j.scriptamat.2016.02.017

Wang J, Wan W (2009) Factors influencing fermentative hydrogen production: a review. Int J Hydrog Energy 34:799–811. https://doi.org/10.1016/j.ijhydene.2008.11.015

Wang D, Czernik S, Chornet E (1998) Production of hydrogen from biomass by catalytic steam reforming of fast pyrolysis oils. Energy Fuels 12:19–24. https://doi.org/10.1021/ef970102j

Wang WP, Thomas S, Zhang XL, Pan XL, Yang WS, Xiong GX (2006) H_2/N_2 gaseous mixture separation in dense Pd/α-Al_2O_3 hollow fiber membranes: Experimental and simulation studies. Sep Purif Technol 52:177–185. https://doi.org/10.1016/j.seppur.2006.04.007

Wang J, Xu S, Xiao B, Xu M, Yang L, Liu S, Hu Z, Guo D, Hu M, Ma C, Luo S (2013) Influence of catalyst and temperature on gasification performance of pig compost for hydrogen-rich gas production. Int J Hydrog Energy 38:14200–14207. https://doi.org/10.1016/j.ijhydene.2013.08.075

Wang N, Chen D, Arena U, He P (2017) Hot char-catalytic reforming of volatiles from MSW pyrolysis. Appl Energy 191:111–124. https://doi.org/10.1016/j.apenergy.2017.01.051

Wang S, Yang X, Xu S, Li B (2018) Investigation into enhancing reforming of biomass-derived glycerol in a membrane reactor with hydrogen separation. Fuel Process Technol 178:283–292. https://doi.org/10.1016/j.fuproc.2018.06.004

Wee JH (2007) Applications of proton exchange membrane fuel cell systems. Renew Sust Energ Rev 11:1720–1738. https://doi.org/10.1016/j.rser.2006.01.005

Williams PT, Besler S, Taylor DT (1990) The pyrolysis of scrap automotive tyres: the influence of temperature and heating rate on product composition. Fuel 69:1474–1482. https://doi.org/10.1016/0016-2361(90)90193-T

World Bioenergy Association, 2019 (n.d.). https://worldbioenergy.org/

Wu JP, Brown IWM, Bowden ME, Kemmitt T (2010) Palladium coated porous anodic alumina membranes for gas reforming processes. Solid State Sci 12:1912–1916. https://doi.org/10.1016/J.SOLIDSTATESCIENCES.2010.06.024

Wu C, Wang Z, Wang L, Huang J, Williams PT (2014) Catalytic steam gasification of biomass for a sustainable hydrogen future: Influence of catalyst composition. Waste Biomass Valoriz 5:175–180. https://doi.org/10.1007/s12649-013-9244-9

Xu P, Jin Y, Cheng Y (2017) Thermodynamic analysis of the gasification of municipal solid waste-NC-ND license (http://creativecommons.org/licenses/by-nc-nd/4.0/). Engineering 3:416–422. https://doi.org/10.1016/J.ENG.2017.03.004

Yang F, Yang G, Feng Y, Xiao B, He M, Liu S, Li J, Luo S, Guo X, Hu Z (2008) Hydrogen-rich gas from catalytic steam gasification of municipal solid waste (MSW): influence of catalyst and temperature on yield and product composition. Int J Hydrog Energy 34:195–203. https://doi.org/10.1016/j.ijhydene.2008.09.070

Yin H, Yip ACK (2017) A review on the production and purification of biomass-derived hydrogen using emerging membrane technologies. Catalysts 7. https://doi.org/10.3390/catal7100297

Yue X-L, Gao Q-X (2018) Contributions of natural systems and human activity to greenhouse gas emissions. Adv Clim Chang Res 9:243–252. https://doi.org/10.1016/J.ACCRE.2018.12.003

Yun S, Ted Oyama S (2011) Correlations in palladium membranes for hydrogen separation: a review. J Membr Sci 375:28–45. https://doi.org/10.1016/j.memsci.2011.03.057

Yun S, Ted Oyama S, Oyama ST (2011a) Correlations in palladium membranes for hydrogen separation: a review. J Membr Sci 375:28–45. https://doi.org/10.1016/j.memsci.2011.03.057

Yun S, Ko JH, Oyama ST (2011b) Ultrathin palladium membranes prepared by a novel electric field assisted activation. J Membr Sci 369:482–489. https://doi.org/10.1016/j.memsci.2010.12.015

Zeng G, Goldbach A, Xu H (2009) Defect sealing in Pd membranes via point plating. J Membr Sci 328:6–10. https://doi.org/10.1016/j.memsci.2008.11.053

Zeng G, Goldbach A, Shi L, Xu H (2012) On alloying and low-temperature stability of thin, supported PdAg membranes. Int J Hydrog Energy 37:6012–6019. https://doi.org/10.1016/j.ijhydene.2011.12.126

Zhang B (2016) Chapter 1 – History–from the discovery of electroless plating to the present BT. In: Amorphous and nano alloys electroless depositions. Elsevier, Oxford, pp 3–48. https://doi.org/10.1016/B978-0-12-802685-4.00001-7

Zhao L, Goldbach A, Bao C, Xu H (2015) Sulfur inhibition of PdCu membranes in the presence of external mass flow resistance. J Membr Sci 496:301–309. https://doi.org/10.1016/j.memsci.2015.08.046

Zhao L, Goldbach A, Xu H (2016) Tailoring palladium alloy membranes for hydrogen separation from sulfur contaminated gas streams. J Membr Sci 507:55–62. https://doi.org/10.1016/J.MEMSCI.2016.01.055

Zhao S, Liao J, Li D, Wang X, Li N (2018a) Blending of compatible polymer of intrinsic microporosity (PIM-1) with Tröger's Base polymer for gas separation membranes. J Membr Sci 566:77–86. https://doi.org/10.1016/J.MEMSCI.2018.08.010

Zhao C, Xu H, Goldbach A (2018b) Duplex Pd/ceramic/Pd composite membrane for sweep gas-enhanced CO_2 capture. J Membr Sci 563:388–397. https://doi.org/10.1016/j.memsci.2018.05.057

Zornoza B, Casado C, Navajas A (2013) Chapter 11 – Advances in hydrogen separation and purification with membrane technology. In: Gandía LM, Arzamendi G, Diéguez PM (eds) Renew. Hydrog. Technol. Elsevier, Amsterdam, pp 245–268. https://doi.org/10.1016/B978-0-444-56352-1.00011-8

Index

Z. Zhang et al. (eds.), *Membranes for Environmental Applications*, Environmental Chemistry for a Sustainable World 42, https://doi.org/10.1007/978-3-030-33978-4